

The copyright of this thesis rests with the author.
No quotation from it should be published without
his prior written consent and information derived
from it should be acknowledged.

BASEMENT FAULT REACTIVATION: THE KINEMATIC EVOLUTION OF THE OUTER HEBRIDES FAULT ZONE, SCOTLAND.

by

Christopher Anthony Butler

**A thesis submitted in partial fulfilment of the requirements for the degree of
Doctor of Philosophy**

Department of Geological Sciences

University of Durham

September 1995



- 6 DEC 1995

DECLARATION

No part of this thesis has been previously submitted for a degree at this or any other university. The work described in this thesis is entirely that of the author, except where reference is made to previously published or unpublished work



C.A. Butler

University of Durham

Department of Geological Sciences
September 1995

Copyright © by C.A. Butler

The copyright of this thesis rests with the author. No quotation or data from it should be published without the authors prior written consent and any information derived from it should be acknowledged.

ABSTRACT

Basement fault reactivation has a profound effect on the response of the continental crust to plate tectonic forces. The Outer Hebrides Fault Zone (OHFZ), a major, (190km long) SE-dipping detachment exposed onshore within the Lewisian basement gneisses of the Outer Hebrides in NW Scotland, has frequently been cited as a 'type' example of a reactivated basement fault. A complex history of movements along this structure, and the possible causes of its reactivation behaviour have been revealed.

The earliest recorded fault zone movements are associated with a belt of upper greenschist facies, thrust-related mylonite which is spatially restricted to the northern part of the archipelago. Mylonitisation post-dates all the main Laxfordian deformation and intrusion events in the host gneisses and is therefore younger than c.1700 Ma. (late Laxfordian). Subsequent reverse faulting at lower P/T conditions occurs throughout the fault zone, and forms large areas of brittle crushing, containing pseudotachylite and ultracataclasite. Existing radiometric dates suggest that the brittle thrusting occurred at c.430 Ma. (Mid Silurian). The fault zone may have been segmented by oblique dextral/south-side-down transfer motion on steeply dipping shear zones in southern Harris between the two thrusting events. Thus, on either side of these transfer zones, the fault rock sequences developed during the early history vary, but later events are common to both fault segments.

Sinistral strike-slip displacements are associated with the development of discrete and anastomosing, low grade phyllonitic fabrics which post-date the earlier thrusting. Increasing deformation and associated fluid channelling through pre-existing, thrust-related anisotropies cause progressive low grade hydration of the fault rocks, which are transformed into green chlorite-white mica phyllonites in regions of highest strain. A late Caledonian (Siluro-Devonian) age for sinistral strike-slip is likely, based on isotopic data and regional considerations. Fluid influx associated with the development of the phyllonite belts appears to reflect a rapid increase in fault zone permeability which may have arisen due to the kinematically-controlled transition from load-strengthening (thrusting) to load-weakening (sinistral strike-slip) behaviour, and the generation of favourably oriented permeability pathways.

The phyllonite belts have preferentially acted as the loci for subsequent low greenschist facies extensional movements. These movements are manifested as low-angle normal faults separating packages of asymmetric, down-dip verging folds. Existing fabrics are either overprinted or reoriented. A direct relationship exists between the degree of retrogression in the phyllonitic rocks and degree to which those rocks have accommodated extension, suggesting that the phyllonites were rheologically softer than the surrounding rocks. A late Caledonian age for extension is likely, and may have been caused by the collapse of the Caledonian orogen at c. 400Ma.

The main offshore, basin bounding fault, the Minch Fault, lies immediately east of, and parallel to the onshore phyllonite belts. The geometry of this Mesozoic structure is probably controlled by the trace of the older OHFZ, and it is proposed that permanent reaction softening, caused ultimately by fluid influx during sinistral strike-slip movement, explains the direction of extension, the architecture of the offshore basins, and the long-lived, absolute and relative weakness of the OHFZ.

ACKNOWLEDGEMENTS

I would like to thank the following for their help and support during the last four years:

- Top of the list is my supervisor, Bob Holdsworth, without whom this thesis would never have come to fruition. I thank him not only for his enthusiastic supervision, advice and general encouragement, but also for the use of his house/ computer/ grass trimmer/ cast-off trousers etc.
- Thanks also to my other supervisor at Oxford Brookes, Rob Strachan, for introducing me to the pleasures of fieldwork in the Outer Hebrides and being generous in his advice throughout.
- Thanks to Amerada Hess Ltd. for their generous sponsorship of this project.
- Numerous islanders made my rather extended stay in the Outer Hebrides more enjoyable than it might have been. Among these, Maggie Cooper and 'the boys' in Claddach Baleshare, Annie and Jackie Morrison in Scalpay, Anne and Donald MacLellan in Lochboisdale and Don MacIntyre (the Stuley boatman) deserve a special mention.
- I'm very grateful to Rick Sibson who visited me in the Outer Hebrides and entertained my ideas on his 'uglification'. I felt less concerned about my task when he suggested I might try to distinguish pseudotachylite from ultracataclasite by hitting it with a hammer and listening (!).
- My friends at Oxford Brookes: the 'two lads' (Burns and Tribe); Richard; Tanya; and Martin have been the source of much insight, good humour and alcohol. Sincerest thanks must also go to Ian Tribe for braving the Park District of Lewis with me as my field assistant.
- My capacity as a structural geologist has benefited from numerous discussions with other like-minded types, past and present in Durham: Donny Hutton, 'Thuggy' Alsop, Michele, Mikey, Andy, Jipper, Roberto, Wayne-ee, Adam, Alun and Sporting-Jonny seem to have been the main protagonists. My heartfelt sympathies go to Jonny, who, having chosen to follow-up this work with his own, now has to try to understand what I meant when I said.....
- Thanks to Dave Schofield for providing me with vast numbers of maps.
- Cheers to my non-structural house/ office mates over the years (Pete, Sue, Stuart, Ivan, Steve, Charlotte and Tim) who probably kept me relatively sane. A great big 'thank-you' is also due to the present inmates of room 223 (Adam, Jo and Jonny) for not complaining when I impressed them with my seniority and chucked them off the computer.
- The technical/secretarial staff at Durham are the real heroes. Thanks to Dave Asbery for making it all work properly and for various bits of my ever-increasing collection of inexpensive furniture. Thanks to Karen for innumerable things, Julie, Ron and George for thin sections, Gerry and Alan for photos, Neville and Dave for computing expertise, and Carol, Lynn and Claire in the office.
- A HUGE thank you to Zoë, for cutting and pasting the old fashioned way all this week. Thanks a million.
- An acknowledgement is also due to all the post-grads I haven't mentioned by name. Thanks for being such a great crowd.
- Last, but certainly not least, very special thanks to Elizabeth, not just for typing a large chunk of data, but for her patience and support of all that this work entailed.

*Dedicated to my parents,
Tony and Jacqueline Butler.*

TABLE OF CONTENTS

Declaration	ii
Abstract	iii
Acknowledgements	iv
Contents	vi

PART ONE - INTRODUCTION

Chapter One: Introduction and overview of fault reactivation	1
1.1 Introduction	1
1.2 The continental tectonic framework of fault reactivation	2
1.3 Fault reactivation: a review of previous work	4
1.3.1 The recognition of fault reactivation	4
1.3.2 Palinspastic reconstructions	9
1.3.3 Indirect stratigraphic evidence	10
1.3.4 Spatial coincidence of modern and ancient structural lineaments	10
1.3.5 Direct stratigraphic evidence	13
1.3.6 Structural evidence	16
1.3.7 Isotopic evidence	18
1.3.8 Implications	18
1.4 An explanation of nomenclature used in this thesis	19
1.4.1 Metamorphic facies	19
1.4.2 Flow	20
1.4.3 Deformation mechanisms	22
Crystal-plastic flow	25
Diffusive mass transfer	25
Frictional grain boundary sliding, fracturing and cataclasis	26
The role of fluids in ductile deformation	27
Grain size effects	28
1.4.4 Fault rocks	29
1.4.5 Shear sense indicators	32
Linear features	32
Sense of movement criteria in the brittle regime	34
Sense of movement criteria in the ductile regime	36
1.5 Thesis outline	41
 Chapter Two: Previous work and the regional geology of the Outer Hebrides	 42
2.1 Introduction	42
2.2 The Lewisian Complex	44
2.2.1 Chronology	44
2.2.2 Composition	46
2.2.3 Structure and metamorphism	49
2.2.4 Regional significance of Lewisian events	54
2.3 The Outer Hebrides Fault Zone	59
2.3.1 General setting and the importance of the Outer Hebrides Fault Zone	59
2.3.2 Definition - The Outer Hebrides Fault Zone	59
2.3.3 Geographical setting	60
2.4 Previous work on the Outer Hebrides Fault Zone	60
2.4.1 Introduction	60
2.4.2 Displacement estimates for the OHFZ	61

2.4.3 The timing of OHFZ movements	62
2.5 The Stornoway Formation	63
2.5.1 Age of the Stornoway Formation	65
2.6 Post Lewisian minor intrusives	65
2.7 Offshore basins	66
2.7.1 The Sea of The Hebrides Basin	66
2.7.2 The North Minch Basin	69
2.7.3 The North Lewis Basin	70
2.8 Possible fault controls on basin formation	72
2.8.1 The Minch Fault / OHFZ	72
2.8.2 The Mid-Minch High	75
2.8.3 Subsidiary structures	76
2.9 Fieldwork methods	77
2.10 The Sub-division of the thesis	78

PART TWO - THE KINEMATIC HISTORY OF THE OUTER HEBRIDES FAULT ZONE.

Chapter Three: The kinematic history of the northern segment of the Outer Hebrides Fault Zone.

3.1 Introduction	80
3.2 Thrust movement	81
3.2.1 Scalpay	83
Geographical setting	83
Local Lewisian Geology	84
Pervasive mylonite formation	85
Cataclasis and fracturing	96
3.2.2 Loch Sgibacleit	98
Geographical setting	98
Local Lewisian Geology	98
Pervasive mylonite formation	100
Fracturing, Cataclasis and pseudotachylite formation	104
3.2.3 Central Lewis	108
3.2.4 Aird Raerinish	110
3.2.5 <i>Conclusions and discussion on thrusting in the northern segment</i>	111
Conclusions	111
Discussion	113
3.2.6 Summary	119
3.3 Strike-slip movement	119
3.3.1 Scalpay	120
3.3.2 The Park district of Lewis	128
3.3.3 Eishken	130
3.3.4 Rubha Vallerip	135
3.3.5 North-east Lewis	136
3.3.6. <i>Conclusions and discussion on strike-slip movement in the northern segment</i>	136
Conclusions	136
Discussion	138
3.3.6 Summary	139
3.4. Low-angle extensional faulting	140
3.4.1 Scalpay and South Harris	140
3.4.2 The Park district of Lewis	143
3.4.3 Eishken	143
3.4.4 Loch Sgibacleit and central Lewis	146
3.4.5 North-east Lewis	146
3.4.6 <i>Conclusions and discussion on low-angle extension in the northern segment</i>	146
Conclusions	146

Discussion	148
3.4.7 Summary	150
3.5 High angle extensional faulting and syn-tectonic sedimentation	150
3.5.1 Scalpay	151
3.5.2 The Park district of Lewis	151
3.5.3 North-east Lewis	152
Syn-tectonic sedimentation	152
3.5.4 Conclusions on steep faulting and syn-tectonic sedimentation	154
Conclusions	155
3.5.5 Summary	155
3.6 Chapter conclusions	156

Chapter Four: the kinematic history of the southern segment of the Outer Hebrides

Fault Zone	160
4.1 Introduction	160
4.2 Thrust movement	161
(i) North Uist and adjacent islands	161
Geographical setting	161
Lewisian geology of North Uist	162
Brittle thrust deformation in North Uist	163
4.2.1 Burrival region	164
West of the thrust base	164
The thrust base	166
East of the thrust base	167
An early, thrust related foliation	171
4.2.2 Eaval	176
4.2.3 Gairbh-eilean	178
4.2.4 Grimsay	179
4.2.5 Loch Steinavat	180
(ii) South Uist and adjacent islands	180
Geographical setting	180
Lewisian geology of South Uist	183
Brittle thrust deformation in South Uist	184
4.2.6 Bealach an Easain	185
4.2.7 Ben na Hoe	190
4.2.8 Eriskay	194
(iii) The Barra Isles	194
Geographical setting	194
Lewisian geology of the Barra Isles	195
Brittle thrust deformation in Barra	197
4.2.9 Castlebay to Otir Mhor	197
4.2.10 Vatersay	199
4.2.11 Halaman Bay, Borge and Greian Head	200
4.2.12 Conclusions and discussion on thrusting in the southern segment	204
Conclusions	204
Discussion	207
4.2.13 Summary	212
4.3 Strike-slip movement	213
(i) North Uist and adjacent islands	214
4.3.1 Burrival to Eigneag Bheag	216
Protophyllonites	216
Phyllonites	220
4.3.2 Ronay	231
4.3.3 Lochportain	232
4.3.4 South Eaval	234

(ii) South Uist and adjacent islands	236
4.3.5 Rubha Rossel	237
4.3.6 Ornish	244
4.3.7 Usinish Bay	246
4.3.8 Rubha Bolum	247
4.3.9 Stuley	249
4.3.10 Conclusions and discussion on strike slip in the southern segment	250
Conclusions	250
Discussion	253
4.3.11 Summary	256
4.4 Extensional movement	257
(i) North Uist and adjacent islands	257
4.4.1 Burrival to Eigneag Bheag	257
4.4.2 Ronay	264
4.4.3 Lochportain	266
4.4.4 South Eaval	269
(ii) South Uist and adjacent islands	271
4.4.5 Rubha Rossel	271
4.4.6 Ornish	275
4.4.7 Usinish Bay	275
4.4.8 Rubha Bolum	275
4.4.9 Stuley	277
4.4.10 Conclusions and discussion on extensional movement in the southern segment	282
Conclusions	282
Discussion	283
4.4.11 Summary	285
4.5 Chapter conclusions	285

PART THREE - SYNTHESIS

Chapter Five: A kinematic model for the OHFZ	291
5.1 introduction	291
5.1.1 Timing of movements	293
5.2 Along-strike differences in the kinematic evolution of the OHFZ	294
5.2.1 The distribution of ductile, thrust -related mylonites	295
5.2.2 The distribution of thrust-related brittle rocks	297
5.2.3 The geometry of phyllonite belts	297
5.2.4 The distribution and direction of low-angle extension	300
5.2.5 The distribution and direction of late, steep normal faulting	302
5.2.6 Summary	303
5.3 The role of the South Harris Shear Zones	303
5.3.1 A possible interaction between the OHFZ and the SHSZ	303
5.3.2 A preliminary investigation of the kinematic evolution of the SHSZ	306
The Langavat Shear Zone	308
The Leverburgh Shear Zone	312
The relative timing of movements	315
5.3.3 An integrated kinematic model for the OHFZ and SHSZ interaction	319
5.4 Estimates of displacement magnitudes on the OHFZ	321
5.4.1 Ductile thrust displacements	321
5.4.2 Brittle thrust displacements	322
5.4.3 Sinistral strike-slip displacements	323
5.4.4 Extension estimates	327
5.4.5 The relationship between fault kinematics and Caledonian plate motions	327
5.5 Summary of the kinematic evolution of the OHFZ	328

Chapter six: Possible causes of weakness and reactivation along the OHFZ	330
6.1 Introduction	330
6.2 Why are faults weak?	330
6.2.1 Transient, syn-tectonic mechanisms of rheological change	332
1 Fluid related processes	332
2 The generation of transient, fine grained reaction products	334
3 The introduction of melt	334
4 Shear heating	335
5 Transformational plasticity	335
6.2.2 Long-lived mechanisms of rheological change	336
1 Favourable orientation of a pre-existing anisotropy	336
2 Permanent reaction softening	340
3 Fabric softening and the formation of CPO's	341
4 Grain size reduction	341
5 Thermal perturbations	342
6 Permeability pathways	342
6.2.3 Conclusions on weakening processes: the importance of fluids	343
6.3 The link between kinematics and fluid flow	343
6.4 Implications for other reactivated basement faults	346
 References cited in the text	 347

Chapter One

Introduction and overview of fault reactivation

1.1 Introduction

It is widely known that many major faults and shear zones in continental crust show evidence of persistent reactivation. Imposition of new far-field stresses commonly reactivates old fault zones rather than creating new ones. There is growing evidence to suggest that fault zones behave as weaknesses compared with the surrounding intact crust, and that these weaknesses may persist for extremely long periods of geological time. Thus, fault zones may experience several phases of movement during their active lifetime, often with marked changes in their sense of displacement.

In much of the published literature, the existence of favourably oriented fractures at high crustal levels is regarded as the only necessity for fault reactivation to occur. At depth however, major faults become broad zones of cataclasis and ultimately ductile shear zones (Sibson 1977a), so the existence of fractures at high crustal levels cannot account solely for the reactivation process on a whole crustal scale. The purpose of this thesis is to investigate the patterns and products of basement fault reactivation by examining a major reactivated fault zone where high level brittle faulting and deeper level cataclasis and ductile shear products are all presently exposed at the surface. Such a study allows insights into the reasons why reactivation occurs at all crustal levels.

A study of the Outer Hebrides Fault Zone (OHFZ) in NW Scotland forms the basis of this project. It is one of the most frequently cited examples of a reactivated basement fault in the British Isles. It is well exposed onshore, and seismic reflection studies suggest that its trace corresponds closely to the location of offshore basin bounding structures. Almost for this reason alone, the OHFZ has achieved its status as a 'type' example of a reactivated fault with a basin forming episode occurring during reactivation. The primary aims of this thesis are to describe the kinematic evolution and style of deformation associated with the OHFZ. No comprehensive onshore study has been carried out on this basement structure since the advent of approaches employing deformation microstructures and kinematic indicators. The secondary aim is to address the problem of why major basement faults such as the OHFZ, once initiated remain vulnerable to reactivation.

1.2 The continental tectonic framework of fault reactivation

The strength of the continental crust

The distribution of seismicity at the earth's surface reflects the distribution of active deformation, and in oceanic areas it is concentrated at lithospheric plate boundaries. The essentially rigid body movements of these oceanic plates is classically cited as a basic tenet of plate tectonics but does not appear to apply equally well to continental regions (Molnar 1988). By contrast, the distribution of seismicity in continental regions is complex and diffuse, occurring in intraplate regions as well as at plate boundaries. In intraplate regions, shallow-focus earthquakes occur, often in distinct belts (e.g. East Africa and western USA) or in broad zones (e.g. eastern USA).

This complex nature of continental deformation compared to the relatively simple nature of oceanic deformation reflects three fundamental mechanical differences between continental and oceanic lithosphere:

1. Continental lithosphere is dominantly felsic and has a relatively lower *total strength* than dominantly mafic oceanic lithosphere. This is probably related to the thickness and strength of sialic crust (Fig. 1.1). Comparisons of total strength indicate that continental lithosphere is weaker than oceanic lithosphere by about a factor of 3 (Vink et al. 1984), whilst a thickened crust leads to a total strength that is half that of normal continental lithosphere (Fig. 1.2). The rheology of the oceanic lithosphere is dominated by olivine, with the strongest region lying in the upper mantle (c. 20 - 60km depth). At this depth range however, continental lithosphere is sialic crust and the constituent minerals (quartz and feldspar) are much weaker. Thus, the total strength is less.

2. Continental and oceanic lithosphere have very different *vertical strength distributions* arising from their very different compositional layering. Continental lithosphere may comprise three (or more) rheologically separate layers (Brace et al. 1980): A seismically active upper crust; an aseismic ductile lower crust; and a strong, occasionally seismic uppermost mantle, which because it lies at greater depths is still not as strong as oceanic *crust* (Chen & Molnar 1983). This strength profile is likely to facilitate decoupling of continental crust from mantle, and separate upper crust with minor faults from ductilely deformed lower crust and mantle. This decoupling process appears to be confirmed by deep seismic reflection profiling (e.g. BIRPS, MOIST and DRUM data [Brewer and Smythe 1984]). Decoupling

enables upper crustal blocks to be driven by flow beneath in the lower crust and mantle and there is abundant evidence for large horizontal translations of such blocks.

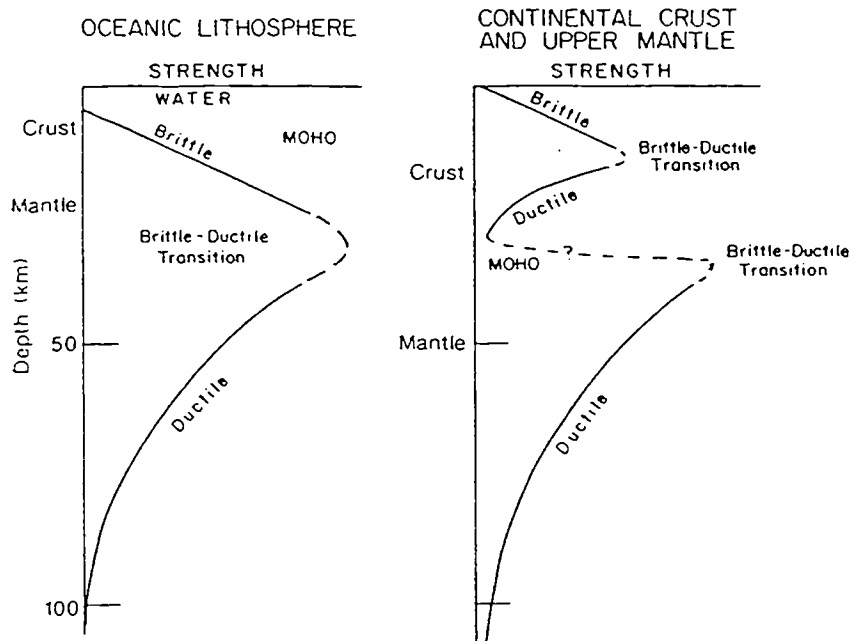


Figure 1.1. Profiles of strength across oceanic and continental lithosphere, based on frictional strengths at shallow depths and ductile flow laws of minerals at greater depths. Note the strong core of oceanic lithosphere at depths of c. 20 - 60 km and the probable weak, ductile region in the lower continental crust. The strengths cannot be usefully quantified due to the uncertainties in the flow laws, and modifications from fluids, melting and mineral impurities. (From Molnar 1988).

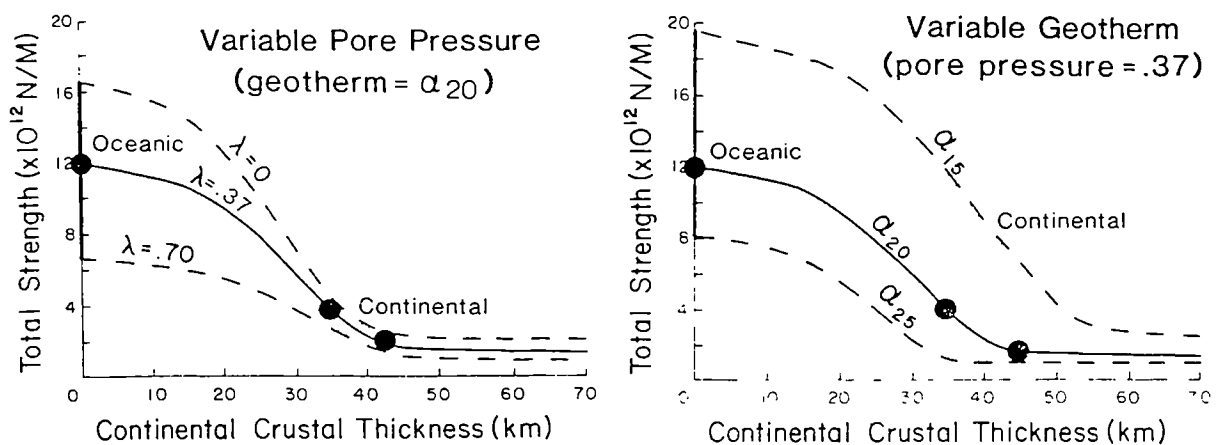


Figure 1.2. Total strength of the lithosphere as a function of continental crustal thickness. Zero crustal thickness corresponds to oceanic crust and olivine controlled rheology. Diagram on the left shows constant geotherm (α_{20}) and varying pore pressure (λ). Diagram on the right shows constant pore pressure ($\lambda = 0.37$) and varying geotherm (α). (From Vink et al. 1984)

3. Continental lithosphere has a very different *lateral strength distribution* in that it contains many old mechanical anisotropies (e.g. weak faults and shear zones). These anisotropies result from the progressive accretionary growth of continental regions that occurs because the buoyancy of continental lithosphere prevents its subduction (McKenzie 1969). During accretion, faults and/or shear zones are incorporated into the continents as a result of the re-stacking and deformation of previously thinned (and therefore more likely to re-thicken) marginal areas (Dewey et al. 1986). The term thrust 'flaking' has been applied to this re-stacking process (Oxburgh 1972), and the flakes exist as rigid bodies separated by rheologically weaker anisotropies. The intrinsic weakness in the lateral strength of the continental crust that such anisotropies create manifests itself in several different ways:

- Deformation is localised into *shear/fault zone networks that separate regions of lower or no strain*. This may be termed '*deformation intensity partitioning*'.
- Regional deformation may be separated into two or more constituent components of the total strain field (i.e. translation +/- rotation +/- simple shear +/- pure shear). This may be termed '*kinematic partitioning*'.
- When far-field tectonic stresses or local body forces are imposed on existing faults and shear zones, renewed failure may occur in the same or in a different shear sense to that which caused fault inception. This is termed *reactivation* and forms the subject matter for this thesis.

1.3 Fault reactivation: a review of previous work

1.3.1 The recognition of fault reactivation

Nearly fifty years ago, Kennedy (1946) noted that the Great Glen Fault of northern Scotland had experienced more than one movement episode. At around the same time, Hills (1946) observed that major faults and shear zones may remain intermittently active through long periods of geological time. Hill's work, based in continental Australia demonstrated that most faults in basement rocks are parallel to older structural fabric trends, and that there was a wealth of independent geological evidence to suggest that these structures had long tectonic histories. He termed this phenomenon "resurgent tectonics", emphasising the intermittent behaviour of fault movement with long periods of quiescence.

Since this early work, many studies have reported the process of fault reactivation. Reactivated faults have been inferred or demonstrated in the published literature by way of one or more of the following six ways.

Fault reactivation can be inferred using:

1. *Palinspastic reconstructions.* Fault reactivation is implied by the lack of abnormally thick basement in regions where cover rocks have been shortened. If continental basement undergoes thinning by normal faulting prior to orogenesis, reversal of movement during shortening prevents overthickening and/ or subduction.
2. *Indirect stratigraphic evidence.* This includes repeated fault scarp breccia deposits and lateral facies variations. Rejuvenation cycles such as these are present in many Mesozoic sedimentary basins (e.g. the Northumbria Basin (Gawthorpe et al. 1989)). Other examples are discussed by Athurton et al. (1989)
3. *Spatial coincidences of modern and ancient structural lineaments.* Magmatism and/or syn-tectonic sedimentation and/or faulting/ earthquake activity (from either modern or historical earthquake records) along ancient faults/ shear zones may constitute a method of inferring fault reactivation.

Fault reactivation can be demonstrated using:

4. *Direct stratigraphic evidence* includes changes in sediment package thicknesses across faults, repeated footwall uplift unconformities, basin inversion geometries and syn-tectonic sedimentation episodes.
5. *Structural evidence* include changes in kinematic history and changes in distribution and nature of deformation within fault and/or shear zones. These in themselves may not be conclusive and may require independent age constraints.
6. *Isotopic evidence* may be attained by directly dating the fault products involved in deformation and/or indirectly dating the fault products by dating cross-cutting units (e.g. igneous intrusions).

Table 1.1 shows a selection of previous fault reactivation studies and the means by which these were recognised. Some of these are enlarged upon below.

Location	Nature and age of weak zone	Nature and age of reactivation	Type of evidence	Reference
Australia	Precambrian intercratonic steeply dipping fault zone 'lineaments' e.g. Ordovician Muckleford fault	Up to and including recent strike-slip movements. Late Tertiary movements on the Muckleford Fault	Geological	Hills 1946 Hills 1960
Scotland	Palaeozoic Great Glen Fault with strike-slip movements	Strike-slip movement in the mesozoic and historic earthquakes	Geological and neotectonic	Kennedy 1946
E. North America	Appalachian fold and thrust belt	Late Mesozoic/Cenozoic rifting and recent seismicity	Geological and neotectonic	Woolard 1958 Sykes 1978
S. and SW. Africa	Late Precambrian Nama fold belt	Modern continental margin fracture zone	Geological	Kennedy 1965
NE. USA	Precambrian Ramapo fault system	Variety of movement directions in Palaeozoic, Triassic and Jurassic. Graben bounding extensional faults	Geological	Ratcliffe 1971
E. Africa	Precambrian intercratonic steep belts	Several fragmentation events up to recent rifting	Geological	McConnell 1972
S. Africa	Damaran-Katangan orogenic belt. (700-450 m.a.)	Reactivations in Mesozoic (Karoo age), Cenozoic magmatism and present seismicity	Geological and neotectonic	McConnell 1972
Turkey	Mudurna extensional faults on Precambrian structural trend	Present strike-slip reactivation	Neotectonic	McKenzie 1972
W. Australia	Darling Fault Zone with normal faulting in the Mesozoic	Thrust faulting associated with present seismicity	Neotectonic	Fitch et al. 1973 Sykes 1978
S. and E. Greenland	Archaean Nagssugtoqidian and Ketilidian mobile belts (2650 m.a.) with transcurent motion	Continued movement in the Phanerozoic	Geological	Bridgewater et al. 1973 Watterson 1975
S. USA (Texas, Arkansas)	Palaeozoic compressional Ouchita-Wichita mountain belt	Triassic, Jurassic and recent reactivations along strike of thrust front	Geological and neotectonic	Nuttli 1973
Himalayas	Pre-existing faults north of Himalayas	Collisional reactivation in the Cenozoic	Geological and neotectonic	Molnar and Tapponnier 1975
Ghana	Late Precambrian/Early Palaeozoic age suture zone in Accra region	Rifting during South Atlantic opening in Mesozoic/Cenozoic and historical seismicity	Geological and neotectonic	Blundell 1976
E. Australia	Palaeozoic orogenic belts east of 138° E	Tertiary continental fragmentation, fracture zones, alkali magmatism (Colchester 1972) and recent seismicity	Geological and neotectonic	Coward 1976
Red Sea	Precambrian age continental fractures	Direction of spreading and control of transform faults from Cenozoic to recent	Geological and neotectonic	Garson and Krs 1976

Table 1.1. Table of previous work on fault reactivation

Brazil and Africa	Precambrian Pernambuco lineament in Brazil and Ngaurandéré fault zone in Africa	Cretaceous reactivation of both during rifting and continental separation	Geological and neotectonic	Gorini and Bryan 1976
SE. USA	Palaeozoic fault system including the Goat Rock Fault in S. Carolina and Georgia	Recent and historic earthquakes on the Goat Rock Fault during reverse motion	Neotectonic	Talwani and Howell 1976
N. Canada	Palaeozoic 'structures' with early rifting	Recent compressional seismicity	Neotectonic	Basham et al. 1977
E. USA	Triassic and Jurassic Brandywine and Stafford fault zones in NE. Virginia and Maryland with extensional geometries	High angle reverse faulting in the late Mesozoic and Cenozoic under horizontal compression	Geological	Mixon and Newell 1977
NE. USA	Precambrian Ramapo fault system with extension in the Mesozoic	Present reverse faulting with seismicity	Neotectonic	Aggarwal and Sykes 1978
Brazil	Amazon basin pre-Mesozoic intercratonic ?suture/?rift	Historical earthquakes on St. Paul's and Romanche fracture zones along strike	Neotectonic	Sykes 1978
Brazil	Precambrian/Early Palaeozoic 'tectonic feature'	Cretaceous reactivation forming the pattern of present -day fracture zones in the S Atlantic	Geological and neotectonic	Sadowski 1978
Malay basin	Basin development up to the end of the Miocene	Erosion due to Inversion at the end of the Miocene/beginning of the Pliocene	Geophysical	Bubb and Hayash 1980
Iran	Mesozoic subsiding continental margin with extensional faulting	Tertiary collisional Zagros mountain belt with recent seismicity	Neotectonic	Jackson 1980
W. USA	Precambrian 'zone of weakness'	Basin and Range oblique/normal reactivation from mid-Miocene to recent	Geological (kinematic analysis)	Zoback and Zoback 1980
Chile	Andean extensional faults	Post depositional shortening by reactivating normal faults as thrusts	Geological (stratigraphic)	Winslow 1981
S. North Sea	Permian to late Cretaceous basin development	Inversion in early to late Cretaceous	Geophysical (seismic and wireline logs)	Glennie and Boegner 1981
S. England	Variscan thrusts in Wessex	1) negative inversion to form Wessex basin by Mesozoic extension 2) positive inversion under Tertiary compression	Geophysical (seismic)	Chadwick et al. 1983
SE USA	Palaeozoic thrust faults in Appalachian orogen. e.g. the Augusta Fault	Triassic extensional reactivation of thrusts to form Riddville basin	Geophysical (seismic and aeromagnetic)	Peterson et al. 1984
W. and Central Europe	Triassic to Early Cretaceous grabens	Alpine Orogeny causes inversion of Mesozoic grabens by reversing fault movement	Geological	Ziegler 1983 Ziegler 1989
N. Atlantic	Late Jurassic/Early Cretaceous extension of the Rockall Trough	Oligo-Miocene inversion	Geophysical (seismic)	Roberts et al. 1983

Table 1.1. Table of previous work on fault reactivation (Continued).

NW. Scotland	Caledonian thrusting in NW. Scotland	Late Palaeozoic/Mesozoic extension	Geophysical (seismic)	Brewer and Smythe 1984
W. North America	Mesozoic/Early Tertiary compressional crustal welt in the Cordilleran hinterland	Tertiary gravitationally induced extensional collapse	Geophysical	Coney and Harms 1984
New Zealand	Late Cretaceous strike-slip zone (the Alpine fault)	Two strike-slip reactivations but since Mid-Tertiary, oblique reverse dextral movement	Geological and absolute dating	White and Green 1985
E. USA (Pennsylvania)	Palaeozoic imbricate thrust sheets	Low angle extension to form Newark Basin bounding faults	Geological (kinematic analysis)	Ratcliffe et al. 1986
W. Australia	Precambrian sinistral strike-slip close to the Darling fault zone (see Blight 1981)	Normal and reverse dip-slip reactivation of the Darling Fault Zone up to the Late Cretaceous	Geological (Kinematic analysis)	White et al. 1986
NE. Africa	Precambrian sutures (the Onib Hamisana and Baraka suture zones)	Late Cretaceous and Tertiary rifting	Geological	Dixon et al. 1987
Peru	Cenozoic to recent thrusts at Ancash	Present-day extension above 4000m	Neotectonic	Doser 1987
Egypt	Extensional Rifting event c. 32 M.a. in the Gulf of Suez	Early Miocene Fault Reactivation (16.5 M.a.) associated with uplift	Geological (sedimentological)	Smale et al. 1988
N. Scotland	Late Caledonian and Variscan thrusts	Extension during the Devonian and Permo-Carboniferous to form basins, and inversion reversing fault motion in late Mesozoic and Tertiary	Geophysical (seismic)	Coward et al. 1989
Central and E. Africa	Precambrian sutures	Mesozoic (Karoo age) rifting and strike-slip reactivation	Geological	Daly et al. 1989
S. America	Circum-Pacific margin basis with normal basin bounding faults	Mid Cretaceous inversion with reverse motion on normal faults	Geological	Dalziel 1989
French Alps	Mesozoic extension creating a complex faulted passive margin	Cretaceous to Pliocene inversion by Alpine Orogeny	Geological	Gillcrist et al. 1989
Antarctica	Proterozoic pseudotachylites in Vestfold Hills	Ductile reactivation of brittle fault rocks constrained by minor intrusives	Geological	Passchier et al. 1990
Scotland	Precambrian, ductile, sinistral shearing in the Gairloch area	At least 4 reactivations since Precambrian with chiefly brittle, dextral sense of shear	Geological (kinematic analysis)	Shiue and Park 1993
Canada	Precambrian Strike-slip motion along Gander-Avalon boundary, Newfoundland	3 phases of post-Silurian reactivation including sinistral and dextral strike-slip	Geological (kinematic analysis)	Holdsworth 1994

Table 1.1. Table of previous work on fault reactivation (Continued).

1.3.2 Palinspastic reconstructions

The idea that fault zones may accommodate various displacements at different times in their history arose through deduction rather than detection. Helwig (1976) pointed out that a space problem existed in shortened orogenic belts. If a decollement surface existed between folded (and shortened) sedimentary cover rocks and the underlying basement rocks, what process prevented the basement from becoming abnormally thick, since this too had to shorten during orogenesis? He realised the problem was diminished if the basement was thin prior to shortening.

This model appears to be borne out by studies in the Zagros mountains of Iran (Jackson 1980), where a Tertiary mountain belt, resulting from the collision of Arabia with Iran, deforms a Mesozoic continental margin (Stocklin 1968). This continental margin is inferred to have been a relatively thin portion of subsiding crust, similar to the present-day Aegean region, where the crust is being actively thinned by normal faulting (McKenzie 1978). In the Zagros region, during the early stages of compression, reversal of the sense of motion on normal faults would shorten the previously thinned basement, returning it to its original thickness and shortening the cover rocks by folding. This avoids over-thickening or subduction of continental material. Present-day reverse faulting observed in the Zagros is at a high angle (40° - 50°), not the more typical 30° predicted by Andersonian or Mohr Coulomb theory, suggesting that the reactivation of normal faults has occurred in compression. In addition, these high angle reverse faults are very similar in dip and orientation to active extensional normal faults in western Turkey (McKenzie 1972). Jackson's model therefore predicts two things:

1. Plate convergence will occur until previously thinned basement is returned by compression to its original thickness, when it either becomes over-thickened, or is partially forced down into the mantle forming a deep crustal root zone. In these cases, the formation of an overthickened region of continental crust leads to substantial uplift forming a mountain range in order to maintain isostatic equilibrium (Bott 1971).
2. During the initial stages of compression, the basement will be thinner and have a higher heat flow than the neighbouring craton.

In the absence of a deep crustal root below active orogenic belts, basement fault reactivation and reversal of movement sense has to be invoked to avoid palinspastic reconstruction problems (Helwig 1976, Butler 1989).

1.3.3 Indirect stratigraphic evidence

Fault reactivation has been inferred for many years on the basis of indirect stratigraphic evidence. Rejuvenation of sediment source areas, stratigraphic thickness and lateral facies changes, and repeated fault scarp wedge deposits have been taken as evidence for multiple movement histories for many faults and fault zones (e.g. the Bala Fault and others in the North Wales Shelf (Gawthorpe et al. *in* Athurton et al. 1989), the Curlew Fault NW Ireland (Philcox et al. *in* Athurton et al. 1989), and the Gulf of Suez faults (Smale et al. 1988)). Such syn-depositional faulting was regarded as evidence for periodic reactivation by a 'stick-slip' mechanism, similar to that operating in the San Andreas Fault.

1.3.4 Spatial coincidence of modern and ancient structural lineaments

The control on location, geometry, magmatism and sedimentation in rift zones of north and east Africa has been attributed to the pre-existence of Precambrian structures (Dixon et al. 1987, Daly et al. 1989). This has largely been inferred from the similar orientations and locations of basement suture zones and displacements of Tertiary ridge troughs and modern-day coastlines. The inherited structures act as weaknesses or 'stress guides' (Dixon et al. 1987) for the subsequent evolution of the rift zones. In order for the pre-existing structures to be utilised again Dixon et al. (1987), suggest two conditions are necessary:

- The structure must be oriented correctly with respect to the new regional stresses
- The structure must be significant both in spatial extent (including depth) and in its strength contrast with the surrounding crust.

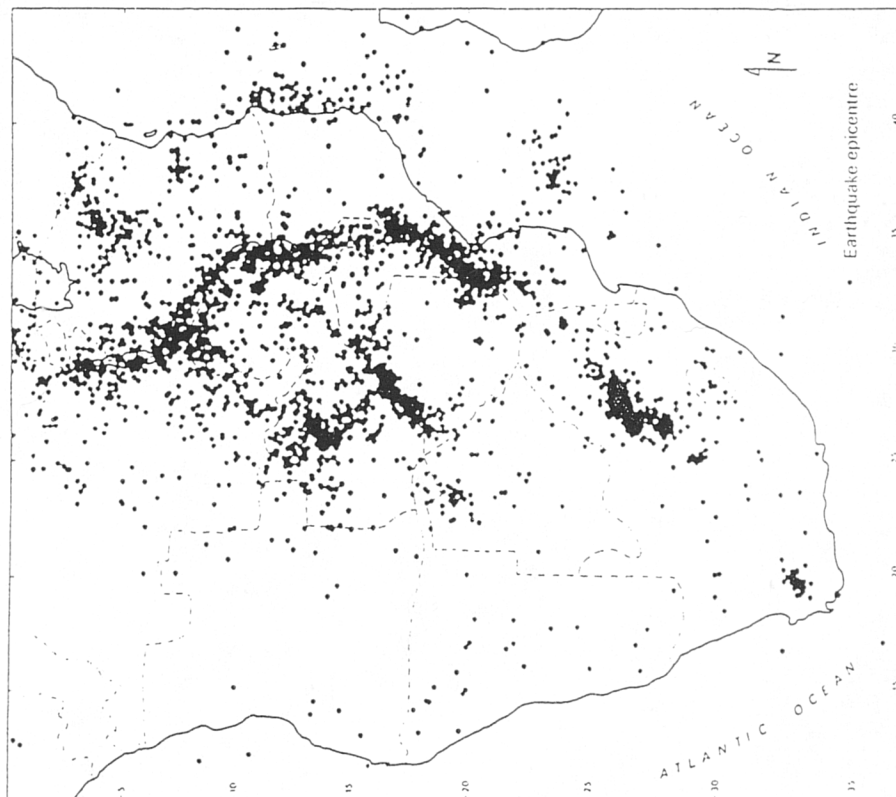
In the Red Sea, the 20° obliquity of the controlling structures with the rift propagation direction appears to be sufficiently close to allow reactivation. The surface extent of the controlling structures suggest that they extend through a significant portion of the lithosphere, and if they represent ancient suture zones, then they may have vertical lithospheric dimensions of 100 - 200 km (Briden et al 1981) and are very likely to extend through the entire lithosphere. Dixon et al (1987). suggest that the contrast in metamorphic grade across part of one of the structures, and the serpentinitised ultramafic rocks with a strong tectonic fabric therein, probably causes a contrast in mechanical properties. The structures therefore act as weak zones, and may be utilised again under renewed tectonic stresses

The most obvious evidence for inferring fault reactivation comes from the occurrence and distribution of neotectonic earthquake shocks in ancient deformation zones. In continental regions, intraplate earthquakes are typically concentrated along pre-existing zones of weakness, such as fault zones, suture zones or failed rifts. These weaknesses also control the distribution of oceanic transform faults, and the shape of continental margins. Present-day earthquake studies and fault plane solutions in the Zagros mountain belt have shown that 20 - 50 km of shortening has occurred chiefly on pre-existing normal faults (Jackson 1980). At Mudurna, Turkey, strike-slip faults result from reactivation of pre-existing extensional structures (McKenzie 1972), showing the ability of a favourably oriented mechanical weakness to accommodate a variety of movements. Those weaknesses near continental margins are especially vulnerable to reactivation. During continental separation, oceanic transform faults are preferentially located near the ends of continental zones of weakness (Fletcher et al. 1978, Sykes 1978). Other intraplate shocks occur parallel, not normal to the strike of the continental margin and reflect the existence of older fold and thrust belts which govern the shape of the continental margin, such as the Appalachian / Caledonian orogen of east USA, Canada, Greenland, Norway, Spitzbergen and the UK (Woollard 1958; Haller and Kulp 1962; Husebye et al. 1975; Lilwall 1976). Thus the Atlantic Ocean developed close to the suture where the ancestral ocean (Iapetus) closed during the last orogeny (Wilson 1966).

A great deal of work has been carried out in Africa, where basement fault and suture zones exert a fundamental control on the geometry and kinematics of present-day rifting. The distribution of recent seismicity is spatially coincident with the intercratonic suture zones which separate tectonic flakes (Fig.1.3). Neotectonic rifting is preferentially located at the margins of older, more stable cratonic areas. These have been fragmented and sutured several times in their history. The East African Rift system always follows pre-existing zones of weakness between cratons (McConnell 1972). Some weaknesses have been reactivated many times over and have been termed "Perennial deep faults" due to their long-lived nature (McConnell 1972). In South Africa, late Precambrian (Pan-African) trends strike parallel to the west coast and have exerted a strong control on the geometry of the present continental margin, Mesozoic fracture zones and alkaline magmatic centres (Kennedy 1965; Fuller 1971).

Figure 1.3. Maps showing the spatial coincidence of ancient intercratonic orogenic belts and historical seismicity.

- A) The geology of southern Africa outlining the main Precambrian Cratonic and orogenic areas and showing how the Phanerozoic rift basins are located almost entirely within the orogenic zones.
- B) The distribution of historical seismic events in Africa. Note how the seismicity is also confined to the orogenic zones. (From Daley et al. 1989).



In South America, similar Precambrian structures with renewed tectonism have controlled the locations of major transform faults involved in the early opening of the South Atlantic (Sykes 1978). The reactivation of Precambrian structural trends by Mesozoic to recent faulting have also been documented in Australia, where historical seismic activity has occurred in response to present-day compressional stresses (Fitch et al. 1973)

In areas of present-day subduction at continental margins, earthquake studies have revealed that fault reactivation involving reversal of movement sense can occur on a much shorter geological timescale than considered previously. The Ancash, Peru, earthquake of 1946 occurred due to the re-use of pre-existing thrust structures in an extensional regime (Doser 1987). The bulk stress regime presently operating in the Andes is however, compressional. Doser (after Dalmayrac and Molnar 1981), accounts for this apparent paradox of local extension by the effect of topographic elevation on the stress field. At high elevations, the vertical stress due to gravity, is inferred to exceed the horizontal, tectonic stress, so that normal faulting results above c. 4000m at Ancash, whilst active reverse faulting occurs at c. 1000m elsewhere. Doser concludes that reactivation occurred because the pre-existing thrust dislocations acted as significant weaknesses and were favourably orientated for the new stress regime.

1.3.5 Direct stratigraphic evidence

Direct stratigraphic field evidence for reverse thrusting along inherited normal faults has been reported from many regions. In South America, up to 40 % of extension occurred in the present-day Chilean Andes prior to some 20 - 40 km of post depositional shortening on high angle reverse faults, as demonstrated by the offset of stratigraphic marker horizons (Winslow 1981). In Terra del Fuego, basement upthrusting along reactivated normal faults accounts for some 5 km of reverse movement on a deformed marginal basin. This reversal of movement has created unusual stratigraphic effects, such as thicker depositional sequences on horsts compared to adjacent grabens, and elsewhere in the basin, undeformed ophiolites sitting on horsts up to 500m above the basin infill.

Large-scale studies of offshore and onshore sedimentary basins and orogenic belts have led to the concept of *inversion tectonics*. *Positive basin inversion* is widely held as 'the transition within a basin from subsidence and net deposition to uplift and net erosion' (Todd & Turner in Cooper et al. 1989). The term *negative inversion* is less widely used but is essentially the opposite, i.e. 'the transition from contraction to extension' (Cooper and Williams in Cooper et al.

1989), and is more pertinent to this study. Both positive and negative inversion are likely to involve reactivation of faults in the opposite sense.

Negative inversion

Peterson et al. (1984) document the results of an interpretation of Consortium for Continental Reflection Profiling (COCORP) seismic data which transected the southern part of the Appalachian Orogen in SE U.S.A. A Triassic basin (the Riddleville Basin), picked out by an aeromagnetic low, was shown to be a half graben with a bounding fault that appears to merge into a pre-existing Palaeozoic detachment. This detachment has a similar geometry to thrust faults which were formed during an earlier collisional episode of the Appalachian Orogeny. They interpreted the basin bounding normal fault as a reactivated thrust fault that splays off a deeper detachment (the Augusta Fault).

Coney and Harms (1984) put forward the suggestion that the Basin and Range of Canada, the U.S.A. and Mexico resulted from gravitationally induced spreading and deep-seated crustal extension of an overthickened crustal welt in the Cordilleran hinterland. This had the effect of reversing earlier compression and superposing Tertiary extensional tectonic fabrics on earlier structural and metamorphic fabrics formed during Mesozoic - early Tertiary crustal shortening.

McClay et al. (1986), suggest that the Devonian basins of N. Scotland resulted from the orogenic collapse of the Caledonian mountain chain soon after the cessation of compressional tectonics. These authors also make the analogy with Coney and Harm's (1984) orogenic collapse model for the Basin and Range, proposing that extension was facilitated by reversal of movement on reactivated compressional structures. Caledonian orogenic collapse has also been well documented from Scandinavia (e.g. Cashman 1990, Fossen 1992, Steltonpohl and Bartley 1993), and the process of orogenic collapse is discussed at length by Dewey (1988).

Positive inversion

Positive inversion structures are most readily recognised from seismic data provided certain requirements are met (Fig 1.4). A basin fill sequence, synchronous with extension (synrift), is a necessity in unequivocal recognition of inversion structures (Cooper & Williams *in* Cooper et al. 1989). In a partially inverted half graben for example, the upper part of the fault causes the elevation of a syn-rift marker horizon to lie above the regional elevation. On the lower part, however, the beds still lie below their regional elevation. The change-over, where the hanging-wall beds are at the regional elevation is termed the *null-point* (Williams et al.

1989). Identification of a null point is critical in the recognition of inversion from seismic data. Also, the post-rift sequence, being longer than the pre-rift, bows upwards in an asymmetric anticline during inversion, such as the Pliocene beds in the Malay Basin (Bubb & Hayash 1980). The degree of inversion can range from partial inversion, where the lower parts of the basin retain their original geometry, to total inversion, where reverse movements along extensional faults are reversed to the null point or beyond (Ziegler *in* Cooper et al. 1989b). This is only considered to be inversion if the degree of extension and compression are of the same order of intensity (cf. de Graciansky 1989). If compression is in the order of magnitude observed in mountain belts then this is not considered inversion. Hayward and Graham (1989) use the example of the moderately inverted Broad Fourteens Basin in the southern North Sea to show that the major basin-bounding, listric, basement fault, which acted as an extensional syn-depositional structure during the Jurassic and Cretaceous, was reactivated as a thrust in the Late Cretaceous. Figure 1.4 shows the possible geometries that could arise from inversion of a simple listric fault system:

- High-angle thrust faults and footwall shortcut thrusts.
- Syn-rift sequences which are elevated above the regional elevation so that wedges exist in complex 'harpoon' or 'arrowhead' geometries.
- In-sequence backthrusts propagating towards the hangingwall. These result from the buttressing effect of the high angle extensional fault.

Many documented examples of inversion have multiple movement histories e.g. the Wessex Basin (Stoneley 1982, Simpson et al. 1989), corroborating the independently derived idea that once a deep crustal fault system has been established it will be re-used to some extent by all subsequent phases of deformation. In the southern North Sea, all major structural elements north west of the Wales-Brabant Massif were inverted during a short compressive event which punctuated the regional subsidence. (Badley et al. 1989). One of these structures, a major extensional fault (the South Hewett Fault), was reactivated twice in a reverse sense; firstly during the late Cretaceous and again in the Miocene, to form a subsequently eroded, monoclinical block. Similarly, a zone of SW-dipping tilted fault blocks, formed by localised Late Jurassic extension, was reactivated in a reverse sense during the late Cretaceous. The cover sequence preserves 'harpoon' geometries indicative of inversion.

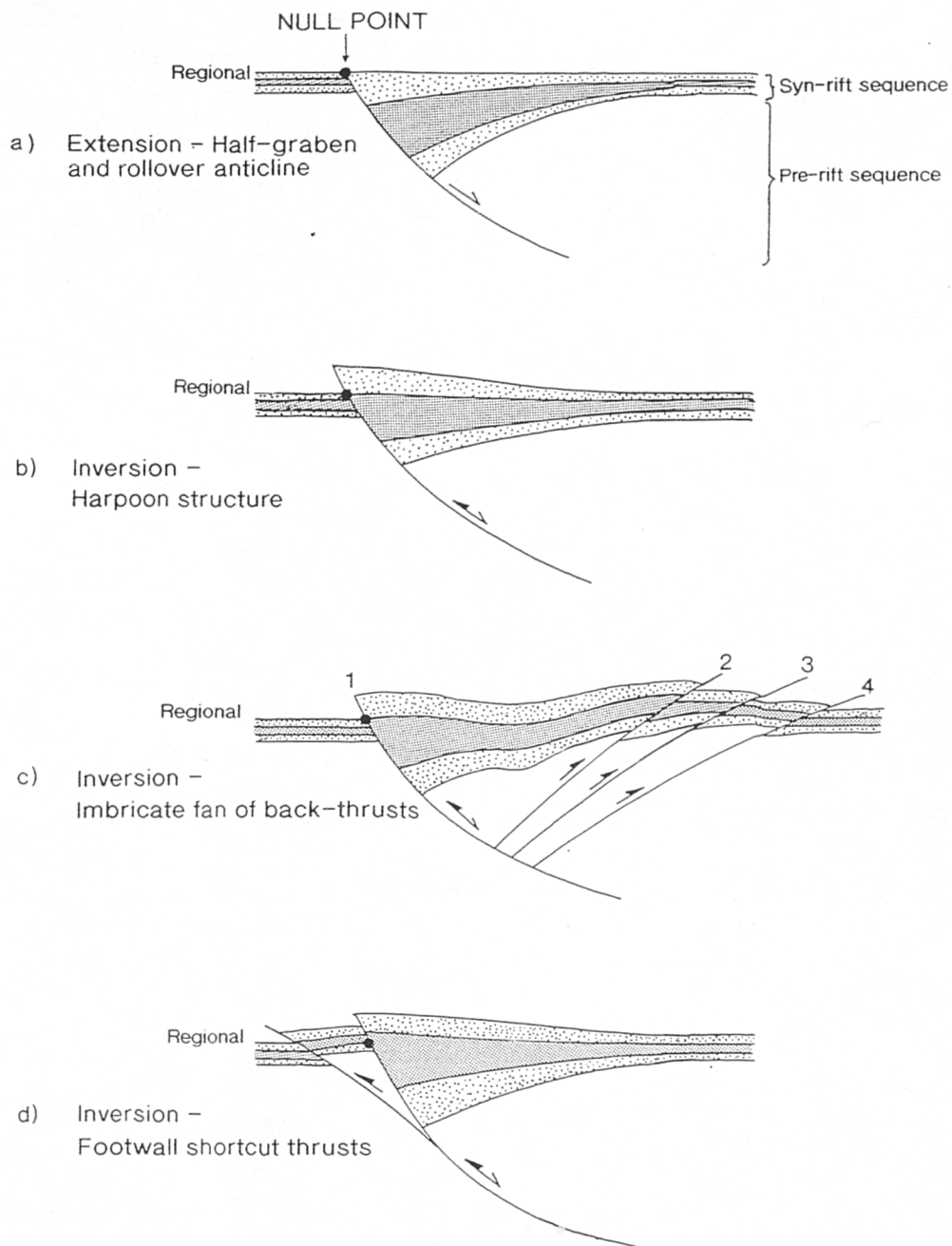


Figure 1.4. Conceptual models for thrust faults developed by the dip-slip inversion of a listric fault system. Note the regional elevation at the top of the syn-rift strata in (a). (From McClay and Buchanan 1992)

1.3.6 Structural evidence

Evidence of fault reactivation from outcrop-scale kinematic indicators has been obtained in the Basin and Range Province of north-central Nevada (Zoback & Zoback 1980). Extension directions have been deduced from fault grooves and slickensides, as well as measured displacements from historic earthquakes. Within this area, it is observed that Mid-Miocene faults locally accommodated recent strain

by oblique-normal slip. Despite a large change in the principal stress direction since the Mid-Miocene, inherited faults appear to be re-activated to accommodate extension, rather than creating new faults in a more appropriate orientation. The cohesive strength on these pre-existing faults was sufficiently low to allow continued slip, despite an obliquity of c. 45° between the pre-existing faults and the new least principal stress direction. These faults may represent a Precambrian zone of weakness (Eaton et al. 1975).

Also in North America, the Newark Basin in Pennsylvania, an early Mesozoic extensional basin, has bounding faults with low angle dips ($25\text{--}35^\circ$), (Ratcliffe et al. 1986). These normal faults lie sub-parallel to a set of imbricate thrust sheets. The latest movement on the basin-bounding faults is interpreted as extensional, from abundant brittle fracturing and extensional faulting in the cores near major contacts. However, away from the border fault, metamorphic mineral lineations, slickenlines and relict S-C fabrics in sub-parallel mylonites, are consistent with thrust faulting in the opposite direction. These authors suggest it is the presence of Palaeozoic, imbricate thrust systems that have controlled the location and geometry of the basin, by reactivation during extension.

Field studies of coupled, orthogonal, Precambrian fault sets in Western Australia (White and Muir 1989) have revealed an even more prolonged history of reactivation, including as many as five, separate tectonic events up to the Holocene. Also in Western Australia, the Darling Fault Zone, a structure close to a major zone of Precambrian shearing (see Blight et al. 1981), has undergone a switch in movement direction during reactivations (White et al. 1986). The results are based on different sets of kinematic indicators that are associated with a change in metamorphic grade. The earlier mylonites are chiefly amphibolite-granulite grade, with sub-horizontal mineral lineations oriented NNE-SSW. Detailed examination of kinematic indicators, suggest these mylonites are dominated by sinistral strike slip movements. The later mylonites have steeply plunging mineral lineations and shear-sense indicators reveal both normal and reverse dip-slip movements have occurred.

More recently, Shihe & Park (1993) present evidence from the Gairloch area of NW Scotland for at least four significant changes in movement direction of brittle-ductile shear zones. Kinematic evidence is given for these movement reversals, which include changes in lineation plunges, and ductile and brittle shear-sense indicators associated with mylonites and cataclasites. The earlier, ductile mylonites generally yield a sinistral sense-of-shear on a SE-plunging lineation, whilst the later cataclasites generally yield a dextral sense-of-shear on NW-plunging or sub-horizontal mineral lineations. Shihe & Park emphasise the fact that the shear zone

network is a major long-lived structure, and may be even more complex than proposed.

1.3.7 Isotopic evidence

Using a combination of fission track age dating of zircons and small-scale shear-sense indicators, White and Green (1985) have shown that the Alpine Fault in New Zealand has experienced at least three stages of fault zone development. A change in mineral lineation, and the presence of rotated feldspar augen, intrafolial folds and shear bands have allowed the kinematics and timing of each fault movement to be deduced. Although dominated since the mid-Tertiary by oblique reverse-dextral strike-slip movements, the fault zone appears to have experienced an earlier strike-slip episode, which focussed on a still earlier strike-slip zone, active from the late Cretaceous.

1.3.8 Implications

Watterson (1975) suggested a mechanism to explain why tectonic lineaments persisted through extended periods of geological time, based on his work on major shear zones in Greenland. He made several important observations:

- If a lineament is an expression of a persisting mechanical weakness along which displacements are localised, then it is also likely to accommodate a variety of movement directions during its active lifetime.
- The weakness would have to affect a major part of the lithosphere and not just the relatively thin upper part, where brittle fracture is the dominant displacement mechanism. (This seismic zone is typically 10 to 15 km depth under a 'normal' geothermal gradient of 20-30°/km (Sibson 1977b))
- The corresponding ductile shear zone below, where aseismic deformation takes place, usually displays a reduction in grain size.

Since the rate of deformation is often strongly dependant on grain size (see section 1.4.3 and chapter 6), Watterson's overall conclusion was that permanent grain size reduction in shear zones, relative to their country rock hosts, leads to long term mechanical weakening and may account for the longevity of major tectonic lineaments. This implies that rocks with bands of different grain sizes will localise strain along suitably oriented belts of finer grained rock.

Intense tectonic fabrics, similar to crustal mylonites, have been observed in upper mantle rocks, now seen in kimberlite pipes and ophiolites, suggesting that similar processes may also operate in the lower part of the lithosphere. Decreases in strength due to grain size reduction could therefore be effective on a lithospheric plate scale. It should be noted that grain size dependant weakening depends upon the non-occurrence of a grain growth recovery phase during periods of fault quiescence between reactivations. An outline of this and other deformation mechanisms will be dealt with in section 1.4.3.

The mechanical causes of reactivation are considered in chapter 6.

1.4 An explanation of nomenclature used in the thesis

1.4.1 Metamorphic facies

The grades of metamorphism discussed in this thesis range from low greenschist facies to granulite facies. These terms are based on the classification scheme of Yardley (1989), after Eskola (1915). The relationship between metamorphic facies, pressure/temperature space and the critical mineral assemblages is summarised in Fig. 1.5a & b.

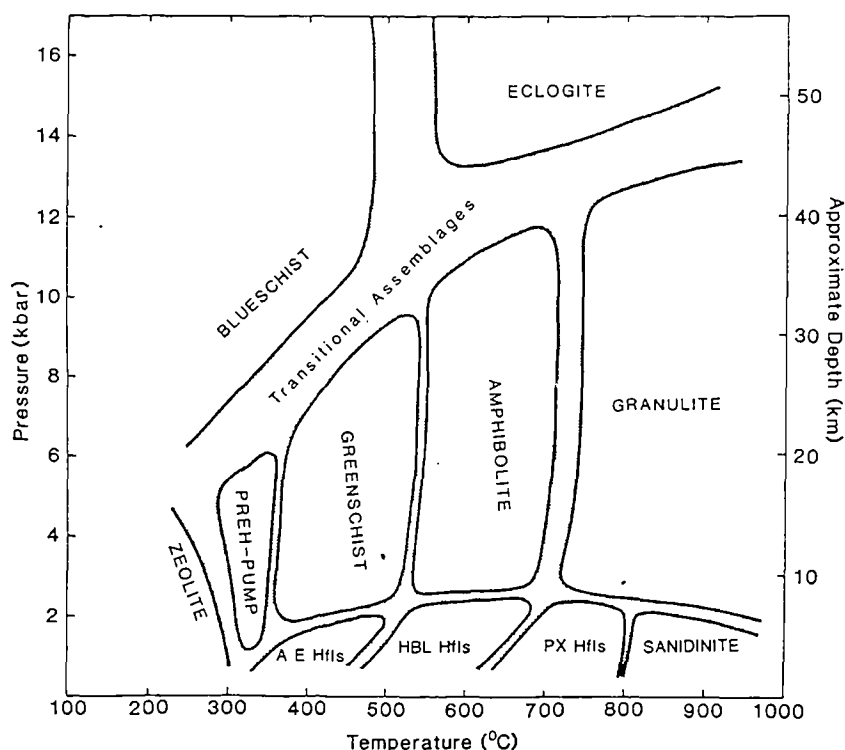


Figure 1.5a. Pressure-temperature diagram showing the fields of various metamorphic facies. Abbreviations used are Hfs = hornfels, AE = albite-epidote, HBL = hornblende, PX = pyroxene, PREH-PUMP = prehnite-pumpellyite. From Yardley (1989).

P/T ratio type classification	Metamorphic facies	Critical mineral assemblages
Low and medium P/T types	Zeolite facies	Zeolite + quartz
	Prehnite-pumpellyite facies	Prehnite +/- pumpellyite + quartz (no zeolite)
	Greenschist facies	Chlorite + epidote + albite + quartz + actinolite + muscovite (no prehnite or pumpellyite)
	Amphibolite facies	Hornblende + plagioclase (andesine or more calcic) + quartz
	Granulite facies	orthopyroxene + clinopyroxene + garnet + plagioclase + quartz

Figure 1.5b. Critical mineral assemblages in metabasites associated with low or medium pressure/temperature space (Modified from Miyashiro 1994)

1.4.2 Flow

The following section on flow is a brief review of terms pertinent to kinematic analysis. The reader is referred to Lister & Williams (1983) and Hanmer & Passchier (1991) for a more thorough discussion.

coaxial and non-coaxial flow

The shear plane, seen in the field, is the mean position of the flow plane during progressive deformation. *Flow* is the instantaneous displacement of particles making up a deforming body. The pattern of particle displacements in homogenous progressive deformation forms either a pure shear (coaxial) flow, simple shear (non-coaxial) flow, or a general shear flow (Fig. 1.6). In homogenous progressive

deformation, all material lines tend to rotate towards a common flow plane. In pure shear, the angular velocities of imaginary material lines which occur perpendicular to each other and coincide with the instantaneous stretching axes, is zero (i.e. they do not rotate and the flow is *coaxial*). All particles within that flow have an average angular velocity of zero and the flow field is symmetrical. In simple shear however, an added component of rigid body rotation transforms the complex velocity field for coaxial flow into the relatively simple non-coaxial velocity field, where the maximum instantaneous stretching axes do not coincide with material lines of zero angular velocity. All particles within that flow have a non-zero average angular velocity and the flow field is asymmetric.

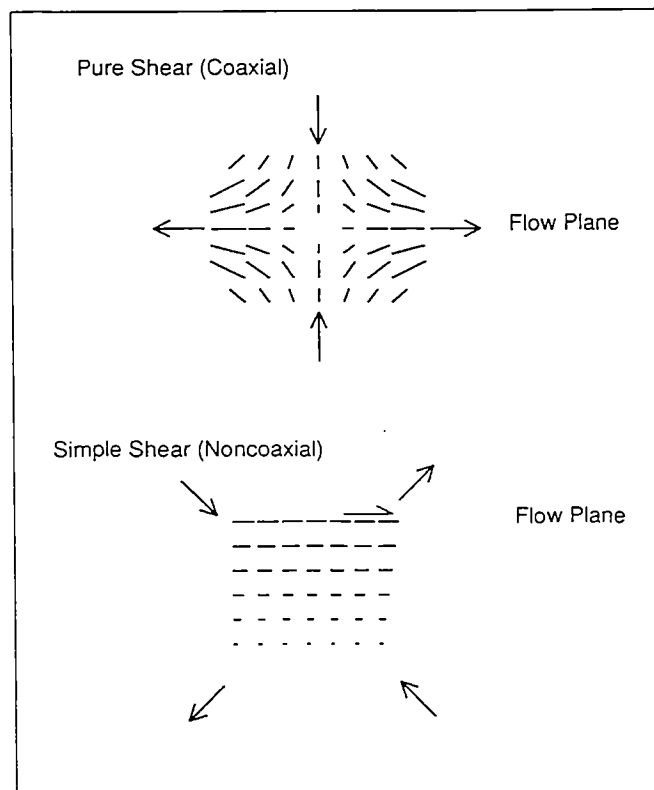
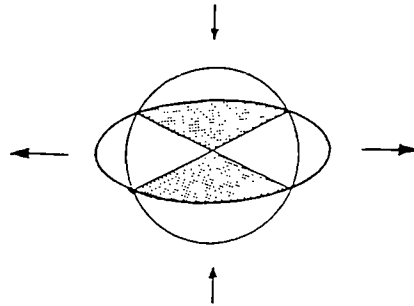


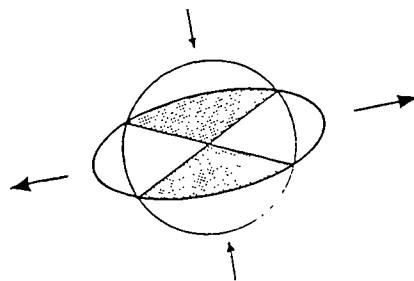
Figure 1.6. Velocity fields representing particle displacements for pure shear and simple shear flows. Instantaneous stretching axes (arrows) are indicated (from Hanmer and Passchier 1991).

The finite deformation resulting from either case can be described in terms of a strain ellipse (ellipsoid in 3D). Fig. 1.7 shows the change in shape of an initially spherical object as it undergoes: a) pure shear; b) general shear; c) simple shear, and also the fields of shortening and extension at any instant in the deformation. The flow in general shear can be considered simply as a combination of pure and simple shear components.

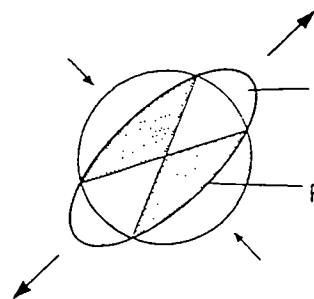
Pure Shear (Coaxial)



General Shear (Noncoaxial)



Simple Shear (Noncoaxial)



Finite Extension

Finite Shortening

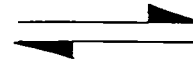


Figure 1.7. Finite strain ellipses for pure, general, and simple shear flows, showing fields of instantaneous shortening (shaded quadrants), and fields of instantaneous extension (unshaded quadrants) separated by two lines of zero stretching rate (modified from Hanmer and Passchier 1991).

1.4.3 Deformation mechanisms

Most rocks forming the earth's lithosphere display a wide range of rheological responses to applied stress. Ultimately, these responses are controlled to a large extent by the mineralogy of the rocks. Specific conditions such as grain size, temperature, pressure, strain rate, fluid activity, etc. govern the way each

constituent mineral deforms (Fig. 1.8). The deformation mechanisms operating in these individual mineral constituents and the ease of activation of the deformation mechanisms of different mineral phases relative to one another, dictate the way in which the whole rock accommodates strain. The ease with which a given rock deforms will be enhanced by the presence of an incompetent phase that deforms easily under specific geological conditions, and inhibited by the presence of a relatively competent phase. The least competent phase in a rock may change over time and strain may therefore be partitioned spatially and temporally (Knipe & Wintsch 1985).

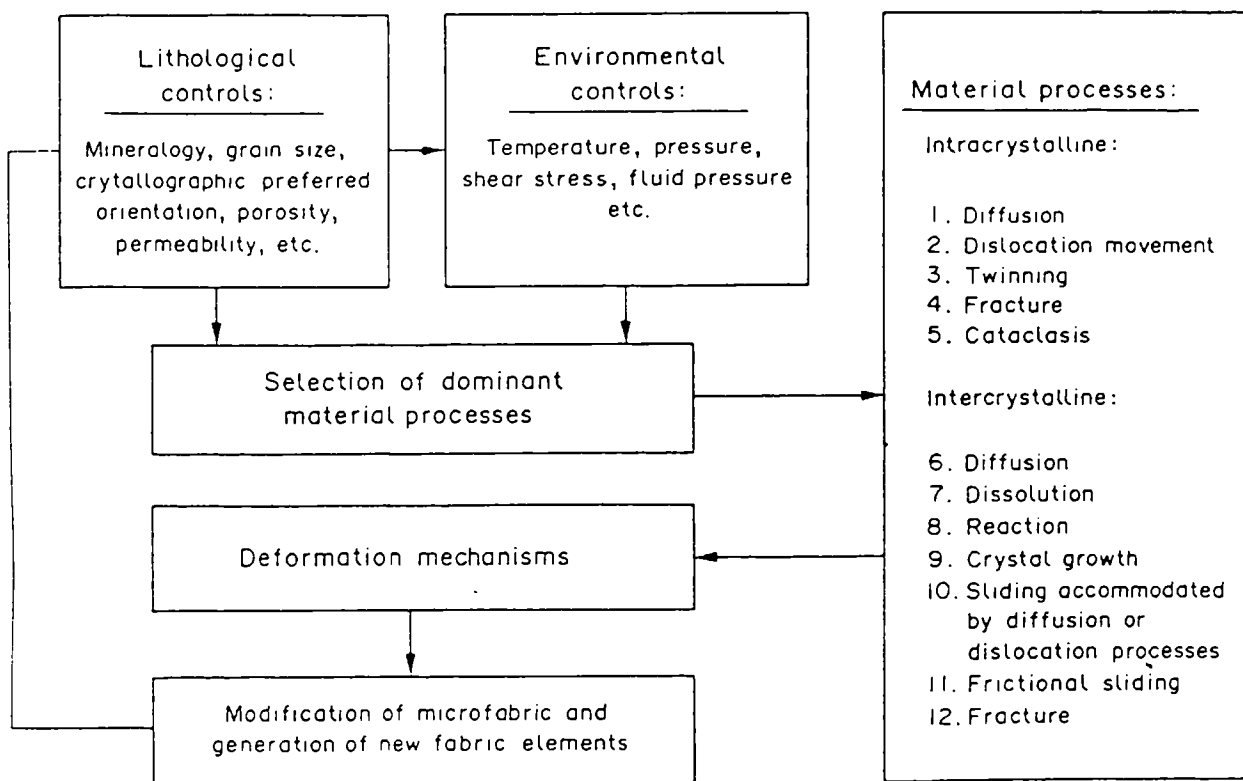


Figure 1.8. Flow diagram illustrating the lithological and environmental variables affecting the material behaviour of a deforming rock body and the interactions between these variables (modified from Knipe 1989).

Direct observation of deformed rocks in the field and experimental deformation studies have shown that two end member classes of deformation may be defined:

- *Ductile deformation* is defined as "A permanent, coherent, solid state deformation in which there is no loss of cohesion on the scale of crystal grains or larger and no evidence of brittle fracturing" (Twiss and Moores 1992).
- *Brittle deformation* is defined as "The breaking of rocks along well-defined fracture planes or zones" (Twiss and Moores 1992).

Experiment has shown that rocks become increasingly ductile with increasing temperature and increasing confining pressure (Heard 1960). If experimental data are correlated with natural conditions, rocks generally become increasingly ductile with depth. Decreasing the strain rate has an effect similar to increasing the temperature, and vice versa. However, the terms 'brittle' and 'ductile', used to describe deformation, can depend on the scale of the observed behaviour. Microscopically brittle behaviour may produce macroscopically ductile flow. The inability to define a simple boundary between brittle and ductile (especially at a macroscopic scale) reflects the wide range of deformation mechanisms which occur over the broad transition (Williams et al. 1994). Paterson's (1969) definition of (macroscopic) ductility is used here: "the capacity for undergoing permanent change of shape without fracturing" because this definition is consistent with the preferred fault rock classification scheme (see section 1.4.4).

The microstructure of a deformed rock can be used in order to assess the dominant deformation mechanisms. This includes the ways in which grains are organised with respect to one another; the grain shapes and character of grain boundaries; and the types and arrangements of internal structures such as twins and dislocations. The many deformation mechanisms can be broadly grouped into three categories (cf. Rutter 1976, Knipe 1989):

- (1) crystal-plastic flow, where grains deform by dislocation creep or twinning;
- (2) diffusive mass transfer;
- (3) fracture, frictional grain-boundary sliding and cataclastic flow.

Fracturing and cataclasis occur under conditions where the other mechanisms cannot operate (i.e. in low temperatures and/or high strain rates and low confining pressures). Crystal-plastic flow is favoured at higher confining pressures, and together with diffusive mass transfer, operate in the process of dynamic recrystallisation. In general, no single process operates alone and the operation of one mechanism will influence the operation of others.

Crystal-plastic flow

Crystals deformed by dislocation glide (cold working) commonly exhibit *undulose extinction* - an imposed curvature in the crystal lattice. If the temperature is high enough for recovery to occur, dislocations present in the lattice may climb or form subgrains. During deformation, new crystal grains may form by the process of *dynamic recrystallisation*. Two different mechanisms may operate to achieve recrystallisation:

- Boundary migration recrystallisation
- Subgrain rotation recrystallisation

The first mechanism of recrystallisation occurs by migration of grain boundaries from unstrained to strained crystals of the same mineral. This migration occurs in the opposite sense to the transfer of material, which is from the highly strained crystal, across the grain boundary, into the unstrained crystal. Grain boundary migration lowers the strain energy of the crystal by reducing the dislocation density. Completely new grains are formed by this process and can become deformed and subsequently replaced. Highly serrated grain boundaries and characteristic bulges of the grain boundary into volumes of strained crystal indicate high mobility and are useful diagnostic features of grain boundary migration recrystallisation.

The second mechanism by which dynamic recrystallisation occurs is subgrain rotation recrystallisation, and requires lower temperature/pressure in order to occur. Subgrain formation occurs when a segment of a crystal becomes separated from the main crystal lattice by dislocation arrays. With progressive misorientation, the boundaries may evolve from low to high-angle boundaries (>c. 3-5°). At c. 10° of relative rotation, the boundary is saturated with dislocations, and any further rotation changes the boundary into a high angle grain boundary of a new grain. In thin section rotational recrystallisation can be recognised by the presence of subgrains which increase in their misorientation progressively from the centre of a crystal to the rim, so that at the boundary itself the subgrains are indistinguishable from the newly recrystallised grains.

Diffusive mass transfer.

Diffusive mass transfer (DMT), involves the transfer of material from one site to another within a rock body. The material transfer occurs from areas of relatively high intergranular normal stress to areas of lower normal stress (cf. Rutter 1983). In general, low strain rates, fine grain size and an active fluid phase promote DMT, but the rate is governed by variations in temperature, strain rate, fluid pressure,

chemical potential, internal strain of mineral grains, and the nature of the grain boundaries.

Diffusion mechanisms can be divided into two main types:

- *Solid state* diffusion through or around grains;
- *Fluid assisted* diffusion by bulk transport or pressure solution.

Field and microstructural evidence for DMT chiefly relies on source (i.e. the site of material loss) and sink (i.e. the site of material gain) mechanisms. Solid state DMT processes leave no characteristic microstructures, but fluid assisted DMT processes however, create stylolites or pressure solution cleavages at source areas and fibrous overgrowths at sink areas. In addition, veins and fibrous mineral growths on joints or faults may indicate the operation of bulk transport mechanisms.

Diffusion rates generally increase with increasing temperature, but because fluids play an important role, diffusive mass transfer is clearly not limited to high-temperature regimes.

Frictional grain-boundary sliding, fracturing and cataclasis.

Frictional grain-boundary sliding

Frictional grain-boundary sliding is the sliding of grains past each other. Deformation is dependent on the amount and strength of intergranular cement, and is facilitated at low effective stress (low confining pressure and/or high pore fluid pressure) where cohesion between grains is easier to overcome. Grain boundary sliding without fracturing is common in fault gouges where the pore fluid pressure is high.

Fracturing

Fracturing occurs through a number of mechanisms which involve the nucleation and propagation of cracks. The cracks behave as free surfaces along which displacement may subsequently occur as deformation continues. Cracks occur by the breaking of atomic bonds, similar to dislocation creep, but in contrast, cracks occur catastrophically and do not generally reform. After a fracture has formed in a rock, the lack of cohesion across it means that it is a plane of weakness. Subsequent deformation occurs by frictional sliding along it.

Cataclasis

At low confining pressures, the differential stress required to form a fracture is *greater* than that which is required to cause frictional sliding on an existing fracture.

This is due to a lack of cohesion on the fault, making the fault weaker. At high confining pressures however, the differential stress required to form another fracture is less than that required to cause sliding on an existing fracture, and a new fracture is formed. If this process is repeated, the rock undergoes *cataclasis*. Cataclasis involves grain-scale fracturing, movement along fractures, frictional grain-boundary sliding, and fragment rotation. Localised cataclasis (in narrow fault zones) is macroscopically brittle, whereas cataclastic flow over a broad area is macroscopically ductile and typically favoured over localised cataclasis at greater depth. Similarly, Intracrystalline cataclasis often results in ductile deformation at the scale of the petrographic microscope. Cataclasis is therefore a process which occurs at all scales and is often preceded by significant grain-scale crystal-plastic flow and occasional macro-scale folding, so deformation takes place through a complex 'brittle-ductile' process (Goodwin & Wenk 1990, Lloyd and Knipe 1992). The description of deformation as 'ductile' or 'brittle' is therefore scale-dependent. *Transient frictional behaviour* (including frictional grain-boundary sliding fracture and cataclasis) may occur episodically within a zone which is dominated by microscopically ductile flow (e.g. Sibson 1980).

The rôle of fluids in ductile deformation.

Fluids generally have a *strain-softening* effect on rock deformation. Briefly, this is accomplished in several ways:

- Reactions are enhanced by the presence of a fluid phase to aid diffusion and the transport of materials from source to sinks. The resultant mineral phases are usually less competent than the reactants, rendering the whole rock less resistant to deformation. The usual result of fluid reactions are hydration reactions which produce phyllosilicates. Phyllosilicates play an important role in focusing both deformation (as the least competent phase in the rocks) and focusing further fluid flow (because of their strong anisotropy). Focused fluid flow may have occurred through fracture formation associated with shear along phyllosilicate domains (Williams 1990) or by channelling of fluids along the well aligned, platy phyllosilicate grains. In both cases, fluids would either have transported material from one part of the system to another or removed material from the system altogether. The net result is a well-developed, mesoscopically visible compositional layering.
- The product of a reaction can have the effect of inhibiting the growth of other mineral phases. Minerals that exist in a rock at a significantly smaller grain size

than their equilibrium grain size, may allow grain size-sensitive deformation mechanisms to operate (Brodie and Rutter 1985) (see next section).

- High pore fluid pressures may reduce the effective stress, enhancing processes such as frictional grain boundary sliding, fracturing and cataclasis.
- The presence of water may reduce the strength of some minerals, especially quartz (Griggs and Blacic 1965). The development of cracks may incorporate water into the crystal lattice before they are subsequently healed (Kronenberg et al. 1986). These water related defects are then able to propagate through the lattice by diffusion.

Grain size effects

Whilst some deformation mechanisms are not affected by grain size (e.g. dislocation creep), many mechanisms are affected by the effective width of the grain boundary relative to the grain diameter. These mechanisms *are* sensitive to grain size. Small grains have larger surface area to volume ratios than large grains, and therefore shorter *intracrystalline* diffusion paths, which allow an increase in the strain rate if the temperature is constant. (Similarly if the strain rate is constant, the smaller grains deform at a lower temperature than the larger ones). *Intercrystalline* diffusion is also facilitated by a decrease in grain size because the volume of grain boundaries has increased for the same volume of rock: In mylonites, diffusion assisted grain boundary sliding is probably the most important grain size sensitive deformation mechanism. An order of magnitude decrease in grain size may result in greater than an order of magnitude increase in strain rate. These two states can be expressed as fields on a deformation mechanism 'map' for a given mineral, consisting of variable stress on one axis and variable grain size on the other (Fig. 1.9). Flow laws are used to calculate the position of the boundary between the regimes. At a constant temperature, reducing the grain size shifts the deformation from the grain size insensitive regime into the grain size sensitive regime and the strain rate will be significantly increased. With decreasing grain size at a constant strain rate, the effect of grain size sensitive creep therefore becomes increasingly important at lower and lower temperatures.

A further consequence of a reduction in grain size may be the promotion of fluid flow by increasing permeability pathways (Sibson 1977a). Fluid flow, as stated previously, may cause strain softening by reducing the effective stress, hydrolytically weaken certain phases, such as quartz, and facilitate the growth of incompetent phyllosilicates.

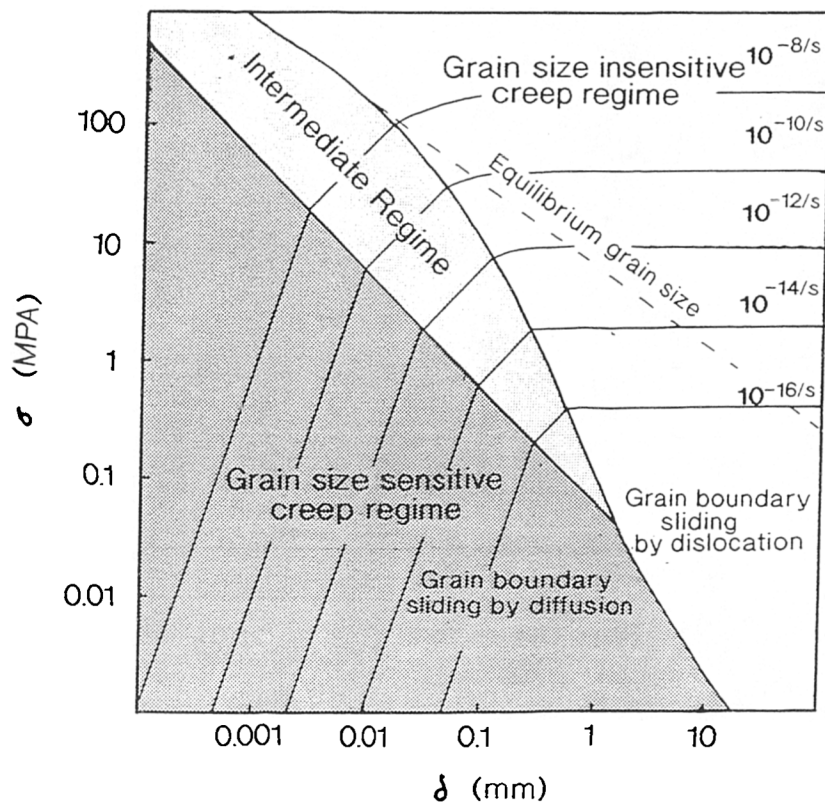


Figure 1.9. Deformation mechanism map for quartz at 500° showing relative positions of deformation fields with varying stress (σ) and grain size (δ). Solid lines show strain rates, and dashed line shows the relationship between equilibrium grain size and stress based on Twiss (1977). Flow laws used to define the regime boundaries are from Gifkins (1976) and the diagram is modified from Williams et al. (1994), after Etheridge and Wilkie (1979).

1.4.4 Fault rocks

Several schemes have been proposed for the classification of fault rocks, nearly all of which are unsatisfactory. Two main approaches have been applied, the first relying on the processes inferred to have operated during deformation, and the second on physical description of fault products.

Of the schemes proposed for classifying fault rocks in terms of their dominant deformation mechanisms, those of White (1982) and Wise et al. (1984) are widely known. The scheme proposed by White (1982) uses nomenclature such as 'c'-type and 'r'-type mylonites, (for rocks derived from the processes of cataclasis and recrystallisation respectively). White (1982) remarks that a "confusing literature" exists, which uses process-derived terminology for description purposes, e.g. the descriptive *term* 'cataclasite' (random fabric cohesive fault rock) and the process of 'cataclasis' (grain comminution). He suggests genetic connotations cannot be avoided using the existing terms. The processes involved in the genesis and evolution of a particular fault rock however, can not only never be proved

beyond doubt, but several mechanisms may act together and/or change with time. A scheme which relies on processes for its terminology (e.g. White 1982) is therefore misleading. White's nomenclature is not vindicated by an existing confusing literature which uses what were originally genetic terms for description only.

Wise et. al. (1984) propose a different approach in which the classification is based around the idea that "the texture of strained rocks is largely a function of the interplay between strain and recovery" (Fig. 1.10). Whilst this is basically correct, this scheme again falls down on its genetic connotations, e.g. the incorrect assumption that all foliated rocks for example, are produced in ductile faults by syntectonic crystal-plastic processes.

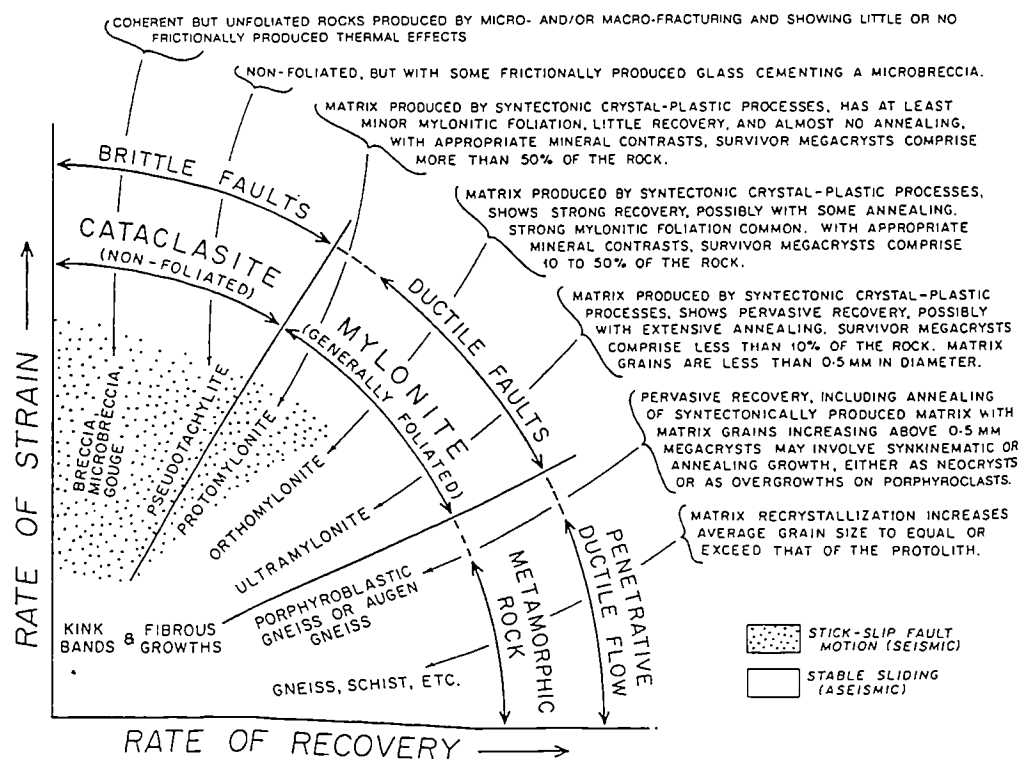


Figure 1.10. Terminology of fault related rocks. Horizontal and vertical scales are variable depending on composition, grain size, and fluids. (From Wise et al. 1984)

Of the classification schemes proposed for classifying fault rocks in terms of their description only, that of Sibson (1977a) is most widely used. Sibson's classification relies on description alone, and separates fault rocks into those with an essentially random shape (and crystallographic) fabric and those that are foliated. A second major division is the presence or absence of *primary cohesion*,

and further subdivisions are made on the nature of the matrix. Using this scheme, fault rocks can be confidently classified without interpretations (Fig. 1.11).

Random fabric		Foliated	
Incohesive	Fault Breccia visible fragments > 30% of rock mass	Incohesive mylonite	
	Fault Gouge visible fragments < 30% of rock mass	Incohesive mylonite	
Cohesive	glass/ devitrified glass	?	
	reduction in grain size dominates; grain growth by recrystallisation and neomineralisation	Crush Breccia Fine Crush Breccia Crush MicroBreccia	(fragments > 0.5cm) (fragments < 0.5cm) (fragments < 0.1cm) 0-10%
		Protocataclasite	Protomylonite
		Cataclasite	Mylonite
		Ultracataclasite	Ultramylonite
	Grain growth pronounced	?	Blastomylonite

Figure 1.11. Textural classification of fault rocks as used in this work. (Modified from Sibson 1977a).

Chester et al. (1985) point out the need to incorporate 'foliated cataclasites' and 'foliated gouges' into fault rock classifications. They suggest that under conditions of brittle failure, where cataclastic deformation mechanisms prevail, fault products with a good foliation can result. This statement is supported by field and experimental evidence. Under the classification schemes proposed by White (1982)

and Wise et al. (1984) a process of cataclasis would have to be inferred. If one applies Sibson's (1977a) descriptive classification rigidly, 'foliated gouges' and 'foliated cataclasites' might be classed as 'incohesive mylonites', because they are foliated and lack primary cohesion. This is not wholly satisfactory because an 'incohesive mylonite' almost certainly has a closer mechanical affinity to a true gouge than to a true mylonite. This scheme is therefore unfortunate in that its descriptive terminology is rooted in inferred processes.

The intention this work's use of Sibson's scheme is not to imply any genetic connotations. Terms such as 'cataclasite' should not be regarded as meaning the rock was necessarily derived through the process of cataclasis, but that it is simply a descriptive term for a cohesive fault rock with a random fabric. The only satisfactory way of classifying fault rocks is to construct a new scheme which like Sibson's (1977a), is based on description and not process, but unlike Sibson's, uses new terminology not linked with deformation processes. Rather than discard existing terminology and create a new terminology, the nomenclature used in this thesis mainly follows that of Sibson (1977a).

1.4.5 Shear sense indicators

In regions of faulted or sheared homogenous crust where there are no offsets of marker horizons, other methods must be used to determine the sense of movement on faults and shear zones. The study of meso- to microscopic- scale geological deformation structures can help elucidate the problem. Firstly the movement direction must be determined by utilising linear features which describe the movement vector on a given fault or shear zone. Once the movement direction has been determined, it should be combined with sense of movement criteria viewed in the plane normal to the shear plane and parallel to the movement vector

It is stressed that no single criterion is infallible, and as the scale of the feature decreases, so the likelihood of erroneous interpretations increases, and as such, as many shear sense criteria as possible should be used together (White et al. 1986).

This section is divided into three main parts: Linear features; sense-of-movement criteria in the brittle regime; and sense of movement criteria in the ductile regime.

Linear Features

Linear features which occur in naturally deformed tectonites fall into one of two categories: Structural; and mineral (Twiss and Moores 1992) Both of these divisions can be subdivided (as shown in fig. 1.12) and nearly all can be used to

determine the movement direction (which is parallel to the lineation) within a sheared surface.

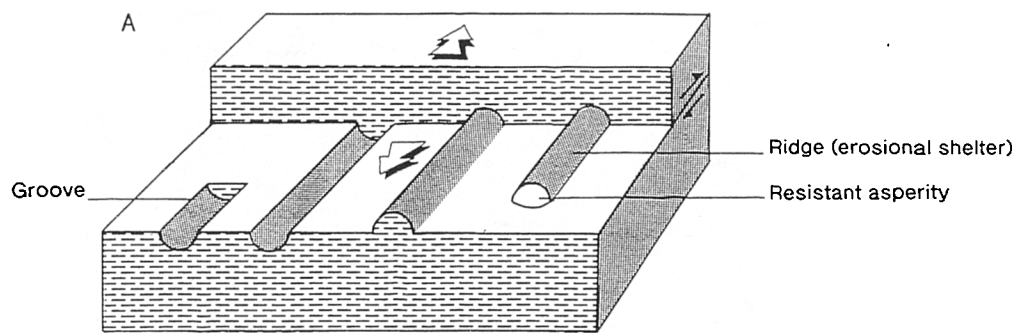
Lineations in tectonites (surficial or penetrative)	Structural	Discrete	Pebbles Ooids Fossils Alteration spots
		Constructed	Hinge lines Intersections Boudin lines Mullions Structural slickenlines
	Mineral	Polycrystalline	Rods Mineral clusters Mineral slickenlines Nonfibrous overgrowths
		Mineral grain	Acicular habit grains Elongated grains Mineral fibers Fibrous vein filling Slickenfibers Fibrous overgrowths

Figure 1.12. Morphological classification scheme for lineations (From Twiss and Moores, 1992)

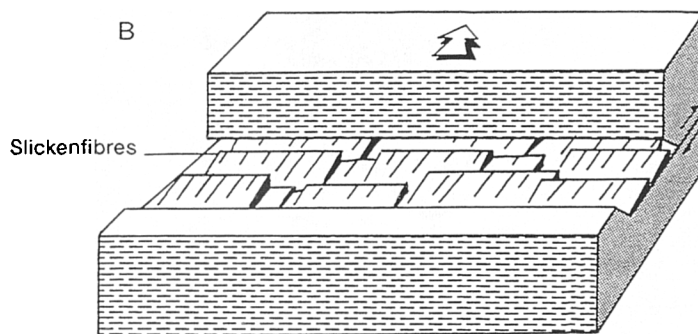
The most important movement direction indicators are:

- *Brittle fault striae* (Fig. 1.13a)
- *Fault plane slickenfibres* (Fig. 1.13b).
- *Ductile mineral lineations*

These may be individual elongate grains or elongate (often polycrystalline) aggregates developed either on a foliation surface or penetratively throughout the entire rock.



Ridge and groove terminations face the opposite way to the movement direction of the missing block.



Slickenfibre growth is by accretion steps in a void left by a fault surface perturbation. Accretion steps face the direction of the missing block.

Figure 1.13. Types of slip parallel movement indicators found on fault surfaces:

A) Ridge and groove striae

B) Slickenfibres

(Modified from Means, 1987).

Sense of movement criteria in the brittle regime

In combination with the sense of movement criteria existing on the fault plane itself, the existence of repeated secondary fractures at an angle to the main fault may provide invaluable information on the movement sense. These may additionally display slickenlines of fibres, but their identification and geometrical position will often suffice.

Following the reviews and terminology of Riedel (1929) Petit (1987) and Swanson (1988) secondary brittle fractures can be divided by way of their orientation and type (striated shear or non-striated tension fracture). The basic orientations are summarised in Fig. 1.14. and their type in Fig. 1.15. The three main types are:

- *R* - shears (Riedel shears)
- *P* - shears
- *T* - fractures (Tensile fractures)

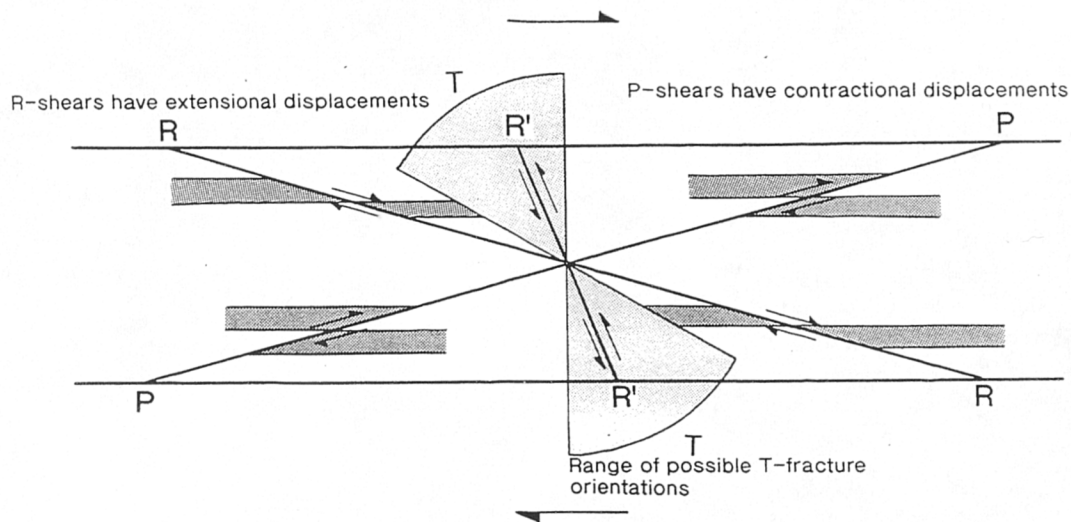


Figure 1.14. Fracture orientation patterns for idealised brittle fault. The pattern illustrated is for dextral layer-parallel simple shear. (Modified from Swanson, 1988).

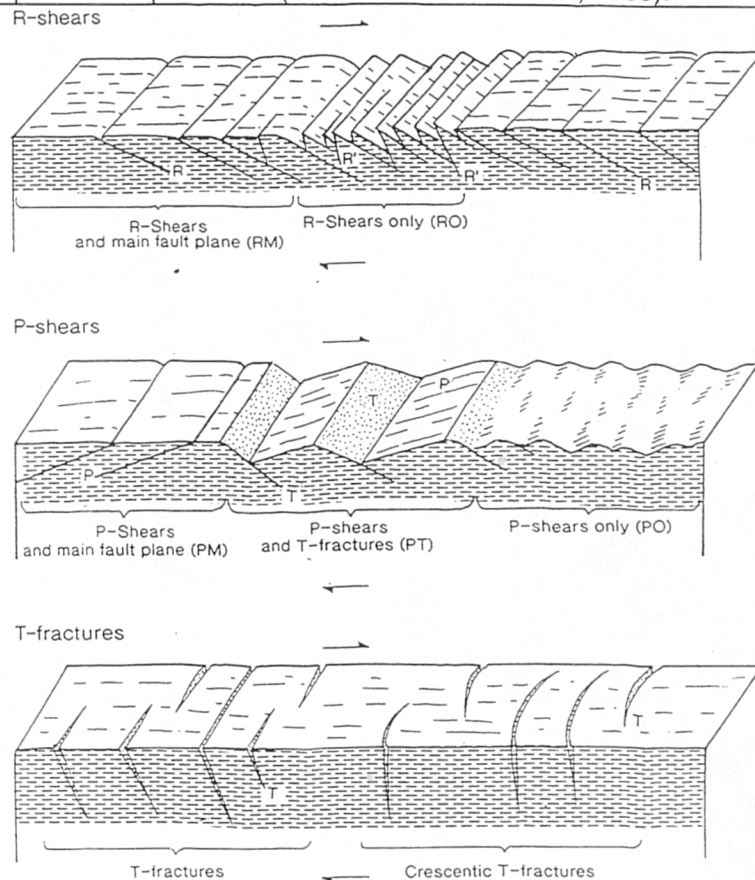


Figure 1.15. Brittle sense of movement determination by repeated secondary fractures (Modified from Petit 1987)

Sense of movement criteria in the ductile regime

When used in combination with movement direction information from mineral lineations, microstructural features within, and/or adjacent to, a ductile shear zone provide criteria for determining the sense of shear of the flow (White et al. 1986). These microstructures can be conveniently sub-divided into three main groups following the review and terminology of Hanmer & Passchier (1991) and references therein. These are:

- Shape fabrics (foliations)
- Inclusions and appendages
- Veins and folds

Shape fabrics

These include: Rotation of a generated foliation (Ramsay & Graham 1970) (Fig. 1.16a); quartz C-axis fabrics (Brunel 1980); C-S fabrics (Berthé et al. 1979) (Fig. 1.16b); asymmetrical extensional shear bands (White et al. 1980) (Fig. 1.16c); and a rotation of deformed markers/pre-existing foliation (Ramsay & Graham 1970).

Inclusions and appendages

Fundamental to the study of inclusions as kinematic indicators, (often described as 'stiff' inclusions if present in a relatively ductile matrix), is whether they have rotated or not. For this reason, most workers (e.g. Passchier and Simpson 1986), have split stiff inclusions into two types:

- σ type clast systems (non-rotated)
- δ type clast systems (rotated)

The most useful geometry for describing flow kinematics is the presence of appendaged or 'winged' porphyroclasts (Passchier and Simpson 1985). The wings (or 'tails' of Simpson and Schmid 1983) are composed of either finer grained recrystallised material of the same composition as the clast, or of reaction softened material (e.g. quartz and white mica resulting from the breakdown of feldspar). These extend along the foliation plane in the direction of shear. Mica 'fish' (Lister & Snoke 1984), pressure shadows, and pressure fringes of minerals precipitated into low pressure areas adjacent to the stiff inclusion bear a close resemblance to the geometry of unrotated σ -type porphyroclasts and can be used in the same way to deduce the sense of shear. Fig. 1.17 shows how winged porphyroclasts can be used to deduce the sense of shear in a flow.

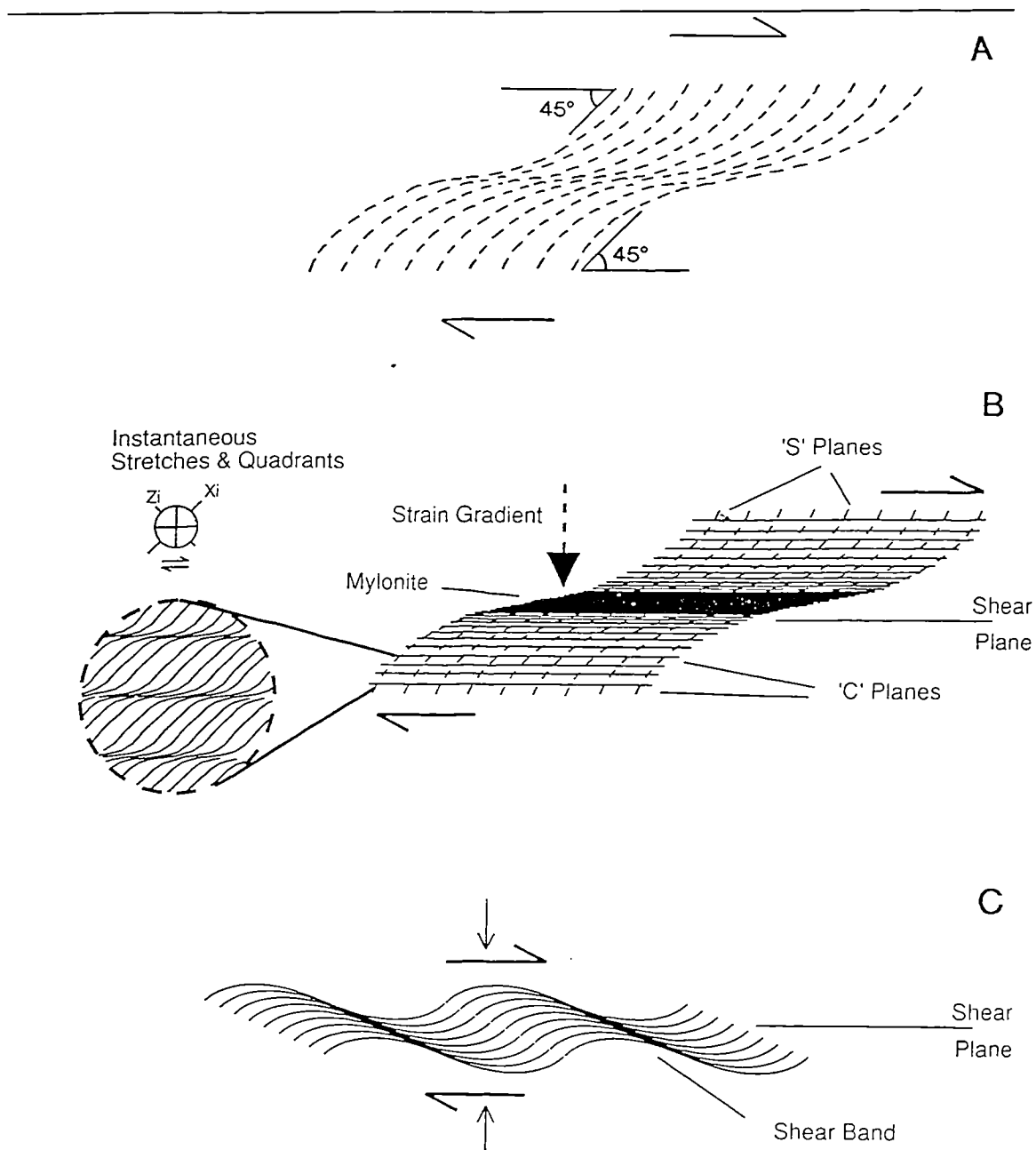


Figure 1.16. Ductile sense of movement determination by shape fabrics:

- a) A homogenous material undergoing progressive simple shear. The generated foliation initiates at 45° to the shear plane and rotates with the finite strain ellipsoid (redrawn from Ramsay and Graham 1970).
- b) C-S fabrics in general non coaxial flow. The extensional (shaded) and shortening (white) quadrants are shown. Each C-plane is a small scale shear zone whose spacing reflects the intensity of deformation. The sense of rotation on the S-planes describes the rotation of the finite strain ellipsoid (after Berthé et al. 1979)
- c) Asymmetrical extensional shear bands in general noncoaxial flow. The shear bands are oblique to the bulk flow direction and are *not* strain sensitive (after Hanmer & Passchier 1991)

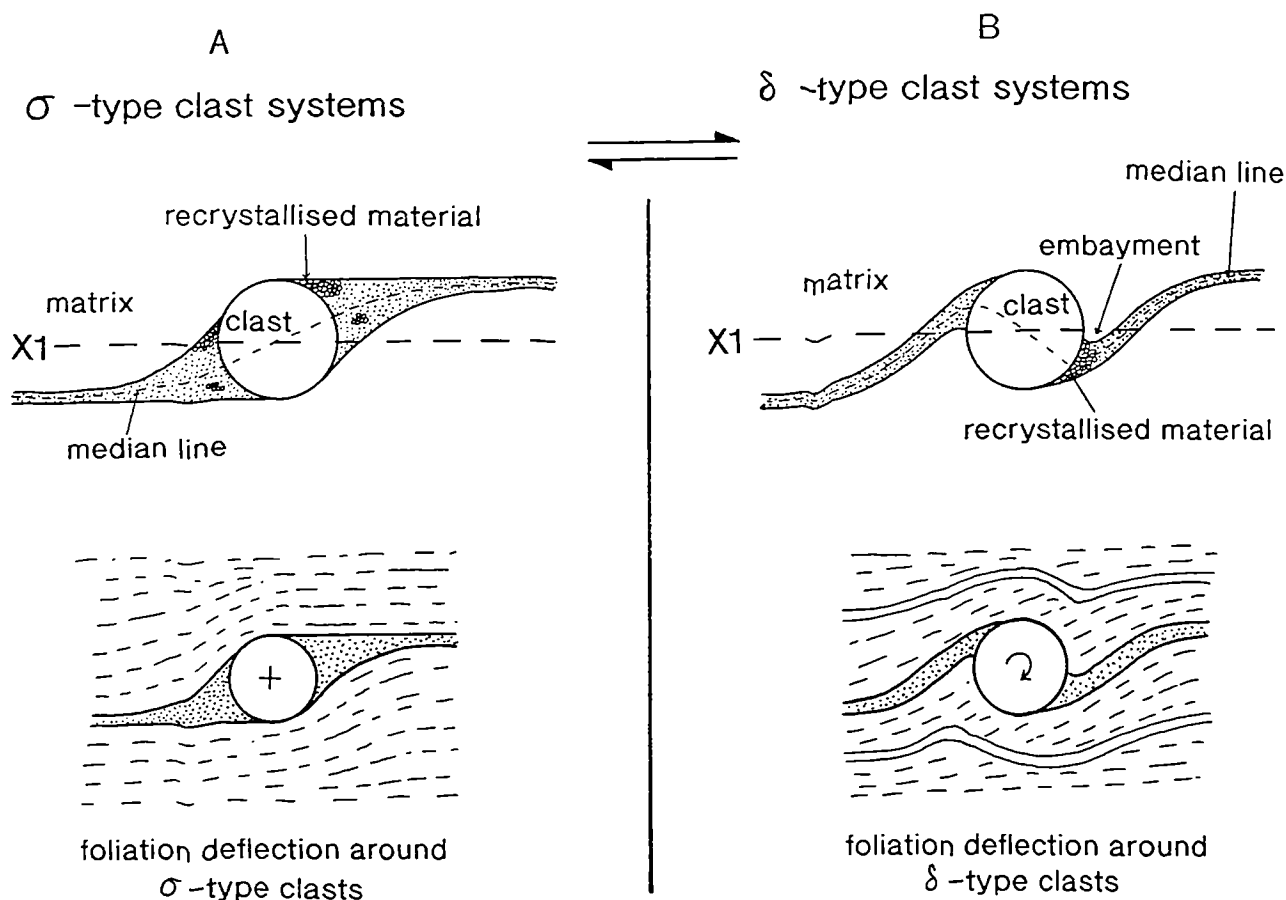


Figure 1.17. Classification of 'winged' porphyroblast systems. (a) σ -type clast system (b) δ -type clast system. Reference plane (X1) approximates the shear plane of the bulk flow. (Adapted from Passchier & Simpson 1986).

Another type of inclusion structure frequently cited as a good kinematic indicator is a 'tiling' or 'domino' structure (Fig 1.18). These structures are not unequivocal and should therefore be supported by other criteria before being used as shear-sense indicators (Hanmer & Passchier 1991)

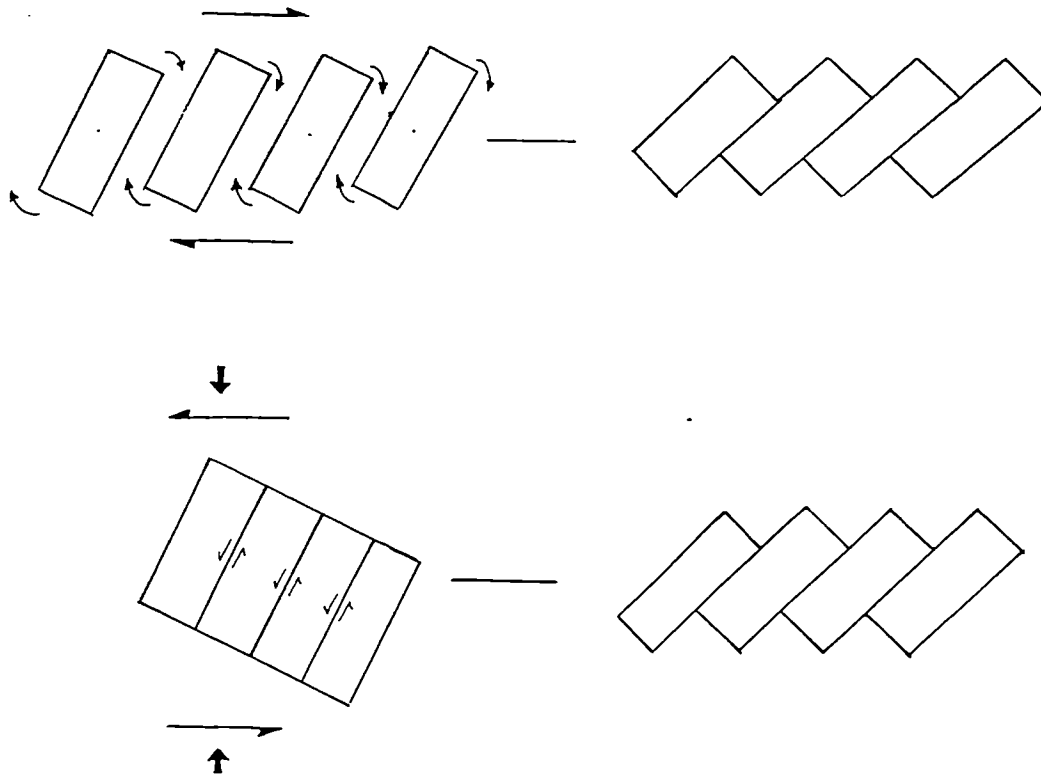


Figure 1.18. Tiling or domino-fault structures. The rotation (tiling) of inclusions in a *dextral* shear zone may produce exactly the same geometry as the rotation of sets of domino-fault structures. Significantly, the domino-faults result from *sinistral* general shear, and as a result, such structures can not be used as sense of shear indicators (after Hanmer and Passchier 1991).

veins and folds

Veins can be useful as kinematic indicators in two senses. Firstly the geometry of the vein itself, either directly or as a result of later deformation, can illustrate the nature of shear. This is illustrated by the en-echelon arrays of dilational tension gashes which are generally thought to have a fixed orientation relative to the maximum instantaneous stretching direction (σ_3). The propagating vein tips open perpendicular to σ_3 , whilst the central portions may rotate in the same sense as the bulk shear (Ramsay and Graham 1970) (Fig. 1.19a). Later deformation can affect a vein in exactly the same way as any other geological surface, -by folding or boudinage (see below). Secondly the fibres within a vein preserve a geometry controlled by the displacement direction of the vein at the time of opening (Fig. 1.19b).

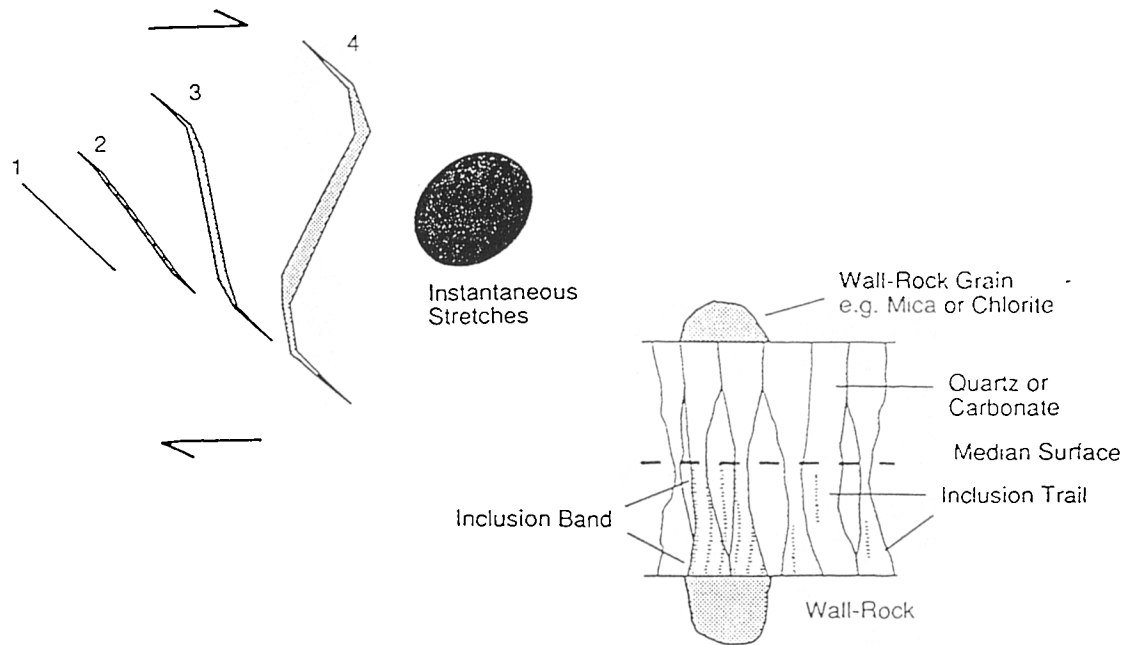
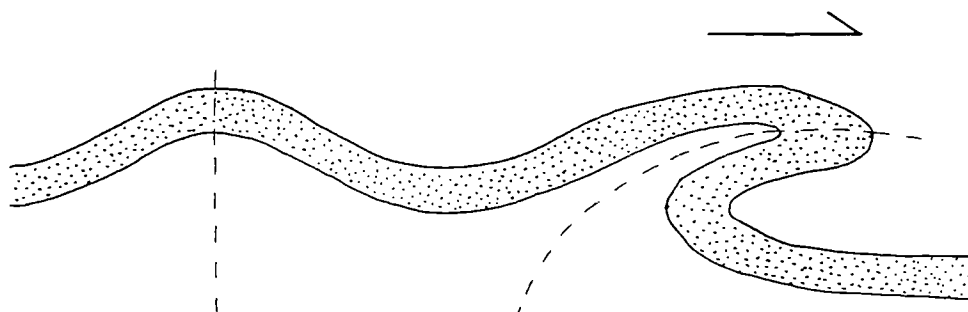


Figure 1.19

a. Sigmoidal tension gashes in dextral shear. Younger tips propagate parallel to σ_1 whilst older dilated central portions rotate with the same sense of vorticity as the flow during progressive deformation (from Hanmer & Passchier 1991).

b. Dilational vein with displacement controlled fibres which track the opening vector during formation. The median line marks the initial fracture and growth is by successive increments at the vein wall. In this example opening is orthogonal to the vein wall (from Hanmer & Passchier 1991).

Folds are less reliable kinematic indicators and should have a regionally extensive, consistent asymmetry, and should not have undergone any significant axis rotation (Fig 1.20). If a consistent asymmetry cannot be proved, this method should be treated with caution, as the plane of observation must be favourably oriented for kinematic analysis, especially in the case of sheath folds.



Rotation of planar fabric elements (axial planes & limbs)

Figure 1.20. Geometry of asymmetric fold in dextral shear. Planar fabric elements rotate with dextral vorticity.

1.5 Thesis Outline

Following this introduction, the thesis follows the format below:

Chapter 2 gives an account of the geology of the Outer Hebrides, based chiefly on previous work. This includes the chronology, composition, and tectono-metamorphic history of the basement Lewisian Gneisses, which form the protolith to the deformation products of the Outer Hebrides Fault Zone (OHFZ). The Outer Hebrides Fault Zone is then introduced, with a section on previous work, putting the present study into context. The only undeformed rocks of the onshore Outer Hebrides, the Stornoway Formation sediments, are then considered, as they place important constraints on the timing of fault zone movement. The offshore basins are then discussed using available seismic data and previously published material. Finally, the fieldwork methods and a discussion on the subdivision of the thesis is presented.

The next two chapters (3 and 4) provide a description of the kinematic history of the Outer Hebrides Fault Zone from the basis of a fundamental geographical division recognised during the present study. The kinematic history of the northern segment (chapter 3) is followed by a kinematic history of the southern segment (chapter 4). In each, the common kinematic history is discussed using macro- and micro-structural evidence. These summaries were deduced from fieldwork carried out during the course of study. In both chapters new field data and observations are presented and interpreted.

In chapter 5, a synthesis of the kinematic evolution of the OHFZ is presented, including the differences between the northern and southern fault zone segments. The possible relevance of the kinematic history of the South Harris shear zones, to the evolution of the OHFZ, is considered, from the basis of new field observations, data and interpretation. A reappraised tectonic model for the OHFZ is presented.

Finally, in chapter 6, the importance of the OHFZ as a key to understanding fault reactivation processes, is discussed.

Chapter Two - Previous work and the regional geology of the Outer Hebrides

2.1 Introduction

The Outer Hebrides, off the coast of NW Scotland, extend for more than 200 km from the Butt of Lewis to Barra Head, and constitute five major, and numerous smaller islands (Fig 2.1). The present project is concerned with the geology and movement history of the Outer Hebrides Fault Zone (OHFZ) which occurs onshore along the eastern seaboard of the Outer Hebridean island chain. For the purposes of this work, the geology of the Outer Hebrides can be conveniently sub-divided into three major parts (Fig. 2.2):

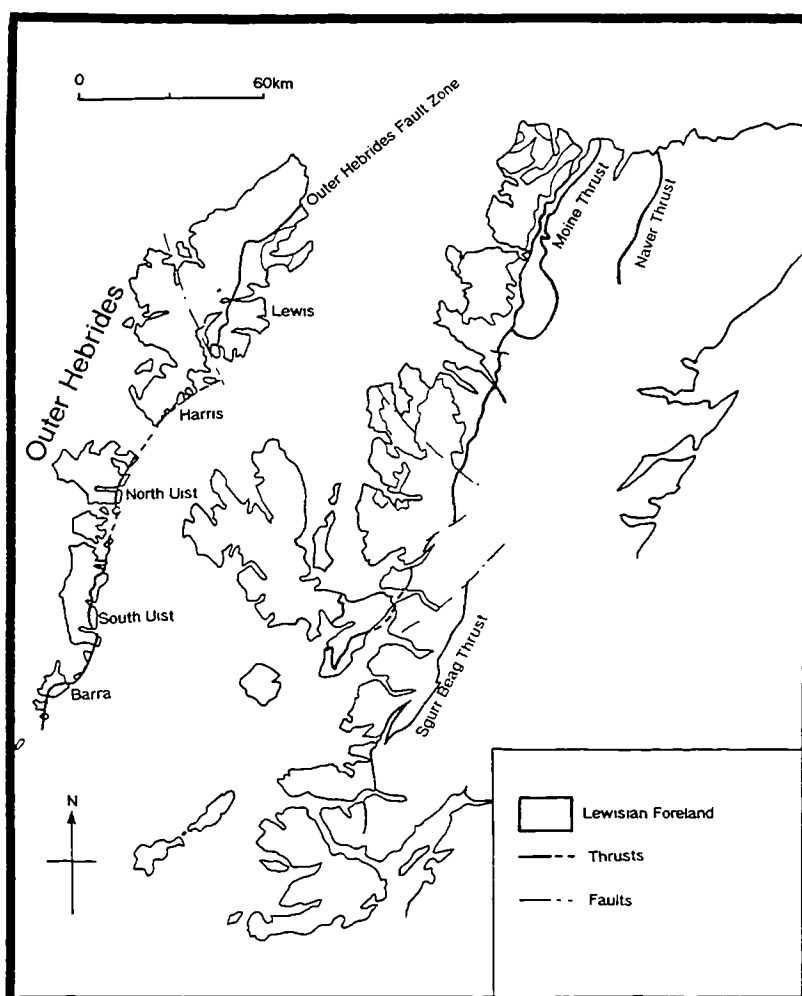


Figure 2.1. Map of the Outer Hebrides and NW Scotland showing the location of the Outer Hebrides Fault Zone and the extent of the Lewisian Foreland. Note the marked parallelism of the Outer Hebrides Fault Zone with major Caledonian thrusts on the mainland. (Re-drawn from Johnstone and Mykura 1989)

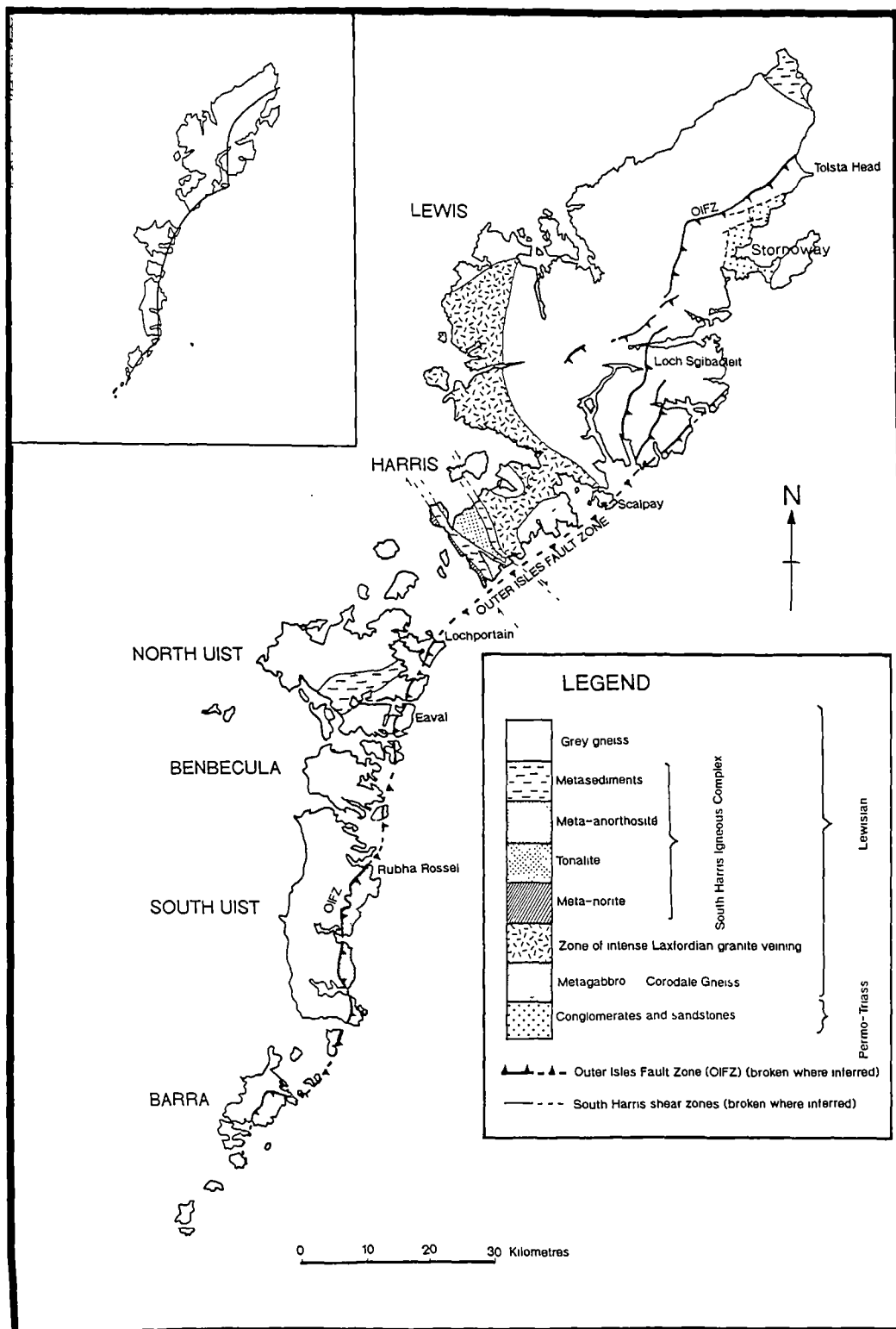


Figure 2.2. Lithological map of the Outer Hebrides. The distribution of Lewisian derived fault rocks associated with the OHFZ is not shown. The OHFZ trace corresponds approximately to three arcs, concave to the ESE (inset).

1. The Lewisian basement gneiss complex (Dearnley 1962, Park and Tarney 1987, Fettes and Mendum 1987)
2. The zone of fault rocks associated with the OHFZ, all of which are derived from the Lewisian gneisses (Sibson 1977b).
3. The conglomerates and sandstone deposits of the Stornoway Formation which are thought by most workers, to be of Permo-Triassic age (e.g. Steel and Wilson 1975).

In addition, the region is intruded by numerous intermediate to basic intrusions (mostly dykes) of Permo-Carboniferous and Tertiary ages. Offshore, the architecture and stratigraphy of three large Mesozoic and Cenozoic basins are apparently controlled by the presence and movement history of the OHFZ (Binns et al. 1974, 1975, Smythe and Kenolty 1975, Brewer and Smythe 1986).

2.2 The Lewisian Complex

2.2.1 Chronology

Most of the Outer Hebrides are composed of an assemblage of gneissose rocks known as the Lewisian Complex. The Lewisian gneisses belong to a widespread group of chiefly high-grade Precambrian metamorphic rocks of late Archaean to Early Proterozoic age that crop out in Scotland (Fig. 2.1), Greenland and Canada, and collectively form an important part of the Laurentian Shield. Much of the chronology of the Lewisian (summarised in Table 2.1), is based on the results of radiometric dating carried out during the 1960's and 70's. The results relied on several types of dating methods including K-Ar and Rb-Sr isotopic age dating. Based on these data, most of the protoliths to the Lewisian are thought to have formed prior to 2800 Ma. (Moorbath et al. 1975).

Two major tectono-metamorphic reworking events have been identified on the Scottish mainland (Sutton and Watson 1951) and are believed to be present in the Outer Hebrides (Dearnley 1962). These are the Scourian event (c. 2900 - 2400 Ma.) and the Laxfordian event (c. 2400 - 1400 Ma.). Separating these two events are a suite of tholeiitic basalt intrusions - the 'Younger Basics' of the Outer Hebrides, or 'Scourie dykes' of the mainland, thought to have been intruded c. 2400 - 2000 Ma. (Chapman 1979, Heaman and Tarney 1989). Most workers suggest these are the same suite, based on chronology, geochemistry and regional correlation (e.g. Fettes et al. 1992). These dykes cut across the Scourian deformation fabrics but are reworked by the effects of Laxfordian deformation. Unlike the Scottish mainland, Laxfordian deformation is relatively intense in most

areas of the Outer Hebrides, and as a result the two distinct phases of Scourian deformation recognised on the mainland (the Badcallian event c. 2700 Ma. and the Inverian event c. 2600 Ma.; following the terminology of Park 1970) have only been applied to rocks in the Outer Hebrides with a large degree of uncertainty (Fettes et al 1992). The termination of the Laxfordian event is marked by the onset of Late Laxfordian migmatisation, and the emplacement of granite and pegmatite intrusions at c. 1800 - 1700 Ma. (Van Breemen et al. 1971).

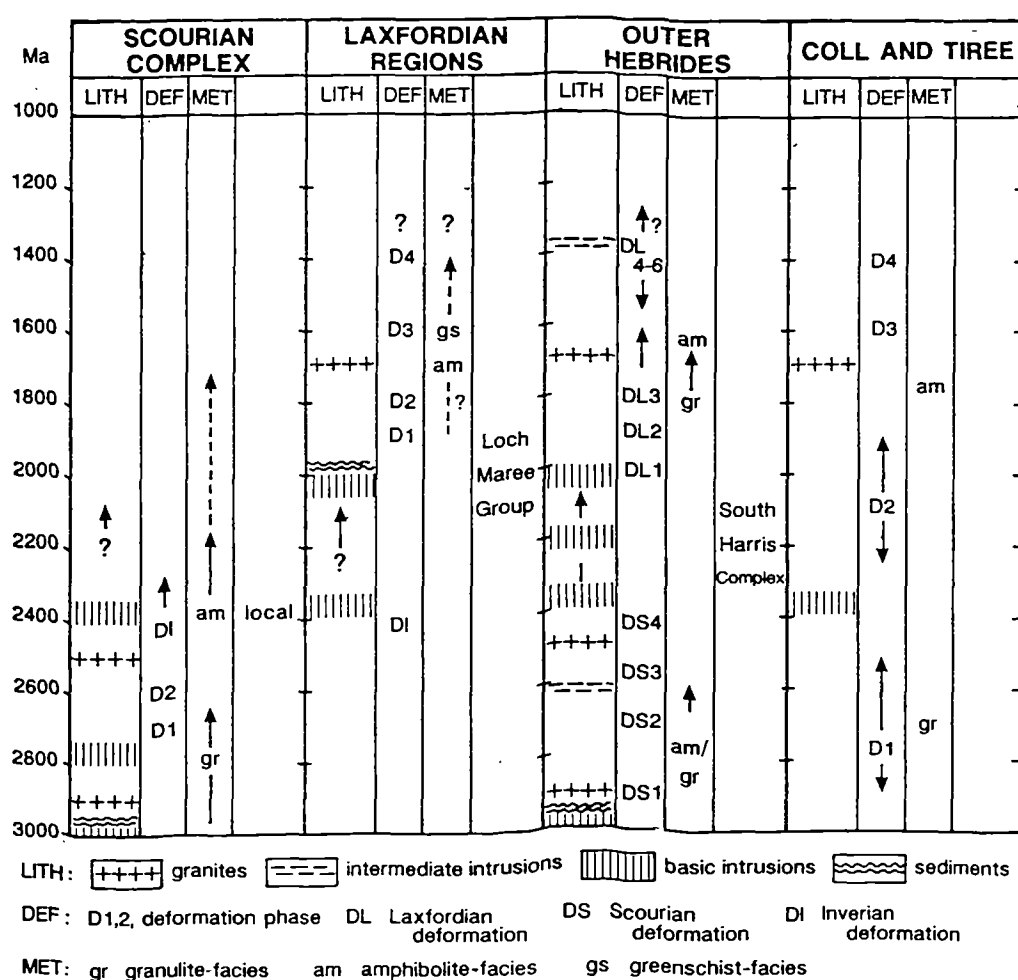


Table 2.1. Correlation of Lewisian between 1) the Scourian complex of the central mainland region; 2) the mainland Laxfordian region; 3) the Outer Hebrides, and 4) Coll and Tiree (From Park et al. 1994)

2.2.2 Composition

The first geological survey carried out in the Outer Hebrides reported a monotonous series of hornblende gneisses (MacCulloch 1819). The heterogeneity of the gneisses was only fully realised following systematic surveys by Jehu and Craig (1923 - 1934) and a study by Dearnley (1962) which compared the Outer Hebridean basement with that of mainland Scotland.

Grey Gneisses

The 'grey Gneisses' were first defined by Dearnley (1962). Acid gneiss constitutes the most common lithology of the region, forming highly weathered, pale grey exposures owing to the large modal percentage of feldspar. The gneisses are medium to coarsely crystalline with inequidimensional grains ranging from 1 - 10mm, comprising quartz (40%), feldspar (45%), with smaller amounts of amphibole and biotite (c. 5 - 10%). The distribution of minerals is even, but inequidimensional grains such as plagioclase laths, acicular amphiboles and biotite sheets are commonly aligned parallel to a rough banding, defined by layers of mafic concentrates.

The acid gneisses are often interlayered with schlieren, pods and lenses of basic and ultrabasic composition of variable thicknesses (typically 5mm-20cm), and on a large scale, forming *distinct bodies up to several hundred metres across*. These basic units have been collectively referred to as the 'Older Basics' to distinguish them from the sometimes similar, post-Scourian intrusions (Younger basics / Scourie dykes) (e.g. O'Hara 1961). Most Older Basic bodies are medium to coarse grained amphibolites, with hornblende and plagioclase the dominant minerals, but locally (eg. in Barra) pyroxene may be present. Grains reach 2 cm in the coarsest material but the majority range between 1 and 5mm and are evenly distributed. They have a layer parallel alignment of amphibole, biotite and thin quartzo-feldspathic concentrates (usually <10% modal volume), compositionally identical with the acid gneisses. This defines a rough banding which is usually parallel to the gross interbanding of acid and basic units.

The dominant protolith of the grey gneisses is probably granodioritic and/or tonalitic igneous intrusive material. The mafic units were probably derived from minor intrusives but lithological differences may, in part, be attributable to metamorphic segregation (Fettes et al. 1992). All the Pre-Scourie dyke rocks were probably derived from both igneous and sedimentary protoliths prior to the 'gneissification' of the Scourian event (Moorbath et al. 1975). The widely held view of a mainly acid or intermediate, igneous pre-metamorphic protolith for the Lewisian rocks was not accepted by some workers (e.g. Dearnley 1962). Compositionally

similar greywackes were thought by some to be the unmetamorphosed precursor to the grey gneisses (e.g. Dearnley and Dunning 1968). However, the geochemical uniformity of the gneisses throughout the North Atlantic region suggests an igneous source, and a sedimentary or mixed source is now regarded by most workers as unlikely (e.g. Fettes et al. 1992). Long, relatively narrow, mappable belts of metasediment and metavolcanics are known to be present in the Outer Hebrides, but where these occur (e.g. S. Harris, (Coward et al. 1969)) they are geochemically highly variable.

Minor Intrusives

Several suites of minor intrusives are known from the Outer Hebrides, the majority occurring as dykes. The most important suite are the Younger Basics or Scourie dykes, but an earlier, *late Scourian suite* of predominantly microdiorites are distinguishable where Laxfordian strain is only moderately developed (e.g. SE Barra: Plate 2.1; see also Francis 1973.). The late Scourian dykes are small scale features (<25cm thick) and are usually fine grained (<1mm), with feldspar (plagioclase and K-feldspar), biotite, hornblende and clinopyroxene forming the main constituents. An early set of pegmatitic and granitic intrusions (up to 10m thick) also pre-date the Younger Basic dykes, but are compositionally similar to later Laxfordian equivalents. These early granitic and pegmatitic suites cut the Scourian country rock fabrics but are cut by Scourie dykes.

The widespread *Younger Basics* or *Scourie dykes*, form laterally continuous, brown or dark grey weathering, metabasite sheets (Plate 2.1). They are fine to medium grained (<0.5mm - 5mm), concordant or slightly discordant and have a poorly defined internal fabric. They are composed of mainly equidimensional plagioclase (mainly oligoclase) and amphibole with smaller amounts of garnet and occasional pyroxene. These are petrographically termed metadolerites (Jehu and Craig 1923, Dearnley 1962, Fettes et al. 1992). In areas of high Laxfordian strain where the dykes are concordant to the gneissose banding, they are virtually indistinguishable from the Older Basics, but may be more uniform in grain size, composition and lateral continuity (Dearnley and Dunning 1968).

The *Late Laxfordian granite-migmatite complex* forms a major granite vein-complex in Harris (Myers 1971), and a more widely distributed suite of pegmatite dykes. The migmatites show evidence of in-situ melting and locally possess cross-cutting geometries. The granite and pegmatite veins form the most easily recognisable set of minor intrusives, because they postdate most of the Laxfordian deformation and are therefore usually highly discordant to the gneissose banding. These rocks have a very variable grain size (1mm in aplites to 2m in pegmatites)

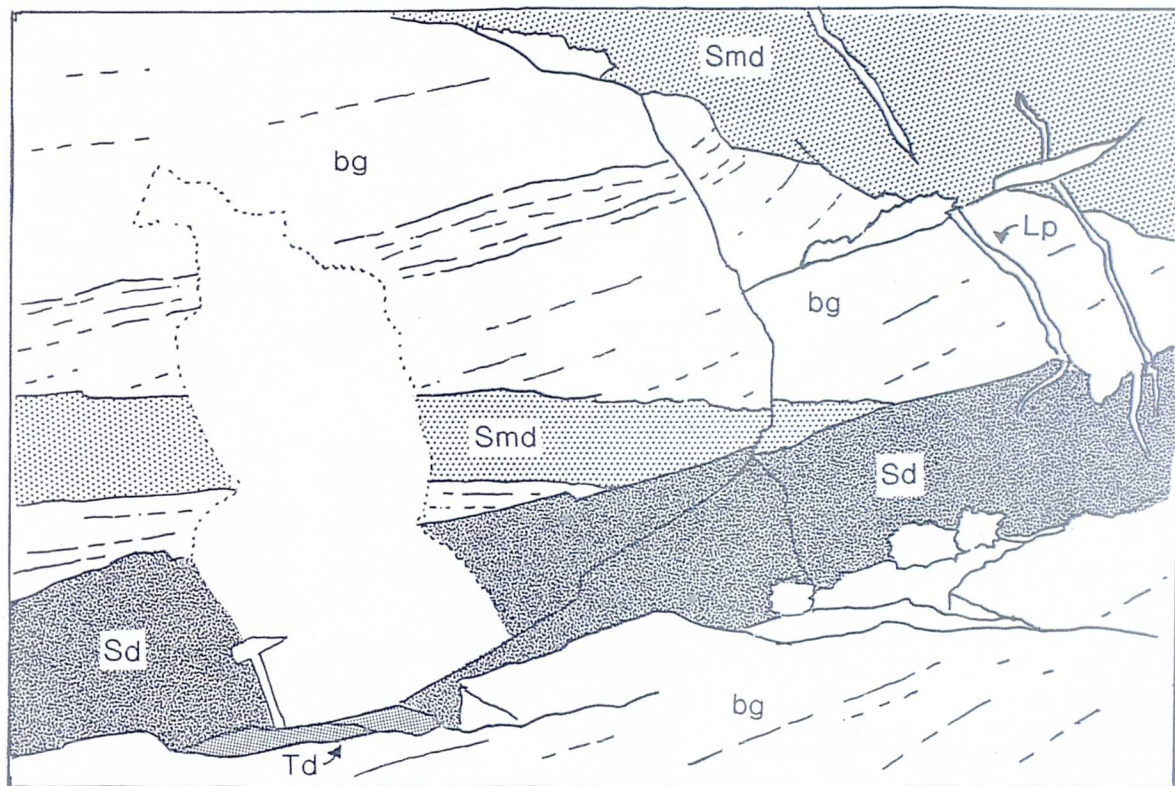


Plate 2.1. Zone of low Laxfordian strain, Easary, SE Barra (NL 702992), showing discordant minor intrusions. Cross-cutting relationships of minor intrusives:

Oldest	bg	Banded Gneiss
	smd	Scourian microdiorites
	Sd	Scourie dykes
	Lp	Laxfordian pegmatites
Youngest	Td	Tertiary dyke

and are chiefly quartzo-feldspathic with a variable dominant feldspar phase. A smaller modal percentage of biotite, muscovite, and accessory minerals such as allanite, is also present.

Major intrusives

Two large intrusive bodies form distinct metamorphosed igneous complexes in the islands (Fig. 2.1). The first is a composite body of meta-gabbro, tonalite, anorthosite and norite, termed the *South Harris Igneous Complex*. It trends NW-SE in S. Harris, and was first recognised during MacCulloch's original survey in 1819. The second is a large pyroxene rich metagabbro, known as the *Corodale gneiss* (Coward 1969, 1972) which trends N-S and occurs east of the OHFZ in South Uist.

Both complexes were believed to be Scourian in age (Dearnley 1963, Coward 1972, Graham 1980) because they appear to post-date most Scourian deformation but are intruded by probable Scourie dykes. Recent whole-rock, Sm-Nd and Pb-Pb isotopic evidence however, suggests that the Corodale gneiss may have been involved in Scourian crustal generation (c. 2800 Ma.) (Whitehouse 1993), and significantly pre-dates the South Harris Igneous Complex, which was intruded at c. 2200 Ma. (Cliff et al. 1983).

2.2.3 Structure and metamorphism

Structure

The present-day structural pattern seen in the islands is thought to be the result of a polyphase structural history spanning some 1100 Ma. The relative timing of each structural event has been deduced by its relationship to dated metamorphic events and suites of minor intrusives. The general history of the Lewisian complex has been built by the correlation of such structural sequences from one area to another. The correlations, however, are not always agreed upon because of the regional variation of structure. Some authors (e.g. Hopgood & Bowes 1972) choose a correlation based on the presumed consistency of fold geometries and orientations. The correlation cited here however, (based on Fettes et al. 1992, after Coward et al. 1970) uses the time relationships between deformation, suites of minor intrusives and dated metamorphic events. The scheme (Table 2.2) shows the structural history of the Lewisian as seen in the Outer Hebrides, with 'd' referring to deformational episodes and the letters 'S' and 'L' referring to Scourian and Laxfordian respectively.

The main NW-SE trending structural grain in the Outer Hebrides (Fig. 2.3) reflects an intense Laxfordian deformation which overprints and reorientates

previous Scourian fabrics. The effects of Scourian deformation are only discernible in areas of low Laxfordian strain, especially in the hinges of major NW-trending Laxfordian antiforms. In these low strain zones 'Younger Basics/Scourie Dykes' lie discordant to the gneissose fabrics. Where Laxfordian strains are high, 'Younger Basics/Scourie Dykes' are concordant to gneissose banding and often resemble 'Older Basic' material. After the initial gneiss forming event (d_{S2}), the main fabric forming event was Laxfordian (d_{L2}), producing NW-plunging tight to isoclinal folds with gently inclined or nearly recumbent axial planes (Plate 2.2a). A further deformation (d_{L3}) was almost coaxial to d_{L2} and formed a later set of tight cusped synforms and broad open antiforms oriented NW-SE (Plate 2.2b, Fig. 2.4,) which can readily be discerned on the foliation map (Fig. 2.3 inset). d_{L4} is only locally developed with laterally variable fold geometries and orientation (Coward 1973).

d _{L5} – d _{L6}	Formation of open warps, restricted cataclasis and retrogression. Initiation of thrusting on Outer Hebrides Thrust Zone. Main pseudotachylite formation.	
d _{L4}	Penetrative deformation of restricted extent	Formation of the Uig Hills – Harris granite complex and related migmatites. Late intrusion of pegmatites (c.1700 Ma)
d _{L3}	Extensive penetrative deformation on steep (mainly NW-trending) axial planes.	
d _{L2}	Extensive penetrative deformation, gently inclined axial planes.	Anorthosite-gabbro (Harris) (c.2250 Ma)
d _{L1}	Opening of dyke fractures, early fabric in dykes	Younger Basic dyke swarm (c.2400 Ma)
d _{S4}	Major shear zones	Diorite-granite suite (Barra) (c.2600 Ma)
d _{S3}	Large asymmetrical folds	
d _{S2}	Regional ductile deformation development of planar – linear fabric system	Regional gneiss-forming episode with accompanying intrusions (c.2750 Ma)
d _{S1}	Penetrative deformation in supracrustal gneisses	

Table 2.2. Lewisian structural history of the Outer Hebrides. d_S = Scourian deformation and d_L = Laxfordian deformation. (Modified from Fettes et al 1992)

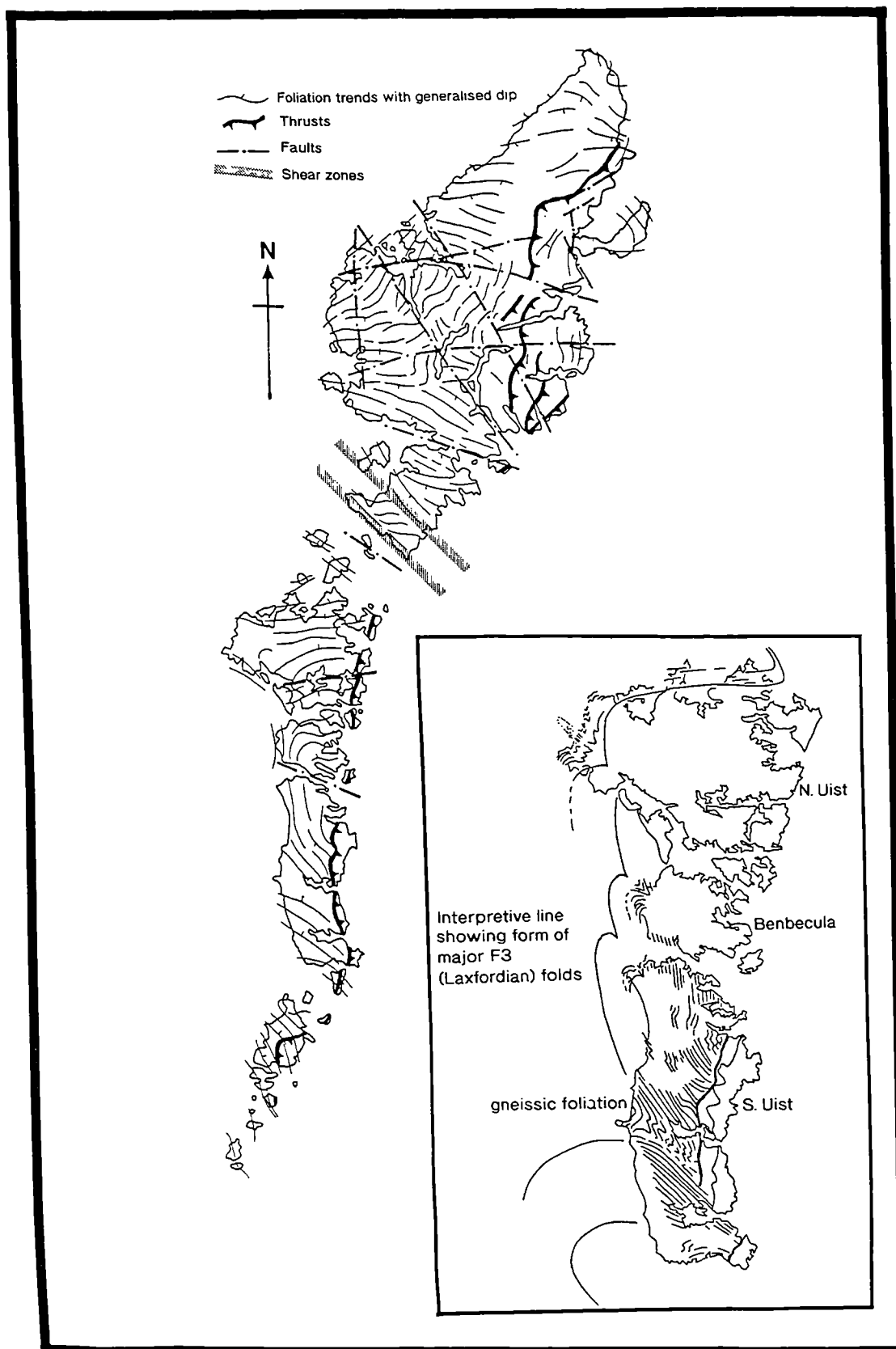


Figure 2.3. Structural map of the Outer Hebrides and (inset) structural map of Uist, showing the dominance of NW-SE trending DL3 foliations and FL3 fold axes. (Modified from Fettes et al 1992 and Coward et al 1970))

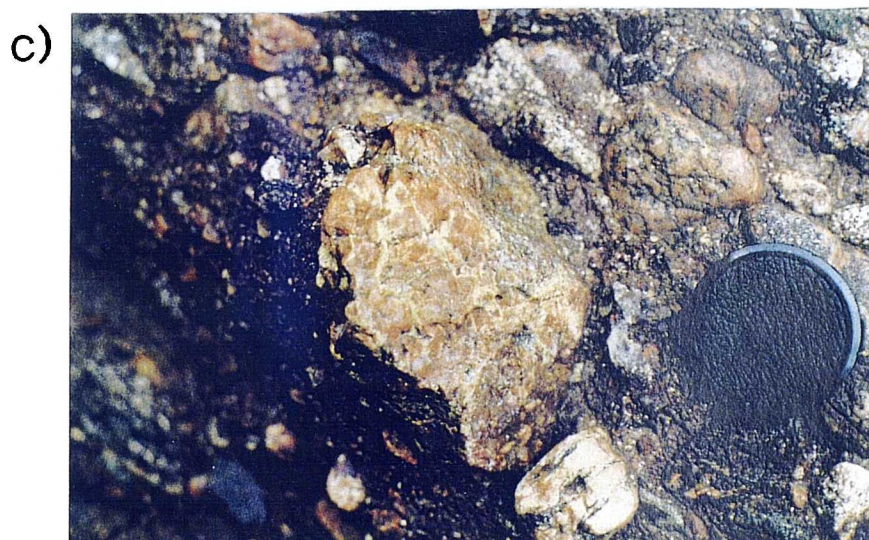
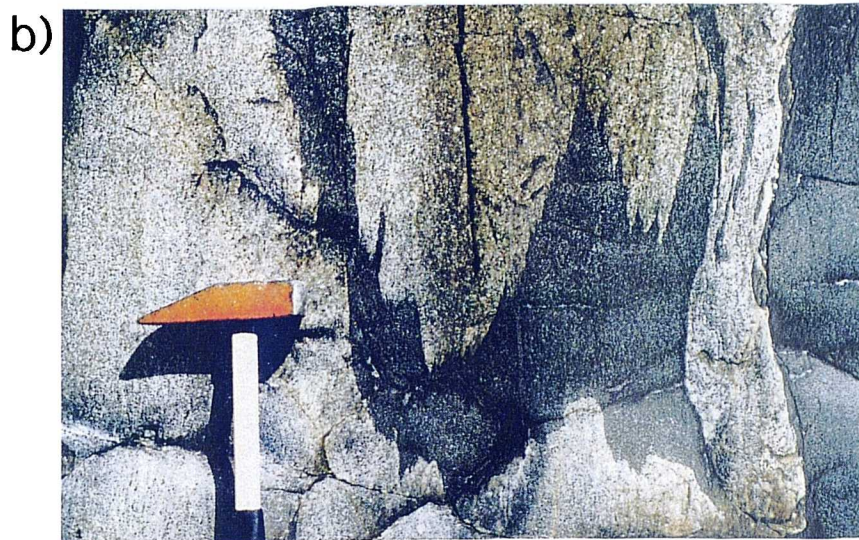
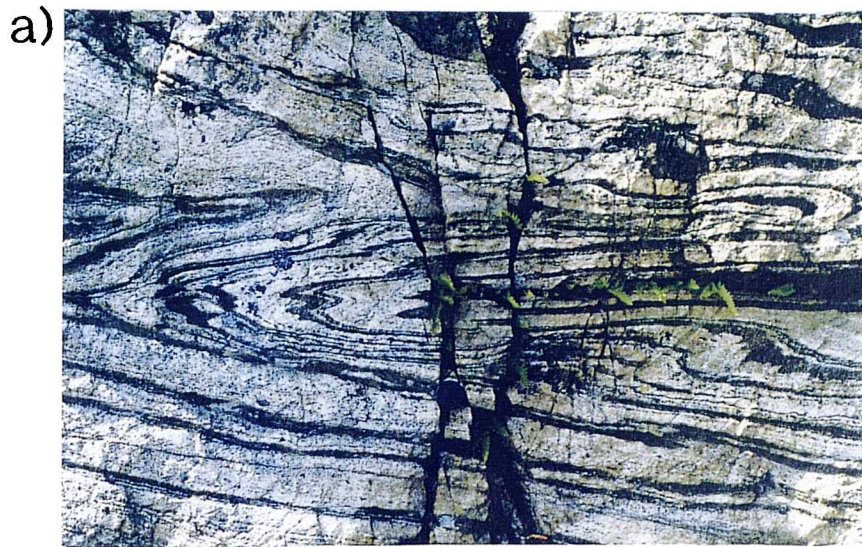


Plate 2.2

a) Laxfordian isoclinal (FL2) folds of Banded Lewisian Gneiss, from Loch Eport, North Uist (NF 895630).

b) Laxfordian upright (FL3) folds of Late Scourian 'Younger Basic' dykes and 'Grey Gneiss', from Garry-a-Siar, Benbecula, (NF 756535).

c) Epidotic and chlorititic material replacing ultracataclasite and/or pseudotachylite in a crushed gneiss clast within the Stornoway Formation conglomerate (from Garrabost [NB 510339]).

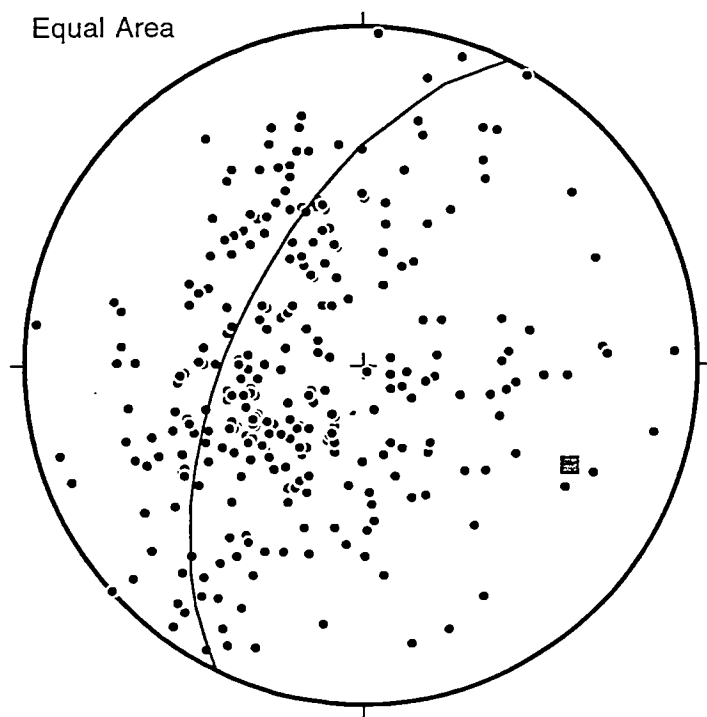


Figure 2.4. Equal area stereonet showing poles to banding in Lewisian basement, folded around NW-SE-trending Laxfordian folds. Great circle shows fold girdle. Data combined from Scalpay, Grimsay and Greian Head.

East of the OHFZ, the structural history of the Lewisian basement prior to faulting is less clear. In South Uist, Coward (1969, 1972) defined a 3 phase sequence of events for the Corodale gneiss thought to be broadly contemporaneous with the main Laxfordian deformation events in the Grey Gneiss further west, despite differences in the styles of deformation in the two units. In Barra, Francis (1973) recognised the same sequence of Laxfordian deformation above and below the fault zone, with the added corollary of a displacement estimate for the Outer Hebrides Fault Zone deduced from the offset of a major Laxfordian synform axis. This will be discussed in more detail in section 2.4.2.

Major Lewisian Shear Zones

There are several sets of shear zones which appear to have been zones of high strain during both the Scourian and the Laxfordian. One major shear zone trends NE-SW along the NW coast of Lewis and appears to curve the surrounding gneissose fabrics in a sinistral sense (Fettes et al. 1992). Discordant Scourie dykes near the shear zone margin are not sinistrally displaced and are therefore postulated to limit shear zone movement to pre-Scourie dyke age (Davies et al. 1975).

A second major set of shear zones occurs in South Harris, coinciding with belts of metasediment. Fettes et al. (1992) consider these NW-SE trending shear zones to be pre-Laxfordian (Inverian) in age because they are also cut by pre-Laxfordian minor intrusions. The Langavat, Leverburgh and Lingarabay shear zones which make up the S. Harris shear zones are believed to be the equivalent of similarly oriented, steep, Inverian shear zones on the mainland (Fettes et al. 1992). Rocks within the shear zones range from coarse grained amphibolites to near mylonites and are thought to have accommodated a dextral motion sense (Graham 1980), or a two-stage reactivation, involving early oblique dextral/thrusting, and later steepening (Coward and Park 1987), (See section 5.3.2 for a reappraisal of the kinematic history of these structures). If the shear belts are originally Inverian structures, they may have been a major controlling element on the margins of the S. Harris Igneous Complex. The metadiorite of the S. Harris Igneous Complex has been dated using Nd-Sm isotopic data at c. 2300 Ma. (Cliff et al. 1983) and is therefore broadly contemporaneous with Inverian shearing (Fettes et al. 1992).

Metamorphism

The earliest metamorphic event recorded is a Scourian granulite facies event forming orthopyroxene and clinopyroxene rich assemblages, such as those present in a few localities in South Uist (Dearnley 1962, Coward 1969). Similar high grade assemblages are known from above and below the fault zone in Barra (Francis 1973), but elsewhere they are obscured by the effects of overprinting during later Laxfordian metamorphism. In common with the Laxfordian regional deformation, the effects of Laxfordian metamorphism are dominant. Contemporaneous with f_L1 and f_L2 is a high amphibolite facies (very locally granulite facies (Coward 1973)) metamorphic episode, succeeded by a lower grade amphibolite facies episode contemporaneous with f_L3 and f_L4 , (which may have been greenschist facies above the fault zone base (Coward 1972)). By far the largest part of the basement preserves evidence for amphibolite facies metamorphism, with abundant growth of garnet and new amphibole (Dearnley 1962, Myers 1970). Areas which preserve granulite facies metamorphism may have escaped amphibolite grade retrogression due to a lack of available water (Fettes et al 1992).

2.2.4 Regional significance of Lewisian events

Scourian

The acidic portion of Lewisian gneiss is believed to have originated at c. 2900 Ma. when a phase of extensive crustal generation is thought to have occurred, marked by the production of vast volumes of tonalite (Park and Tarney 1987).

These authors suggest crustal thickening occurred by the underplating of tonalitic magmas, produced by partial melting of a mafic source in a subduction zone. Geochemical evidence suggests that the mafic/metasedimentary portion of the gneisses may have originated as subducted oceanic floor material at around the same time (Weaver and Tarney 1980). The two main components probably became tectonically intercalated soon after, during the Scourian tectono-thermal event (Fig 2.5 a) (Park and Tarney 1987). If underplating was the dominant mechanism of crustal addition, most of the crust would have had to pass through a high grade (upper amphibolite facies) metamorphic phase. This would account for the absence of low-grade Scourian rocks in the Lewisian. In addition, Park and Tarney (1987) suggest that the extremely long-lived ductility of the lower crust (which results from underplating), is consistent with the presence of extremely disrupted mafic layers and the relative abundance of mafic lenses. These authors suggest the mafic material may have been stripped from a subducting oceanic slab and was tectonically emplaced into a ductile, lower crustal keel.

The metamorphic peak (granulite facies), probably occurred c. 2700 Ma. followed by the initiation of mid-crustal shear zones in the Inverian, which segmented the Lewisian crust (Fig. 2.5 b). Coward and Park (1987) have constructed a model for the kinematics of the Lewisian based on the interpreted movement histories of Lewisian shear zones in mainland Scotland and the Outer Hebrides. They suggest that the kinematics of the shear zones are the result of the relative movements of two Archaean 'plates' in the region of the present N. Atlantic. In their reconstruction the Lewisian lies directly along strike of the Nagssugtoqidian belt of W and E. Greenland (Fig 2.6 a). This belt is placed between the two relatively stable 'plates' to the N and S. The kinematic history of the Lewisian can be interpreted by changes in the plate convergence vector. Movement directions on the Lewisian shear zones appear to indicate an Inverian N-S convergence. This explains the dominantly dextral transpressional regime seen in Scotland, and the dominantly sinistral transpressional regime seen in W. Greenland (Fig 2.6 b).

Scourie Dykes

Between the Inverian and the Laxfordian (2400 - 2000 Ma.), large volumes of mafic magma were emplaced in the form of Scourie dykes (or 'Younger Basics') during two periods of intrusion (Heaman and Tarney 1989). These dykes appear to have been emplaced dilationally, implying major crustal extension. (Park and Tarney 1987). Coeval with the youngest Scourie dykes are the Loch Maree Group metasediments and metavolcanics in mainland Scotland (Fig. 2.5 c), (Park and Tarney 1987), and the South Harris Igneous Complex (Dearnley 1963, Cliff et al.

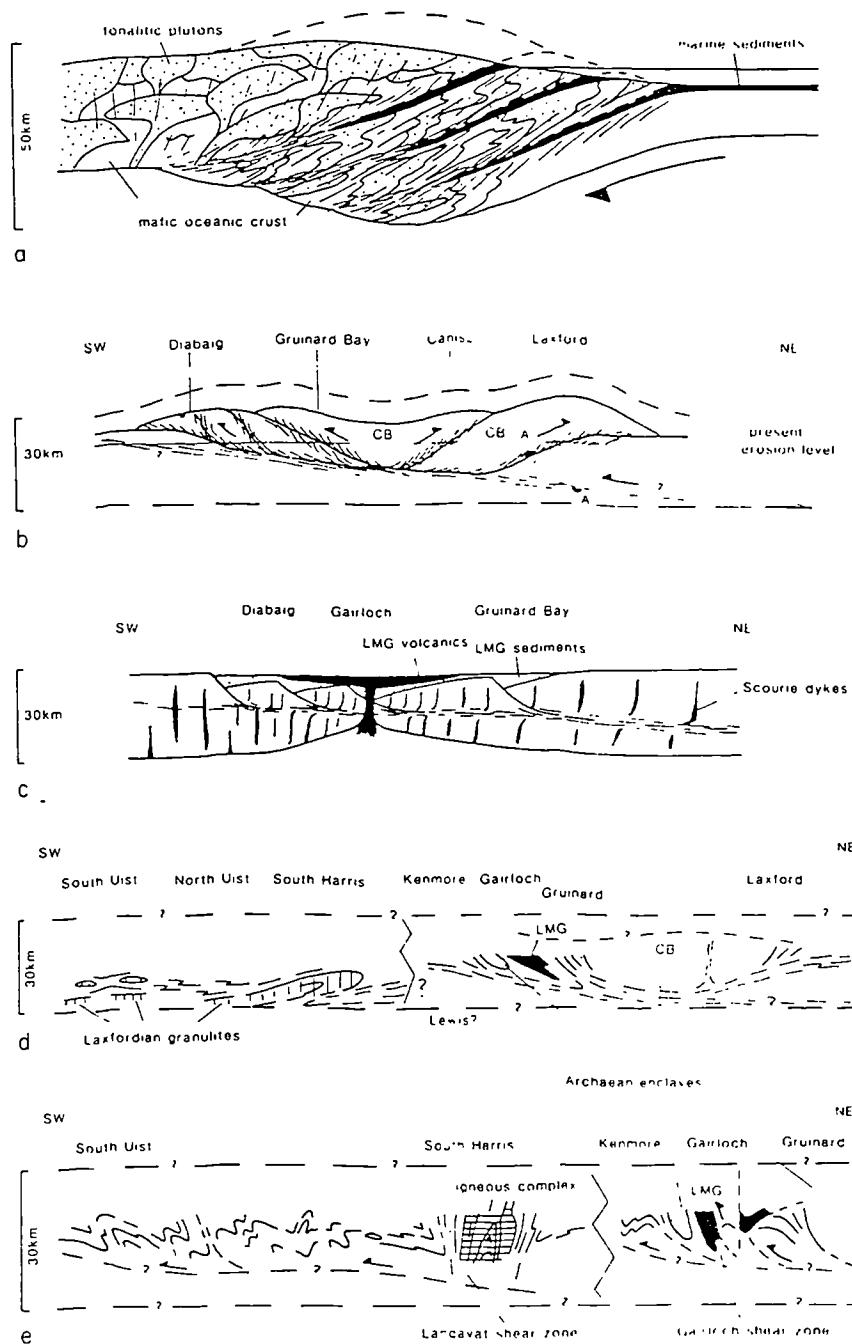


Figure 2.5. Schematic section perpendicular to the strike of Proterozoic structures, illustrating the possible early evolution of the Lewisian in Scotland.

- A) The Badcallian gneiss-forming event
- B) The Inverian Event. Note that deep-crustal granulites are transferred from A to A'
- C) Emplacement of Scourie dykes and Loch Maree Group (LMG). Extension is oblique to the line of section.
- D) Early Laxfordian (dL1 and dL2) events. Note that the relative positions of the Outer Hebrides and the mainland sections is speculative, but that the former represents a deeper crustal level. CB - Central Block.
- E) The late Laxfordian (dL3) event. There is a strike slip component on both the Langavat and Gairloch Shear Zones and movement is therefore oblique to the line of section

(From Park and Tarney, 1987, and Coward, 1984)

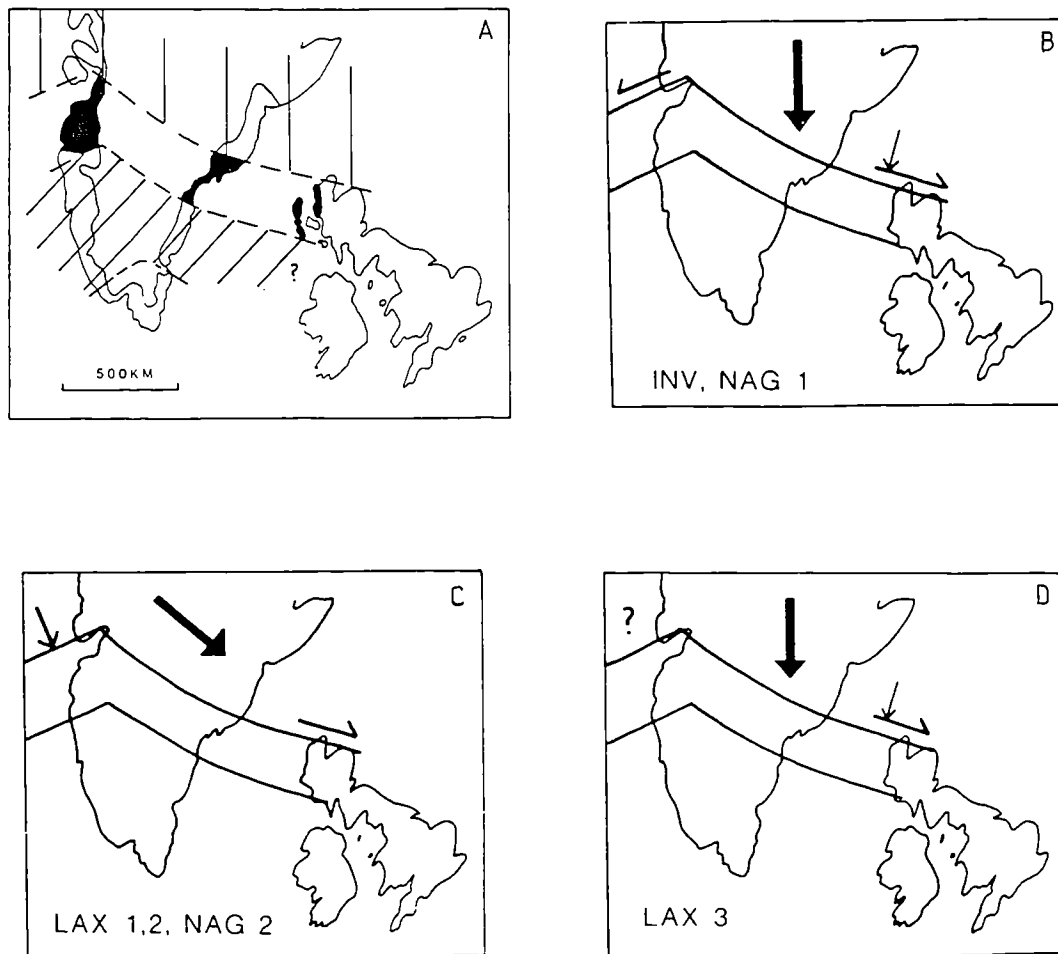


Figure 2.6. Reconstruction of the Early Proterozoic belts of Greenland and Scotland after removing the effects of N. Atlantic opening. The restoration is based on the removal of oceanic crust and on the assumption of an average 50% thinning of continental crust on the continental shelves. The Nagssugtoqian/Lewisian belt is marked in black on diagram A) and appears to be between two more stable 'plates' to N and S. Diagrams B), C), and D) summarise the interpreted changes in the convergence vector between the two 'plates' through the Inverian, early Laxfordian and late Laxfordian.

(From Coward and Park, 1987)

1983). Park and Tarney (1987) interpret the metavolcanic rocks as indicative of continued, but more rapid, extension, with lower crustal thinning accompanied by localised, upper crustal rifting. The early Proterozoic igneous rocks of the Outer Hebrides, however, are not obviously related to the volcanics of the mainland.

Laxfordian

A change in the plate movement vector to a NW-SE convergence during the early Laxfordian (2000-1800 Ma.) adequately explains both the presence of NW-directed dextral strike-slip on Lewisian shear zones, and the thrust-sense deformation present in W. Greenland (Fig 2.6 c) (Coward and Park 1987). The structures developed in the Outer Hebrides during the early Laxfordian are chiefly recumbent (Fettes and Mendum 1987), which Coward (1984) suggests indicate the existence of a major shear zone flat in the Outer Hebrides, compared with steeper structures of the same age, probably developed within shear zone ramps, in mainland Scotland. The metamorphic peak (granulite facies), during the Laxfordian (c. 1800 Ma.), is restricted to the Corodale gneiss, (although some authors regard the Corodale gneiss as upper amphibolite facies, e.g. Coward 1972), and areas of S. Harris. In S. Harris, the relatively high crustal level of adjacent, amphibolite grade areas later moved downwards with respect to S. Harris along boundary shear zones (Park and Tarney 1987). These shear zones are believed to be responsible for the local generation of migmatites in S. Harris (Coward 1984). The granitic injection complex of S. Harris post-dates most of the Laxfordian deformation, and is spatially and chronologically linked with the migmatites.

Finally, a NNW-SSE convergence is thought to have occurred in the late Laxfordian (c. 1600 Ma.), by widespread evidence for dextral transpression along the Lewisian shear zones (Coward and Park 1987) (Fig. 2.6 d). Park et al. (1987) and Park and Tarney (1987) regard the movements along South Harris shear zones and most of the upright, NW-SE trending folds (dL3 - dL6) as products of late Laxfordian deformation.

Post-Laxfordian

Cliff and Rex (1989) proposed that the Lewisian gneisses of the northern Outer Hebrides were affected by a tectono-thermal event of approximate 'Grenville' age (c. 1100 Ma.). These authors sampled biotite-hornblende gneisses in a 50 km, N-S traverse, and showed that Rb-Sr biotite ages differ across the Langavat shear zone in South Harris. The block to the south of the shear zone possesses biotite ages older than 1300 Ma., whilst the northern block possesses biotite ages of c. 1100 Ma. They suggest that two crustal blocks are present, which may have been separated by kilometre-scale displacements on the Langavat shear zone during the 'Grenville' event. The displacements were thought to preferentially uplift the northern block, and may have provided a source area for the Torridonian.

2.3 The Outer Hebrides Fault Zone

2.3.1 General setting and importance of the Outer Hebrides Fault Zone

The Outer Hebrides Fault Zone (OHFZ) is one of the largest crustal dislocations in the British Isles. It is exposed onshore in the eastern Outer Hebrides, NW Scotland and can be traced along strike for some 190 km. The fault strikes NNE-SSW and dips on average c.25° ESE under the Minch. It cuts homogeneous Lewisian gneiss along its entire length and therefore does not displace any stratigraphic marker horizons. In plan, the fault zone consists of three arcs, concave to the ESE, clearly visible on the geological map (Fig. 2.2 Inset). Seismic reflection profiling indicates that the fault zone is traceable through most of the crust in NW Scotland to a depth of c. 24km (Smythe et al 1982), and that it may even cut the Moho (Peddy 1984).

The OHFZ has been chosen as the study area for this work on basement fault reactivation for several reasons:

- It is very well exposed
- It has been well studied previously, both onshore (Sibson 1977a, Lailey et al 1989, Walker 1990,) and offshore (e.g. Brewer and Smythe 1984), (see section 2.7) but there seems to be little agreement as to its kinematic history. It has been variously described as a thrust (Sibson 1977a), a predominantly extensionally reactivated thrust (Walker 1990) and a normal fault (White and Glasser 1987, Wernicke 1986).
- There has been no comprehensive field-based analysis of the kinematic history of the OHFZ since the advent of kinematic analysis using microstructures (cf. section 1.5).
- It has frequently been cited as a 'type' example of a reactivated, continental basement fault. (e.g. Smythe 1982, Smythe et al. 1982, Brewer and Smythe 1984, White and Glasser 1987, Walker 1990, Huyghe and Mugnier 1992).
- A great variety of fault rocks are associated with the OHFZ (e.g. Sibson 1977a), suggesting that it exposes deformation zones formed at several different crustal levels during its history. This affords the ability to study the processes that may facilitate deformation and reactivation in both the brittle and ductile regimes.

2.3.2. Definition - The Outer Hebrides Fault Zone

There has been little consistency in the naming of the OHFZ, with early terms such as "Hebridean Main Belt" (Dougal 1928) and "Hebridean Thrust"

(Kurstén 1957) not being widely accepted. Other terms, such as "Outer Isles Thrust Plane" (Dearnley 1962) are unsuitable as they imply the existence of a single fault surface. The most commonly used terms combine a geographical designation, with the noun "Thrust", "Fault", "Thrust Zone" or "Fault Zone". Nearly every possible permutation of these terms have been used by previous workers (e.g. Outer Hebrides Thrust (Sibson 1977b, Brewer & Smythe 1984, Maddock 1986), Outer Hebrides Fault (Lailey et al. 1989, Huyghe & Mugnier 1992), Outer Hebrides Thrust Zone (Fettes et al. 1992), Outer Isles Thrust (Coward 1969, Smythe et al. 1982, Blundell et al. 1985), Outer Isles Fault (Stein 1988), Outer Isles Fault Zone (Butler et al. 1993). In the present work however, the fault zone is referred to as "The Outer Hebrides Fault Zone" after White and Glasser (1987), and Walker (1990), because the term is geographically accurate and has no kinematic implications.

2.3.3 Geographical setting

The OHFZ is traceable along the eastern seaboard of the Outer Hebridean island chain and corresponds to the shape of that coastline. (Fig. 2.3) The fault zone is known from seismic data to continue north along the strike of the onshore trace for a short distance into the North Lewis Basin and southwards into the Sea of Hebrides (Binns et al. 1974, Chesher et al. 1983).

The topography of the islands is chiefly the result of glacial activity and is mostly very low-lying and gently undulating. The only areas of substantial relief occur in the east of the islands, corresponding to the trace of the more erosion-resistant fault products of the OHFZ, and in the region of Harris where the geology is substantially different (see section 2.2). In contrast to the gently sloping western coast that holds numerous beaches, the east coast drops sharply and possesses many inlets. The inland exposure in the Outer Hebrides is generally poor, owing to the vast expanses of blanket peat moorland. On the eastern side of the islands however, the exposure is usually very good, especially on the coast, although north-facing slopes are often highly weathered and lichen-covered.

2.4 Previous work on the Outer Hebrides Fault Zone

2.4.1 Introduction

The earliest investigators of the geology of the Outer Hebrides (MacCulloch 1819, Heddle 1888, Dougal 1928) noted the presence of unusual rock types, such as 'basaltic paste', 'trap-shotten gneiss' and 'argillaceous schist'. These were probably the first reports of deformation products relating to the Outer Hebrides Fault Zone, and could refer to the fault rocks 'pseudotachylite', 'pseudotachylite

breccia' and 'phyllonite'. Between 1923 and 1934, Jehu and Craig systematically mapped the whole island chain and postulated a major causal structure for the belt of 'flinty crush rock' which occurred on the eastern side of the islands (Jehu & Craig 1923, 1925, 1926, 1927, 1934). They stated that the belt of crush zones and shear lines rested on a *thrust* plane and, in doing so, gave the first kinematic connotation for the fault zone.

Later 20th century workers have refined the early work by focussing on the geology of local areas that include parts of the fault zone, (Kurstén 1957, Hopgood 1964, Bowes and Hopgood 1969, Coward 1969, Francis 1969, Francis and Sibson 1973, Sibson 1977b) but the concept of a major thrust remained throughout. The fault zone has also served as the major field area for workers studying specific fault zone processes which are particularly well displayed, e.g. pseudotachylite generation, (Maddock 1986, 1992, Kelley et al. 1994) and the mechanics of fault reactivation (Huyghe and Mugnier 1992).

An important study of the OHFZ was carried out by Sibson (1977b) who proposed that the fault zone had experienced a late component of down-dip extension following the initial thrusting. This seems to be corroborated by seismic reflection data collected in adjacent offshore regions (Smythe 1982, Smythe et al 1982) which showed that a significant basin-forming phase of extension had occurred along a structure which appears to correspond to the position of the OHFZ. The relative importance of thrusting has been questioned, with some authors (e.g. White and Glasser 1987) preferring a relatively insignificant thrust phase, followed by an important phase of extension (largely based on microstructural evidence). Wernicke (1986), using seismic evidence only, has suggested that the fault zone is a result of extension, with no earlier thrusting required to account for the observed geometries. Other authors (e.g. Dearnley 1962, Francis 1969, Coward, 1969, Piper 1992 and Lisle 1993) have postulated significant strike-slip displacements between the Outer Hebrides and the Scottish mainland. Earlier workers based these ideas of strike-slip movement on the along-strike correlation of zones of different metamorphic grade, whilst Piper (1992) and Lisle (1993) suggest a bulk sinistral offset has occurred, based on palaeomagnetic evidence and the orientation of Scourie Dykes respectively. The latter authors suggest that the nearby Minch Fault, which roots into the OHFZ at depth (Stein 1988) is responsible for the apparent strike-slip motion.

2.4.2 Displacement estimates for the OHFZ

Estimates for the amount of displacement on the OHFZ have been made based on the correlation of regional structures across the fault zone (Francis 1969,

1973 and Sibson 1977b), and by deformed strain markers (Sibson 1977b). Sibson (1977b) estimated finite reverse-slip motion to be 10 +/- 5 km with translation from ESE to WNW, normal to the fault zone strike. This implies a vertical uplift of the hanging wall of 4.2 +/- 2.1 km. However, since no stratigraphic marker horizons are displaced, all but one of Sibson's displacement estimate methods are indirect strain measurements. The direct estimate (c. 7.5 km of dip-slip motion without rotation), using the displacement of a major Laxfordian (f_L3) synform axis (after Francis 1973), is only pertinent to Barra. A critique of this displacement estimate is provided in section 5.3.4.

2.4.3 The timing of OHFZ movements

The timing of movements on the OHFZ has also been contentious in recent years and further confused because the important distinction between fault *inception* and *subsequent fault movement* has rarely been made.

Evidence for both inception and/or subsequent fault zone movement relies on either:

- Stratigraphic and cross-cutting relationships, both onshore and offshore, or;
- Isotopic dating of fault rocks.

OHFZ inception

Using onshore cross-cutting relationships, chiefly the relative timing of faulting with minor intrusions, the relative timing of faulting with the deposition of the Stornoway Formation, and the marked parallelism of the OHFZ with the Caledonian-age Moine Thrust (Fig. 2.1), most workers favour a Caledonian age for *inception* of the thrust motion (e.g. Francis & Sibson 1973; Sibson 1977a, Sibson 1977b; Coward 1980; Macaudiere & Brown 1982; Maddock 1986; White & Glasser 1987; Walker 1990; Kelley et al. 1994). A Proterozoic origin (Coward 1969, 1972, Fettes & Mendum 1987, Smythe 1987, Lailey et al. 1989) and a post-Caledonian origin (Wernicke 1986) have also been suggested however.

Isotopic age dating of fault rocks (e.g. K-Ar dating of phyllonites (Sibson 1977b), and Ar-Ar dating of Pseudotachylites (Kelley et al. 1994)) has revealed dates in the range c. 450-400 Ma. and have been suggested as indicative of Caledonian fault *inception*. These dates are broadly coeval with available isotopic age dates for thrusting on the Caledonian age Moine Thrust in mainland Scotland (Van Breemen et al. 1979, Kelley 1988).

If these age dates of OHFZ fault rocks are correct, then a post-Caledonian *inception* for the OHFZ is impossible (cf. Wernicke 1986). These age dates do not

come from the earliest fault rocks however (see chapter 3), and may therefore date fault rocks associated with reactivation after fault inception. Thus, a post-Laxfordian, pre-Caledonian age for inception cannot be precluded.

Subsequent OHFZ movements

Although onshore stratigraphic relationships are useful for determining the age of fault inception, they are less useful for determining the age of subsequent movements because these may be focused offshore. Offshore seismic data has been used to try to constrain periods of extension and inversion on the basin bounding faults, of which the partially reactivated OHFZ is the most important (Stein 1988). Using this method, Stein (1988) suggests basin development occurred by extensional movement on the partially reactivated OHFZ (the Minch Fault) during the Torridonian and the Carboniferous with a period of basin inversion in the latest Jurassic and Early-Mid Cretaceous. Stein's chronology of fault movements however, relies on the correct stratigraphic correlation of seismic reflections, which are not well constrained by independent data, e.g. boreholes. O' Neill and England (1994) suggest that movement on the Minch Fault did not control the deposition of either the Torridonian or the Carboniferous. Torridonian basin fill, is thought to be pre-rift (Nicholson 1992), and Carboniferous sediments, if present, constitute a relatively thin sequence (< 250m thick) (O' Neill and England 1994). These authors suggest that syn-depositional Minch Fault movement was chiefly restricted to the Devonian (Caledonian orogenic collapse) and the Triassic.

2.5 The Stornoway Formation

Overlying the Lewisian gneiss in the region of Stornoway in Lewis (Fig. 2.2), are a series of red-brown conglomerates, coarse sandstones, and mudstones of the Stornoway Formation, with an estimated thickness of c. 4000m (Steel & Wilson 1975). These rocks were well studied in the early part of the century (Dougal 1928, Steavenson 1928, Peach & Horne 1930, Jehu & Craig 1934,) but there is less recent work (Steel & Wilson 1975, Storetvedt & Steel 1977). They constitute the only unmetamorphosed and undeformed rocks of the region, and cover a small area from Arnish point in the south (NB 426303) to Allt Raonadale (NB 516434) in the north.

The red colouration, persistently coarse-grained nature, lack of fossils and locally derived clast composition suggest the Stornoway Formation was deposited in an arid climates as an alluvial fan sequence, (Steel & Wilson 1975). These workers

(Steel 1971, Steel & Wilson 1975,) have suggested the existence of three depositional units each of which contains the following two main types of sediment:

1. Conglomeratic rocks, which were probably deposited in a fault-controlled, alluvial fan environment building out laterally S and SE-wards towards the basin axis;
2. Sandstones and mudstones (probable alluvial floodplain deposits), which interfinger the conglomerates and may have accumulated from a NE flowing river system on the local palaeoslope.

Within each of the three depositional units, it was suggested that the nature of the sedimentation reflects the rate of fault controlled subsidence. The formation's bounding faults are thought to accumulate c. 4km, of downthrow, equal to the true thickness of the succession (Steel & Wilson 1975). The fault blocks are inferred to be syn-sedimentary and rotational, and as a result, the basement may exist quite close to the surface (Steel & Wilson 1975) (Fig. 2.7). They suggest that the fault movement and related sedimentation took place in 3 phases:

- The lower unit accumulated synchronously with movement on the eastern faults.
- Movement on these faults ceased and following a sedimentary overlap, the middle unit was deposited against an active fault further west.
- The upper unit was then deposited in the same way.- by cessation of faulting on the previous fault, and accumulating against the faults which now constitute the western boundary.

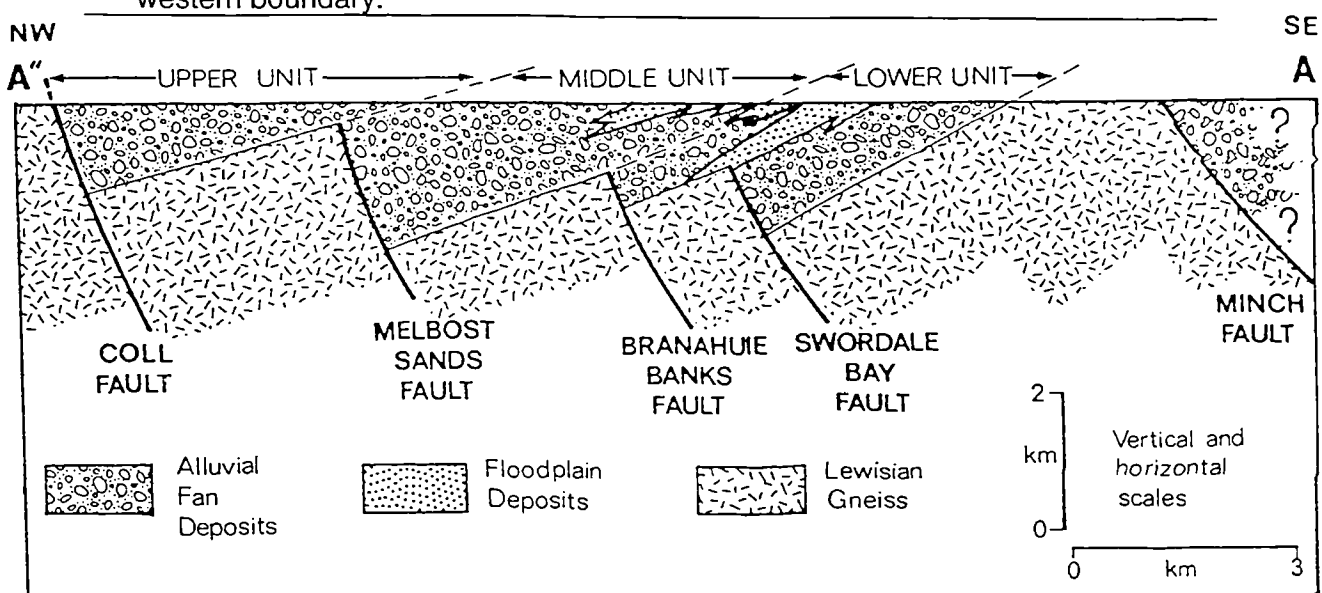


Figure 2.7. Cross section (roughly NW-SE) through the Stornoway Formation, showing the suggested structural configuration of the western Minch Basin margin (as outlined in the text). The base of the cover succession is thought to be highly diachronous (from Steel and Wilson 1975).

The western basin margin would have therefore migrated c. 15 km onshore and to the west of the Minch Fault trace with the greatest extent of the formation filling the deepest region of the asymmetric, Permo-Triassic age, North Minch Basin (section 2.7)

2.5.1 Age of the Stornoway Formation

Because the formation is unfossiliferous, estimates of its age have largely been based on comparative evidence from other similar successions of known age. Three possibilities have been favoured by previous workers: Torridonian (Steavenson 1928, Jehu & Craig 1934), Devonian, (Kurstén 1957), and Permo-Triassic, (Steel 1971, Steel and Wilson 1975, Storetvedt & Steel 1977). Despite a superficial resemblance to the Diabaig Group (Jehu & Craig 1934), or basal horizons of the Applecross Formation of the Torridonian, no exotic pebbles are present in the Stornoway Formation (Peach & Horne 1930), unlike other Torridonian conglomerates. In addition, geophysical measurements on the sediments have proved seismic velocities comparable to those of the Inner Hebrides Triassic deposits and significantly different from those of the Torridonian Sandstone (Steel & Wilson 1975). Furthermore, as fault rocks, including relict (probably Caledonian) pseudotachylites clearly derived from the adjacent OHFZ occur in the mainly undeformed Stornoway Formation (see section 2.4.3) (Plate 2.2c), a Precambrian age for the formation seems unlikely. A Late Permian - Triassic age is considered the most probable, based on superficial similarities with the New Red Sandstone deposits of Wester Ross and Sutherland. These mainland deposits are also mainly conglomeratic and contain locally derived clasts (Johnstone and Mykura 1989). The most convincing evidence for a Permo-Triassic age for the Stornoway Formation comes from palaeomagnetic studies on the lowermost fine grained horizons (Storetvedt and Steel 1977), which suggest an age of c. 250 (+/- 50) Ma., and a shallow borehole study (Binns et al. 1974), sited near the Minch Fault, east of Benbecula, which again concluded a late Permian age for the formation. If the late Permian - Triassic ages of Storetvedt & Steel (1977) and Binns et al. (1974) are correct, this sets a youngest age limit on the onset of OHFZ movement onshore of c. 250 Ma

2.6 Post-Lewisian minor intrusives

Several suites of minor intrusives, mainly dykes, cut the Lewisian rocks throughout the Outer Hebrides. Most belong to one of two suites: a *Permo - Carboniferous suite* of quartz - dolerite and lamprophyric (camptonites and

monchiquites) compositions; and a later suite of *Tertiary dolerites and basalts*. The earlier suite can be taken as Permo-Carboniferous on the basis of a large number of age determinations in the range 330-320 Ma that have been obtained in petrologically similar camptonite-monchiquite swarms in Orkney, the Ross of Mull and elsewhere, and Rb-Sr age determinations from the Outer Hebrides (Fettes et al. 1992).

The later suite are more abundant and petrologically similar to dykes of known Tertiary age from Skye and Mull. Both suites lie in NW-SE trending swarms, discordant to the country rock foliation, and both post-date all major deformation associated with movement on the OHFZ. They can therefore be used to place a youngest possible age limit on the onset of fault zone movement onshore of c. 320 Ma., and a total age range for possible onshore movements of c. 1380 Ma.

2.7 Offshore basins

The Stornoway Formation is thought to be the onshore development of a much greater extent of basin fill offshore. Three basins have been identified off the eastern and northern coasts of the Outer Hebrides based on borehole and geophysical (gravity, magnetic and seismic) data. From south to north these are: the Sea of the Hebrides Basin, the North Minch Basin, and the North Lewis Basin (Fig. 2.8). Each of them have a similar age, stratigraphy and basement control, and are discussed below:

2.7.1 The Sea of The Hebrides Basin

This, the largest of the three offshore basins, is bound to the west by the Minch Fault and to the north by a Torridonian structural high (the Mid-Minch High) (Binns et al. 1975, Stein 1988). To the east, the basin margin is controlled by the Lewisian and Torridonian structural high which lies close to the Camasunary-Skerryvore fault (Fig. 2.8), (section 2.8). The basin is markedly asymmetric in shape, the deepest part occurring near the Minch Fault (Binns et al 1974). South of Barra, a syncline is developed close to the Minch Fault, the approximate trace of which is clearly visible on the Bouger anomaly gravity map (Fig. 2.9). The northwestern limb of the syncline is gradually truncated further south, causing an apparent steepening of the gravity gradient (Binns et al. 1975).

West of the Minch Fault, sediments of Permo-Triassic to Early Jurassic age and Carboniferous reworked miospores have been identified from drill core SH. 207 (Binns et al. 1974). East of the fault, the basin contains up to 3 km of similar Mesozoic sediments, with a seismic character comparable to those further west, and

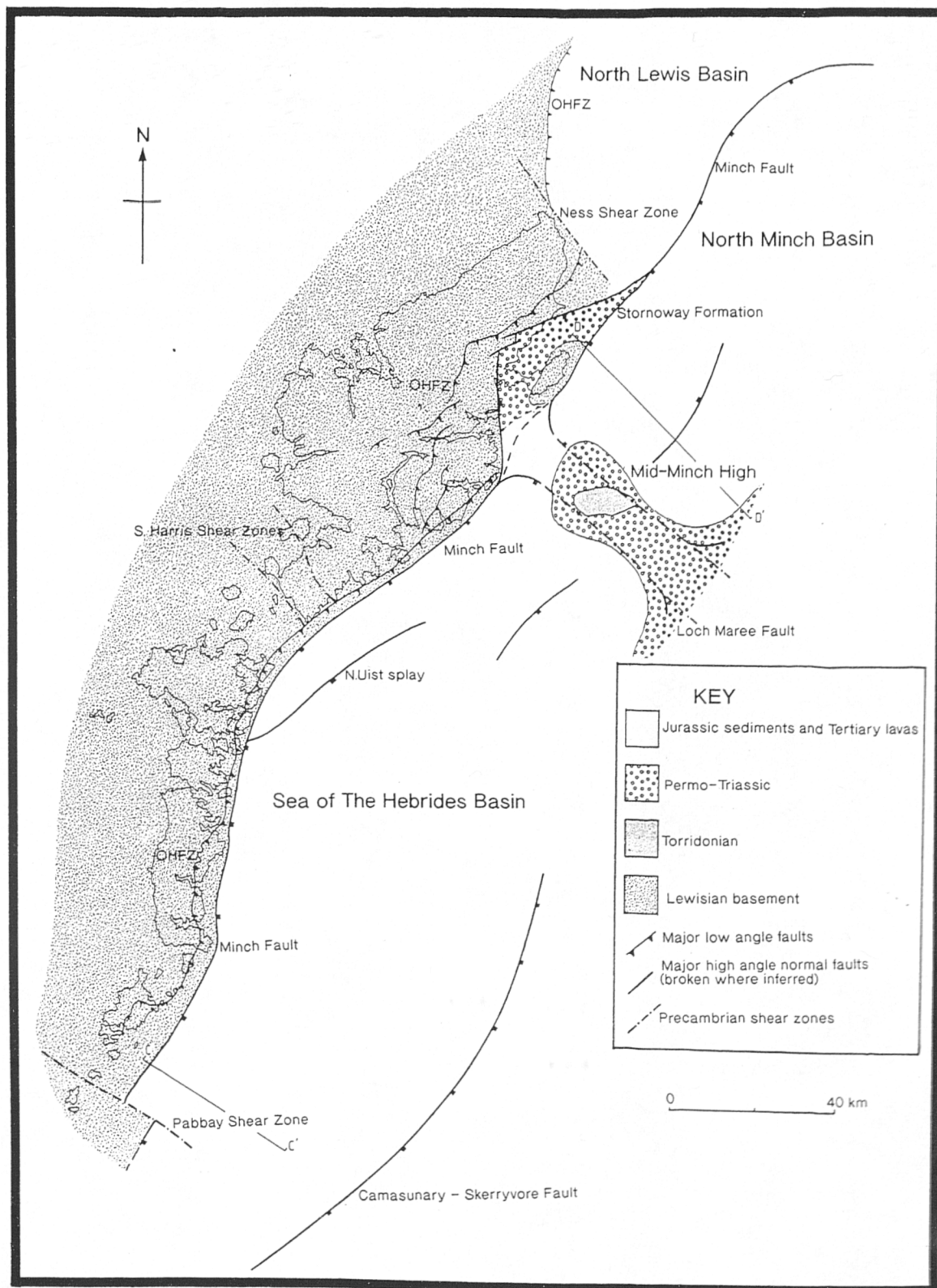


Figure 2.8. Solid geology of the area between the Outer Hebrides and the Scottish mainland based on boreholes and surface sampling. (redrawn from and modified from Binns et al. 1975, Cheshier et al. 1983, Cheshier and Smythe 1986 and Stein 1988).

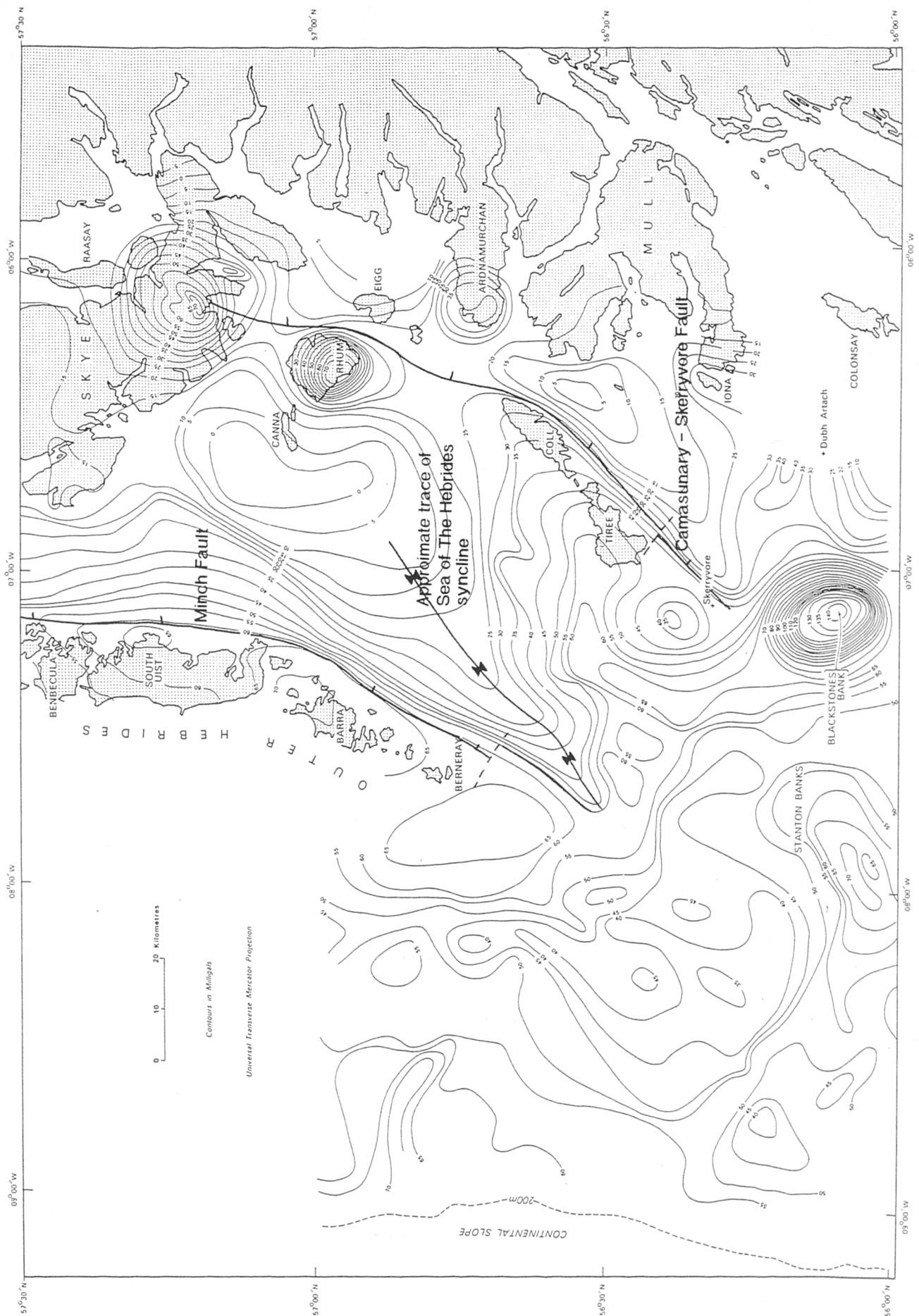


Figure 2.9. Bouguer anomaly gravity map of the Sea of Hebrides (from Binns et al. 1975).

is thought to be floored by Precambrian and possibly Palaeozoic basement (Binns et al. 1974, 1975). These sediments are partially overlain and intruded by Palaeogene lavas and sills which, on nearby Mull and Skye, reach a thickness of c. 1 km. The lavas have locally downwarped to accommodate successive Tertiary sediments (Smythe and Kenolty 1975). One of these small basins adjacent to the Minch Fault has been sampled by a borehole and comprises carbonaceous clays and sands of Oligocene age (Evans et al. 1991). The basin therefore has been interpreted as containing mainly Permo-Triassic-Jurassic sediments, overlain by a thin Tertiary/Quaternary succession (Fig. 2.10).

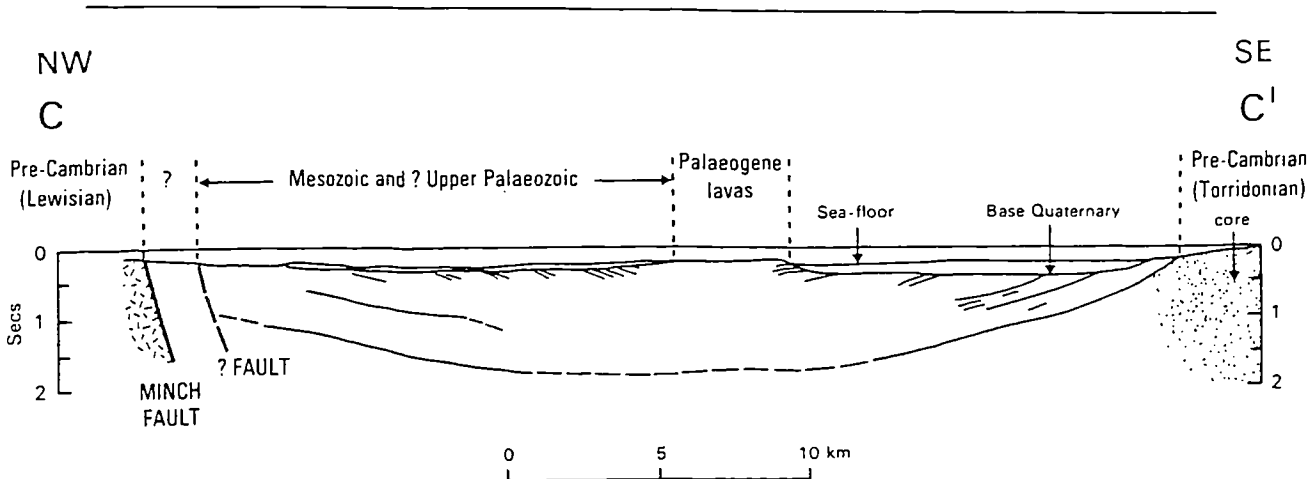


Figure 2.10. Section C - C' across the Sea of The Hebrides Basin; from deep and shallow seismic profiles. For location see Fig. 2.7. (from Binns et al. 1975).

2.7.2 The North Minch Basin

To the north of the Sea of The Hebrides Basin, and separated from it by the Mid-Minch High (section 2.8), is the North Minch Basin. It is also highly asymmetric, bounded in the west by the Minch Fault, but it remains relatively open to the North. It appears to have had a strong tectonic control during its development, giving rise to a half-graben geometry with westerly-dipping sedimentary reflectors, easily seen on the BIRPS GRID 10 seismic section (Fig. 2.11, and Fig. 2.12)

The Stornoway Formation (section 2.5) can be seen on shallow seismic profiles to the west of the Minch Fault adjacent to the main basin (Binns et al. 1975). The onshore evidence for a Permo-Triassic age for these rocks is corroborated offshore by palaeontological evidence further south (Binns et al 1974). Permo-Triassic age sequences in the basin, east of the Minch Fault are highly reflective but the base is poorly defined.

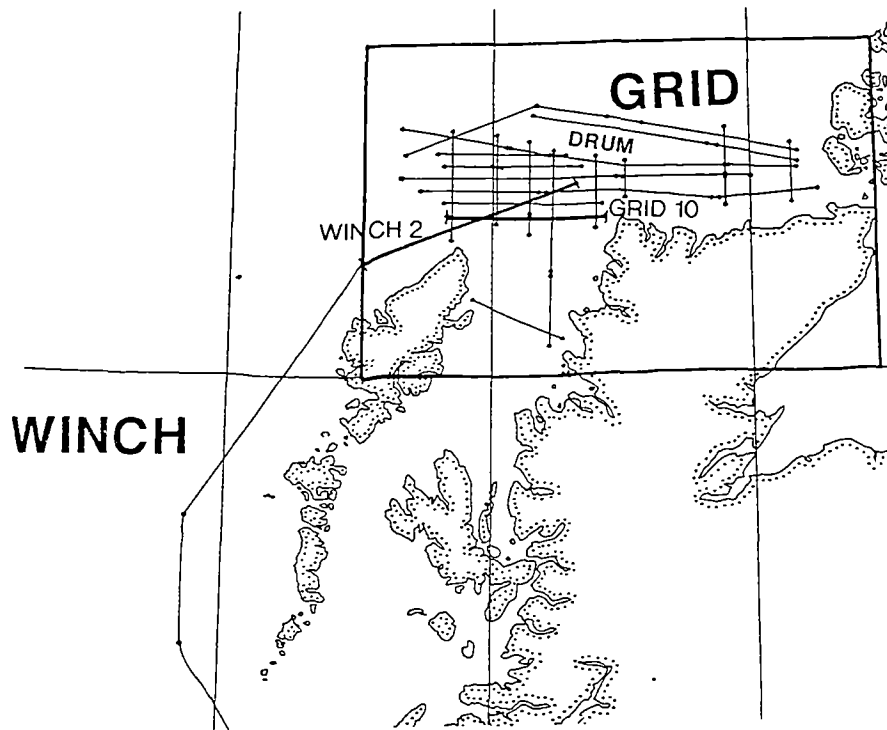


Figure. 2.11. Location map for BIRPS deep seismic refraction profiles.

In the main basin, a borehole sample of Middle Jurassic age has been recovered, and is thought to correspond to c. 4 km of seismically reflective sandstones and shales (Chesher et al. 1983). The top 0.7 km of this succession is a sequence of poorly bedded, low seismic velocity sediments of Quaternary age. Another borehole has revealed a complete Quaternary succession in this unit (Graham et al. 1990). Generally the stratigraphy is similar to the Sea of the Hebrides Basin (Fig. 2.13) :- a chiefly Mesozoic fill, the base of which is probably Permo-Triassic, passing up into a thicker Jurassic succession, and capped by much thinner Cenozoic deposits (Binns et al. 1975, Chesher et al. 1983),

2.7.3 The North Lewis Basin

This is the north westerly continuation of the North Minch Basin and is also a half-graben. Underlying the westerly dipping sedimentary reflectors of the North Lewis Basin is a major reflective zone, visible on the BIRPS WINCH 2 profile, corresponding to the trace of the OHFZ (Fig 2.11 and Fig. 2.14). The Minch Fault does not continue further north and is therefore not the major controlling element on the North Lewis basin development (Brewer and Smythe 1986).

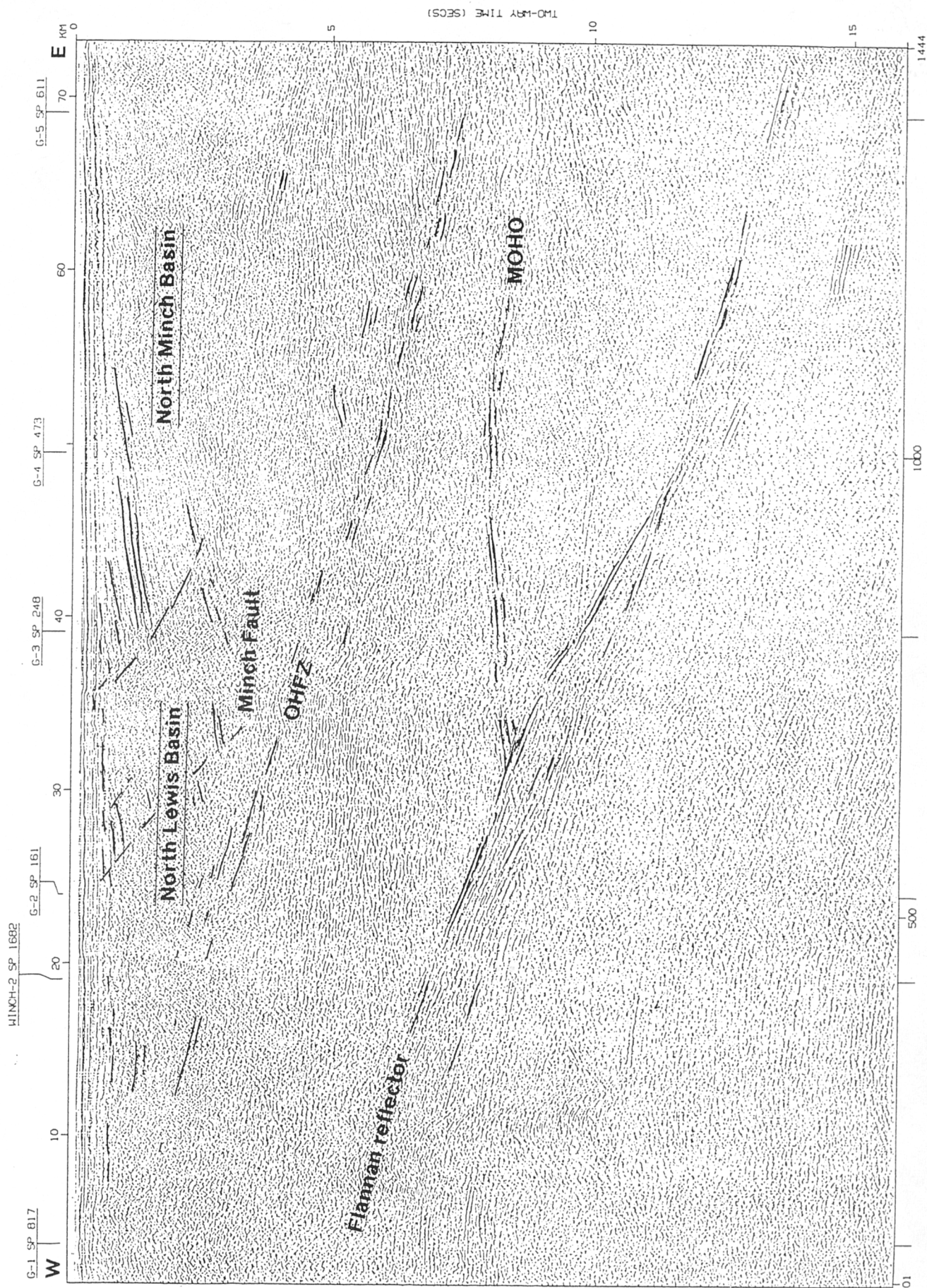


Figure 2.12. BIRPS (GRID 10) deep seismic profile. For location see Fig. 2.11.

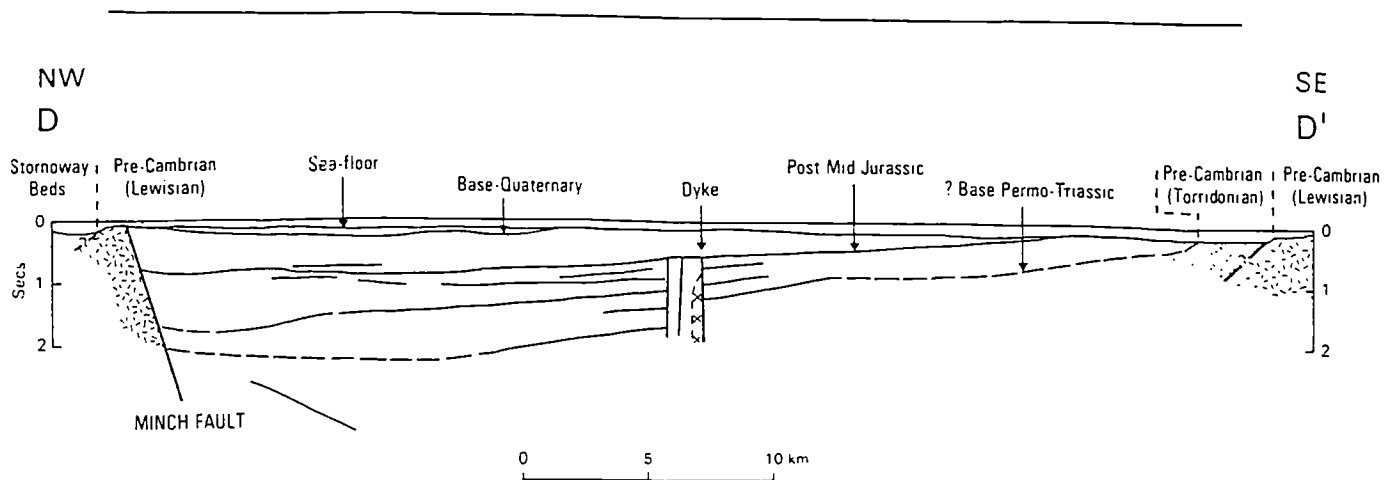


Figure 2.13. Section D - D' across the North Minch Basin, from deep and seismic shallow seismic profiles. For location see Fig. 2.7. (from Binns et al. 1975).

2.8 Possible fault controls on basin formation

2.8.1 The Minch Fault / OHFZ

The western margins of the Sea of Hebrides and North Minch Basins are controlled by the Minch Fault, a NE-SW trending set of faults with a steep dip to the SE (McQuillin and Binns 1973, Stein 1988). The structure is clearly visible on gravity and magnetic profiles, as a result of the strong physical contrast between the Lewisian gneisses to the west and the Jurassic mudstones to the east (Chesher 1983). The location of the Minch Fault appears to be strongly influenced by the location of the OHFZ onshore, and the former has clearly acted as a locus for late Palaeozoic (Devonian) and younger normal movements (Smythe 1982, Brewer et al. 1983). Regional extension may have partially reactivated the OHFZ at depth (Stein 1988), creating the wedge-shaped, hanging-wall basins by basement block rotation, and giving rise to westerly-dipping sediment packages (Blundell 1984). Some workers regard the Minch Fault as a possible strike-slip fault during its pre-Mesozoic history (Dearnley 1963, Piper 1992, Lisle 1993), but it has clearly acted as an extensional fault and is a major structure which has controlled basin evolution since Permo-Triassic times (Steel and Wilson 1975).

Extent

According to existing seismic reflection data, the Minch Fault appears to be a single structure along the southern part of its trace (Chesher 1983, cf. Stein 1988), separating into several strands near the mouth of Stornoway Bay. Several of these fault strands occur onshore and are thought to be responsible for downthrowing the Stornoway Formation (section 2.5). The onshore development of the basin margin

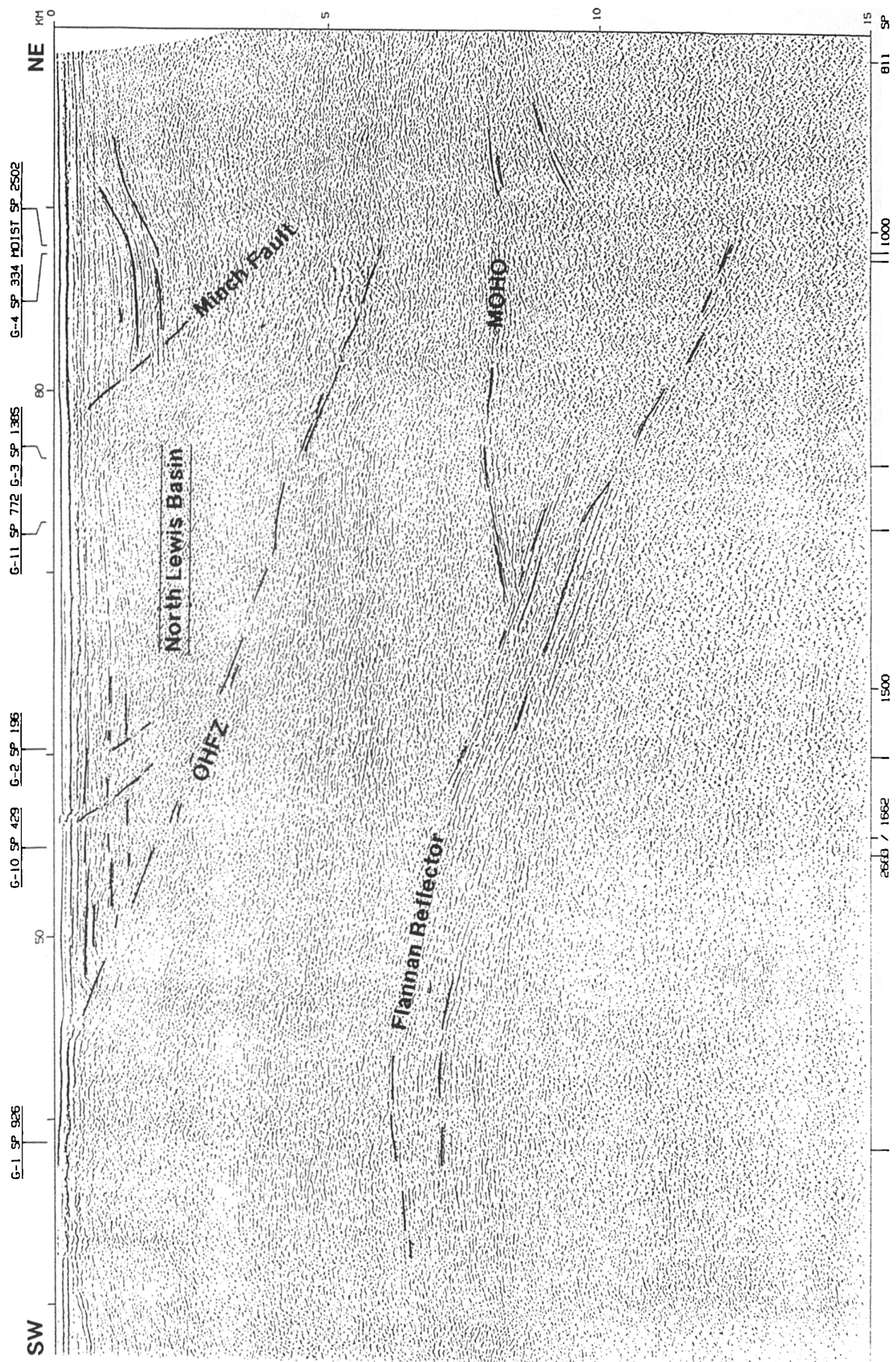


Figure 2.14. BIRPS (WINCH 2) deep seismic reflection profile. For location see Fig. 2.11.

and the offshore trace of the Minch Fault may be linked at depth south of Stornoway Bay (Fig. 2.8). At around this point the trace of the Minch Fault and the trace of the OHFZ diverge, and the character of the basin appears to change. The sediments no longer dip towards the fault, but dip basinwards above the Minch Fault north-east of the Eye Peninsula. North of Lewis, where the trace of the OHFZ appears to have significantly departed from the trace of the Minch Fault, the OHFZ becomes the major tectonic control on the evolution of the North Lewis Basin,

Where the Minch fault begins to converge with the Camasunary-Skerryvore Fault, the Mesozoic outcrop narrows. This is probably due to the intersection of the Minch Fault with the southeastern limb of The Sea of The Hebrides syncline (Binns et al. 1975). South of the Outer Hebrides, the OHFZ does not form a strong seismic reflection, and the Sea of The Hebrides basin has died out, implying either that the OHFZ fundamentally controls the lateral extent of the basin, or that OHFZ seismic reflections are not strong where the fault zone did not experience extension (Brewer and Smythe 1986). These authors prefer the former interpretation because other faults that experienced no extension, e.g. The Wind River Thrust, Wyoming, do provide strong seismic reflections (Smithson et al. 1979). Most authors agree that the complex of sheared and unsheared Lewisian rocks onshore could easily produce reflections on seismic data through the processes of spatial interference and ray focussing, without undergoing extensional movement (Fountain et al. 1984, Reston 1987, Stein 1988).

Movement history

Principal normal movements on the Minch Fault, with syn-tectonic deposition have been postulated for the Permo-Triassic, middle/late Jurassic, and the post - Eocene (Hudson 1964, Steel 1971, Binns et al. 1975, O' Neill and England 1994). Blundell (1984) and Stein (1988) regard the deeper reflectors visible on the BIRPS MOIST profile, parallel and north of GRID 10 (Fig. 2.11 and 2.12), as possible Torridonian deposits, whilst Brewer and Smythe (1986) regard a Devonian age for these sediments as also possible. Recent evidence however, suggests that significant syn-depositional movement on the Minch Fault only occurred during the Devonian (Caledonian orogenic collapse), and Triassic rifting (O' Neill and England 1994), although some workers regard the Minch Fault as a possible strike-slip fault during its pre-Mesozoic history (Dearnley 1963, Piper 1992, Lisle 1993). The Permo-Triassic sediments are present onshore as the Stornoway Formation, (Steel and Wilson 1975), and seismic reflectors offshore, interpreted as Triassic sediments, are observed to thicken towards the fault, indicating syn-depositional fault movement (O' Neill and England 1994). The Middle Jurassic sediments of the

Inner Hebrides, which are traceable offshore using seismic data, are believed to be derived from a Lewisian source west of Skye (Hudson, 1964), but are interpreted as chiefly post-rift sediments by O' Neill and England (1994). Stein (1988) suggests that a period of basin inversion occurred in the latest Jurassic / Early cretaceous,, with uplift in the footwall of the Minch Fault and Mid-Minch High. Probable further uplift was associated with Palaeogene lava extrusion (Emeleus 1983), and close to the scarp of, and possibly truncated by, the Minch Fault is an outlier of Eocene basaltic lava, which indicates post-lava movement of the fault (Binns et al. 1975).

Displacement

The amount of displacement on the Minch Fault appears to be laterally variable. In the Sea of The Hebrides, for example, the throw on the Minch Fault appears to be highest at the southernmost and northernmost sections (Brewer and Smythe 1986). In the central part (adjacent to South Uist), the throw on the fault decreases, and the gravity gradient is therefore less steep (Fig. 2.9). The deepest part of the Sea of The Hebrides basin is at the northern end, adjacent to the highest topography onshore (S. Harris). Brewer and Smythe suggest that the Outer Hebrides block remained a positive structure through much of its history as a result of isostatic footwall uplift on the Minch Fault. In addition, the present elevation of the Outer Hebrides can be explained by the 10% isostatic footwall uplift, (using the criterion of Jackson and McKenzie 1983), predicted for a fault with 3-4km sedimentary infill in its hanging-wall (Brewer and Smythe 1986). This important suggestion implies that uplift associated with the latest movements along the OHFZ is largely responsible for the presence of the Outer Hebridean island chain.

2.8.2 The Mid-Minch High

The Mid-Minch High is an upstanding NW-SE trending basement ridge currently separating the Sea of The Hebrides Basin from the North Minch Basin. It has been imaged on commercial seismic data (Stein 1988), and appears to coincide with two major Precambrian structural lineaments on the Scottish Mainland. The northern margin of the basement high coincides with the lateral continuation of the transition zone at Gruinard Bay, separating dominantly granulite facies Scourian rocks in the north from dominantly amphibolite facies Laxfordian rocks in the south (Sutton and Watson 1951). The southern margin appears to be the lateral continuation of the Gairloch Shear Zone/Loch Maree Fault, another Precambrian shear zone (Fig. 2.15) (Stein 1988).

Palaeocurrent evidence from the Permo-Triassic basins of mainland Scotland and the Stornoway Formation of Lewis suggests that the Sea of The

Hebrides Basin and the North Minch Basin were partially separated in their early history by the Mid-Minch High (Steel and Wilson 1975). This had the effect of partially closing both basins at adjacent ends. Subsequent deposition in the Mesozoic and Cenozoic was influenced by the divided basin architecture.

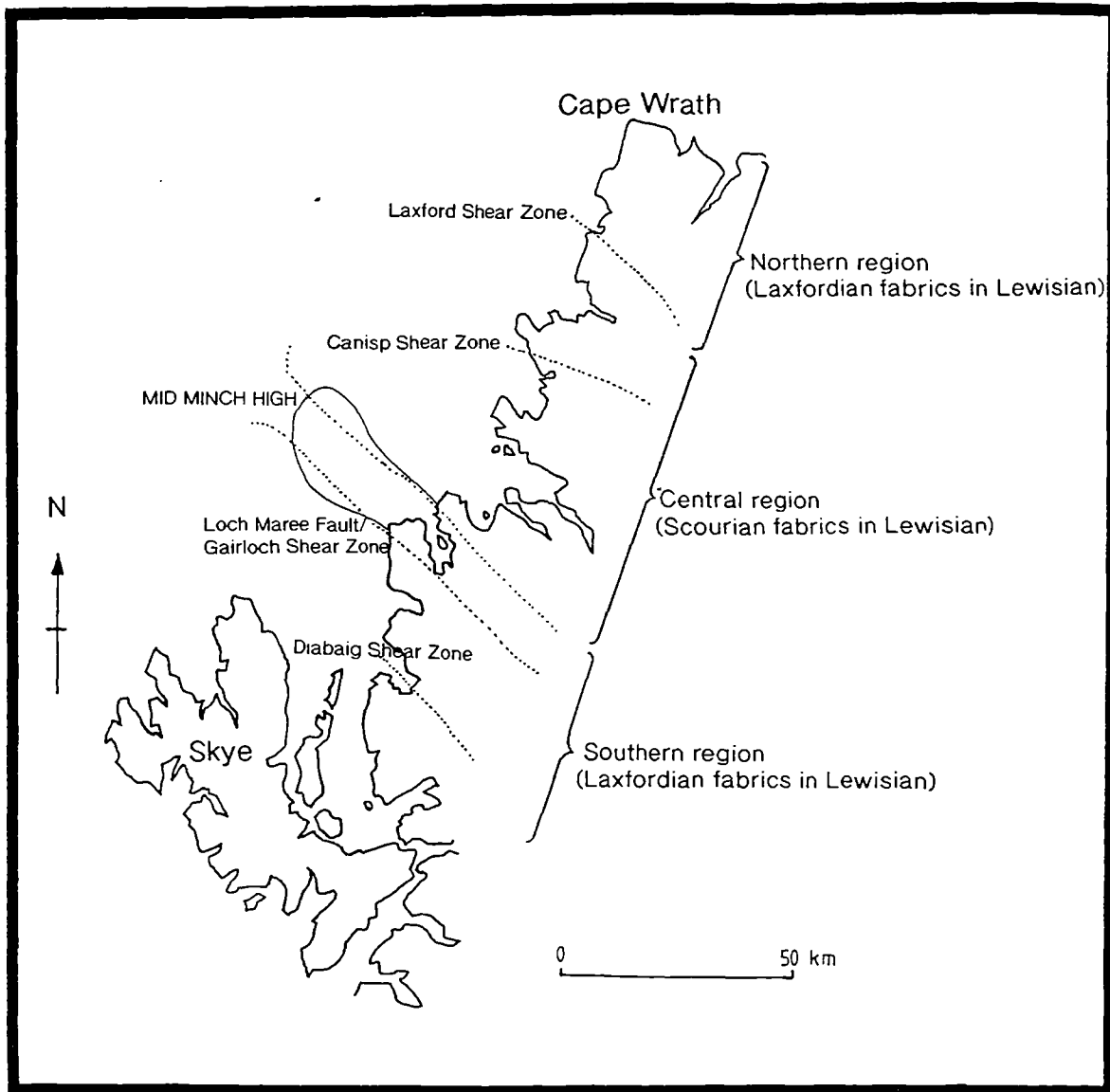


Figure 2.15. Map showing the lateral continuation of Precambrian mainland shear zones to the Mid-Minch High.

2.8.3 Subsidiary structures

Stein (1988) suggests that the relationship between the Minch Fault and the OHFZ is not a straightforward example of geological inheritance. If this was the case, he argues that the Minch Fault would reactivate the OHFZ along its entire length. In the North Lewis Basin however, the OHFZ appears to be sinistrally offset by a NW-SE trending structure called the Ness Shear Zone (Stein 1988) (Fig.2.8).

Here, the OHFZ is en-echelon to, and west of the relatively linear Minch Fault, and it is the OHFZ which appears to control the basin margin. In this locality the sinistral Ness Shear Zone, which has an onshore expression is thought to be responsible for the location of the North Lewis Basin (Stein 1988).

Another fault which roots into the Outer Hebrides fault at depth is present on the seismic data presented by Stein (1988). He believes that this structure, which is essentially a splay of the Minch Fault, is a consequence of a NW-SE sinistral offset of the OHFZ in N.Uist. Stein's evidence for the existence of this lineament, the N. Uist Shear Zone, comes from thematically mapped landsat images, although no evidence of this shear zone has been found by the present author, and there appears to be no significant displacement of the OHFZ onshore.

The last major offshore basin-controlling structural element is the Pabbay Shear Zone (Fig. 2.8), another NW-SE trending Precambrian structure which appears to truncate the OHFZ (Stein 1988). This structure is apparent from seismic data and effectively marks the southern termination of the hanging-wall basins. South of this shear zone, sedimentary basins have a very different geometry, apparently uncontrolled by the OHFZ.

2.9 Fieldwork methods

The OHFZ has been mapped and studied at several localities along its length, selected on the basis of good exposure and previous mapping coverage. In addition to interpretations made by mapping a large number of areas, previous work has also been re-interpreted. Most notable amongst these are the PhD works of Coward (1969), Sibson (1977b), and Walker (1990).

A total of 11 months were spent in the field between 1991 and 1994. Mapping was carried out on a scale of 1:10 000 in Scalpay, Seaforth Head, Raerinish Point, the Park District of Lewis, South Harris, Lochportain, Grimsay, N.Uist road sections, Burrival, Eaval, Eigneag Bheag, Ben na Hoe, the S. Uist 'Rubhas', Triuirebheinn, Stuley, Eriskay, Greian Head, Central Barra, SW Barra and Vatersay. Mapping on a scale of 1:25 000 was carried out in Tolsta, Arnish, Garrabost, Central Lewis road sections, Eishken, and Ronay.

The purpose of studying so many locations was not to construct definitive geological maps of the area, (most of these localities have been studied previously and, with the exception of the relatively inaccessible Park District of Lewis, very good maps are already available - see Sibson 1977b, Fettes et al. 1993). The aim was to gain structural data and kinematic information from as many parts of the fault zone as possible.

Transport was mainly by car and on foot. However, the islands of Stuley and Ronay, and the Park District were all accessed by boat from Lochboisdale, Grimsay and Tarbert.

2.10 The sub-division of the thesis

In the course of the following two chapters, a common kinematic history will be referred to, which differs markedly from those previously suggested. In the important work on the OHFZ by Sibson (1977b), reference is made to thrust inception (D_0), a main phase of thrusting (D_1), a recovery phase of lag-sliding (D_2), and finally, a phase of late, near surface faulting at competence boundaries (D_3). Most workers since Sibson have retained this sequence, regarding it as correct, but have placed different degrees of importance on different phases (e.g. White and Glasser (1987) regard the extensional D_2 phase as being more important than the compressional D_1 phase). In this work however, 'D' numbers have been discarded, as they give the impression that each deformation phase is mutually exclusive, which, from the present study, is thought to be unlikely. In addition, a previously unrecognised phase of sinistral strike-slip is incorporated into the kinematic history, so that the entire sequence can be re-written as:

- 1) Ductile thrusting
- 2) Brittle thrusting
- 3) Sinistral strike-slip
- 4) Extensional gravity-collapse
- 5) Late, steep, extensional faulting

In addition to the proposed kinematic history, Sibson (1977b) also recognised two major structural trends:

- A major change across strike, from brittle faulting in the west, to ductile shearing in the east of the fault zone.
- A progressive decrease from south to north along strike, in the proportion of brittle to ductile deformation.

The present study has shown that the fault rock sequences undergo a major abrupt change along strike, and this change occurs in the region of South Harris. This contrasts with the progressive along-strike change proposed by Sibson (1977b), and suggests that at least two fault zone segments are presently exposed

onshore. These segments appear to be linked by the NW-SE trending shear zones in South Harris (Fig. 2.3) which may therefore have been active as transfer zones early in the history of the OHFZ (see chapter 5 for a full discussion).

It is apparent that neither a strictly chronological report, nor a strictly geographical report on the evolution of the OHFZ would be wholly satisfactory. Both approaches would involve a great deal of unnecessary repetition. The bulk of the present work on the OHFZ may be sub-divided *geographically* into two separate parts, based on the differences in the observed fault rock sequences from each fault zone segment. In each segment, where a common fault rock sequence appears to be present, the evolution of the fault zone segment may be treated *chronologically*. The discussion of the kinematic history of the OHFZ, based on this two-fold subdivision, is therefore separated into the following two chapters.

Chapter Three

The Kinematic history of the northern segment of the OHFZ

3.1 Introduction

The northern segment of the OHFZ occurs as a diffuse band (c. 18km wide at maximum) of fault-related deformation in the eastern half of Lewis and Harris, extending from Port Geiraha, in Lewis, to Rubha Vallerip in South Harris and passing through key field localities (Fig. 3.1). The various fault rock types present include mylonites and phyllonites, cataclasites, fault breccias and pseudotachylites. These are developed to varying degrees. The diverse nature of the fault rocks reflects a polyphase movement history along the OHFZ. This chapter is sub-divided into four major sections, with each section devoted to a kinematically distinct set of structures:

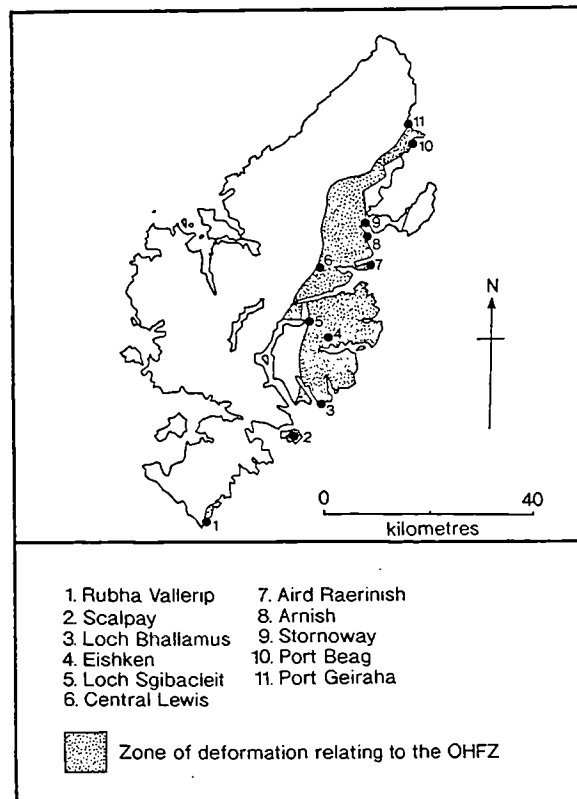


Figure 3.1. Map of the northern Outer Hebrides, showing the broad zone of deformation related to the OHFZ, and major field localities. (Modified from Fettes et al. 1981)

1. a) *Ductile thrust movement*, associated with high greenschist facies, early ductile mylonite formation and b) *brittle thrust movement*, resulting in later brittle faulting, cataclasis and pseudotachylite generation;
2. *Sinistral strike-slip movement*, associated with retrogression of the high grade gneisses, early mylonites and brittle fault rocks to form moderately or shallowly dipping, low greenschist facies phyllonites;
3. *Low-angle extensional faulting*, forming moderately or shallowly-dipping faults and folds, which are often focused into pre-existing phyllonite belts, extending the crust by utilizing pre-existing fault zone fabrics;
4. *High-angle extensional faulting*, which forms brittle structures, including those which bound the conglomeratic sediments of the Stornoway Formation. They appear to be associated with the formation of the large Mesozoic basins in the hangingwall of the OHFZ.

In each section, the localities described are prefaced by a brief description of the local Lewisian geology. The timing of each event is not discussed here unless direct field evidence is available. This is dealt with in greater detail in chapter 5

3.2 Thrust movement

The earliest deformation within the OHFZ relates to a major phase of ductile thrusting, which results in a wide band of upper greenschist facies mylonites. This band of variably mylonitic deformation is traceable through much of eastern Lewis, and is inferred to pass through the isthmus currently overlain by the main outcrop of the Stornoway Formation (Fig. 3.2). Thrust-related brittle rocks are also present, but are not always spatially coincident with the mylonites (Fig. 3.3). In general, mylonites are best developed in the southern part of the northern segment (e.g. Scalpay), whilst cataclasites are best developed in the northern part (e.g. Port Beag). Both types of deformation are present in the central region (e.g. Loch Sgibacleit), where important inferences can be made regarding their relative timing. Thrust-related rocks have been studied at several localities, including Scalpay, Loch Sgibacleit and parts of central and eastern Lewis, and are treated in turn, from south to north, below:

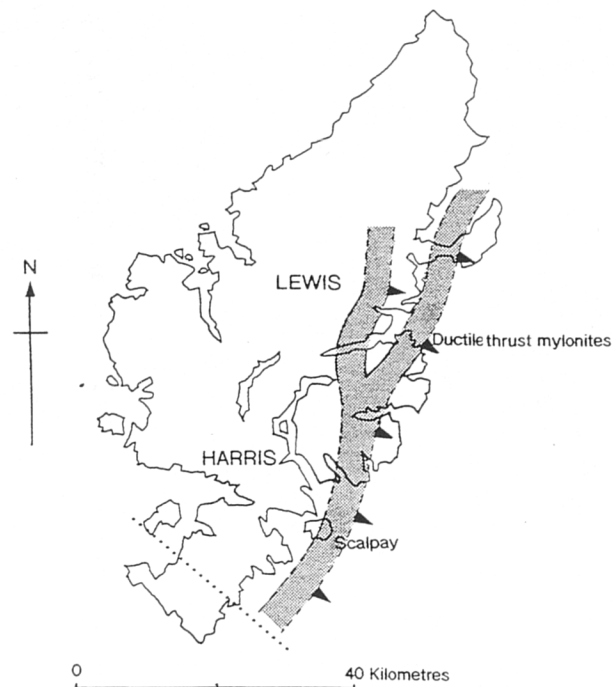


Figure 3.2. Map of the northern Outer Hebrides showing the extent of ductile mylonitic deformation relating to early thrust-sense movement on the OHFZ. Constrained by reconnaissance mapping during the present work.

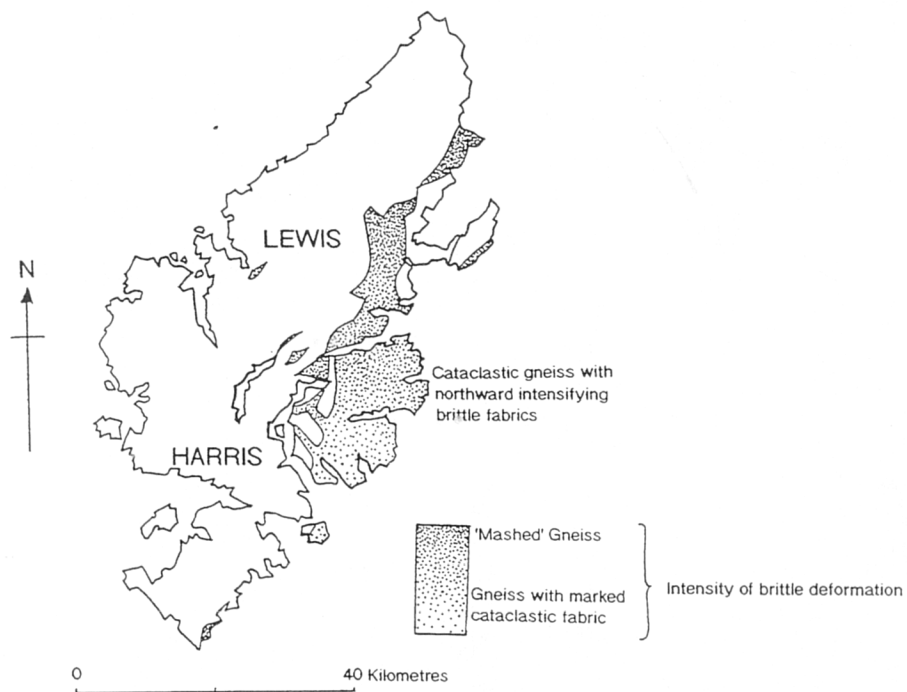


Figure 3.3. Map of the northern Outer Hebrides showing the extent of brittle cataclastic deformation relating to later thrust-sense movement on the OHFZ. Intensity of stipple corresponds to intensity of brittle deformation.

3.2.1 Scalpay

Geographical setting

The island of Scalpay is situated off the SE coast of N Harris at the mouth of East Loch Tarbert, and has an area of 10km² (Fig. 3.4). The terrain is typically undulating with extremely good exposures on the coast and inland, although the latter are often highly weathered.

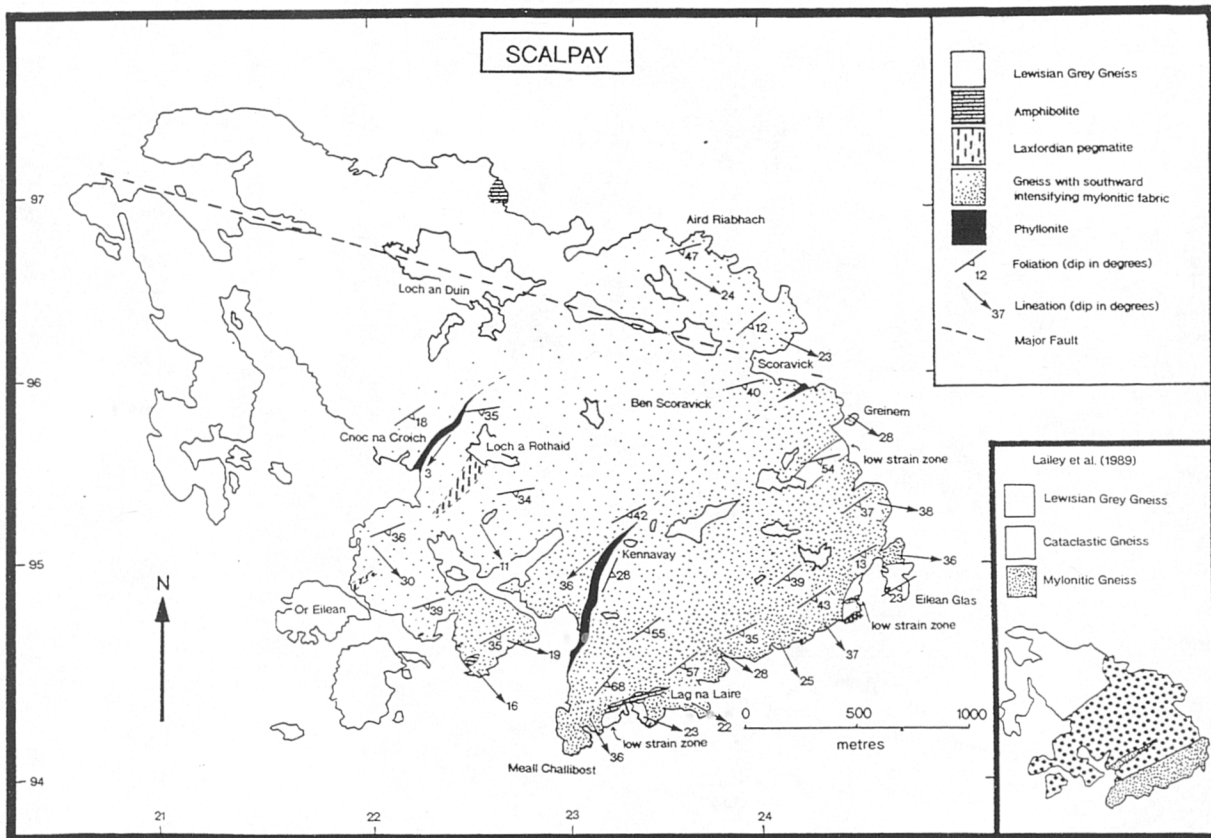


Figure 3.4. Geological map of Scalpay (with inset map after Lailey et al. 1989).

Local Lewisian geology

The geology of Scalpay is dominated by medium-grained, heterogeneously deformed amphibolite facies gneisses of the Lewisian complex. (A full description of constituent rock types in the Lewisian Gneisses is provided in section 2.2.2). Scourie dykes (Younger Basics) and large areas of extensive Laxfordian pegmatite veining are present in the 'Grey Gneiss' host rock. Laxfordian pegmatites are particularly well developed between Or Eilean (NG 219950) and Loch a' Rothaid (NG 226956). The gneiss also appears to be migmatised in places, with locally coarse grained quartzofeldspathic veins often cross-cutting gneissose banding. In contrast to sharply defined pegmatite contacts, migmatite contacts with unmigmatised, host acid gneisses are diffuse and gradational.

Minor folds of gneissose banding are common throughout Scalpay, and mainly post-date 'Younger Basic' dykes. These ESE-plunging, upright minor folds are therefore probably Laxfordian (F_{L3}) in age (see section 2.2.3 and table 2.2). Earlier (presumably F_{L2}) folds are present, and are characterised by gently inclined axial planes dipping to the SE (Fig. 3.5). No evidence of a syn-fold cleavage occurs in either generation. Laxfordian folds are most common in the Grey Gneisses of NW Scalpay where original (?Scourian) banding is also preserved. These structures, are largely obliterated in areas where subsequent thrust-related deformation has occurred.

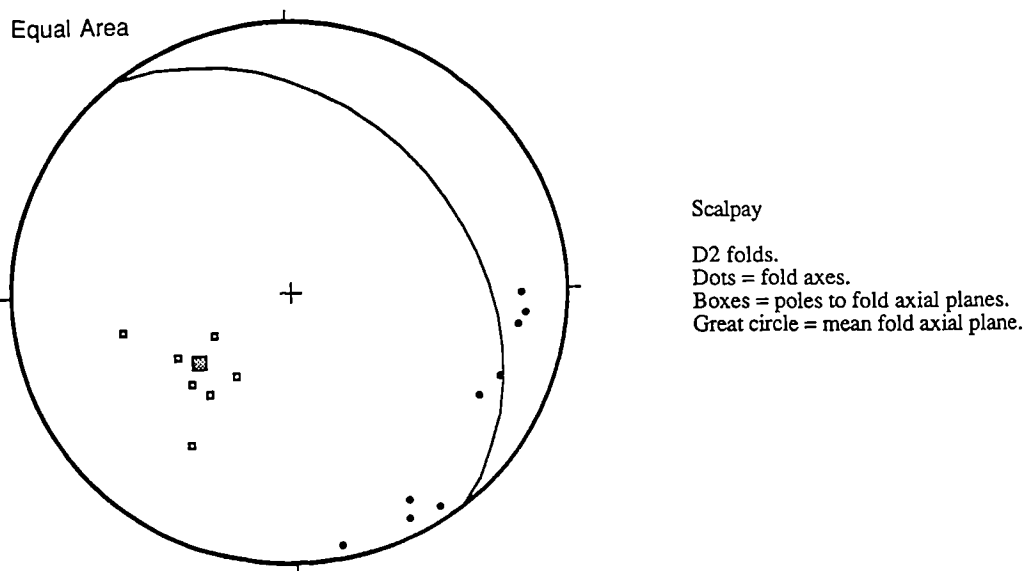


Figure 3.5. Equal area stereonet of Laxfordian f_{L3} fold axes and poles to Laxfordian f_{L3} fold axial planes from Scalpay.

Pervasive mylonite formation

Macrostructure

An extensive (c. 1km wide) belt of ductile mylonites crops out on the SE side of Scalpay (Plate 3.1a), constituting c. 600m of exposed vertical thickness. Although the geological maps presented by the I.G.S. (Fettes et al., 1981, 1992), and Lailey et al. (1989) suggest that the mylonites occur as discrete bands, the mylonitic overprint is widespread, gradually becoming stronger towards the SE of the island. Low-strain augen occur within the mylonites, usually in strain shadows adjacent to large basic and ultrabasic pods. In these low-strain augen, relict Lewisian features, including early Laxfordian isoclinal folds and discordant 'younger basic' dykes, may still be preserved. Three major low-strain 'windows' of this type have been observed, at Lag na Laire (NG 232942), Eilean Glas (NG 245946), and south of Greinem (NG 245955).

The pervasive mylonites are pale grey or cream coloured and often colour banded, a feature probably inherited from the compositional layering in the gneissic protolith. Quartz (c. 30%) and plagioclase (mainly labradorite/bytownite) (c. 25%) are the dominant minerals, with minor amounts of K-feldspar (5-10%), amphibole (c. 10%), biotite (c. 5%), chlorite (c. 5%), epidote (c. 5%) and muscovite (c. 5-10%). The mylonites are most readily distinguished by the presence of elongate quartz ribbons streaked out along foliation surfaces.

The dominant tectonic fabric present in the mylonites is that of a gently to moderately SE-dipping foliation defined by grain alignments, re-oriented compositional banding, quartz ribboning and elongate mineral aggregates. This foliation consistently dips at c. 35°, and lies at high angles to the strike of the gneissose banding in the NW of the island (Fig. 3.6). The gradual reorientation of gneissose banding from a NW-SE trend to a NE-SW trend occurs NW of Cnoc na Croich (NG 219952), where the regional strike reorientates by c. 90°. In SE Scalpay, in areas where banding can still be discerned, the mylonitic foliation is sub-parallel to banding, suggesting that banding has been significantly re-orientated on a regional scale by mylonitisation.

A linear fabric, defined by quartz rods and elongate quartz-feldspar aggregates, is also well developed in the mylonites. It plunges at c. 35°, just east of the true dip of the mylonitic foliation (Plate 3.1b and Fig. 3.6), indicative of dip-slip movement during mylonitic deformation. An intersection lineation also occurs locally, due to the intersection of the mylonitic foliation with pre-existing banding, and shows a highly variable orientation in regions where banding has been folded (e.g. the low strain augen at Lag na Laire, NG 233942).

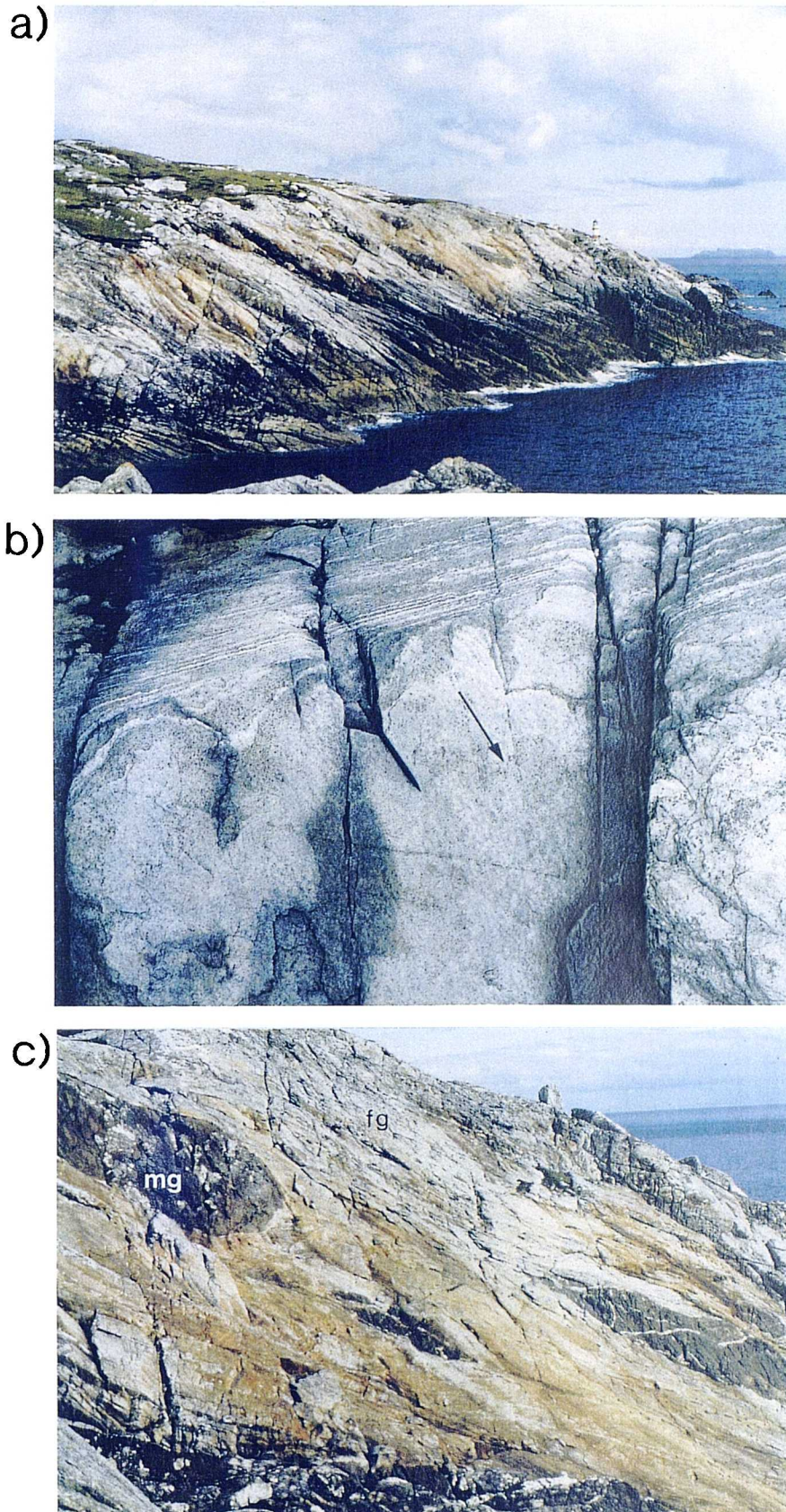


Plate 3.1 Ductile mylonites

a) View NE from east of Lag na Laire towards Eilean Glas (NG 238943). Ductile, felsic mylonites wrap lenticular mafic pods and dip shallowly SE. Cliff section is c. 30m high.

b) Mineral elongation lineation (marked by arrow) developed in the ductile mylonites of SE Scalpay (NG 247951). the mineral lineation is defined by elongate quart-feldspar aggregates.

c) Elongate boudins of mafic gneiss (mg) developed in felsic gneiss (fg). The boudin on the left of the photo is c. 2m thick.

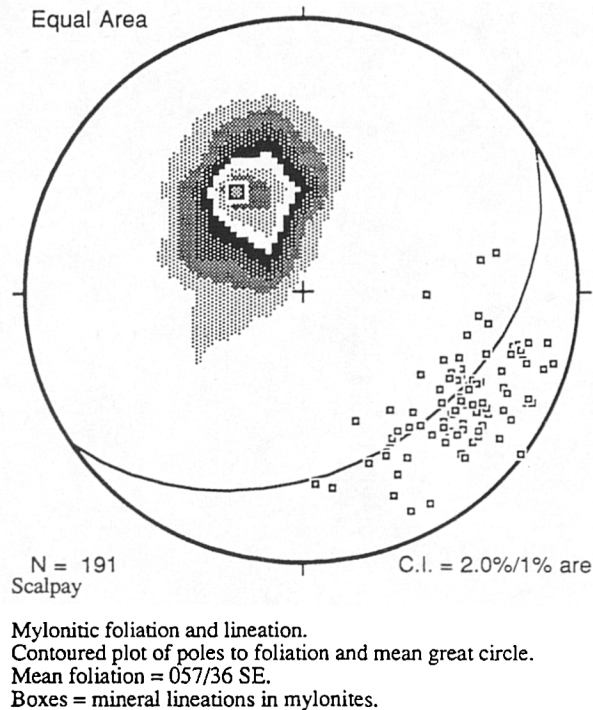


Figure 3.6. Equal area stereonet of contoured poles to early pervasive mylonite foliation and mineral stretching lineation from Scalpay.

The mylonites are predominantly of acidic composition, reflecting the high modal percentage of quartz and feldspar in the gneissic protolith. However, layers and boudins of internally unsheared amphibolitic gneiss are also present, with recrystallised quartz occupying the low strain zones between boudins. Some of the larger deformed mafic pods have an internal foliation whose orientation differs markedly from that of the surrounding mylonite. This internal foliation is thought to be a relict Lewisian fabric which suggests that the acid components of the gneisses were more readily reworked during mylonitisation. The boudins lie with their long axes parallel to the SE-plunging mineral lineation and their short axes consistently normal to the foliation (Plate 3.1c), and may be indicative of foliation-normal shortening, as envisaged for thrust-parallel, extensional strain models (Sanderson 1982, Holdsworth and Grant 1990).

Shear criteria are numerous and particularly common in mylonitised pegmatites. These criteria include asymmetric extensional shear bands, asymmetric feldspar porphyroclasts, minor fold vergence and asymmetric and rotated amphibolite pods, (Plates 3.2a and 3.2b). The mylonitic foliation often occurs axial planar to folds of gneissose banding, and the asymmetry of such folds may also give a sense-of-shear indication. All criteria give an overall top-to-the-NW, thrust sense-of-shear.



Plate 3.2. Kinematic indicators in ductile mylonites

a) Delta-wrapping of amphibolite pod within 'Grey Gneiss' of SW Scalpay (NG 231943). Top-to-the NW sense-of-shear is displayed by anticlockwise rotation of the clast and the growth of quartz pressure tails.

b) Laxfordian pegmatite with thrust deformation fabrics from Lag na Laire, (NG 231942). Top-to-the-NW sense-of-shear is displayed by the orientation of secondary 'c'-planes (c) relative to the shear foliation (s).

Microstructure

Mylonites have been sampled throughout Scalpay, and are observed to become progressively more evolved from the Lewisian gneiss protolith towards the SE coast (Plate 3.3a, b, c). These changes include:

1. A reduction in grain size from c. 1mm to < 100 μm ;
2. The generation of ductile quartz ribbons and 'core and mantle' structures;
3. The dynamic recrystallisation of quartz by rotational recrystallisation;
4. The brittle deformation of feldspars and amphiboles;
5. The replacement of feldspar by sericite and epidote;
6. The replacement of hornblende by actinolite, biotite and chlorite;
7. The generation of a planar and linear fabric by grain alignments and preferred orientation during phyllosilicate growth.

Each mineral phase responds differently to the deformation, providing an indication of the overall temperature, pressure and fluid conditions during mylonitisation. It should be noted that for reasons discussed in section 3.2.5, retrogression^{to low greenschist facies} is regarded as post-deformational and is therefore treated elsewhere (see section 3.3.1)

In quartz, the mylonitic fabric is defined by ribbons which are nearly always polycrystalline. Quartz ribbons generally occur as one of two types: *Type-1*, polycrystalline ribbons (using the terminology of Boullier and Bouchez, 1978), have relatively large monocrystalline cores (usually 2-5mm long), which show significant undulose extinction and deformation lamellae. These are surrounded by mantles of undeformed recrystallised quartz of much finer grain size (c. 200 μm), (Plate 3.4a and b). In this type of ribbon, subgrain misorientations in the relict core region become progressively greater towards the mantle region (Plate 3.4b and c), and the process of rotational recrystallisation is believed to have operated. The more common *Type-2*, polycrystalline ribbons, comprise totally recrystallised and undeformed quartz with no evidence of the original deformed grain (Plate 3.5a). The grain size is c. 100 - 300 μm and generally uniform, with polygonal geometries. Grain boundaries are often oriented at c. 120° to each other in the manner of *type-2(a)* ribbons of Boullier and Bouchez (1978), suggesting a relatively high degree of interfacial stability. When viewed through a sensitive tint plate, the quartz ribbons often show a colour uniformity characteristic of strongly aligned quartz c-axes.

Occasionally, quartz appears to show textures indicative of grain boundary migration recrystallisation, involving bulge nucleation (Plate 3.5b). These

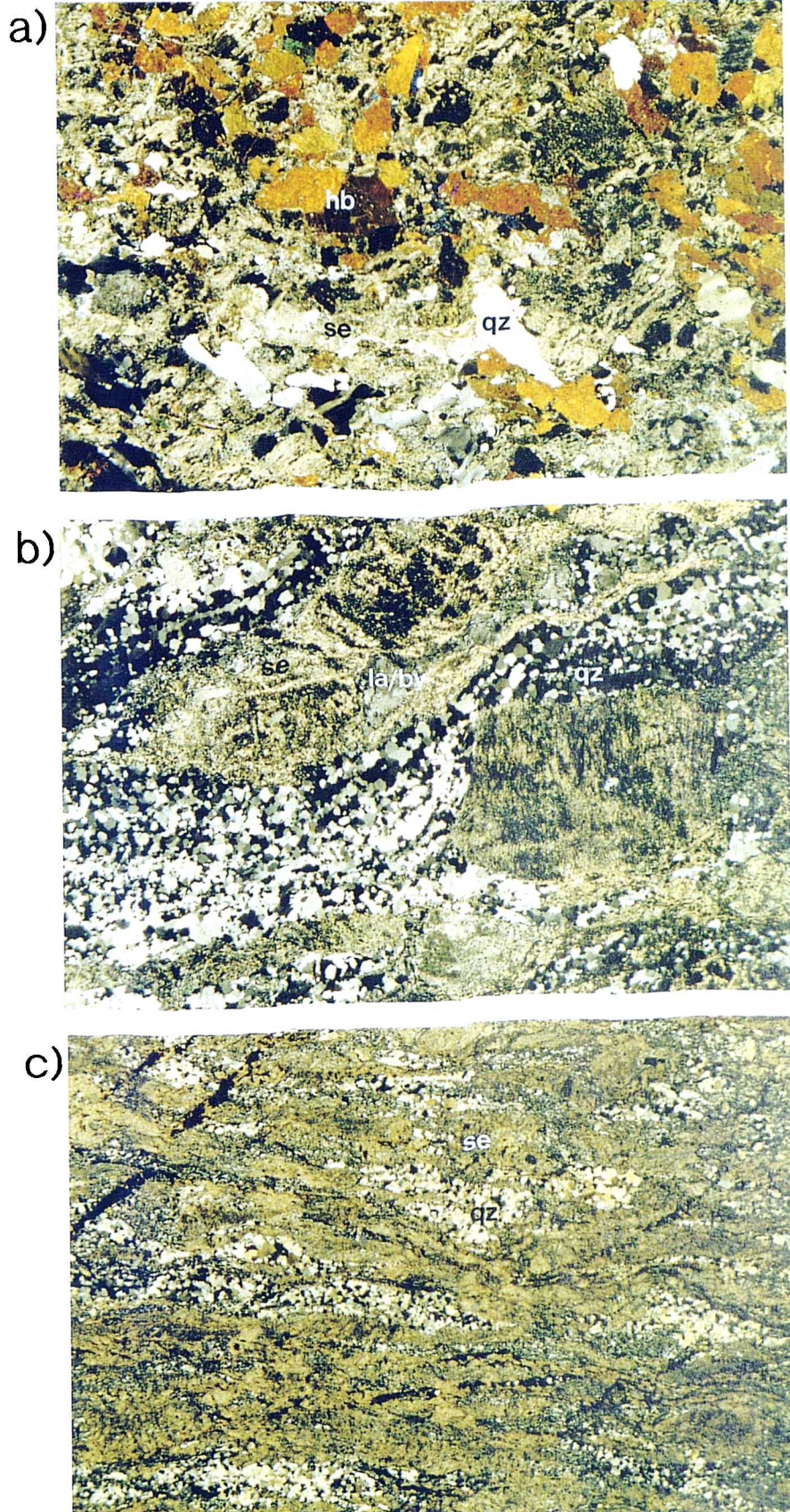


Plate 3.3 Textural evolution from 'Grey Gneiss' protolith to ductile mylonite

a) Lewisian 'Grey Gneiss' from the low-strain 'window' at Lag na Laire, (NG 232942). Quartz (qz), hornblende (hb) and sericitised feldspar (se) are the main constituents. Field of view is 3.3 cm. Photographed in crossed polarised light (XPL).

b) Moderately mylonitised acid gneiss from S of Loch a' Rothaid (NG 225951). Quartz (qz), and sericitised feldspar (se) are the main constituents, with minor relict labradorite/bytownite (la/by). Field of view is 2 cm. (XPL)

c) Highly mylonitised acid gneiss from Kennavay (NG 233951), close to the upper contact with the Kennavay Phyllonite belt. Quartz (qz) and sericite (se) are the main constituents. Field of view is 20 mm (XPL)

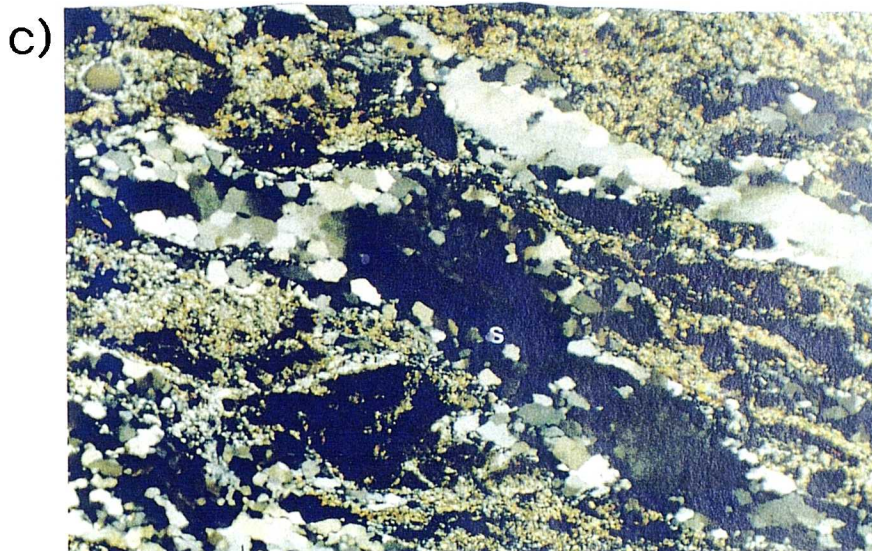
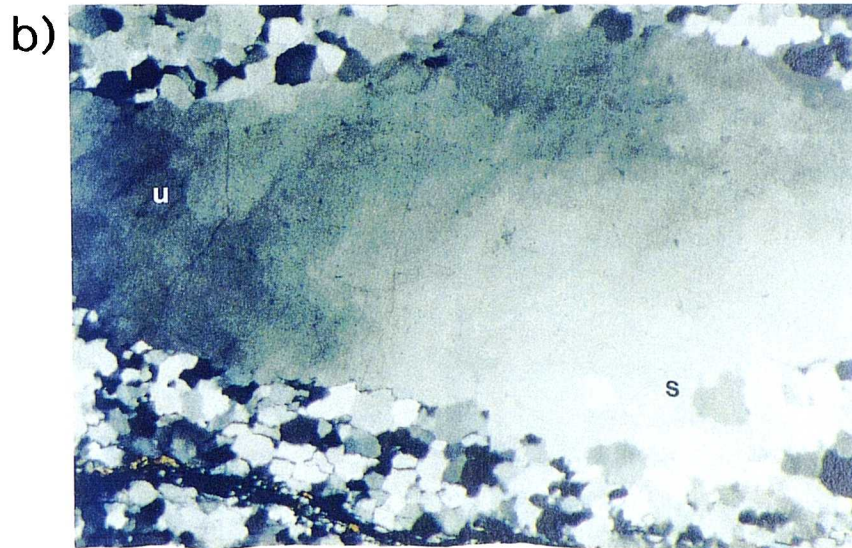
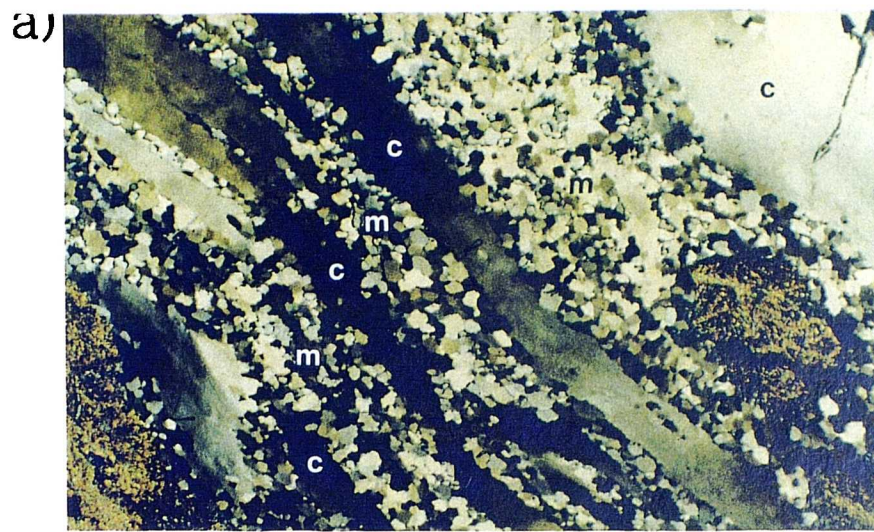


Plate 3.4 Deformational behaviour of quartz in ductile mylonite

a) Mylonitised Laxfordian pegmatite from Kennavay (NG 233951) displaying 'core and mantle' structure. Elongate, monocrystalline quartz cores with undulose extinction (c) are surrounded by mantles of finer grained, unstrained, recrystallised quartz (m). Field of view is 6mm. (XPL)

b) Mylonitised Laxfordian pegmatite from Kennavay (NG 233951) displaying 'core and mantle' structure. Monocrystalline quartz core displays undulose extinction (u) and incipient subgraining (s). Field of view is 3mm. (XPL)

c) 'Core and mantle' structure from mylonite at Lag na Laire (NG 232942), displaying subgraining by rotational recrystallisation. Subgrains (s) become progressively misoriented with respect to the relict grain from the core to the mantle. Field of view is 3mm.

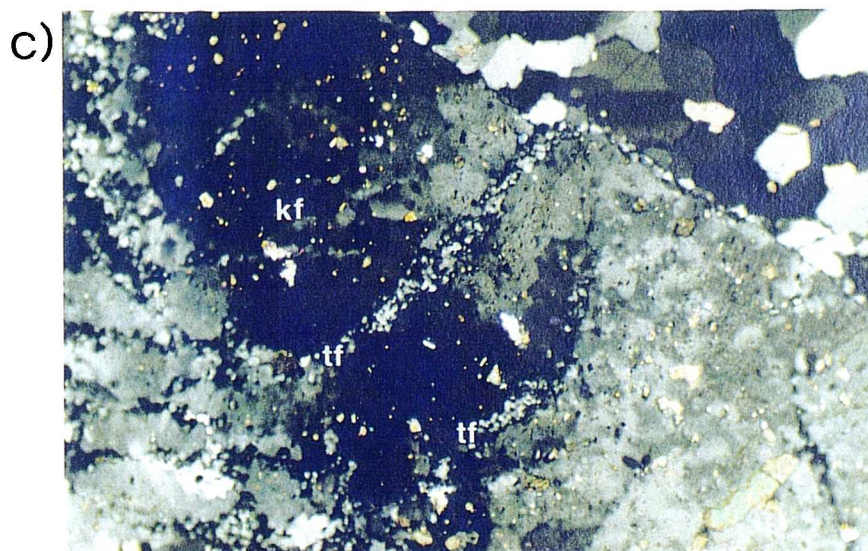
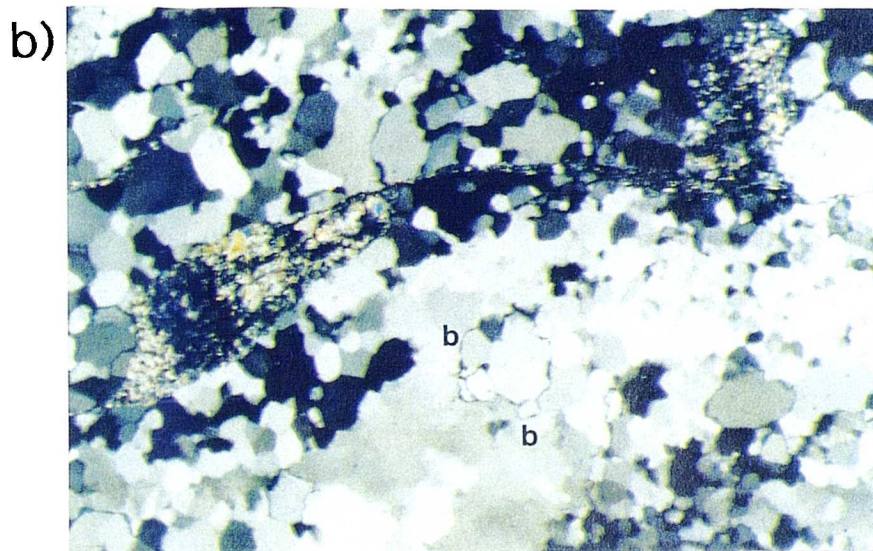
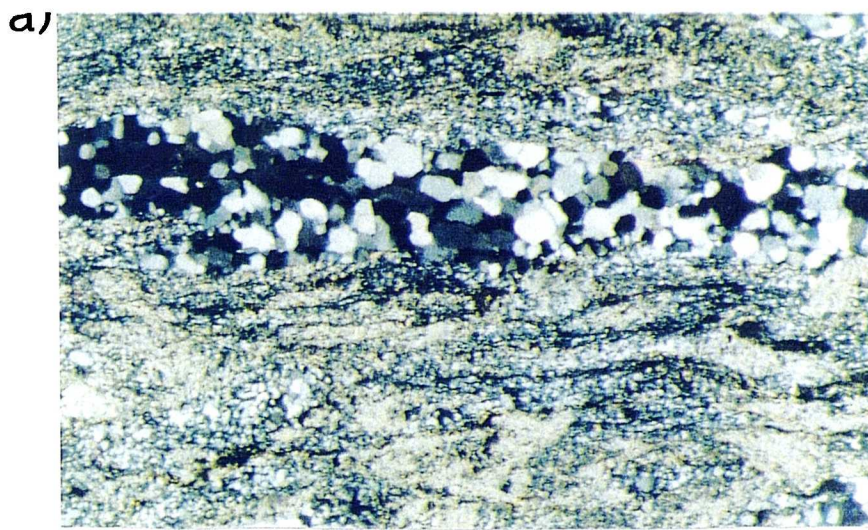


Plate 3.5 Deformational behaviour of quartz and feldspar in ductile mylonite

a) 'Type 2' polycrystalline quartz ribbon, with unstrained and recrystallised quartz grains, from the highly mylonitised acid gneiss of Kennavay (NG 233951), close to the upper contact with the Kennavay Phyllonite belt. Field of view is 6mm. (XPL)

b) Moderately mylonitised acid gneiss from from S of Loch a' Rothaid (NG 225951). Fully recrystallised quartz grains with textures indicative of grain boundary migration involving the nucleation of bulges (b). are shown. Field of view is 4mm. (XPL)

c) Moderately mylonitised acid gneiss from from S of Loch a' Rothaid (NG 225951). K-feldspar (kf) displays brittle transgranular fractures(tf) hosting recrystallised fine grained k-feldspar. Field of view is 4mm. (XPL)

microstructures, indicative of deformation at higher grades (amphibolite facies or above), (Hirth and Tullis 1992), are relatively rare and most evidence suggests recrystallisation of quartz occurred by rotation of sub-grains.

Plagioclase (labradorite/bytownite) and K-feldspar by contrast, deform in a brittle manner, with no evidence for ductile behaviour. Many feldspars have been pseudomorphed by sericite during later retrogression, but original grain shapes are fractured, with recrystallised quartz occupying the fractures. Where late-stage retrogression of K-feldspar to sericite is minor, brittle transgranular fractures occasionally host fine grained K-feldspar aggregates (Plate 3.5c). These are not annealed cataclastic fragments of the original grain, as they appear to be internally undeformed, and may be fully recrystallised subgrains in healed microcracks.

The mafic content of the mylonites is nearly all unretrogressed hornblende, with minor amounts of biotite and chlorite. The amphiboles appear to have remained metastable during deformation. Minor alteration to chlorite probably relates to later retrogression (see discussion in section 3.2.5.). Pristine actinolite has grown in tensional microcracks (Plate 3.6a) and some hornblendes have been plastically deformed (Plate 3.6b).

Kinematic indicators are numerous in thin section, and include shear bands and fractured displaced feldspars, whose shear sense is consistent with top-to-the-NW thrust displacements.

Metamorphic conditions during deformation

The presence of biotite and relatively unaltered, coarse hornblende within these mylonites (eg. at NG 232945), suggests that little retrogression from the amphibolite facies banded gneisses accompanied early mylonitisation. However, the deformational behaviour of the main felsic minerals indicates lower grades of metamorphism. Core and mantle quartz ribbons (Type-1 polycrystalline ribbons) are characteristic of low-mid greenschist facies (Simpson 1985), but the dominance of polygonal type-2 polycrystalline ribbons suggests that the degree of recovery was high, and that metamorphic grades of mid-high greenschist facies (Boullier and Bouchez 1978, Hirth and Tullis 1992) prevailed during deformation. Quartz recrystallisation largely occurred by rotation of the crystal lattice, a process which occurs at lower metamorphic grades (c. greenschist facies), rather than by grain boundary migration recrystallisation, which occurs at higher grades (Simpson, 1985, Hirth and Tullis 1992). Feldspar deforms in a brittle manner, often possessing rotationally recrystallised healed microcracks. In general, feldspar does not recrystallise at grades lower than upper greenschist facies.

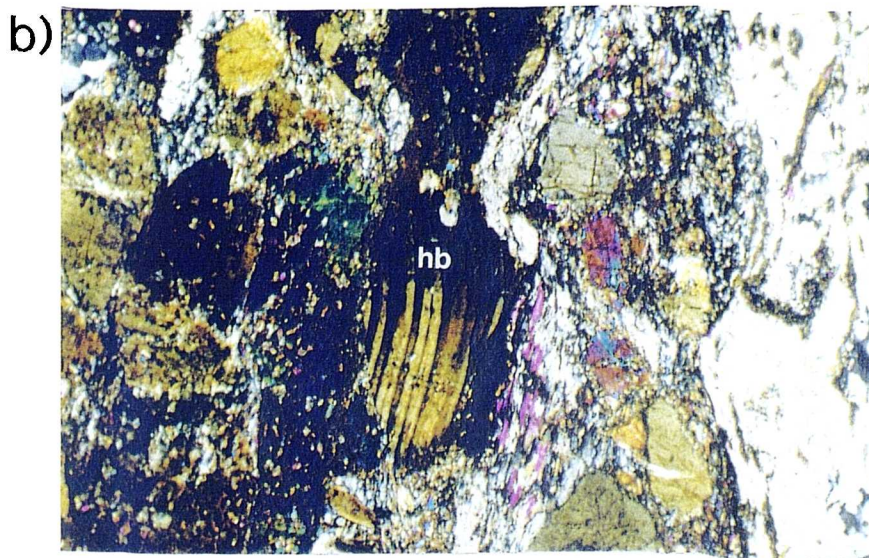
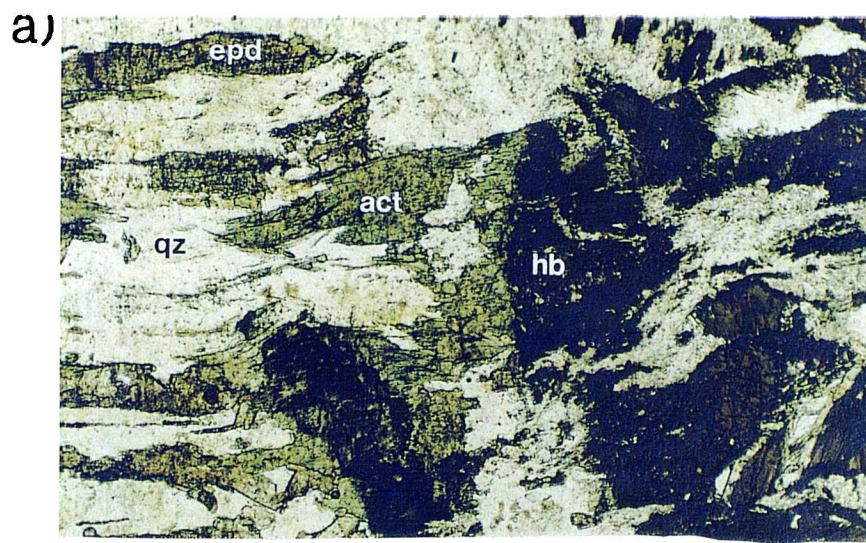


Plate 3.6

a) Amphibolitic mylonite (Younger Basic dyke) at Lag na Laire (NG 232942). A tensional microcrack (pale region on the left of the photo) hosts quartz (qz) and epidote (epd) and has allowed pristine actinolite (act) to grow from relict hornblende (hb) grains. Field of view is 3mm. Photographed in plane polarised light (PPL).

b) Amphibolitic mylonite at Lag na Laire (NG 232942), showing plastically deformed hornblende (hb). Field of view is 3mm. (XPL)

c) Contact between amphibolitic (Younger Basic dyke) and quartzo-feldspathic mylonite at Lag an Laire (NG 232942). A quartz-filled tensional microcrack occurs in the amphibolitic material but not in the quartzo-feldspathic material. Field of view is 6mm. (XPL)

(Obee and White 1985) but starts to deform ductilely at lower amphibolite facies (Fitz Gerald and Stunitz 1993). The generally ductile behaviour of quartz, with extensive rotational recrystallisation, and brittle behaviour of feldspar with only minor recrystallisation, sets a maximum deformation temperature of c. 450°C or upper greenschist facies (Burg et al. 1984, Obee and White, 1985, Simpson, 1985).

The presence of bent hornblendes and the growth of new actinolite is consistent with high greenschist facies metamorphic conditions (Simpson, 1986). If high greenschist facies prevailed during deformation, the relatively pristine hornblendes in these mylonites may reflect a lack of available water. Retrogression of the relict Lewisian amphiboles to biotite or chlorite is therefore effectively prevented (Beach 1976). The high modal percentage of chlorite in these rocks may result from later fluid influx (see section 3.2.5). High greenschist facies is regarded as the metamorphic peak during this phase of deformation.

Clearly, certain mineral phases exert stronger controls on the rheology of the rock as a whole than others. Despite the chiefly brittle behaviour of plagioclase and K-feldspar, the quartzo-feldspathic units accommodate deformation in a chiefly ductile manner, in contrast to the brittle deformational behaviour of amphibolitic material. This relationship is exemplified by the behaviour of quartz-filled, tensional microcracks which occur in amphibolites, but do not continue into the quartzo-feldspathic material (Plate 3.6c). This suggests that *crystal plastic* rather than *brittle fracture* processes accommodated the deformation in the quartzo-feldspathic material, and that ductile minerals, e.g. quartz, are the dominant phases in controlling rheological behaviour of quartzo-feldspathic material. The differing deformational behaviour of different rock units, or different phases within the same rock unit, highlights two important points:

- 1) The difficulty in classifying fault rocks, when two or more deformation mechanisms have occurred synchronously. If a genetic fault-rock classification scheme is applied to these rocks, a subjective estimate of the dominant process is required. The complex nature of naturally occurring fault rocks therefore validates classification schemes based on observation only (e.g. Sibson 1977a).
- 2) The confusion, in previous work on Scalpay, between 'cataclastic' gneiss and 'mylonitic' gneiss, when in fact, they are both mylonites *sensu stricto*, (being cohesive and possessing a foliation), (Sibson 1977a). They are regarded in the present work as the same unit. The subdivision of the mylonite, by previous workers, into "gneiss with a marked cataclastic fabric" and "gneiss with mylonitic fabric" (Lailey et al 1989), or

"microbreccia" and "c-type mylonite" (Walker 1990), has been brought about by the decrease in the amount of brittle relative to ductile deformation at the grain scale, superficially suggesting an apparent increase in palaeotemperature, (noted by Sibson 1977b) from NW to SE.

The apparent increase in paleotemperature from NW to SE probably reflects a slight rheological weakening, brought about by the collapse of the load-bearing framework by mechanical grain comminution of framework-supporting minerals (e.g. the 'rounding' of feldspar grains), (Handy 1990). Where strain is highest in the mylonites, feldspar porphyroclasts undergo the greatest amount^{of} brittle comminution and therefore clast size reduction. When the size of these clasts has been sufficiently reduced, a breakdown of the framework occurs and quartz becomes more important in controlling the bulk rheology. The regions where ductile deformation is dominant therefore reflects an increase in strain. The increase in palaeotemperature toward the SE coast of Scalpay, inferred by Sibson (1977b), may therefore be an apparent one.

Cataclasis and fracturing

Evidence for brittle deformation is widespread throughout Scalpay but previous workers have not made the distinction between brittle deformation of individual phases during large-scale, ductile mylonitisation, and brittle deformation of all phases which entirely post-dates the mylonitisation. On both the I.G.S. survey map (Fettes et al. 1981, 1992), and that presented by Lailey et al. (1989), a NE-SW trending boundary is drawn from the eastern side of Loch an Duin (NG 229964) to Cnoc na Croich (NG 219952). This supposedly separates 'undifferentiated gneiss' to the NW from 'cataclastic gneiss' to the SE (Fig. 3.4 inset). Sibson (1977b) also refers to a 'cataclastic foliation' present in the mylonites, and Walker (1990) suggests 'microbreccia' occurs in the vicinity of this boundary

Although this boundary is an important one, being the site of later phyllonite generation (see section 3.3.1), present mapping has revealed that no breccia (*sensu stricto*) exists, and that the 'cataclastic' rocks referred to by Lailey et al. (1989), are, in nearly all aspects, identical to those referred to here as mylonites. Using the classification scheme of Sibson (1977a), the presence of a foliation in the 'cataclastic' rocks suggests they are better termed mylonites. Grain comminution by fracturing and cataclasis results in the frequent presence of rounded porphyroclasts of competent phases (e.g. feldspar), (Plate 3.7a). The strong foliation however, results from elongate feldspar aggregates and quartz ribbons.

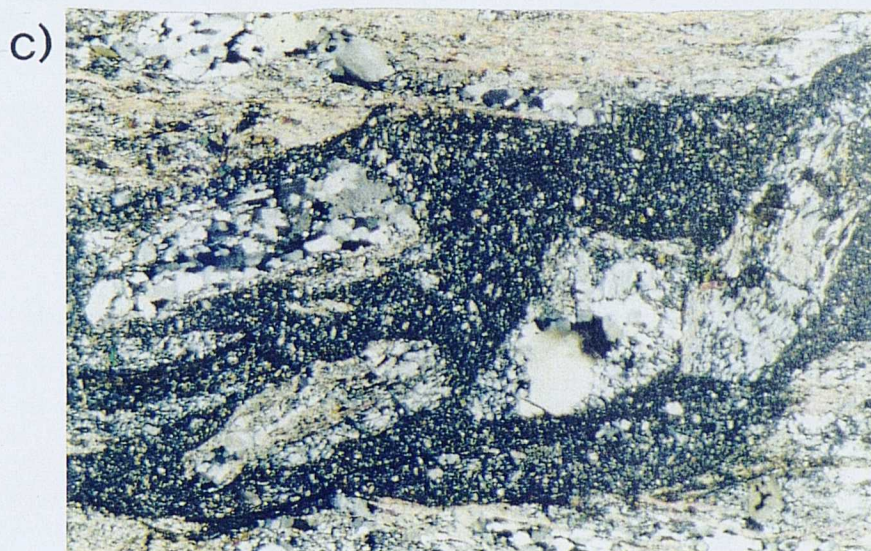


Plate 3.7

a) Mylonitic, quartzo-feldspathic gneiss from NW of Cnoc na Croich (NG 220960). Plagioclase appears as rounded porphyroclasts in a ductile quartz matrix.

b) Brittle deformation of Lewisian Grey Gneiss, SE Scalpay (NG 242945). Thrusts cause top-to-the-NW displacements of gneissose banding. The minor extensional displacements and quartz veining are related to later deformation.

c) Cataclasite vein in felsic gneiss from Kennavay (NG 232950). The larger relict quartz grains in gneiss fragments show undulose extinction. Field of view is 9mm. (XPL)

Evidence for post-mylonitic brittle deformation on Scalpay is geographically widespread but infrequent. Brittle deformation overprints ductile fault rocks and undeformed gneisses to similar degrees, but the kinematics of this deformation are best observed in areas where mylonitisation is poorly developed (e.g. NW Scalpay or low strain augen in the mylonite belts). At these localities original gneissose banding is often faulted in a reverse sense. Top-to-the-NW senses of motion are preserved on steeply dipping reverse faults, but the magnitude of displacement is only in the order of a few centimetres (Plate 3.7b). Occasionally, in localised areas of brittle crushing, green coloured epidote and/or grey cataclasite occur along microfaults with thrust displacements. In thin section, these cataclasites are recognised by a fine grained groundmass surrounding clasts of host material (Plate 3.7c). Tensional microcracks which splay off the main fault strands are also present, and their asymmetry also gives a thrust sense-of-shear. More than one generation of faulting is indicated by several generations of cross-cutting microfaults. Brittle crushing is generally restricted to the area east of the main phyllonite belts (Fig. 3.4), but does not appear to post-date phyllonite formation (see section 3.3.1).

3.2.2 Loch Sgibacleit

Geographical setting

The area studied around Loch Sgibacleit covers c. 3.5 km², and extends for c. 1km north and south of Loch Sgibacleit and the Seaforth River (Fig. 3.7). The northern side extends from Beinn Iobhair (NB 293168), to the northern arm of Loch Sgibacleit (NB 315168), and the southern side extends from Lagan Dubh (NB 302155) to Cleit na Ceardaich (NB 313153). The relief in the area is comparatively high, with excellent exposure on the hills of Mullach Breac Malagair (172m) (NB 301166), Creag na h-Uamha (265m) (NB 306153), and Cleit na Ceardaich (168m) (NB 313153). Exposure in the low ground between hills is generally poor.

Local Lewisian geology

The geology of the Loch Sgibacleit region is dominated by medium grained, heterogeneously deformed Lewisian Grey Gneisses, similar to those on Scalpay. In contrast however, amphibolites are not subordinate to acid gneisses and locally constitute c. 50-60% of the basement rocks. Large pods (c. 200m thick) of amphibolite are observable in regions where overprinting structures are not well developed. Amphibolite facies mineral assemblages in the basement rocks are comparable to those seen elsewhere. The gneissose banding is well developed and dips shallowly

eastwards. Discordant to the banding are numerous Laxfordian pegmatites, and cm-scale 'Younger Basic' dykes, which suggests this area formed a zone of low Laxfordian strain prior to deformation along this part of the OHFZ.

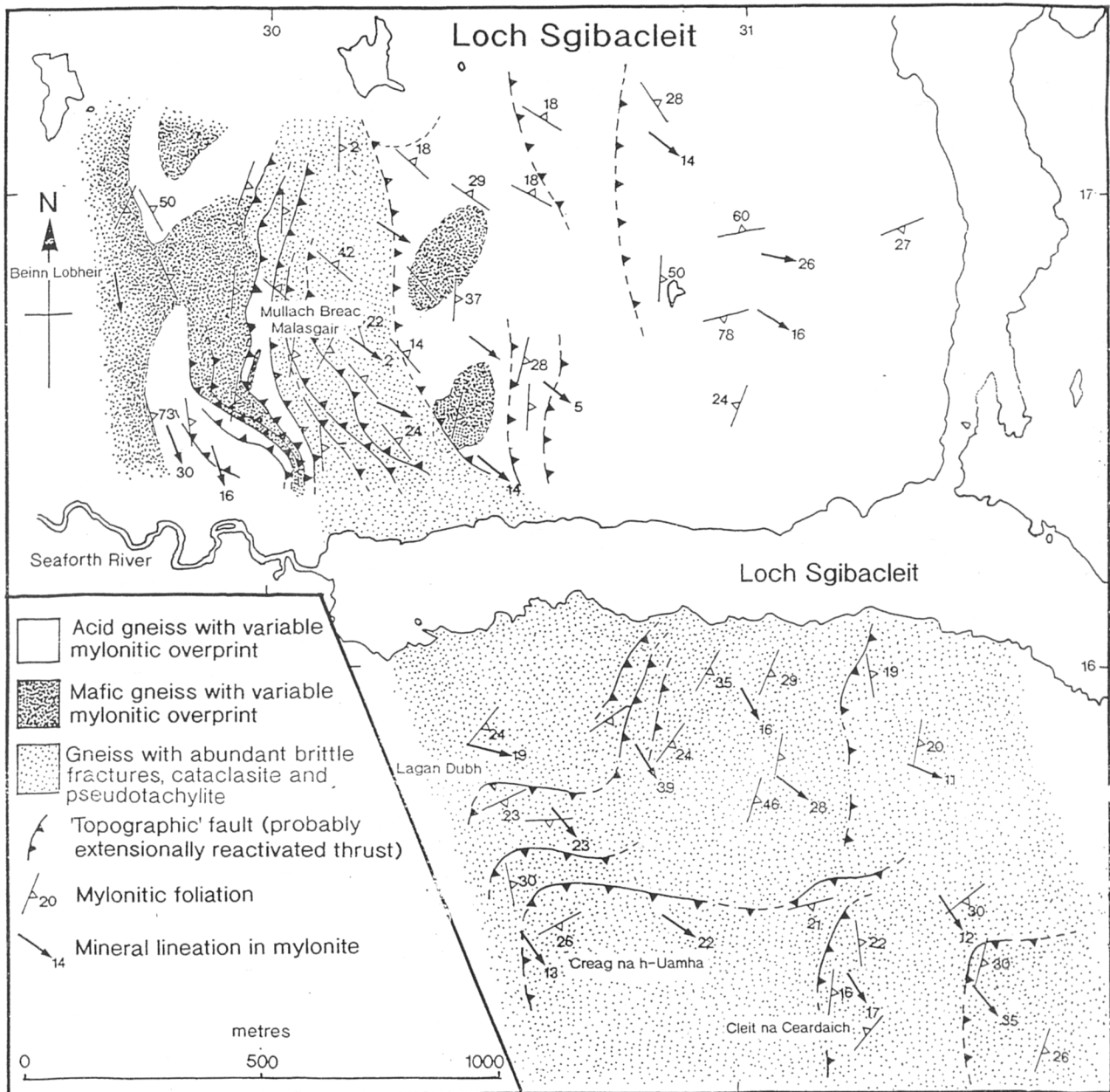


Figure 3.7. Geological map of the Loch Sgibacleit area.

Pervasive mylonite formation

Macrostructure

Sub-parallel to, and probably controlled by the Lewisian banding are a suite of mylonitic rocks, similar to those seen on Scalpay. These crop out on the western sides of Mullach Breac Malagair (NB 301166) and Creag na h-Uamha (NB 306153) and extend eastwards, to define a NNW-SSE trending belt c. 1km wide, and c. 350m thick.

The mylonitic overprint is heterogenous, with highly strained zones of extremely fine grained, well foliated ultramylonites, often near lithological contacts, grading into less mylonitised regions, and ultimately into unmylonitised gneiss. In the low strain regions, the foliation is observed to be axial planar to relict isoclinal folds (probable Laxfordian F2 folds), which may have been reoriented during mylonitisation. In the higher strain regions, finely foliated, dark grey or brown coloured mylonites occur, which often show disrupted, relict gneissose colour banding. Relict pegmatites are frequently reoriented into parallelism with the mylonitic foliation, and are deformed internally. The mineralogy of the mylonites directly reflects that of the protolith, with the typical assemblage: quartz (c. 35%); plagioclase (c. 40%); K-feldspar (c. 10%) amphibole (c.10%), and minor quantities of biotite; garnet; epidote, and opaques. Most of the plagioclase is labrodorite/bytownite (c. 30% Na, 70% Ca). Chlorite is totally absent in these mylonites, and feldspars are not sericitised.

The foliation in the mylonites is very well defined by quartz ribbons and grain alignments and dips shallowly (c.20°) E on the northern side of the Seaforth River, and c. 20° SE on the southern side. A mineral elongation lineation, defined by quartz rods and felsic aggregates is present, and plunges shallowly (c. 15°) SE (Fig. 3.8a and 3.8b). On the southern side of the Seaforth River, this lineation is almost directly down-dip, whilst on the northern side, it plunges slightly clockwise of the true dip, suggesting that an oblique-slip movement occurred in this northern region. The minor discrepancy in fabric orientations north and south of the Seaforth River may have arisen as a result of post-mylonitic movement and/or rotation related to a late E-W trending fault in the Seaforth/Sgibacleit valley. Boudins of amphibolite are common in the mylonites, and their orientations appear to indicate an apparent layer-parallel extension. This geometry is consistent with the strain models proposed by Sanderson (1982) and Holdsworth and Grant (1990), to account for the parallelism between fabrics and thrusts in regions of differing strain intensity.

Kinematic indicators are common in the mylonites and include asymmetric boudins, shear bands and asymmetric σ porphyroclasts of feldspar (Plate 3.8a). All indicate top-to-the-NW thrust displacements.

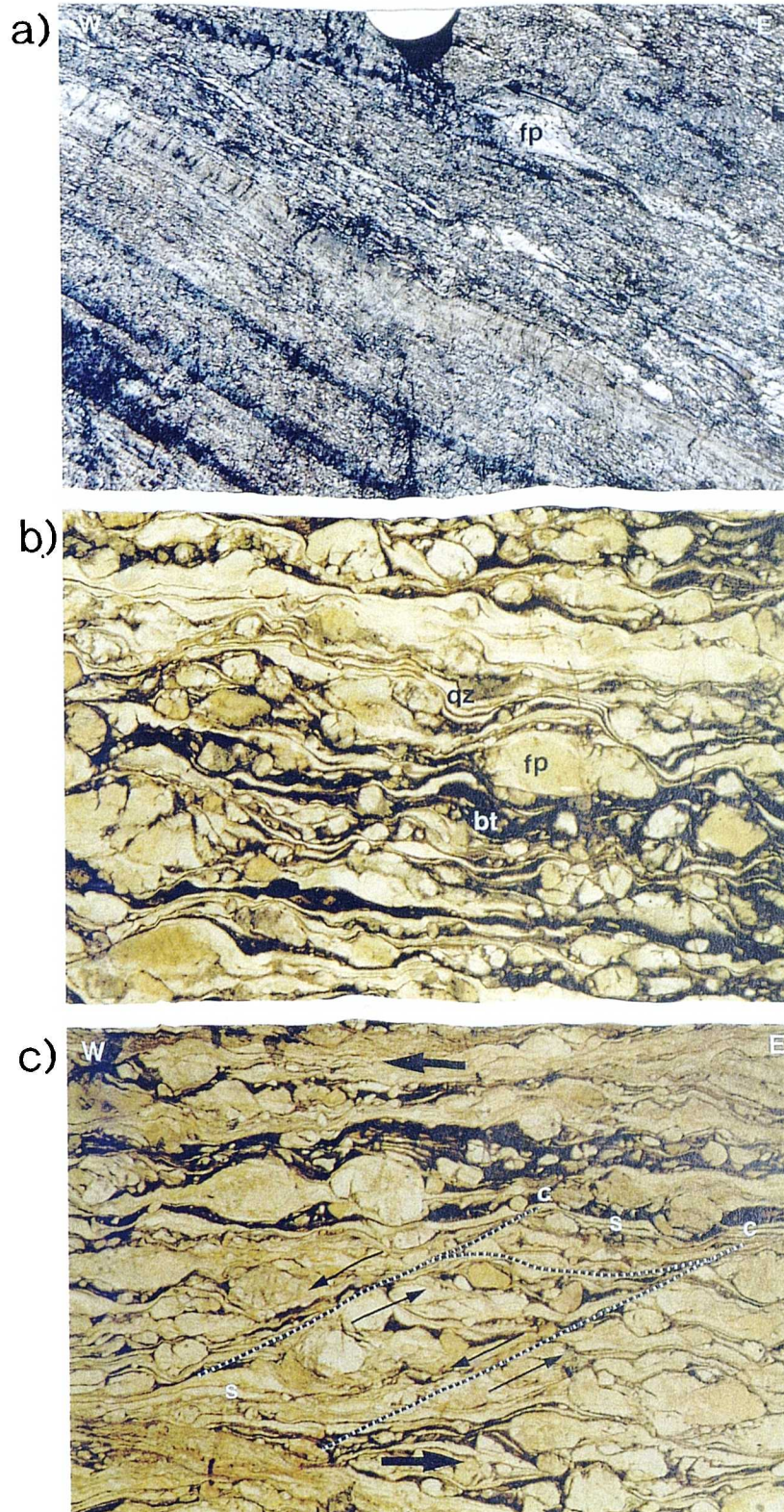


Plate 3.8. Loch Sgibacleit mylonites

a) Mylonitic quartzo-feldspathic gneiss from the south side of Mullach Breac Malasgair (NB 302165). The non-rotated or porphyroclast of feldspar (fp), in the upper right of the photo, possesses asymmetric quartz pressure tails indicative of top-to-the-west sense of shear.

b) Mylonitic quartzo-feldspathic gneiss from north of the summit of Creag na h-Uamha (NB 306156). Rounded feldspar porphyroclasts (fp) are wrapped by elongate quartz ribbons (qz) and amorphous material partially composed of unchloritised biotite (bt). Field of view is 2cm. (PPL)

c) Mylonitic quartzo-feldspathic gneiss from the south side of Mullach Breac Malasgair (NB 302165). Asymmetric extensional shears (c) occur between porphyroclasts and displace quartz ribbons (s). The overall shear sense is top-to-the-west. Field of view is 2cm. (PPL)

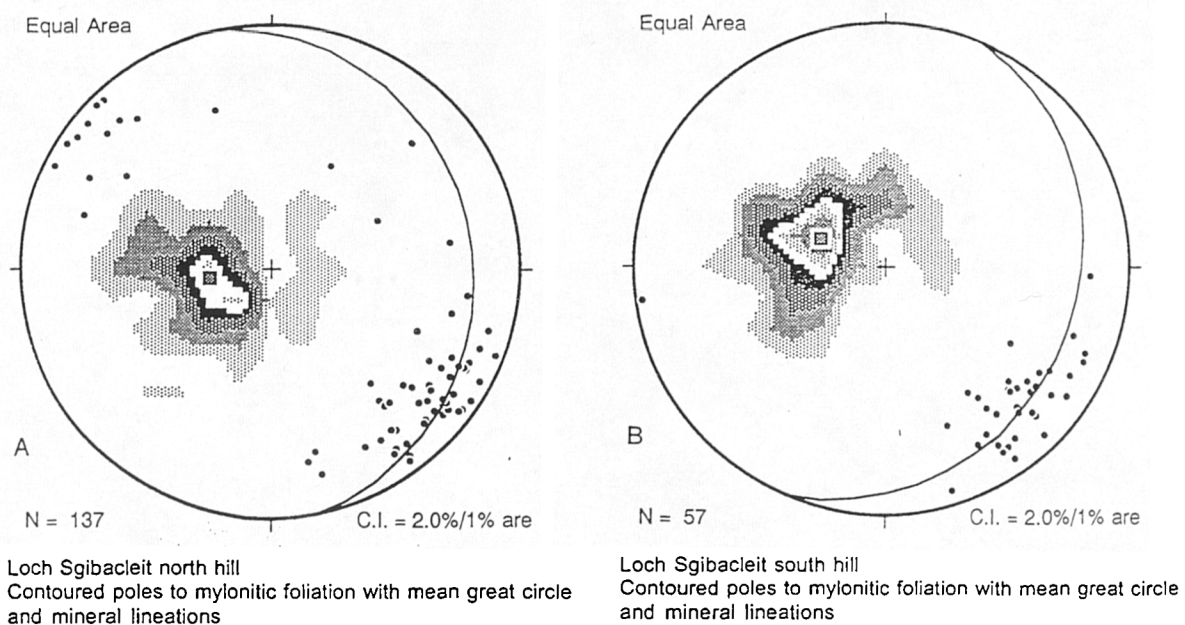


Figure 3.8 a. Equal area stereonet of contoured poles to early pervasive mylonitic foliation, and mineral stretching lineation from north of the Seaforth River, Loch Sgibacleit region.

b. Equal area stereonet of contoured poles to early pervasive mylonitic foliation, and mineral stretching lineation from south of the Seaforth River, Loch Sgibacleit region.

Microstructure

The microstructures in pervasive mylonites from the Loch Sgibacleit region share many similarities with those observed on Scalpay. Quartz deforms ductilely with significant dynamic recrystallisation, forming either *type-1*, *type 2a*, or *type 2b* polycrystalline ribbons, (using the terminology of Boullier and Bouchez 1978). Generally, core and mantle structures and monocrystalline relicts are more subordinate to fully recrystallised fine grained polycrystalline types in these rocks. Where original grains remain, subgrains are discernible near the margins and rotational recrystallisation is believed to be the dominant recrystallisation mechanism. In contrast to the Scalpay mylonites, the most commonly observed quartz ribbons are *Type-2b* polycrystalline ribbons, showing preferred alignments of recrystallised grains. Polygonal grain boundaries are rare, and the grain size is finer (c. 100 μm).

Plagioclase and K-feldspar show abundant evidence for brittle behaviour. Porphyroclasts of both feldspar types show rounded grain shapes as a result of

cataclastic comminution. These porphyroclasts occur in a quartz ribbon matrix and are also internally brittlely deformed, displaying undulose extinction, indicative of high dislocation densities within the grains. Microfractures are common, and are often filled with grains of recrystallised quartz. There is little evidence for widespread ductile deformation, or recrystallisation of feldspar, and in contrast to the Scalpay mylonites, nearly all feldspar grains are unsericitised.

Amphiboles are also unaltered and show chiefly brittle deformation features. Their grain margins have been cataclastically comminuted to form rounded porphyroclasts arranged in discrete bands which probably relate to the relict gneissose banding. Rusty-brown amorphous material forms thin layers (<0.5 mm) which wrap around porphyroclasts of amphibole or feldspar, and are partly composed of unchloritised biotite. Extremely fine grained dark brown or greenish brown material constitutes another matrix component, and is extremely common in ultramylonites (Plate 3.8b). This may have the same composition as the host rock, but the minute grain size makes identification uncertain.

Shear sense indicators are numerous in thin section and include asymmetric extensional shear bands (Plate 3.8c) and asymmetric folds of quartz ribbons. Porphyroclasts are generally symmetrically wrapped by ribboned quartz, and indicate apparent flattening strains. Walker (1990) has conducted quartz c-axis analyses on these mylonites and the results are consistent with top-to-the-NW-directed thrusting.

Metamorphic conditions during deformation

The mylonites preserve index minerals indicative of amphibolite facies metamorphism, which is, however, inconsistent with the pressure and temperature constraints provided by deformation microstructures. The mineral assemblages are probably metastable and may have been preserved across a range of temperatures and pressures. They are therefore unlikely to be syn-tectonic with respect to OHFZ deformation, and are probably relict Lewisian features.

The deformation microstructures indicate that a high greenschist-grade of metamorphism prevailed during deformation, comparable to that inferred from the Scalpay mylonites. The most common (*type 2b*) quartz ribbons have aligned recrystallised grains and probably formed at mid-upper greenschist facies. This is also consistent with the observed dominance of rotational recrystallisation of quartz over grain boundary migration recrystallisation, and the brittle deformation of feldspar and amphibole (Simpson 1985). No recrystallisation of feldspar is apparent but low temperature dislocation glide dominated processes are likely to have caused the

widespread undulose extinction encountered in feldspar porphyroclasts. The lack of deformed monocrystalline quartz also suggests that a high greenschist grade of metamorphism accompanied deformation (Boullier and Bouchez, 1978, Simpson, 1985). Texturally and kinematically, these mylonites are very similar to those on Scalpay and are inferred in the present work to be part of the same laterally continuous belt.

Fracturing, cataclasis and pseudotachylite formation

Macrostructure

Both the E-dipping gneissose banding and mylonitic foliation appear to have acted as planes of preferential failure during later brittle faulting. Comparison of Figs. 3.8a and b and 3.9a and b, show the marked parallelism of the two sets of structures. Occasionally, however, faulting occurs at a high angle to the foliation and the mylonitic fabric in these regions appears to be significantly re-oriented.

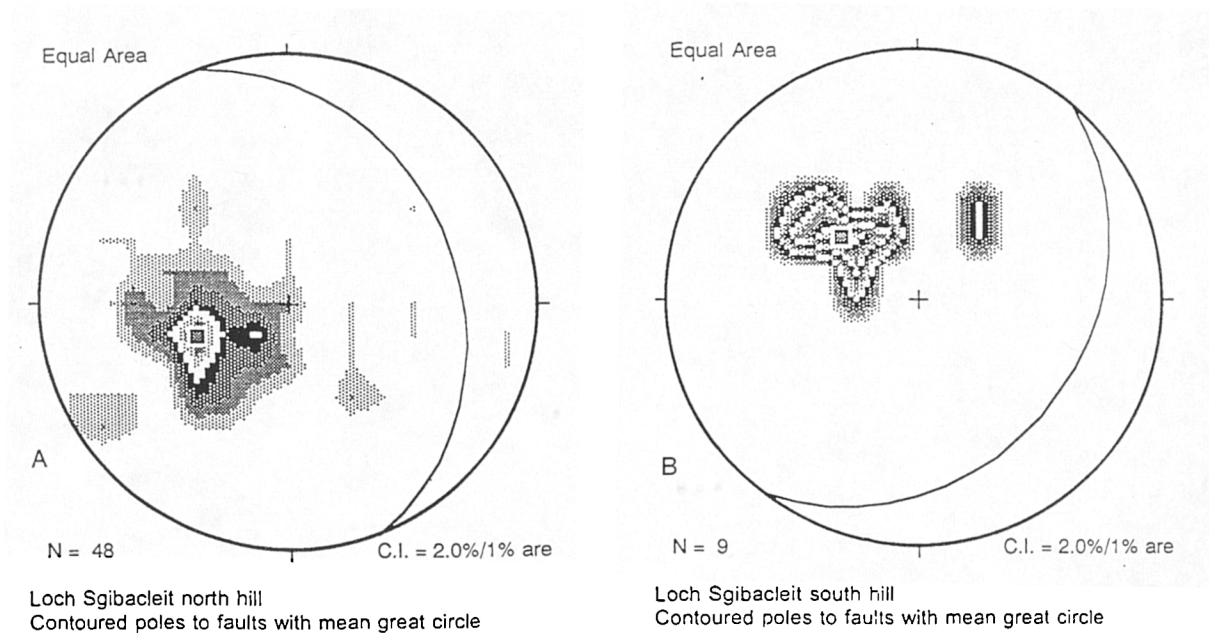


Figure 3.9 a. Equal area stereonet of contoured poles to faults from north of the Seaforth River, Loch Sgibacleit region.

b. Equal area stereonet of poles to faults from south of the Seaforth River, Loch Sgibacleit region.

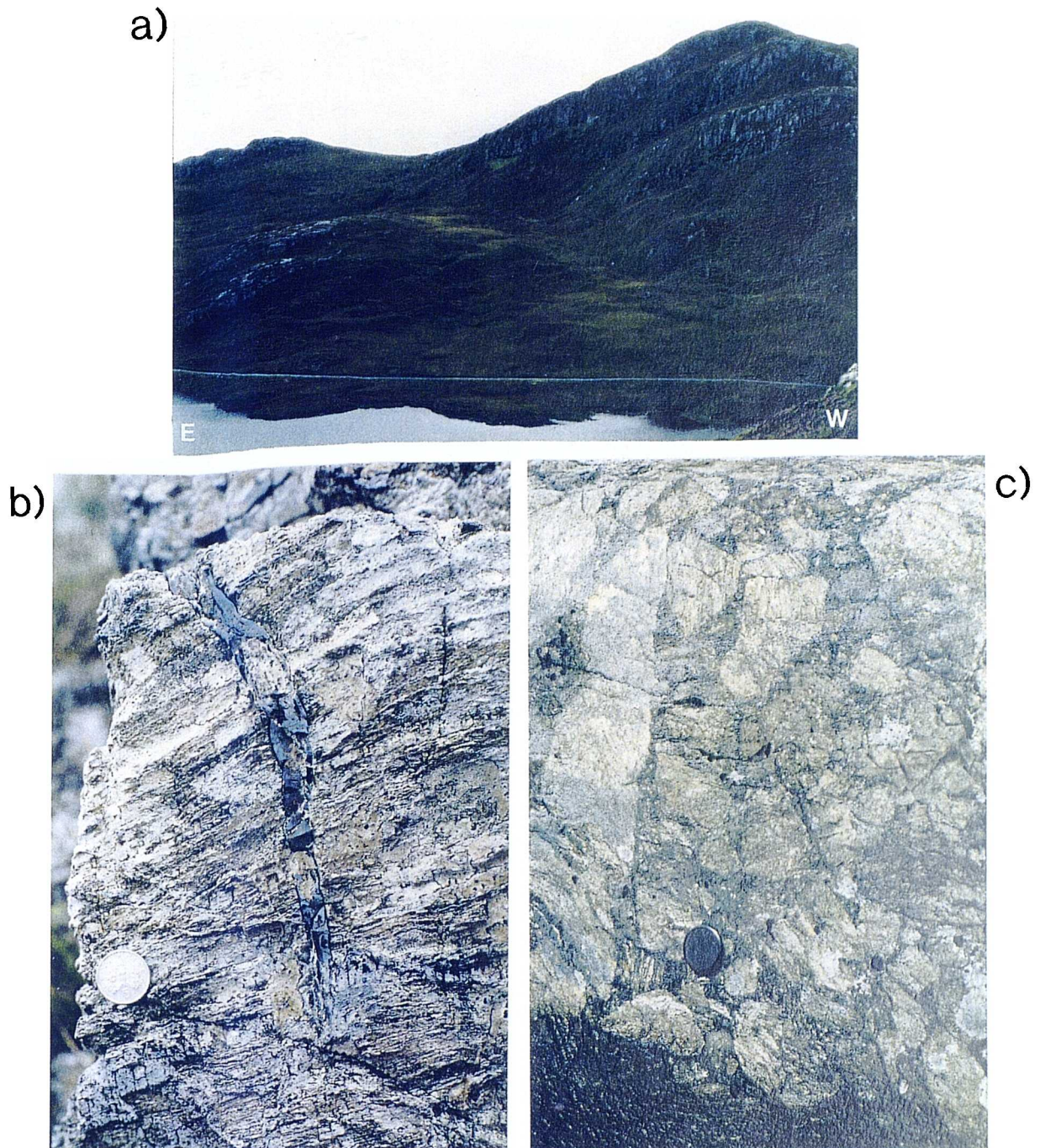


Plate 3.9 Loch Sgibacleit brittle faulting

a) View from Mullach Breac Malasgair across Loch Sgibacleit to the north side of Creag na h-Uamha (NB 306156). Three 'topographic' faults can be observed dipping from upper right to lower left.

b) Mylonitic quartzo-feldspathic gneiss from Cleat na h-uamha (NB 308159), hosting dark grey, discordant pseudotachylite injection vein. Note the chilled margins (darker coloured fringes) on the vein.

c) Pseudotachylite quasi-conglomerate injecting mylonitic quartzo-feldspathic gneiss from Mullach Breac Malasgair (NB 302167).

Large-scale, N-S striking faults, up to several hundred metres in length, appear to bound the lower boundary of the mylonite belt, and continue to occur throughout the belt. The intersections of the fault surface with the topographic surface often causes marked changes in slope gradient which have been referred to as 'topographic thrusts' by previous workers (e.g. Sibson 1977b). These faults often occur in groups (Plate 3.9a) and were mapped as thrusts by Sibson (1977b). No displacement markers for these faults have been found, however, and their movement sense remains enigmatic. Given that no 'topographic' faults appear to be cross-cut by other features, it seems very likely that these faults are relatively late structures.

Several generations of smaller-scale, concordant and discordant meso- and microfaults are very common and are observed to cross-cut each other. Most strike N-S with a variety of dip angles, but in contrast to the larger 'topographic' faults, displacement markers and riedel (R) shears are often present. It should be noted that linear displacement indicators, such as fault grooves and slickensides, are rarely preserved on these meso- and microfaults, but those that are present are observed to plunge down-dip. Apparent displacements on discordant microfaults are in the order of a few cm's, and display both reverse- (c. 48% of those faults measured) and normal- (c.52% of those faults measured) senses of movement. No overall uniformity regarding the relative timing of reverse and normal microfaulting has been deduced. Concordant microfaults are also extremely common in the mylonites and appear to focus into the most ultramylonitic layers. Small-scale folds of the mylonitic foliation are often associated with microfaults, and show vergence directions indicative of both up-dip and down-dip movement.

Both reverse and normal microfaults frequently possess fault-parallel veins of grey cataclasite or black/brown-coloured pseudotachyite. These fault rocks are very extensively developed, and do not appear restricted to thrusts as previously proposed (Sibson 1977b). Pseudotachylites show a variety of geometries, including <1 mm- c.10 cm thick pinch-and-swell fault-veins, <1 mm - c.50 cm-thick injection veins (Plate 3.9b), and c.10 cm - c.3 m - thick injection complexes or breccias, enclosing well-rounded clasts (c. 10-20cm in the larger breccias) of well-foliated, mylonitic host rock (Plate 3.9c). Pseudotachylite injection veins frequently adopt 'T fracture' orientations, similar to those documented by Grocott (1981) and Swanson (1988) (see section 1.4.5), and may display top-to-the NW, reverse movement (Fig. 3.10a), or top-to-the-SE, normal movement. The bounding envelopes of pseudotachylite breccias (comprising paired shear fractures) are usually concordant to the surrounding foliation, and the injection veins, generated by the paired shears, intrude inwards with respect to the bounding

shears. Breccias may be associated with secondary 'R-shears', which usually indicate top-to-the SE, *normal* movement (Fig. 3.11b).

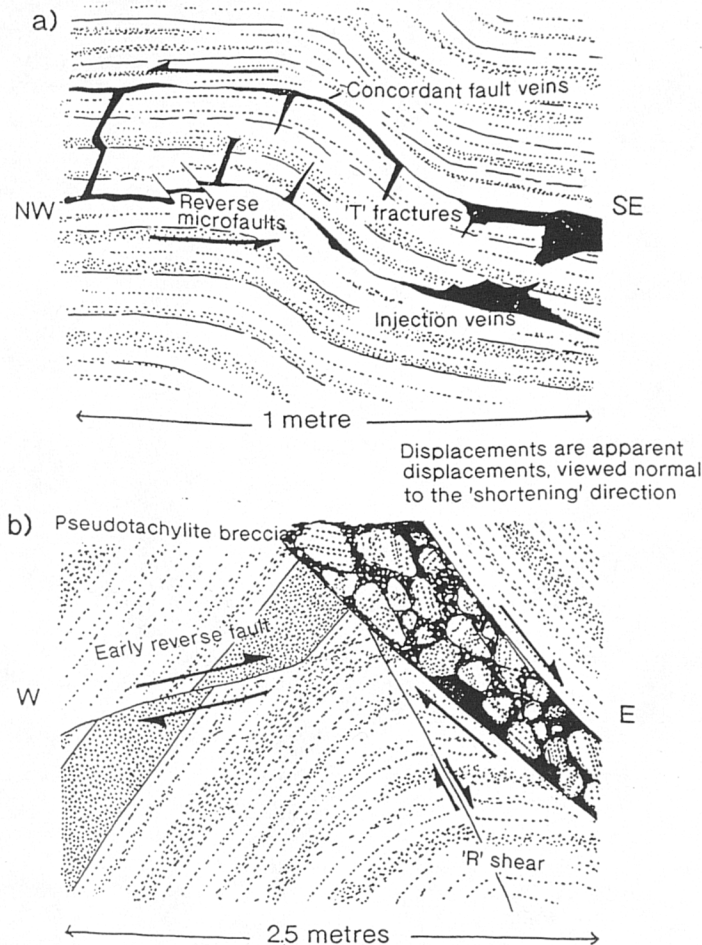


Figure 3.10. Field sketches of structural geometries commonly associated with pseudotachylite injection complexes and pseudotachylite breccias:

a) The geometry of pseudotachylite injection veins, which adopt 'T'-fracture orientations in injection complexes demonstrate that generation took place in a thrust regime, displacing top-to-the NW;

b) Barren 'R'-shears outside breccia envelopes, suggest that injection took place in an extensional environment displacing top-to-the SE.

Pseudotachylite crush zones (c. 10m thick) form extensive belts (traceable for c. 100 m) containing pseudotachylite, ultracataclasite and ultramylonite, with little material of grain size >1mm. These belts are highly strained mylonitic areas where later microfaulting and cataclasis, (with their associated fault rock products) are at their greatest intensity. The largest crush zones are well developed close to the lowermost

'topographic' faults in the region of Mullach Breac Malasgair (NB 131166), but are laterally discontinuous.

Some pseudotachylites appear to have experienced open folding, which Walker (1990) assigned to Laxfordian reworking. Since all the OHFZ fault rocks are inferred to post-date Laxfordian reworking (see section 3.2.5), folding is likely to be due to much later deformation, probably during extensional fault reactivation (see section 3.4).

Microstructure

Pseudotachylite fault and injection veins locally disrupt the mylonitic (Plate 3.10a) and ultramylonitic foliation (Plate 3.10b and c). Mylonites however, have never been observed to deform pseudotachylite injection veins. All brittle fracturing therefore appears to post-date mylonitisation (cf. Sibson 1977b), (see discussion in section 3.2.5). No retrogression appears to accompany brittle deformation and the presence of large volumes of pseudotachylite may have implications for the amount of fluid present during this phase of deformation (see conclusions in section 3.2.5).

3.2.3 Central Lewis

The pervasive mylonite belt studied in detail on Scalpay and around Loch Sgibacleit is laterally continuous and reconnaissance mapping has traced the belt north as far as Achmore (NB 310300), where it disappears into a large area of sparse exposure. A second strand links into the first at Gravir (NB 380155) and trends NNE-wards to Marvig (NB 190415). This eastern splay is lost at the mouth of Loch Erisort (NB 420210), but crops out again on the eastern side of Aird Raerinish (NB 430250). It is inferred to continue this NNE trend and pass beneath the cover rocks on the Stornoway isthmus (Fig 3.2).

In central Lewis, the belt of thrust-sense mylonites c. 500m thick, shows characteristics consistent with the Loch Sgibacleit mylonites further south, although the intensity of thrust-sense brittle overprint is usually less. Quartz deforms in a ductile manner, forming well developed ribbons. These are either polycrystalline *type 1* or *type 2* forms, and suggest that deformation occurred at greenschist facies (Boullier and Bouchez 1978). Both feldspar and hornblende are largely unaltered and appear as cataclastically deformed, rounded, rigid clasts within the quartz ribbon matrix. Amorphous brown-green material also wraps the clasts. Feldspars often show undulose extinction, indicative of high dislocation densities within the crystal lattices.

In central Lewis, thrust-sense brittle deformation appears to have affected a wider area than thrust-sense ductile deformation. At Springcorrie (NB 230 325), c. 11

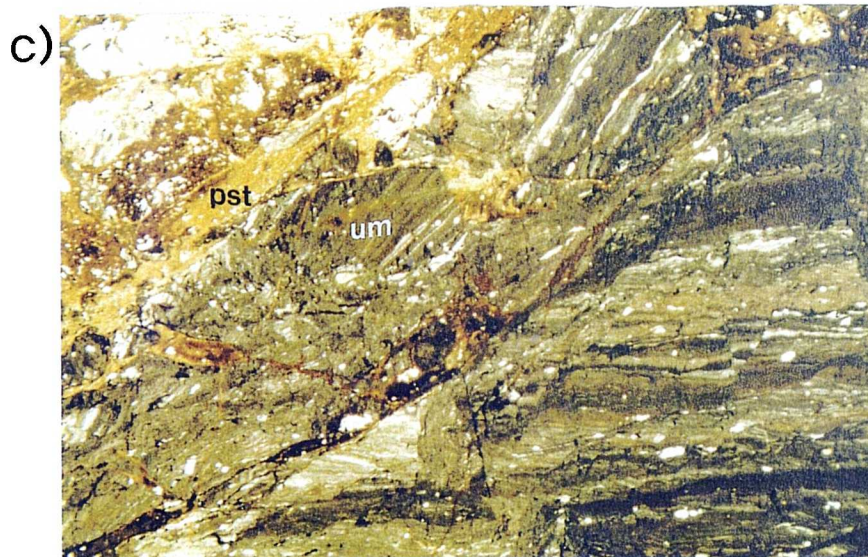
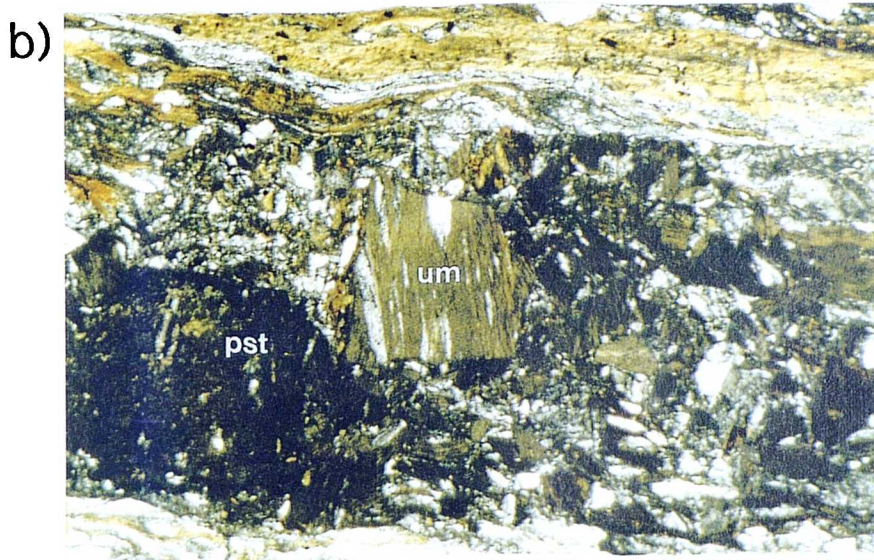
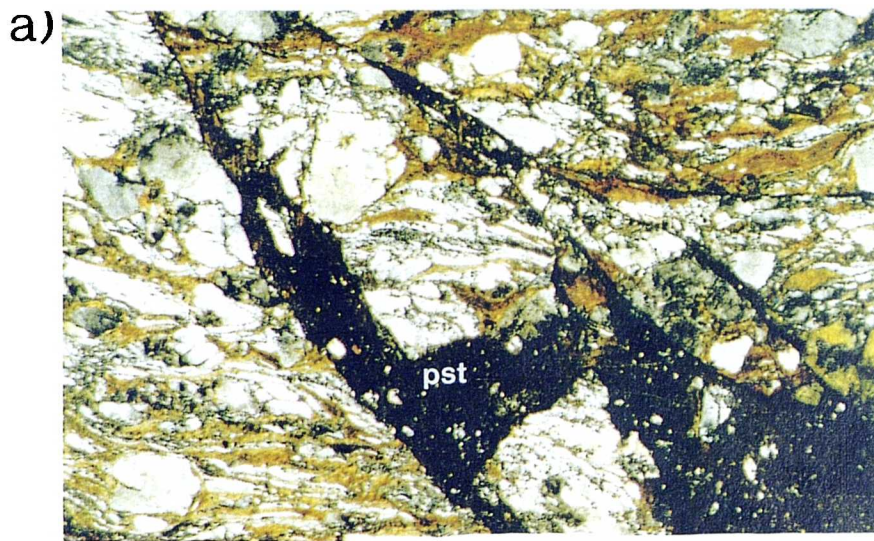


Plate 3.10 Loch Sgibacleit pseudotachylite

a) Pseudotachylite injection veins (pst) disrupting mylonitic gneiss from Mullach Breac Malasgair (NB 302165). Clasts of country rock within the pseudotachylite veins preserve quartz ribbons and feldspar porphyroclasts. Field of view is 1.4 cm. (XPL)

b) Pseudotachylite (pst) disrupting ultramylonitic gneiss from Mullach Breac Malasgair (NB 301166). Clasts of country rock within the pseudotachylite are extremely fine grained and possess aligned quartz/ feldspar clasts. Ultramylonite clasts (um) are significantly misoriented with respect to the foliation outside the veins. Field of view is 1.2 cm. (XPL)

c) Ultramylonitic gneiss (um) cross-cut by discordant microfaults possessing light brown pseudotachylite, from west of Malasgair (NB 169300). Field of view is 3 cm. (XPL)

km east of the early mylonite belt, there is no evidence of pervasive ductile deformation overprinting the Lewisian fabrics. Small fault and injection veins of pseudotachylite are common however, and are generated on surfaces concordant to banding. Discordant microfaults without pseudotachylite are also common and consistently show thrust-sense, top-to-the-NW displacements.

3.2.4 Aird Raerinish

The small peninsula of Aird Raerinish (NB 420250) (Fig. 3.11), is the north-easternmost outcrop of early ductile mylonite in the OHFZ. Here, the dominant lithologies are acid gneisses similar to those seen elsewhere, and Laxfordian granite and pegmatite intrusive bodies. The eastern side of the peninsula has been variably affected by ductile mylonitisation and brittle crushing. A well developed, NNE-SSW trending belt of heterogeneous mylonite c.140m thick is exposed on the extreme east coast, extending from Braigh an Stac (NB 428241) to Raerinish Point (NB 430250), and c.200 m inland. The effects of ductile shearing are gradually less well developed westwards, but a thinner belt of mylonite, c. 80m thick, occurs near the summit of Beinn Mhor (NB 426245). In contrast, brittle faulting with cataclasite generation is abundant throughout the area.

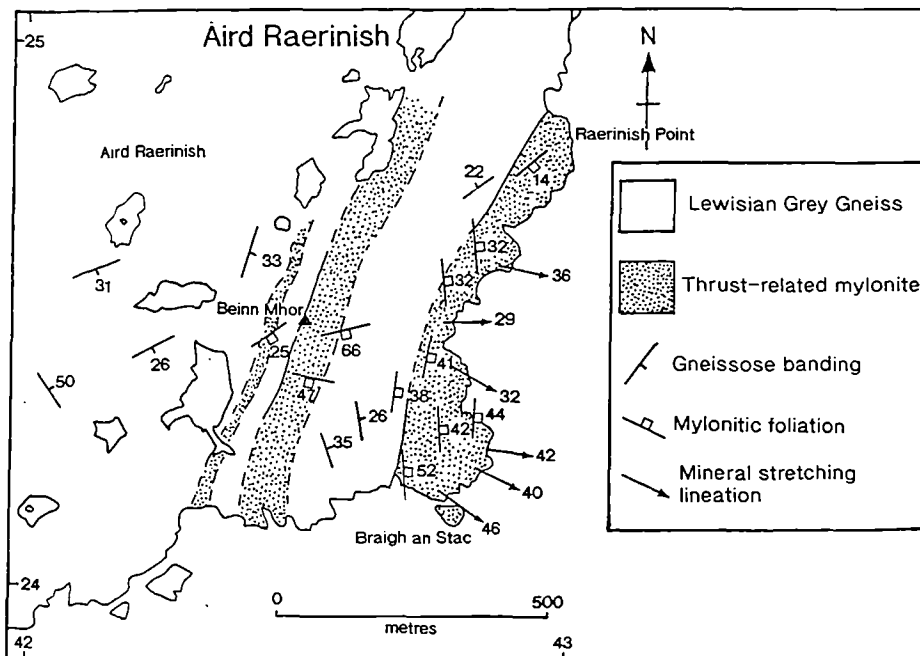


Figure 3.11. Geological Map of Aird Raerinish , eastern Lewis.

The mylonites are fine grained and similar to those observed elsewhere, in that the well developed colour banding and mineralogy (quartz (c.30%), feldspar (c. 30-40%) (mainly Ca rich plagioclase), and amphibole (c.20%)) is largely inherited from the banded gneissose protolith. The mylonitic foliation, defined by quartz ribbons and elongate feldspar aggregates, dips much more steeply than elsewhere (c. 50° to the SE), and has clearly not been controlled by the orientation of pre-existing gneissose banding, which is locally variable (Fig. 3.11, stereonet a). A strong, ESE plunging mineral elongation lineation, defined by quartz ribbons, feldspar aggregates and aligned hornblende porphyroclasts, is developed on the mylonitic foliation surfaces, and mostly plunges down-dip (Fig. 3.11, stereonet b). Shear sense indicators parallel to this lineation include asymmetric σ porphyroclasts of feldspar, asymmetric amphibolite boudins and minor asymmetric folds. All indicate a top-to-the NW sense-of-shear.

Both mylonitic and non-mylonitic gneisses host abundant microfractures and moderately developed cataclasites. Microfractures cross-cut the mylonites, which suggest that the mylonites formed relatively early in the structural history of the region. Rare NW-SE trending upright folds of probable Laxfordian age occur in less mylonitised areas, and the strong mineral lineation disappears.

These mylonites were noted and classified as phyllonites by Sibson (1977b). However, the present study has shown that this unit is petrologically and kinematically dissimilar to the phyllonites observed from Scalpay, and more akin to the pervasive, higher grade early mylonites. Minor retrogression occurs west of the main mylonite belt, where amphibole is pseudomorphed by chlorite, and cross-cutting veins of epidote occur, suggesting that minor hydration occurred very locally, in irregular non-planar zones. These are probably late-stage developments, post-dating mylonitisation, since the original amphibolite facies gneiss assemblages are largely retained in the mylonite and appear to have remained metastable during mylonitic deformation.

3.2.5 Conclusions and discussion on thrusting in the northern segment

Conclusions

The earliest phase of deformation on the OHFZ has generated a NE-SW-trending band of heterogeneously developed ductile mylonites at least 5 km wide, which dips moderately to the SE. This band is cross-cut and post-dated by brittle fracturing and cataclasis, which is less restricted in extent. In general, ductile mylonitic fabrics become *less* apparent from the south of the area to the north. Conversely, brittle

deformation, including pseudotachylite and cataclasite formation, becomes *more* apparent in the same direction. In the central area of Lewis, around Loch Sgibacleit, both ductile and brittle deformation products are developed to similar degrees.

The evolution of deformation style observed in the thrust-sense fault rocks of the northern OHFZ, is as follows:

1. Pervasive, heterogenous, high greenschist facies mylonite;
2. Discrete brittle faults:
3. Discrete pseudotachylite and cataclasite generating faults, probably coeval with the above.
4. Generation of large-scale topographic faults

The kinematic regime

Both ductile and brittle deformation appear to be associated with large-scale NW-directed thrusting. Whilst evidence for thrusting is readily observable in the ductile mylonites, brittle deformation is less obviously thrust-related. Top-to-the-NW thrusts, top-to the SE backthrusts, W-dipping normal faults and E-dipping normal faults have all been observed, and the large-scale kinematics of brittle deformation are therefore uncertain.

The best evidence for large-scale brittle kinematics comes from around Seaforth Head, where the field relationships of brittle microfaulting and pseudotachylite/cataclasite generation are extremely complex. Both barren and non-barren faults, showing a variety of shear senses, cross cut each other, and are therefore regarded as being broadly coeval. Overall compression during brittle deformation has not been proved beyond doubt, but brittle deformation producing large amounts of pseudotachylite is probably facilitated by a load strengthening, rather than a load-weakening environment (Sibson 1977a, 1993). In a load strengthening environment, the frictional shear strength of a fault increases as shear stress across the fault rises (Sibson 1977a, 1993), maintaining friction on the pseudotachylite generating surface. Paradoxically however, pseudotachylite fault breccias appear to be hosted by apparent normal faults, and the extremely local provenance of pseudotachylite melt (Maddock 1992) suggests that normal faulting probably *generated* such breccias. Although the complex cross-cutting relationships of thrust and normal faults *could* be well explained by several closely timed reversals in fault-zone movement, alternative, equally viable and less complicated interpretations also exist:

- Most deformation may have occurred in a reverse faulted (load strengthening) regime, with relatively minor gravity-induced adjustments occurring as aftershocks between major thrust phases.
- Overall thrust sense of shear may produce block rotations and complex minor normal fault arrays to accommodate strain during one sense of movement.

Pressure, temperature and fluid conditions during deformation

As stated previously, microstructures in the early mylonites are consistent with deformation at high greenschist facies. Amphiboles are metastable during deformation, however, suggesting that little retrogression from amphibolite facies occurred. The change to large-scale brittle thrusting appears to have caused little change in the amphibolite facies mineral assemblages present. Brittle deformation may therefore have occurred at either the same metamorphic grade as the ductile deformation, (In this situation high strain rates or high pore fluid pressures are required to account for the change from ductile to brittle deformation), or, at low grades, where the amphibolite facies assemblages are metastable. A lack of available water may have prevented retrogression in this situation. Since there is little evidence for embrittlement due to fluid influx or increasing strain rates, deformation is believed to have occurred at lower P/T conditions than those accompanying mylonitisation. The high grade assemblage is therefore a relict feature.

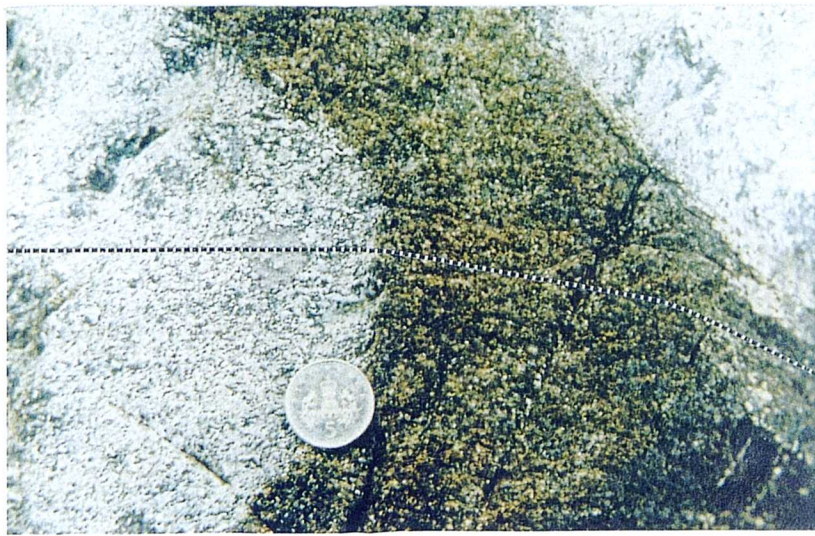
Discussion

Timing of early mylonitisation

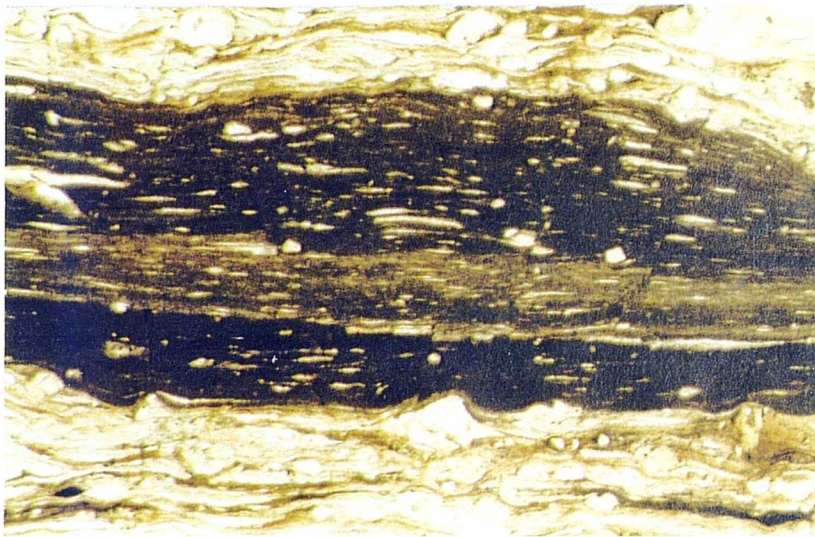
Lailey et al. (1989) suggested that thrust-related mylonites on Scalpay (NG 231942) are cut, and therefore post-dated by, Scourie dykes ('Younger Basics'). This evidence puts fault inception earlier than 2400 -2000 Ma (Heaman and Tarney 1989). The present work has been unable to corroborate this conclusion for several reasons:

- Although the dykes lie at an angle to the mylonitic foliation, they do *not* cross-cut it. The mylonitic fabric can be traced continuously from the country rock through the dykes (albeit slightly refracted). This suggests that mylonitisation *post-dates* dyke intrusion, (Plate 3.11a). Sibson (1977b) correctly noted that the dykes are folded, and that the foliation lies axial planar to these folds. If the foliation developed during the folding episode, the intrusion of the dykes must pre-date the fabric forming event.

a)



b)



c)

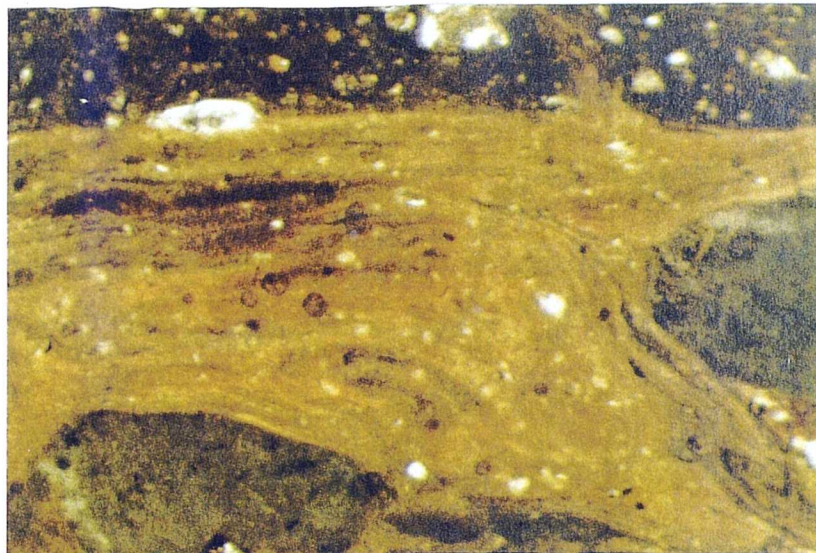


Plate 3.11

a) Folded 'Younger Basic' dyke from Meall Challibost SW Scalpay (NG 232942). The fold hinge shows an axial planar, refracted, foliation which clearly cross-cuts both the quartzofeldspathic gneiss and the mafic dyke material.

b) Ultramylonite from Mullach Breac Malasgair (NB 301166) with aligned clasts of felsic gneiss. Field of view is 1cm. (PPL)

c) Flow banded brown pseudotachylite, from west of Malasgair (NB 300169). Field of view is 4mm. (PPL)

- The country rock in the vicinity of the dykes is only weakly mylonitic and is interpreted as a protomylonitic low-strain zone. The dykes are not sufficiently deformed to be rotated into parallelism with the foliation.
- Elsewhere in the high-strain mylonites, similar small-scale amphibolites are parallel to, and significantly boudinaged by the country rock foliation, If these are Scourie dykes, they are undoubtedly post-dated by shear deformation.
- Lailey et al. (1989) suggest that the dykes show their original intrusive geometries on the basis that apophyses are still present. The present work has found only one apophysis-like structure (at NG 239944), formed by the tectonic juxtaposition of two separate amphibolite bodies along a brittle thrust plane, and not during intrusion.
- Nearby pegmatites (presumably Laxfordian) which always cross-cut the amphibolite dykes are often highly mylonitised (Plate 3.2b). It is inconceivable that these later intrusions have been disrupted by a foliation which pre-dates the amphibolite dykes.

It is therefore concluded that there is no evidence at this locality for fault zone inception prior to the intrusion of 'Younger Basic' dykes or Laxfordian pegmatites. Since Laxfordian pegmatites are internally disrupted by these mylonites, both on Scalpay and around Loch Sgibacleit, the earliest possible age of mylonitic deformation is Laxfordian (c. 1700 Ma).

Fettes and Mendum (1987) and Fettes et al. (1992), suggest that early thrusting may have been coeval with Laxfordian granite veining. These authors cite examples where:

- granite sheets, possessing an internal foliation, have been thrust over banded gneisses. Both these rock types are cross-cut by aplogranites with only local shear effects;
- aplogranites and pegmatites, possessing strong internal fabrics, cross-cut granites and banded gneisses which are only weakly foliated or unmodified.

These observations have not been corroborated by the present work, but suggest that thrust fabrics are heterogeneously developed in different intrusions, consistent with variations of deformation intensity in Laxfordian pegmatites on Scalpay. Moreover, thrust-related deformation may be interpreted as later than the intrusions in both examples. It is conceivable that the mylonitic deformation is significantly younger than the Laxfordian veining episode (see chapter 5).

The relative timing of mylonitisation and retrogression.

In Scalpay, the effects of ubiquitous retrogression are present and have altered the assemblages of both undeformed gneissic protolith and fault rocks. In the mylonites, most of the feldspar has been replaced by sericite, and original hornblende by biotite or chlorite, but this retrogression is regarded in the present work as post-mylonitisation in age for three reasons:

- The majority of microstructural palaeotemperature indicators in the mylonites are consistent with high greenschist facies metamorphism accompanying deformation, and incompatible with the low grades of deformation and water-rich environment inferred by the retrograde reaction products.
- Retrograde minerals do not always occur in mylonites. The lack of retrogression in the mylonites of Loch Sgibacleit, for example, suggests that low grade conditions did not prevail during mylonitisation at this locality.
- The retrograde reaction products show little evidence of deformation, contrasting with the obvious deformation in the original grains

The contemporaneity of ductile and brittle thrusting?

Previous workers have recognised the crucial importance of the Seaforth Head/Loch Sgibacleit area to the understanding of the mechanical behaviour of the OHFZ. Sibson (1977b) regarded the area as evidence for the coeval operation of ductile shearing and brittle faulting, and concluded that the local behaviour of the fault zone is "intermediate between the essentially brittle pseudotachylite-ultracataclasite crush zones and the ductile mylonitic shear zones, whilst elsewhere in the fault zone, these two types of deformation are separately developed" (Sibson 1977b). From observations made in thin section, he concluded that "a shape fabric has been superimposed on some pseudotachylite fault veins after their formation, to form ultramylonites". Sibson's interpretation for this coeval ductile and brittle deformation is a plastico-viscous critical state, which fails under brittle conditions if the strain rate is increased slightly. Walker (1990) however, regards the two events as separate, but suggests pseudotachylite generation occurred in two phases. She suggests that the brown pseudotachylites around Loch Sgibacleit were generated very early in the structural history of the region, and cites examples where pseudotachylites are folded during Laxfordian reworking (see section 3.2.2).

The present study has re-examined the relationships of ductile to brittle deformation. Both in the field and in thin section, pseudotachylites only appear to show a shape fabric in *concordant* fault veins. If this shape fabric has arisen as a result of continued mylonitisation after pseudotachylite generation, both discordant fault veins *and* discordant injection veins should also show disruption, or a cross-cutting mylonitic fabric. No shape fabrics have been observed by the writer in either type of *discordant* veins, and shape fabrics must therefore have arisen through a different mechanism.

There are two possible mechanisms for this apparent mylonitic fabric:

- Some dark-coloured concordant, crypto-crystalline veins with apparently aligned clasts, may be ultramylonites, whose grain size is too fine to be resolved by a petrological microscope. Where these occur in the absence of intrusive geometries and in highly strained mylonites (Plate 3.11b), this is almost certainly the case.
- Some apparent mylonitic fabrics *do* occur in rocks with intrusive geometries. These are very often brown, a characteristic peculiar to some pseudotachylites from Lewis (Walker 1990), and show evidence of flow-banding (Plate 3.11c). In this situation, the shape fabrics are thought to be alignments brought about during flow of pseudotachylite whilst still molten, a process documented widely in the existing literature (Macaudi re and Brown 1982, Berlenbach and Roering 1992).

There is no evidence for brittle deformation having been post-dated by renewed thrust-related upper greenschist facies mylonitisation. Ductile and brittle deformations are therefore not coeval.

The embrittlement of mylonites: A lowering of P-T conditions or an increase in strain rate?

The change in deformation style from chiefly ductile to chiefly brittle deformation conditions observed in the thrust-sense fault rocks of the northern OHFZ, may have resulted from one or more mechanisms outlined below:

1. An increase in strain rate.
2. A lowering of P/T conditions.
3. An increase in fluid pressure.

Although the presence of pseudotachylite in these rocks does not necessitate a fluid-absent environment (Killick 1990, Magloughlin 1992), the combination of large

volumes of pseudotachylite, and the extremely high melting point of acid gneiss host (c. 800°C), suggests that brittle deformation occurred in the absence of water (Sibson 1977a) (see section 4.2.12 for a full discussion). In the absence of any geological evidence for the presence of a tectonically active fluid phase in these rocks, fluid pressure changes are thought to be an unlikely mechanism for this change in deformation style. The change from large-scale ductile thrusting, to large scale brittle thrusting, is therefore regarded as resulting from one of two possible mechanisms:

- Brittle deformation may have formed at roughly the same grade as the ductile mylonites, with increasing strain rates to account for the change in fault behaviour, (originally suggested by Sibson (1977b)),
- Brittle deformation may have occurred at much lower metamorphic grades than the ductile mylonitic deformation. The lack of observed retrogression in the brittle rocks may be due to the inferred water-absent conditions

The first explanation is considered unlikely because fluctuations in strain rate should theoretically promote a return to ductile conditions after brittle behaviour ceased. Nowhere are brittle deformation products observed to be cross-cut by ductile deformation (cf. Sibson 1977b). The second explanation is therefore preferred, but does not establish whether the change in deformation style is due to two exclusive (and possibly widely separated) thrusting events, or part of a single progressive thrusting event involving a gradual lowering of P/T conditions over time. Discussion of both models is provided in chapter 5.

Strain estimates

Using crude strain estimates from Scalpay, based on boudinaged and folded basic layers, and the obliquity of the foliation compared with the large-scale OHFZ, Sibson (1977b) concluded that an up-dip displacement of 1.8 - 3 km may have occurred during early mylonitisation. His strain estimates assume a progressive simple shear during deformation, but as he states, "no account is taken of boudin flattening, which has certainly taken place to some extent". This interpretation would appear to be confirmed by the presence of symmetrically wrapped amphibolite boudins and porphyroclasts, and the lack of fabric deflections from low to high strain zones. In addition, the pre-shear geometry of the features he uses as strain markers are not known. Sibson's strain estimate is therefore probably unreliable. No useful strain

estimates presently exist for early thrust sense motion on the OHFZ, but the large thickness of mylonite (c. 600 m on Scalpay), suggests significant thrust displacements (on the scale of several km) may have occurred.

3.2.6 Summary

- The distribution of thrust-related deformation is heterogenous.
- Fault inception and the onset of mylonitisation occurred either during or after the late Laxfordian (c.1700 Ma).
- Upper greenschist facies ductile mylonites are overprinted by brittle deformation products including pseudotachylites and cataclasites.
- Both ductile and brittle deformation appear to be associated with NW-directed thrusting.
- Ductile and brittle deformation phases appear to be exclusive events. There is no return to ductile deformation after the onset of brittle deformation.
- The change in deformation style is probably due to a lowering of P/T conditions and not an increase in strain rate and/or fluid pressures.
- Retrogression, where observed is regarded as post-deformational.
- Existing thrust displacement estimates are regarded as inconclusive.

3.3 Strike-slip movement

A second suite of fault rocks post-dates the early ductile and brittle thrust-related deformation, and forms discontinuous bands and lenses of phyllonitic mylonite (phyllonite). These rocks have a lower grade (low greenschist) assemblage than the earlier thrust-related mylonites and their areal extent coincides with pre-existing zones of ductile and brittle thrust-related deformation (Fig 3.12). Evidence is presented which suggests that these rocks were formed under conditions of sinistral strike-slip on the OHFZ. Rocks deformed during regional strike-slip motion have been studied in detail in Scalpay, the Park district of Lewis, Eishken and parts of north-east Lewis (Fig. 3.1).

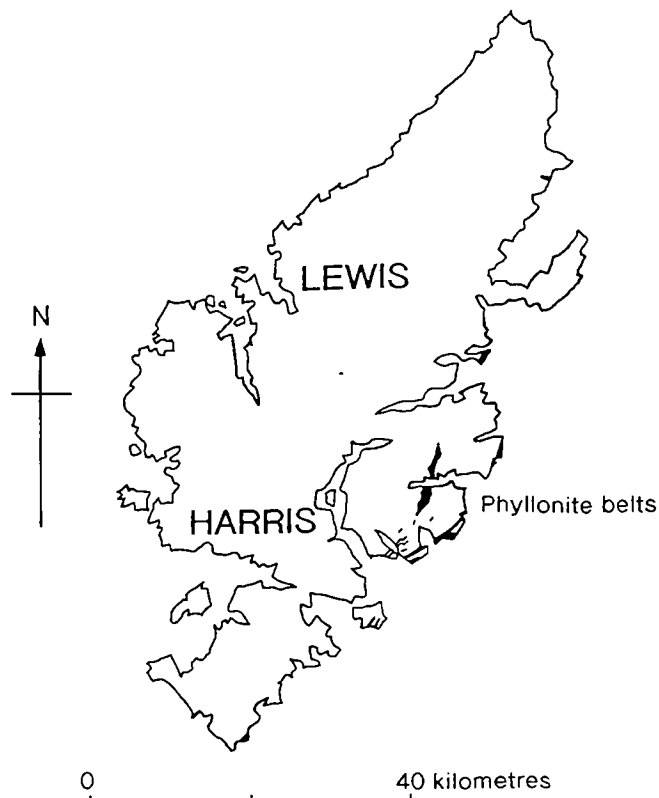


Figure 3.12. Map of the northern Outer Hebrides showing the extent of ductile phyllonitic deformation relating to sinistral strike-slip movement on the OHFZ. (Modified from Fettes et al. 1981)

3.3.1 Scalpay

Macrostructure

Sub-parallel to the early, thrust-related mylonitic foliation in Scalpay (Fig. 3.4) are several SE-dipping belts, c. 500 - 1000 m in lateral extent, of fault-bounded green phyllonite, which many authors (e.g. Sibson (1977b), Walker (1990) and Fettes et al. (1991)) do not differentiate from the higher grade, pervasive mylonites discussed above. Previous workers have generally regarded these two fault rock types as resulting from the same deformational event, but having undergone different intensities of strain and retrogression. Walker (1990) for example, assigns the name 'c'-type mylonites to both fault rock types. The present work suggests that the phyllonite belts developed consistently later than the pervasive mylonites, and under different pressure, temperature and fluid conditions.

Phyllonite belts occur at several locations across the island and are best exposed at Cnoc na Croich (NG 224956) and Kennavay (NG 232 950), where large (c. 10 - 15m thick) belts of phyllonite occur. In contrast to the thrust-related mylonites, the

phyllonitic fabric is never cross-cut by the effects of brittle thrust-sense deformation. Phyllonite generation is therefore inferred to largely post-date brittle thrust-sense deformation.

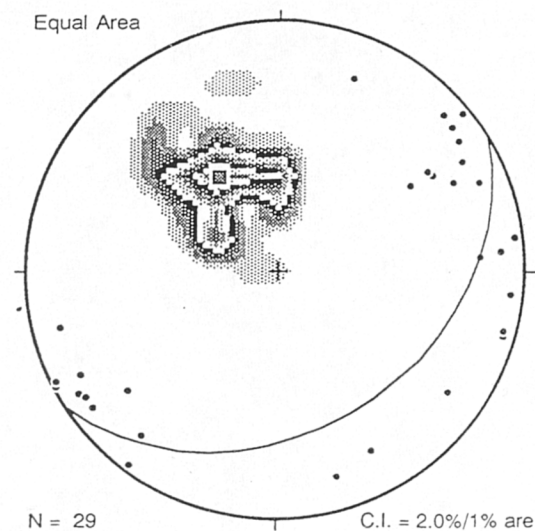
The phyllonites are characterised by a green-grey weathering colour (occasionally cream) and a well developed fissility. Phyllonites are usually fine grained (<2mm), but porphyroclasts of pink feldspar (up to 10 cm) are abundant. These porphyroclasts often occur in distinct bands and may represent disrupted Laxfordian pegmatites. The mineralogy of the matrix is difficult to ascertain in the field due to its fine grain size, but the colour is chiefly derived from the large modal percentage of chlorite, formed largely from the breakdown of mafic relicts in the gneiss, (e.g. hornblende). Quartz and feldspar are present in lesser quantities. Most feldspar has been altered to sericite and epidote.

Thinner discrete bands of shear-banded phyllonites are very common and penetrate all lithologies, but are spectacularly exposed in Laxfordian pegmatites. They are recognised by unusually large porphyroclasts of feldspar surrounded by an epidote and chlorite rich matrix, occasionally with quartz ribbons and /or quartz pressure tails (wings) on some of the porphyroclasts. Phyllonite bands also occur preferentially at lithological contacts, especially between gneisses and pegmatites or gneisses and amphibolites, and are believed to reflect the zones of highest strain in the pre-existing mylonite. The apparent correlation between the intensity of strain in the finer grained regions and the degree of retrogression noted by Sibson (1977b) is believed to result from the exploitation of the highest strain thrust-related mylonites by a new deformation regime which eventually formed phyllonites.

In general, the fissility of the phyllonites results from a well defined foliation, which has a waxy, micaceous sheen which is somewhat phyllitic. The foliation dips c. 40° SE-wards, and a sub-horizontal mineral stretching lineation, defined by chlorite fibres and elongate, sericitised feldspar aggregates, is developed on the foliation surfaces (Fig. 3.13). Numerous kinematic indicators are present and include asymmetric extensional shear bands and asymmetric folds. The kinematic interpretation of these rocks varies from those suggested by previous workers.

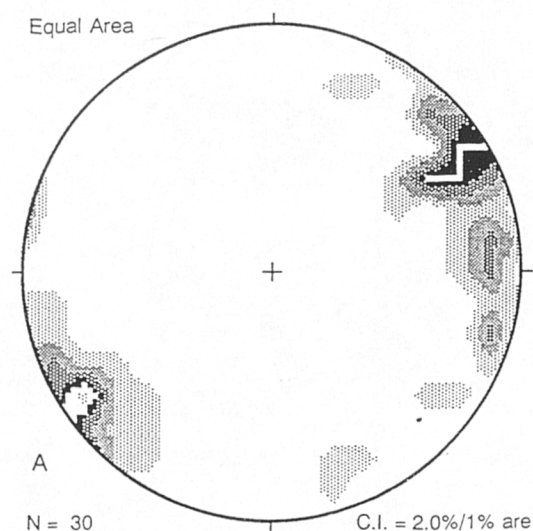
The phyllonitic foliation dips c. 40° SE (Fig. 3.13), at low angles to the phyllonite belt margins and the earlier pervasive mylonite foliation. Asymmetric extensional shear bands (c. 1 - 2cm apart) displace the phyllonitic foliation in a sinistral sense, indicating top-to-the NE sense-of-shear (Plate 3.12a). A well developed mineral elongation lineation, defined by aligned quartz ribbons, fibrous chlorite and pseudomorphed feldspar aggregates on phyllonitic foliation surfaces, trends NE-SW, parallel to the

strike of the regional foliation and the trace of the OHFZ. This lineation is believed to be the same as that referred to by Walker (1990), (see below), as the intersection lineation, but has a different orientation to the intersection lineation (banding / mylonite), seen elsewhere on Scalpay (Fig.3.14). It is thought to be a probable indicator of the local shear zone movement vector at the time of mineral growth.

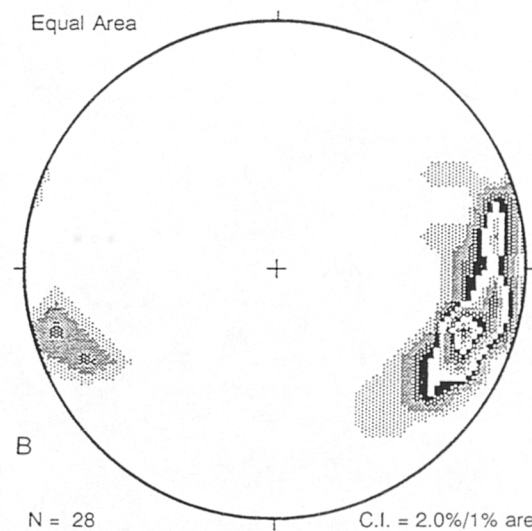


Scalpay
Contoured plot of poles to phyllonitic foliation with mean great circle, and
Mineral lineations in phyllonite

Figure 3.13. Equal area stereonet of poles to phyllonitic foliation and mineral stretching lineations in phyllonites from Scalpay.



Scalpay
Contoured mineral lineations in phyllonite



Scalpay
Contoured intersection lineation of banding and mylonitic foliation

Figure 3.14. Equal area stereonet of mineral lineations in phyllonites, and intersection lineation of banding/mylonitic foliation from Scalpay.

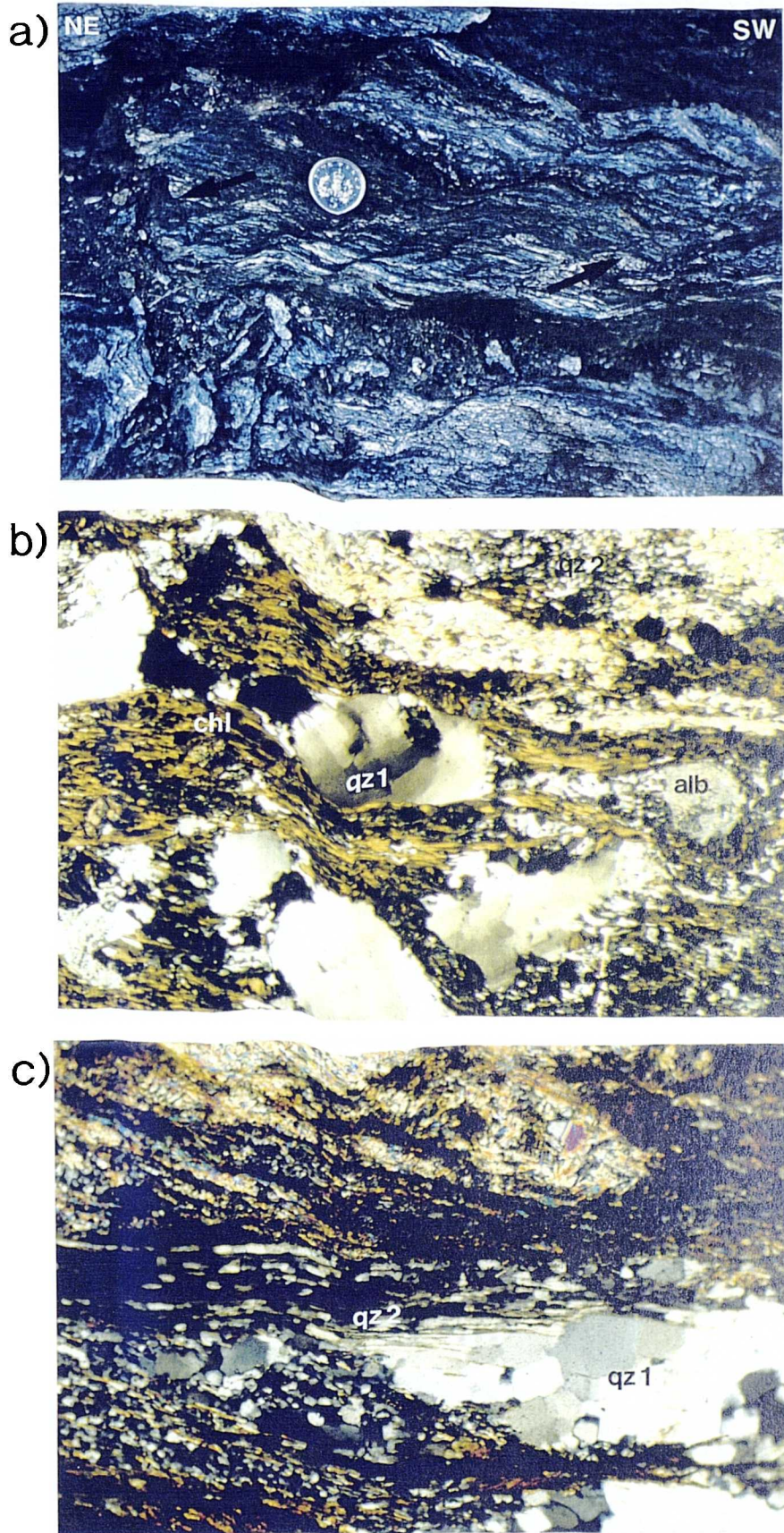


Plate 3.12 Scalpay phyllonites

a) Asymmetric extensional shear bands in phyllonite from Cnoc na Croich, Scalpay (NG 224957). View is down dip, and demonstrates sinistral top-to-the-NE, sense-of-shear.

b) Quartz microstructures from Cnoc na Croich phyllonite belt on the NW coast of Ardsheinish (NG 221953). Relict quartz grains (qz1) show undulose extinction indicative of cold working. Recrystallised quartz grains (qz2) are undeformed. Chlorite (chl) and sericitised albite (alb) occupy the rest of the slide. Field of view is 4mm. (XPL)

c) Phyllonite from Kennavay (NG 233951). Very fine grained quartz ribbons (qz2) occur between epidote rich material and relict subgrained quartz (qz1). The fine grained elongate grains may be stretched recrystallised grains. Field of view is 4mm. (XPL)

The phyllonite belt at Cnoc na Croich (NG 219952) has been studied in detail by Walker (1990). She suggests two sets of phyllonite bands (c. 10-20 cm thick), occur in this belt, both possessing shear sense indicators:

1. Set 1 dips moderately to the NW. Down-dip verging folds within this set suggest a normal dip-slip motion occurred, displacing top-to-the NW. Normal sense shear bands in this set produce a strike-parallel intersection lineation.
2. Set 2 dips at around 20° ESE, cross-cutting set 1 and displacing it sinistrally. Walker regarded the sinistral shear as not regionally important.

Several discrepancies arise by comparison with the present work however:

- The phyllonite belt does not ^{appear to} possess two sets of phyllonite bands.
- fabrics within the phyllonites dip moderately SE. No NW-dipping fabrics have been observed.
- Walker's plate 4.2c ^{appears to have been} presented in reverse, so that the foliation appears to dip NW, when in fact it dips SE.
- Walker's 'set 2' phyllonite bands have not been observed.

On the NE coast of Scalpay, directly along strike from the larger phyllonite exposures at Cnoc na Croich and Kennavay are localised belts of non-retrogressed mylonite. South of the bay at Scoravick (NG 244958), a localised mylonitic zone of very high strain, associated with a brittle fault, possesses strike-parallel mineral lineations and sinistral shear-sense indicators similar to the larger phyllonite belts. Although the belt appears to be of a higher metamorphic grade than the larger phyllonite belts, it probably significantly post-dates the pervasive mylonite belt and its apparent lack of retrogression may reflect a lack of water availability either during or after this phase of deformation. This zone is inferred to be the along-strike continuation of the Kennavay phyllonite belt on the basis of its localised nature and common kinematics.

In some Laxfordian pegmatites (eg at Kennavay NG 233951), thin discrete phyllonite belts usually contain asymmetric extensional shear bands and asymmetric porphyroclasts which suggest top-to-the-E or NE strike-parallel movement occurred in the phyllonites. In some of the thin discrete phyllonite belts, however, kinematic

indicators suggest that thrust sense motion may have occurred (e.g. S.E. of Aird Riabhach, NG 240965). Asymmetric feldspar porphyroclasts and asymmetric extensional shear bands occasionally show an anomalous top-to-the-W or NW shear sense which may be important in assessing the relationship between fault zone movement and the onset of phyllonitisation (see section 3.3.6).

Microstructure

All lithologies on Scalpay show the effects of retrogression, which are most pronounced in the phyllonites. The low-grade assemblages are not reworked by the high greenschist facies mylonites. They are therefore regarded as the result of a later phase of ubiquitous, retrograde metamorphism, associated with sinistral strike-slip on the OHFZ. The belts of phyllonite, where the effects of retrogression are most pronounced, have the assemblage:

Quartz - chlorite - sericite - epidote -opaque minerals (including pyrite) +/- calcite.

Quartz (< c.15% by volume) exists in a variety of states, including isolated grains, fine grained recrystallised aggregates and ribbons. Most of the larger quartz grains show undulose extinction, with little or no subgraining or adjacent recrystallisation. The co-existence of these cold-worked large grains with fine grained, fully recrystallised, polycrystalline (type 1 and 2) ribbons suggests that a large range of pressures and temperatures have affected these rocks (Plate 3.12b), but probably at different times. The heterogeneity in quartz microstructures in the phyllonites may reflect the wide range of pre-existing quartz microstructures. This preservation of microstructural relicts makes those microstructures produced *during* phyllonitisation difficult to determine, although the preservation of large cold worked grains suggests that other mineral phases (e.g. phyllosilicates) have taken up much of the ductile deformation.

Some of the subgrains and recrystallised quartz grains, however, appear to show the same effects of cold-working as the larger grains; a feature not observed in the apparently undeformed recrystallised grains in the earlier mylonites. Both original and recrystallised grains therefore appear to have experienced at least one low temperature deformation.

In the phyllonites, feldspar has been almost completely replaced and often pseudomorphed by extremely fine grained white mica, except where coarse grained protoliths, e.g. pegmatites, have been incompletely retrogressed. The newly formed

sericite often adopts a preferred alignment, parallel to the phyllonitic foliation and is visible, in thin section, as bands of high birefringence which separate bands of quartz aggregates. Rarely, feldspar is replaced by calcite.

All amphibole and biotite have been replaced by chlorite in the phyllonitic material. Chlorite flakes often show a preferred alignment and occasional small scale folds. Opaque minerals, which include pyrite cubes, are largely restricted to areas where chlorite has formed. They appear entirely undeformed and do not possess pressure tails (wings), suggesting they may be post-deformational.

Discrete slip planes parallel, or at a low angle to the main foliation are common in the phyllonites and are defined by extremely fine grained sericite, chlorite, and possible clay minerals. Very fine grained ribboned quartz, which may have been derived from previously recrystallised material also occurs in these areas (Plate 3.12c). Extensional displacements of marker bands on these slip planes, suggest that they acted as asymmetric extensional shear bands. They displace top-to-the-NE, consistent with larger scale kinematic indicators. Additional kinematic indicators include both δ and σ asymmetric porphyroclasts. These are usually of feldspar pseudomorphs, but occasionally unaltered feldspar porphyroclasts occur in areas that appear to have escaped retrogression, (e.g. south of the bay at Scoravick (NG 244958). The asymmetry of non-rotated (Plate 3.13a) and rotated types (Plate 3.13b) indicates a top-to-the-NE shear sense.

Metamorphic conditions during deformation

The replacement of hornblende and biotite by chlorite and epidote suggests that the grade of metamorphism which prevailed during thrusting and mylonite formation, has been reduced. The presence of the index mineral chlorite, without biotite (cf. Sibson 1977b who regarded biotite as present), indicates that metamorphism occurred at low greenschist facies. Replacement of feldspar by sericite, and comparatively low temperature deformation of quartz, is also consistent with this hypothesis. The ubiquitous presence of chlorite fibres and calcite in some phyllonites, suggests that retrograde metamorphism may have occurred in the presence of a fluid phase, and that some minerals may have precipitated from solution. These phyllonites may therefore have acted as diffusive mass transfer (DMT) sinks. Although no true pressure solution cleavage has been observed, phyllonitic slip planes may have acted as fluid channelways, and sources for the removal of material, and the possibility that these phyllonites acted as DMT sources has not been ruled out.

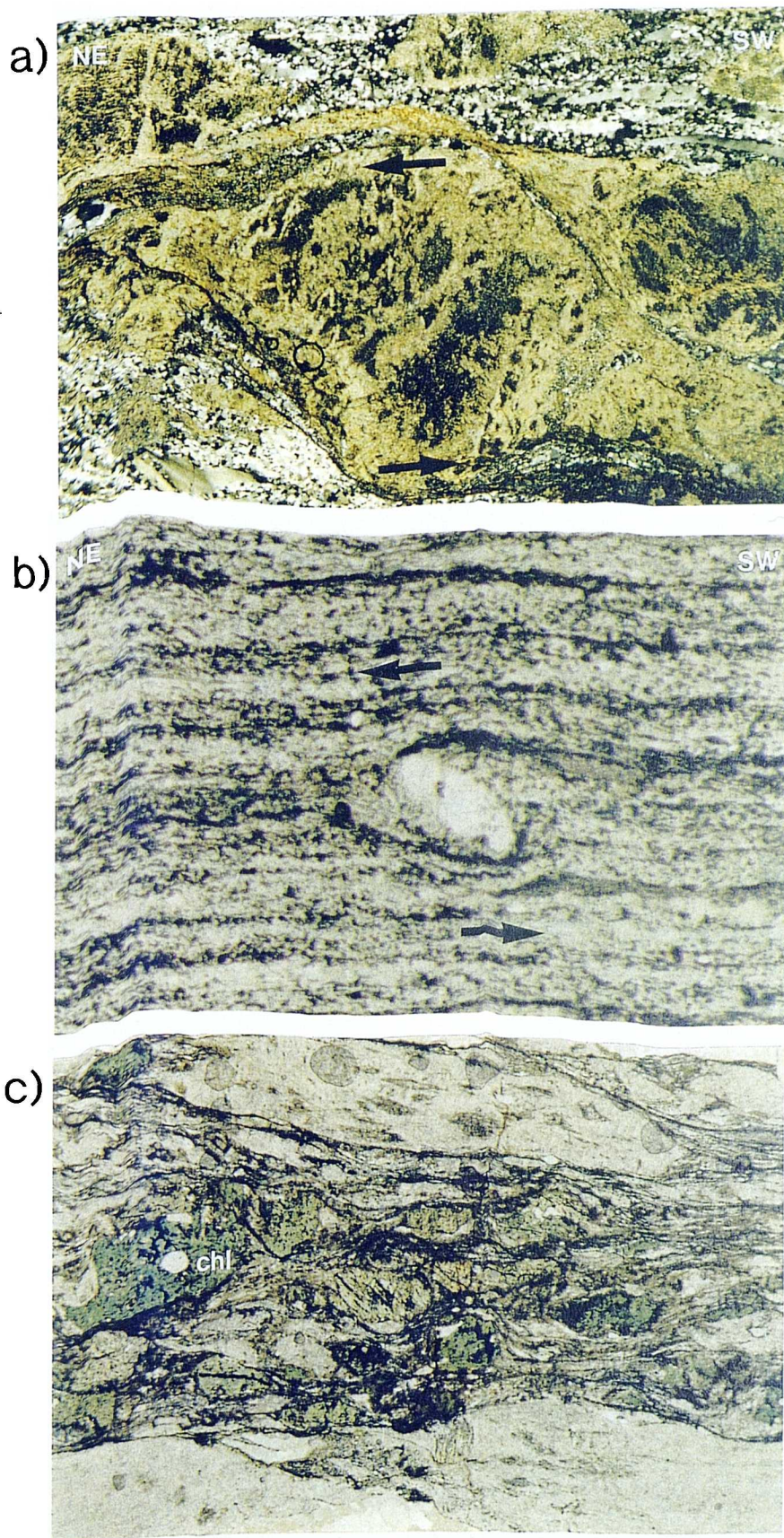


Plate 3.13 Scalpay phyllonites

a) Phyllonitised pegmatite from Kennavay (NG 233951).

Large σ porphyroblast of partially sericitised albite displays top-to-the NE sense of shear. Field of view is 3.5cm. (XPL).

b) Discrete phyllonite from south of Scoravick (NG 244958).

δ porphyroblast of albite possesses asymmetric chlorite and opaque mineral -rich tails indicative of top-to-the-NE sense-of-shear. Field of view is 5mm. (PPL)

c) Discrete phyllonitic layer deforming chlorite-rich amphibole pseudomorphs (chl). The shear foliation post-dates chloritisation, as chlorites are pulled-apart and sheared during deformation.

(NB 286009), where the unretrogressed mylonitic unit dips more steeply SE than the phyllonites, and the mineral elongation lineation plunges down-dip to the SE.

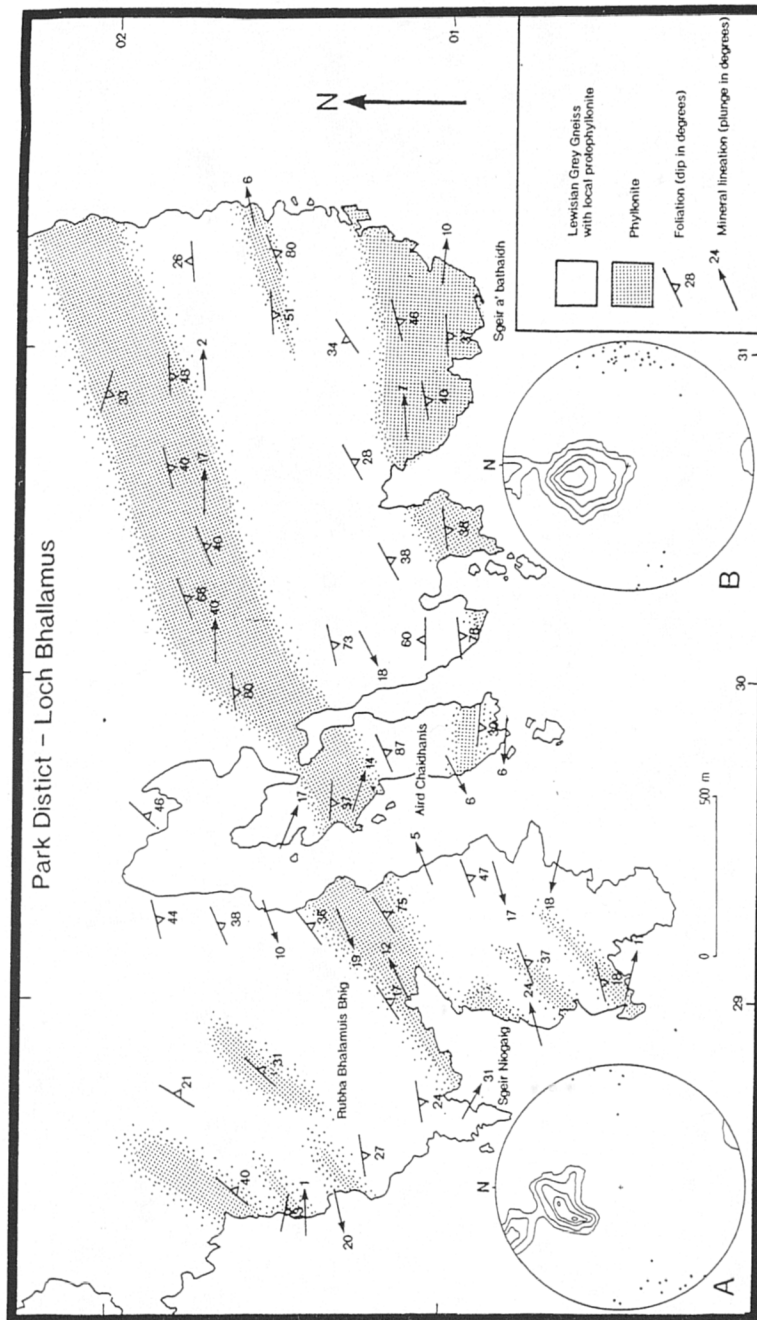


Figure 3.15. Geological map of the area around Loch Bhallamus, southern Park district, Isle of Lewis. Equal area stereonets of:

- Poles to protophyllonitic foliation and mineral lineation in protophyllonites.
- Poles to phyllonitic foliation and mineral lineation in phyllonites

Retrogressed belts of green-weathering phyllonite overprint the deformed gneisses. The phyllonite belts are extremely well developed but often laterally discontinuous, and adopt a regional NE-SW trend. The belts have diffuse margins over c.100m, where the phyllonitic fabric within the belt becomes protophyllonitic and ultimately grades into unphyllonitised gneiss. The lithology is often extremely fissile with a very fine grain size (<1mm). Chlorite, epidote and sericite (replacing hornblende and feldspar) are the dominant minerals, with minor quantities of original quartz. Smaller, m-scale, high strain zones occur throughout the protophyllonitic material, which have locally retrogressed to form thin, discrete phyllonites, similar to those exposed on Scalpay.

The phyllonitic foliation orientation is variable across the study area. Adjacent to the phyllonite belts, a protophyllonitic foliation trends ENE-WSW, striking clockwise of the belt margins by c. 12° and dipping c. 50° SSE. Within the phyllonite belts, the phyllonitic foliation is also oblique to, and clockwise of the belt margins by c. 12°, but dips more shallowly c. 35° SSE. Very well developed mineral elongation lineations defined by quartz rods, quartz-feldspar aggregates and new chlorite fibres are consistently developed parallel to foliation strike, plunging at low angles to the WSW in the protophyllonitic material, and at low angles to the ENE in the phyllonitic material. Occasionally (e.g. on the west side of Aird Chaidhanis (NB 295014), the lineation is extremely strong in the phyllonite and the rock may be classed as an L-tectonite. The structural relationships are summarised in figure 3.16.

Shear sense indicators include the map-scale geometry of the phyllonitic foliation relative to the phyllonite belt margins, asymmetric σ wrapping of amphibolite lenses, small, steeply dipping cm-scale shear zones (Plate 3.14a) and extensional shear bands. These structures suggest that the dominant movement at this time was sinistral strike-slip, identical to that inferred from the Scalpay phyllonites. The regional fabric is oriented more towards E-W, however, and the displacement direction is therefore slightly different. The hanging-wall of the OHFZ appears to have been displaced laterally to the ENE.

3.3.3 Eishken

The largest single belt of phyllonite mapped by the writer in the northern Outer Hebrides stretches c. 3km from the north shore of Loch Shell (NB 319109) to a region of poor exposure near Lochan nan Uidhean Beaga (NB 330140) (Fig. 3.17). Most of the central portion of the belt is obscured by peat bog, but the western margin coincides with an area of good exposure on the east slopes of Beinn Gearaidh Raistail

(NB 318114), where it lies adjacent to undeformed and unretrogressed banded Lewisian gneiss.

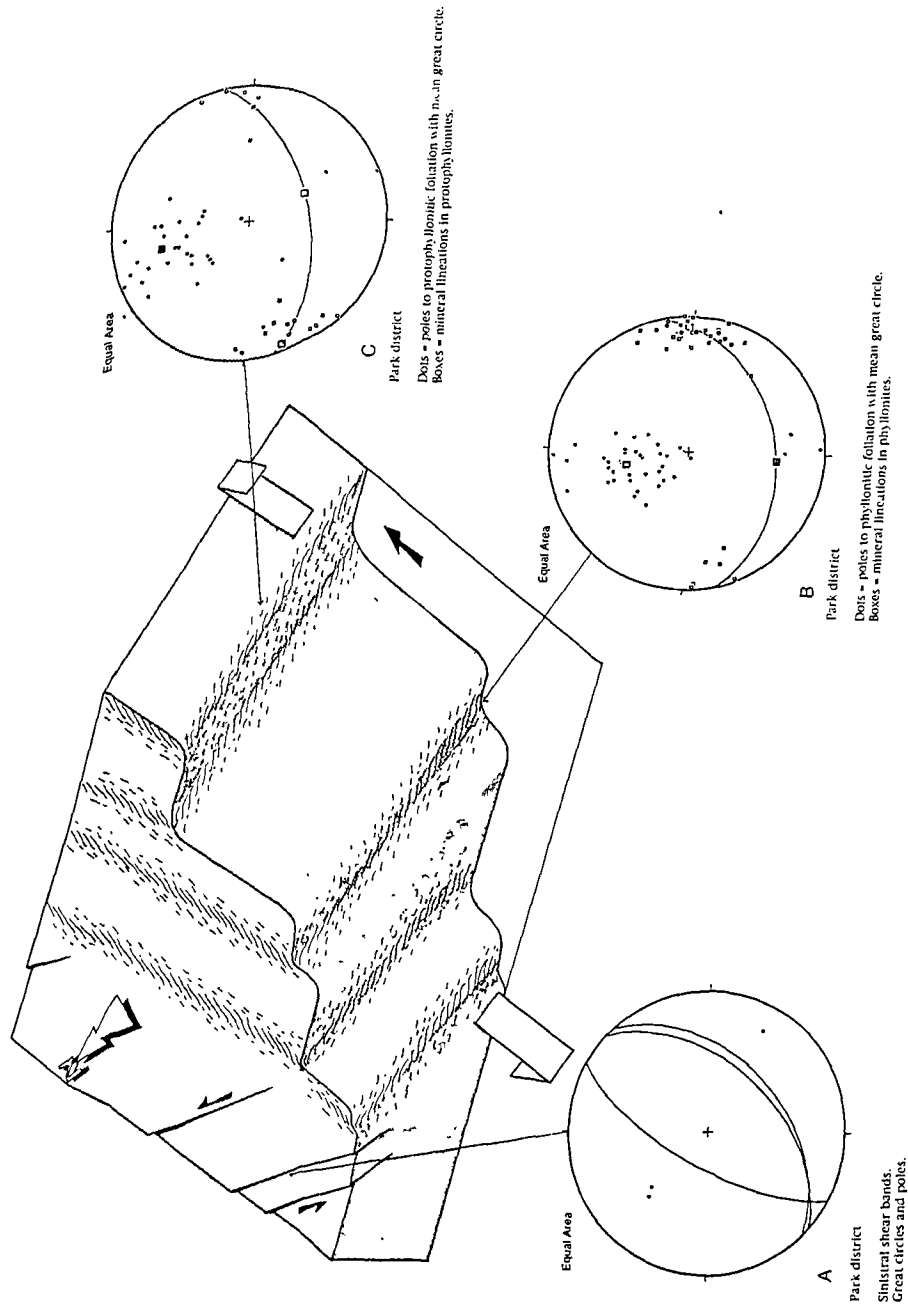


Figure 3.16. 3-D block diagram of structural relationships relating to sinistral strike-slip, in the southern Park district of Lewis. Equal area stereonet of:

- sinistral shear bands
- Poles to phyllonitic foliation and mineral lineation in phyllonites
- Poles to protophyllonitic foliation and mineral lineation in protophyllonites.

a)



b)

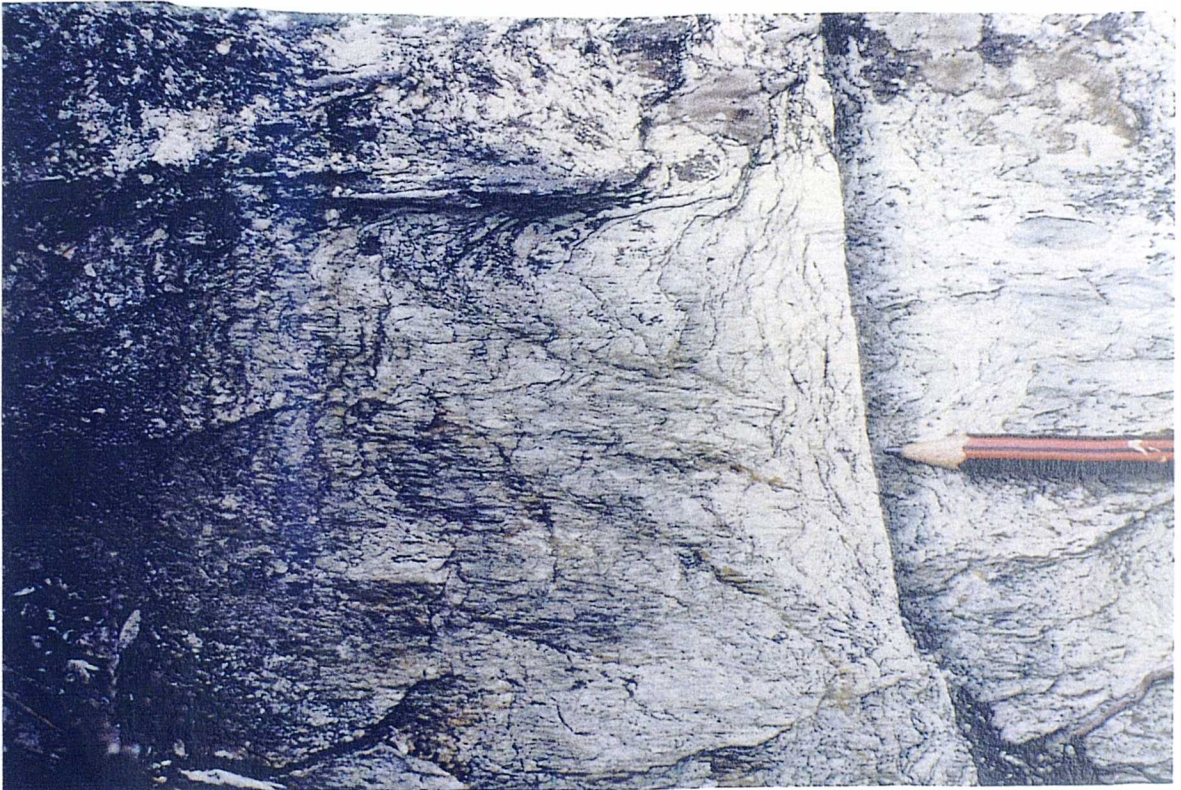


Plate 3.14 Lewis phyllonites

a) Steeply dipping shear zone in partially phyllonitised quartzo-feldspathic pegmatite, from E of Loch Bhallamus (NB 302010). Shear zone is oriented NE-SW and sense of shear is sinistral.

b) Mineral stretching lineation defined chiefly by quartz ribbons in phyllonite from Cleite na Uidhe, Eishken (NB 319122). Lineation is subhorizontal and oriented WNW-ESE.

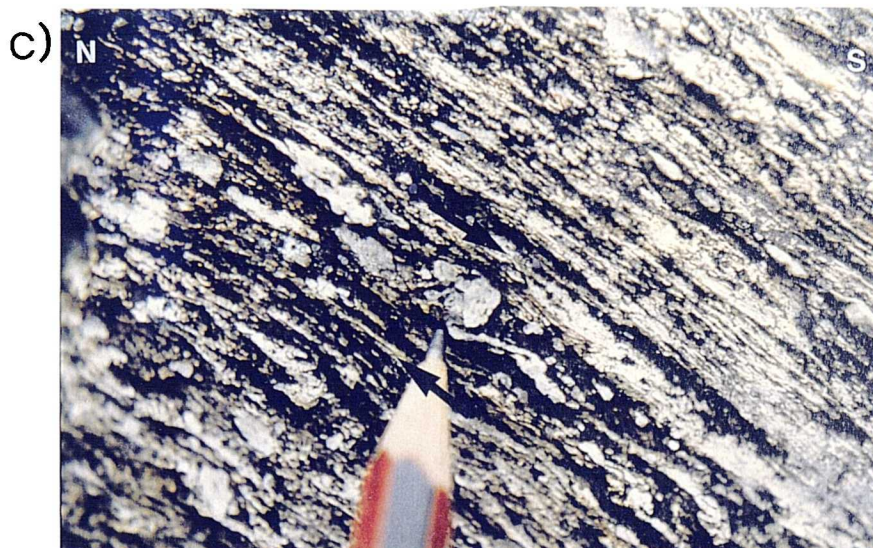
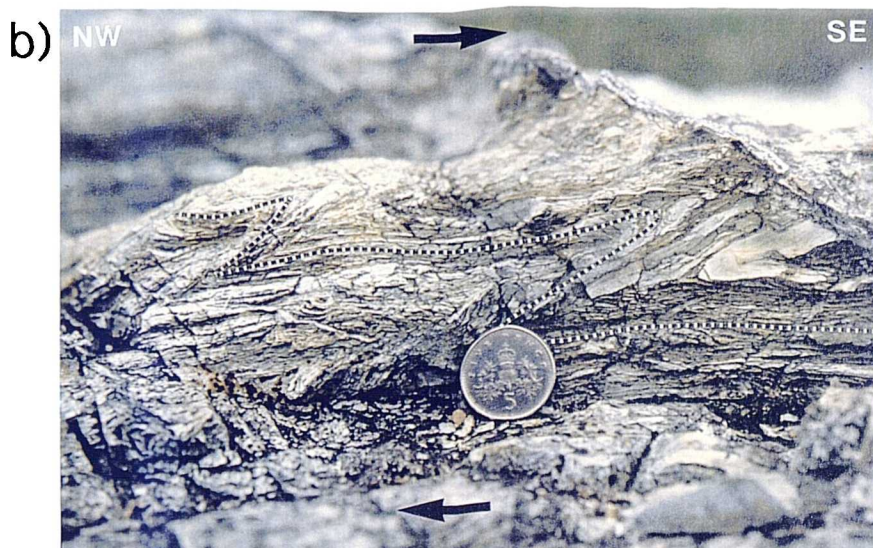


Plate 3.15 Extension-related structures from Scalpay and Lewis

a) SW-verging fold/ fault package from the Kennavay phyllonite belt, S of Kennavay (NG 231947). Note the extensional detachment faults above and below the fold package.

b) SE-verging, extension-related, chevron folds from Airigh Bhinneach Eishken (NB 326132).

c) δ porphyroblast of relict quartz and feldspar aggregate, from Airigh Bhinneach Eishken (NB 326130). Asymmetric quartz tails indicate a top-to-the-S sense-of-shear.

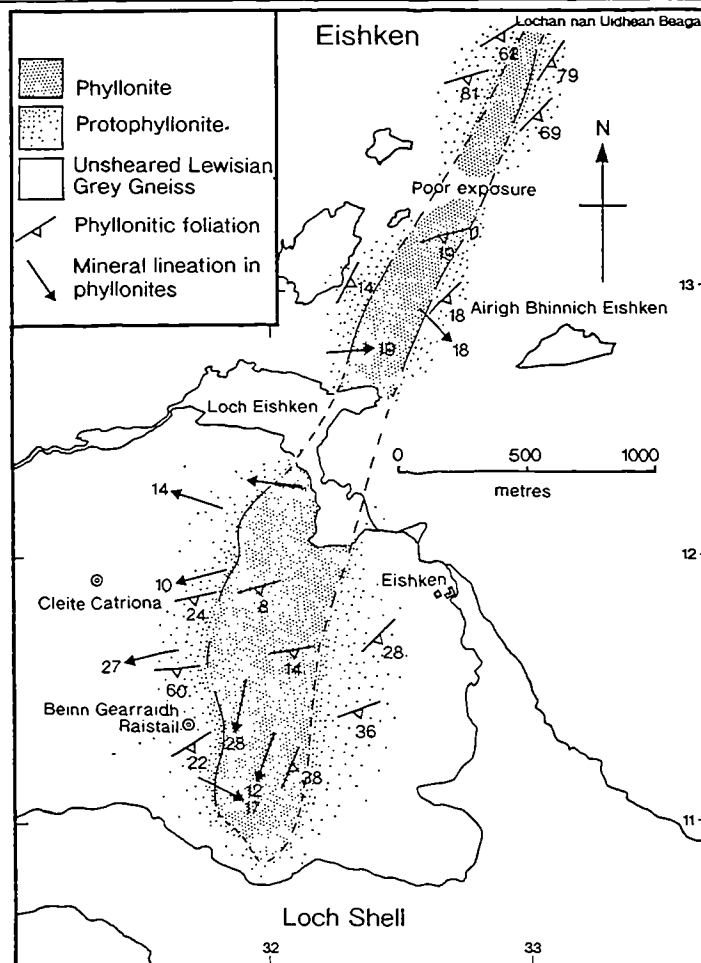


Figure 3.17. Geological map of the area around the Eishken Estate, northern Park district, Isle of Lewis.

The belt lies sub-parallel to the gneissose banding of the country rock, and entirely post-dates extensive brittle faulting, pseudotachylite generation and cataclasis in the host gneiss. The lithology is characteristically green and platy, with a metamorphic assemblage comparable to phyllonites from Scalpay and around Loch Bhallamus, comprising: chlorite - sericite - epidote - quartz and opaques. Amphiboles are never observed in the phyllonite belt, but are abundant in the host rock, indicating a spatially restricted, but complete retrogression to chlorite grade, (low greenschist facies).

The foliation within the phyllonite belt dips shallowly southwards and is unusually oriented at a high angle to the belt margins (Fig 3.18a). The mineral elongation lineation is well defined by elongate quartz ribbons and chlorite pseudomorphs (replacing hornblende) and shows a shallow plunge mostly variable

between E-W (strike-parallel) and SE (oblique to both dip and strike of the foliation) (Plate 3.14b and Fig 3.18b). The high angle between phyllonitic foliation and belt margins can not easily be explained as a result of strike-parallel movement alone. A degree of post-phyllonitic deformation and re-orientation is likely (see section 3.4.3). Significantly, both the strong fissility and retrogression of the phyllonites become less well defined nearer the belt margins, and in these areas, the mineral lineations are less obvious, and trend NE-SW. It is thought that the belt margins preserve clearer evidence for strike-slip movement, which is largely overprinted by subsequent deformation in the central portion of the belt.

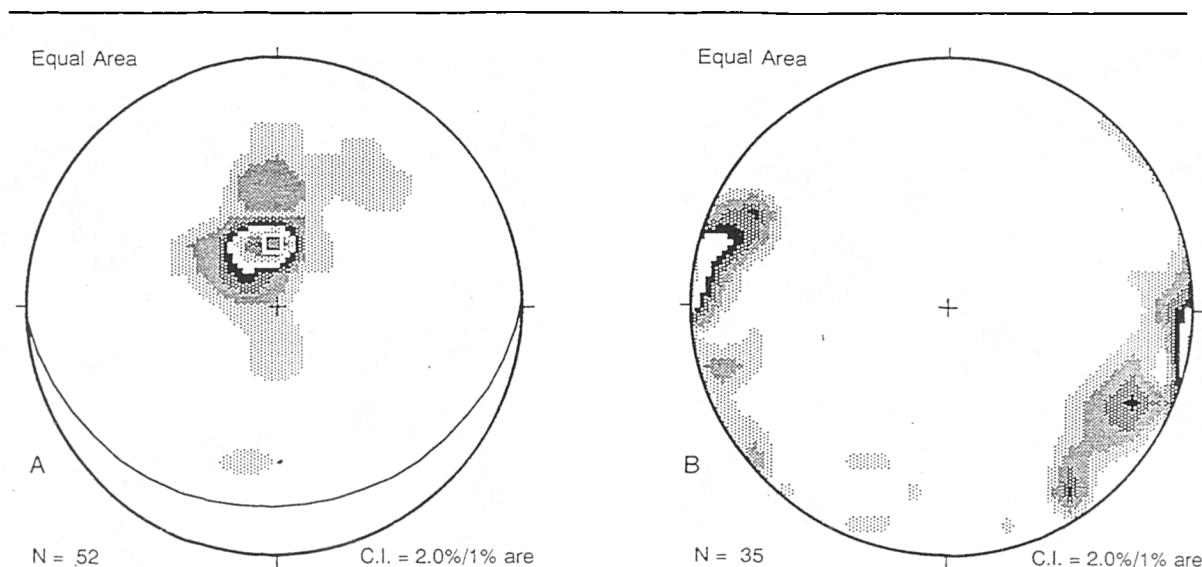


Figure 3.18. Equal area stereonets of:

- a) poles to phyllonitic foliation;
- b) mineral stretching lineations in phyllonites from Eiskén.

3.3.4 Rubha Vallerip

In S. Harris (see Fig. 3.1 for location), a small exposure of phyllonite very similar to phyllonites observed on Scalpay is present at Rubha Vallerip (NG 060830). In contrast to the mylonitised, banded gneiss protolith of the Scalpay phyllonites however, this belt is derived from extensively crushed and cataclased anorthosite of the South Harris Igneous Complex (see Section 2.2.2). In addition, these rocks do not appear to have undergone any ductile, thrust-related mylonitisation, and may therefore have a greater affinity with southern segment fault rocks (see chapter 4). A thickness of c. 20 - 30m of grey-green phyllonite is exposed onshore, bounded on the NW side by crushed anorthosite. The SE side is not exposed. Quartz, feldspar, chlorite, epidote and

sericite constitute the dominant minerals. The phyllonitic foliation dips shallowly towards the SE (c. 25-30°) but in contrast with other localities, the well defined mineral lineation, defined by quartzo-feldspathic aggregates, plunges eastwards. Kinematic indicators are rare in the Rubha Vallerip exposures but exhibit a top-to-the-E shear sense when present. This mineral lineation is thought to be a strike-slip lineation partially reoriented by subsequent deformation (section 3.4).

3.3.5 North-east Lewis

A small (50m wide) belt of blue-grey, phyllonite-like rocks have also been observed SE of the pier at Port nam Bothaig near Port Beag in north-east Lewis (NB 541462) (see Fig. 3.1 for location), and post-dates all brittle deformation. Both Jehu and Craig (1934) and Sibson (1977b) regarded these NNE-dipping rocks as calcareous mylonites because the unit contains abundant calcite, mostly in veins. The assemblage bears a superficial resemblance to that of the phyllonites, with chlorite, sericite, opaque minerals and quartz as the dominant groundmass phases, but original plagioclase is evident, and retrogression is therefore less well developed. In addition, a possible mineral lineation strikes at 011°, consistent with sinistral movement on the NNE-trending fault zone at this location. No ductile shear-sense indicators have been observed in the field or in thin section, and the unusual strike, perpendicular to the trace of the OHFZ, makes the true affinities of this unit uncertain.

3.3.6 Conclusions and discussion on strike-slip movement in the northern segment

Conclusions

Post dating thrust-related ductile *and* brittle fault rocks, are a suite of ductile phyllonites and protophyllonites which have developed heterogeneously across the northern Outer Hebrides. It is suggested that the retrogression of high grade mylonites occurred preferentially in discrete bands, where fluids were channelled through planar anisotropies in the pre-existing crust, and caused local hydration reactions and retrogression. The anisotropies were probably the most highly strained thrust mylonites, or large brittle faults, since the resulting phyllonites always have a close spatial association with highly deformed protoliths, and are usually concordant to a pre-existing foliation, where present.

The kinematic regime

The mineral elongation lineation in the phyllonites is parallel to strike and indicates that movement was dominantly strike-slip. Asymmetric extensional shear band fabrics are the dominant shear criterion present and nearly always display a sinistral sense-of shear with the SE side moving NE-wards. These kinematic indicators are indicative of sinistral strike-slip motion on the OHFZ, either during or post-dating phyllonite formation.

Pressure, temperature and fluid conditions during deformation

In general, the phyllonites appear to have formed at lower temperatures and pressures than the pre-existing pervasive mylonites. Metamorphic assemblages rich in newly crystallised epidote and chlorite but absent in biotite in the phyllonites are indicative of an accompanying retrogressive, lower greenschist facies metamorphism in the presence of large amounts of hydrous fluid. Deformation probably occurred through a number of mechanisms, but diffusive mass transfer (DMT) by fluid flux is believed to be the dominant mechanism. Crystal-plastic deformation may also have occurred, especially in newly precipitated minerals such as chlorite, and the marked absence of brittle fracture processes indicates that ductile deformation mechanisms dominated. This more ductile deformation style associated with phyllonite generation, compared to the brittle deformation style associated with the late stages of thrusting, should not be taken as evidence for an increase in P/T conditions. Deformation occurred without brittle failure, probably as a direct result of fluid induced retrogression to a weaker rheology.

Most authors (e.g. Sibson 1977b, Walker 1990) regard the phyllonites as the highest strain zones within the pervasive mylonites. They suggest that the lower grade of the former resulted from retrogression preferentially focussing into the higher strain zones, but that both rock types were originally generated by thrusting. Sibson (1977b) inferred an increase in palaeotemperature towards SE Scalpay, on the evidence of synkinematic biotite from phyllonites at the extreme SE coastline. Only small discrete phyllonites have been observed from this area however, and the rare biotites which are present only occur in incompletely phyllonitised pegmatite. These biotites are regarded in the present work as pre-strike-slip, and evidence for incomplete retrogression during the phyllonitisation event. No biotite has been found in phyllonites derived from finer grained protoliths (i.e. banded gneiss) and Sibson's evidence cannot be confirmed. The phyllonitic rocks are therefore regarded in the present work as post-dating the bulk of NW-directed thrusting.

Discussion

The change in kinematics from thrusting to strike slip

The anomolous SE plunging mineral lineations present in the phyllonites (Fig 3.19) are likely to have two different origins:

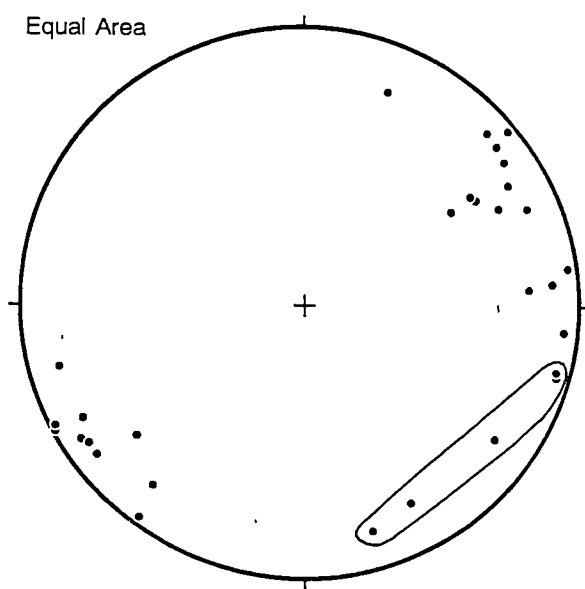


Figure 3.19. Equal area stereonet of mineral lineations in phyllonites from Scalpay, with anomalous SE plunging lineations highlighted.

1. Most SE plunging mineral lineations have a close relationship to a wealth of structures which indicate normal-sense kinematics. These include normal-sense shear band fabrics and apparent dextral / down-dip verging asymmetric folds in the phyllonites on Scalpay, referred to by Walker (1990). They are observed to deform the sinistral shear band fabrics and therefore post-date the strike-slip event. These structures are therefore related to a different kinematic regime, (see section 3.4.1).
2. Top-to-the-W or NW shear sense indicators, accompanied by rare, SE plunging mineral lineations in some of the thin discrete lower greenschist facies phyllonites may be evidence for either:
 - thrust-sense movement which occurred *prior to* phyllonitisation. A thin belt containing thrust-sense kinematic indicators may have been preferentially retrogressed over the surrounding mylonites due to the higher strain and finer grain

size of the discrete belt. This belt may have remained largely unaffected by subsequent strike-slip deformation and therefore preserve earlier features;

- Thrust-sense movement having occurred *during* phyllonitisation. Lower greenschist facies phyllonites produced during thrusting are therefore accompanied by top-to-the-NW kinematic indicators (e.g. asymmetric feldspar porphyroclasts in the discrete phyllonite SE of Aird Riabhach, NG 240 965). It is notable that thrust-sense kinematic indicators have only been observed in thin (cm-scale) phyllonites, suggesting that the larger phyllonite belts preferentially accommodate sinistral strike-slip motion. The change in movement direction from thrust-sense to sinistral-sense of shear may therefore be progressive.

3.3.7 Summary

- Ductile deformation overprints and post-dates ductile and brittle thrust-related deformation.
- Phyllonite development is heterogeneous, forming large areas of metamorphic retrogression and discrete planar belts of phyllonite.
- The geometry and orientation of the phyllonite belts are chiefly dependant on pre-existing anisotropies, e.g. belts of high strain ductile thrust-related mylonite or brittle faults.
- The metamorphic assemblages and fibrous overgrowths of hydrous minerals in the phyllonites suggest fluid-assisted retrogression to low-greenschist facies metamorphism occurred.
- Fluid influx appears to have preferentially localised in discrete anisotropies (forming phyllonite belts). The finer grained, higher strained protoliths may have enhanced permeability and assisted retrogression in localised zones.
- The ductile phyllonites preserve syn-deformational kinematic indicators giving a consistent sinistral strike-slip sense of motion, with the SE, hanging-wall side giving top-to-the NE sense of shear.
- Retrogression is regarded as coeval with sinistral strike-slip and diffusive mass transfer (DMT), and crystal plastic deformation mechanisms appear to be the dominant deformation mechanisms.
- Some phyllonitisation may have occurred during the latter stages of thrusting, preserving local thrust-sense fabrics in thin zones of discrete phyllonite development

3.4 Low angle extensional faulting

Post-dating the rocks derived from thrusting and sinistral strike slip are a suite of extensional structures. These are preferentially localised into, and therefore spatially coincident with, pre-existing belts of phyllonite generated during sinistral strike slip. Mylonites with accompanying chlorite-grade assemblages have developed in places, but the pre-existing lithologies are largely unaltered. Thus, no significant change in metamorphic conditions between the strike-slip and extensional 'events' is obvious.

3.4.1 Scalpay and South Harris

Late, semi-brittle folding of the regional mylonitic fabric is observed from several localities in Scalpay (see Fig. 3.4). Sibson (1977b) noted folds of the mylonitic foliation at the lighthouse (NG 247948), which he regarded as (D2) 'lag' structures. The best examples of late folds, however, occur in the largest belts of phyllonite, which are presumably rheologically weaker than the surrounding mylonites. These folds are chiefly inclined or recumbent, asymmetric, with open to close inter-limb angles, rounded hinges, and a SW vergence (Plate 3.15a). Fold axes are horizontal or gently SE-plunging and possess wavelengths between 5 and 30cm. The pre-existing NE-SW-trending, strike-parallel lineation is folded during this phase of deformation and a new, SE- to SW-plunging mineral lineation of quartz and feldspar aggregates and chlorite fibres, is generated. A change in movement vector is therefore inferred.

The asymmetry of 'Z' - shaped folds in the Scalpay phyllonite belts invokes a dextral strike-slip sense of movement in the phyllonites, opposite to the preceding sinistral strike-slip. This relationship is unique to Scalpay in the northern Outer Hebrides because most structures south of Stornoway, inferred to be coeval with gravity collapse, suggest extension was directed S or SSE. This fold asymmetry may be consistent however, with the south directed collapse vector inferred from the Park district and Eishken phyllonites (see sections 3.4.2 and 3.4.3). Under conditions of top-to-the-south extension, an oblique normal/dextral differential shear component may have been generated in the Scalpay region, and caused clockwise rotation of S-verging folds (Fig. 3.22). The new, apparently SW-verging, orientation is thus a function of *local* re-orientation and does not necessarily require a *regional*, dextral strike-slip displacement.

a)



b)



c)

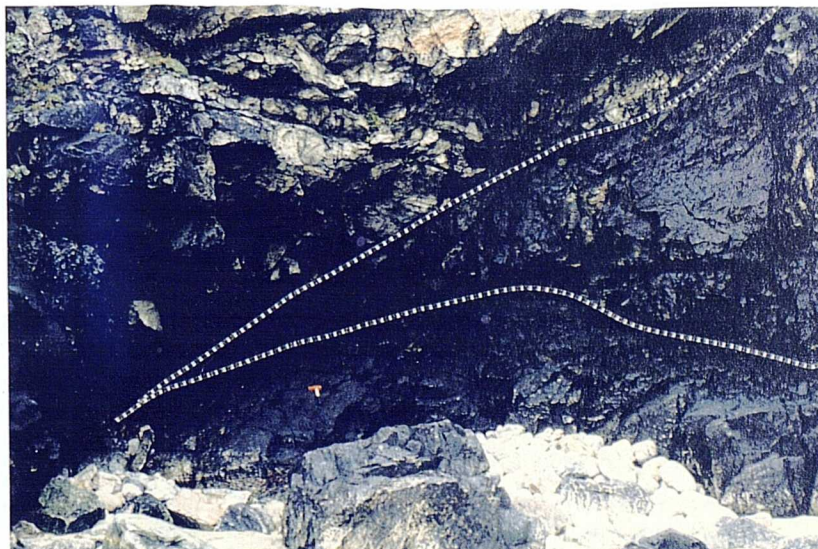


Plate 3.16 Extension-related structures from Lewis

a) Curviplanar, low-angle, extensional faults from Traigh Geiraha, near Gob Hais (NB 538495). The faults cut banded, Lewisian, 'Grey' Gneiss, and displace a Laxfordian pegmatite extensionally, c. 4m toward the NE.

b) S-verging extensional 'collapse' fold from S of Cleit na Uidhe, Eishken (NB 318119). The fold axis is parallel to a well defined, pre-existing mineral stretching lineation, relating to earlier movement.

c) Partially reactivated thrust from beach S of Gob Hais (NB 537494). The large detachment running from upper right to lower left is a hanging-wall short-cut fault displacing yellowish 'Mashed Gneiss, in a normal sense. The curviplanar, low-angle fault is an earlier thrust, displacing top-to-the-N.

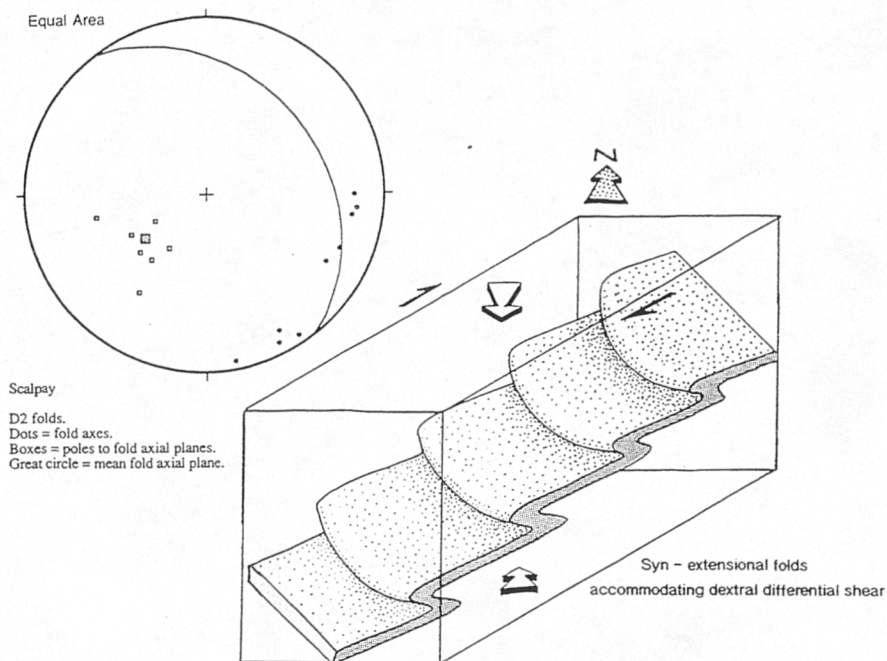


Figure 3.20. 3-D block diagram of extensional collapse folds (D2) from Scalpay. A southward directed collapse vector is envisaged, which causes a dextral differential shear couple, and SW verging folds. Equal area stereonet of poles to collapse fold axial planes and collapse fold axes.

Parallel to the dominant NE-SW striking tectonic fabric in SE Scalpay are numerous low-angle detachment faults. These are particularly well developed within, and bounding the larger belts of phyllonite, and also occur parallel to the mylonitic foliation. This suggests that the presence of a pre-existing foliation is the most important control on localisation of deformation. Low-angle normal faults also occur close to thin discrete belts of phyllonite (< 2m thick) (e.g. SE of Aird Riabhach, (NG 240965)) demonstrating the tendency of low angle faults to exploit the most highly strained and/or most highly retrogressed regions. In general, the detachment faults have a close spatial association with the late folds (D2 folds of Sibson 1977b) and may be broadly coeval. Some faults also occur in non-phyllonitic regions, however, and possess SE-plunging slickensides or striae, and duplex-like structures in some of the larger examples. These kinematic indicators consistently give a top-to-the-SE displacement and suggest that the SE-directed extension on some detachments may be non-coeval with the SW-verging folds. This apparent change in the extension direction is discussed in section 3.4.6.

At Rubha Vallerip in S. Harris (NG 060830), extension to the E or SE is believed to have partially re-oriented a mineral lineation which originally trended NE-SW. The

present E-W orientation is consistent with this clockwise reorientation, and inferred to result from a switch to oblique transtension from sinistral strike slip. This process has been *inferred* in parts of the southern segment of the OHFZ (see section 4.4.1).

Some extensional brittle faulting is associated with the development of quartz tension gash arrays both on Scalpay and extensively at Rubha Vallerip, where N-S trending quartz veins cross-cut the phyllonitic foliation.

3.4.2 The Park district of Lewis

Small-scale folds are abundant in the ENE-WSW-trending phyllonite belts around Loch Bhallamus (NB 294315), and are entirely restricted to the highly strained and retrogressed phyllonites (see Fig. 3.15). The folds are mm-cm-scale structures which are described from other localities by Sibson (1977b) as D2 'lag' folds. They are open to close, often chevron-like, with angular hinges and straight limbs, and slightly curvilinear axes. An axial planar crenulation cleavage is occasionally present. The fold axes are mostly oriented parallel to the strong mineral stretching lineation derived from the earlier strike-slip movement. Fold vergence is consistently down the dip of the phyllonitic foliation. Since the dip of the regional foliation in the Park district is somewhat different to that inferred further south (see section 3.4.1), the displacement direction is also locally different and towards the S or SSE. This interpretation is corroborated by the existence of asymmetric extensional shear bands which are often located in close proximity to the collapse folds and overprint the phyllonitic fabric. All shear bands indicate top to the S or SSE as the dominant displacement direction. These relationships are summarised in figure 3.20).

No brittle detachment faults of the type bounding the phyllonite belts on Scalpay are present and no control on the localisation of faulting appears to be exerted by the strongly developed phyllonitic foliation. This is probably due to the local orientation of the phyllonite belts, which trend at a higher angle to overall strike of the fault zone than those on Scalpay. Brittle extensional faults, which are moderately to steeply dipping and strike NNE-SSW *are* present, and cross-cut fabrics in both the pre-existing gneiss and the phyllonites. These probably relate to a later phase of extension (section 3.5).

3.4.3 Eishken

The NNE-SSW trending phyllonite belt at Eishken (NB 320115), also displays the effects of post-phyllonitic deformation (see Fig. 3.17). Brittle-ductile, chevron-like folds with down-dip vergence, similar to folds associated with extension from Scalpay, Loch Sgibacleit and the Park District are abundant in the Eishken phyllonite (Plate

3.15b). They are usually developed on a mm - cm scale, have shallow, NNW-dipping axial planes, shallow WSW-plunging axes, and consistently verge SSE-wards. An axial planar pressure solution cleavage is occasionally developed. A crenulation cleavage often intersects the original foliation and the resulting intersection lineation is parallel to the fold axes and often also parallel to the mineral lineation. Where the orientation of all linear fabric elements coincide, e.g. east of Cleite Catriona (NB 318119), a strong L-tectonite with a pencil-cleavage results.

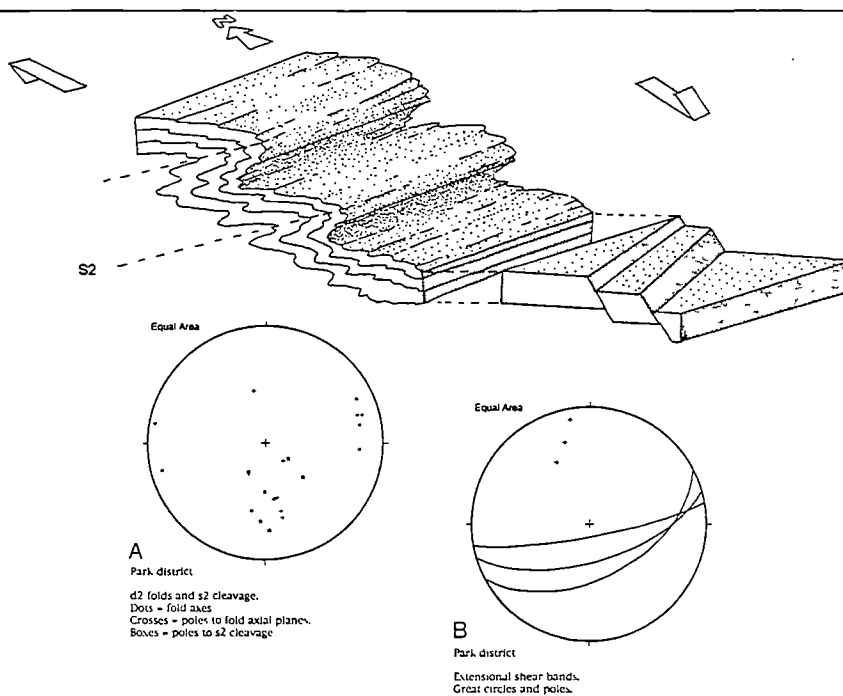


Figure 3.21. 3-D block diagram of structural relationships relating to low angle extension, in the southern Park district of Lewis. Equal area stereonets of:

- a) poles to (D2) fold axial planes, fold axes, and poles to cleavage (S2)
- b) extensional shear bands.

The E-W trend of the phyllonitic foliation, at a high angle of obliquity to the N-S trending belt margins, and the SSE-verging folds can be adequately explained by the effects of extensional collapse (Fig 3.21). Following the sinistral strike-slip movement, top-to-the-south extension is inferred to have caused clockwise reorientation of the foliation in the central part of the belt relative to the belt margins. Passing from the western margin of the belt into the centre, a dextral differential shear component generated the observed reorientation of both foliation and mineral lineation. Relict foliation and mineral lineation orientations are retained close to the belt margins. A south-directed collapse vector is substantiated by the presence of small scale kinematic

indicators, which include asymmetric folds of both the foliation and cross-cutting quartz veins, and asymmetric δ porphyroclasts of feldspar (Plate 3.15c), all of which indicate a top-to-the-south sense-of-shear.

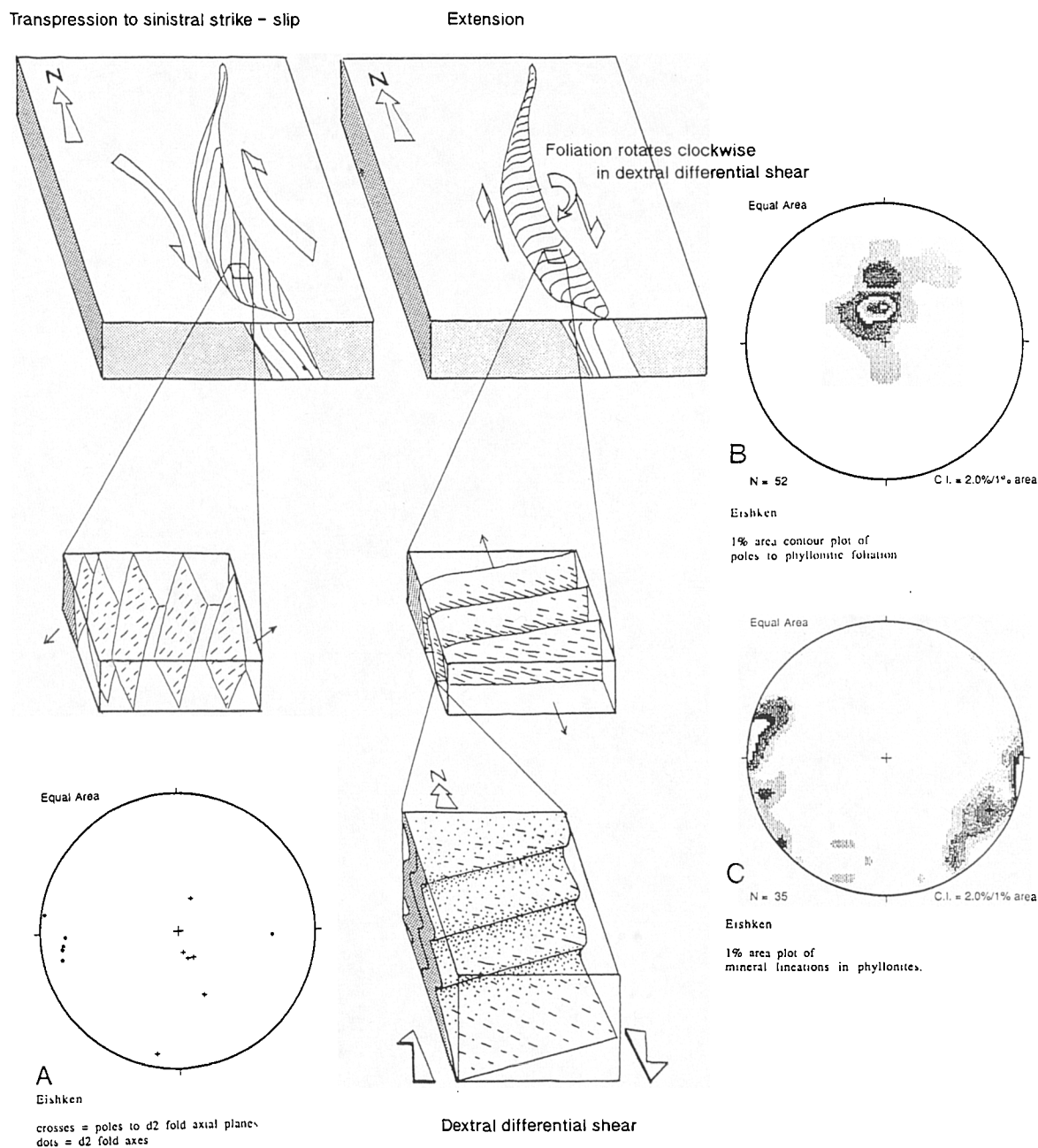


Figure 3.22. 3-D block diagram of structural relationships relating to extension, from Eishken, central Lewis. Equal area stereonet of:

- poles to (d2) fold axial planes and fold axes
- contoured poles to phyllonitic foliation
- contoured mineral lineations in phyllonite

3.4.4 Loch Sgibacleit and central Lewis

Microfaults with normal-sense displacements are common in the deformed rocks of central Lewis and around Loch Sgibacleit (see Fig. 3.7). Most of the faults which cross-cut pseudotachylites and cataclasites have normal displacements, and probably relate to a later phase of large-scale extensional reactivation. Many of these 'late' normal faults do not possess pseudotachylite and cataclasite and are spatially associated with down-dip, SE verging brittle-ductile folds of the mylonitic foliation. These folds often possess angular hinges, sometimes with a fracture cleavage, and bear resemblances to brittle-ductile, extension-related structures in heavily retrogressed phyllonites observed elsewhere. The folds are never cross-cut by thrusts, and the combination of these characteristics may make it possible to distinguish later, extension-related normal faults from earlier thrust-related normal faults.

3.4.5 North-east Lewis

North of Gob Hais, and around Port Geiraha (NB 535499) (see Fig.3.1 for location), the Lewisian gneisses are relatively intact, with SW-dipping banding and occasional relict Lewisian folds. The rocks here are moderately fractured and heavily retrogressed, with abundant chlorite, sericite and epidote. Using the terminology of Fettes et al. (1981), Fettes et al. (1992, after Jehu and Craig 1934), they are probably best termed 'cataclastic' rather than 'mashed' gneiss. Evidence for low-angle brittle normal movement on curvilinear faults is present at Gob Hais (NB 538495), and in the well exposed sea stacks of Traigh Geiraha (NB 537497) (Plate 3.16a). At this location, displaced Laxfordian pegmatites display normal, top-to-the-NE senses of shear.

Similarly, normal faults in the 'mashed' gneisses of Port Beag (NB 544466) also show downthrows to the NE. The regional implications of this faulting are not clear, but the low-angle nature of the structures, and their obvious affinities to low-angle detachments seen elsewhere, suggest that they may relate to extensional collapse on the OHFZ.

3.4.6 Conclusions and discussion on low-angle extension in the northern segment

Conclusions

Overprinting fabrics related to sinistral strike-slip are a suite of structures, including faults and folds, which relate to extensional reactivation. These structures are 'passive', in that the direction of extension appears to be largely controlled by the dip of the pre-existing foliation, and displacements are generally down the palaeoslope. For

this reason, extension is believed to result from the influence of gravity and not from tectonic forces, which promote 'active' extension.

Extensional 'collapse' structures are preferentially located in pre-existing phyllonite zones, suggesting that these rocks are rheologically weak, and tend to localise subsequent deformations. Where extensional detachment faults occur in non-phyllonitised host-rock, phyllonites are either completely absent (e.g. Loch Sgibacleit) or may be present in a non-ideal orientation for reactivation (e.g. the southern Park district of Lewis).

The kinematic regime

All structures which post-date the sinistral strike-slip-related deformation, show geometries indicative of extensional movement. 'Collapse' folds display a ruck-like geometry, suggesting a sticking point on the slip surface has caused localised hanging-wall compression, and fold vergence is always down-dip.

Conditions of deformation

Brittle-ductile behaviour during gravity induced collapse is likely to have occurred under low P-T conditions. Few new minerals have grown during this phase of deformation, and the low greenschist facies phyllonites have not been metamorphically altered. The presence of chlorite fibres aligned with the extension direction in some phyllonites suggests the presence of a fluid phase and the operation of DMT deformation mechanisms. A pressure solution cleavage, axial planar to the collapse folds in the Park district and Eishken, suggests the removal of material via solution. Thus, the phyllonites appear to have acted as both DMT sources and sinks during gravitational collapse.

Discussion

Pre-existing fabric controls on the extensional displacement direction

It seems likely that the arcuate swing in the OHFZ trace from a NNE trend in S. Harris, through a NE trend in Scalpay, and ultimately to an ENE trend in the Park district, is partially responsible for two observed geographical differences in extensional fault behaviour;

- Localisation of detachment faults
- Extensional 'collapse' vector

Detachment faults

The SE-dipping phyllonite belts in Scalpay are bounded by normal detachment faults. In contrast, the phyllonite belts in the Park district, around Loch Bhallamus are not fault-bounded, but have gradational margins. The pre-existing phyllonitic anisotropy in Scalpay is therefore inferred to be both rheologically weak, and ideally oriented for extensional reactivation, focussing both brittle-ductile folds and extensional detachments into the phyllonite belts. By contrast however, the Park district phyllonites (which are presumably rheologically similar to those on Scalpay) are inferred to be less favourably oriented. The ENE orientation has prevented extensional brittle faults from focussing into the phyllonite belts. Significantly, the faults observed around Loch Bhallamus in contrast to those on Scalpay, cross-cut the phyllonites, often at high angles, and may relate to later, high-angle extension (see section 3.5).

'Collapse' vector

The collapse fold vergence direction in the Park district is also controlled by pre-existing fault zone architecture, and displaces top-to-the-S or SSE. Significantly, the well-developed strike-parallel mineral lineation, in the Eishken and Park district phyllonites, is parallel to the collapse fold axes (Plate 3.16b). This strong linear anisotropy may have 'corrugated' the foliation and formed a strong structural control, effectively preventing the range of fold axis orientations observed elsewhere. In Scalpay, detachment faults displace top-to-the-SE, down the dip of the pre-existing foliation, but the fold geometries within the phyllonite belts are not controlled by the foliation and do not verge directly down-dip. The collapse-fold vergence in Scalpay is anomalously SW-directed, and probably results from a dextral shear couple, generated by top-to-the-S extension on a NE-SW trending phyllonite belt. The change from top-to-the-S extension indicated by fold vergence to top-to-the-SE extension indicated by brittle detachment faults suggests a protracted history of extensional collapse may have occurred, involving a change in extension direction.

A marked bimodality in the inferred collapse direction is apparent in northern Lewis. North of Stornoway, extensional faults appear to displace towards the NE, whilst south of Stornoway, folds and faults indicate a SSE or S collapse vector (except in Scalpay, discussed below). It is thought that this bimodality may be related in some way to the presence of the Mid-Minch high, a culmination of Lewisian basement and Torridonian cover rocks, stretching from the region of Raerinish Point (NB 430250) in Lewis towards Gruinard Bay in mainland Scotland. North of this structure, collapse is towards the NE, and south of it, towards the SSE.

3.4.7 Summary

- Brittle-ductile deformation, forming ruck-geometry 'collapse' folds and faults, overprints and therefore post-dates deformation relating to sinistral strike-slip.
- Extensional deformation has preferentially focused into the phyllonite belts. Relatively little extension is accommodated outside the phyllonite belts
- The pre-existing low-greenschist facies assemblages in the phyllonites are not altered by the extension event.
- Diffusive mass transfer (DMT), deformation mechanisms dominate during extension and include the removal of material from pressure solution 'source' areas and the deposition of material as fibrous growths. Crystal plastic and brittle fracturing deformation mechanisms also operate during extensional movement.
- Kinematic indicators associated with down-dip plunging mineral elongation lineations mainly give down-dip, normal senses of shear.
- The extension directions are 'passively' controlled by the orientation and geometries of the pre-existing fabric, suggesting extension may have resulted from gravitational collapse. In areas where pre-existing fault-zone fabrics are not ideally oriented for reactivation, extensional faults cross-cut the fabrics.
- Collapse fold axes form parallel to pre-existing mineral lineations, suggesting that a strong control on fold orientation is provided by a linear fabric element.
- In Scalpay, the extensional collapse direction is dictated by the regional orientation of the fault zone further north. A dextral differential shear component results, and folds verge anomalously SW.
- The inferred collapse vector shows a marked bimodality in Northern Lewis. This is believed to relate to the presence of the Mid-Minch High offshore.

3.5 High-angle extensional faulting and syn-tectonic sedimentation

The final major deformation 'event' to have affected the northern Outer Hebrides, involves a set of steeply dipping, highly brittle faults which cross-cut all previous structures, and are believed to be the last manifestation of onshore tectonic activity on the OHFZ. These faults consistently show normal, down-dip displacements, and are probably associated with the development of the Sea of the Hebrides, North Minch and North Lewis basins. The faults are developed to varying extents throughout the OHFZ, but are more common close to the eastern coasts, especially in Lewis.

Close to Stornoway, they act as bounding faults to the (?Permo-Triassic) Stornoway Formation sediments (discussed in section 2.5).

3.5.1 Scalpay

Small scale, N-S trending normal faults, which dip moderately to steeply E, are common in the gneisses and mylonites of Scalpay. They are generally small and have typical displacements of only c. 5 cm. Larger m-scale normal faults occur along the north coast of Scalpay, and fault splays forming extensional duplexes are occasionally present in these structures. The orientation of these faults appears to be strongly influenced by anisotropies such as the SW-NE-striking mylonitic foliation and/ or gneissose banding. Most faults displace top-to-the SE, directly down-dip, but a second, (possibly conjugate) set is also apparent (Fig. 3.23) and displaces top to the SW.

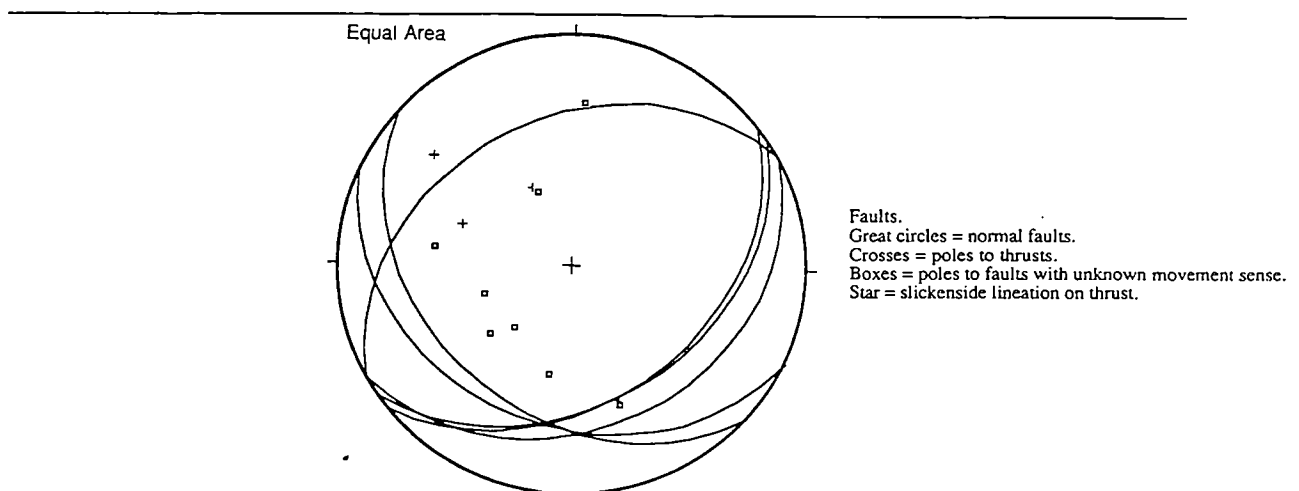


Figure 3.23. Equal area stereonet of late-stage high angle normal faults from Scalpay.

3.5.2 The Park district of Lewis

No evidence for the 'D₃' phase of late-stage faulting (Sibson 1977b) has been found, but the moderately-dipping 'topographic' faults around Loch Sgibacleit, that Sibson regarded as thrusts, may have been produced by large-scale normal movement (see section 3.2.2). These faults are planar, possess SE plunging striae indicative of dip-slip movement, and appear to have escaped the effects of folding (D₂ lag-sliding folds of Sibson, 1977b), commonly associated with extensional collapse elsewhere, and may therefore post-date most of the deformation. Alternatively, 'topographic' faults may be earlier brittle thrusts, generated during overall top-to-the-NW compression, that have experienced late-stage, normal-sense reactivation, and redefinition. In either

case, dip-slip movement which post-dates all previous deformation is envisaged to have occurred on these faults.

3.5.3 North-east Lewis

South of Gob Hais, on a well exposed beach section at NB 537494, steep normal faults displace earlier low-angle normal faults and low-angle thrusts, extensionally (Fig 3.24), and in one case, normal movement appears to have partially reactivated a low-angle thrust by way of a hanging-wall short-cut fault. (highlighted on Fig. 3.24 and Plate 3.16c). The deformation regime for all these structures is either brittle or sub-brittle and these events may be closely timed. The steeper set of normal faults in Fig. 3.24, appears to form a conjugate set similar to that observed in Scalpay, and serves to thin the section.

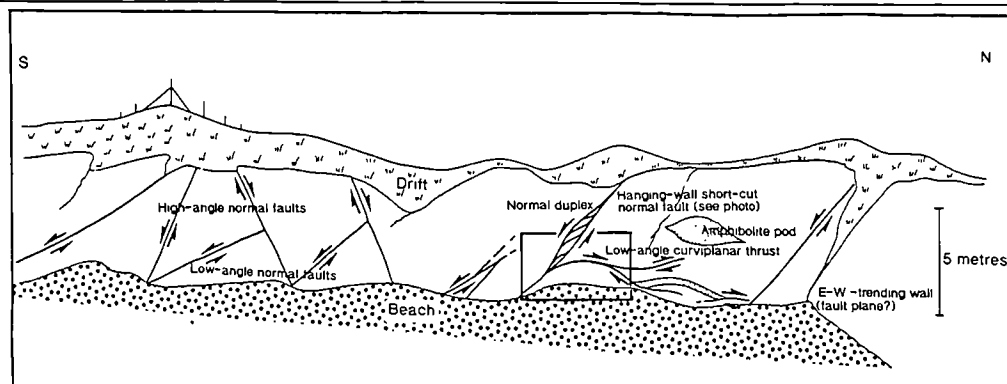


Figure 3.24. Sketch section of low-angle and high angle faults from south of Gob Hais (NB 537494).

At Arnish (NB 425304), steep faults with 0.5 cm of incohesive foliated and non-foliated gouge are present. Displacement of marker bands, show that some faults have normal senses of movement. These steep faults are superficially similar to basin bounding faults observed around Stornoway, and may be synchronous with basin development.

Syn-tectonic sedimentation

Offshore basin development may have occurred synchronously with widespread, moderate-to-high-angle brittle normal faulting onshore. Part of the western margin of the North Minch Basin is believed to be exposed west of the town of Stornoway in Lewis (Steel and Wilson 1975). Eastwards from the margin, unmetamorphosed and undeformed conglomeratic sediments of the Stornoway

Formation (described in section 2.5) overlies the basement gneisses. Conclusions derived from the structure of the basin margin and clast composition within the conglomerates, have important consequences regarding the timing of onshore movement on the OHFZ. The Stornoway formation has been studied in detail at several localities, including Dun Mor (NB 515340), Roisnis an Ear (NB 511339) Allt Raonadale (NB 516434) and Arnish Point (NB 428303).

Structure of the Stornoway Formation

The Stornoway Formation has a shallow (c. 30°) WNW dip in the east which decreases westwards to c. 10-15° WNW near Stornoway (Steavenson 1928). The eastern boundary with the Lewisian is an irregular erosional unconformity and is well displayed at Roisnis an Ear (NB 511339), and at a small outlier at Dun Mor (NB 515340) near Garrabost on the Eye Peninsula. At the latter location, the immediate contact shows numerous filled hollows and Neptunian dykes of mudstone in the gneiss. In contrast, the western and southern contacts with the Lewisian are largely not exposed, but have been inferred to be defined (Steel & Wilson 1975), by steeply dipping (c. 50°) normal faults, one of which is exposed on the northern boundary near the mouth of Allt Raonadale (NB 516434). Identical, subparallel faults occur in the adjacent basement and have a normal displacement. Steavenson (1928) noted that within 1 - 3m of the faulted contacts, the conglomerates are generally shattered, with minor red-coloured gouge-filled fractures. Faults within the formation are not confined to regions adjacent to faulted contacts however. Some moderately dipping faults with clayey red gouge have been observed immediately adjacent to the unconformities at Dun Mor (NB 515340) and Roisnis an Ear (NB 511 339), and are *believed to relate to* minor post-depositional extension. Away from the contacts the sediments are homogeneous and free of cross-cutting faults.

Sedimentary structures in the Stornoway Formation are infrequent, but occasional cross laminations in the coarse sandstone lenses indicate a current flowing from southwest to northeast. Similarly, possible pebble imbrication in the largely massive, structureless conglomeratic horizons corroborate this conclusion. Other than the bounding faults, no tectonic structures are present.

Composition

The conglomerates contain subangular or rounded clasts of up to 2m but most are pebble or cobble sized (c. 5-10 cm). The clasts are locally derived Lewisian gneisses of acid and basic compositions in varying states of alteration and iron

staining. Pegmatites, (presumably of Laxfordian age) and metabasites, (possible 'Younger Basics') are also present. Examples of cataclased and brecciated gneiss, frequently injected with pseudotachylite and/or ultracataclasite are common, but constitute a relatively minor portion (<10%) of the total clast composition. The pseudotachylite is usually devitrified and replaced with epidote and chlorite (see section 2.5 and Plate 2.7), which Dougal (1928) identified as epidosites and flinty crush pebbles. The "lenticular seams and nests of soft, chocolate-coloured sandstone" described by Peach & Horne (1930) are finer grained derivatives of the same parent rock. The matrix in both the conglomerates and the sandstones is often calcareous and occasional patches of calcite are present, filling the spaces between clasts.

Implications for a lower age limit on fault zone movement

The presence of cataclastic and crushed gneiss, and the frequent occurrence of epidote rich veins of replaced ultracataclasite and/or pseudotachylite as clasts within the Stornoway Formation, suggest that the sediments post-date most brittle movement on the onshore Outer Hebrides Fault Zone. The basement close to the Stornoway Formation is relatively unaffected by fault zone movement and the provenance of the sediments is probably extremely local. This may explain why a low modal percentage (<10%) of all clasts are fault products.

The bounding faults to the Stornoway Formation are unaltered and free of cross-cutting faults. This suggests that they post-date all onshore movement on the OHFZ. They may be synchronous with very similar, high-angle faults commonly observed in NE Lewis, and are probably syn-depositional. The only tectonic structures *within* the formation are minor faults, close to the basin bounding faults and unconformity. These gouge-filled fractures relate to minor extension after sediment deposition and are probably not generated by renewed tectonic activity on the OHFZ.

3.5.4 Conclusions on steep faulting and syn-tectonic sedimentation

Steeply dipping brittle faults cross-cut all other structures, and are therefore regarded as the last manifestation of tectonic activity on the OHFZ in the northern Outer Hebrides. The change from low-angle normal faulting to high angle normal faulting has been documented in parts of mainland Scotland (Holdsworth 1989). The change in fault geometry represents a change from 'thin skinned' reactivation of pre-existing structures by gravity, to whole-crustal 'thick skinned' faulting brought about by tectonic extension and culminating in the formation of the Mesozoic basins offshore.

Conclusions

The kinematic regime

The lack of kinematic indicators on these steeply dipping faults, makes detailed analysis difficult, but most faults south of Stornoway displace marker bands extensionally, and appear to extend to the south or east. North of Stornoway, extension directions are unknown, but they probably extend to the east (as inferred from faults bounding the Stornoway Formation sediments) or the NE, displacing low-angle NE-directed extensional detachment faults.

Pressure, temperature and fluid conditions during deformation

The very brittle nature of deformation, lack of new minerals or recrystallisation, suggests that deformation occurred at very low P/T conditions, representative of near-surface crustal depths.

Timing of onshore extension

Whilst extensional movement on the OHFZ may have continued offshore as a result of partial reactivation of the structure at depth (Stein 1988, Huyghe and Mugnier 1992), the cessation of onshore movement on the OHFZ can be confidently postulated as earlier than the Permo-Triassic. Clasts of several fault rock types in the Permo-Triassic Stornoway Formation conglomerates put the main onshore movement before sedimentation. In addition, the lack of cross-cutting faults in the succession suggests that no significant onshore movement post-dated sedimentation. This suggests that Walker's (1990) inferred Tertiary phase of phyllonitisation is unlikely to be correct.

3.5.5. Summary

- High-angle extensional faults cross-cut all previous deformation and are probably the last manifestation of onshore OHFZ movement
- The faults displace extensionally to the E or SE and are best developed on the east coast
- A second, possibly conjugate, W-dipping fault set is also occasionally developed
- The faults are syn-depositional, acting as bounding faults to the Stornoway Formation
- The Stornoway Formation is largely free of cross-cutting faults and OHFZ products are common clast constituents in the Stornoway Formation, suggesting that deposition post-dates all onshore OHFZ movement.

- A younger age limit on OHFZ movement of Permo-Triassic is probable

3.6 Chapter conclusions

Field evidence demonstrates a polyphase deformation history for the northern Outer Hebrides region. After Scourian and Laxfordian deformation of the Lewisian gneisses, early ductile movement on the OHFZ was responsible for re-orienting regional gneissose fabrics from a dominantly NW-SE trend in the western parts of the Lewis and Harris to a NE-SW trend, east of the fault zone trace. Once this shear foliation had been generated, it acted in part as a zone of preferential reactivation during the subsequent, protracted history of fault zone movement.

Distribution of fault rocks

The distribution of deformation products relating to the OHFZ is geographically variable. A NNE-SSW trending, wide and bifurcating belt of ductile mylonites, which dip moderately SE, formed in response to the earliest fault movement. These rocks were generated during bulk compression, in a NW-directed overthrust setting, and are strongly developed in the southern part of the islands and become apparently less well-developed further N. Brittle deformation, probably also generated by thrusting, was in part focused into areas of ductile deformation, occupying the eastern side of the islands. The distribution of brittle rocks is more widespread than the preceding ductile rocks. Examples of brittle deformation including pseudotachylite generation, are known from areas significantly west of the main deformation zone. In addition, brittle deformation is abundant in areas where ductile deformation is absent, e.g. north of Stornoway, in Lewis. In general, brittle deformation occurs across the entire fault zone, but in contrast to its ductile precursor, is less well developed in the southern part of the islands, and better developed in the north. Both ductile and brittle deformation phases are present in the central region, an area which also coincides with maximum pseudotachylite generation.

Overprinting these ductile and brittle rocks are a suite of phyllonites and protophyllonites. These are subparallel to the mylonitic foliation, and dip dominantly SE (or S, where the fault zone swings from NNE to ENE). They are foliation-concordant belts of green, highly retrogressed ductile rocks, with newly formed fabrics. These belts are most common in the central part of the fault zone; thinner phyllonite strands are developed in the southern part. They may represent fluid channelways, where hydrous

fluid has fluxed along pre-existing anisotropies, (e.g. highly strained mylonites or brittle concordant faults), and retrogressed the high grade assemblages in the immediate vicinity.

Faults and folds associated with a passive phase of brittle-ductile extensional collapse are virtually exclusively developed in the zones of phyllonite, suggesting that a large rheological contrast existed between phyllonitised and non-phyllonitised rock. The NNE-SSW-trending weak strands of phyllonite are host to down-dip verging folds and low-angle detachments. In areas where phyllonites are oriented in a roughly E-W orientation (e.g. the Park district of Lewis), down-dip verging folds are still focussed into these areas, but brittle detachments are markedly oblique, trending NNE-SSW and cross-cutting the phyllonites. Where phyllonites are absent, collapse folds form locally in the early mylonites (e.g. Loch Sgibacleit). Where phyllonites *and* early mylonites are absent (e.g. north of Stornoway), collapse folds are absent altogether, and brittle *extensional* faults are the only expression of gravitational collapse.

The final manifestation of OHFZ-related movement is a period of high-angle normal faulting, synchronous with sedimentation and inferred to be associated with the evolution of hanging-wall basins. This represents a shift in the extensional driving force from gravity-driven 'thin skinned' tectonics, to tectonically driven 'thick-skinned' tectonics.

Changes in Kinematics

The kinematic history of the northern segment of the OHFZ involves:

1. Ductile thrusting (forming mylonites);
2. Brittle thrusting (forming cataclasites, pseudotachylites, and abundant microfractures);
3. Ductile sinistral strike-slip (forming phyllonites and protophyllonites);
4. Brittle-ductile extension (mainly *deforming* phyllonites);
5. Brittle extension (forming ubiquitous, steep normal faults);

The kinematic history of the entire northern segment of the OHFZ may be summarised as a traditional 'D-number' sequence (Fig. 3.25) or as a continuum (Fig. 3.26).

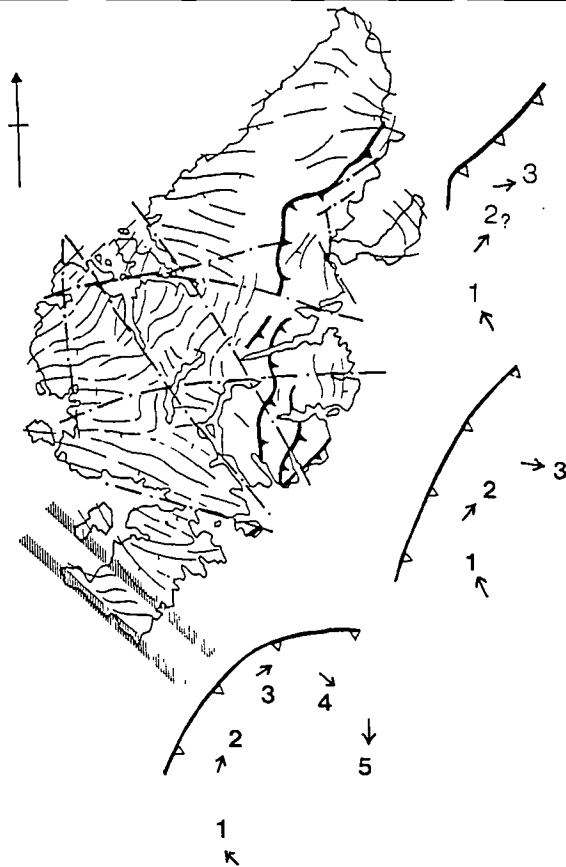


Figure 3.25 Map of the northern Outer Hebrides showing the inferred motion of the hanging-wall block. Magnitudes of displacement are not known, and are not implied by the diagram.

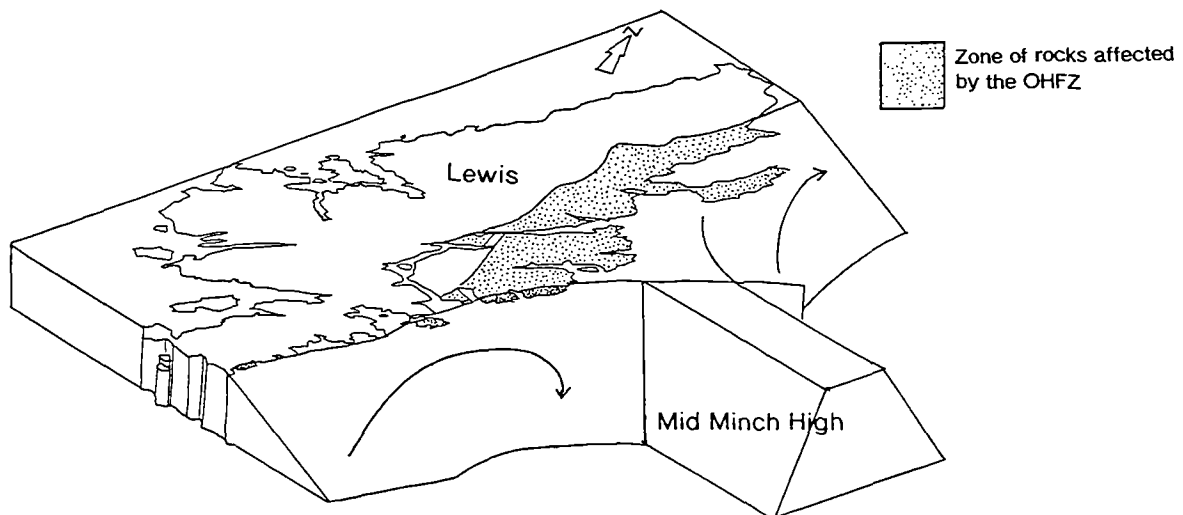


Figure 3.26. 3-D block diagram of the kinematic evolution of the onshore trace of the northern segment of the OHFZ, prior to the offshore motion on the Minch Fault. The footwall block, and the motion vector of the hanging wall block are shown. Note the S or SSE-directed collapse vector south of the Mid-Minch High and the NE-directed collapse vector north of the Mid-Minch high.

Changes in deformation conditions

The earliest mylonites in the OHFZ are high greenschist facies rocks, with quartzo-feldspathic components deforming dominantly by crystal plastic deformation mechanisms, and the mafic components deforming dominantly by brittle fracture. Such high greenschist facies mylonites probably formed at c. 350-450°C, and c. 2-6 kb.

The embrittlement associated with later thrusting has previously been assigned to high strain rates (Sibson 1977b) at the same P-T conditions. This interpretation is thought to be unlikely based on new field evidence. A lowering of P-T conditions, moving the fault zone through the brittle-ductile transition into the brittle field, is regarded as responsible for the change in deformation mechanisms. The lack of retrogression is attributed to fluid-absent conditions. This is corroborated by the large amounts of pseudotachylite present, which are widely regarded as having developed by frictional melting in fluid-free conditions (Sibson 1977a, although cf. Magloughlin 1992).

A subsequent return to ductile conditions during strike-slip is not due to a rise in P-T conditions, but reflects a change to a rheologically weaker deforming medium. This has the same effect as a return through the brittle-ductile transition into the ductile field. The weak rocks result from complete retrogression to low-greenschist facies, brought about by hydration reactions between high greenschist assemblages and ingressed fluid. The dominant deformation mechanisms were probably diffusive mass transfer mechanisms due to the large volumes of neocrystallised minerals e.g. fibrous chlorite and calcite, precipitated from solution. These low greenschist facies phyllonites probably formed at c. 300°C, and c. 2-3kb.

During extension, deformation which focussed into the weak units, probably occurred close to the brittle-ductile transition for hydrated phyllonites, since both ductile and brittle products of this 'event' are preserved. In contrast to the earlier phyllonitisation, the belts of phyllonite acted as DMT sources during extension, with pressure solution cleavages defining where material has been removed. Deformation may have occurred at slightly lower P-T conditions than during strike-slip. Brittle, normal faulting with no fluid flow or ductile behaviour suggests that near-surface conditions prevailed during basin-forming extension.

Chapter Four

The Kinematic history of the southern segment of the OHFZ

4.1 Introduction

The southern segment of the OHFZ is a narrow (<5 km wide at maximum) belt of fault-related deformation on the eastern side of the southern Outer Hebrides. The belt extends c. 90km from Sandray, south of Barra, to the small islands in the sound of Harris, and has been studied at several key localities (Fig 4.1). Fault rock types present are similar to those noted in the northern segment and include cataclasites, pseudotachylites, fault breccias and phyllonites. Significantly, however, mylonites of the type noted from the northern segment are not present in the southern segment. This chapter is subdivided into three major sections, based on the observed changes in kinematics associated with different fault rock types:

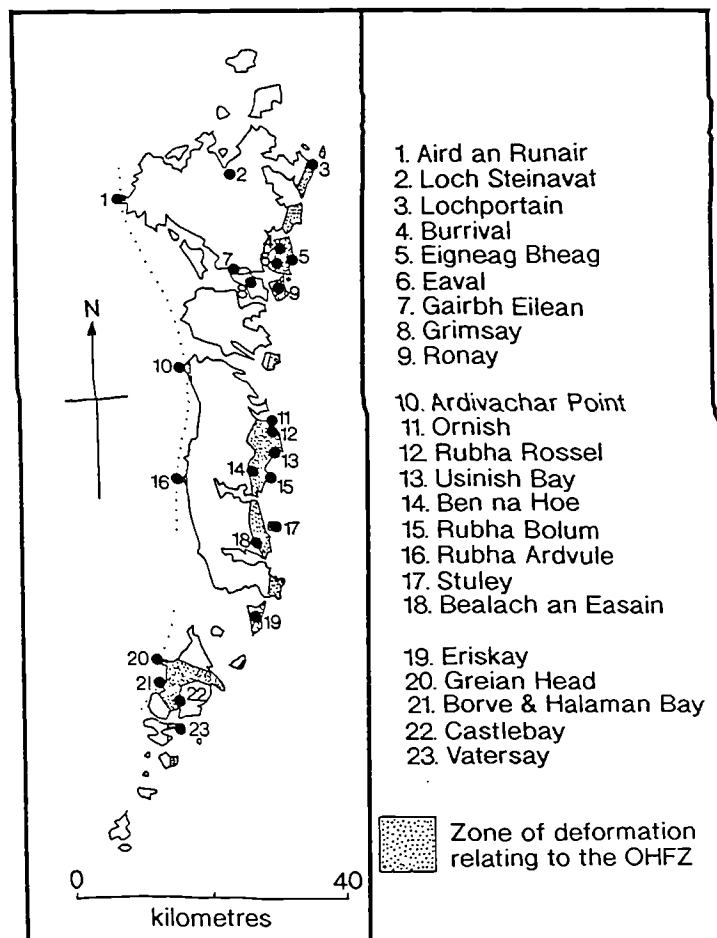


Figure 4.1. Map of the southern Outer Hebrides, showing the eastern zone of deformation related to the OHFZ, and major field localities. (Modified from Fettes et al. 1981.).

1. *Thrust movement*, which caused widespread brittle faulting, cataclasis and crushing, and the development of a large cataclasite / pseudotachylite crush mélange;
2. *Sinistral strike-slip movement*, with associated retrogression of the mineral assemblages in the pre-existing fault rocks, to form shallow-dipping, low-greenschist facies phyllonites;
3. *Extensional movement*, forming moderately to shallowly-dipping normal fault and fold packages. These preferentially focus into pre-existing phyllonite belts and passively extend the crust.

In each section, the locality descriptions are prefaced by a description of the local Lewisian geology. The timing of each movement phase is discussed in chapter 5

4.2 Thrust movement

In contrast to the early ductile deformation of the northern segment, the earliest deformation event to have affected the gneisses of the southern segment appears to have been brittle. Brittle deformation products are mainly restricted to a narrow strip of land parallel, and adjacent to, the eastern seaboard of the Uists. Brittle rocks have also been noted from western coastal promontories in South Uist and Barra (Fig. 4.1), and several localities in central North Uist. Thrust-related rocks of the southern segment have been studied at several localities, described in turn below. For convenience, the descriptions have been sub-divided into three main regions: North Uist; South Uist; and Barra.

Localities which show the best examples of characteristic structural features of the OHFZ have been rigorously described. To avoid repetition, only the salient features of other localities are outlined.

(i). North Uist and adjacent islands

Geographical setting

The island of North Uist (including the adjacent islands of Gairbh Eilean, Grimsay and Ronay) is the third largest island of the Outer Hebrides and occupies an area of c. 350km² (Fig. 4.2). Most of this area is extremely flat lying, with low, undulating moorland and complex networks of lochs and lochans. Only in the

eastern part of the island does the topography rise to significant levels. This marked change in relief, forming the hills of North Lee (262m), South Lee (281m), Burrival (140m) and Eaval (347m), is due to the onshore extension of erosion-resistant fault rocks associated with the OHFZ. Rock exposure is generally good in this area, but poor further west. Coastal exposure is good and accessible, but inland exposures are often weathered and lichen-covered, especially on north facing slopes.

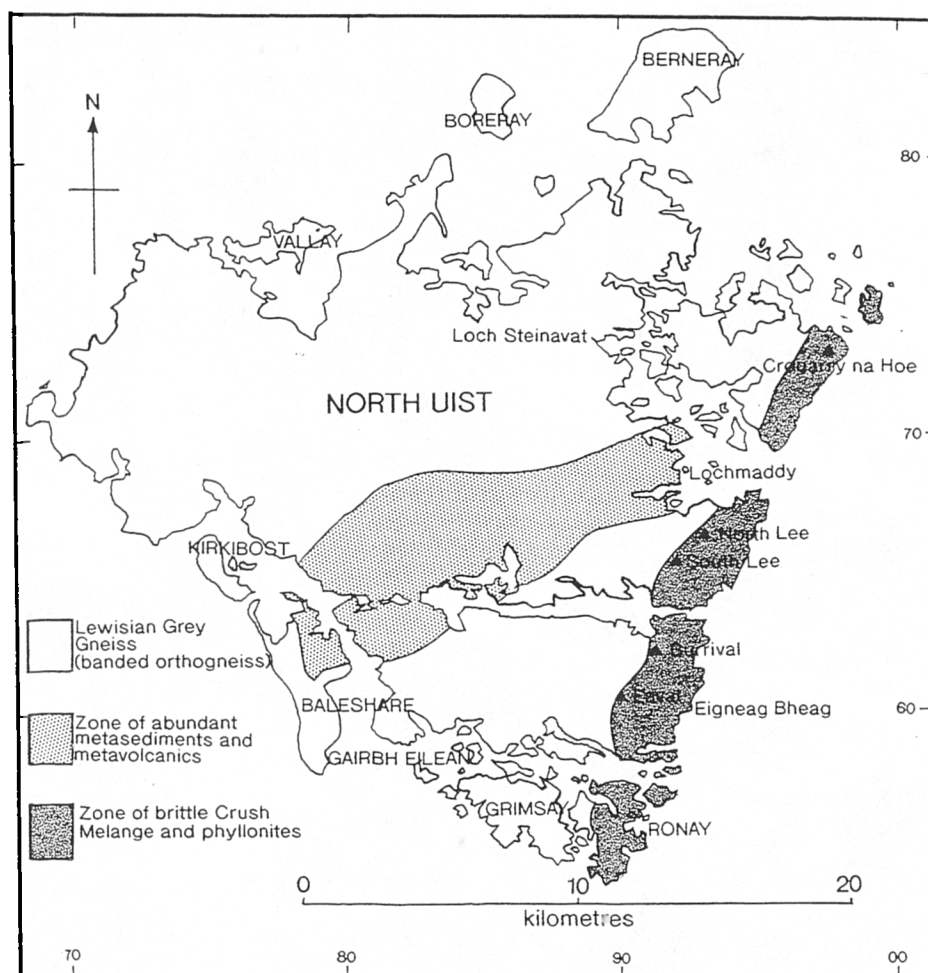


Figure 4.2. Simplified geological map of N.Uist and adjacent islands. (Modified from Fettes et al. 1992).

Lewisian geology of North Uist

The main lithology of North Uist and adjacent islands is chiefly heterogeneously deformed, amphibolite grade 'Grey Gneiss' of the type described previously (see chapter 2). The main unit present is a medium grained (c. 2-3mm), banded, acid orthogneiss with abundant sheets, pods, lenses and schlieren of 'Older Basic' material at various scales. Quartz (c.30%), plagioclase (mainly bytownite/ labradorite) (c. 30%), K-feldspar (c. 15%), biotite (15%) and hornblende

(c.10%) are the dominant minerals, with minor amounts of epidote and accessory minerals, including allanite.

In the central part of North Uist, a large E-W-trending belt of metasedimentary paragneiss, composed mainly of pelites and semi-pelites, is present (Coward et al. 1969). These contain discontinuous (mm-cm scale) quartz (c. 20%) and plagioclase (c. 20%) rich layers interbanded with biotite (30%), garnet (c. 15%) and hornblende (c. 15%) rich layers. The grain size is usually fine (1-2 mm), but large porphyroblasts of garnet occasionally reach 5 cm in diameter.

Post-Scourian intrusive 'Younger Basic' material is present, in the form of amphibole and plagioclase-rich concordant sheets (c. 2cm to 5m thick), although the high Laxfordian strain in this area obscures most of the discordant dyke contacts. Where Laxfordian strain is low (e.g. Garry-a-Siar, western Benbecula (NF 756536)), however, discordant intrusive contacts can be observed. Mafic material, composed mainly of hornblende (c. 50%), plagioclase (c. 40%) +/- garnet (c. 10%) is often agmatized by quartzo-feldspathic dykes (5mm - 1m), including aplites, granites and pegmatites, related to late Laxfordian granite veining. Remobilised layers and injected dykes of acidic material relating to Laxfordian migmatization are also present in places.

At least four phases of major pre-thrust folding have been recognised in the southern segment (Coward et al. 1970), corresponding to the major tectonothermal episodes of the Scourian and Laxfordian events outlined in chapter 2. These folds are largely obscured by later faulting close to the trace of the OHFZ.

Brittle thrust deformation in North Uist

Most of the Lewisian gneisses in the eastern part of North Uist are affected by early brittle deformation to varying degrees. Deformation occurs by several different brittle processes, discussed by Sibson (1977b). These include:

1. Microfault chopping;
2. Cataclasis;
3. Pseudotachylite generation.

Sibson (1977b) also includes the generation of an 'early cataclastic foliation' in this list, but this has been reinterpreted in the present work, and is discussed separately (see section 4.3.10). An essentially gradational series of fault rocks occurs, by the increasing intensity of one or all of these processes.

Sibson (1977b) regarded the series of fault rocks as divisible into four major geographical domains, depending on the dominant style of deformation. These

domains are listed below, and form the basis for the order of locality descriptions in this section.

1. The area west of the main belt of deformation, where *localised brittle failure* has occurred in the grey gneisses.
2. The *pseudotachylite-ultracataclasite crush zones*, which lie along parts of the western boundary of the fault zone.
3. The '*Crush Melange*' which makes up most of the fault zone rocks, and has been further sub-divided (Fettes et al. 1981, 1992) into:
 - 'Mashed Gneiss' (Jehu and Craig 1926): An intensely crushed lithology where the amount of microfaulting and cataclasis is so intense that no original gneissose banding is present. This occurs in the vicinity of, and above, the fault zone base defined by Sibson (1977b).
 - 'Cataclastic Gneiss' with a marked cataclastic overprint: An Intermediate unit where vestiges of the original banding become more common as the intensity of faulting and cataclasite generation decreases. This lithology occurs above the fault zone base, and becomes more common further east.
4. The 'Braided Mylonite Belts' which penetrate the Crush Melange.

It should be noted that the fourth domain is associated with later fault zone movements under a different kinematic regime, and is thus considered in a later section (see section 4.3).

4.2.1. Burrival region

The area between the small hill of Burrival (NF 909622) and the coast at Eigneag Bheag (NF 925600) (c.6 km²) has been studied in detail, and provides a typical example of the state of deformation in the '*Crush Melange*' of North Uist (Fig. 4.3).

Macrostructure

West of the thrust base

In the flat ground NW of Burrival (NF 906626), pristine, hornblende-bearing, amphibolite facies Lewisian Grey Gneisses with evidence of Laxfordian F2 and F3 folding, and granite veining/migmatisation (see section 2.2.2) occur, hosting small-scale, localised brittle faults, (up to several metres long). These faults usually dip

c.30-40° ENE or WNW and have down-dip plunging slickensides or striae. Displacements of well constrained marker horizons show that both thrusts and normal faults occur together and are probably coeval. Compressional movements dominate, however (c. 65:45 ratio of thrust to normal faults), and average apparent displacements are in the order of 1-10 cm on each thrust (Fig 4.4). In places, syn-thrust folding has occurred, but is only distinguishable from relict Lewisian folding (the 'false drag' folds of Sibson 1977b), with independent kinematic evidence, such as shear bands. The amphibolite facies mineralogy remains largely unaltered.

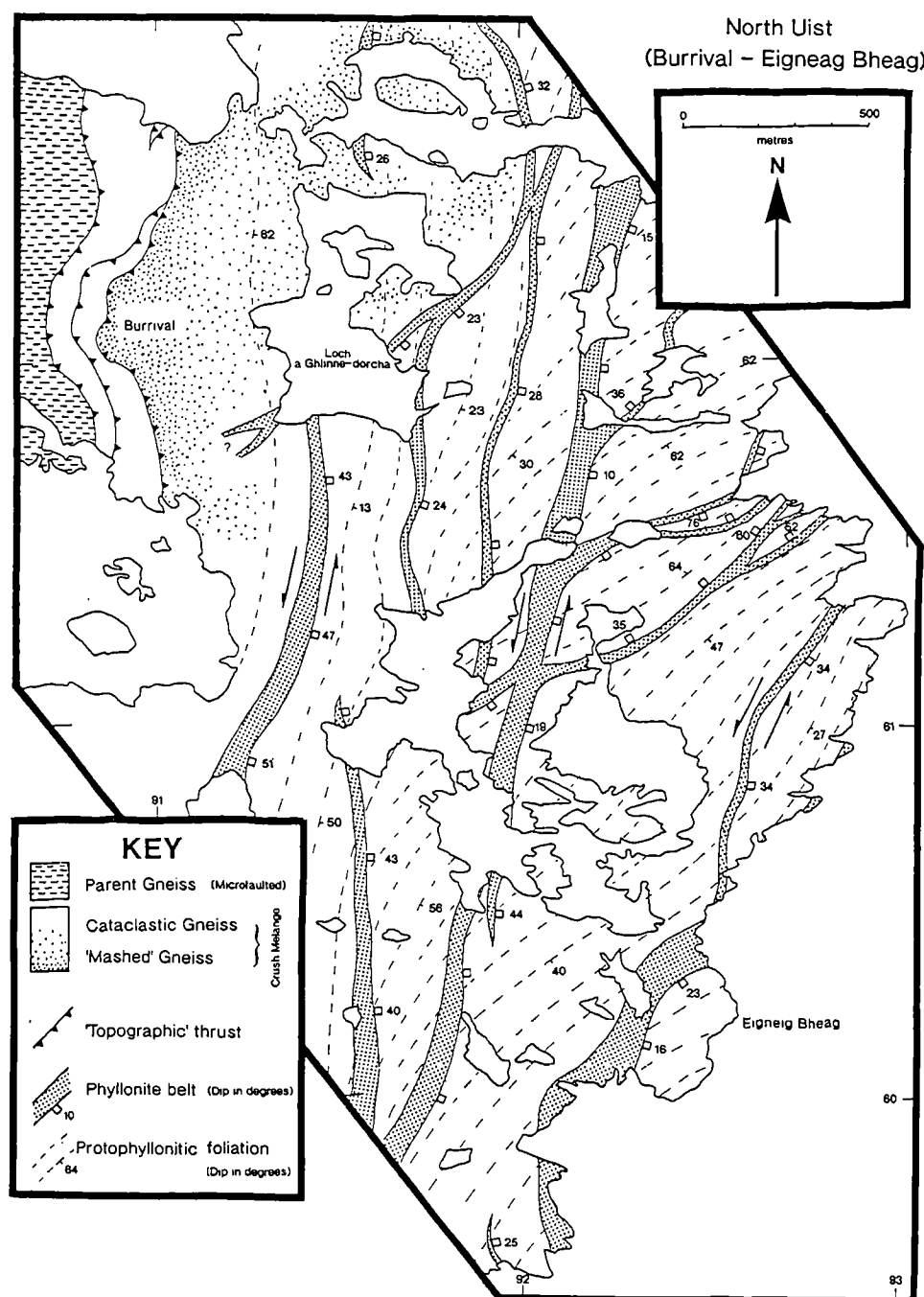


Figure 4.3. Geological map of the Burrival-Eigneag Bheag region of N.Uist.

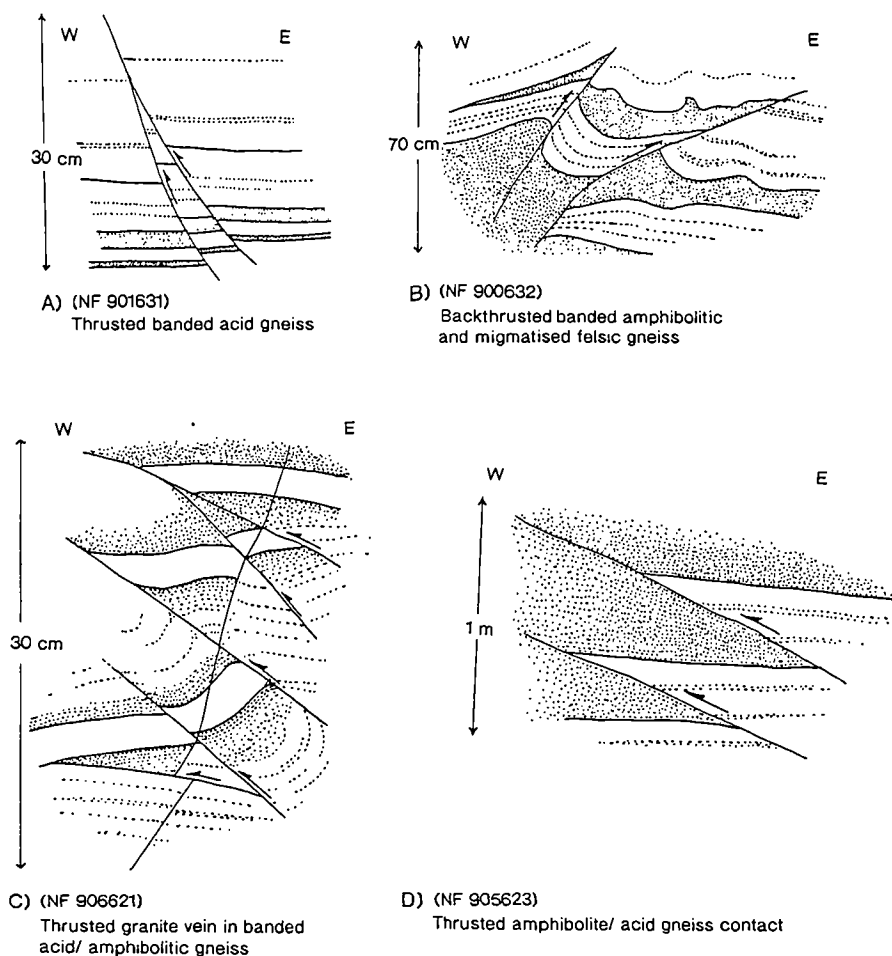


Figure 4.4. Field sketches of typical thrust geometries in the banded gneisses west of Burrival, N.Ulst.

The thrust base

Further east, at Burrival (NF 909622), the relatively intact gneisses are truncated by rocks of the 'Crush Melange', "an essentially chaotic jumble of partially retrogressed metabasite pods set in a matrix of crushed and sheared acid gneiss" (Sibson 1977b). This abrupt contact, termed the "thrust base" by Sibson (1977b), is marked by the most westerly faults in a series of stacked, large-scale, E-dipping faults, which, individually, can be traced laterally for several hundred metres along strike (Plate 4.1a). These large-scale fault planes extend throughout the melange. Where these intersect the topographic surface, a marked break in slope occurs. These 'topographic' faults dip at c. 25-35° ESE. In the material between individual topographic fault planes, minor concentrations of pseudotachylite/ ultracataclasite occur, usually in discontinuous-discordant, or discontinuous-concordant fault veins (c. 1mm- 5cm thick), but also in concordant breccia zones up to 1-2m thick. Isolated examples of discordant pseudotachylite injection veins exhibiting flow structures

also occur close to the westernmost topographic faults (e.g. at NF 908621). Sibson (1977b) regarded the topographic faults as having generated much of the nearby pseudotachylite, but the present work has not corroborated Sibson's suggestion that pseudotachylite concentrates close to the fault surfaces. Above the melange base, the volume of pseudotachylite appears to gradually decrease from west to east, throughout the whole melange, irrespective of the proximity to topographic fault surfaces. The pseudotachylite distribution is probably governed by the degree of microfaulting, which is also observed to decrease eastwards.

A particularly well exposed topographic fault occurs on the southern slope of Burrival (NF 908619), where a complete section through the structure is exposed. Approximately 30cm of highly weathered, epidotic cataclasite, with numerous minor faults, occurs along the exposed fault trace. A well preserved down-dip, SE-plunging slickenside lineation is present, and the geometry of minor faults, (including the presence of extensional, top-to-the west, riedel (R) shears, and asymmetric extensional shear bands) suggests this topographic fault preserves evidence for top-to-the-west thrusting.

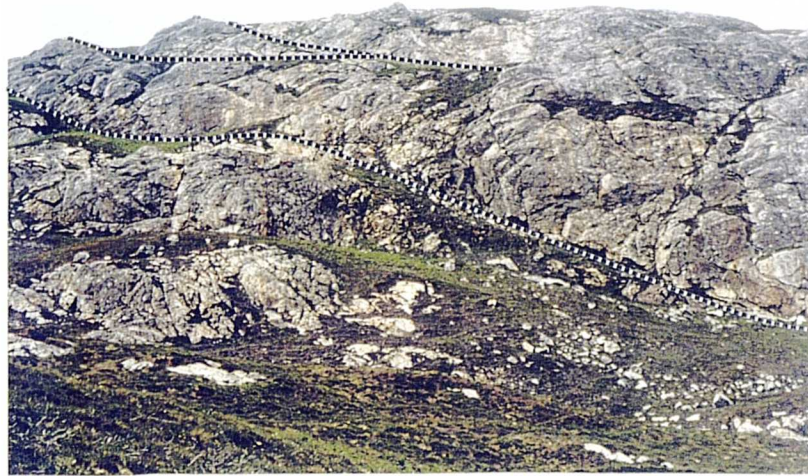
Topographic faults which occur *within* the melange often show subsidiary riedel (R) shears which suggest a top-to-the east sense of shear (e.g. SE of Burrival summit, NF 912621). These extensional displacements become more apparent further east, and are thought to reflect later reactivation (see section 4.4.1).

East of the thrust base

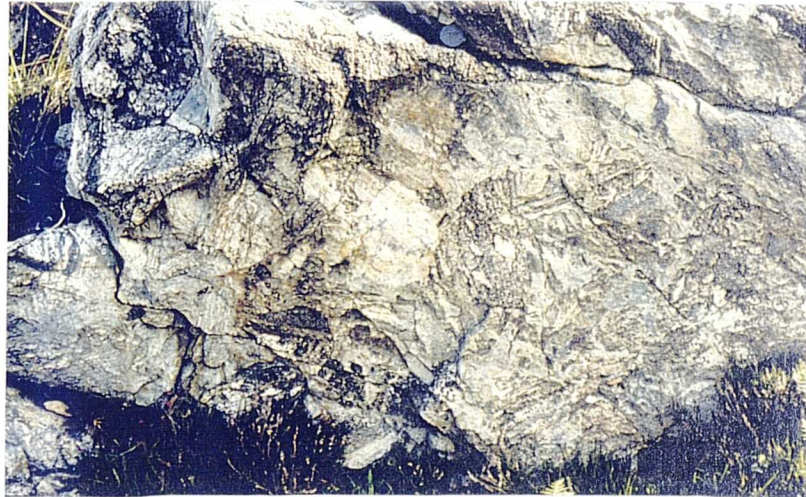
The Crush Melange is chiefly composed of crushed, pale grey- or cream-coloured acid gneiss with occasional pods of relatively intact, brown-weathering amphibolitic material, which become progressively more common further east. The amphibolite pods occur on several scales and occasionally achieve dimensions of about 100m, e.g. at Eigneag Bheag (NF 925602). They often preserve internal fabrics, defined by lithological layering or grain alignments. Such fabrics are usually significantly mis-oriented to any observed fabrics outside the pod, or fabrics within other pods. They are probably relict Lewisian features, whose orientations suggest that a significant degree of clast rotation has occurred within the melange. Where vestiges of relict Lewisian gneissose banding are present within the melange (e.g. west of Loch a Ghlinne-dorcha NF 912619), no consistent banding orientation exists, and the vestiges are undoubtedly reoriented.

The mineralogy of the clasts in the Crush Melange is largely the same as those of the undeformed banded Grey Gneiss. Quartz, plagioclase and K-feldspar dominate in the felsic portions, whilst hornblende and bytownite/ labradorite plagioclase (plus minor quartz, garnet and biotite) dominate in the mafic portions.

a)



b)



c)



Plate 4.1. N.Uist brittle thrust deformation

a) Topographic faults from south side of Burrival, N.Uist (NF 909619). Approximate height of exposure is c. 60m.

b) Typical 'Mashed Gneiss' from south side of Burrival (NF 918620).

c) Close-up of same locality showing microfractured clast in cataclasite matrix, which is itself microfractured.

The assemblage is typical of amphibolite facies metamorphic grades, and is presumably inherited from the amphibolite facies Lewisian Grey Gneiss protolith. Parts of the melange material are retrogressed, especially the cataclasite matrix. Chlorite, epidote, and sericite are extremely common in both matrix and as vein material. Occasionally the mafic material of the melange contains more biotite than hornblende, suggesting a retrogression to low greenschist facies has occurred. These low greenschist facies minerals are probably not syntectonic, however, and may relate to deformation under a different kinematic regime (see section 4.3).

In its most deformed state ('Mashed Gneiss'), the Crush Melange preserves no evidence of original gneissose fabrics. It has the appearance of being shattered, with innumerable, small, and apparently randomly oriented brittle or semi-brittle faults and hairline fractures accommodating little or no displacement. This gives the unit a characteristic 'blocky' weathering (Plate 4.1b).

Veins and minor irregular concentrations of grey cataclasite and/ or ultracataclasite are commonly associated with microfaults, especially at the faulted contacts between acid and basic gneisses. These cataclastic products are distributed evenly throughout the melange, and their grain size is characteristically extremely variable. Larger clasts are often microfaulted or *cataclastically* ^{deformed} themselves, revealing earlier phases of faulting and cataclasis (Plate 4.1c). Similarly, the whole unit is often further cut by fractures, with or without cataclasite/ ultracataclasite. Clearly, microfaulting and cataclasis are polyphase and/or progressive and occur on several different scales as part of a continuous process.

Occasionally, microfaults occur with a thin (<1cm) vein fill of brown or green epidote/ chlorite/ sericite rich material. The grain size of the vein fill material is usually too small to be resolved with the naked eye, but is probably retrogressed ultracataclasite or completely devitrified and altered pseudotachylite. The heavily weathered and altered state restricts positive field identification of pseudotachylites to two forms:

- Fault-bounded quasi-conglomerates, containing rounded clasts;
- Veins with a flow texture, chilled margins or devitrification structures.

White and Glasser (1987) point out that SEM studies are often the only way to make a distinction between pseudotachylite and ultracataclasite. No vitric pseudotachylite has been positively identified in the rocks of the Crush Melange.

The distribution of microfaults within the melange appears to be widespread, but the density of these structures gradually decreases from west to east, away from the melange base. Microfaulting constitutes an extremely important type of

deformation in North Uist, but little sense has been made of these structures in previous studies. White and Glasser (1987) refer to areas in the crush melange where blocks of country rock are separated by ultracataclasite or slickensided surfaces. Sibson (1977b) refers to 'microfault chopping' as one deformation style out of four that affects the melange. Both of these previous studies conclude that the microfaulted structure of the melange, especially the 'Mashed Gneiss', is too chaotic to make coherent sense. During the present study however, an attempt has been made to classify the dominant microfault orientations. Measurements were concentrated on microfaults with the following characteristics:

- Larger microfaults (i.e. those extending for >30cm);
- Microfaults forming part of a similarly oriented array;
- Microfaults possessing an altered cataclasite/ pseudotachylite vein fill (chiefly composed of very fine grained epidote and chlorite).

This procedure attempts to eliminate the possibility of measuring joints or tension cracks with no displacements. Although microfault orientations within the melange are extremely variable, they also show a preferred tendency towards a roughly N-S orientation, with a moderate or shallow easterly dip (Fig. 4.5). A secondary group of shallow, west-dipping types lies at a low angle to the local Lewisian banding.

The highly deformed nature of the gneiss means that original gneissose marker bands are few and fault displacements are therefore often difficult to determine. In addition, where gneissose banding *is* present, displacements are only apparent displacements because fault planes and movement direction indicators on them are rarely seen in the same exposure. Most exposed fault surfaces dip moderately west or east and have down-dip plunging slickensides or striae. Displacements of well constrained marker horizons show that both thrusts and normal faults occur together and are probably coeval. Compressional movements dominate however (c. 60:40 ratio of thrust to normal faults), and average observed displacements are in the order of 1-10cm. Extensional and compressional displacements are observed to be present on microfaults, dipping both westwards and eastwards in approximately equal numbers. Cross-cutting relationships of microfaults and/ or cataclastic vein material suggests several episodes of microfaulting occurred, and no consistencies exist between the sense of displacement on earlier, and later structures. Where pseudotachylite breccias and quasi-conglomerates are present, they often occur in the zones between the generating fault surfaces and subsidiary riedel (R) shears, a phenomenon also noted at other localities in the OHFZ (see section 4.2.11). This geometry is

consistent with extensional displacement on the generating fault surface, and suggests that pseudotachylite breccias/ quasi-conglomerates preferentially occur in *local* zones of extension (see also section 3.2.2. and Fig. 3.11b).

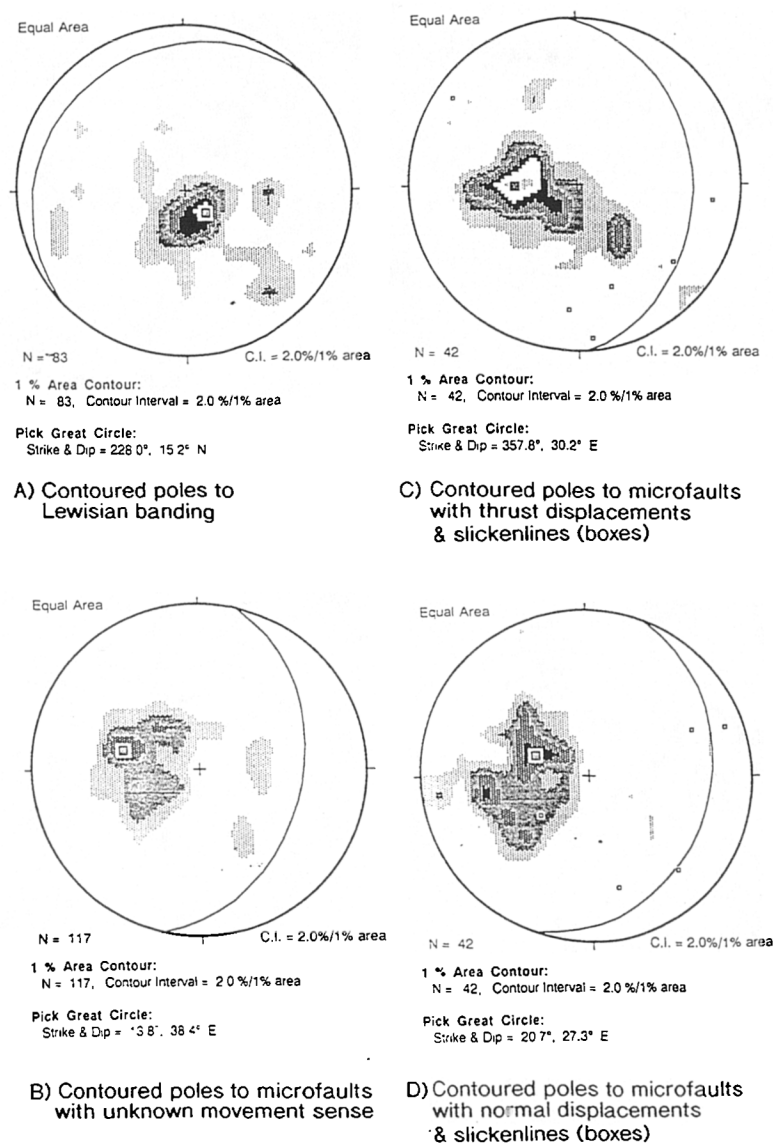


Figure 4.5. Equal area stereonet of Lewisian banding and microfaults within the Crush Melange of N. Uist.

An early, thrust-related foliation

Areas which show a coherent and consistently oriented thrust-related fabric within the Crush Melange are rare, but occasionally occur close to the 'thrust base' on the western slopes of Burrival (NF 908622). This thrust 'fabric' preferentially occurs in the hangingwalls or occasionally the footwalls of cm - m scale faults and comprises zones (typically <50cm thick) of crudely foliated melange material with closely spaced anastomosing networks of semi-brittle microfaults which parallel the

larger structures. These zones of intense brittle deformation, which have been generated by microfaulting, cataclasis and mechanical re-orientation and comminution of grains, constitute *part* of what Sibson (1977b) refers to as the "early cataclastic foliation". Apparent thrust-sense fabric swings above these zones may be due to the preservation of rare, relict Lewisian folds; the 'false drag' folds of Sibson (1977b) (e.g. at NF 908619), and not a result of true thrust-sense 'drag' on these structures. Despite the lack of displacement indicators, these semi-brittle, intensely microfaulted zones are associated with the development of down-dip plunging slickenfibres and mineral lineations. They are therefore thought to be related to dip-slip movements. True contemporaneity with cataclasis can be discounted however, because this foliation always appears to cross-cut and post-date cataclasis; *clasts of foliated melange material misoriented by cataclasis have never been found*. As this 'fabric' is usually localised in only one wall of the adjacent fault, a degree of later reactivation may have occurred. A further discussion of Sibson's 'early cataclastic foliation' is provided in section 4.3.10.

Microstructure

All mineral phases within the crush melange gneisses have responded to deformation in a brittle manner. Quartz grains display undulose extinction due to the large dislocation densities within the grains. Very little recovery has occurred although a few unstrained, possible rotationally recrystallised subgrains are apparent at grain boundaries. Most subgrains however, show sweeping undulose extinction, suggesting that brittle 'cold working' continued after minor recovery. Most fine grained quartz grains in the Crush Melange rocks are the product of cataclasis and brittle comminution of larger grains. These grains form along discrete fracture surfaces which may be intracrystalline or transcrystalline (Plate 4.2.a). No evidence for ductile behaviour of quartz (e.g. ribboning) has been found.

Plagioclase and K-feldspar are nearly always pseudomorphed by sericite in the Crush Melange (Plate 4.2b). Original feldspar, where present, deforms in a very brittle manner, by transcrystalline microfracturing and cataclasis (Plate 4.2b). The retrogressive sericite is largely undeformed and probably entirely post-dates brittle deformation and may be synchronous with later deformations (see section 4.3). Mafic minerals, e.g. hornblende and minor biotite, are also intensely cataclastically ^{deformed} and comminuted, but remain metastable, however, with only minor alteration to chlorite in places.

Zones of brown amorphous cataclasite and ultracataclasite commonly cross-cut the rock in randomly oriented veins and fractures. The small grain size usually makes mineral identification difficult, but quartz, sericite, mafic material (probably

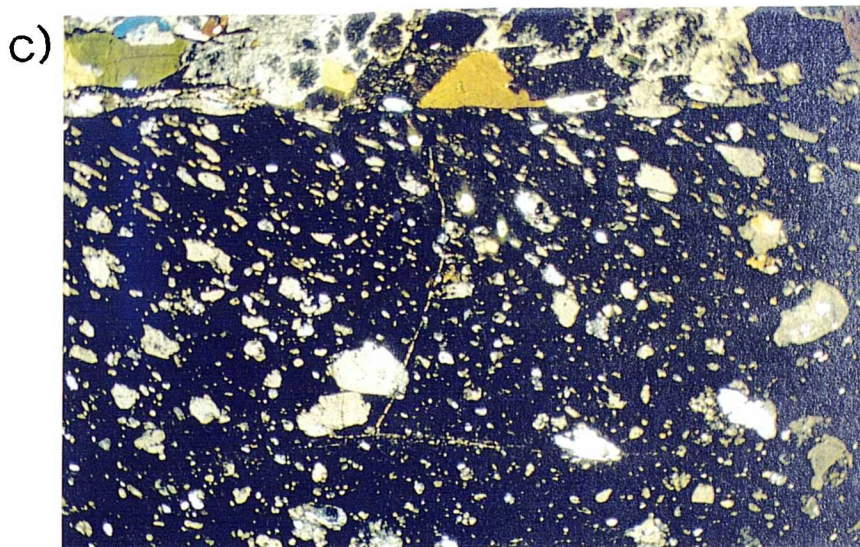
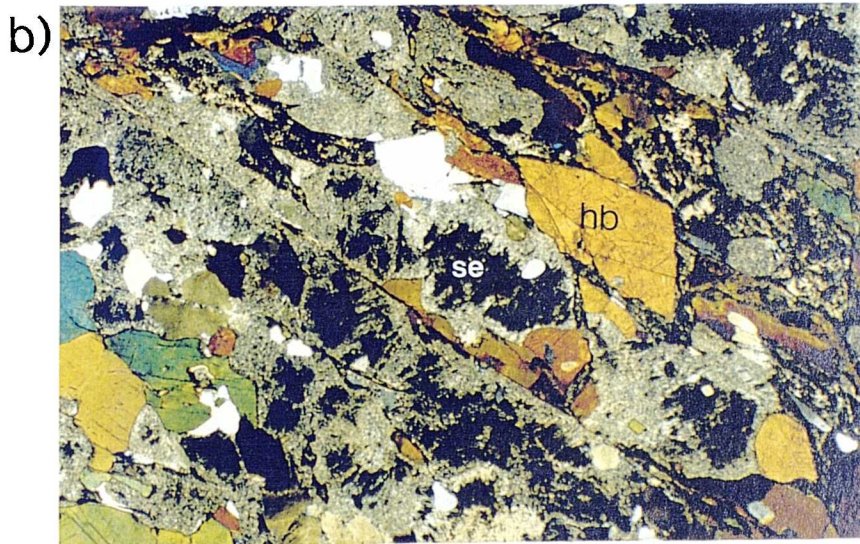
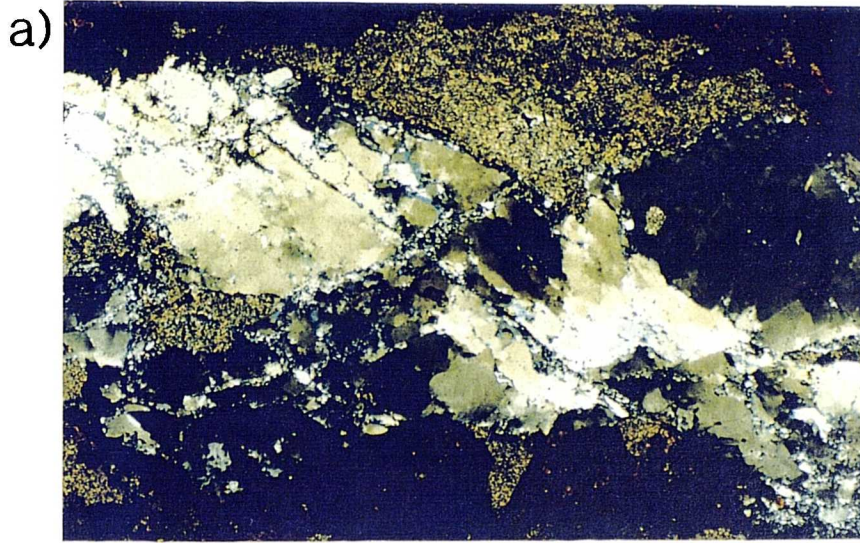


Plate 4.2. Brittle thrust deformation, N.Uist

a) Transcrystalline brittle fractures in quartz from the Burrival region (NF 907621). The larger grains show undulose extinction and the fractures host very fine grained comminuted quartz due to cataclasis. Field of view is 3mm. (XPL)

b) Partially sericitised feldspars (se) and original hornblendes (hb) from Burrival (NF 909618). Transcrystalline fractures with minor cataclasis cross-cut the photo. Field of view is 6mm. (XPL)

c) Fault vein of pseudotachylite from Burrival (NF 909618) showing strong shape fabric of clasts close to contact with vein wall. Field of view is 12mm. (XPL)

hornblende) and later epidote and chlorite are constituent minerals. Other veins and fractures are filled with devitrified pseudotachylite, which, in thin section, is also brown, amorphous and very fine grained. Isotropic, glassy pseudotachylite is never preserved. Clasts of locally derived country rock within the pseudotachylite are randomly oriented and may be rounded. In rare instances along fault veins, the clasts adopt a strong shape fabric which appears to indicate vein-parallel simple shear (Plate 4.2c). This fabric is not observed outside the vein, and appears to stop at the vein walls. Rather than being a mylonitic overprint after pseudotachylite injection (cf. Sibson 1977b), this fabric is thought to be a syntectonic fabric, generated by flow within a viscous melt. This process has also been observed by other workers elsewhere, e.g. Berlenbach and Roering (1992) at Witswatersrand, South Africa.

Veins of epidote and chlorite cross-cut all other melange constituents and are very late in the deformation sequence (see section 4.3). The epidote and chlorite observed in the cataclasite/ ultracataclasite veins are probably also of this generation, and shows a tendency to associate with the most chaotically fractured regions (Plate 4.3a). The fractured zones may provide fluid pathways to induce subsequent alteration.

Metamorphic conditions during deformation

Sibson (1977b) regarded the Crush Melange as developing at low-greenschist facies, owing to the large amount of chlorite, calcite, epidote and sericite developed during partial retrogression of the amphibolite grade gneisses. He does not, however, state evidence for syn-tectonic development of these phases. This work has found no evidence for syntectonic retrogression and regards these minerals as later, post-tectonic products, synchronous with renewed fault zone movement in a different kinematic regime. Without the effects of syntectonic greenschist facies retrogression, the interpretation of the Crush Melange may be very different.

The very brittle nature of all the mineral phases associated with early fault zone deformation, which includes microfaulting, cataclasis, ultracataclasis and pseudotachylite generation, suggests that low pressure/ temperature conditions and/ or high strain rates and/ or high pore fluid pressures prevailed during early fault zone motion. In general, quartz does not deform in a brittle manner above 300°C, at which point, 'type 1' quartz ribbons develop (Boullier and Bouchez 1978), unless strain rates/ pore fluid pressures are high.

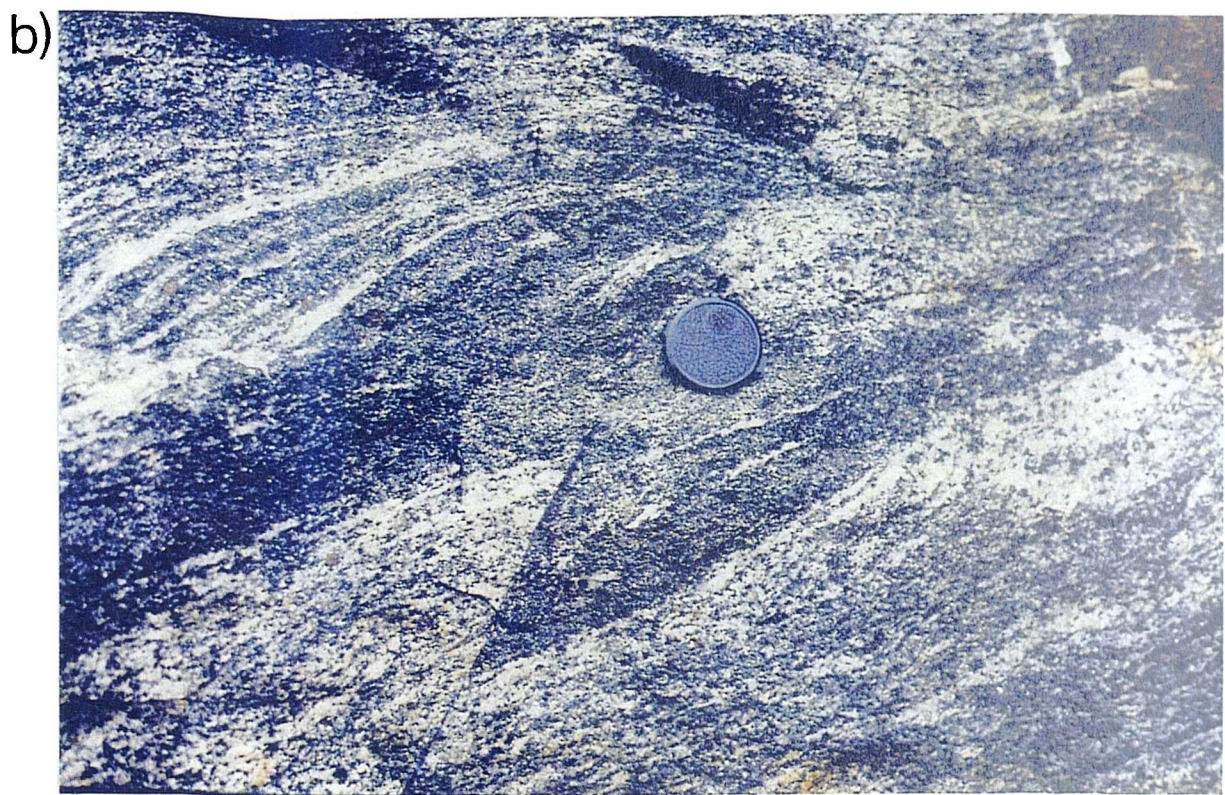
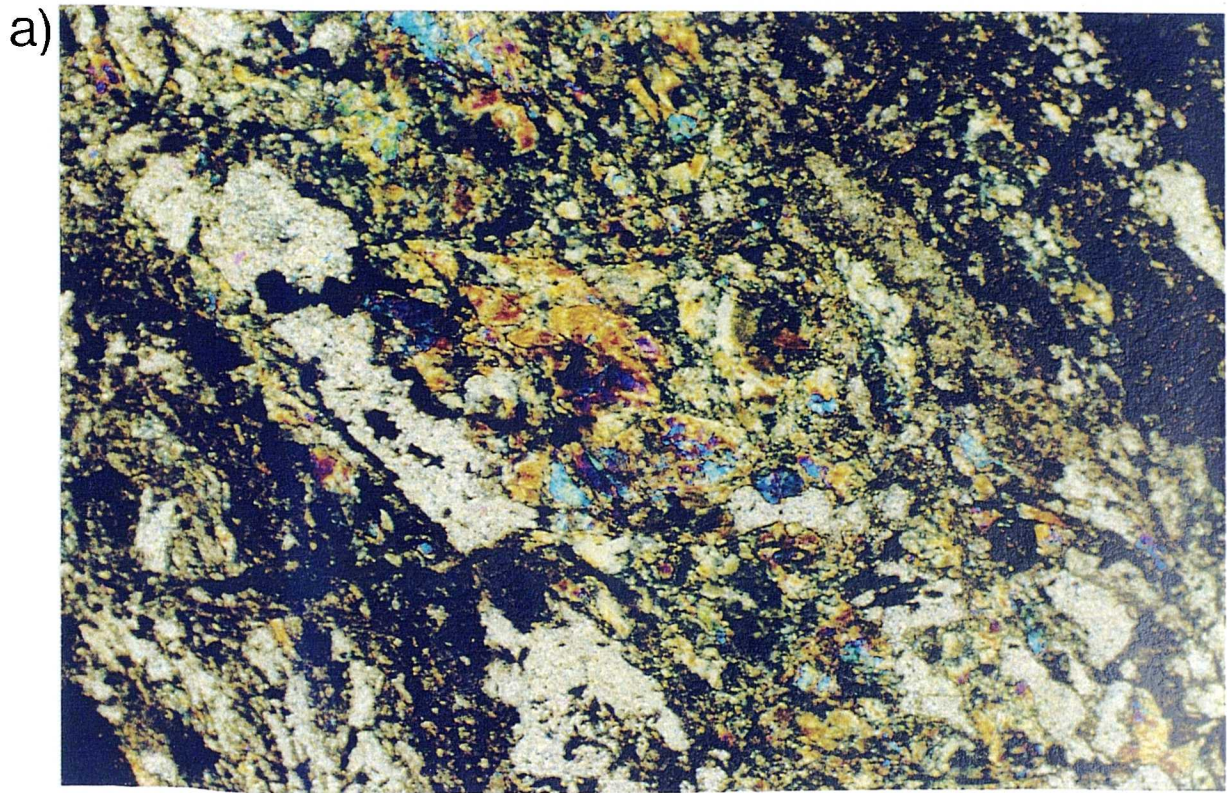


Plate 4.3 Brittle thrust deformation in N.Uist

a) Extremely strongly ^{deformed} ~~Cataclastically~~ region of 'Mashed Gneiss' from Burrival (NF 910624), showing the growth of secondary epidote. Field of view is 3mm. (XPL)

b) Backthrust in banded gneiss from Grimsay (NF 856562), with pinch-and-swell fault vein of pseudotachylite.

The mineral assemblage however, suggests that pressure-temperature conditions may have been higher. The presence of unaltered hornblende and biotite suggests that no low-temperature thermal re-equilibration took place, and a temperature of at least 450°C prevailed. This apparent co-existence of high grade (amphibolite facies) assemblages with low grade deformation microstructures is discussed in section 4.2.12.

4.2.2. Eaval

Close to the summit of Eaval (NF 899606), the largest hill on North Uist, a discontinuous, dark green coloured *pseudotachylite/ cataclasite crush zone*, c. 20 - 30 m thick occurs (see North Uist location map; Fig. 4.2). This zone of intense brittle deformation, dipping east at c. 25° and bounded by large (m-scale) thrust planes with SE-plunging striae, continues northwards along strike to crop out on the western scarp slopes of North Lee and South Lee (Sibson 1977b). The crush zone is absent from the low hills of Burrival (140m), Ben Hacklett (116m) and Crogarra na Hoe (154m) to the north, and Beinn a Charnain (115m) on Ronay to the south. Sibson (1977b) suggests that the marked change in relief between the high hills (>250m), which possess the crush zone, and the low hills (<155m), which do not, is clearly related to the erosive resistance of the crush zone.

Internally, the crush zones are extremely complex, composed of randomly oriented and random sized fractured gneissic fragments (30-60% of the rock), set in a matrix (c. 40-70%) of extremely fine grained ultracataclasite, cataclasite and pseudotachylite. The relative amount of ultracataclasite to pseudotachylite is difficult to ascertain, even in thin section, since both are heavily retrogressed, and the pseudotachylite is completely devitrified. The whole unit is fractured by a large number of apparently randomly oriented, low-angle to high-angle microfracture sets, displacing both extensionally and compressionally. No uniformity exists, in either the orientation, or the shear sense of late, continuous, cross-cutting fractures, or early, discontinuous cross-cut fractures. Outside the crush zone, however, pseudotachylite-bearing microfaults invariably possess injection veins in T-fracture orientations indicative of overall top-to-the-west compression. It is thought, therefore, that a compressional thrust-setting prevailed during crush zone generation.

The origin of the crush zones is uncertain but they may be the product of a large number of pseudotachylite injection phases ("multiple jerk" features of Sibson 1977b), combined with cataclastic comminution processes and microfaulting.

On the southern slopes of Eaval, where no pseudotachylite/ ultracataclasite crush zone occurs, an area of extensive localised brittle failure has been generated.

It is significant to note that the Lewisian banding in this region is quite steep, and microfaulting orientations are somewhat different to those from further north (see section 4.2.1). A prominent set of microfaults trends N-S, with a shallow to moderate easterly dip. These faults are cross cut by pseudotachylites, and may have provided a suitable low-angle anisotropy for the focus of the larger 'topographic' faults which are not cut by pseudotachylites and are therefore later. Two more prominent microfault arrays with displacements in the order of 2-3 cm, appear to form a conjugate set (Fig. 4.6):

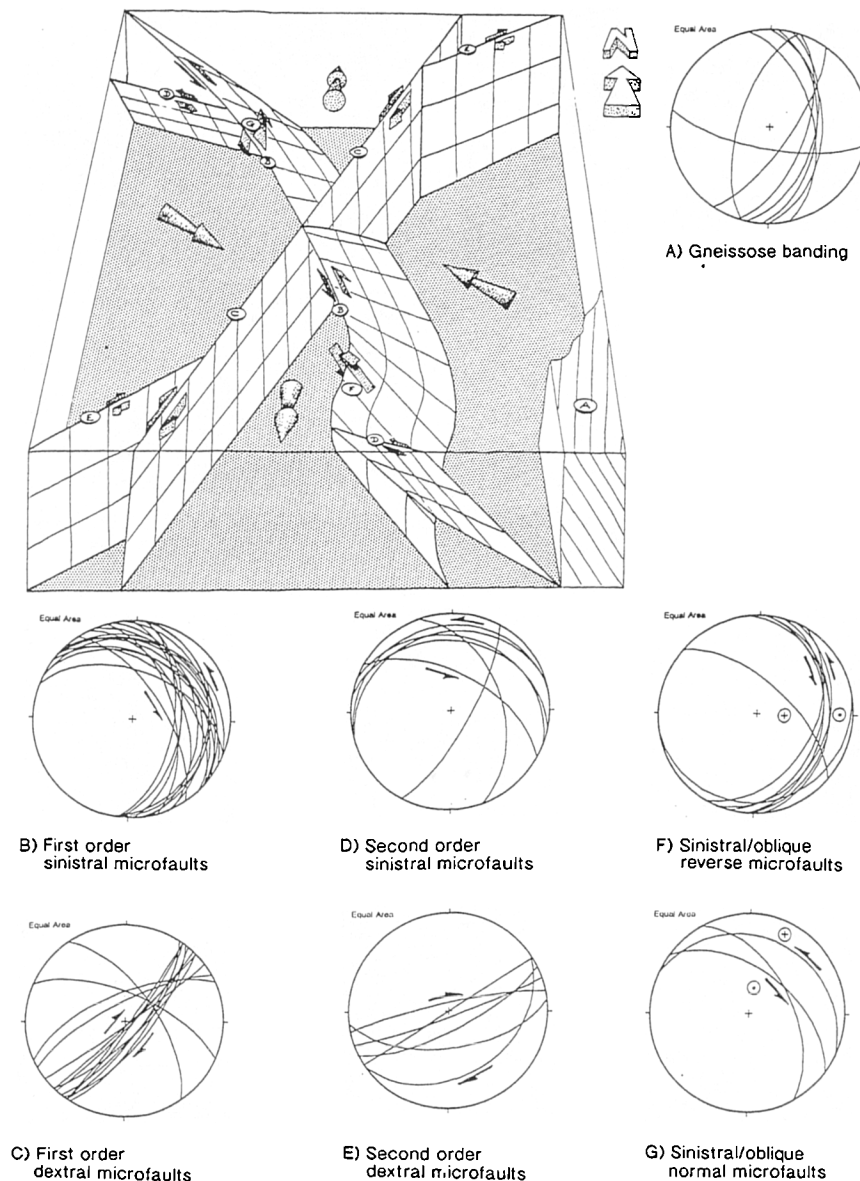


Figure 4.6. Block diagram of typical microfault orientations at Eaval, N.Uist, illustrating a first order conjugate fault set. The 7 equal area stereonets show orientations of gneissose banding and microfaults (labelled A to G on the diagram).

- The first array, oriented NW-SE, and dipping moderately NE, displaces marker bands sinistrally and generates pseudotachylite. A 2nd-order sinistral fault array forms subsidiary faults in Riedel (R)-shear orientations with respect to the 1st-order array. Very rarely, a 3rd order sinistral array is present.
- The second array, oriented NE-SW, and dipping very steeply SE, displaces marker bands dextrally, and also generates pseudotachylite. A 2nd-order dextral array forms subsidiary faults in Riedel (R)-shear orientations with respect to the 1st-order array.

No pseudotachylite has been generated on 2nd-order faults in either array. This conjugate faulting, which accommodates E-W shortening and N-S extension, has not been observed at Burrival, where the orientation of Lewisian banding is much shallower (see Fig. 4.5) and even subhorizontal in places. These observations suggest that the orientation of pre-existing banding in the gneisses may control the style and kinematics of brittle shortening along the OHFZ.

Metamorphic conditions during deformation

The pressure/ temperature conditions which prevailed during pseudotachylite/ ultracataclasite crush zone development are essentially the same as those which prevailed during Crush Melange development. The intense cataclasis requires high confining pressures to prevent reactivation of the same failure surface (Twiss and Moores 1992). The large amount of post-tectonic retrogression virtually obliterates the original assemblage, but it is thought likely that the original gneiss assemblages remained metastable during crush zone-related deformation (see section 4.2.12).

The large pseudotachylite/ ultracataclasite crush zone, not seen at Burrival, suggests some degree of strain localisation occurred, where the magnitude and frequency of individual slip events far exceeded those in the surrounding Crush Melange. The reason for this localisation, which is still essentially cataclastic, is presently unknown but may relate to the difference in pre-existing banding orientation described above.

4.2.3 Gairbh-eilean

The c.250m long road section on the small island of Gairbh-eilean (NF 847588) linking the islands of North Uist and Grimsay c. 5km west of the thrust base, provides good examples of *localised brittle failure* in relatively intact gneiss (Fig 4.2). Here, pristine, banded Lewisian Grey Gneisses are occasionally cut by small (cm/ m-scale) faults, often bearing pseudotachylite. The pseudotachylite

occurs in a variety of states: Concordant fault veins displaying pinch-and-swell geometries (c. 2-10 mm thick); discordant fault veins (<2cm thick) often appearing green in colour due to alteration to epidote and chlorite; injection veins (c. 1cm thick) with occasional chilled margins; and vein networks. Most faults strike NNW-SSE, parallel to the gneissic foliation, and dip moderately ENE. Movement direction indicators such as slickensides or striae are rare, because fault surfaces are usually unexposed. Rare, exposed fault surfaces bear slickenlines plunging close to, or directly down dip. Apparent sense of displacement indicators are numerous due to the banded nature of the gneiss which provides abundant marker horizons. Apparent, thrust-sense displacements of marker bands along both east-dipping, pseudotachylite-bearing, and pseudotachylite-barren faults, and a minor, east-dipping, thrust duplex in a deformed Laxfordian pegmatite, suggest pseudotachylite generation occurred during compressive brittle failure. In addition, pseudotachylite injection veins are observed to adopt Riedel (R)-shear orientations, consistent with overall top-to-the-west thrusting.

4.2.4. Grimsay

In Grimsay (Fig. 4.2), the Lewisian gneisses possess both pseudotachylite-bearing microfaults and pseudotachylite-barren microfaults. These show mutual cross-cutting relationships, suggesting a contemporaneous generation. Both concordant and discordant faults are present, but a strong preference for the former is observed (Fig. 4.7). The focusing of faults onto pre-existing anisotropies is exemplified by the common occurrence of faulted Laxfordian pegmatite margins, e.g at Gearradubh (NF 855576). Most faults dip E or ESE, at moderate or low angles, but a few dip west. Fault surfaces are only rarely exposed, and down-dip (usually SE-) plunging slickensides are present. Sense of displacement indicators include displaced gneissose banding, drag folds and occasionally in semi-brittle faults, shear band fabrics. Most examples give a thrust sense-of-shear displacing top-to-the-west (Plate 4.3b), less frequently, top-to-the-east, with displacements in the order of 3-10cm. Very fine veins of epidote (<0.5 mm thick) probably coincide with faults which have experienced very localised retrogression.

Fresh, unaltered pseudotachylite fault and injection veins are common on Grimsay, and where well developed, create ladder networks and breccias. Typically, fault veins are traceable over several metres, exhibiting pinch-and-swell geometries, with vein thicknesses variable between <1mm and >2cm. The largest injection veins achieve thicknesses up to 25 cm. Pseudotachylite breccias host irregular or rounded clasts of unaltered Lewisian Grey Gneiss up to 10cm in diameter. Sibson (1977b) suggests these breccias were generated by several

phases of injection, or 'multiple jerk' faulting. The gneissose banding is often completely reoriented within these structures, making the offsets and shear sense difficult to determine.

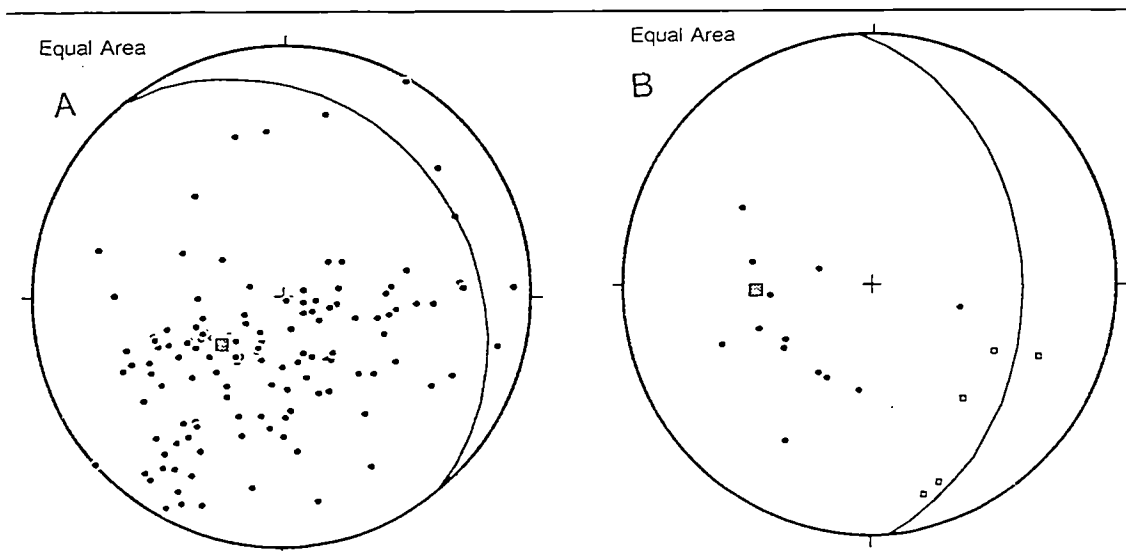


Figure 4.7. Equal area stereonet showing: A) Poles to Lewisian banding with mean great circle; and B) Poles to microfaults (dots) and slickensides (boxes) from Grimsay, N.Uist.

4.2.5. Loch Steinavat

The quarry south of Loch Steinavat (NF 875738) (Fig. 4.2), exposes folded gneisses and intrusives, which are cut by m-scale brittle faults, dipping moderately to the E or SE. No slickenlines are present, so all observed displacements are apparent. Several small-scale extensional fault duplexes are developed along these detachments and appear to displace top-to-the E or SE. Closely associated with the large-scale faults, but significantly not along them, are pseudotachylite veined microfaults and fractures. All veins are discordant to the foliation, and a progressive sequence of pseudotachylite development, first proposed by Sibson (1977a & b), involving fault veins, injection veins, ladder networks, breccias, and quasi-conglomerates (Fig. 4.8) is presently exposed. It is unclear whether the pseudotachylites developed coevally with the larger extensional faults, but their close spatial association does not preclude this possibility.

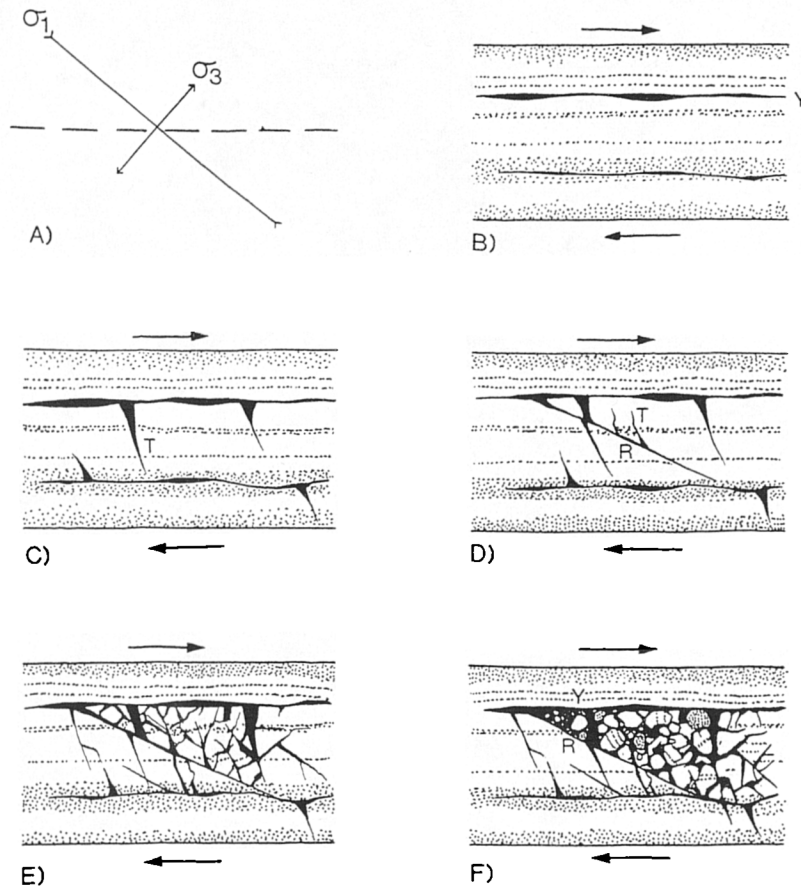
(ii). South Uist and adjacent islands

Geographical setting

South Uist is the second largest island in the Outer Hebrides, occupying an area of c. 370 km² (Fig. 4.9). In contrast to North Uist and Benbecula to the north, much of the island has substantial relief, culminating in the hills of Hecla (606m),

Ben Corodale (527m) and Beinn Mhor (620m). These hills occur in the east of the island, coinciding with the onshore trace of the OHFZ. Again, the eastward rise in relief is due to the presence of erosion-resistant fault rocks. Exposure is generally good in the east, but is obscured by large tracts of coastal 'machair' further west.

Top to the right sense of shear applies throughout



- A) Initial stress system
- B) Concordant fault vein of pseudotachylite in layer-parallel 'Y-shear' orientation (using the terminology of Swanson 1988). Veins commonly exhibit pinch-and-swell lensing
- C) Discordant injection veins of pseudotachylite splay off fault veins in 'T-fracture' orientations
- D) Discordant fault vein of pseudotachylite in 'R-shear' orientation splays off concordant fault vein. 'T-fracture' injection veins splay off newly formed 'R-shear'
- E) Erratic injection veins coalesce to form ladder networks and pseudotachylite breccias
- F) Fracturing, attrition, abrasion and thermal ablation contribute to clast rounding and clast rotation occurs. Pseudotachylite quasi-conglomerate results and is often best developed in apexes of 'Y-shear' and 'R-shear' intersections

Figure 4.8. Schematic, progressive sequence of events leading to pseudotachylite development from concordant fault vein to pseudotachylite quasi-conglomerate. (Modified from Sibson 1977a and b).

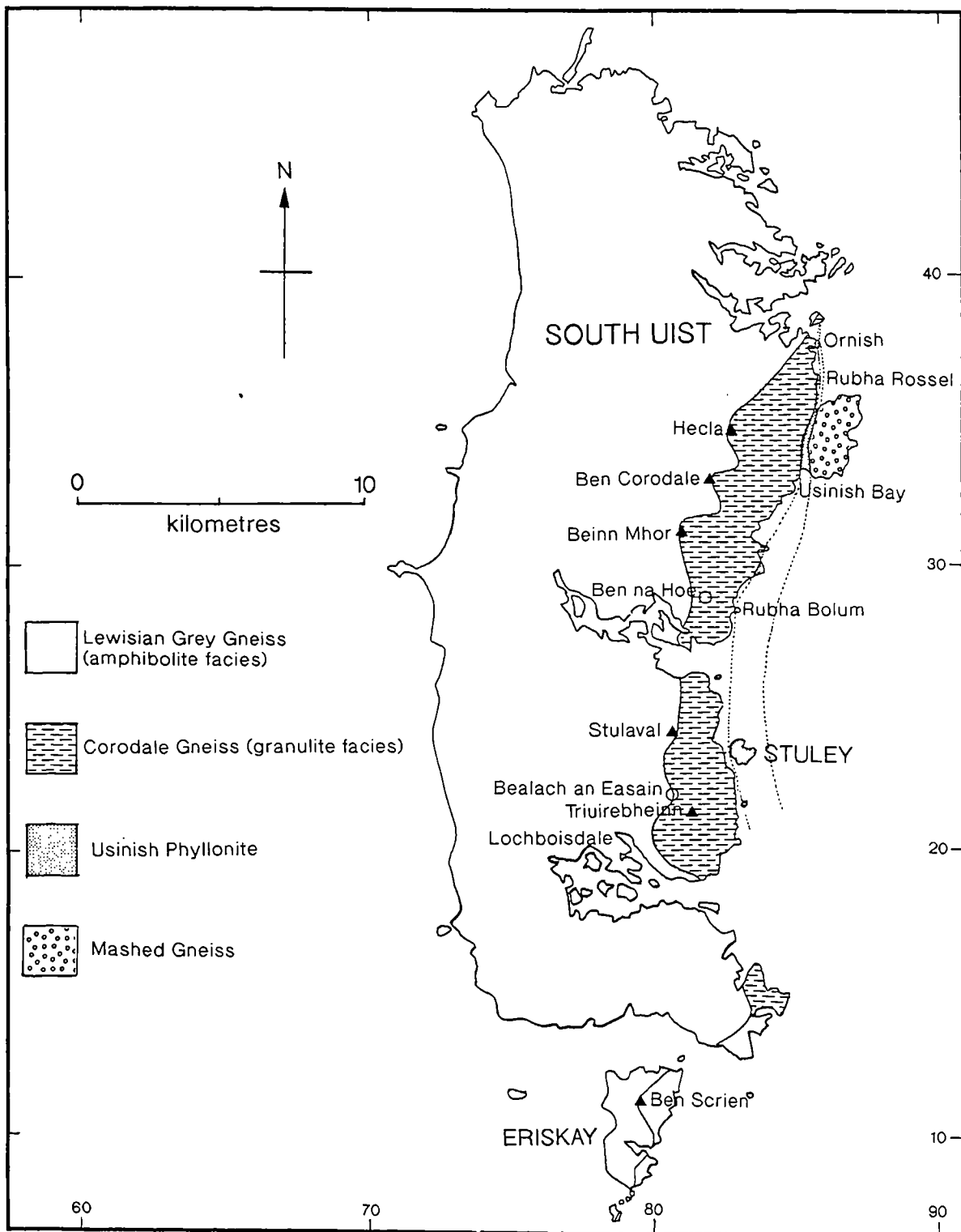


Figure 4.9. Simplified geological map of South Uist (modified from Fettes et al. 1992).

Lewisian geology of South Uist

The background Lewisian geology of South Uist is divisible into two major regions. The western part of the island, occupying the region below the OHFZ trace is composed of banded quartzo-feldspathic Grey Gneiss, similar to that observed elsewhere (see chapter 2 for a full description), with subordinate metasediments and 'Older Basics'. These rocks are intruded by numerous Scourie Dykes (Younger Basics) and Laxfordian pegmatites. The state of overprinting Laxfordian strain is often highly variable. In low Laxfordian strain areas, marked discordancies occur between late Scourian 'Younger Basics' and the pre-existing banded gneiss (Coward 1972). At least four separate deformation episodes have been observed in the Grey Gneisses (Coward et al. 1970, Coward 1972, 1973). Much of the NW-SE structural 'grain' of the region is due to the dominance of upright, NW-plunging Laxfordian F3 folds (see Fig. 2.3), (Coward et al. 1970).

Above the OHFZ trace, the rocks are markedly different. Coward (1972) has sub-divided these 'Eastern Gneisses' (using the terminology of Dearnley 1962) into three main units:

1. Corodale Gneiss
2. Mashed Gneiss
3. Usinish Mylonites

The latter two units are regarded in the present work as related to the evolution of the OHFZ and not directly related to Lewisian geology. These two units are considered during the locality descriptions (section 4.2.6 and thereafter).

The largest, and the only unit which pre-dates OHFZ movement east of the OHFZ is the Corodale Gneiss, a granulite facies, meta-igneous body of uncertain age. Most workers regard it as late Scourian, contemporaneous with Scourie Dyke intrusion (c. 2.2 - 2.4 Ga) (e.g. Fettes et al. 1992), but recent work (Whitehouse 1993), has suggested this body may be older (c. 2.8 Ga.).

The Corodale Gneiss is a north-south trending body stretching from Luirsay Dubh (NF 866405) in the north, to Rubha na h-Ordaig (NF 846150) in the south. It is bound on its western side by the trace of the OHFZ 'base' and on its east side by a line parallel to the east coast of South Uist. Dearnley (1962) adopted the term 'pyroxene-granulite' for the Corodale gneiss, owing to the large amount of clinopyroxene and orthopyroxene present, and the granulite facies grade of metamorphism preserved. The unit is medium to coarse grained (c. 2-5mm),

composed of felsic layers with interbanded mafic layers or pods, and has the assemblage:

plagioclase - garnet - hornblende - clinopyroxene (diopside) - orthopyroxene (hypersthene).

Quartz is subordinate or absent. Coward (1972) reports the presence of an original igneous layering, and a spatial separation of different lithological units which he proposes as the result of magmatic differentiation. The unit also shows abundant evidence for a polyphase deformation and metamorphic history. A tectonically derived foliation, assigned the name "F1" by Coward (1972), with minor syntectonic recrystallisation is commonly observed in the Corodale Gneiss. The F2 and F3 fold phases which fold and refold this foliation are tentatively correlated by Coward (1972) with the F2 and F3 fold phases observed in the Grey Gneisses further west. This preservation of the regional structure above the fault base has not been observed anywhere north of this part of the OHFZ.

Brittle thrust deformation in South Uist

The eastern half of South Uist is extensively disrupted by the effects of brittle deformation. Both the Lewisian Grey gneiss and the Corodale gneiss show the similar effects of brittle deformation as seen in North Uist. Microfaulting, pseudotachylite generation and cataclasis are abundant, and are best developed close to the contact between Grey Gneiss and Corodale Gneiss.

By comparison with North Uist, no Crush Melange exists in South Uist, as relatively little pervasive crushing is apparent within the Corodale gneiss. A few small eastern promontaries (the largest of which is the Usinish Peninsula at NF 860350) however, are composed of extremely brittlely deformed 'Mashed' Gneiss, similar to that observed further north.

Localised brittle failure is apparent from below the fault base, but South Uist is host to the thickest and most continuous pseudotachylite/ ultracataclasite crush zones developed along the OHFZ. Two main geographical domains are apparent in the South Uist region; an area (chiefly at the 'thrust base') of crush zone formation; and an area (chiefly below the 'thrust base') of localised brittle failure. These two domains form the basis for the locality descriptions below.

4.2.6. Bealach an Easain

The area around Coire na Cuilc (NF 808205) exposes a section through a large *pseudotachylite/ ultracataclasite* crush zone, separating western banded Grey Gneiss from eastern Corodale Gneiss (Fig. 4.10).

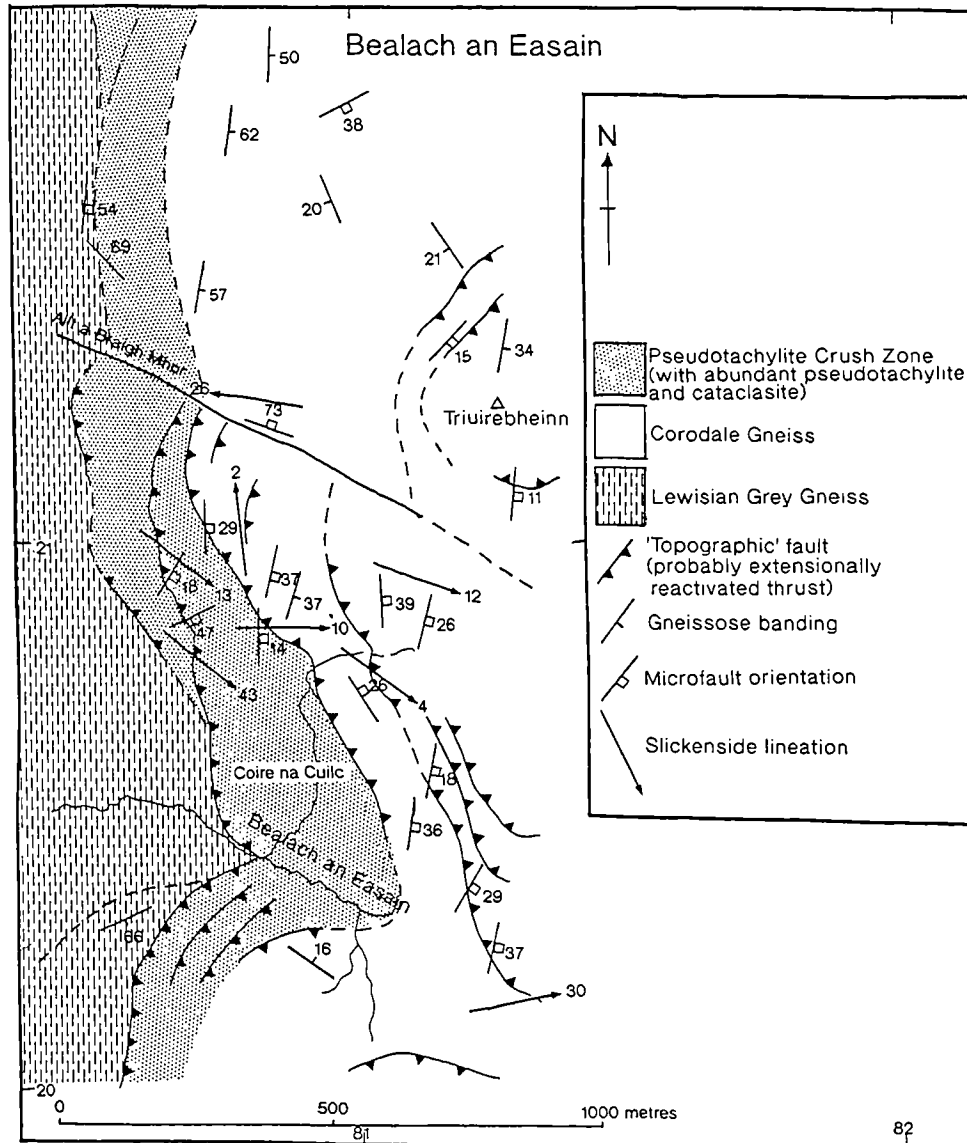


Figure 4.10. Geological map of Bealach an Easain, S. Uist.

Macrostructure

In the Lewisian gneisses below the fault base, numerous brittle fractures (traceable for up to 2-3m), with cm-scale displacements, cut through the gneissose banding and Laxfordian F2 and F3 structures. Pseudotachylite fault and injection veins are extremely common along these faults, and typically range between 1mm and 2cm in thickness. Displacements are largely compressional (c. 60:40 ratio of thrust to normal faults), but displacement direction indicators are not usually

exposed, and thus displacements are only apparent. Very little metamorphic degradation of the hornblende-bearing western gneisses has occurred, and amphibolite facies assemblages are preserved. At the fault 'base', the gneiss is extremely cataclastically ^{deformed} and existing structures, (including banding) are virtually obliterated.

Separating the Lewisian Grey Gneiss from the overlying Corodale Gneiss, are several topographic faults, which occur as stacked, laterally continuous fault planes, dipping at c. 25 - 40° (Fig. 4.11). Where the fault planes are not directly exposed, the trace of the faults can be delineated by marked breaks in slope, at least 6 of which occur on the SW slope of Triuirebheinn (NF 808208). The topographic faults are subparallel to each other, but linking splays between individual fault strands also occur, (e.g. between Coire na Cuilc (NF 807206) and Allt a' Bhraigh Mhoir (NF 807213)). Movement direction indicators on the topographic faults, including fault striae and slickenfibres, usually plunge to the SE. Secondary ESE-dipping R-shears are commonly developed in the region of topographic faults, especially in the immediate footwalls, and mostly display geometries consistent with top-to-the-ESE movement (Fig. 4.12). Small m-scale normal fault duplexes are also developed occasionally (e.g. at NF 808210). Infrequent ENE-WSW trending fault slickensides also occur, and are associated with top-to-the ENE movements, suggested from R-shear orientations. At NF 813202, the ENE plunging slickensides are observed to overprint the SE plunging slickensides, suggesting that reactivation of these structures has occurred. The material isolated as 'screens' between the topographic faults varies from west to east. In the west of the region, a 25-30m thick pseudotachylite/ ultracataclasite crush zone occurs, whilst in the east, Corodale Gneiss with localised brittle microfaulting occurs.

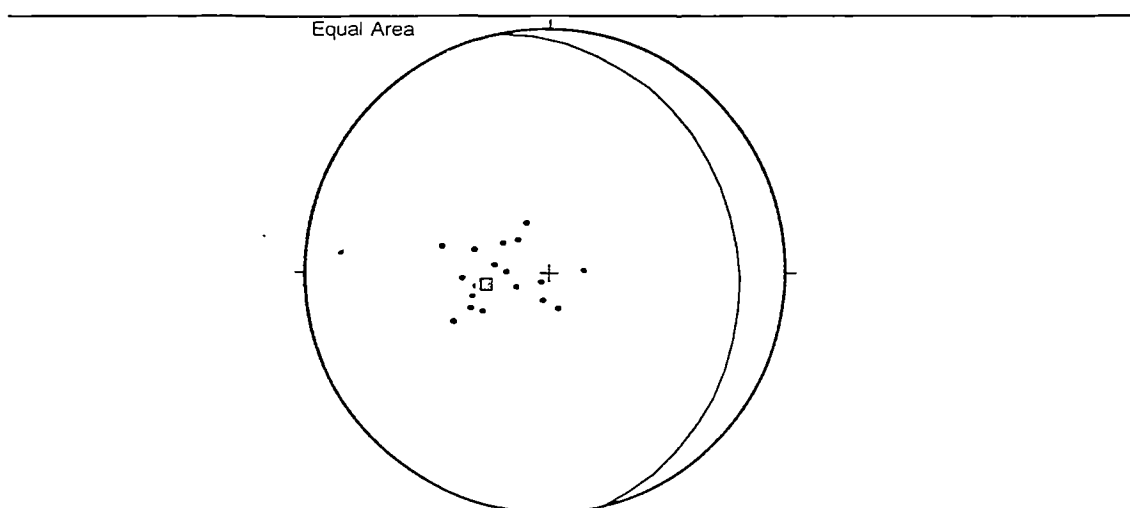


Figure 4.11. Equal area stereonet of poles to topographic faults with mean great circle from Bealach an Easain.

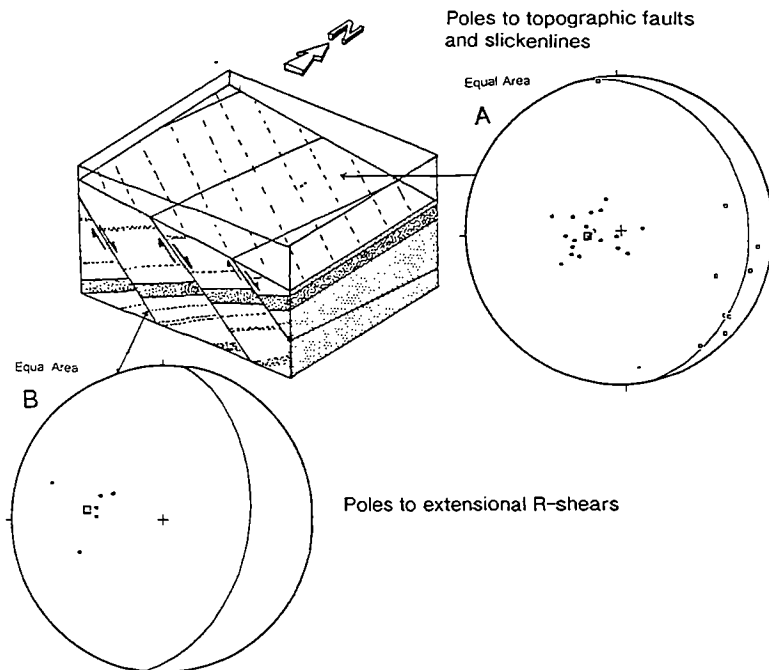
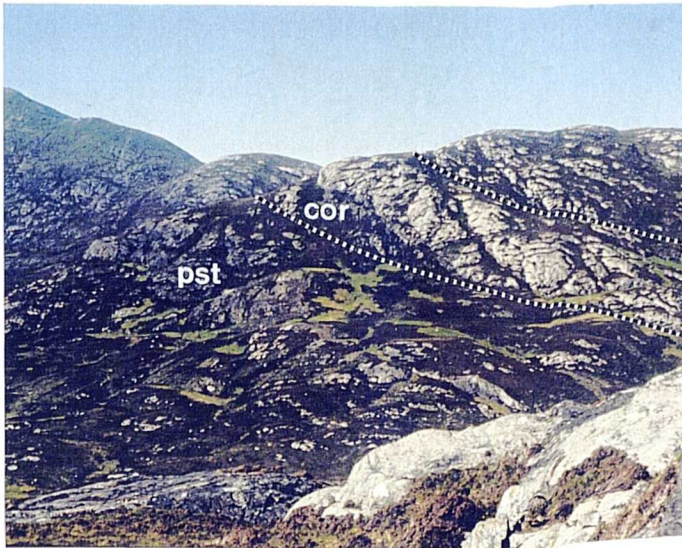


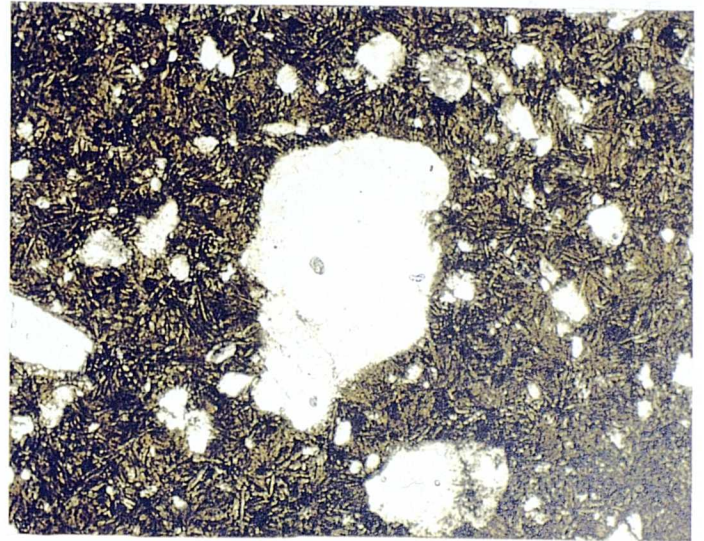
Figure 4.12 Block diagram of topographic fault and R- shear geometries from Bealach an Easain, S.Uist. Equal area stereonets of poles to extensional R-shears with mean great circle and poles to topographic faults (dots) with mean great circle and slickenlines (boxes).

The major pseudotachylite/ ultracataclasite crush zone (termed the Outer Isles Crush Zone by Coward 1969) forms an obvious east-dipping band 20-30m thick which is significantly darker in colour than the surrounding gneiss (Plate 4.4a). The band can be traced northwards towards Stulaval (NF 806240) and southwards to Beinn Ruigh Choinnich (NF 804197). In detail, the crush zone is extremely fine grained, black, massive, and contains gneiss fragments, usually on a mm-cm scale. It appears structureless, except for numerous, orthogonal, closely spaced joints, which give the rock a shattered appearance. Frequently, individual fault and injection veins of pseudotachylite are discernible within the crush zone, and several phases of pseudotachylite generation (the 'multiple Jerk' mechanism of Sibson 1977b) have undoubtedly occurred.

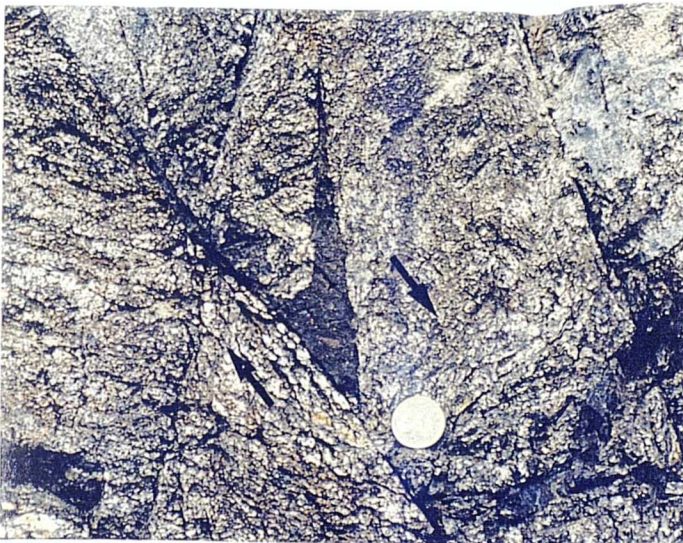
Discrete, pale green or cream-colored zones of alteration, < 2cm thick, pervade much of the crush zone material in E-W trending, subvertical veins, altering the pseudotachylite to epidote, sericite and chlorite. Small dilational jogs are sometimes present along these veins, and show sinistral sense displacements. Coward (1969) describes the veins as evidence for incipient phyllonitisation. No evidence has been found which links them to phyllonitisation, however, and an entirely separate origin cannot be discounted. E-W trending subvertical quartz veins frequently coincide with these epidote veins and may have acted as loci of devitrification in the pseudotachylites.



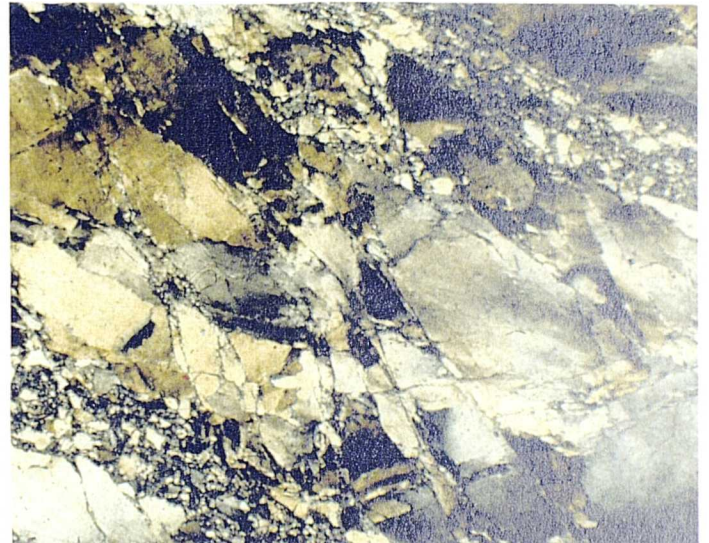
a)



b)



c)



d)

Plate 4.4 Brittle thrust deformation in S.Uist

a) View north from Bealach an Easain (NF 808210) towards Stulaval, showing large pseudotachylite/ ultracataclasite crush zone (pst), topographic faults and Corodale Gneiss (cor).

b) Pseudotachylite from bealach an Easain (NF 810208), showing devitrifying stellate spherulites. Field of view is 2.5mm. (PPL)

c) Pseudotachylite injection vein in T-fracture orientation showing normal sense of shear, from Eriskay (NF 794112).

d) Brittle deformation of quartz from Barra (NL 666 886) showing undulose extinction (cold working) of relict grains, transcrystalline fractures, and cataclased quartz within those fractures. Field of view is 5mm. (XPL)

In the heavily faulted and fractured Corodale gneiss above the crush zone, the Laxfordian, ESE-dipping 'F1' fabric described by Coward (1969, 1972) is still discernible as elongate feldspar aggregates in places (e.g. at NF 808209). The F1 fabric lies subparallel to the crush zone and bounding topographic faults, and has clearly acted as a control on their geometry. Cross-cutting this early fabric are minor black, devitrified pseudotachylite fault and injection veins with pinch-and-swell geometries. They are c. 2mm-2cm thick, and show evidence of brown-coloured chilled margins <1mm thick. Pseudotachylite fault veins, like the topographic faults are also often concordant to the Corodale Gneiss F1 foliation, and have been controlled by this pre-existing fabric. Where the fabric has been folded, pseudotachylite is occasionally injected along curved surfaces (e.g. at Creag na h-Inghinne (NF 813205). Injection veins in T-fracture orientations, along pseudotachylite-bearing faults, give evidence of chiefly top-to-the SE normal movements. The degree of pseudotachylite generation drops off from west to east, away from the fault base.

Microstructure

In thin section, little more can be made of the pseudotachylite/ultracataclasite crush zone that is not discernible in the field. The unit is dark brown or black, extremely fine grained and very occasionally isotropic. The extremely fine grain size of the material makes mineral identification impossible at the scale of thin section. Clasts within the crush zone are quartzo-feldspathic, and show quartz grains with undulose extinction and brittle transcrystalline fractures. Both plagioclase and K-feldspar are apparent, but alteration to sericite and epidote is advanced. Some pseudotachylite injection veins and breccias within these crush zones show incipient devitrification, in the form of stellate spherulites, radiating from gneissic inclusions (Plate 4.4b)

Cross-cutting and therefore post-dating the crush zone, are tiny anastomosing hairline fractures filled with calcite, epidote, quartz and chlorite in several sets. Alteration zones immediately adjacent to these veins and of various thicknesses are marked by a discolouration ('bleaching') of the dark amorphous groundmass. These veins are exactly the same type as those noted on a larger scale, and probably relate to later, post-tectonic fluid flow along the fractures.

Metamorphic conditions during deformation

The extremely brittle nature of the deformation, including the generation of cataclasite and ultracataclasite appears to suggest a low P-T environment. As

already noted however, all metamorphic retrogression is late, and the amphibolite facies gneiss assemblage is metastable throughout brittle deformation. These possibilities are discussed in section 4.2.12.

4.2.7. Ben na Hoe

A narrow strip of land between Beinn nan Caorach (NF 815295) and Meall Mòr (NF 810274) exposes a well defined contact between the western banded Grey Gneiss and the overlying Corodale Gneiss (Fig. 4.13). A large *pseudotachylite-ultracataclasite crush zone* is apparent between the two units for much of this area.

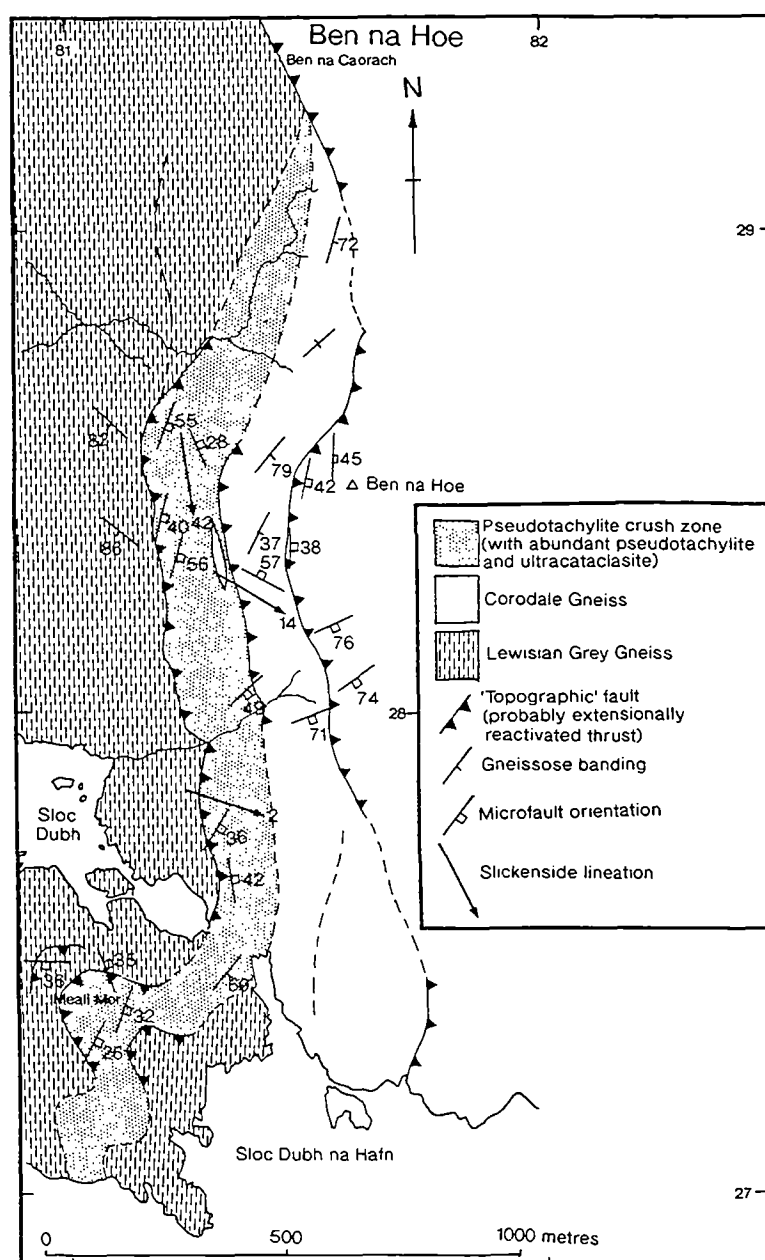


Figure 4.13. Geological map of Ben na Hoe, S.Uist.

Below the fault base, the Lewisian Grey Gneiss is banded and possesses Scourian folds and discordant, Late Scourian Younger Basics, indicative of low Laxfordian strain. The banding in the gneiss dips steeply to the SW, in sharp contrast to the moderate easterly dipping topographic faults above. Very little fabric control on fault geometry is observed in the Grey Gneiss. As the fault base is approached from the west, the intensity of brittle fracturing increases, especially within 10m of the fault base. Little microfaulting and pseudotachylite generation is observed further west, and the gneisses remain intact.

At the fault base, a laterally continuous topographic fault occurs, with two more faults picked out by marked breaks in slope further east. These faults, unlike those at Bealach an Easain are infrequently directly exposed, but share the tendency to form as stacked families, moderately dipping between ENE and ESE (Fig. 4.14a). The intensity of brittle fracturing and the amount of generated pseudotachylite increases dramatically within 1 metre of the westernmost topographic fault. Subsidiary faults subparallel to the larger structures possess well-defined slickensides, which plunge dominantly SSE, at a low-angle to strike. Kinematic indicators parallel to this lineation are often contradictory, and the movement sense remains enigmatic. A second, less well developed linear fabric is also apparent on some topographic faults, and comprises ENE plunging fault striae. Secondary R-shears with a steeper dip than the topographic faults dip between ESE and ENE, indicative of bulk top-to-the-east normal faulting (Fig 4.14b). The continuity of these structures, and the fact they are never cross-cut by the effects of minor faulting suggests that they are relatively late features of the fault zone. A very late, ESE-WNW-trending open fold is discernible, both in the field, and from the change in orientation of both topographic faults and normal R-shears (Fig. 4.15) (N.B. The apparently steeper fold axis deforming the R-shears, compared to that deforming the topographic faults is due to the pre-fold geometry). This phase of folding is very late in the structural history of the region and is not thought to be regionally significant.

Above the lowest topographic fault, a large pseudotachylite-ultracataclasite crush zone occurs c. 30m thick. This zone, picked out at a distance by a dark coloured, positively weathering ridge, is laterally continuous for over 2 km, but appears to pinch-out south of Beinn nan Caorach (NF 815292). This pinching-out may be due to the northward reduction in vertical separation between the bounding topographic bounding faults. North of this area Grey Gneiss lies directly underneath Corodale gneiss. Coward (1969) marks 4 individual subparallel crush zones on his map of the Ben na Hoe region. No evidence for more than one crush zone has been found during the present work, however. The crush zone is composed mainly

of black, extremely fine grained pseudotachylite and/ or ultrataclasite, with very little coherent structure. Clasts of both grey gneiss and (subordinate) Corodale gneiss are common on various scales, and appear to become dominant over the finer grained matrix towards the top of the crush zone. Compared to the crush zone base, the crush zone top contains relatively little pseudotachylite, and locally possesses a lower pseudotachylite content than that of the immediately adjacent Corodale gneiss, in the topographic fault hangingwall.

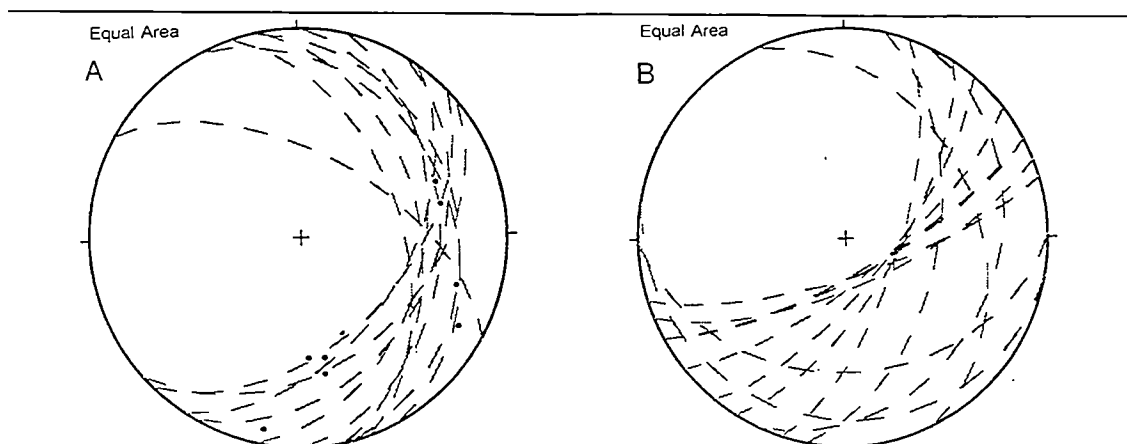
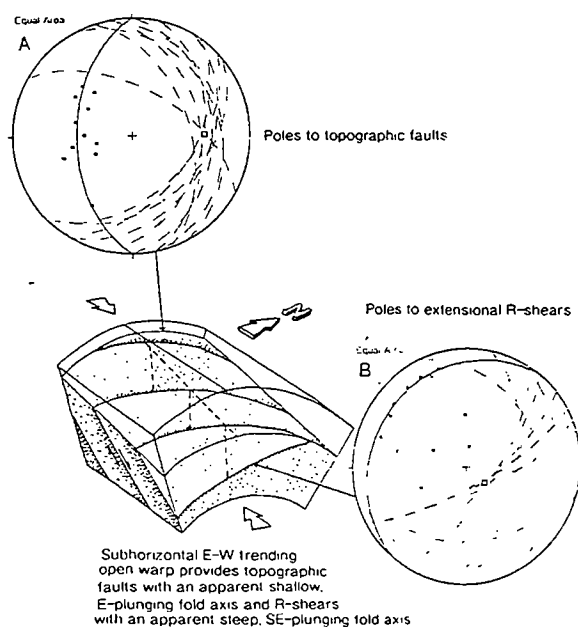


Figure 4.14. Equal area stereonets of: A) topographic faults (dashed great circles) with slickensides (dots); and B) subsidiary R-shears (dashed great circles) from Ben na Hoe, S. Uist.



Note: Pre-fold geometry shows R-shears strike clockwise of topographic fault:

Figure 4.15 Block diagram of topographic fault and R- shear geometries from Ben na Hoe, S.Uist. Equal area stereonets of: A) topographic faults (dashed great circles), poles to topographic faults (boxes), fold girdle (solid great circle) and fold axis (solid box); and B) extensional R-shears (dashed great circles), poles to extensional R-shears (boxes), fold girdle (solid great circle) and fold axis (solid box) .

Above the crush zone, pyroxene and garnet bearing Corodale gneiss occurs, containing much less quartz than the Grey Gneiss. This is directly juxtaposed against the crush zone by the intervening topographic fault. There is no evidence to support Coward's (1972) map which shows a laterally continuous thin sliver of Grey Gneiss *above* the crush zone. Moreover, a small 100m long lens of Corodale gneiss actually occurs *within* the crush zone at NF 813284 (see Fig. 4.13). Present work has shown that an intervening Grey Gneiss unit does occur, but is restricted to the region SE of Meall Mòr (NF 812273).

The dominant foliation in the Corodale gneiss is the 'F1' foliation of Coward (1969), defined by elongate feldspar aggregates and aligned ortho- and clinopyroxenes. This trends NE-SW and dips steeply SE, at a high angle to the moderately dipping faulting and crush zone envelopes. It appears that banding in this unit, like the Grey Gneiss, exerted little control on topographic fault orientation.

Microfaults are abundant in the Corodale gneiss, and >50% show thrust-sense, top-to-the-west displacements, often with minor cataclasite development or pseudotachylite generation. In general, the pseudotachylite content of the Corodale Gneiss is higher than that of the Grey Gneiss. Pseudotachylites mainly form in c. 2mm thick veins or vein networks, but some pseudotachylite breccias (c. 50cm thick) also occur. The envelopes to the breccias are parallel to the topographic faults and minor thrusts, and are likely to have been generated by minor thrusting. Injection veins are present on many fault veins and may reach thicknesses of c. 25cm. Some pseudotachylite-bearing faults however, show apparent normal displacements to the SE. From these observations, it seems likely that:

- Topographic fault orientations were controlled by pre-existing minor faults and not the orientation of gneissose banding, as observed elsewhere,
- Pseudotachylite generation occurred on thrusts *and* normal faults, but no consistent cross-cutting evidence has been found which elucidates whether both these types occurred as a result of overall compression, or as a result of reactivation in a different shear sense. For reasons outlined in section 4.2.12, it is thought unlikely that a regionally significant extension event generated the pseudotachylite. In addition, the juxtaposition of granulite facies Corodale Gneiss structurally above amphibolite facies Western Gneiss, has long been suggested as the result of an overthrust setting (e.g. Jehu and Craig 1925) and is difficult to reconcile with extensional movement.

4.2.8. Eriskay

The southwestern slopes of Ben Srien (NF 793110) on the island of Eriskay (Fig. 4.2) preserve excellent evidence for *localised brittle failure* west of the fault zone base. The Lewisian Grey gneissose banding in this region dips predominantly shallowly ($20\text{--}30^\circ$) to the east or northeast, and forms a strong geometrical control on the orientation of subsequent brittle fracturing (Fig. 4.16). East-dipping, concordant pseudotachylite breccia envelopes c. 20cm thick, and individual fault veins are common, and often possess injection veins which form in T-shear orientations (Plate 4.4c). Both normal and reverse faults are apparent from these geometries as well as from displaced marker bands, with apparent displacements in the order of 10-20cm. Slickenfibres plunge down the dip, so the apparent displacements on these faults may closely approximate the true displacements. In this area, normal faults appear to dominate over reverse faults. In areas where Lewisian folds occur, banding orientation is effectively ignored, and the faults are observed to cross-cut the pre-existing structures. Several laterally traceable topographic faults occur parallel to this fabric, and possess slickensides and subsidiary R-shears indicative of top-to-the-east, normal motion. These topographic faults are never cross-cut by pseudotachylite veining, and therefore post-date the earlier pseudotachylite generating faults.

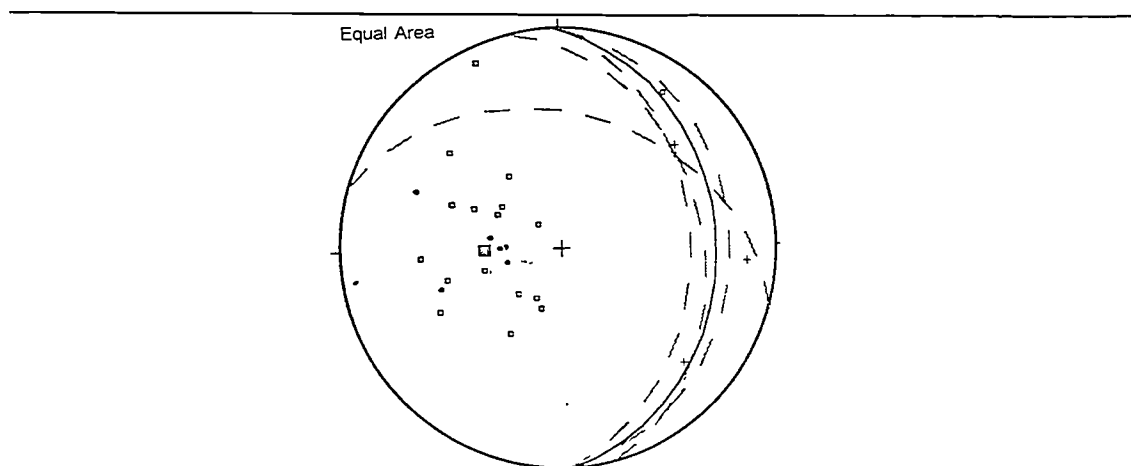


Figure 4.16. Equal area stereonet of Lewisian banding (dashed great circles), faults (boxes), pseudotachylite bearing faults (dots), slickensides (crosses) and mean fault orientation (solid great circle), from Eriskay.

(iii). The Barra Isles

Geographical setting

The islands of Berneray, Mingulay, Pabbay, Sandray, Vatersay and Barra are the most southerly of the Outer Hebridean island chain. Of these, only

Sandray (not visited during the present work), Vatersay and Barra possess features associated with the Outer Hebrides Fault Zone (Fig. 4.17).

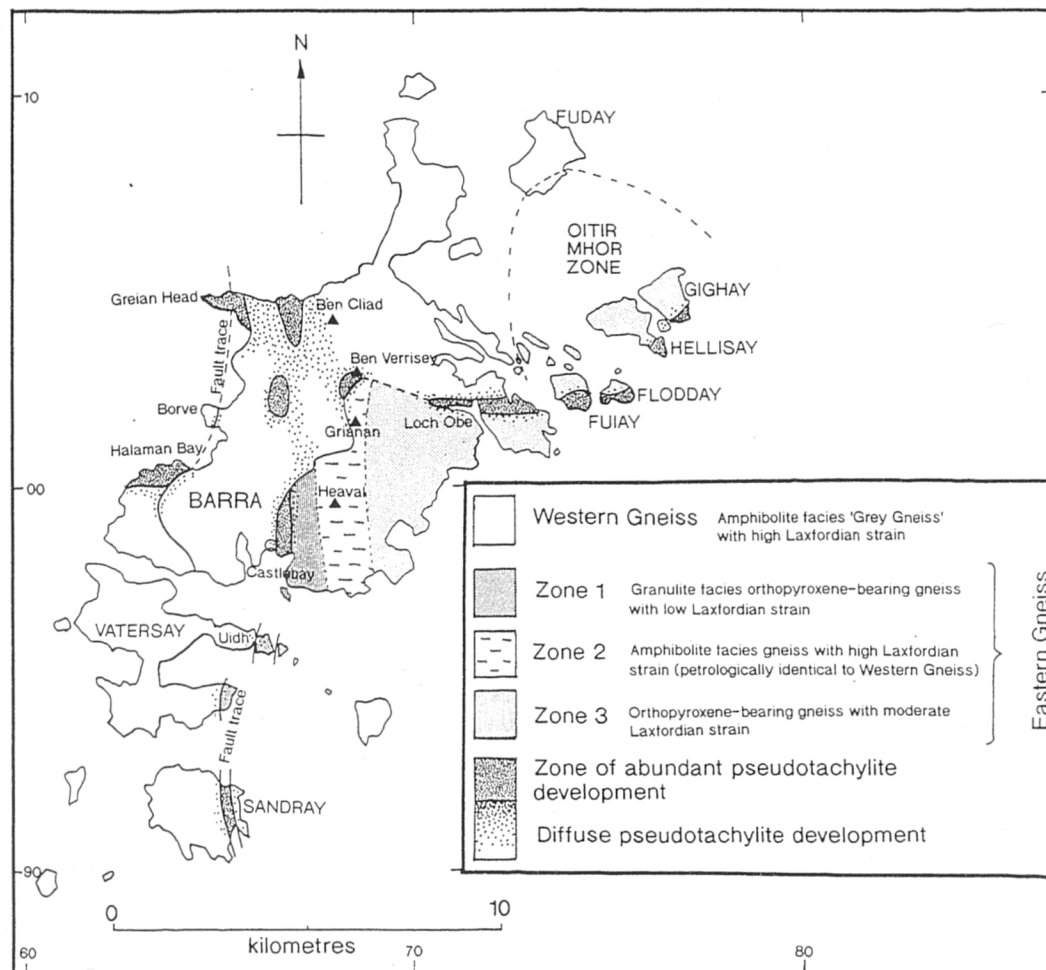


Figure 4.17. Geological map of the Barra Isles (modified from Francis 1973 and Fettes et al. 1992).

In contrast to much of the Uists, the topography of the Barra Isles is rugged, culminating in the hill Heaval (383m) in south-central Barra. Erosion resistant fault rocks, characteristic of the Uists, are not well developed in the area. Exposure is generally good and accessible.

Lewisian geology of the Barra Isles

There are two main lithologies in Barra, separated into western and eastern regions by the trace of the OHFZ base. The 'Western Gneisses' are heterogeneously deformed amphibolite grade banded Lewisian Grey Gneiss described previously (see chapter 2). These are typically medium grained (2-3mm) acid orthogneiss, interbanded with older basic material. The assemblage: quartz (c. 30%); plagioclase (c. 30%); K-feldspar (c. 15%) and hornblende (c. 10%), is typical. Garnet is often present in small amounts. The 'Eastern Gneisses' by contrast,

preserve evidence for granulite facies metamorphism, which Dearnley (1962) regarded as early Laxfordian, but which is now thought by most workers to be preserved Scourian metamorphism (e.g. Fettes et al. 1992). Orthopyroxene-bearing banded acid and basic units, and clinopyroxene and orthopyroxene bearing basic dykes (Correlated with the Scourie dyke suite of mainland Scotland by Francis, 1969 (after Dearnley 1962)) are present in the eastern Gneisses.

The two-pyroxene-bearing Scourie dykes are preserved in a variety of tectonic states above the fault base in Barra, which is dependant on the intensity of overprinting Laxfordian strain. Francis (1969) divided the eastern region into 3 zones:

1. A zone of least deformation, where granulite facies Scourie dykes are markedly discordant to the gneissose banding.
2. A zone of intense deformation, where amphibolite facies Scourie dykes are concordant to the gneissose banding and often folded and/or boudinaged.
3. A zone of moderate deformation, where partially amphibolitised (mostly granulite facies) Scourie dykes are often folded but still preserve discordant relationships.

A region of pyroxene-bearing gneiss has been mapped west of the fault trace by Francis (1973). This area, comprising the islands of Gighay (NF 765048), Hellisay (NF 755044) and the SE part of Fudhay (NF 735085), was termed the Oitir Mhór Zone by Francis (1973). These rocks, which strongly resemble the eastern gneisses, lie west, instead of east, of the fault zone. Francis regarded this anomaly, as an inlier of deeper level (infra-structural) granulite facies Eastern Gneiss occupying the core of a major Laxfordian antiform whose limbs were derived from supra-structural, retrogressed, amphibolite facies western Gneiss. A simpler explanation for this anomaly arises if the trace of the contact between Western and Eastern Gneiss is reinterpreted (see discussion in section 4.2.12)

Four Laxfordian deformation events have been recognised on Barra in the Western Gneiss (Francis 1973) (outlined in chapter 2). The most important deformation phases are the 'F2' event, which produced recumbent isoclinal folds, and the 'F3' event, which refolded the earlier folds and produced the regional structure.

In Barra, Laxfordian 'F3' folds are preserved *above* the thrust base. A comparison of the trend of these structures with those below the thrust base have been used previously to elucidate fault zone movements (Francis 1973, Sibson 1977b). A critique of this method of displacement estimation is provided in Chapter 5.

Brittle thrust deformation in Barra

In marked contrast to the extensive brittle thrust deformation in North and South Uist, relatively little deformation associated with OHFZ movement is preserved in Barra. Microfaulting, pseudotachylite generation, and a minor amount of cataclasis occur, but no large pseudotachylite/ ultracataclasite crush zones of the type observed at Eaval (NF 899606) Bealach an Easain (NF 808205) and Ben na Hoe (NF 813285) are present. Similarly, no Crush Melange or Mashed Gneiss occurs.

4.2.9. Castlebay to Otir Mhor

Macrostructure

The trace of the OHFZ in Barra is marked by a topographic break which runs north from Castlebay (NL 666983) for c. 2.5km (Fig. 4.17). North of Heaval (NF 678007), the trace is observed to swing north-eastwards, chiefly as a result of the topography, before continuing north towards Ben Verrisey (NF 685027). Previous workers (e.g. Francis 1973, Sibson 1977b, Fettes et al. 1992) suggest the fault trace undergoes a major right-angle bend at this location, to continue eastwards towards Loch Obe (NF 710020). The present work has failed to corroborate this inferred major change in strike, and a possible alternative fault trace is discussed in section 4.2.12.

In contrast to other parts of the OHFZ, only one topographic break marks the fault zone trace, and corresponds to a laterally extensive NNE-SSW trending brittle fault which dips east at c. 25°, subparallel to the banding in the Eastern Gneisses.

The quartzo-feldspathic gneissose footwall rocks and the pyroxene-bearing, microdioritic hangingwall rocks are both injected with minor amounts of pseudotachylite. Pseudotachylite occurs in concordant and discordant fault veins as well as injection veins. In areas where veining is very well developed, 'multiple jerk' vein networks and breccias occur (using the terminology of Sibson 1977b). The envelopes to the pseudotachylite breccias are usually also parallel to gneissose banding and dip moderately east. A contrast in the behaviour of pseudotachylite exists between those veins formed in the hangingwall and those formed in the footwall. The banding in the hangingwall rocks remains intact along the length of the fault trace, and the pseudotachylite content quickly dies off immediately east of the fault trace. By contrast, the footwall rocks are intensely and incoherently microfractured, crushed and injected with pseudotachylite for up to 40m west of the fault trace. Between Grianan (NF 680015) and Ben Verrisey (NF 685027), the trace

of the fault zone becomes obscure. Very little microfaulting and pseudotachylite generation is apparent and faulting may be relatively minor at this locality.

For much of the observed length of the topographic fault, N-S trending parallel faults, in both the hangingwall and footwall, are often barren of pseudotachylite, and occasionally possess ESE-plunging fault striae (Fig. 4.18). Sense-of-displacement indicators are rare but small, discontinuous, discordant, E-dipping microfaults usually show apparent compressional displacements in the order of a few cm, displacing top-to-the-W or NW (c. 70:30 ratio of thrust to normal faults). Apparent displacements on similar, W-dipping faults occasionally show extensional displacements, but again mainly displace top-to-the-W. This suggests that the deformation occurred in a thrust, top-to-the-west kinematic regime. In addition, the change in metamorphic grade across the fault zone, from amphibolite facies in the west to granulite facies in the east has been cited by previous workers (e.g. Jehu and Craig 1925), as evidence to suggest the fault is a major thrust.

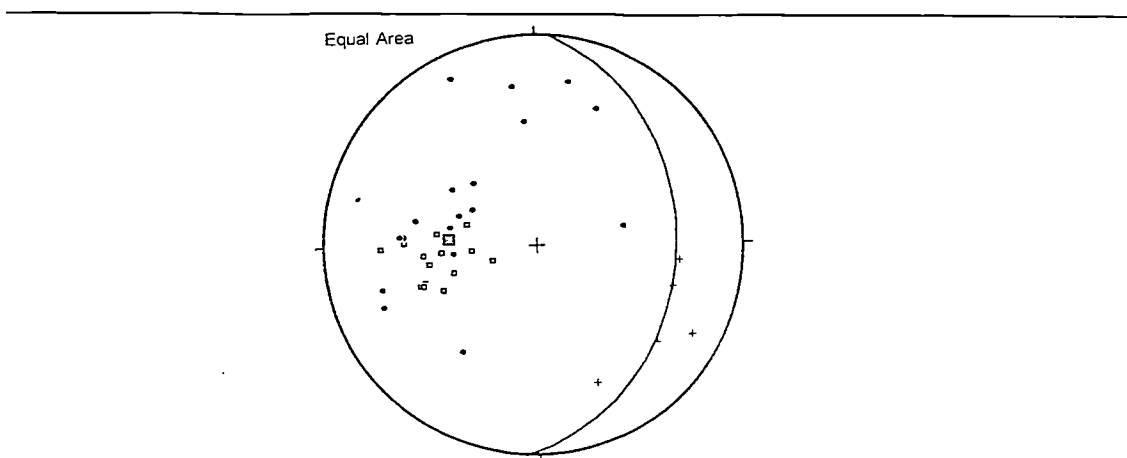


Figure 4.18. Equal area stereonet of faults (boxes), pseudotachylite bearing faults (dots) and fault striae (crosses) from Barra.

Microstructure

The deformation associated with the fault zone in Barra is extremely brittle. Quartz shows evidence for 'cold working' by the common occurrence of grains with undulose extinction. This manifests itself in the field as blackened or 'bruised' quartz grains. Quartz 'subgrains' only occur in transcrystalline fractures and are therefore not true rotationally recrystallised subgrains, but the comminuted products of cataclasis (Plate 4.4d). All other minerals deform in a brittle manner also. Feldspars are fractured and comminuted, but in comparison to similar rocks from North and South Uist, remain metastable, with only partial retrogression to sericite. Hornblende, biotite and pyroxenes also remain metastable, but are often intensively fractured and faulted.

Metamorphic conditions during deformation

The amphibolite facies assemblage, brittle style of deformation, and high pseudotachylite content of these rocks, suggests P-T and fluid conditions during deformation were the same as those accompanying Crush Melange formation (see section 4.2.1) and ultracataclasite/ pseudotachylite crush zone development (see section 4.2.2). The lack of any large area of crushing and the lack of stacked topographic fault families in Barra (cf. North and South Uist) is unlikely to relate to differing P-T-fluid conditions but may be due to the lower frequency and/ or magnitude of fault slip events.

4.2.10. Vatersay

The Uidh peninsula in NE Vatersay (NL 655960) is joined with Creag Mhor (NL660956) by a small sand-covered isthmus (Fig. 4.19). This topographic hollow coincides with the trace of the OHFZ as it continues southwards from Castlebay in Barra (NL 665983). A similar topographic expression of the fault trace is encountered on the western slope of Am Meall (NL 648944) further south. Although the fault trace is never directly exposed, the adjacent Western Gneisses in the fault footwall, and the Eastern Gneisses in the hangingwall, contain abundant microfaults and pseudotachylite veins within 400m of the fault trace. No large-scale pseudotachylite/ ultracataclasite crush zone occurs (cf. IGS map. Fettes et al. 1992).

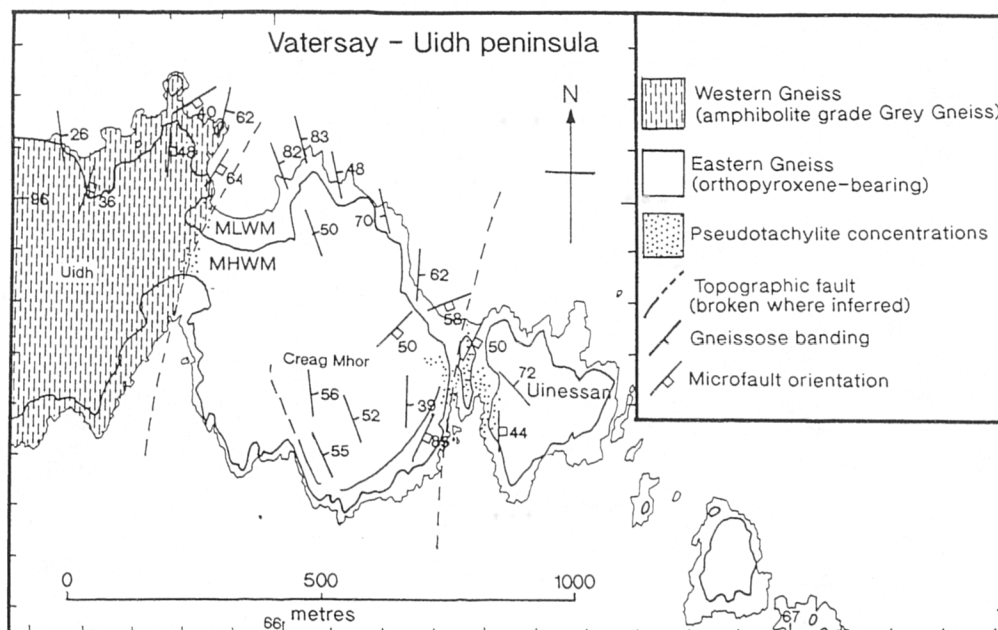


Figure 4.19. Geological map of Uidh, Vatersay.

The Eastern Gneisses are orthopyroxene-bearing diorites, with abundant clinopyroxene and garnet. They retain their original gneissose banding, which trends dominantly NNW-SSE and dips moderately or steeply ENE (Fig. 4.20a). Cross-cutting microfaults strike between NE-SW and NW-SE, with most trending N-S, and become more abundant close to the inferred trace of the inexposed topographic fault (Fig. 4.20b).

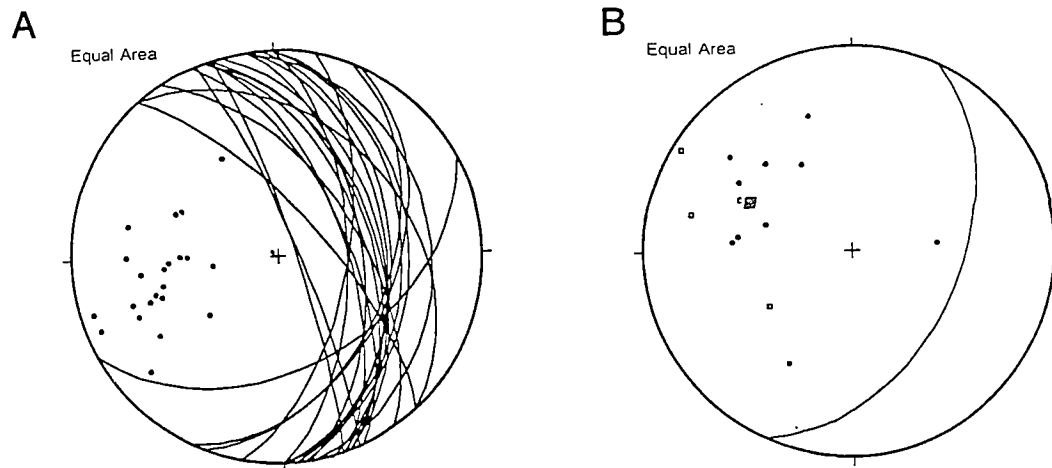


Figure 4.20. Equal area stereonet of: A) banding in Eastern Gneisses (great circles) and poles to banding (dots); and B) poles to microfaults (boxes) and pseudotachylite-bearing microfaults (dots), with mean great circle.

A secondary topographic fault occurs within the Eastern Gneiss immediately west of Uinessan (NL 664956), and a localised zone of intense pseudotachylite veining is generated. Concordant fault veins of pseudotachylite are common and dip c. 40-50° E, reflecting the relatively steep dip of the gneissose banding in this region. Another shallow SE dipping major fault occurs at Creag Mhor (NL 660956), but this does not appear to focus pseudotachylite development. Subsidiary faults in apparent R-shear orientations suggest extension, displacing top-to-the-east, has occurred on this structure, although no conclusive linear movement direction criteria have been found. It is thought that this structure has accommodated late extensional reactivation and is akin to the detachment faults observed in the Uists (see section 4.4).

4.2.11. Halaman Bay, Borge and Greian Head

A roughly N-S trending zone of abundant pseudotachylite veining occurs c. 3km west of the inferred main fault trace on Barra. This zone is exposed only on the most western peninsulas, and in particular, the southern side of Halaman Bay

(NF 644005), the southern side of Borge Point (NF650015), and Greian Head (NF 653048) (Fig. 4.21).

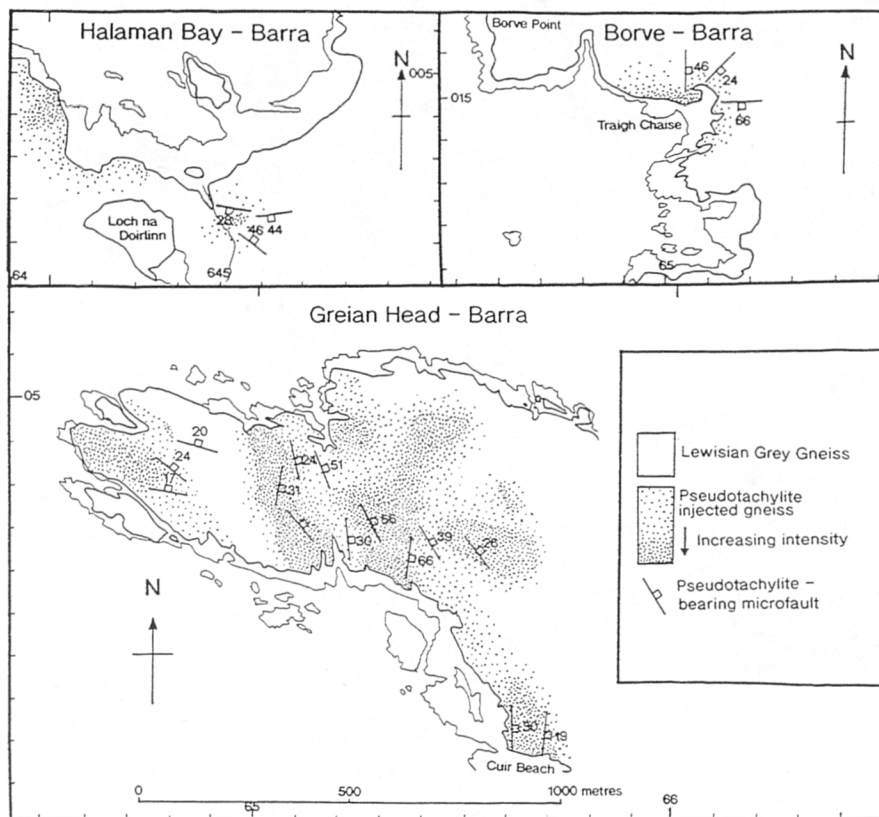


Figure 4.21. Geological maps of Halaman Bay, Borge, and Greian Head, Barra.

The Western Gneisses in these localities retain their original N-S striking, moderately E-dipping gneissose banding. The gneisses are uncrushed and relatively free of microfaults. In localised zones however, pseudotachylite generation on microfaults is abundant. At Traigh Chaise (NF 650015), a 5m wide zone of intense brittle deformation occurs, and 'single and multiple jerk' fault veins of pseudotachylite occur (using the terminology of Sibson, 1977b). Single jerk fault veins of pseudotachylite c.1mm - 2cm occur in mostly discordant, subvertical arrays, trending roughly E-W to the N-S trending banding. By contrast, multiple jerk faults, generating large injection veins (c. 5cm thick), ladder networks and breccias (with envelopes up to 50cm thick) are usually concordant to the foliation, dipping gently or moderately east. This relationship is reversed at Halaman Bay (NF 644005), where the zone of brittle rocks occurs over a much wider area (up to 500m), and breccia envelopes are markedly discordant to banding, and dip moderately N or S. An unexposed topographic fault is inferred to dip moderately east at this location, and can be traced southward as a marked break in slope on Ben Tangaval (NF 000635).

At Greian Head (NF 653048) and Cuir Beach (NF 656041), spectacular exposures of pseudotachylite-injected Western Gneiss occur. Pseudotachylite occurs as concordant and discordant fault and injection veins, ladder networks, breccias, and quasi-conglomerates (Plate 4.5a), frequently with chilled margins. The pseudotachylite complex is concordant to banding, trending NNW-SSE and dipping shallowly or moderately ENE (Fig. 4.22). Several phases of pseudotachylite injection have occurred, and cross-cutting veins are common (Plate 4.5b). Pseudotachylite quasi-conglomerates often form in the zone between R-shears and the main fault strands as a result of the coalescence of injection veins generated by both faults (Plate 4.5c). Clasts of gneiss entrained in these conglomerates are observed to become larger and less rounded away from the fault intersections, so that a quasi conglomerate grades first into a breccia and then into a ladder network over a distance of only 1.5m from the intersection point.

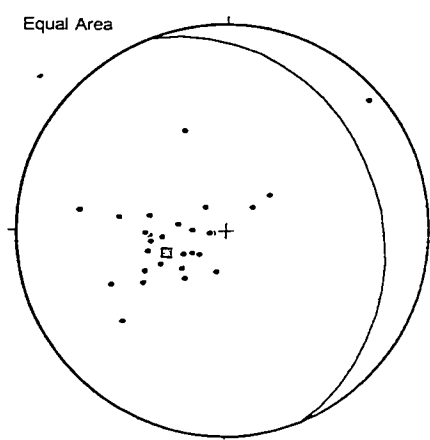


Figure 4.22. Equal area stereonet of poles to pseudotachylite-bearing microfaults with mean great circle, from Greian head, Barra.

Apparent microfault displacements in western Barra, deduced from offset marker bands in the gneiss, are usually between 2 and 10 cm, but no fault planes directly expose linear fault movement indicators. Both reverse and normal apparent shear senses occur. Reverse indicators dominate however (>60%), especially along multiple-jerk breccias and ladder networks, or along faults with larger apparent displacements (c. 2m). Apparent normal displacements are always confined to single jerk microfaults, and may therefore have important implications regarding the relative timing of reverse and normal movements (see section 4.2.12). Pseudotachylite injection veins adopt T-fracture or R-shear orientations, consistent with thrusting. Most of the deduced kinematic information in the region suggest a compressional, top-to-the-W or WSW shear sense regime prevailed during pseudotachylite generation.



Plate 4.5 Pseudotachylite injection complexes in Barra

a) Pseudotachylite quasi-conglomerate pavement from Cuir Beach (Greain Head), Barra (NF 656041).

b) Cross-cutting pseudotachylite breccias from Greian Head, Barra. (NF 652049)

c) Pseudotachylite quasi-conglomerates from Cuir Beach, Greian Head, Barra (NF 656041). The pseudotachylite ponds at the intersection of the generating fault (Y) and the subsidiary R-shear, forming a transition from quasi conglomerate (at the apex) to ladder network (further left).

The origin of this belt of pseudotachylite microfaulting, and its disassociation from the main fault trace, is not fully understood. Similar zones of pseudotachylite generation occur along the western coasts of North and South Uist at Aird an Runair, Ardivachar Point and Rubha Ardvule (see Fig. 4.1), and it is thought that the zones could be laterally continuous. Francis (1969) did not speculate whether the west Barra zone was part of the OHFZ, or whether it predated it. Sibson (1977) thought that the apparent truncation of this belt by the OHFZ in Barra made the latter suggestion a distinct possibility. Since the present work regards this cross-cutting relationship as unlikely (see discussion below), there is little evidence to support either viewpoint, and the origin of this belt remains enigmatic.

4.2.12. Conclusions and discussion on thrusting in the southern segment

Conclusions

The earliest phase of deformation in the southern segment of the OHFZ has generated a large, roughly NNE-SSW trending belt of very brittle deformation, in a highly deformed hinterland zone c. 5km wide which dips moderately eastwards. Brittle deformation affects broader regions of the foreland, up to 20km west of the fault base, where the Lewisian Grey Gneisses are subject to localised brittle failure. The narrow zone separating the foreland and hinterland regions of the OHFZ hosts stacked families of topographic faults, which envelope discontinuous pseudotachylite/ ultracataclasite crush zones.

The change in deformation style observed in the thrust sense fault rocks of the southern OHFZ from west to east is as follows:

- Discrete brittle faulting
- Discrete pseudotachylite and cataclasite generating faulting
- Localised zones of extremely intense ultracataclasis and pseudotachylite crush zone generation
- Pervasive crushing and cataclasis
- Extremely localised zones of coherent fabric development
- Generation of large-scale topographic faults

Although no chronology is implied by this list, the discrete faulting may be relatively early in the deformation sequence, whilst later phases of movement along topographic faults may have occurred after thrust deformation ceased.

Fault rock distribution

The large-scale distribution of deformation products into zones of very intense brittle deformation (the crush zones and/ or Crush Melange), and wider adjacent region of localised brittle failure, has been likened to the experimental behaviour of rocks in the laboratory. Sibson (1977b) satisfactorily explains this distribution, by drawing the analogy between the scattered, localised brittle failure west of the fault base and the microfracturing that occurs in laboratory uniaxial test specimens prior to major failure. He cites Scholz (1968), who found that microfracturing of the specimen under load occurs at a fraction of the ultimate strength, and that at about 90% of the ultimate failure stress, the microfractures cluster around the locus of the final fault plane. The earlier, more diffuse deformation is therefore thought to be the immediate precursor to the final development of the fault zone proper.

The kinematic regime

Brittle failure in the southern segment of the OHFZ appears to be associated with top-to-the west thrusting. Ambiguous displacements of marker horizons are common, however, and the overall kinematics of the region are locally complex. East of the fault base in North and South Uist, a variety of west and east dipping faults dominate the chaotic fracture patterns with both apparent reverse and normal displacements. These faults cross-cut each other and are probably therefore coeval.

Sibson (1977b) suggests that the Crush Melange of North Uist is the result of a major thrusting event along the OHFZ. White and Glasser (1987), however, cite evidence of bulk extension from syntectonic quartz veins within the melange, and conclude that an extensional origin for the melange could be equally viable. The extensional quartz fibres referred to by White and Glasser are only reworked by very late, extensional reactivation-related deformation, and may therefore be relatively late features, unrelated to the generation of the Crush Melange (see section 4.4.1).

The lack of displacement markers in the Crush Melange makes kinematic analysis uncertain. More useful information about fault zone kinematics can be gained from the less deformed Lewisian gneisses further west. Fault surface lineations, where present, are usually slickensides, composed largely of epidote and chlorite. These plunge down-dip and suggest dip-slip movements dominate. In most localities, the well preserved banding west of the Crush Melange shows a dominance of N-S trending compressional thrusts and backthrusts over extensional faults and faults with significantly different orientations.

At Eaval (NF 899606), the style of compressional faulting is different. Compared to the microfaults observed elsewhere in North Uist, the faults at Eaval are comparatively steeply dipping and form two conjugate sets with dextral and sinistral strike-slip motion. These accommodate E-W shortening, similar to the thrusts and backthrusts elsewhere. These conjugate strike-slip faults probably developed due to the unfavourable (steeply dipping) orientation of the pre-existing Lewisian gneissose banding anisotropy.

In South Uist, kinematic evidence is often ambiguous. Barren microfaults in the Corodale and Lewisian Grey Gneiss mainly show top-to-the-west thrust sense displacements. Some subordinate pseudotachylite veins however, adopt 'T-fracture' orientations indicative of top-to-the SE normal movement. This apparent extension along pseudotachylite generating faults is common to both fault segments (see also section 3.2.2) and may be the result of minor gravity induced adjustments occurring as aftershocks after the main compressional slip event. This interpretation is corroborated to some extent by observations on Barra, where extension-related pseudotachylites are always produced along 'single jerk' microfaults. These possible aftershock adjustments are then replaced by 'multiple jerk' events during renewed compression. Alternatively, overall thrusting may produce block rotations with localised normal movements to accommodate strain during compression. Theoretical considerations suggest that a major compressional structure is more likely to have developed the features observed because thrusts are *load strengthening* faults and therefore have a greater capacity for storing elastic strain energy (Sibson 1974, 1993).

This theoretical fault strength consideration also applies to the large pseudotachylite/ ultracataclasite crush zones generated in North and South Uist, and the intense pseudotachylite veining developed in the Western Gneisses of Barra. These 'multiple jerk' features are unlikely to have formed in a *load weakening*, extensional environment. Independent, direct kinematic evidence is also apparent from these areas. In Barra, The geometry of 'multiple-jerk' pseudotachylite generating faults and their subsidiary R-shears is consistent with top-to-the-west thrusting.

Many of the larger, more continuous faults, such as the 'topographic' faults coincide with the highest density of compressional microfaulting, associated pseudotachylite generation; occasional brittle shear sense indicators suggest a west-directed thrust-sense association. They are laterally continuous, however, are never cross-cut by the effects of cataclasis or faulting, and often possess extensional shear sense indicators, indicative of top-to-the SE movement. In rare instances, two different movement direction indicators are preserved on the same

fault surface. These major anisotropies may therefore have been reactivated and redefined by later deformation and not necessarily with the deformation regime responsible for the Crush Melange as a whole.

Pressure, temperature and fluid conditions during deformation

The deformation products associated with early movements on the OHFZ cannot be equated with the preserved metamorphic assemblage in a straightforward relationship. The deformation is extremely brittle and pervasive in all mineral phases, including quartz. In a 'normal' continental geothermal gradient (c. 30°C per km) (Sibson 1973), a temperature of <300°C at <10 km is required to account for this behaviour (Boullier and Bouchez 1978). The preserved mineral assemblages however, show no evidence for syntectonic retrogression from amphibolite facies or locally granulite facies. Unaltered hornblendes are common in the Grey Gneiss, and unaltered orthopyroxenes frequently occur in the Eastern Gneisses. These assemblages are only in equilibrium above 500°C. To account for this 200°C discrepancy in the inferred palaeotemperature, specific conditions of fluid pressure and/or strain rate are required. These are discussed in the following section.

Discussion

Deformation conditions: high or low grade?

The discrepancy in inferred palaeotemperature between the non-retrogressed amphibolite facies mineral assemblages and the very brittle style of deformation in the early thrust-sense deformation along the OHFZ may be explained in two ways (Table 4.1)

Until recently, high water content of fault rocks were thought to be incompatible with pseudotachylite generation. Sibson (1975), argues that pseudotachylite can only be generated if the frictional heat is enough to cause melting, which, in medium-coarse grained, acid, crystalline rocks, is c. 800°C (Sibson 1973). The heat generated by the fault, in turn, depends on the frictional strength of the fault. According to Sibson (1973, 1975), if water is held at a roughly constant volume around the fault plane, sufficient frictional heat will not be generated and pseudotachylite will not form. Fluids also cause hydrolitic weakening of quartz (Griggs, 1967) and promote crystal-plastic flow and reaction softening (Magloughlin 1992), again reducing the likelihood of pseudotachylite generation. Dry rock conditions and a shallow depth range (c. 1-10 km according to Sibson,

1975 or 1.5-15km according to Techmer et al. 1992) were therefore thought to be necessary to account for rocks with a high pseudotachylite content.

1) Deformation occurred at high grade	2) Deformation occurred at low grade
Amphibolite facies mineral assemblages were in equilibrium during <i>amphibolite facies deformation</i>	Amphibolite facies assemblages were not in equilibrium (i.e. metastable) during deformation at <i>lower grades</i> than amphibolite facies.
<i>Fluids</i> may or may not have been present but <i>were unimportant</i> and did not affect the assemblage	<i>Fluid-absence and/ or rapid exhumation prevented retrogression</i> (re-equilibration) to a lower grade assemblage
<i>High strain rates and/ or high pore fluid pressures were required</i> to promote brittle fracturing at amphibolite facies	<i>High strain rates and/ or high pore fluid pressures were unnecessary</i> to account for brittle deformation at lower than amphibolite facies

Table 4.1 Two alternative high grade and low grade deformation scenarios, and their respective causal factors, required to account for a discrepancy in inferred paleotemperature during brittle thrusting.

Magloughlin (1992), however, argues that water serves to reduce the melting point of rock, reduce the viscosity of pseudotachylite melt and create hydrofractures, which serve to effectively evacuate the fluid from the fault surface and maintain frictional strength. This has been borne out by observations during high speed drilling (Killick 1990), where frictional melting has occurred in a water-saturated rock. Thus, the presence of pseudotachylite cannot apparently be used as a reliable indicator of a dry environment.

It should be noted, however, that Magloughlin (1992) cites evidence for pseudotachylite generation in *pelitic* rocks, and concedes that melting may have occurred at lower temperatures than those required to cause melting in medium - coarse grained quartzofeldspathic rocks with a high shear strength, such as Lewisian Gneisses. In coarse-grained gneisses, such as those cut by the OHFZ, much higher temperatures (c. 800°C) are required to generate melt and the absence of water may be more important in generating frictional heat. For this

reason, fluid-absence is regarded as a favourable condition for pseudotachylite generation along the OHFZ.

If the assumption is made that fluids were *absent* during deformation, high pore-fluid pressures are not regarded as a viable explanation of deformation behaviour. Although the large degree of cataclasis could be well explained by fluid pressure, cataclasis is probably due to high confining pressures at depth, which have the effect of making a new fracture easier to form than continuing movement along an existing fracture (Twiss and Moores 1992), (see also chapter 6). In this case, the simplest explanation for the co-existence of high grade assemblages with low grade deformation microstructures is deformation at low grades without re-equilibration of the metamorphic assemblages due to fluid absent conditions.

If the assumption is made that fluids were *present* during deformation, the assemblage *must* have been in equilibrium to prevent retrograde reactions to lower grades. In this case, the simplest explanation of the observed features is the operation of very high strain rates. Some authors also regard high strain rates as necessary for the generation of pseudotachylite (Sibson, 1975, Killick 1990, Berlenbach and Roering 1992). If deformation occurred at amphibolite facies, under conditions of a 'normal' continental geothermal gradient (c. 30°C per km) (Sibson 1973), a temperature of c. 550°C and a pressure of 5 kb, at c. 18km depth is probable. Under these conditions it is unlikely that several observed features would occur:

1. Pseudotachylite would not quench quickly enough to prevent crystallisation
2. Microfractures in cataclasites would anneal
3. Brittle quartz would undergo considerable recovery during periods of fault quiescence, and possibly ductile creep.

None of these features have been noted, and deformation is therefore regarded as having occurred at lower grades than amphibolite facies.

Although the metamorphic conditions during Crush Melange development are somewhat conjectural, a combination of periodic high strain rates and low metamorphic grades in the absence of water, are likely to have operated. In this combined scenario, high strain rates and moderate to high confining pressures would produce pseudotachylites and cataclasites. Pseudotachylites may in fact be the manifestation of the highest strain rate events in a 'background' of cataclasite generation.

A possible alternative fault trace in Barra

Very little field evidence exists which supports a right-angled strike-swing in the fault trace at Ben Verrisey (NF 685027) on Barra. The footwall and hangingwall rocks are identical at this location, and cannot be used to discern the fault trace. Similarly, no obvious topographic break exists to delineate the fault trace. A zone of diffuse pseudotachylite generation *does* trend ESE-WNW from Loch Obe (NF 710020) to Greian Head (NF 647049), but it is debatable whether this is the main fault trace.

A more obvious topographic break continues north from Ben Verrisey (NF 685027) to Ben Cliad (NF676043), and pseudotachylite generation is more intense at this location. Fig. 4.23a and b show the widely accepted fault zone trace (e.g. Fettes et al. 1992) and a possible reinterpretation of the fault zone trace. Interestingly, the maps of most previous workers on the Barra region (especially that of Jehu and Craig (1923) who were not prejudiced by knowledge of the OHFZ in South Uist and Eriskay), can be reinterpreted to account for the possibility of a non-bending N-S trending fault zone. This reinterpretation provides a simple explanation why orthopyroxene-bearing (granulite facies) rocks resembling the eastern gneisses are found apparently west of the accepted fault zone trace in the Oitir Mhor Zone of Barra (Francis 1973).

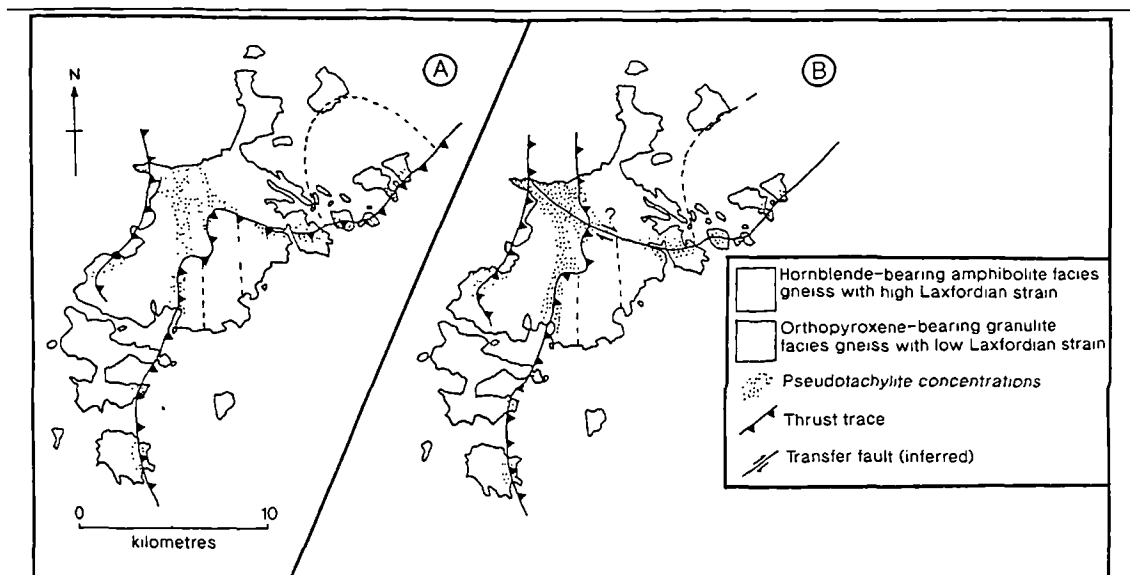


Figure. 4.23. Simplified geological maps of the Barra region. A) widely accepted fault zone trace (based on Francis 1973 and Fettes et al. 1992). B) Possible reinterpretation of fault zone trace.

The *corollaries* of this reinterpretation are:

1. The displacement estimate for the fault zone based on the apparent offset of a major Laxfordian F3 antiform across the fault (Francis 1973, Sibson 1977b) (outlined in section 2.4.2) is invalid (see section 5.4.2). This displacement

estimate also requires c. 30° of clockwise hangingwall rotation (Sibson 1977b). This is regarded as unlikely because the banding orientations in both west and east regions are presently subparallel (Fig. 4.24), and no independent evidence for major block rotation has been found.

2. The trace of the fault zone in Barra does not match along strike with the trace of the fault zone in Eriskay (see also Fig. 4.25a and b).

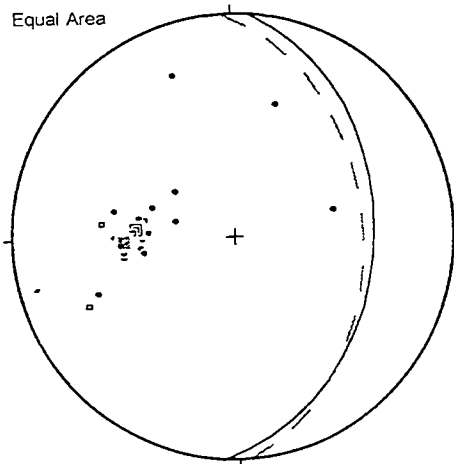


Figure 4.24. Equal area stereonet showing poles to gneissose banding in Western Gneiss (dots) with mean great circle (solid line) and Eastern Gneiss (boxes) with mean great circle (dashed line).

The fault trace in Eriskay (the OHFZ) may not be the same structure as the fault trace in Barra (Fig. 4.25a). Coward (1969) and Sibson (1977b) report the existence of extensive and intense pseudotachylite development (including well developed breccias and quasi conglomerates) on the west coast of South Uist, at Ardivarchar Point (NF 738460) and Rubha Ardvule (NF 710300), and on the west coast of North Uist at Aird an Runair (NF 687705) (Fig. 4.1). These fault rocks have developed between 10 and 25km west of the main fault base, and are interpreted by Coward (1969) as the deformation products of an older fault zone. If the fault trace on Barra continues north instead of veering east, a lateral continuation through these localities is possible. The belt of pseudotachylite injected rocks which splays eastwards on Barra may therefore be a subsidiary structure linking with the main fault trace. Alternatively, a late displacement on a NW-SE trending transfer structure in the sound of Barra has accommodated apparent dextral displacement of the OHFZ trace (Fig. 4.25b). Similar dextral displacements have been reported on similarly oriented transfer zones in South Harris (see section 5.3.2).

Although these suggestions are merely conjectural, the first explanation is regarded as unlikely because it has the consequence of placing granulite facies eastern gneisses in Barra, along strike from amphibolite facies western gneisses in

South Uist. The second explanation is more likely but the timing of transfer movement is problematical (see section 5.3.3).

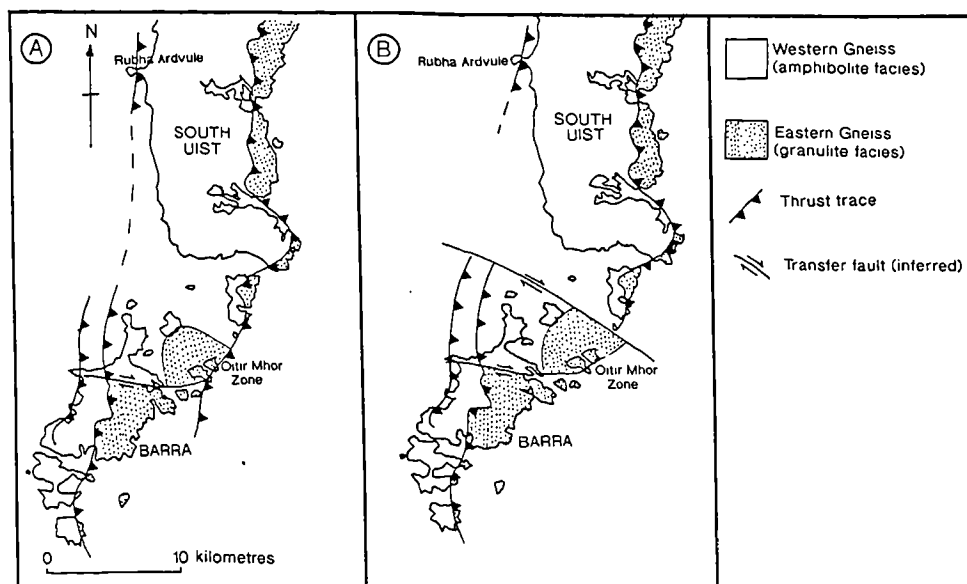


Figure 4.25. Geological maps of the South Uist/Barra region. A) Possible lateral continuation of the fault zone trace from Greian Head, Barra to Rubha Ardvule S. Uist. B) Possible dextral transfer zone in the sound of Barra. The fault zone trace in Barra may have been dextrally displaced relative to Eriskay.

4.2.13 Summary

- Brittle deformation is heterogeneous, forming diffuse belts of localised brittle failure and narrower belts of E-SE-dipping Crush Melange and/ or pseudotachylite/ ultracataclasite crush zones. The crush zones probably result from either the presence of a lithological contrast or an unfavourable pre-existing banding orientation.
- The geometry and kinematics of brittle faults are strongly controlled by the orientation of pre-existing anisotropies e.g. banding.
- Brittle deformation appears to be associated with overall top-to-the-W thrusting, although second-order extensional movements' may have occurred during aftershocks.
- Some topographic faults were probably reactivated during later extensional movement.
- The coexistence of brittle microstructures and amphibolite facies assemblages requires that the assemblages were metastable during low-grade deformation, due to lack of available water.

- The large volumes of pseudotachylite generated during brittle deformation suggests that both low-fluid conditions prevailed and strain rates were periodically high.
- Retrogression is regarded as post-deformational.
- Thrust displacement estimates using displaced fold axes across the fault zone are regarded as inconclusive.

4.3. Sinistral strike-slip movement

Cross-cutting, and therefore post-dating, the brittle thrust-related deformation in the southern segment of the OHFZ, are a suite of low greenschist facies rocks comprising phyllonitic mylonites (phyllonites) and phyllonitic protomylonites (protophyllonites) (Fig. 4.26).

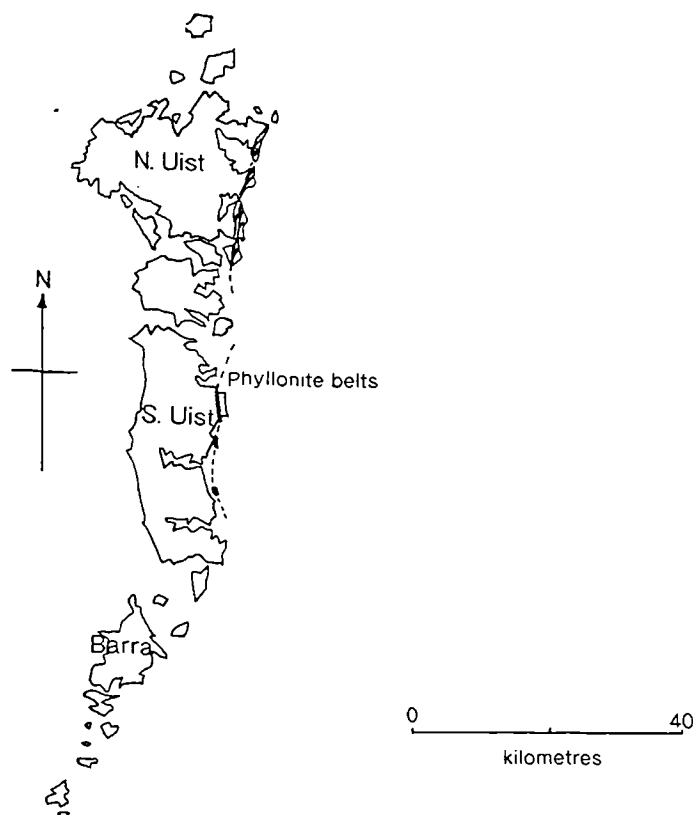


Figure 4.26. Map of the southern Outer Hebrides showing the extent of ductile phyllonitic deformation relating to sinistral strike-slip movement on the OHFZ (modified from Fettes et al. 1981).

The division in this study between protophyllonites and phyllonites is somewhat arbitrary, because a gradation occurs both in the metamorphic and the tectonic state of the rocks. For the purposes of this study, true *phyllonites* are defined as 'foliated fault rocks which have experienced total retrogression to low

greenschist facies, promoting phyllosilicate growth'. *Protophyllonites* are less well foliated and have undergone only partial retrogression to low greenschist facies.

The phyllonitisation process has begun to occur ubiquitously throughout the pre-existing fault rocks of the southern segment, but the process is only well advanced in discrete zones. These zones host foliated, green phyllonites in laterally extensive belts of variable thickness, which can be traced on land for up to 5 km along strike. In South Uist, the largest phyllonite belt (termed the Usinish Mylonite by Jehu and Craig 1925) is inferred to be over 20 km long and c. 1km. at its widest. The protoliths to the phyllonites are crushed and fractured gneisses of the Crush Melange. An obvious contrast therefore exists between these phyllonites and those of the northern segment, where a greater variety of protoliths occur. Furthermore, in the southern segment, phyllonite belt geometry undergoes an obvious lateral change. In north Uist and Ronay, the phyllonites occur in braided networks, not observed in the northern segment. Further south however, the braided phyllonite belts have become a single belt (termed the Usinish Mylonite by Jehu and Craig 1925).

All the phyllonitic rocks of the southern segment are essentially petrographically identical, and are therefore only described in detail in the Burrival - Eigneag Bheag section (section 4.3.1), below. The structure of these rocks however, varies considerably with location, and thus, each locality has a separate structural description.

Evidence is presented which suggests that the southern segment phyllonitic rocks, like those of the northern segment, were formed under conditions of sinistral strike-slip on the OHFZ. For convenience the localities have been grouped into two main regions: North Uist and South Uist. No phyllonitic rocks have been found in Barra or adjacent islands. If phyllonites *are* laterally continuous southwards, it is likely that they crop out offshore to the east of Barra.

(i). North Uist and adjacent islands

Several anastomosing belts of green phyllonite (c.5 - 50m thick), surrounded by less well developed protophyllonite, cut through the Crush Melange of eastern North Uist (Fig. 4.27). Most phyllonite belts trend roughly NNE-SSW and dip at low angles to the SE or ESE, but there are significant variations. Sibson (1977b) subdivides the networks into four main orientations:

- | | | |
|---------|------------|----------------|
| • Set A | NNE strike | 15-35° dip ESE |
| • Set B | NE strike | 20-50° dip SE |
| • Set C | NE strike | 20-50° dip NW |

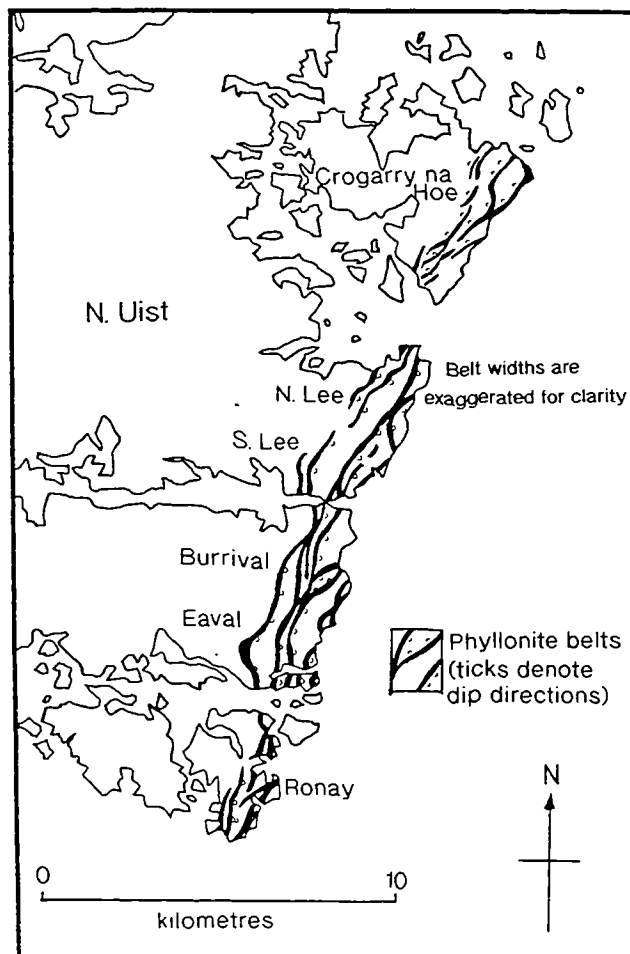


Figure 4.27. simplified geological map of the eastern part of N.Uist, showing the anastomosing nature of the phyllonite belts (modified from Fettes et al. 1981 and Sibson 1977b).

This classification scheme is somewhat arbitrary however, because some belts strike directly N-S, and the strike of the phyllonite belts is observed to swing locally through 30 or 40°. Overall, the dip values of the phyllonites are not very variable and therefore do not appear to be a good criterion for distinction. The belts did not develop sequentially, as no cross-cutting relationships occur. The present work has shown that few belts dip at more than 45°, but corroborates Sibson's observation that SE-dipping belts dominate over NW-dipping belts south of Lochmaddy, and vice versa north of Lochmaddy. The significance of these observations is further discussed in section 4.3.10.

Augen, lenses and laterally continuous belts of the less retrogressed protophyllonitic material between the phyllonite belts, occupy a larger area than the phyllonites and are individually structurally thicker (c.100- 500m thick). The boundaries between phyllonites and protophyllonites are always gradational (unless separated by a later detachment fault) and one is never cross-cut by the other. This

process is independent of scale and has also been observed in outcrop and in thin section. On a medium scale (m to 10's of m), the pods rich in mafic minerals do not often adopt the phyllonitic fabric and remain as low strain enclaves within the phyllonite belt. The foliation wraps these enclaves and is particularly intense at the margins. On a small scale (μm -mm), clasts of chlorite/epidote rich material are wrapped by highly elongate phyllosilicate aggregates. Phyllonitic and protophyllonitic fabrics share metamorphic and structural characteristics, and are therefore regarded as coeval.

Commonly, the phyllonite boundaries are faulted, but these faults are a result of a later deformation phase (see section 4.4).

4.3.1. Burrival to Eigneag Bheag

The area between the hill of Burrival (NF 909622) and the coastal promontary of Eigneig Bheag (NF 925600) has been mapped in detail and affords the best section through the phyllonite and protophyllonite belts of North Uist (Fig 4.28). In general, phyllonites are best developed in the east of the area, which may partly be a function of the quality of exposure. The relatively clean coastal exposures south of Eigneag Bheag (NF 921596) are replaced by lichen covered outcrops further west, which tend to erode more readily than the surrounding protophyllonitic Crush Melange. Thus, the phyllonite belts are often only represented by topographic lows in the central part of the study region.

Macrostructure

Protophyllonites

Protophyllonites occur between belts of phyllonite throughout the Burrival region, and are recognised in the field by the presence of a crude foliation in the pre-existing cataclastic rocks of the Crush Melange (Plate 4.6a). Typically, original melange material constitutes c. 90% of the whole rock. Protophyllonitic rocks are usually grey to greenish-grey in colour and have variable mineral assemblages depending on the degree of retrogression, which, in these rocks, is extremely heterogeneous. A gradation occurs between the poorly retrogressed rocks of the Crush Melange, which largely retain the amphibolite facies mineralogy of their banded gneiss protolith, to totally retrogressed phyllonites, where the assemblages show no evidence of grades higher than low greenschist facies. Typical protophyllonites, where only partial retrogression has occurred, are composed of quartz (30 - 35%), sericite (30 - 40%), chlorite (5 - 10%), epidote (5 - 10%) and calcite (1 - 10%) with minor amounts of (relict) feldspar (including plagioclase (An <30%) and K-feldspar (3 - 10%)), and mafic minerals, including biotite, actinolite and

hornblende (2 - 5%). Modal percentages are highly variable in individual samples, due to the variable state of retrogression. Epidote, chlorite and calcite often occur in randomly oriented veins and hairline fractures, which are probably pre-existing microfaults.

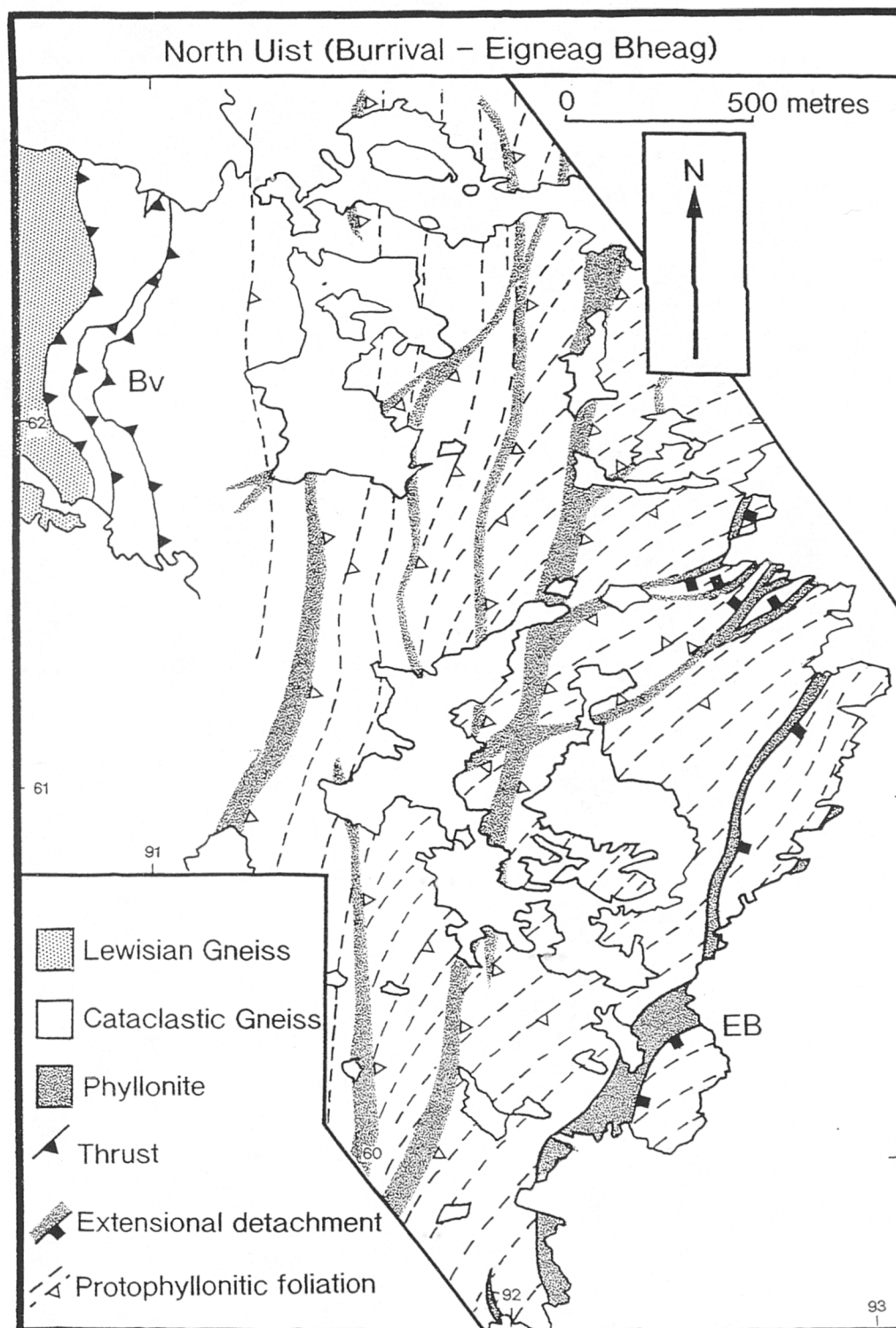


Figure 4.28. Geological map of the Burrival-Eigneag Bheag region.

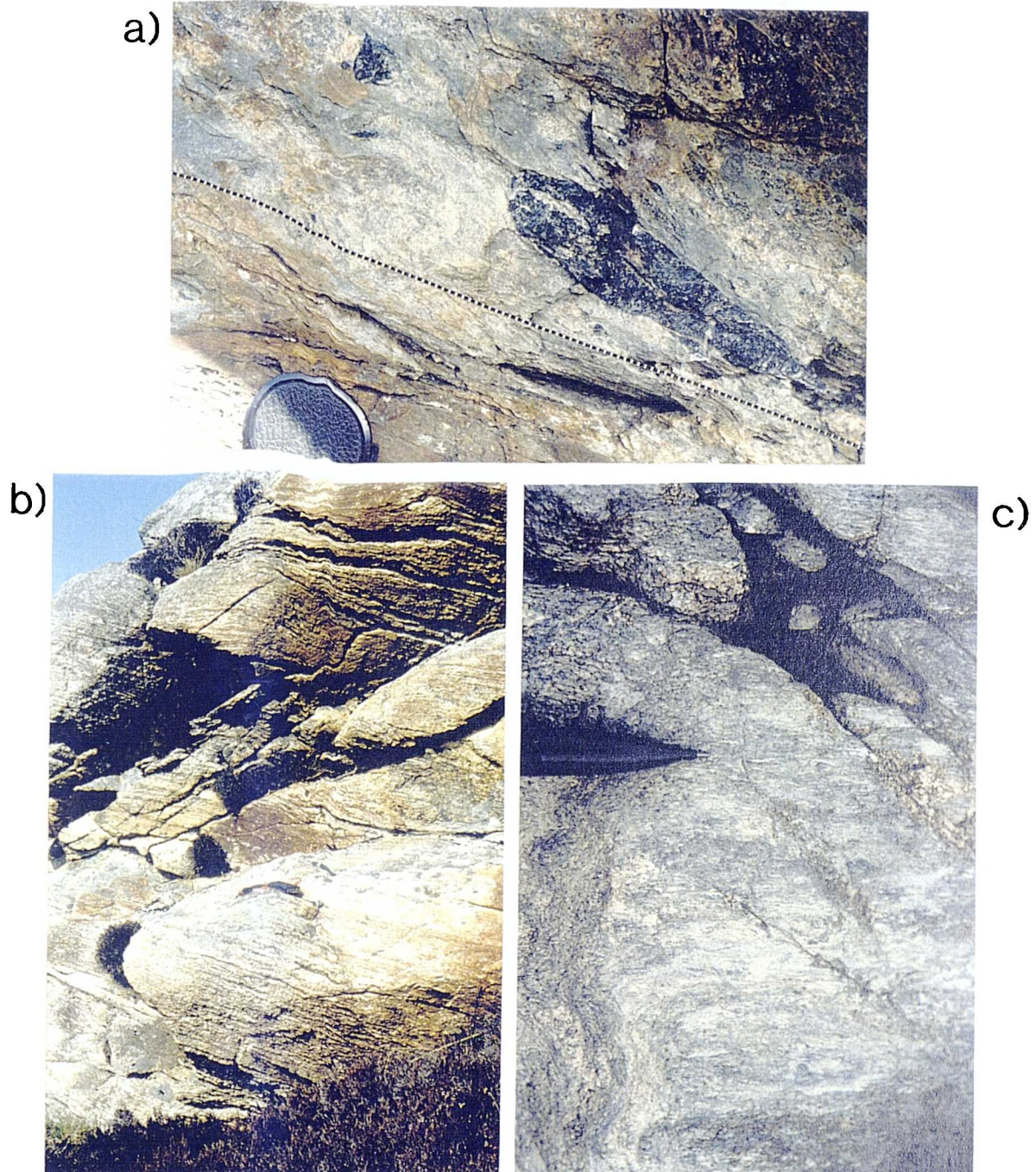


Plate 4.6 N.Uist phyllonites and protophyllonites

a) 'Mashed Gneiss' with mafic clasts and cataclasite matrix from Burrival region (NF 909620), showing the development of a cross-cutting protophyllonitic foliation.

b) Extremely well developed protophyllonitic foliation developed in the immediate hangingwall of a topographic fault from Burrival (NF 908621).

c) Strike-parallel mineral elongation lineation on a protophyllonitic foliation surface, from Burrival - Eigneag Bheag region (NF 926606).

The dominant fabric in protophyllonite, is a poorly to moderately developed foliation, defined by aligned phyllosilicates, including chlorite and occasionally biotite, and termed the "early cataclastic foliation" by Sibson (1977b). Quartz is also present along foliation surfaces where it is usually elongate and ribboned. In thin section, the plastically elongated ribbons are composed of undeformed, recrystallised quartz grains. In contrast, feldspars appear to have been deformed in a brittle manner, and comminuted. This foliation occurs throughout the melange but is often best developed close to large (m-scale) faults, e.g on Burrival (NF 908622) (Plate 4.6b).

The protophyllonitic foliation has a regionally variable orientation, which is discernible on the geological map (Fig 4.28). In the west of the region, between Burrival (NF 913618) and the phyllonite belt at NF 920610, the foliation strikes N-S and dips shallowly eastwards (Fig. 4.29a). East of the phyllonite belt at NF 920610, it swings clockwise through c. 40°, to strike NE-SE and dip moderately to shallowly SE (Fig. 4.29b). In the extreme east of the region at Eigneig Mhór (NF 930613), an anticlockwise swing is observed, so that the foliation strikes NNE-SSW, and dips moderately to shallowly ESE in this area. Locally (e.g. at NF 926616), the foliation dips NW but this is unusual for the Burrival region, and is discussed in greater detail in the following section and in section 4.3.10.

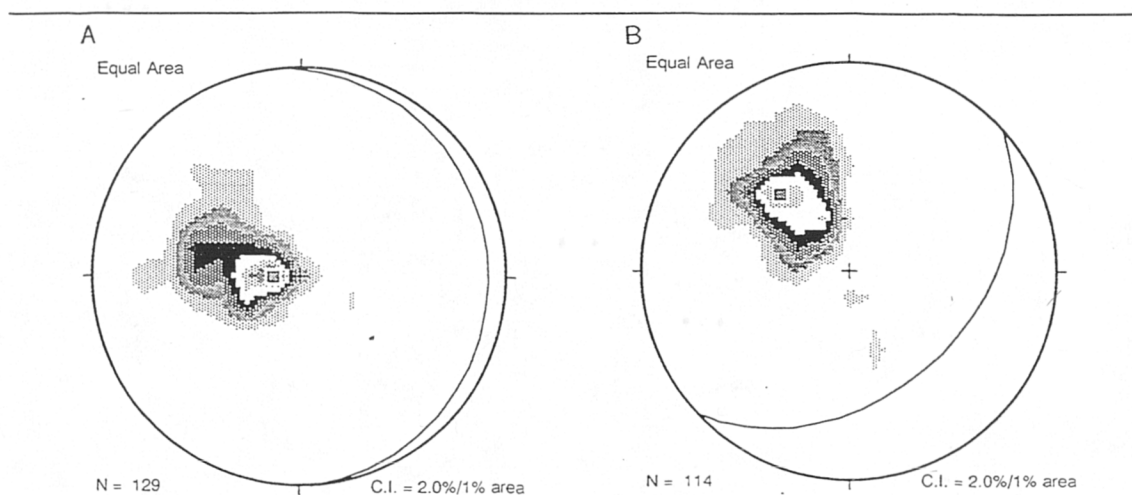


Figure 4.29. Equal area stereonet of: A) Contoured poles of protophyllonitic foliation with mean great circle from the Burrival region; and B) Contoured poles of protophyllonitic foliation with mean great circle from the Eigneag Bheag region .

A linear fabric is also apparent within these rocks, defined by elongate quartz/ feldspar aggregates, syntectonic chlorite fibres and occasionally quartz rods (Plate 4.6c). The fibrous and/ or elongate mineral growth discounts Sibson's interpretation of this lineation as the result of the "intersection of sets of

complementary shear zones". The mineral elongation lineation is observed to plunge at very shallow angles NE or SW, parallel to the strike of the foliation (Fig. 4.30). The linear fabric orientation indicates the probable local movement direction of the shear zone during mineral growth. Kinematic indicators, including foliation swings in cm-scale shear zones, cm-mm scale shear bands (e.g. at NF 923616) (Plate 4.7a) and asymmetric clasts, are numerous, and when observed in conjunction with the mineral lineation, may be used to constrain a consistent sense of sinistral strike-slip motion on the fault zone, displacing the hangingwall laterally to the NE.

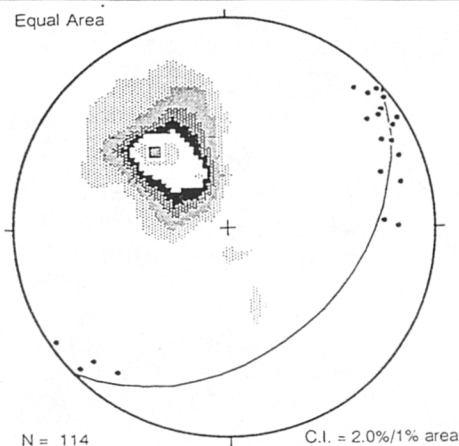


Figure 4.30. Equal area stereonet of contoured poles to protophyllonitic foliation with mean great circle and mineral lineations (dots) from the Eigneag Bheag region.

Where relict gneissose banding, or microfaulted lithological contacts are discernible in the melange, the 'early cataclastic foliation' is observed to cross-cut them. In some places, veins of cataclasite and/or pseudotachylite are observed to be cross-cut by the foliation (e.g. NF 920605). This fabric is never cross-cut by the effects of brittle cataclasis, microfaulting, or pseudotachylite generation, however, and is therefore not contemporaneous with these thrust-sense deformation processes (cf. Sibson 1977b). In addition, most of the kinematic evidence also suggests that the generation of protophyllonite was not contemporaneous with thrusting, although a thrust-sense ductile fabric *is* present in the west of the region. This latter fabric is not regarded as coeval with the brittle thrusting event described above and is discussed more fully in section 4.3.10.

Phyllonites

Several discrete belts of phyllonite occur in the Burrival/ Eigneag Bheag region, the thickest (c. 50m thick) and best exposed of which occurs immediately south of Eigneag Bheag (NF 922600). This N-S to NNE-SSW trending belt, and

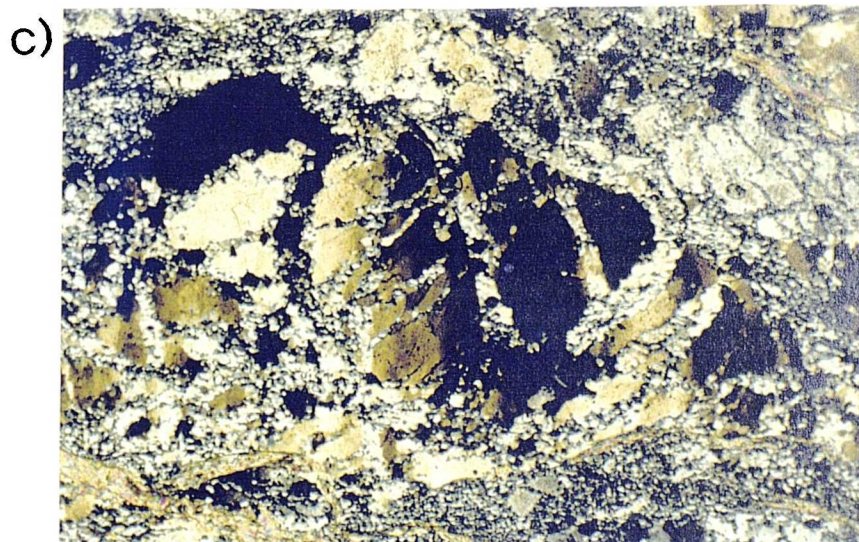


Plate 4.7 Phyllonites and protophyllonites from N.Uist.

a) Small-scale sinistral shear zone in protophyllonite from Eigneag Bheag (NF 923616).

b) Asymmetric 'curve-in' of phyllonitic foliation at shear zone margin. Sense of shear demonstrated is sinistral (top-to-the-NE), from Eigneag Bheag (NF 919595).

c) Brittle deformation in quartz from Eigneag Bheag region (NF 924604), showing tension fractures with recrystallised quartz. Field of view is 3mm. (XPL)

several more similarly oriented belts further west are the most common type encountered ("Sibson's (1977b) set A"). A small number of NE-SW trending phyllonite belts around NF 926615 correspond to Sibson's sets B and C. These are essentially splays from the main belt. The southern splay, which bifurcates towards the NE dips anomalously towards the NW. It should be noted that this orientation is not due to folding (cf. Sibson 1977b), but is probably due to the wrapping of a large low strain zone, only the keel of which is now exposed at NF 923613. The equivalent SE dipping splay c. 200m to the north is probably part of the same wrapped belt (see section 4.3.10 and Fig 4.49).

Phyllonite belt margins are usually fault bounded, by low angle detachment faults accommodating normal movement (see section 4.4). In belts where later deformational overprint has not occurred, the phyllonite belts have gradational margins. The degree of retrogression and intensity of strain in the belts reduce gradually, over a distance of 2-5m, into the protophyllonitic regions. Phyllonite belt margins are difficult to observe away from the coast due to the poorer quality of the exposures.

The phyllonites are extremely well foliated, green or blue coloured rocks. Like the protophyllonites, these rocks are never seen to be cross-cut by the effects of brittle crushing and therefore post-date most brittle deformation. They are fine grained (<2mm) and chiefly composed of quartz, chlorite and epidote, the latter two being the cause of the lithology's greenish colouration. These minerals were derived from the breakdown of mafic minerals (e.g. hornblende) and feldspars respectively. A large proportion of the lithology is composed of sericitised feldspar, and very little of the original protolith assemblage (with the exception of quartz) is preserved. These belts of total retrogression are coincident with the zones of the most intensely foliated phyllonite, and it seems likely that Sibson's (1977b) observation, "(that) a direct correlation (exists) between the intensity of shearing and the extent of retrogression", is correct.

The foliation, which is phyllitic or occasionally schistose, is responsible for the extreme fissility of these rocks in places. The orientation is variable both regionally and locally, but in general dips c. 30° SE (Fig. 4.31a and b).

A mineral elongation lineation, defined by fibrous chlorite, quartz ribbons and stretched sericite feldspar pseudomorphs is present on the foliation surfaces. The plunge of this lineation is variable between a sub-horizontal, NE-SW direction and a shallow-plunging, S direction, with most plunging E or ESE (Fig. 4.32). In the NW-dipping belts, the lineation usually trends subhorizontally NE-SW. A direct correlation exists between the state of strain/ retrogression and the orientation of this lineation. Most extremely well foliated and retrogressed material occurs in the

centre of the phyllonite belts and possesses an E to SE-plunging lineation. This probably reflects a later phase of deformation which has focussed into the most retrogressed material (see section 4.4.1). The sub-horizontal NE-plunging lineation however, which occurs throughout the protophyllonites and mostly in the margins of the phyllonite belts is earlier and linked with the state of deformation *during* retrogression. Kinematic indicators associated with this sub-horizontal mineral lineation suggest an interpretation of the regional kinematic evolution of the phyllonites that differs from the previous work of Sibson (1977b), White and Glasser (1987) and Walker (1990).

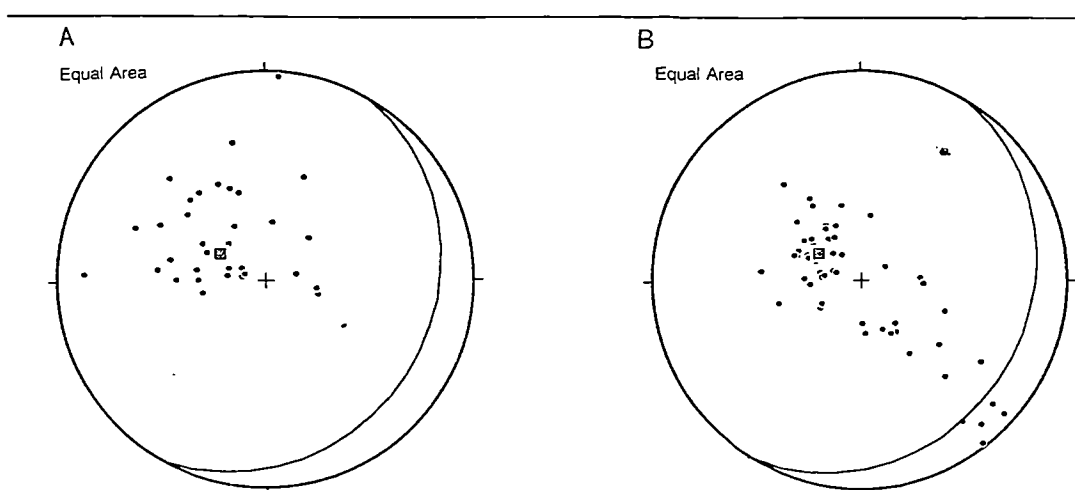


Figure 4.31. Equal area stereonet of: A) Poles to phyllonitic foliation with mean great circle from the Burrival region; and B) Poles to phyllonitic foliation with mean great circle from the Eigneag Bheag region.

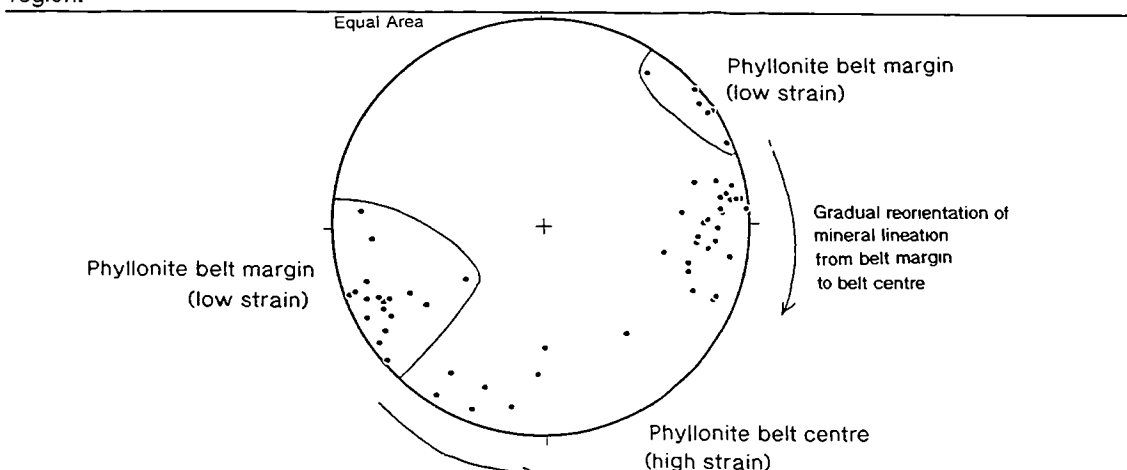


Figure 4.32. Equal area stereonet of mineral lineations in phyllonites from the Eigneag Bheag region.

Sibson (1977b) describes the phyllonite belts as either possessing "thrust-sense" or "lag-sense" structures, and suggests these two types of feature occurred during phases of thrusting (D1) and extension (D2) respectively. Whilst there is abundant evidence for extension within the belts (see section 4.4), the evidence for thrusting described by Sibson is somewhat equivocal. Sibson (1977b) describes the

asymmetric "marginal curve-in" of the schistosity along the phyllonite belt margins as being indicative of heterogeneous simple shear in a west-directed thrust sense, likening the shear zone fabrics to those described from elsewhere in the Lewisian by Ramsay and Graham (1970) (Fig 4.33). There are problems with Sibson's conclusions however:

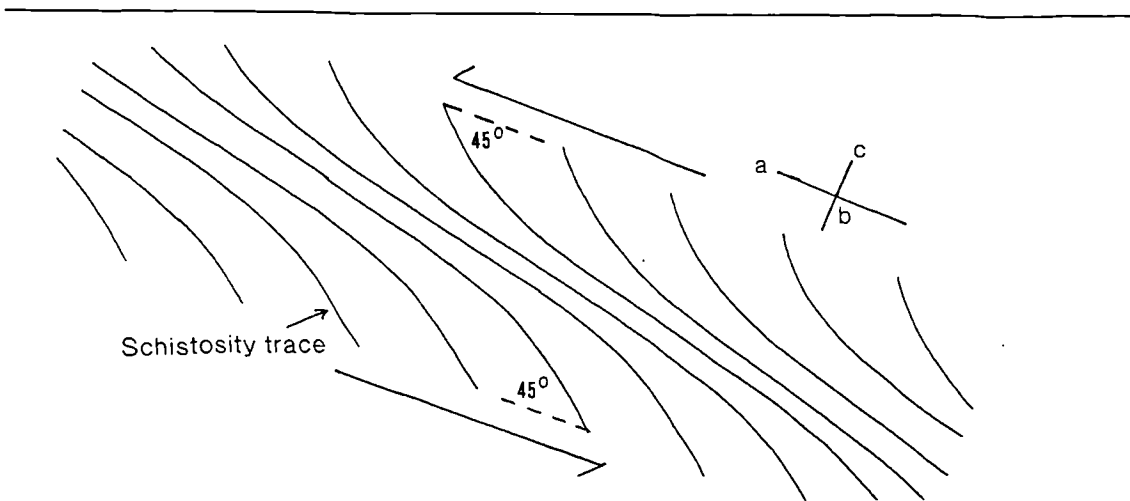


Figure 4.33. Profile section of a 'thrust sense' shear zone with kinematic axes a, b, and c, (section lies in the X-Z planar trajectory of finite strain) (from Sibson 1977b).

- The asymmetric 'curve-in' of the schistosity on the edge of some shear zones suggests a transport direction which is roughly top-to-the-W (e.g. at Eigneag Bheag NF 921596). Apparently opposite senses of motion however, are demonstrated using the same criterion, on other belts, e.g. at NF 926616). This method of shear sense determination is only reliable when the mineral lineation is normal to the arc of curvature. If the mineral lineation deviates from this orientation (e.g. at Eigneag Bheag NF 921596), the apparent curvature may be due to relict folding or reorientation during later reactivation.
- The E- ESE- plunging stretching lineation, with boudinaged feldspar porphyroclasts and ribboned quartz, is not related to thrusting. The lineation is nearly always observed in the centre of the phyllonite belts, where strain and retrogression are at their maximum. This lineation is associated with normal shear sense indicators and relates to a later phase of extensional movement (Sibson's D2 lag-sliding phase. See section 4.4.1).
- Occasional, N-S oriented, en-echelon tension gashes, which Sibson (1977b) suggests developed during thrust-sense simple shear, are also related to later extensional movement (see section 4.4.1).

- A simple shear environment invoked by Sibson for the phyllonite belts is probably over-simplified. A significant amount of pure shear occurred, either during initial movement phases or during subsequent ones. This is evident in the marked parallelism of shear zone margins and internal foliations within some shear zones, and the common occurrence of apparently flattened feldspar boudins. Sibson's strain estimates, based on shear zone geometry and a simple shear supposition, are therefore likely to be inaccurate.

White and Glasser (1987) also disagree with Sibson's conclusions. Although these authors state that the fault rocks encountered in North Uist are the result of a two phase development (namely the Crush Melange and the phyllonites), they suggest that both phases occurred during net extension. Microstructural evidence from the Crush Melange and the phyllonites, including lag-folds and shear bands, is presented in their work to support this. They conclude that no unequivocal evidence for thrust sense motion exists in the Uists.

Walker (1990) agrees with the D1 (thrust) followed by D2 (extension) model of Sibson (1977b), but suggests that microstructures in the phyllonites are consistent with extension only, and that there is no evidence for thrusting after the formation of the Crush Melange. She also suggests that the phyllonitic rocks, whilst preserving evidence for an extensional development, only became true phyllonites after a much later (Tertiary) phase of fluid ingress.

The present study has shown that several interpretations of White and Glasser (1987) and Walker (1990) are incorrect. In the less strained/ retrogressed marginal areas of the phyllonite, where relict strike-parallel mineral elongation lineations are evident, several types of shear sense indicator are apparent:

- m to cm-scale shear bands, preserved in the field and in thin section;
- marginal 'curve-in' of phyllonitic foliation at the margins of phyllonite shear zones (where consistent with the mineral lineation orientation) (Plate 4.7b);
- The asymmetry of the large (kilometre-scale) protophyllonitic fabrics outside the mylonite belts (Fig. 4.28);
- The asymmetry of shear zone fabrics within the phyllonite shear zone.

All reliable shear sense indicators are consistent with sinistral strike-slip on the fault zone during phyllonitisation. The inclined foliation on which this strike-slip motion has taken place is a relict feature, inherited from the pre-existing thrust phase. It is thought that relict low-angle thrusts acted as preferential pathways for localised and

total retrogression. Partial retrogression, forming protophyllonites, was probably ubiquitous throughout the rest of the melange.

Microstructure of phyllonites and protophyllonites

In the phyllonitic material, all the original amphibolite facies gneissose assemblages have been replaced by low greenschist facies minerals, indicative of retrograde reactions. The retrograde minerals formed largely depend on the mineralogy of the protolith; in the phyllonitic amphibolites, quartz is a very minor component, and in the phyllonitised pegmatites, quartz is a major component whilst chlorite is minor. In most of the high strain phyllonites the main products are:

(quartz) - sericite - chlorite - epidote - opaque minerals (especially pyrite) +/- calcite.

These minerals replace chiefly plagioclase (although albite is sometimes still present), amphibole (including both hornblende and actinolite), biotite, and garnet, all of which are only recognisable by their pseudomorphs, or partial pseudomorphs in the protophyllonites. The higher strain phyllonites show no pseudomorphs.

Quartz occasionally constitutes up to 20% of the whole rock and preserves a variety of deformation microstructures. Isolated quartz grains usually show strong undulose extinction and occasionally brittle fracturing (Plate 4.7c). Tension fractures between pulled apart quartz grains are often filled with undeformed fibrous quartz, chlorite and sericite. Grains are occasionally ribboned, and may be monocrystalline ribbons, or *type 1* polycrystalline ribbons (using the terminology of Boullier and Bouchez 1978) (Plate 4.8a). No fully recrystallised *type-2* ribbons have been positively identified. In general, recrystallised grains are not as common as isolated relict grains and they mainly occur at existing grain boundaries. The dominant recrystallisation mechanism is rotational recrystallisation, involving the progressive misorientation of subgrains from the relict grain towards the fully recrystallised mantle region. In very rare examples, grain boundaries show complex interlocking bulges, and recrystallisation by grain boundary migration recrystallisation is believed to have operated. The co-existence of these apparently bulge nucleated recrystallised quartz grains, which usually form at P-T conditions of at least amphibolite facies (Hirth and Tullis 1992, Twiss and Moores 1992), with apparently cold worked grains, with fractures and undulose extinction, suggests that they are relict microstructures that are not contemporaneous with phyllonitisation. The preservation of such relict features suggests that other mineral phases, with features conducive to deformation at low P-T conditions, (e.g. phyllosilicates with

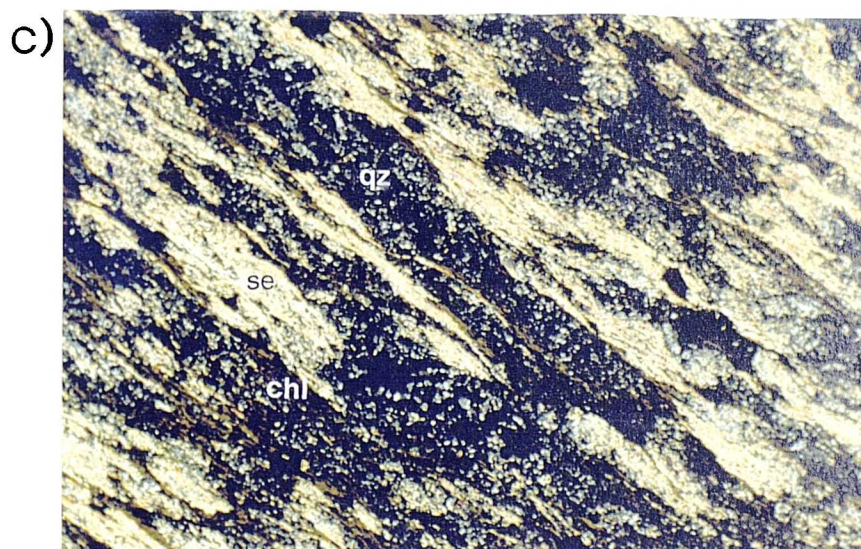
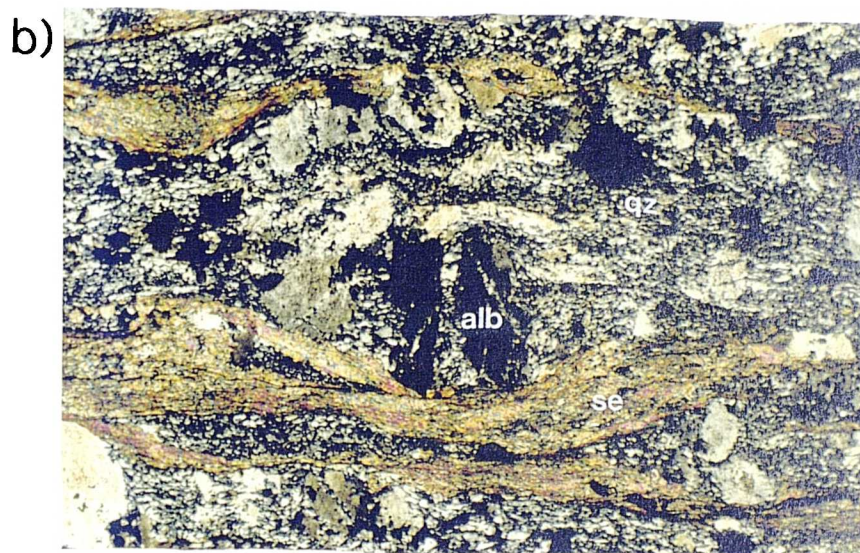
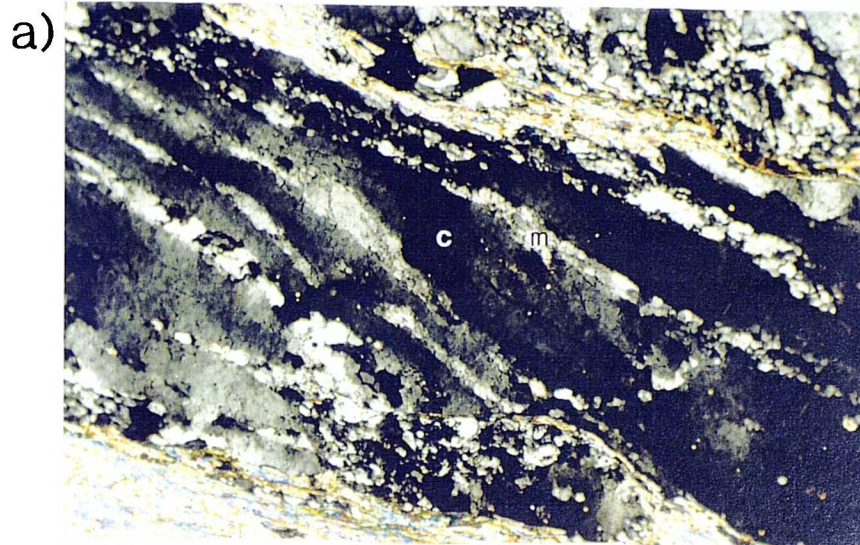


Plate 4.8 Phyllonites and protophyllonites from N.Uist

a) Monocrystalline ribbons of quartz (c) with thin mantles (m) of recrystallised subgrains, from north of Eigneag Mhor (NF 926616). Field of view is 3mm. (XPL)

b) Segregated quartz (qz) and sericite (se) bands in phyllonite from Eigneag Bheag (NF 925604). Tensional fractures in relict albite porphyroclast (alb) possess recrystallised quartz. Field of view is 3mm. (XPL)

c) Sericite (se) and chlorite (chl) screens segregating fine grained, fully recrystallised quartz ribbons (qz), from Eigneag Bheag (NF 925604). Field of view is 3mm. (XPL)

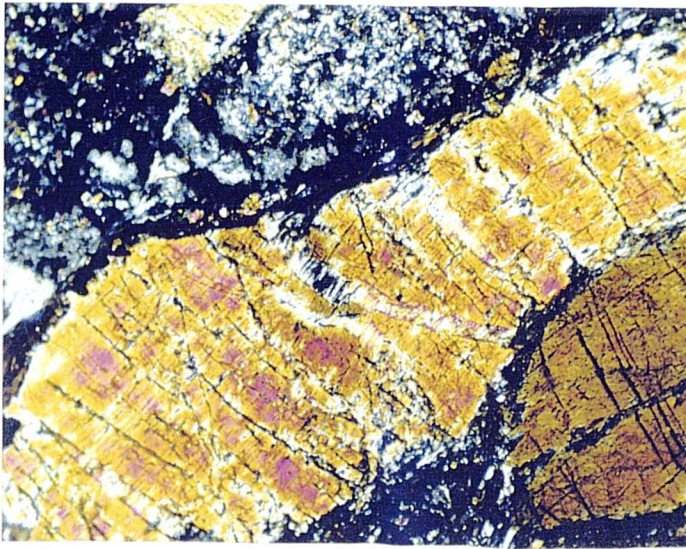
abundant foliation-parallel surfaces for intercrystalline slip), may have accommodated most of the later, lower temperature deformation.

The deformational behaviour of plagioclase and K-feldspar is only observable in the protophyllonitic units, because complete retrogression (to white mica, epidote and occasionally calcite), and subsequent deformation, obliterates all evidence of pseudomorphs in the higher strain phyllonites. In the protophyllonites, cores of non-sericitised plagioclase are often preserved within mantles of completely altered sericite. Where relict twinning is apparent, an albitic composition can be deduced. All feldspars show abundant transcrystalline fracturing, with recrystallised fibrous minerals (including quartz, chlorite and sericite) occupying the low pressure pull-aparts between grain fragments (Plate 4.8b). Feldspar subgrains are occasionally apparent close to grain boundaries or transcrystalline fractures. These subgrains are internally undeformed, and show progressive misorientation from core to mantle regions. They are therefore interpreted as having formed by rotational recrystallisation as oppose to cataclastic comminution. In the phyllonitic material, the sericitic product of feldspar retrogression is strongly aligned parallel to the phyllonitic foliation and forms 'screens' which isolate ribboned quartz (Plate 4.8c).

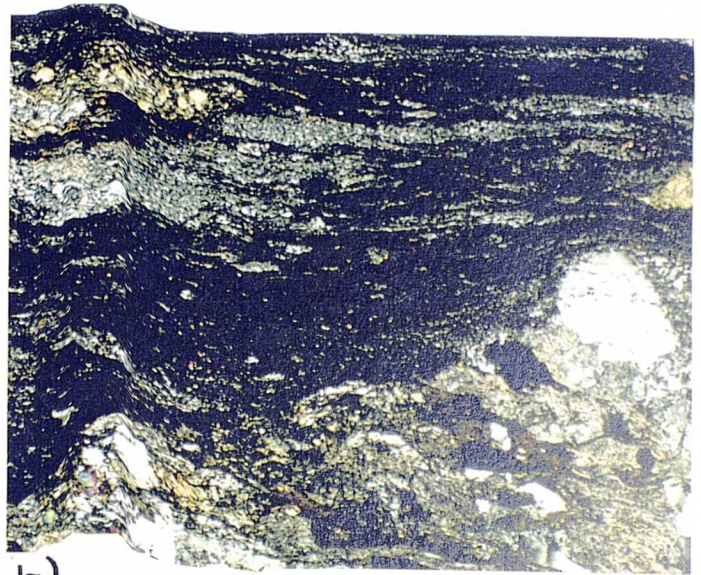
Where hornblendes are incompletely retrogressed to chlorite, pull-apart tension fractures separate grain fragments, and host fibrous chlorite, sericite and quartz (Plate 4.9a). No ductile behaviour of amphibole has been identified.

With the exception of transcrystalline fractures, virtually all fabric elements, including quartz ribbons, sericite laths and chlorite fibres, are strongly aligned. Quartz and sericite show a strong preferred orientation and a high degree of intercrystalline slip is inferred. Where veins of relict cataclasite or pseudotachylite have been phyllonitised, grain size increase up to c. 100 μm is apparent. These zones of fine grain size show many ductile microstructures, including grain ribboning and alignment of recrystallised quartz grains and phyllosilicates (Plate 4.9b). It appears that such regions have focused higher ductile strains than the surrounding coarser material on account of their initially finer grain size.

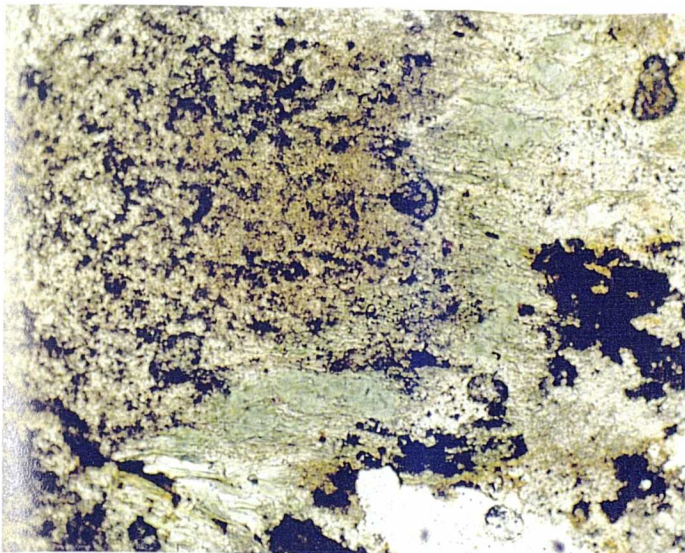
On foliation surfaces, quartz and chlorite fibres in tensional pull-aparts have grown parallel to the NE-SW mineral elongation stretching lineation (Plate 4.9c). Discrete, foliation-parallel pressure solution surfaces occur, and are visible as thin, dark-coloured, continuous layers (Plate 4.9d). Many slip surfaces, however, lie at a low angle to the foliation and when viewed parallel to the quartz/chlorite fibres, show extensional displacements indicative of bulk top to the-NE sense of shear, consistent with larger scale kinematic indicators. Asymmetric porphyroclasts are



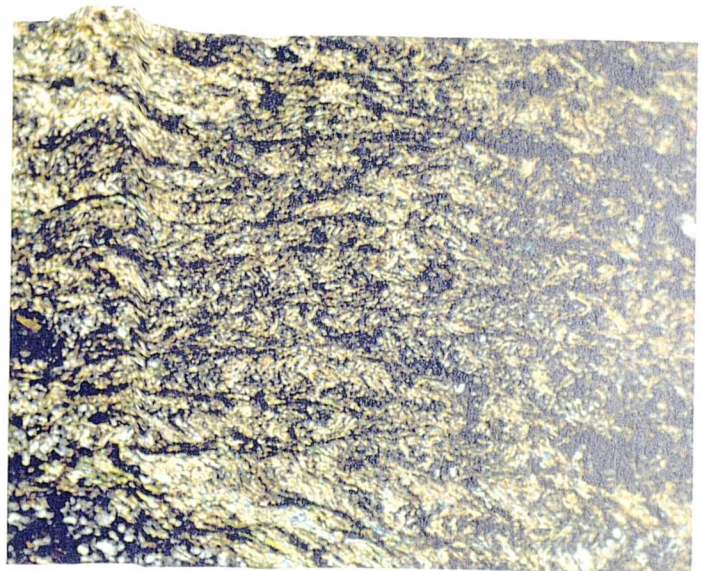
a)



b)



c)



d)

Plate 4.9 Phyllonites and protophyllonites from N.Uist

a) Relict hornblende porphyroblast in protophyllonite from Eigneag Bheag (NF 925602). Tensional fractures host fibrous white mica (sericite). Field of view is 1mm. (XPL)

b) Relict zone of fine grained cataclasite (upper part of photo) and coarser grained gneiss (lower part) from Eigneag Bheag (NF 922601). The finer grained material has deformed in a ductile manner, with ribboning and alignment of grains. Field of view is 5mm. (XPL)

c) Phyllonitic foliation surface with NE-SW trending chlorite fibres, from Eigneag Bheag (NF 921601). Field of view is 1mm. (PPL)

d) DMT pressure solution cleavage in phyllonite from Eigneag Bheag (NF 925604). Field of view is 1mm (XPL)

rarely found in these phyllonites, and where they do exist, give inconsistent shear senses.

Metamorphic conditions during deformation

In the most altered and highly strained phyllonitic material, the original mineral assemblages indicative of amphibolite facies in the cataclastically ^{deformed} gneissic protolith have been replaced by new assemblages. Feldspars (mostly plagioclase) are strongly sericitised, and a large proportion of the whole rock is composed of white mica and epidote (c. 50%). Relict amphiboles, including hornblende derived from the Lewisian Grey Gneiss, are replaced by chlorite. Garnets are also totally replaced and may be recognised by their chlorite pseudomorphs. These assemblages suggest that the grade of the protolith has been significantly reduced to low greenschist facies.

Most of the deformation microstructures preserved, including the presence of ubiquitous undulose extinction in quartz and the brittle fracturing of feldspars, are also indicative of low P-T conditions. Quartz microstructures, including monocrystalline ribbons with subordinate, rotationally recrystallised mantle regions, and undulose extinction within the core regions, suggests the prevalent metamorphic conditions during phyllonitisation approximated low greenschist facies (Boullier and Bouchez 1978, Simpson 1985). The presence of rare, high grade microstructures, e.g. bulge nucleated, (grain boundary migration) recrystallised quartz grains, and rotationally recrystallised feldspars, which are not observed below upper greenschist facies (c. 450° C) (Obee and White 1985, Fitzgerald and Stunitz 1993) is thought to be a relict, (possibly original gneissose) feature.

Non-silicates include calcite, and iron ores (usually pyrite), both of which are apparent throughout the phyllonitised rocks. The presence of calcite and fibrous chlorite in tension cracks between fractured grains and pressure shadows (especially around opaque minerals) suggests that these minerals have precipitated from solution, and that the phyllonites acted as DMT sinks. In addition, the phyllonites are likely to have acted as the source for the removal of material in solution, because of the presence of pressure solution cleavages.

The orientation of chlorite fibre growth is consistent with the kinematic regime, and retrogression is therefore unlikely to post-date sinistral strike-slip motion. In addition, reworking of retrograde minerals appears to have taken place prior to and during late extensional fault zone movements (see section 4.4.1). The retrogression therefore, probably either pre-dates, or is synchronous with strike-slip motion. The fact that the material deposited in DMT sinks has the same composition as the products of retrogression, suggests that retrogression was syn-

tectonic (Beach 1982). Detailed geochemical studies are required however, before this can be confidently proposed.

4.3.2. Ronay

The island of Ronay shares many characteristics of the Burrival/ Eigneag Bheag area in the development and subsequent evolution of the phyllonites and protophyllonites. The island can be split into two halves, the west being dominated by fault rocks produced by top-to-the-west thrusting, whilst a zone c. 1km wide on the east of the island is dominated by fault rocks associated with phyllonite development (Fig 4.34). The present work has focussed on a small area of phyllonite, c. 60m thick, and adjacent protophyllonite north of Bagh na Caiplich (NF 903560). Here, green, chlorite-grade phyllonites have developed heterogeneously over the cataclastic gneisses of the Crush Melange, occurring as N-S or NE-SW trending phyllonite belts separated by augen of lower strain protophyllonites. Pseudotachylite and ultrataclasite concentrations are occasionally discernible (e.g. at NF 904562), but are overprinted by a phyllonitic or protophyllonitic fabric. The rocks are essentially petrographically identical to those further north.

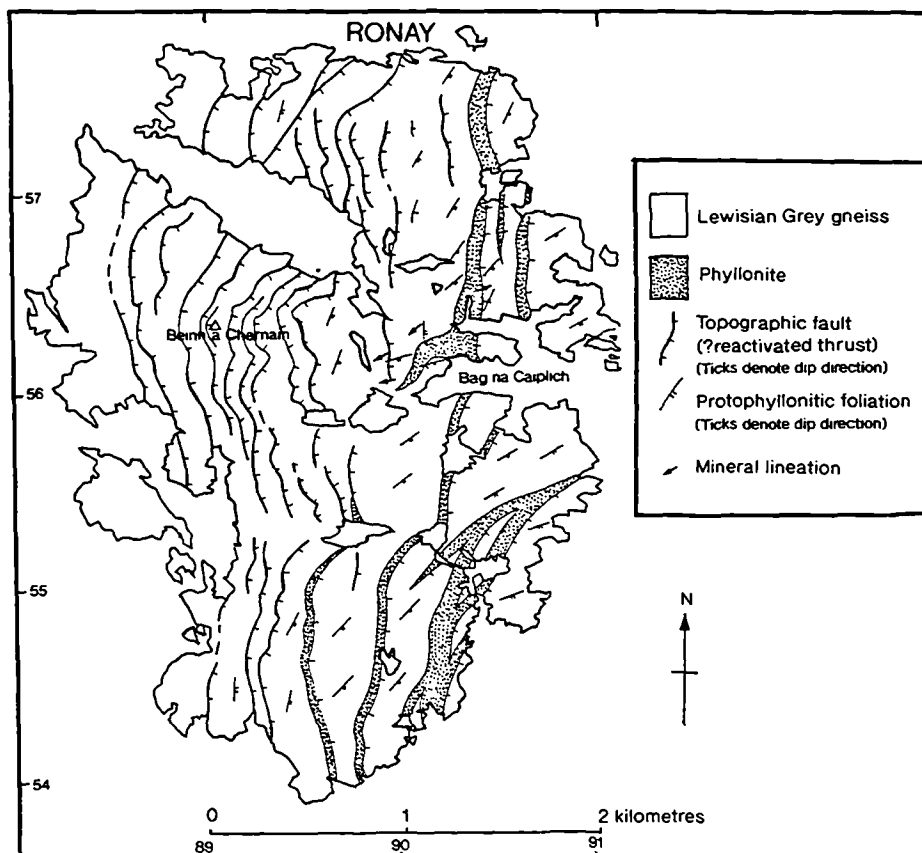


Figure 4.34 Geological map of Ronay (modified from Sibson 1977b).

The phyllonitic foliation, defined by aligned phyllosilicates and elongate quartz/ feldspar aggregates, is moderately developed, trends NE-SW and dips shallowly SE (Fig. 4.35a). In the lower strain protophyllonites, where the foliation is often only poorly defined, a clockwise strike swing, similar to that noted in the Burrival/ Eigneag Bheag area is apparent from the west of the melange to the east. A poorly developed sub-horizontal NE-SW trending mineral lineation, defined by elongate quartz or fibrous chlorite pseudomorphs of amphibole, is developed on some protophyllonitic foliation surfaces parallel to strike (Fig. 4.35b). A similarly oriented mineral lineation is present in the higher strain phyllonites. Kinematic indicators parallel to this lineation, including sheared, relict ultramafic pods, and asymmetric quartz/ feldspar porphyroclasts, suggest sinistral strike-slip motion occurred on these foliation surfaces displacing the hanging-wall to the NE. No E-W or NW-SE trending mineral lineations have been found in the phyllonites of Ronay.

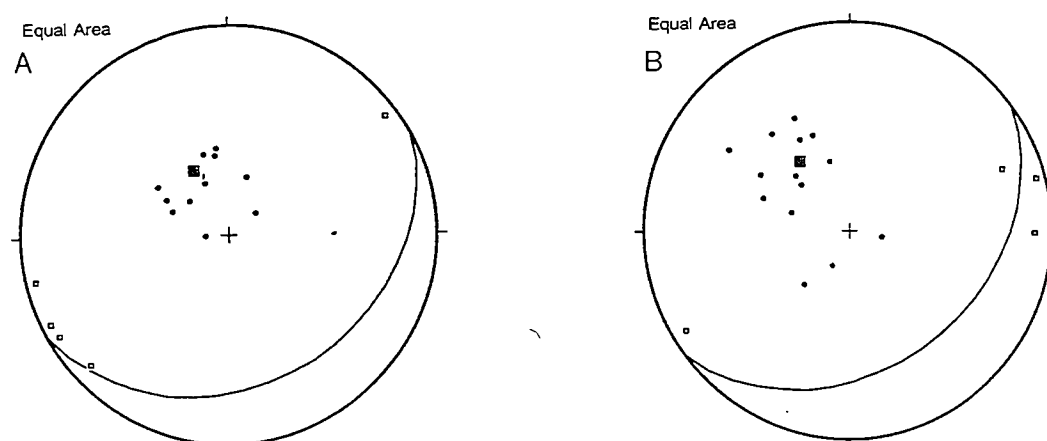


Figure 4.35. Equal area stereonet of: A) Poles to phyllonitic foliation (dots) with mean great circle and mineral lineations (boxes); and B) Poles to protophyllonitic foliation (dots) with mean great circle and mineral lineations (boxes), from Ronay.

In the protophyllonites, original quartz appears 'bruised', suggestive of high dislocation densities within grains. It is unknown whether this cold working is synchronous with phyllonitisation or the response to previous or subsequent deformation.

4.3.3. Lochportain

East of Lochportain, on the NE tip of north Uist, several NE-SW trending belts of phyllonite and protophyllonite cut through the 'Mashed' gneiss of the Crush Melange (Fig. 4.36). NE of Crogarra na Hoe (NF 979388), a protophyllonitic foliation which cross-cuts acid, basic and pegmatitic relicts in the Crush Melange, becomes progressively more phyllonitic further SE. A belt of well foliated, green,

chloritic phyllonite, c. 200m thick, crops out between the bay at Rubha an Duine (NF 975380) and Leac na Hoe (NF 980385) and can be traced SW for c. 300m into a region of poor exposure. The phyllonite belt dips shallowly (c. 30°) NW, and can thus also be traced north-westwards along the northeast coast for c. 400m, a region which both Sibson (1977b) and Walker (1990) mapped as being phyllonite-absent. The eastern phyllonite margin occurs offshore.

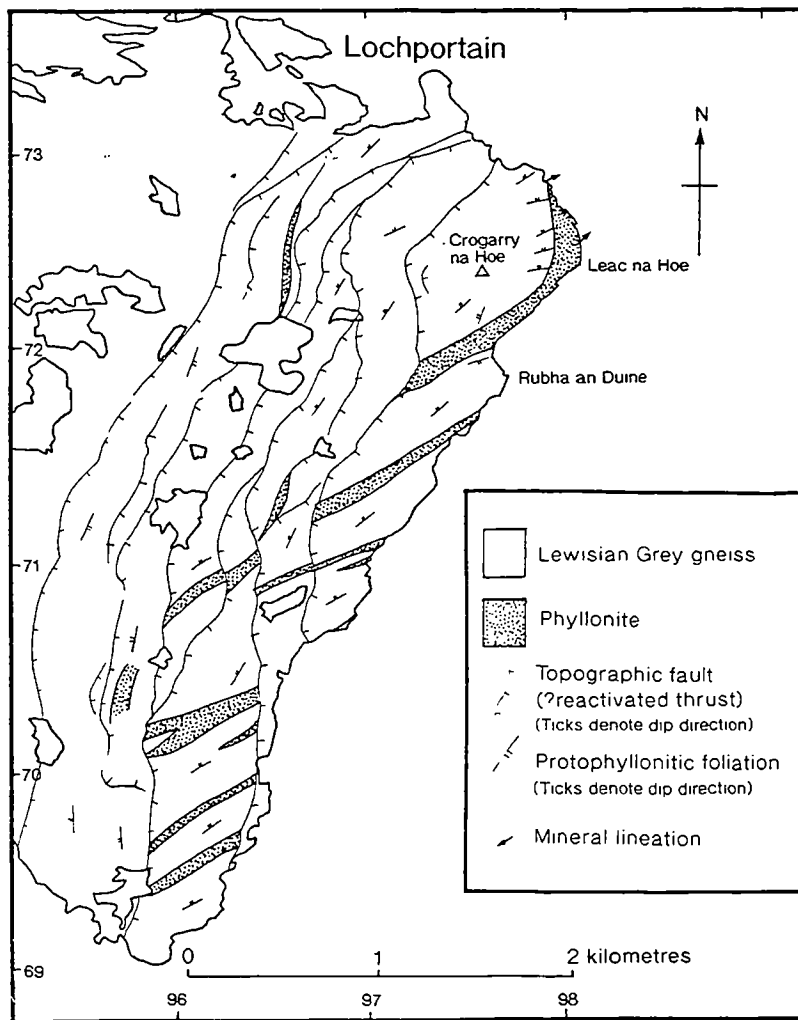


Figure 4.36. Geological map of the Lochportain region (modified from Sibson 1977b).

The phyllonites and protophyllonites of the Lochportain region have structural characteristics not observed elsewhere in North Uist. The phyllonitic foliation, defined by aligned phyllosilicates and quartz/ feldspar aggregates, strikes predominantly ENE-WSW and dips predominantly to the NNW, similar to the area north of Eigneag Mhor (NF 927615) in the Burrival region (described above) (Fig. 4.38a). The lower strain protophyllonites possess a NW-dipping fabric, but are locally much more variably oriented, probably as a result of wrapping large lower strain 'clasts' (Fig. 4.38b). A subhorizontal mineral stretching lineation, defined by

phyllosilicates (including fibrous chlorite replacing amphibole), feldspar aggregates, often partially replaced by epidote, is present in both high and low strain phyllonitic material and also trends NE-SW. Rarely, elongate blebs of pre-existing crushed acid gneiss c. 50-100cm are aligned with the mineral stretching lineation in the protophyllonitic material. Kinematic indicators parallel to this lineation have not been found, but it is thought that sinistral strike-slip motion, inferred from phyllonitic and protophyllonitic material elsewhere in North Uist was responsible for the mineral lineation orientation.

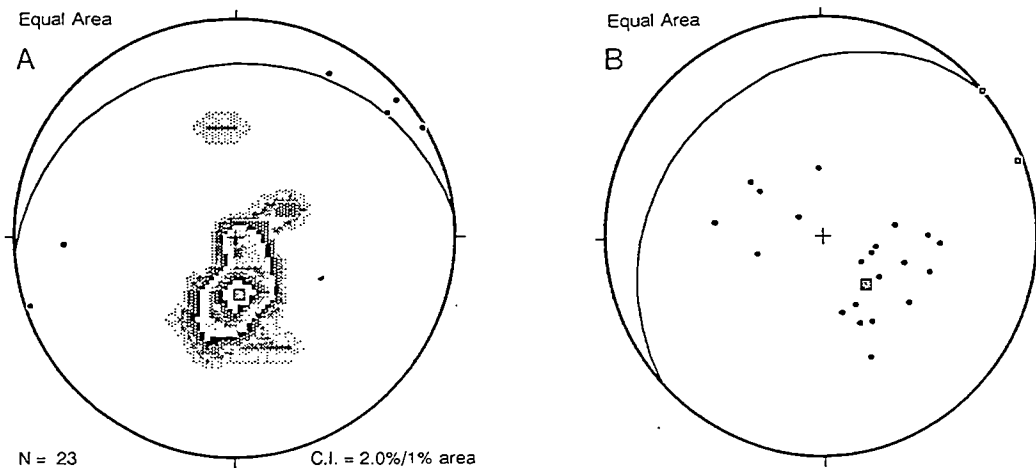


Figure 4.38. Equal area stereonet of: A) Contoured poles to phyllonitic foliation with mean great circle and mineral lineations (dots); and B) Poles to protophyllonitic foliation

In certain parts of the Lochportain region the phyllonitic foliation strikes NW-SE and dips shallowly NE; an orientation which is unique to this region and which is believed to relate to later reorientation during extensional reactivation (see section 4.4.3)

4.3.4. South Eaval

In the region between Beinn na-h-aire (NF 900590) and the eastern tip of the peninsula south of Bagh Moraig (NF 920586), five N-S striking, well foliated green phyllonite belts cross-cut the 'Mashed' and cataclastic gneisses of the Crush Melange. Between these belts, less foliated protophyllonitic areas occur (Fig. 4.39). The extremely well foliated phyllonites appear to be coincident with areas within the melange where cataclasis was extensive, and individual veins of altered ultracataclasite and pseudotachylite are occasionally discernible, but are always cross-cut by the phyllonitic foliation.

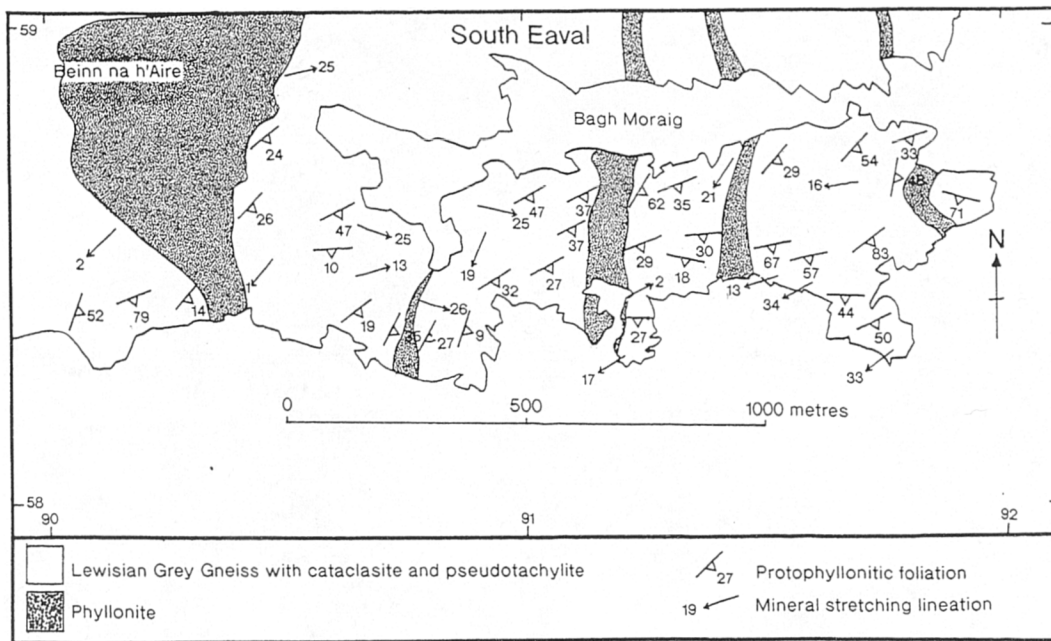


Figure 4.39. Geological map of the South Eaval region.

The phyllonitic and protophyllonitic foliations dip consistently to the SE, but a significant spread of mineral lineation plunges, between NE and SW, occurs (Fig. 4.40). The NE-SW trending mineral lineation, which dominates outside the phyllonite belts can be traced through a clockwise reorientation to plunge E or S in the phyllonite belts, (e.g. at NF 908583). This reorientation is due to the focussing of later extensional reactivation in to the most phyllonitised areas (see section 4.4). The 'curve-in' of the foliation at the margins of the phyllonite belts induces a local strike-swing of up to 60°, and mainly show geometries consistent with sinistral strike-slip (e.g. at NF 904584 and NF 915585) (Fig. 4.41).

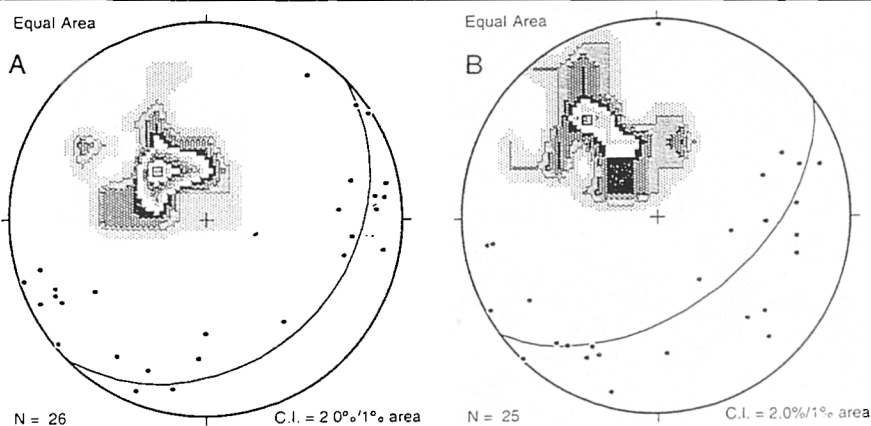


Figure 4.40. Equal area stereonet of contoured poles to: A) Phyllonitic foliation with mineral lineations (dots); and B) Protophyllonitic foliation with mineral lineations (dots), from Eaval, N.Uist.

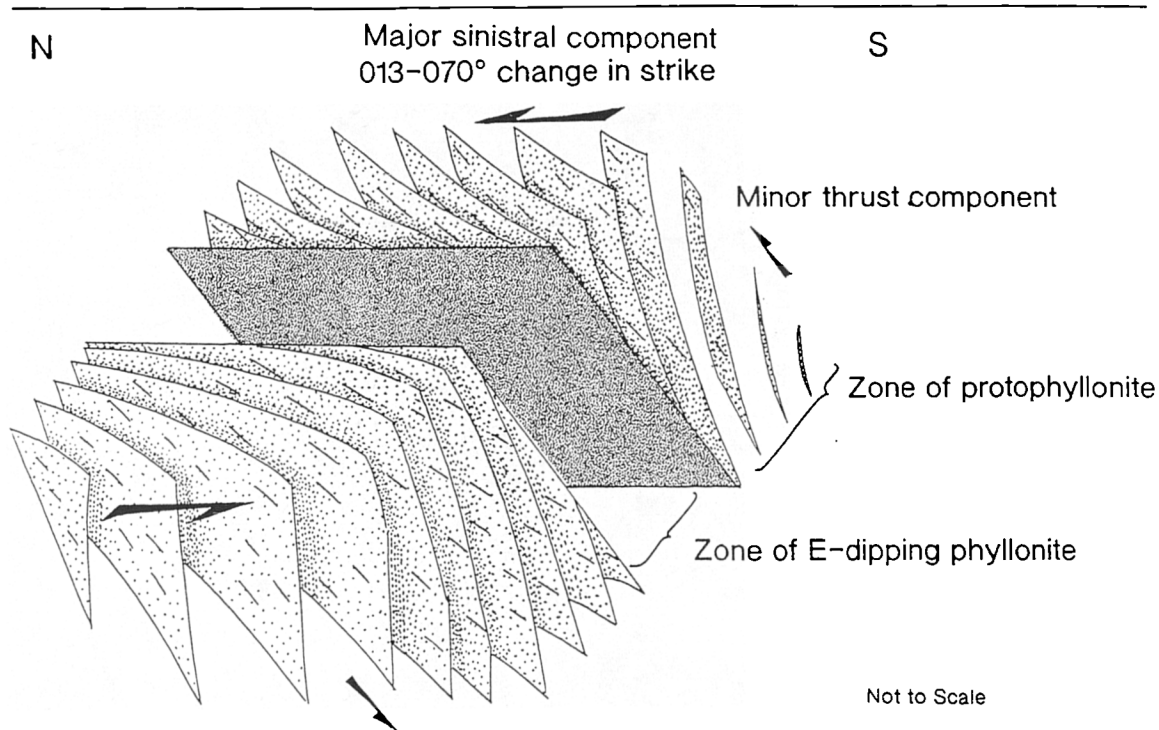


Figure 4.41. Schematic block diagram showing swing of protophyllonitic foliation into phyllonite belt, consistent with sinistral motion.

(ii). South Uist and adjacent islands

In contrast to the braided nature of the phyllonite belts in North Uist, the phyllonites of South Uist appear to be confined to a single N-S trending belt, termed the Usinish Mylonite by Jehu and Craig (1925). This term is somewhat misleading since these rocks are virtually identical to the phyllonites in North Uist. Thus, the Usinish *Mylonite* is hereafter referred to as the Usinish *Phyllonite*.

The Usinish Phyllonite belt is mainly exposed in a series of east coastal 'Rubhas' (promontories) and islands, but is inferred to be a continuous belt, at least 15km long (Fig. 4.42). The belt is only c. 10m thick at its northernmost exposure (Ornish NF 858376) where both upper and lower contacts are exposed, but is at least c. 200m thick at its southernmost exposure (Stuley; NF 830235), although the contacts of the belt are not exposed at this locality.

The Usinish phyllonite belt strikes N-S and dips shallowly to moderately eastwards or southeastwards. Locally, however, the phyllonitic foliation dips in other orientations, but this is *probably* due to either subsequent deformation, or the 'wrapping' of low strain pods. No evidence for the progressive northward steepening of the foliation reported by Walker (1990) has been found.

Protophyllonites are not well developed in South Uist, due to the non-braided nature of the phyllonite belt. The phyllonitic foliation does become less intense however, in the immediately adjacent gneisses. Protophyllonitic material is rarely

observed more than 100m from the Usinish Phyllonite belt. Occasionally, low-strain pods (up to several metres) occur within the phyllonite belt in which the cataclastic and microfaulted nature of the protolith can still be discerned. The homogeneity of the Usinish Phyllonite means that a petrographic description at each of the localities studied would prove repetitive. Thus, a petrographic description pertinent to the whole unit is provided in the following section only.

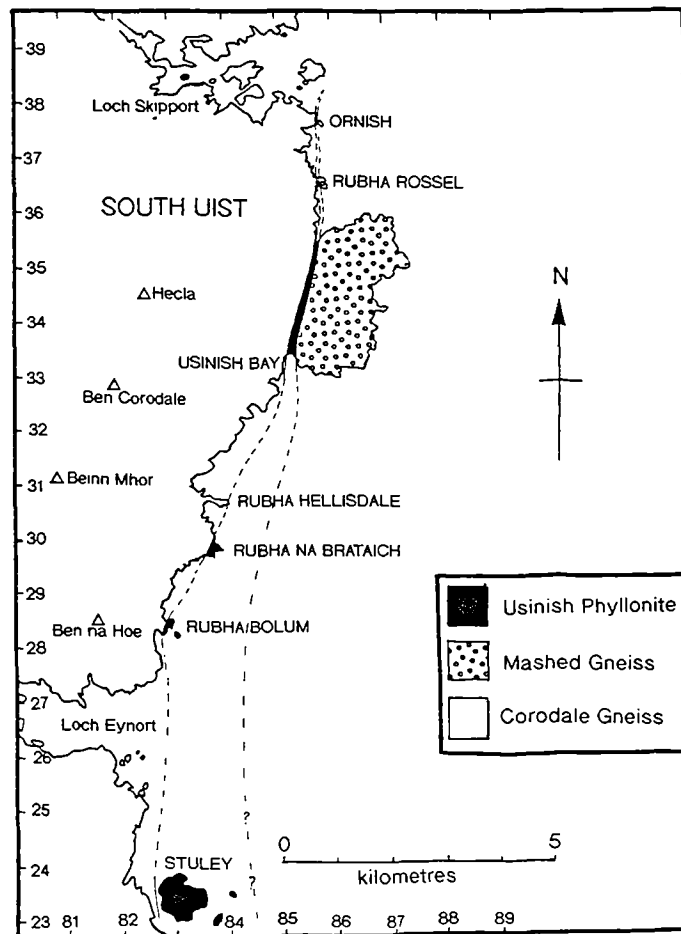


Figure 4.42. Simplified geological map of the eastern part of S. Uist, showing the trace of the Usinish Phyllonite.

Usinish Phyllonite contacts with the adjacent gneisses are nearly always faulted, but these faults are due to a later deformation phase (see section 4.4).

4.3.5. Rubha Rossel

The small promontory of Rubha Rossel (NF 858365) exposes a small sliver of Usinish Phyllonite c. 30m thick, sandwiched between the Corodale Gneiss to the west and Mashed Gneiss to the east (Fig 4.43a).

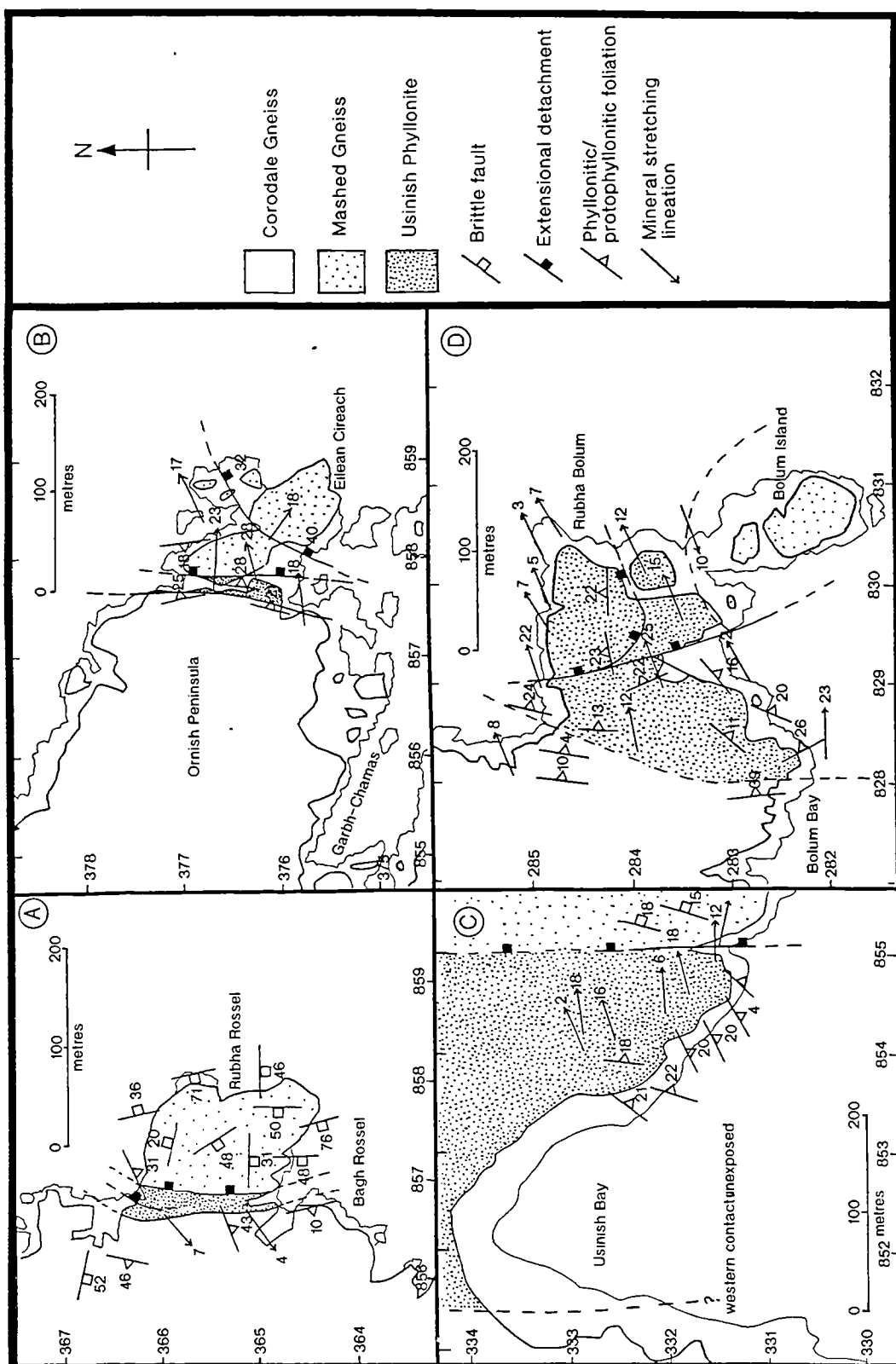


Figure 4.43. Geological maps of: A) Rubha Rossel; B) Ornish; C) Usinish Bay; and D) Rubha Bolum, S.Uist

Macrostructure

The Corodale Gneiss (rich in orthopyroxene, clinopyroxene and garnet), which lies structurally below the phyllonite, shows evidence of normal and reverse microfaulting. The Mashed Gneiss, which lies structurally above the phyllonite is intensely fractured, and contains veins, up to 1cm thick, of pseudotachylite/ultracataclasite partially altered to epidote. The deformation in both units relates to earlier thrust-sense motion on the OHFZ (see section 4.2). A crude phyllosilicate-defined foliation is also developed, and relates to the phase of phyllonite development.

The best exposure of true phyllonite occurs on the northern side of Rubha Rossel, where clean coastal outcrops of green-grey, intensely foliated and fissile phyllonite occur. The rock is fine grained (<2mm grain size) and rich in chlorite, epidote, and sericite. In coarser grained regions, remnants of K-feldspar and plagioclase crystals (up to 1cm) occur, and probably represent zones where Laxfordian pegmatites have been phyllonitised. Feldspar is usually replaced by epidote and/ or sericite and hornblende is replaced by chlorite. Quartz is probably the only mineral of the original protolith assemblage, and otherwise near-total retrogression to low-greenschist facies has occurred.

The phyllonite foliation is extremely well developed, and has a variable orientation. Most foliation surfaces strike NE-SW, with a moderate southeasterly dip (Fig. 4.44). This orientation lies clockwise of the strike of the phyllonite belt as a whole, and undergoes a sigmoidal strike-swing. Across the belt, a 9° anticlockwise swing from an ENE-WSW trend in the west, to a NE-SW trend in the centre occurs, and a further 43° clockwise swing to a ESE-WNW trend in the east occurs (Fig 4.45). In general, the strain and intensity of foliation development decreases from the base of the unit to the top (from west to east).

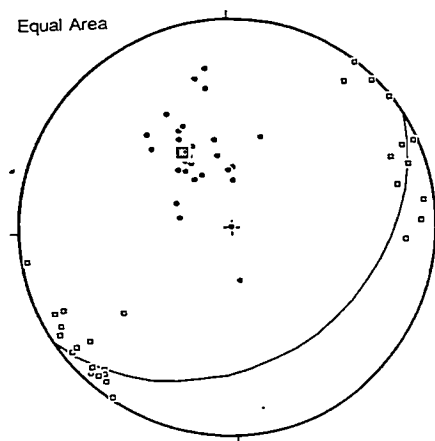


Figure 4.44. Equal area stereonet of poles to phyllonitic foliation (dots) with mean great circle, and mineral lineations (boxes), from Rubha Rossel, S. Uist.

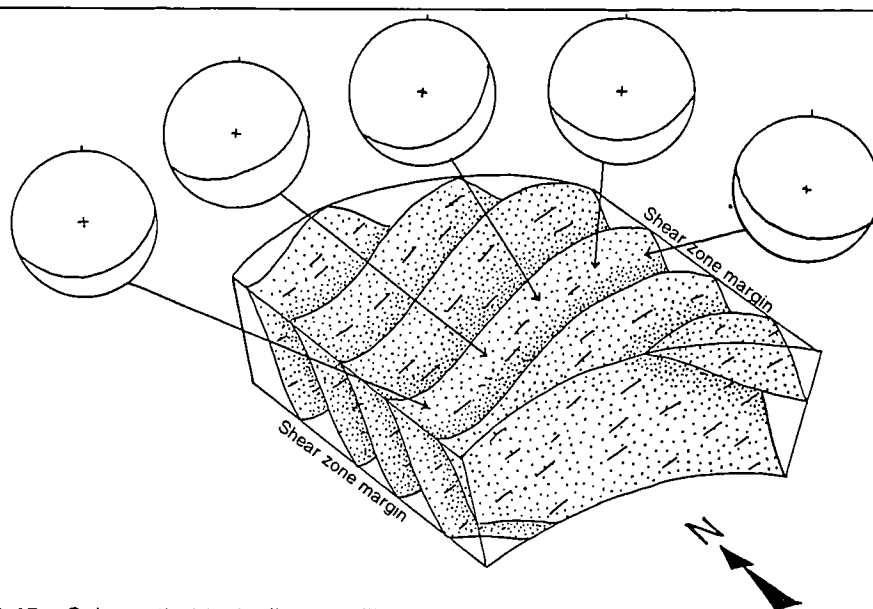


Figure 4.45. Schematic block diagram illustrating the swing in foliation orientation due to sinistral shear (each stereonet shows foliation orientation across the phyllonite belt).

A very well developed mineral lineation, defined by quartz rods, and elongate feldspar and mafic pseudomorphs (chiefly fibrous chlorite and epidote), trends subhorizontally NE-SW and is affected by the foliation swing described above (Fig. 4.44). This lineation is not an intersection lineation (cf. Coward 1969, 1972). The plunge of the mineral lineation is variable between NE and SW, and results from a large-scale, open 'warp' of the phyllonite foliation (discussed in section 4.4.5). Parallel to this lineation, is a minor cm-m-scale swing in the foliation trace. (Plate 4.10a) This schistosity swing is compatible with the overall sinistral-sense of shear inferred from the map-view strike-swing. A top-to-the-NE sinistral strike-slip sense of motion is interpreted for this phyllonite belt.

A subordinate SE-plunging mineral lineation is developed in only the most highly strained phyllonite near the base of the unit, and relates to later extensional reactivation (section 4.4.5).

Microstructure

The Usinish Phyllonite belt as a whole is rather homogeneous and shares many petrographical similarities with the braided phyllonite belts of North Uist. A microstructural description pertinent to the entire Usinish Phyllonite belt is provided here.

The assemblage of the phyllonite protolith has been replaced by lower grade minerals as a result of retrogression. The assemblage: Quartz (10 - 20%), sericite (25 - 40%), chlorite (20 - 30%), epidote (20 - 30%), opaque minerals (5 - 10%), +/-

calcite, +/- biotite, is typical of the phyllonite, but relict grains of plagioclase (0 - 5%), K-feldspar (0 - 5%) and hornblende (0 - 10%) are occasionally present. Quartz and epidote are noted to become less common in regions where relict amphiboles and feldspars are preserved, and may reflect the primary compositional layering of the unit.

Quartz usually exists as isolated grains and polycrystalline ribbons, with the latter dominating. The larger monocrystalline grains always display undulose extinction, indicative of high dislocation densities in the crystal lattice, due to dislocation creep without recovery. The polycrystalline quartz ribbons occur as either *type 1*, core and mantle structures, or *type 2*, fully recrystallised aggregates (using the terminology of Boullier and Bouchez 1978). Subgrains occur throughout these *type 2* ribbons and may occasionally show a preferred alignment (*type 2b* ribbons) (Plate 4.10b). In contrast to the relict, non-recrystallised larger grains, very little undulose extinction has been observed in these ribbons, and recrystallisation therefore probably post-dates all cold working. The gradual misalignment in the crystal lattice from core to mantle, inferred by the extinction behaviour of individual subgrains, suggests that grains recrystallise by rotational recrystallisation only. Relict grains of monocrystalline quartz with undulose extinction occasionally show brittle intracrystalline and transcrystalline fracturing, with dilatational pull-aparts. These fractures form loci for rotational recrystallisation in the relict grain and the gaps between fragments are usually filled with fibrous chlorite +/- sericite.

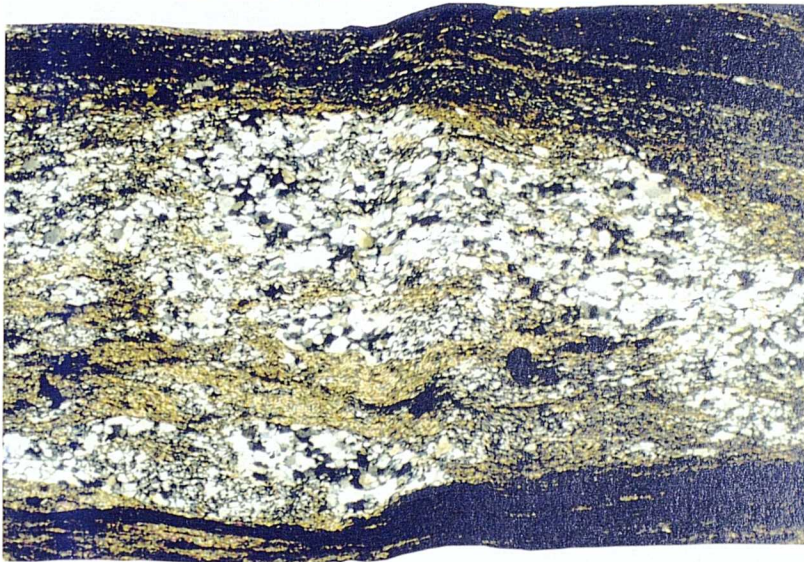
The protolith feldspar in the Usinish Phyllonite has been largely retrogressed to fine-grained sericite. The phyllosilicate forms strong, foliation-parallel alignments, between ribbons of recrystallised quartz or fine grained epidote. Where original feldspar has been partially replaced by sericite, the original grain exhibits undulose extinction due to cold-working. Brittle intracrystalline and transcrystalline fractures are commonly filled with recrystallised quartz and fibrous chlorite. Occasional epidote porphyroblast pseudomorphs of feldspar are apparent and display tensional intracrystalline fractures. These pulled-apart fragments are filled with fibres of chlorite, which on foliation surfaces lie parallel to the strong NE-SW trending mineral lineation observed in the field. A well defined pressure solution cleavage, visible as thin, closely spaced, foliation parallel, dark coloured layers is apparent in areas of alteration to sericite and/ or chlorite.

Amphiboles are only rarely preserved, and occur where retrogression to chlorite is incomplete. Relict hornblendes are pulled apart, with fibrous chlorite growth between fragments (Plate 4.10c). Like sericite, chlorite shows a strong preferred alignment and screens of chlorite often separate ribbons of recrystallised quartz.

a)



b)



c)

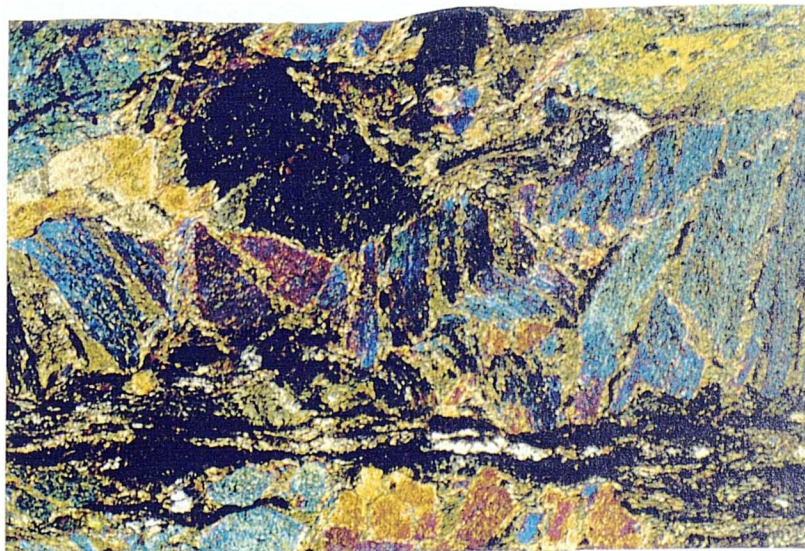


Plate 4.10 Phyllonites from S.Uist

a) Asymmetric swing in foliation trace from Rubha Rossel, S.Uist (NF 858366), consistent with top-to-the-NE sinistral shear.

b) 'Type 2b' quartz ribbon surrounded by fine grained sericite showing preferred alignment of subgrains, parallel to ribboned grain margins, from Rubha Bolum (NF 829283). Field of view is 3mm. (XPL)

c) Relict hornblendes in phyllonite from Rubha Bolum (NF 830284). Tensional fractures between grain fragments are filled with fibrous chlorite. Field of view is 3mm (XPL)

Kinematic indicators are numerous in thin section and include asymmetric extensional shear bands and asymmetric minor fold pairs. The folds are defined by layers of epidote-rich material interleaved with layers of sericite-rich material. Quartz and chlorite fibre growth in tensional fractures between grain fragments is often oblique to the fracture walls. The asymmetric nature of these fibres also give a shear sense. Asymmetric δ porphyroclasts also occasionally occur (Plate 4.11a), but most clasts in the Usinish Phyllonite are markedly symmetrical. All kinematic indicators give a dominant sinistral sense of shear of top towards the NE or ENE, parallel to the mineral stretching lineation. Top-to-the E shear senses are also apparent in places, and in general become more common from north to south, along strike. This top-to-the-E shear sense is believed to result from subsequent extensional reactivation of the phyllonite belt (see section 4.4).

Metamorphic conditions during deformation

The P-T conditions during phyllonite development can be deduced from both the metamorphic assemblages present, and the deformational behaviour of the existing phases.

The replacement of amphibolite and granulite facies minerals in the 'Mashed Gneiss' and Corodale Gneiss protoliths respectively, with lower grade, hydrous mineral assemblages in the phyllonite belt is evidence for retrogression in the presence of a fluid phase. The presence of chlorite, replacing hornblende is indicative of low greenschist facies metamorphism. No Corodale Gneiss-derived pyroxenes are present in the phyllonite, and complete retrogression to chlorite is likely to have occurred. Feldspars, including bytownite/ labradorite plagioclase in the gneissic protolith have undergone alteration to sericite and/or epidote, and where plagioclase has only been partially altered at grain rims, a core of albite is preserved. The fibrous phases (chlorite, sericite and quartz) which occupy the tensional pull-aparts in relict grains (feldspar and/or monocrystalline quartz), or in pseudomorphs of relict grains (usually epidote), are evidence for the precipitation of these minerals from solution, and the large-scale behaviour of the phyllonite as diffusive mass transfer (DMT) sink.

The microstructures preserved in existing minerals are consistent with the dominantly low-greenschist facies retrograde assemblage. The undulose extinction and occasional brittle fracturing observed in both quartz and feldspar relicts is indicative of low P-T conditions. The presence of *Type 1* core and mantle quartz ribbons and *Type 2* polycrystalline ribbons in quartz is similarly indicative of low - mid greenschist facies metamorphism (Boullier and Bouchez 1978). The rotational recrystallisation of quartz in these ribbons approximates low-greenschist facies

(Boullier and Bouchez 1978 Simpson 1985). The non-recrystallised feldspars suggest that deformation occurred at less than mid-greenschist facies (<350° C) (Fitzgerald and Stunitz 1993).

A pressure solution cleavage, defined by thin, black, closely spaced, foliation parallel layers is often present in these rocks, suggesting that material may have been removed by DMT, as well as added. Although the relative timing of retrogression and deformation is often difficult to determine (Rutter and Brodie 1985), a pre-tectonic fluid ingress and retrogression is not thought to have occurred, due to the fresh, undeformed nature of chlorite replacing hornblende and sericite replacing feldspar. Metamorphism-enhanced deformation localisation is therefore unlikely. A post-tectonic fluid ingress and retrogression is also thought to be unlikely, due to the strong alignment of precipitated chlorite fibres, consistent with the kinematic regime *during* deformation. It could be argued that chlorite grew mimetically on existing fibrous amphibole, but no partial replacement has been observed. The fluid ingress and retrogression is therefore regarded as synchronous with deformation.

4.3.6. Ornish

The Ornish peninsula and the adjacent island of Eilean Cireach (NF858376) hosts the most northerly outcrop of Usinish Phyllonite (Fig 4.43b). The belt is no more than 10-12m thick and is largely exposed below the high water mark.

The adjacent Corodale Gneiss to the west, and Mashed Gneiss to the east have a crude protophyllonitic fabric, but its orientation is highly variable. The foliation in the underlying Corodale Gneiss 'grades' into higher strain material, whereas the upper contact with mashed gneiss is less gradational and a discrete late fault occurs at the strain boundary (see section 4.4.6). The phyllonite is petrographically identical to that observed at Rubha Rossel, being green-grey, fine grained and rich in retrograde phyllosilicates (see section 4.3.5 for a full petrographical description). The extremely well developed foliation strikes NNE-SSW, and has a shallow easterly dip (Fig. 4.46). Unlike the Rubha Rossel phyllonite, however, the foliation is sub-parallel to the strike of the belt as a whole. The mineral lineation, defined by feldspar aggregates and fibrous chlorite plunges between ENE and E in the main part of the belt, but swings to plunge NE close to the upper contact with the Mashed Gneiss (Fig. 4.46). It is thought that the present fabric orientation is chiefly due to extension (section 4.4.6), and only the belt margins preserve evidence for strike-parallel movement. No kinematic indicators were found.

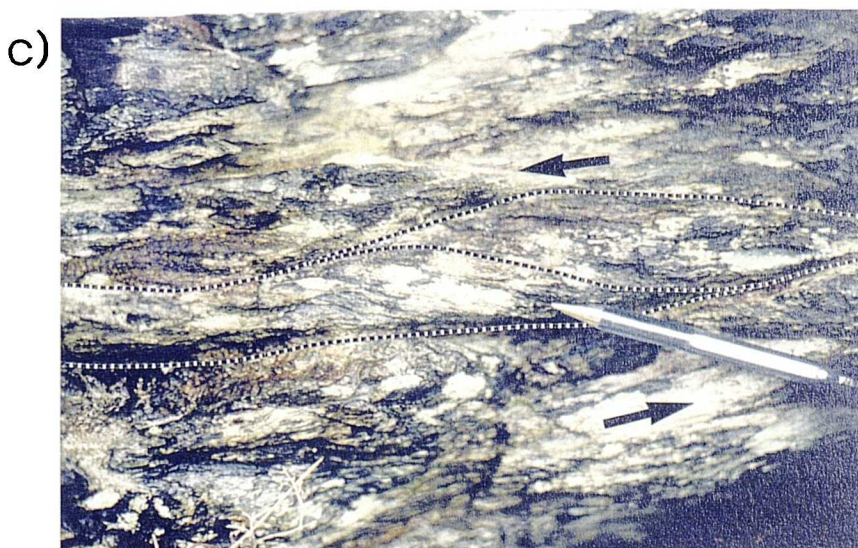
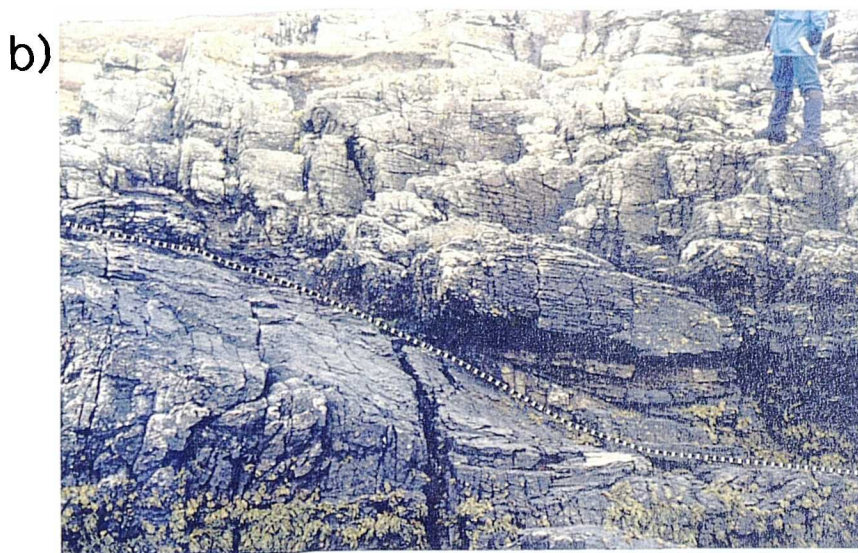
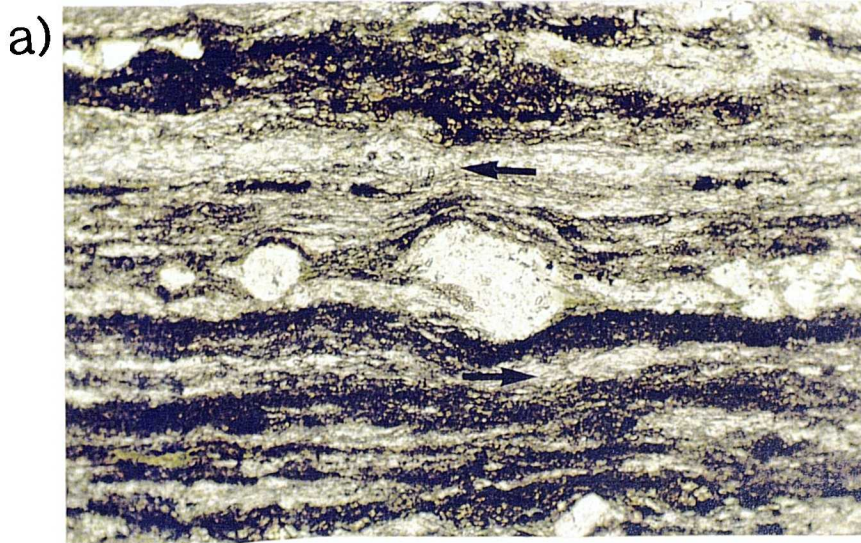


Plate 4.11 Phyllonites from S.Uist.

a) Asymmetric, rotated δ porphyroblast of albite, consistent with top-to-the-NE sinistral shear, in phyllonite from Rubha Rossel (NF 858366). Field of view is 1.3mm. (PPL)

b) Low strain protophyllonitic 'Mashed Gneiss' clast (lower left of photo) wrapped by high strain phyllonite (upper right) at Rubha Bolum (NF 830283).

c) High strain phyllonite from Rubha Bolum (NF 830284) with asymmetric shear band fabric indicative of top-to-the NE sinistral shear.

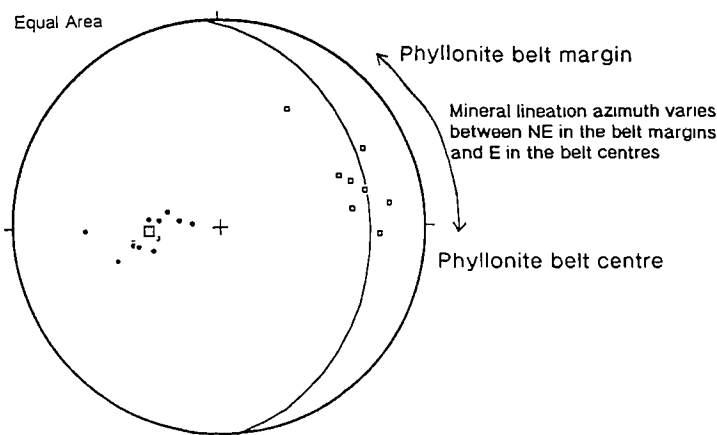


Figure 4.46. Equal area stereonet showing poles to phyllonitic foliation (dots) with mean great circle, and mineral lineations (boxes), from Ornish, S.Uist.

4.3.7. Usinish Bay

The southerly extension of the Usinish phyllonite belt continues on land for c. 3km, and is indicated by a wide topographic hollow between Molatuath (NF 857354) and Usinish Bay (NF 852334) (Fig. 4.43c). Although the Corodale Gneiss and Mashed Gneisses are well exposed to the west and east respectively, the Usinish Phyllonite is only exposed in the east part of Usinish Bay. The lower contact with the Corodale Gneiss is not exposed, whilst the upper contact with the Mashed Gneiss is marked by a complex set of later detachment faults (see section 4.4.7).

The phyllonites in Usinish Bay show a marked upward (eastward) reduction in the amount of chlorite. Towards the top of the unit, chlorite is subordinate to original quartz and feldspar, and it is likely that these rocks were derived from quartz-rich Mashed Gneiss, not Corodale Gneiss, which has relatively little quartz.

The phyllonitic foliation strikes NE-SW, and dips shallowly SE, clockwise of the N-S trace of the belt (Fig. 4.47). Laxfordian pegmatite relicts are observed to be disrupted by this foliation. The phyllonitic lineation plunges NE at the top of the belt (in the quartzo-feldspathic-rich zone), and ESE in the more chloritic zones, near the base of the unit (Fig. 4.47). It is thought that extensional deformation may have reoriented the strike-parallel lineation in the more retrogressed and highly strained material. Kinematic indicators were not found.

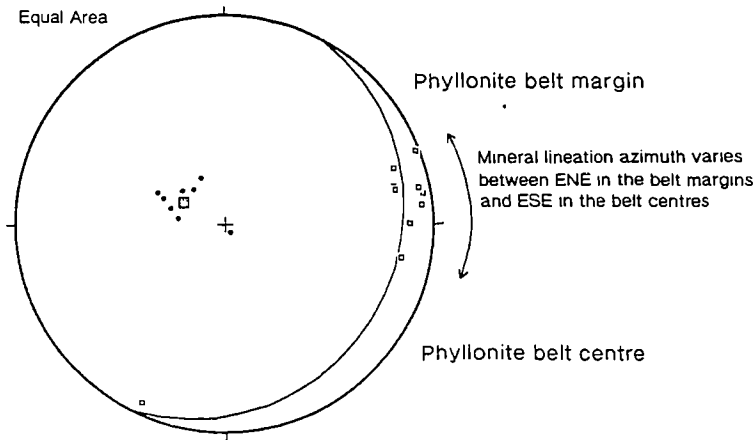


Figure 4.47. Equal area stereonet of poles to phyllonitic foliation (dots) with mean great circle and mineral lineations (boxes), from Usinish Bay, S. Uist.

4.3.8. Rubha Bolum

Excellent exposures of the Usinish Phyllonite and adjacent Corodale Gneiss occur at Rubha Bolum (NF 828284) (Fig. 4.43d). The characteristically brown weathering Corodale gneiss in the west of the area is heavily fractured and cataclastically ^{deformed} and is rich in retrogressed minerals such as chlorite and epidote. A crude protophyllonitic fabric is present in this unit, forming a shallow east dipping foliation with a poorly developed NE-SW trending mineral lineation. The intensely crushed Corodale Gneiss has a gradational contact over c. 5m with the structurally higher phyllonitic material. This contact is marked in the field, by a change from brown to an overall greenish-grey weathering colour and an intensification in the phyllonitic foliation.

At the SE tip of Rubha Bolum, at a lower structural level, a small outcrop of quartzo-feldspathic Mashed Gneiss occurs, which continues towards Bolum Island. The phyllonitic foliation is observed to de-intensify into the Mashed Gneiss, so that earlier brittle features, including cataclasite veins and randomly oriented microfaults may still be discerned. Occasionally, veins of relict cataclasite are still discernible in the main body of the phyllonite, but they are always overprinted by the phyllonitic foliation.

The phyllonite unit shows evidence of compositional banding, parallel to the foliation, with quartzo-feldspathic layers interbanded with more chloritic layers. This may represent an original banding in the gneiss, and hence a control on the orientation of phyllonite fabric orientation. Alternatively, the phyllonitisation and associated shearing may have reoriented the relict banding into parallelism with the foliation. Relict Laxfordian granites/ pegmatites (c. 2-3 cm thick) are also present, and lie parallel to the overprinting foliation. The high modal percentage of quartz in

the phyllonite suggests that most of the phyllonite is derived from the acid Mashed Gneiss to the east, rather than the mafic Corodale Gneiss to the west.

In the most phyllonitic part of the area, abundant evidence for the ductile behaviour of quartz and brittle behaviour of feldspar is present. Blue-grey 'bruised' quartz ribbons are common, indicating the operation of dislocation creep (cold working) deformation mechanisms. Feldspar, however, deforms in a brittle manner, with newly recrystallised quartz infilling fractures between feldspar grains. On the SE tip of Rubha Bolum (NF 830284), the reverse relationship is observed. Altered feldspar pseudomorphs (replaced by sericite and epidote), appear to be deforming in a ductile manner, whilst bruised quartz grains appear to be behaving as rigid porphyroclasts.

The orientation of the phyllonitic foliation is locally variable. The peninsula of Rubha Bolum can be divided geographically into two halves, each with a structurally distinct domain, separated from the other by a late detachment fault (see section 4.4.8 and Fig. 4.65:

1. In the western half of the peninsula, the extremely well developed phyllonitic foliation strikes NNE-SSW, with a shallow ESE dip (Figs. 4.43 and 4.48).
2. In the eastern half of the area, the phyllonitic foliation strikes ENE-WSW and dips shallowly NNW, c. 120° anticlockwise of the western half (Figs. 4.43 and 4.48).

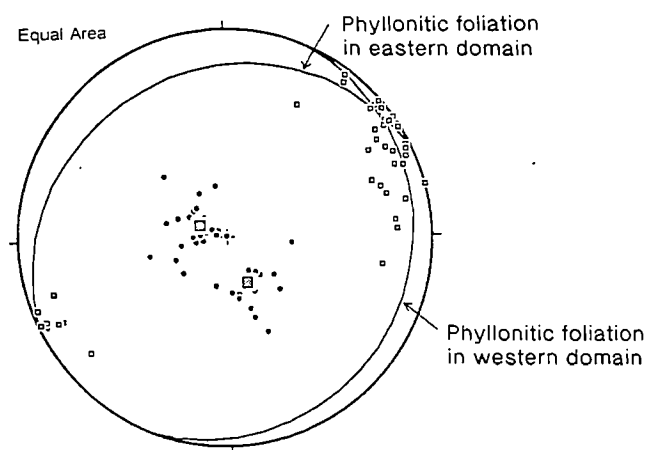


Figure 4.48. Equal area stereonet of two populations of poles to phyllonitic foliation (dots) with mean great circles and mineral lineations (boxes), from Rubha Bolum, S. Uist.

The mineral stretching lineation in *both* regions, defined by rodded quartz and elongate feldspar aggregates, trends close to NE-SW, and is assumed to be contemporaneous in both domains (Fig. 4.48). This means that 120° of rotation of one domain relative to the other is unlikely. It is therefore suggested that the northerly dip of the foliation on the eastern side is the result of the presence of the low strain 'clast' of Mashed Gneiss on Bolum Island, around which the foliation has wrapped, influencing the local dip direction (Plate 4.11b). Late movement on a detachment fault (see section 4.4.8) probably juxtaposed the east domain foliation, affected by the proximity of the clast, against the western domain foliation whose orientation was unaffected.

The low-strain enclave of Mashed Gneiss on Bolum Island is at least 100m thick. This may explain why the I.G.S mapping programme (Fettes et al. 1992) marked the eastern boundary of the entire Usinish Phyllonite belt west of Bolum Island. This boundary is regarded as suspect for two reasons:

1. An upper boundary for the phyllonite at this location requires a large decrease in phyllonite width between Usinish Bay (NF 852334) and Stuley (NF 830235), when regionally, the Usinish Phyllonite belt appears to be undergoing an overall increase in width (Fig 4.42).
2. The Mashed Gneisses on Bolum Island and the adjacent tip of Rubha Bolum do *not* lie at higher structural levels than the phyllonite. (cf. the IGS map, Fettes et al. 1992). (*See Plate 4.11 b*).

Kinematic indicators parallel to the well developed NE-SW trending mineral lineation in both domains are rare, but a small 1cm wide shear zone at NF 829284 in the eastern domain, shows an asymmetric fabric swing displaying a top-to-the-NE sense-of-shear, consistent with regional sinistral strike-slip on the OHFZ (Plate 4.11c).

4.3.9. Stuley

The southernmost outcrop of Usinish Phyllonite is on the island of Stuley (NF 830235) (Fig. 4.42 ; see also Fig. 4.66). The island is composed entirely of low greenschist facies chloritic phyllonite covering an area of c. 1km², and thus constitutes the widest exposure of this unit in the southern segment of the OHFZ. The phyllonite belt is at least c. 250m thick. The original foliation has been virtually obliterated by a second foliation, related to subsequent extension, which dips very shallowly to the west in most parts. Late warping of this often subhorizontal foliation

results in a locally highly variable dip direction. Very little evidence is preserved of the strike-slip event which generated this phyllonite. All the deformation features relate to extensional reactivation of the phyllonite belt (see section 4.4.9).

4.3.10 Conclusions and discussion on strike-slip movement in the southern segment

Conclusions

Post-dating the heterogeneous, thrust-related, brittle deformation, are a suite of ductile phyllonitic rocks. These occur as dominantly N-S or NNE-SSW trending braided networks in North Uist, and as a single N-S trending belt in South Uist. It is suggested that localised planar zones of *retrogression* developed due to fluid channelling into the previously dry OHFZ through zones of locally increased permeability, causing hydration reactions and the production of low greenschist facies assemblages. The anisotropies were probably large brittle thrusts.

Fault rock distribution: The large scale geometry of the phyllonite belts

In the west of the 'Crush Melange' of North Uist, at Burrival (e.g. at NF 908622), a crude protophyllonitic foliation is developed and occurs preferentially close to large faults (see Plate 4.6b). Sibson (1977b) regarded this close association between faults and fabrics as indicative of a close temporal association, i.e. the protophyllonitic foliation developed coevally with large scale thrusting. However, this suggestion is inconsistent with the dominantly strike-parallel movement direction indicators associated with the foliation throughout the rest of the Crush Melange. An alternative, kinematically viable, scenario is that two separate and locally different kinematic regimes gave rise to similar features and that the close spatial association between them is due to the control of one type of structure on the other. Specifically, the location and geometry of the strike-slip-related foliation is controlled by the earlier pre-existing thrust anisotropy. This is corroborated to some extent by field relationships further east in the Crush Melange, where the degree of retrogression and strain is higher. Here, 'topographic' faults appear to pass eastwards into phyllonite belts with a very similar orientation. Such large anisotropies could act as pathways for localised retrogression and may explain the belt-like nature of phyllonitic foliation development.

The anastomosing nature of the phyllonite belts in North Uist, which Sibson (1977b) broke down into four categories based on orientation (see section 4.3) can be explained by a model in which laterally elongate, flattened and irregularly sized low strain 'clasts' are enveloped by a network of anastomosing high strain shear

zones (Fig. 4.49). The orientation of these clasts undergoes a degree of clockwise rotation from west to east and probably reflects the imposed sinistral shear. As the 'clasts' are wrapped by higher strain material (the phyllonite belts), the orientation of the phyllonite belts depends on:

- The orientation of the clast, affecting the strike of the phyllonite belts;
- The erosional cut surface, affecting both the dip magnitude and sometimes the dip direction of the phyllonite belts.

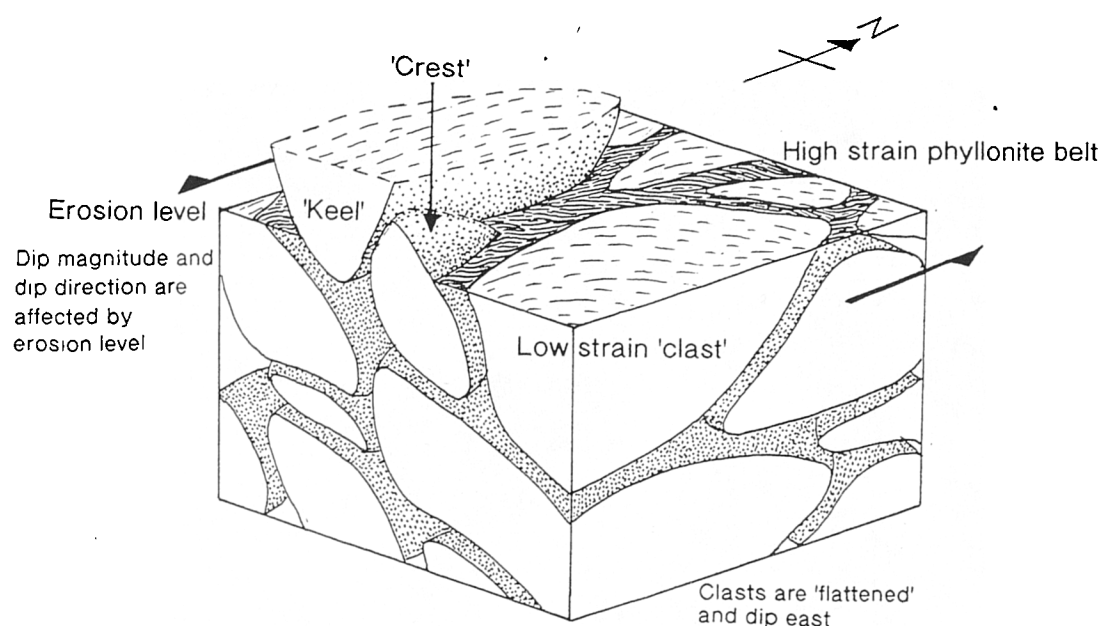


Figure 4.49. Schematic block diagram of low strain protophyllonitic 'clasts' wrapped by anastomosing, high strain phyllonite belts in the Crush Melange of North Uist.

NW-dipping belts are probably subordinate to SE-dipping belts due to the flattened nature of the clasts in a SE-dipping plane. The erosion level will therefore usually cut the lower and upper surfaces of the clast when they are parallel and SE dipping. Only if the erosion level cuts the extreme top (crest) or the extreme bottom (keel) of the clast will an 'anomalous' NW-dipping belt be encountered. In the Eigneag Mhor region, a clast *crest* is inferred at NF 924610, which explains the SE dipping phyllonite belt on its SE side (NF 926610) and the NW-dipping phyllonite on its northern side (NF 924613) (Fig 4.50). The same NW dipping belt forms a high strain wrap to a clast *keel* at (NF 923614). The corresponding SE-dipping belt to this keel occurs c. 300m NW at NF 922615.

The North Uist region of phyllonitic and protophyllonitic deformation may be described as clast-supported, due to the large ratio of protophyllonitic 'clasts' to phyllonitic matrix in the area. The non-anastomosing nature of the phyllonite belts

in South Uist however may be described as matrix supported, as large-scale low strain zones are few (e.g. Rubha Bolum; see section 4.3.8). Furthermore, all strike-slip-related deformation is focussed into one major belt which is thicker than any individual belt making up the braided network further north. This may be due to strain/ fluid localisation along the pre-existing contact between the meta-igneous Corodale Gneiss body and the Western Gneiss derived 'Mashed' Gneiss.

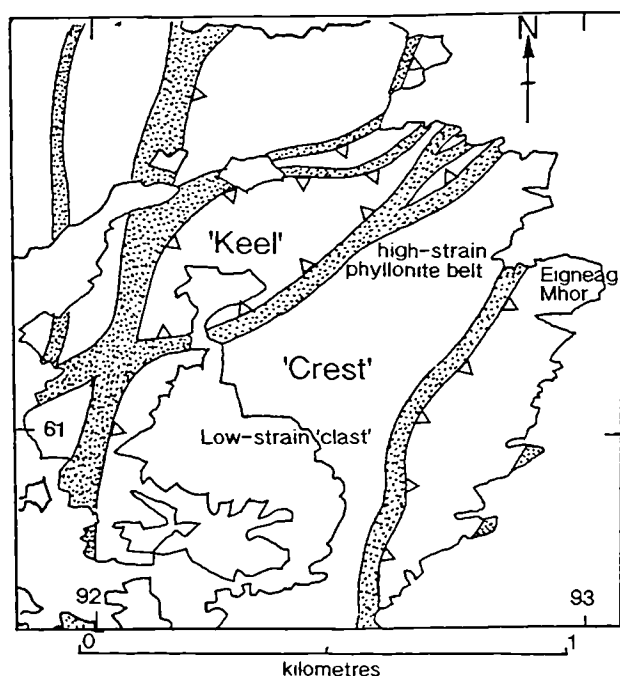


Figure 4.50. Geological map of part of the Burrival Eigneag Bheag region of eastern N.Uist, showing low-strain 'clasts' (protophyllonite) and high strain matrix (phyllonite).

Kinematic regime

Mineral stretching lineations in the phyllonites and protophyllonites of North and South Uist show a variable orientation which bears a relationship to the state of strain and retrogression. The low-strain, protophyllonitic areas show a strike-parallel mineral lineation, which rotates clockwise into a down-dip orientation as the protophyllonite accommodates higher strain and metamorphic retrogression. Thus, in the centre of the phyllonite belts, a down-dip orientation predominates. This association between state of strain, retrogression and mineral stretching lineation orientation is believed to show the effects of focussing subsequent reactivation (see section 4.4), and as such, only the lower strain protophyllonites or the marginal zones of some phyllonites preserve evidence for the kinematic regime operative *during* phyllonite development.

The strike-parallel mineral lineations in the protophyllonites are indicative of regional strike-slip motion on the OHFZ. Kinematic indicators parallel to the

movement vector, including asymmetric shear bands, asymmetric folds and asymmetric porphyroclasts, display a dominantly sinistral sense of shear with the eastern, hangingwall block moving northwards with respect to the western footwall block.

In South Uist, the proportion of high strain phyllonite to low strain protophyllonite is greater than in North Uist, and the deformation related to regional strike-slip motion is therefore often overprinted, especially towards the southern end of the belt. Most mineral lineations plunge shallowly between NE and E, and associated shear sense indicators suggest movements occurred during extension with a component of sinistral strike slip.

Pressure, temperature and fluid conditions during deformation

The phyllonites and protophyllonites of the southern segment of the OHFZ appear to have formed under very different P/ T/ fluid conditions than both the original gneissic protoliths and the thrust-related fault rocks. Metamorphic assemblages are dominated by newly recrystallised chlorite, epidote and sericite, replacing amphiboles, feldspars and, in South Uist, pyroxenes. Deformation is thought to have occurred in conjunction with retrogressive, low-greenschist facies metamorphism. Most of the metamorphic reactions are hydrous reactions, and can not occur without additional water (Beach 1976). Fluid flux into the shear zones facilitates diffusive mass transfer (DMT) dominated deformation mechanisms. Crystal-plastic deformation and intercrystalline slip are probably also increased as a result of the replacement of gneissose assemblages by the weaker retrograde reaction products. The greenschist facies, ductile deformation which overprints and post-dates the brittle thrust -related deformation is therefore probably due to changes in fluid conditions rather than an increase in P/T conditions. Evidence cited in section 4.2.1 and summarised in section 4.2.12, suggests that P/T conditions during brittle thrusting may have even been higher than those prevalent during ductile strike-slip.

Discussion

The kinematic regime of Sibson's "early cataclastic foliation"

Sibson (1977b) termed the pervasive fabric developed extensively within the Crush Melange, the "early cataclastic foliation". He regarded it as having been produced by early *thrust-sense* deformation, but could not readily explain the obvious regional strike swing apparent from the geological map of the area (Sibson pers comm. 1993) (Fig. 4.28). In his description of this fabric, he cites the close proximity of the foliation with large thrusts in the west of the melange as evidence

for the syn-thrust foliation development throughout the melange. The present work has shown that at least two types of foliation exist in different parts of the melange, which were not separately distinguished by Sibson (1977b):

1. A poorly developed fabric of closely spaced, semi-brittle microfaults and brittle comminuted and re-oriented grains developed extremely locally close to brittle thrusts in the western part of the melange, and possessing down-dip plunging mineral lineations, preferentially preserved in the west of the melange. (see section 4.2.1 for a full description).
2. A poorly developed fabric of comminuted and stretched grains developed pervasively throughout the rest of the melange, and possessing strike-parallel mineral lineations (see section 4.3.1 for a full description).

Both these fabrics are similar in appearance in the field, but preserve different kinematic information. The former fabric, which provided Sibson with the information for his interpretation appears to be thrust-generated, and the latter by strike-slip movement.

It is significant to note that no clasts possessing the 'early cataclastic foliation' have been observed in the thrust-related cataclasites of the Crush Melange, as would be expected if the two fault rocks were contemporaneous. Conversely, the foliation is commonly observed to cross-cut the products of early thrusting. The 'early cataclastic foliation' is therefore due to a later phase(s) of deformation which post-dates the cataclasis, microfaulting and pseudotachylite generation associated with the development of the Crush Melange.

The obvious difference in movement direction orientation preserved in the two foliations requires that either both foliations were generated at different times under different kinematic regimes, or both were generated contemporaneously by a transpressional strain which was spatially partitioned. The similarities of these two foliations appear to favour the latter model, but no conclusive evidence has been found to discount either model.

A revised structural correlation of the Eastern Gneisses of South Uist

Previous workers have debated whether the Usinish Phyllonites of South Uist form part of the fault zone or pre-date it. Jehu and Craig (1925) regarded the phyllonites as coeval with the OHFZ-related crush zones, and suggested that differing strain rates were responsible for the markedly different fault rocks. Kursten (1957) regarded the brittle thrust products as later than the Usinish Phyllonites, on

the tentative (and incorrect) correlation of low angle faults in the Usinish Phyllonite with thrust-related pseudotachylite generation elsewhere.

Coward (1969, 1972) regards the Usinish Phyllonite as entirely pre-dating the fault zone, and the result of intense contact strain between the Corodale Gneiss and the Mashed Gneiss, prior to thrust inception.

Sibson (1977b) refutes Coward's interpretation, citing several lines of evidence why the Usinish Phyllonites are part of the OHFZ. Most of these suggestions are supported by the findings of the present study. The evidence against Coward's hypothesis are as follows:

- A marked parallelism occurs between the belt of Usinish Phyllonite and the dip envelope of the OHFZ.
- Petrographically identical phyllonites are very common in the rest of the OHFZ,
- Pseudotachylite generating faults are unlikely to occur in a region where a rheologically weak belt of phyllonite (Usinish Phyllonite) already exists (Sibson 1977b) because sufficient elastic strain energy to cause brittle pseudotachylite failure could not be stored where crystal-plastic deformation mechanisms in the phyllonitic unit would bleed away strain energy (Sibson 1977a, 1977b). This constrains the generation of phyllonitic material to a time which entirely post-dates the syn-pseudotachylite thrusting.
- The correlation between structures in the Grey Gneisses, the Corodale Gneiss and the Usinish Phyllonite are tenuous at best (see Sibson 1977b). The style of deformation associated with foliation development in the Corodale gneiss and the Usinish Phyllonite are very different and unlikely to be of the same age. The Laxfordian age foliation in the Corodale gneiss is produced by high temperature deformation microstructures, including ductile ribboning of feldspars. By contrast, feldspar deformation in the Usinish Phyllonite is by brittle comminution, and unlikely to be Laxfordian.

This information, which negates the idea of a pre-existing (Laxfordian) phyllonite belt prior to thrust deformation on the OHFZ, leaves only two viable alternative interpretations of the Eastern Gneisses. Sibson (1977b) favoured the idea that the phyllonites and brittle thrusts are entirely post Laxfordian (probably Caledonian) but may have developed synchronously at different crustal levels. He did not believe that the phyllonites were later because elsewhere in the OHFZ (e.g.

Seaforth Head, Lewis), mylonites are seen to be penecontemporaneous with pseudotachylite generating faults. This evidence can now be discounted however, because the thrust-related mylonites at Seaforth Head are not the same as the phyllonitic rocks which constitute the Usinish Phyllonite. Mylonites at Seaforth head formed at different times and under different conditions from the Usinish Phyllonites (see section 3.2.2 for a full account). There is, in fact, no evidence for renewed pseudotachylite faulting after the generation of phyllonite, and it seems likely that phyllonites entirely post-date this phase of brittle thrusting. The observed continuity between the Laxfordian S1 foliation in the Corodale gneiss and the foliation of the Usinish Phyllonite noted by Coward (1969, 1972) is apparent. The retrogressive low greenschist facies event responsible for the development of the Usinish Phyllonite also pervaded the Corodale gneiss. Mimetic chlorite/ epidote overgrowths did not destroy the earlier Laxfordian S1 foliation, giving the appearance of a pre-Laxfordian, low-greenschist event. This conclusion is corroborated by Sibson (1977b) who examined Coward's thin sections and found no evidence to discount a late stage, post-Laxfordian retrogression.

4.3.11 Summary

- Ductile deformation overprints and post-dates brittle thrust-related deformation
- In North Uist, ductile deformation is heterogeneous, forming anastomosing shear zone networks of phyllonite, separating lower strain augen of protophyllonite.
- In South Uist, ductile deformation is more homogeneous, forming a single planar belt of phyllonite at the zone of high contact strain between the meta-igneous Corodale Gneiss body, and the brittlely deformed acid 'Mashed Gneiss'.
- The geometry and orientation of the phyllonite belts are chiefly dependant on pre-existing anisotropies, e.g. brittle faults.
- The metamorphic assemblages in the phyllonites suggest fluid-assisted retrogression to low-greenschist facies metamorphism occurred.
- Fluid influx appears to have preferentially localised in pre-existing anisotropies (forming phyllonite belts) where permeability may have been locally enhanced.
- The ductile phyllonites preserve syn-deformational kinematic indicators only in their lower strain portions, and show a consistent sinistral strike-slip sense of motion, with the SE, hanging-wall side giving top-to-the NE sense of shear.
- The higher strain phyllonites are loci for subsequent extensional reactivation, and therefore evidence for sinistral shear is obliterated in most regions.
- Retrogression is regarded as syn-sinistral shear.

- Diffusive mass transfer (DMT), and crystal plastic deformation mechanisms dominated during strike-slip motion.
- A phase of sinistral transpression is thought to separate purely thrust-sense deformation from purely strike-slip deformation, and may have manifested itself in the apparent spatial partitioning of dominantly thrust-sense fabrics in the west and dominantly strike-slip fabrics in the east.

4.4. Extensional movement

A suite of extensional structures overprint and therefore post-date the deformation associated with thrusting and strike-slip movements. Whilst the locations of these extensional structures are not exclusively restricted to the pre-existing phyllonite belts, a very strong spatial coincidence between these two exists. Extensional structures show many similarities to those noted from the northern segment of the OHFZ (see section 3.4), but the intensity and distribution of extension-related deformation is greater in the southern segment

(i). North Uist and adjacent islands

The braided phyllonite networks of eastern north Uist are host to abundant small-scale folds, faults and shear bands associated with regional extension. The extension direction is chiefly controlled by the local orientations of shear zone fabrics, which in this region are variable (see section 4.3 and figs 4.28 and 4.36). The geometry of the majority of late structures suggests that a passive extensional movement occurred, down the dip of the pre-existing foliation. Anomalous 'up-dip' verging folds are apparent in Lochportain and parts of the Burrival/ Eigneag Bheag region, and are discussed in section 4.4.10.

4.4.1. Burrival to Eigneag Bheag

Late folding of the phyllonitic/ protophyllonitic fabrics is chiefly restricted to the phyllonite belts and higher strain areas in the protophyllonites (Fig. 4.28). The best examples of late folds occur at Eigneag Bheag (NF 922600) where chevron folds are developed on different scales (Plate 4.12a). These have been described previously as 'D2 lag folds' by Sibson (1977b). They are typically recumbent or inclined, asymmetric with open, close and occasionally tight inter-limb angles. They usually have angular hinges and straight limbs, but examples with rounded hinges have been observed at other localities in the Burrival/ Eigneag Bheag region. Fold axes are sub-horizontal and are locally markedly curvilinear, their orientations mainly varying between 010° and 060°, and possessing a curvature of up to c. 50°.

Fold wavelengths vary between 1 and 50cm. The fold axes often lie parallel to the pre-existing NE-SW trending mineral lineation, especially in the less phyllonitic areas (Fig 4.51).

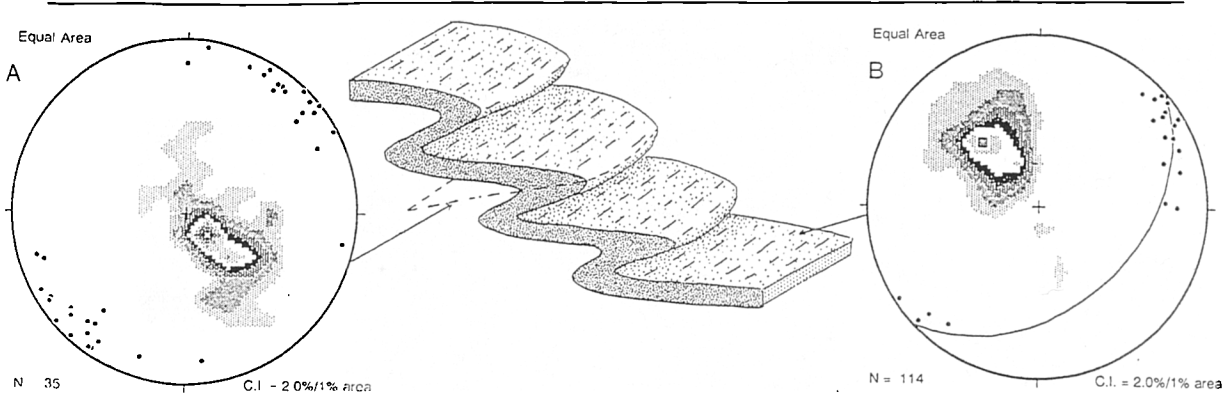


Figure 4.51. Block diagram showing typical fold geometry associated with low angle extension in the less phyllonitic parts of the Eigneag Bheag region. Equal area stereonets of: A) Contoured poles to fold axial planes and fold axes (dots); and B) Contoured poles to protophyllonitic foliation and mineral lineation (dots).

Fold vergence is almost always 'down-dip' and usually varies between E and SE, depending on the local orientation of the phyllonitic foliation. On the SW side of Loch an Tomain (NF 917607), the local phyllonitic foliation dips anomalously NW however (see section 4.3.1), and the fold vergence is also towards the NW. Again, these NW-verging folds are overturning down the dip of the foliation and possess axes parallel to the NE-SW trending strike-slip-related mineral lineation. Some anomalous 'up-dip' fold vergences also occur however:

- At NF 923616 the foliation dips SE but some of the folds verge NW, with an asymmetry suggestive of NW directed *thrusting*.
- At NF 923614 and NF 928615 the foliation dips NW, but some of the folds verge SE, with an asymmetry suggestive of SE-directed *thrusting* (Plate 4.12b).

Both these types of 'up-dip' verging folds are clearly later than the phyllonite generating event and unrelated to the much earlier thrusting. These can be explained as small parasitic 2nd-order 'collapse' folds which have been refolded in the same stress regime by 1st-order collapse folds. The up-dip verging folds now occupy regions on the short limbs of the larger structures (Fig. 4.52).

A swing in the strike of the phyllonite foliation is apparent between the margins and the centres of some of the phyllonite belts (e.g. at NF 920612 and NF 916607). In the belt margins, the foliation strike is parallel to the strike of the belt,

but in the centres, a clockwise swing of up to 40° is often observed (Fig 4.53). Phyllonite belts from the northern segment (e.g. Eishken) also have this geometry, and have been interpreted as the result of top-to-the-south extensional reactivation. The strike-swing in the phyllonites of the southern segment is more difficult to reconcile with this process, since extensional reactivation is not inferred to be southward-directed (see section 4.4). The strike swing may be related to SE-directed extension, however, which alters both the foliation and lineation orientations (see below) in the most retrogressed parts of the belt.

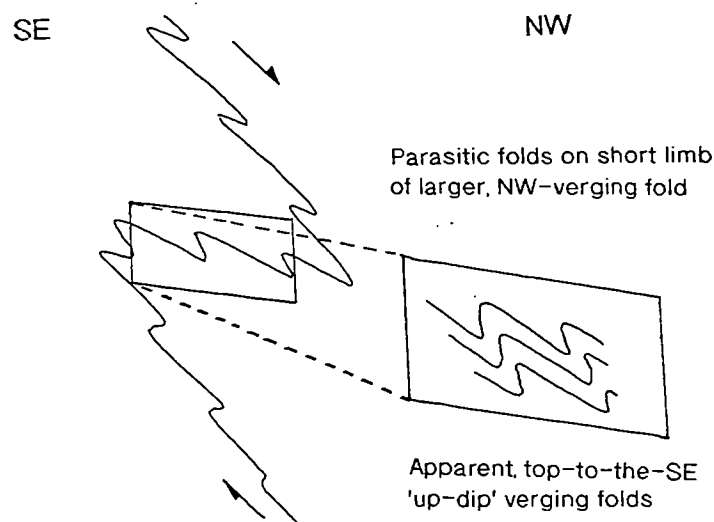


Figure 4.52. Diagram showing the generation of small-scale parasitic folds on larger scale structures with an apparent opposite sense of vergence.

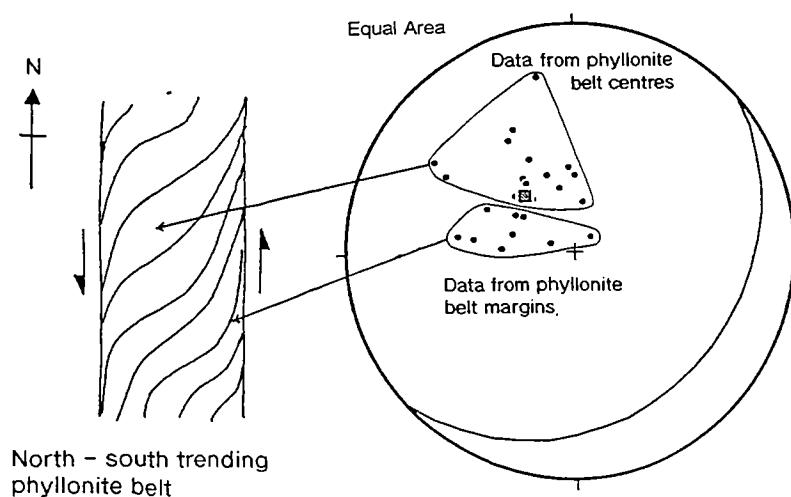


Figure 4.53. Diagram showing the foliation swing encountered in a typical phyllonite from the Burrival - Eigneag Bheag region. Equal area stereonet showing poles to phyllonite foliations and mean great circle.

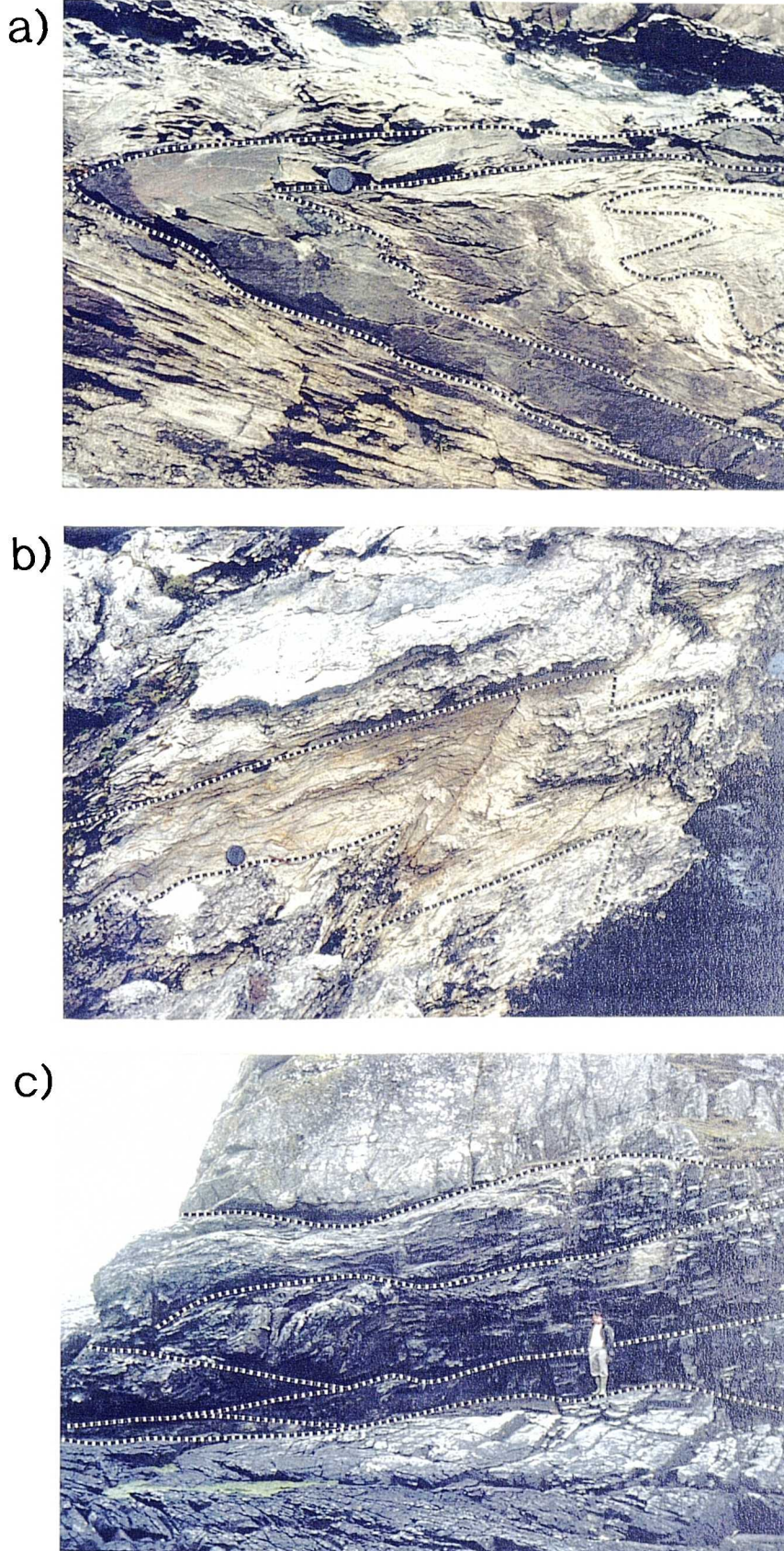


Plate 4.12 low-angle extensional structures from N.Uist

a) Large SE-verging chevron fold from phyllonite at Eigneag Bheag (NF 921596). Vergence is down dip.

b) SE-verging chevron folds from N of Eigneag Mhor (NF 928616). Vergence is up-dip.

c) Fault/fold geometries from Eigneag Bheag (NF 921597). Major faults, separating SE-verging fold packages, are picked out.

A clockwise re-orientation of the mineral lineation of c. 40° occurs during extension and can be observed in the transition from the protophyllonitic areas into the intensely deformed, central parts of many phyllonite belts (Fig. 4.54). In the phyllonite, the reoriented mineral lineation plunges SE or ESE and is defined by elongate feldspar pseudomorph aggregates, quartz rods, and fibrous chlorite. Where D2 'lag' folds are present in the phyllonite, this lineation is folded (Fig 4.55). An axial planar crenulation cleavage is occasionally developed in the most intensely folded areas, and forms an intersection lineation with the folded layers trending NE-SW. The lack of elongate mineral aggregates separates this strike-parallel lineation from the earlier strike-slip-related mineral lineation. The new axial planar foliation may itself carry a new extension-related SE or ESE plunging mineral lineation.

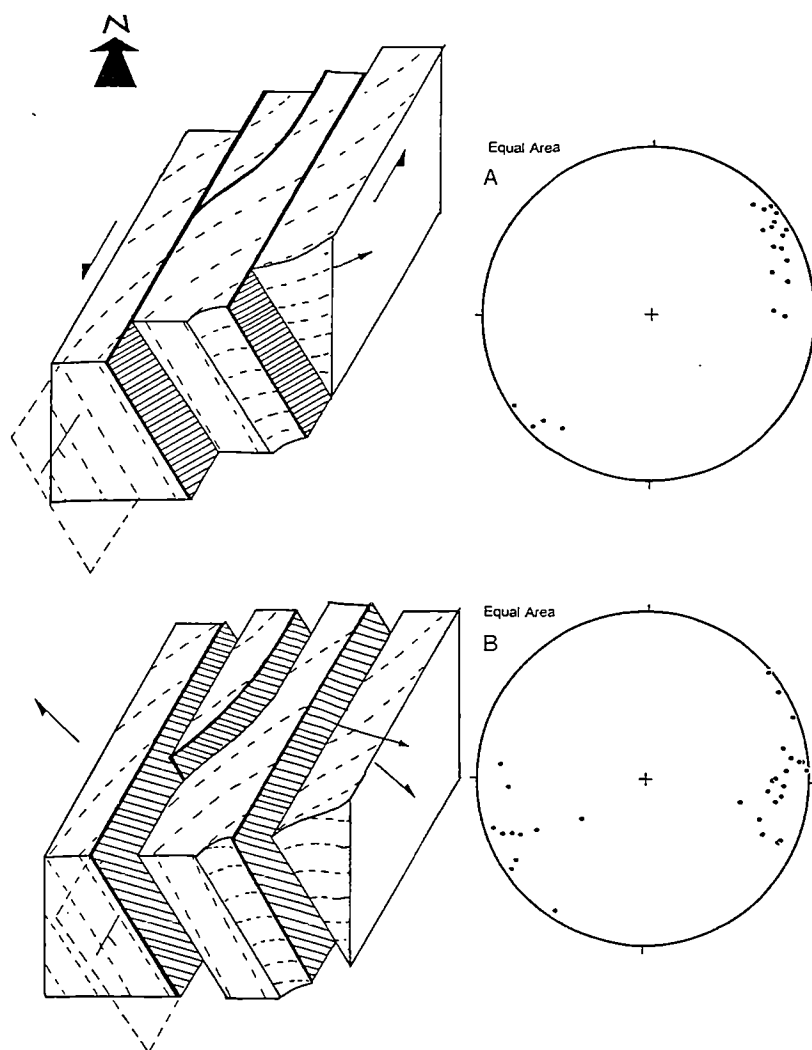


Figure 4.54. Block diagrams showing the reorientation of mineral lineations in phyllonites from Burrival - Eigneag Bheag. Equal area stereonet of: A) Mineral lineations in protophyllonites (relict lineations in their original orientation); and B) Mineral lineations in phyllonites (reoriented lineations).

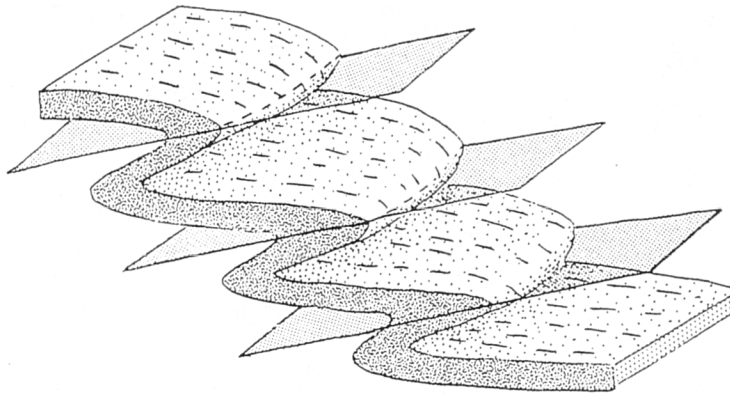


Figure 4.55. Block diagram showing typical fold geometry associated with low angle extension in the high strain phyllonites of the Eigneag Bheag region. The reoriented mineral lineation is folded..

Asymmetric extensional shear bands are developed in many of the phyllonite belts (e.g. south of Eigneag Bheag (NF 921596)) and have characteristically weathered-out 'C'-planes' and positive 'S' planes. Shear bands show a variety of displacement directions, but most strike NNW-SSE, and appear to extend in a direction which is slightly anticlockwise of the dominant fold vergence direction. Shear bands are very rarely folded (although some open warps appear to post-date them), but shear bands may cross-cut folds, suggesting shear band generation may have been slightly later (Fig. 4.56).

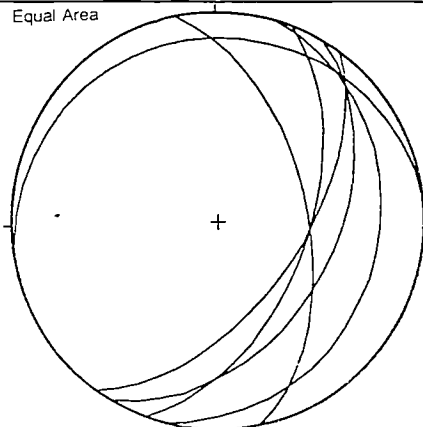


Figure 4.56. Equal area stereonet of asymmetric extensional shear bands (great circles) from Burrival - Eigneag Bheag.

Networks of low-angle detachment faults are abundant in the Burrival/ Eigneag Bheag region, and are usually parallel to the local foliation in either their footwall or hangingwall regions. These faults commonly separate packages of folded phyllonite from non-folded phyllonite, but may also occur *within* fold packages (Plate 4.12c) (Fig. 4.57). They focus into either extremely phyllonitised zones, or Mashed Gneiss/ phyllonite margins. An association exists between the regions of highest strain in the phyllonite and the location of the detachment faults. The faults possess down-dip plunging slickenlines in many examples, and the

geometry of secondary Riedel (R) -shears (e.g. south of Eigneag Bheag at NF919595) suggests normal motion has been accommodated on these structures, usually displacing top-to-the-E or ESE (Fig. 4.57). Minor, subsidiary faults parallel to the larger detachments also displace markers extensionally. In NW-dipping detachment faults, subsidiary R-shears suggests displacement is top-to-the NW. Rarely, the SE-dipping detachment faults cut up-section in P-shear orientations, locally becoming compressional thrusts, displacing top-to-the E (Fig. 4.57). The detachment faults are occasionally folded into very open warps, but no strong folding of these structures has been observed.

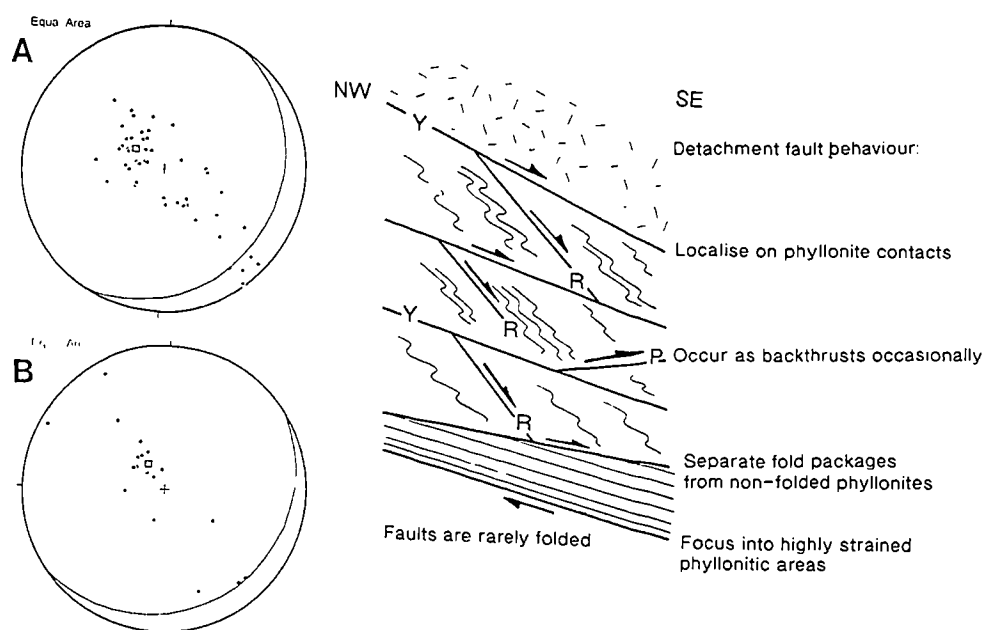


Figure 4.57. Typical behaviour of detachment faults in the Burrival - Eigneag Bheag region. Equal area stereonet of: A) poles to phyllonitic foliation with mean great circle; and B) poles to detachment faults with mean great circle.

The timing of folding and detachment faulting is uncertain but the close spatial association of the two sets of structures, including the effect of fault configuration on the geometry of folds and the cross-cutting nature of faults, suggests that they are coeval, and similar to those described as 'gravitational collapse' features from mainland Scotland by Holdsworth (1989).

Late stage quartz and quartz-chlorite veining is common in the phyllonites and protophyllonites of the Burrival/ Eigneag Bheag region. These are usually 1mm to 1cm thick and extend laterally for several metres in some examples. They are commonly planar or (rarely) sigmoidal and occasionally fibrous, with quartz fibres growing at a high angle to the vein walls. The veins occur preferentially in the less

phyllonitic material, and may be isolated or occur as en-echelon tension gashes. A N-S-striking and subvertical orientation is predominant in individual veins, but the veins within the arrays are usually subvertical and oriented NNW-SSE (Fig. 4.58).

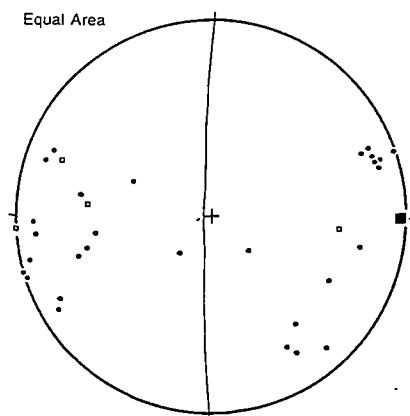


Figure 4.58. Equal area stereonet of poles to extension-related quartz veins (dots) with mean great circle and vein fibres (boxes), from Burrival - Eigneag Bheag.

At least two generations of quartz and quartz-chlorite veining have occurred, and several extension increments are probable. Most quartz veins (which include a dominant N-S-trending set and an earlier, more variably oriented set) cross-cut the phyllonitic foliation, but a few veins are reworked by extension-related 'lag' folds, (e.g. at NF 921619). The reworked veins are blackened by cold-working (dislocation creep) and are dominantly NW-SE-trending. This relationship requires an overlap in timing between extensional movements and veining (see discussion in section 4.4.10).

Very late, subvertical faults which are traceable for 10's of metres, are also apparent in the Burrival/ Eigneag Bheag region. These are oriented NE-SW or NW-SE, cross-cutting all previous structures, and have zones of up to 20 cm of incohesive breccia, which is often mineralised with vuggy calcite and/or haematite. Dilational jogs suggesting sinistral displacements are apparent on both trends, but movement direction indicators have not been found. The displacements associated with these late faults are in the order of a few metres (Sibson 1977b). Their origin is uncertain.

4.4.2. Ronay

Unlike those at Eigneag Bheag, the Ronay phyllonites (Fig 4.34), which are not as highly strained, do not show significant re-orientation of the NE-SW trending mineral lineation, and little evidence of extension-related folding is present. Shear

bands which cross-cut and displace the foliation within the phyllonites, however, displace top-to-the-east, suggestive of later E-W extension (Fig. 4.59a)

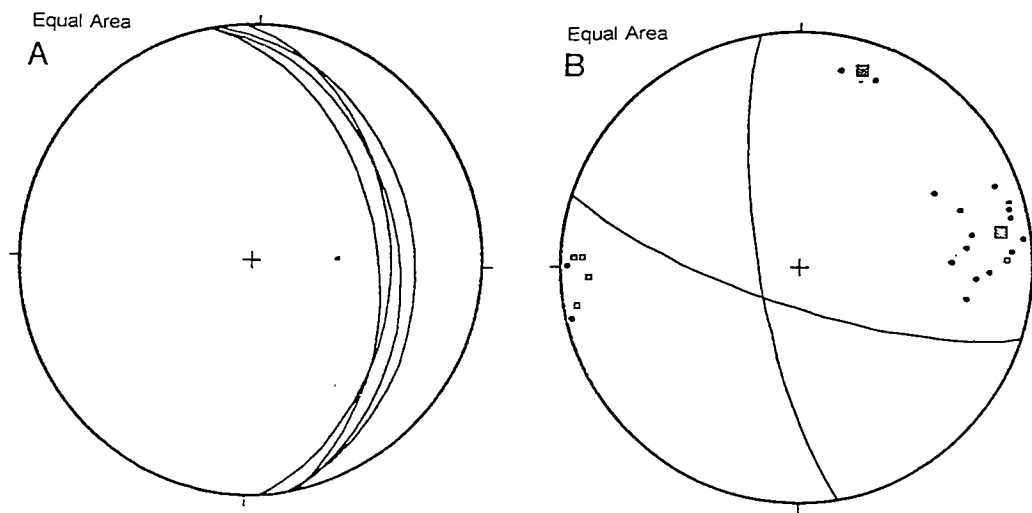


Figure 4.59. Equal area stereonets from Ronay of: A) Asymmetric extensional shear bands (great circles); and B) poles to two populations of quartz veins (dots) with mean great circles and slickenfibres (boxes),.

At (NF 904565), a phyllonite lies directly below an earlier pseudotachylite-ultracataclasite crush zone. These two units have been juxtaposed by a large (m-scale) N-S striking detachment fault, with down-dip, E-plunging fault grooves and subsidiary Riedel (R) shears indicative of normal motion. Other detachment faults also show evidence of late extension. North of Bagh na Caiplich (NF 904562), the N-S striking fault, bounding the top surface of a phyllonite belt, truncates the phyllonitic fabric and possesses ridge and groove structures indicative of top-to-the-ENE extension. The foliation in the hangingwall is markedly misoriented with respect to the footwall at this locality and may have been caused by rotation during extension.

Late quartz veining within the phyllonites and protophyllonites on Ronay is common. A dominant subvertical, N-S trending set often possesses quartz fibres indicative of opening orthogonal to the vein walls, in an E-W orientation (Fig. 4.59b). Occasionally, veins within this N-S trending set possess asymmetric curved quartz fibres whose geometry records a history of initially NW-SE oblique extension, followed by orthogonal E-W opening. In rare instances, quartz fibres within the cross-cutting veins have grown syntaxially upon existing elongate quartz grains in the protophyllonitic foliation, so that the foliation appears to be continuous through the vein, despite its earlier development.

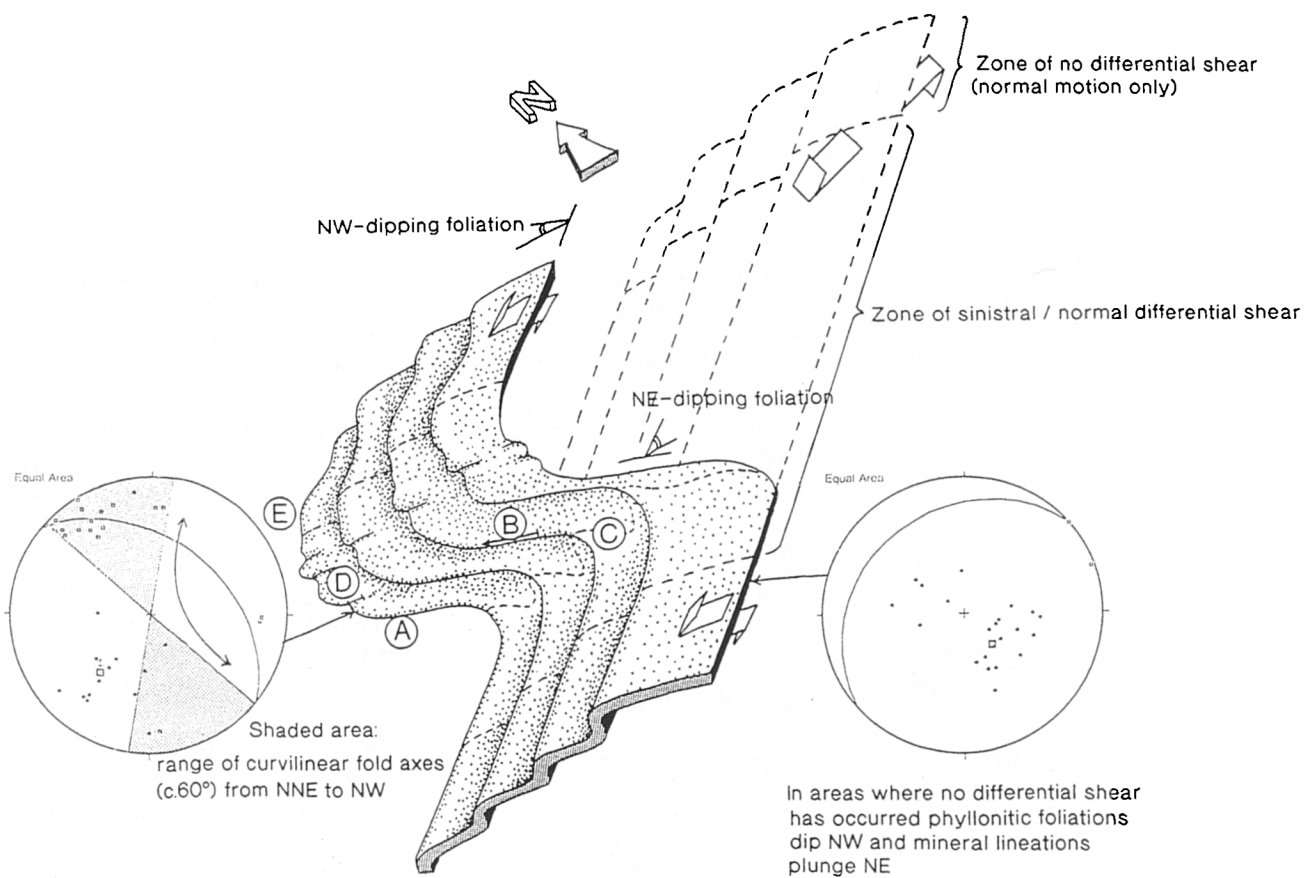
4.4.3. Lochportain

Late folding of the phyllonites and protophyllonites is extremely complex in the Lochportain region (Fig. 4.36). In most cases where folding is apparent, mm-cm scale asymmetric folds have developed which are open to close with rounded hinges. Their axes are subhorizontal and oriented NE-SW, subparallel to the pre-existing strike-slip related mineral lineation. Fold vergence is usually down the dip of the foliation (e.g. at NF 975382), which dips NW in this region. This sense of vergence is opposite to that observed in most, but not all parts of N.Uist (see section 4.4.1), and suggests that extension was passive, and collapsed towards the NW.

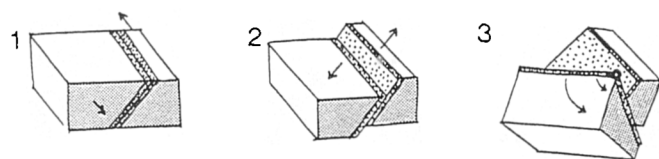
Several deviations in both the local foliation orientation and the local fold vergence directions are apparent at NF 978388. These are numbered below and summarised in Fig. 4.60:

1. The phyllonitic foliation strikes NW-SE and dips NE, having undergone a strike-swing of c. 90° (marked A on Fig. 4.60).
2. Folds axial planes strike NW-SE, having undergone the same strike swing, but axes are no longer subhorizontal. Here, fold axes have a shallow plunge towards NW (marked B on Fig. 4.60)..
3. Folds verge locally 'up-dip', showing apparent thrust-sense geometries. The vergence direction, having undergone the same 90° strike swing is no longer 'down' to the NW but is 'up' to the SW (marked C on Fig. 4.60)..
4. Minor, disharmonic, symmetric and upright shallow E-plunging folds are parasitically developed on the larger structures (marked D on Fig. 4.60).
5. NW-plunging folds are extremely curvilinear through c. 60° in less than 50cm and may plunge NNE (marked E on Fig. 4.60).

These anomalous fold relationships can be explained by the effects of differential shear and rotation during extension (Fig. 4.60). Specifically, an anticlockwise strike-swing and back-rotation of a NW-verging fold package has occurred. This strike-swing may have been induced by relative block rotations between the two large low-strain protophyllonitic 'clasts' which form the upper and lower boundaries to this phyllonite belt.



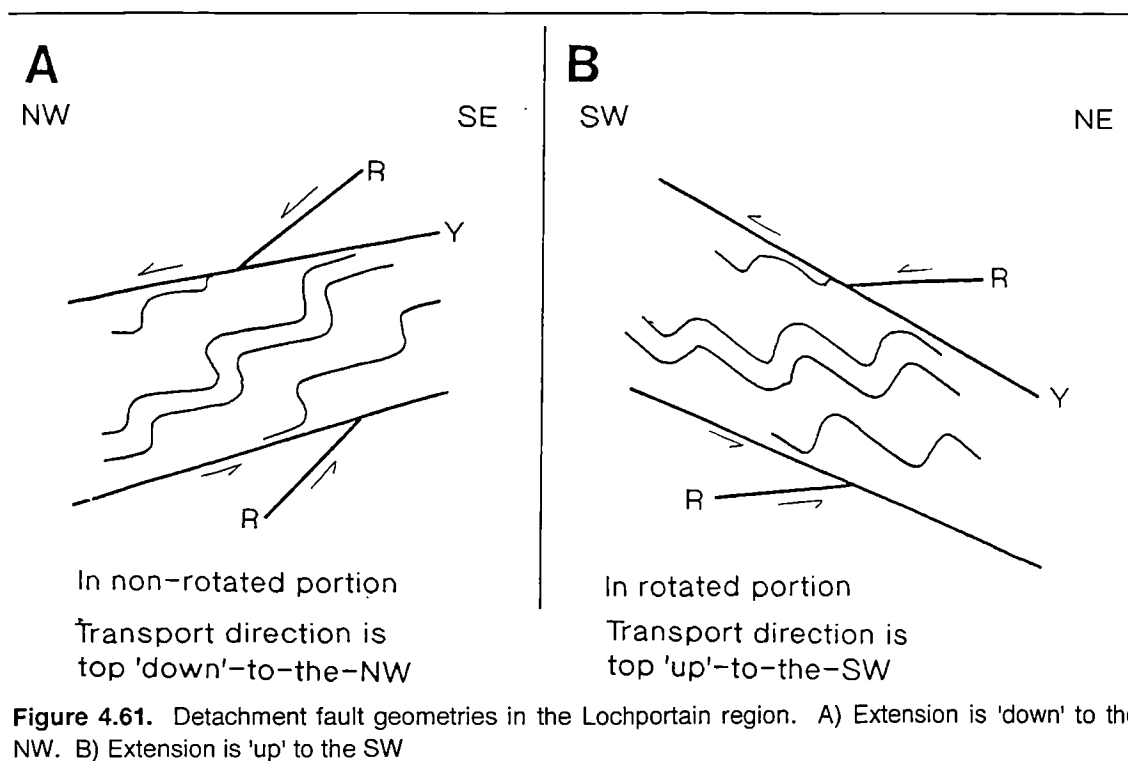
Sequence of events :



- 1) Sinistral strike-slip
 - 2) Extension, causing NW-verging 'collapse' folds
 - 3) Scissor faulting between clasts
- N end extends faster than S end
Normal / sinistral differential shear causes back-rotation of the central part of the fold package.
Folds in the central part therefore verge 'up-dip' to the SW

Figure 4.60. Summary block diagram of complex folding in the Lochportain region. Equal area stereonet of : A) poles to fold axial planes (dots) with mean great circle, and fold axes (boxes). The shaded area denotes the range of curvilinearity of fold axes; and B) poles to phyllonitic foliation (dots) and mean great circle.

Extensional detachment faulting is also common in the Lochportain region. The map-scale geometry of phyllonites and topographic faults clearly shows the later cross-cutting behaviour of the latter (Fig. 4.36), a field relationship at odds with Sibson's (1977b) interpretation of these faults as earlier thrusts. Detachment faults lie sub-parallel to the protophyllonitic foliation, despite local deviations in foliation orientation. They often localise along lithological contacts, including at NF 978388, the contact between poorly phyllonitised 'mashed' gneiss and more strongly phyllonitised material. They separate packages of extension related folds, often with the effect of significantly misorientating one set of folds relative to the other (up to 80°), and rotation on such faults, about an axis at 90° to the fault surface, is likely. Detachment faults are often curvilinear, and possess subsidiary faults indicative of extensional top-to-the-NW movement (Fig. 4.61 a).



More complex detachment fault orientations are present in the region thought to have been affected by relative 'clast' rotations. Where the foliation strike has swung through 90° to trend NW-SE and the foliation dip direction has been reversed so that it dips NE (e.g. at NF 978388), the detachment faults possess Riedel (R)-shears which display apparent 'up-dip' thrust sense motion to the SW, consistent with the up-dip SW verging folds of the region (Fig. 4.61b) (Plate 4.13a). On restoring the effects of strike-swing and back rotation, the detachments displace extensionally 'down' to the NW, consistent with passive extensional

collapse. Rare examples of asymmetric extensional shear bands elsewhere in the phyllonite also suggest extensional top-to-the-NW displacements.

Quartz veining, with average individual veins c. 1mm -1cm thick, is common in the phyllonites and protophyllonites of Lochportain. All veining appears to post-date folding as no reworked veins have been observed. A dominant subvertical, N-S orientation exists, indicative of E-W extension.

4.4.4. South Eaval

As already noted (section 4.3.4), the phyllonites in the Bagh Moraig region (NF 915585) (Fig. 4.39), show significant reorientation of the NE-SW trending mineral stretching lineation, to adopt an E-W or NW-SE trend in the more phyllonitic areas. This reorientated lineation is folded by down-dip, SE-verging collapse folds of the type seen at Eigneag Bheag (NF 922600), which are sporadically developed in parts of the phyllonite (Fig. 4.62a). No anomalous 'up-dip' vergence directions are present, and thus, a top-to-the-SE extension direction is implied.

In rare examples of marginal 'curve-in' between protophyllonite and phyllonite where the arc of curvature is at 90° to the mineral lineation, the foliation swing displays a geometry consistent with extension, and probably results from the effects of normal-sense reactivation. Detachment faults are not as frequently developed in the south Eaval area as elsewhere within the melange, and only become common towards the east coast. Detachment faults usually dip E or SE (Fig. 4.62b), and subsidiary R-shears suggest fault movement was normal and top-to-the-east.

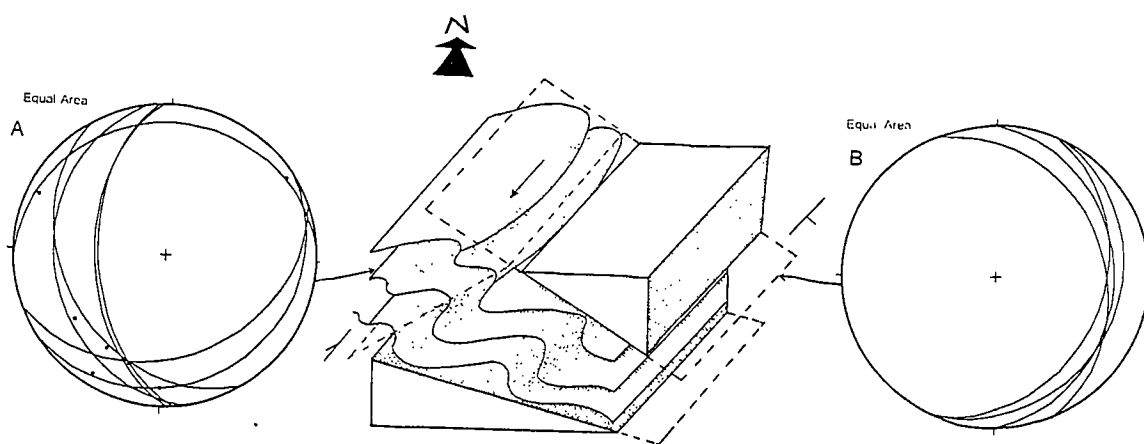


Figure 4.62. Block diagram of fold and detachment fault relationships in the south Eaval region. Equal area stereonets of: A) Extension-related fold axial planes (great circles) and fold axes (dots); and B) Detachment faults (great circles).

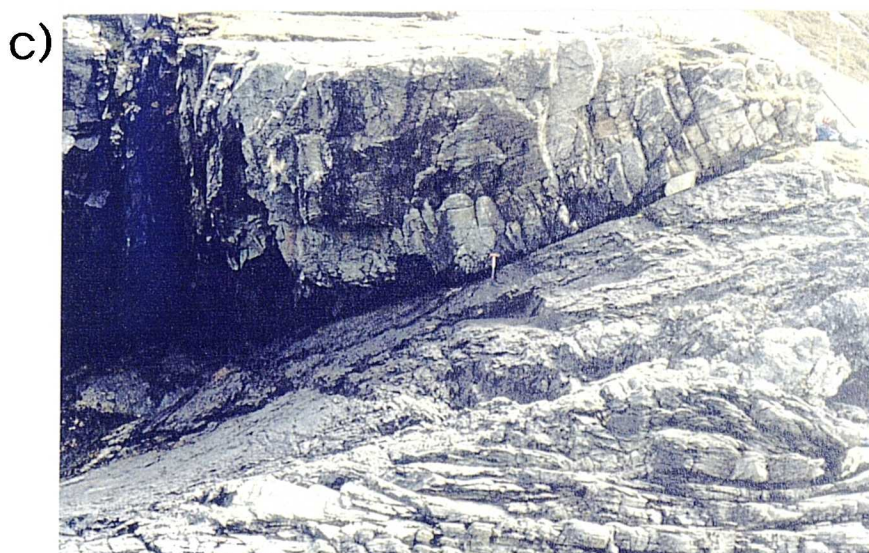
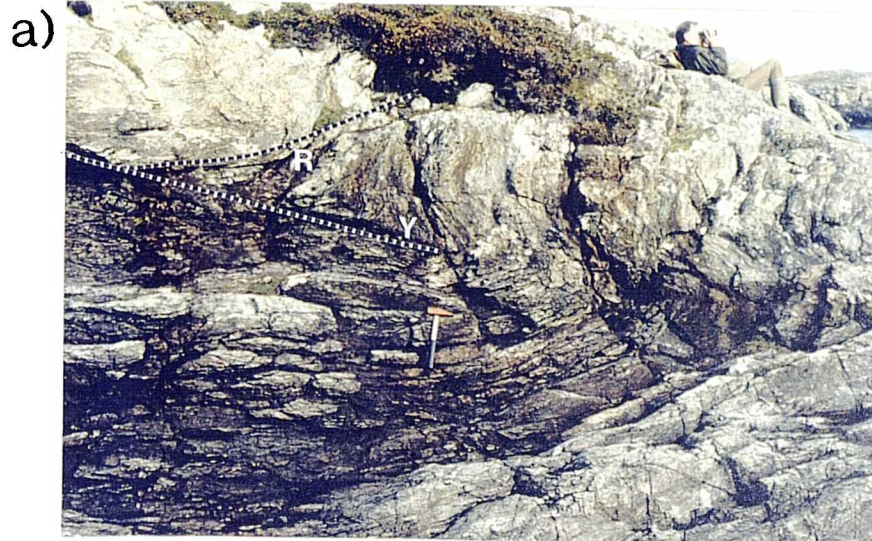


Plate 4.13 Low angle extensional structures from N. and S. Uist

a) Complex fold/ fault geometry from Lochportain, N.Uist (NF 978388). Fold vergence is 'up-dip' towards the SW and R-Shears suggest thrusting towards the SW.

b) N-S trending quartz vein array in footwall of large detachment fault from Eaval, N.Uist (NF 918583).

c) Large detachment fault separating 'Mashed Gneiss' above from Usinish Phyllonite below (from Rubha Rossel, S.Uist) (NF 858366).

Several sets of quartz and quartz-epidote veins are developed in, and around the phyllonites. A dominant, subvertical N-S set with E-W oriented quartz fibres, is again apparent, but other sets, which are cross-cut by, and therefore pre-date this, include both NW-SE and NE-SW sets (Fig. 4.63). These earlier sets are usually moderately east-dipping and sometimes concordant with the foliation. Vein arrays are frequently associated with detachment faults, but are observed to be truncated by such features (e.g. at NF 918583). Quartz vein arrays do not usually inject the hangingwall and the footwall at the same location (Plate 4.13b), and some extensional fault movement probably post dates extension-related veining in this area.

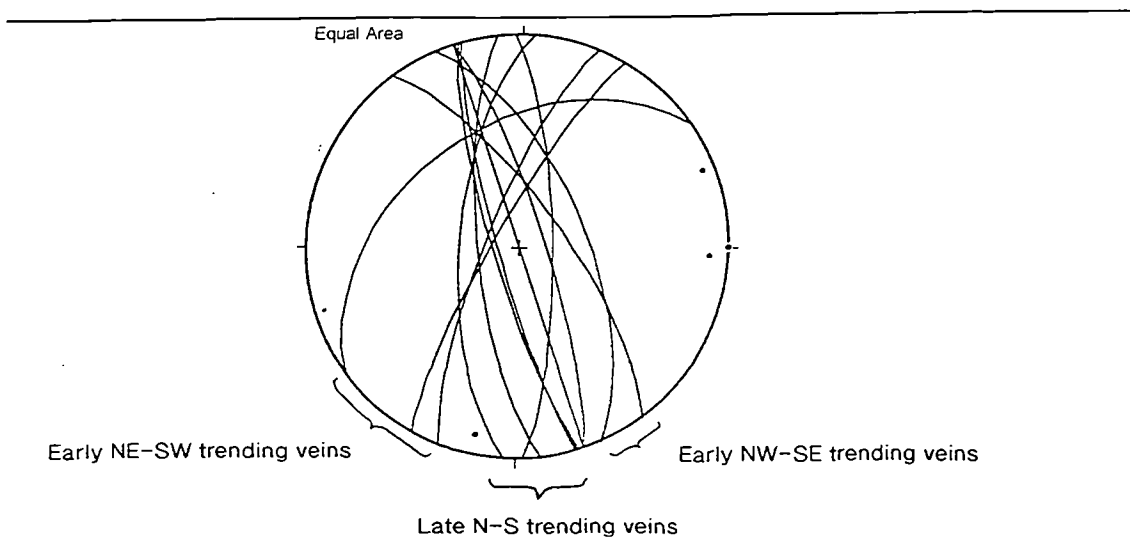


Figure 4.63. Equal area stereonet of quartz veins (great circles) and fibres (dots) from the south Eaval region.

(ii). South Uist and adjacent islands

Extensional reactivation of the OHFZ in South Uist, is mainly confined to the N-S trending Usinish Phyllonite belt. Large-scale extensional detachment faults are common, both at the contacts of the phyllonite, and within the phyllonite belt itself, showing a preference to locate either at zones of pre-existing high strain or at strain gradient boundaries. Folds of the phyllonitic fabric (the 'D2' lag folds of Sibson, 1977b) are common and a second phyllonitic fabric (S2), lies axial planar to the folds.

4.4.5. Rubha Rossel

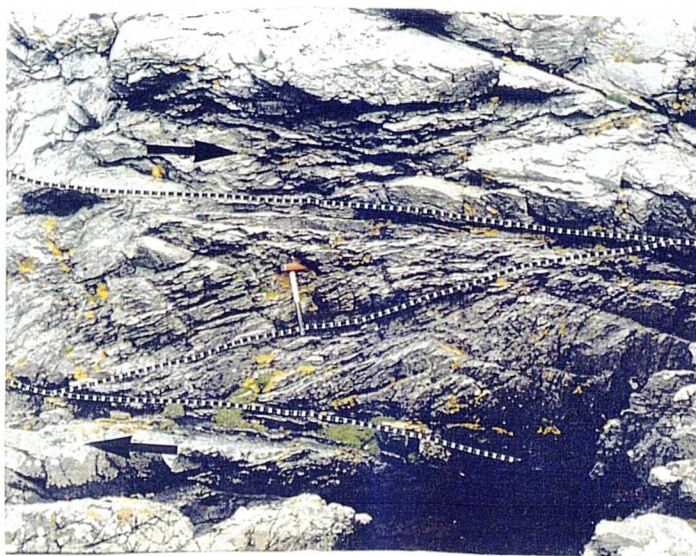
The small sliver of phyllonite at Rubha Rossel (NF 858365) is host to several large-scale detachment faults (Fig. 4.43a). The Mashed Gneiss, which lies to the east of the phyllonite is juxtaposed above it by a moderately ENE-dipping normal fault (Plate 4.13c) which is laterally extensive for c. 100m. Linear movement

direction indicators are absent along this fault, but a cm-scale foliation swing in the immediate footwall phyllonites, into a 2-3 cm thick brecciated zone, gives an apparent normal displacement to the E or NE. A similarly oriented fault bounds the lower phyllonite contact, but the movement sense on this structure is not known. Within the phyllonite body, several more anastomosing detachment faults occur, separating rock packages of differing strain intensities (Fig. 4.64a). Near the base of the phyllonite belt, where the strain, and intensity of foliation development is high, a fault bounded package c. 50 cm thick, shows a structural geometry which is different from that of the rest of the unit (Fig. 4.64). The foliation trace in the phyllonite package strikes ENE-WSW, with a gentle SSE dip, and the mineral lineation plunges dominantly to the ENE or E (Fig. 4.64b). Both of these fabric elements are significantly clockwise of their counterparts in the less foliated regions (see section 4.3.5). Moreover, when viewed normal to regional strike, the foliation swing has the opposite sense of apparent asymmetry (Plate 4.14a). A top-to-the SE sense-of shear is demonstrated in this package.

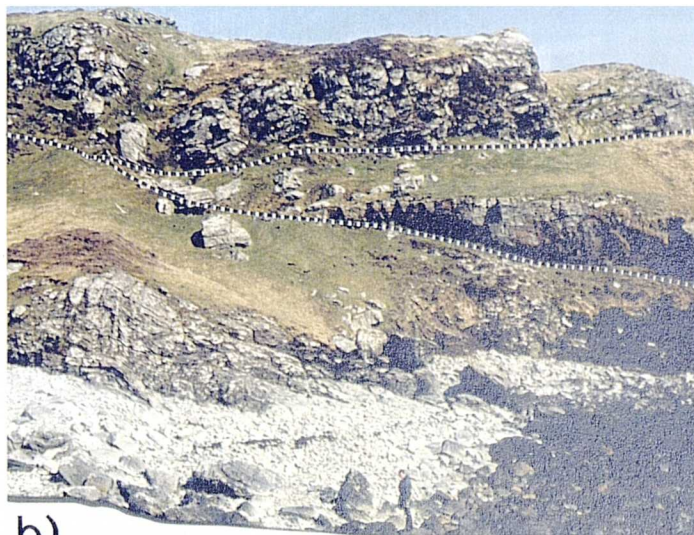
Folding of the phyllonitic foliation at Rubha Rossel is not intense, and no *examples* of the tight E-W trending folds described at this locality by Coward (1972) have been found. A large scale fold, which serves to buckle the foliation is present however (Fig. 4.64). This very open upright structure trends roughly N-S and is markedly non-cylindrical. Smaller, possibly parasitic, cm-scale N-S trending warps are also present, and may represent incipient extensional folds (Sibson's (1977b) 'D2' lag folds). The origin of both the large-scale and small-scale open folds is enigmatic, and two possible explanations exist:

- The 'warping' entirely post-dates the phyllonite formation. This requires a later deformation event, and either relates to extensional reactivation (forming fold geometries unique to this locality) or a different deformational event not observed elsewhere.
- The structure pre-dates the phyllonite formation, and controls the present phyllonite geometry. A large low-strain 'clast' may exist at depth, around which the foliation wraps. Similar small-scale low-strain pods may account for smaller-scale warps (e.g at NF 8575 3663).

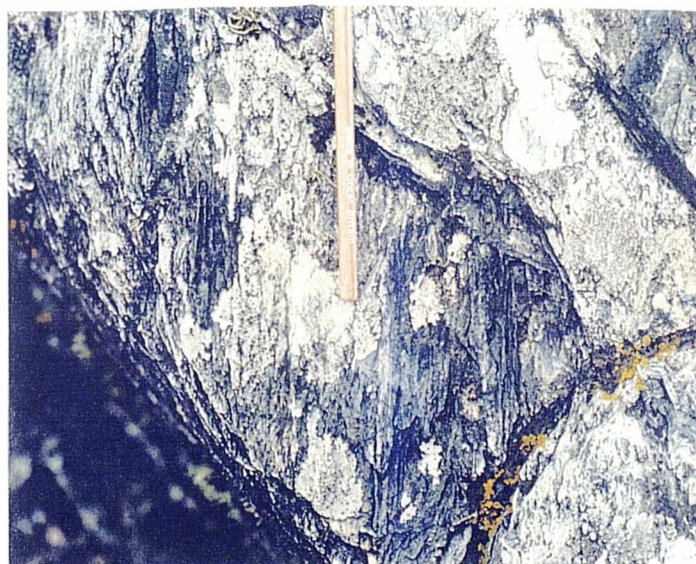
The process of low-strain zone wrapping has been observed on a large-scale elsewhere along the OHFZ, and throughout the OHFZ on a small-scale. Late generation open warping of the phyllonite however has not been observed elsewhere along the OHFZ. For these reasons, the latter explanation is preferred.



a)



b)



c)



d)

Plate 4.14 Low-angle extensional structures from S. Ulst.

a) High strain package of phyllonite bound by detachment faults at Rubha Rossel (NF858366). Asymmetric shear foliation suggests top-to-the-SE motion.

b) Converging detachment faults at Rubha Bolum (NF 829284). Phyllonite foliation below the detachments (in the foreground) has a different orientation to phyllonite foliation above the detachments.

c) Extremely well developed, E-W trending mineral stretching lineation, defined by rodded quartz from stüley (NF 832231).

d) Quartz veins parallel to S1, folded during regional extension (D2), from Stüley (NF832231).

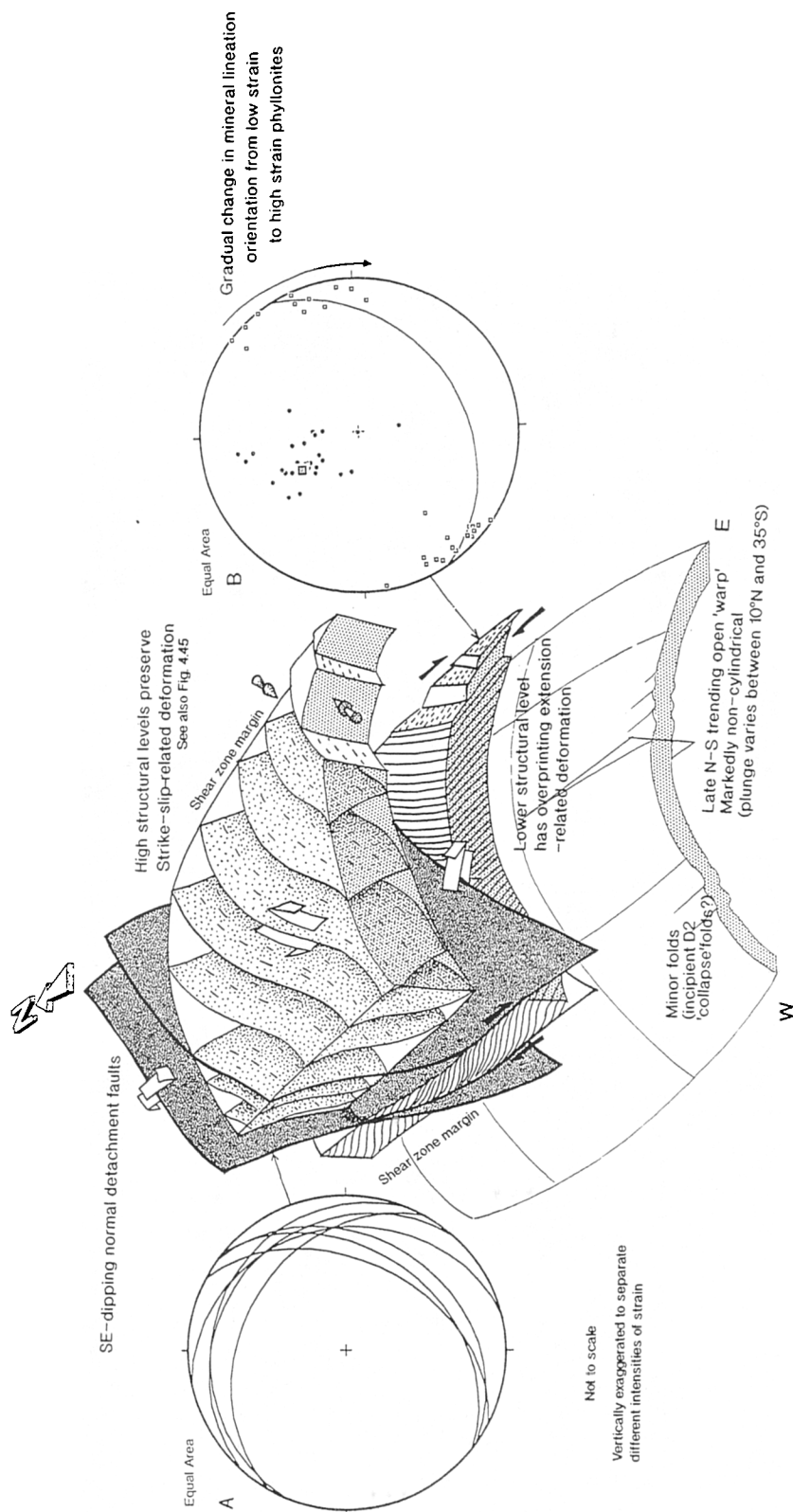


Figure 4.64. Summary block diagram of foliation/lineation and detachment fault relationships at Rubha Rossel, S.Uist. Equal area stereonets of: A) Detachment faults (great circles); and B) poles to phyllonitic foliation (dots) with mean great circle and mineral lineations (boxes).

4.4.6. Ornish

The thin phyllonite belt at Ornish (NF 858376) (Fig. 4.43b) has focused several m-scale E- or SE-dipping detachment faults which are concordant to the phyllonitic foliation. The most prominent fault effectively separates the small island of Eilen Cireach, composed of Mashed Gneiss, from mainland South Uist, and forms the upper contact to the Usinish Phyllonite at this locality. Slickensides are present on the underside of this fault and plunge southeastwards. Subvertical ENE-WSW quartz tension gashes are present in the immediate fault footwall, and have opened NNW-SSE, subparallel to the fault slickensides. It is thought that top-to-the SE or SSE extension occurred on these detachment faults. The mineral stretching lineation, as already noted in section 4.3.6, has been rotated clockwise in the centre of the phyllonite belt. This is also believed to result from late extension. There are no extension-related folds at this locality.

4.4.7. Usinish Bay

Similar extension-related structures are observed in the phyllonite at Usinish Bay (NF 854332) (Fig. 4.43c). In contrast to Ornish, however, isolated examples of cm-scale open to close, SE-verging folds similar to the D2 'lag' folds of Sibson (1977b) are present.

Very few obvious detachments are present in the Usinish Bay phyllonites, but this may be due to the concordant nature of the faults. In the overlying Mashed Gneiss, however, a complex low-angle faulted contact with the phyllonite occurs. These structures strike N-S with a shallow or moderate east dip. Displacement of marker bands suggests *apparent* extension (top-to-the-east), but no linear movement direction indicators are preserved.

4.4.8. Rubha Bolum

Evidence of folding during regional extension is rare at Rubha Bolum (NF 828284) (Fig. 4.43d). Detachment faults are well developed, however, and are usually concordant to the phyllonitic foliation and occasionally converge (Plate 4.14b). The main NNW-SSE trending detachment splits the peninsula into two structural domains (already discussed in section 4.3.8) (Fig. 4.65a). This fault dips shallowly SE and has poorly developed east-plunging slickensides and a zone of friable fault gouge, c.20cm thick. Kursten (1957) regarded this fault as a thrust, but subsidiary hangingwall, SE-dipping R-shears suggest top-to-the-E, normal motion has occurred. Ridge and groove structures are present on the undersides of other

low-angle E-dipping detachments and also suggest top-to-the east (normal) senses of displacement.

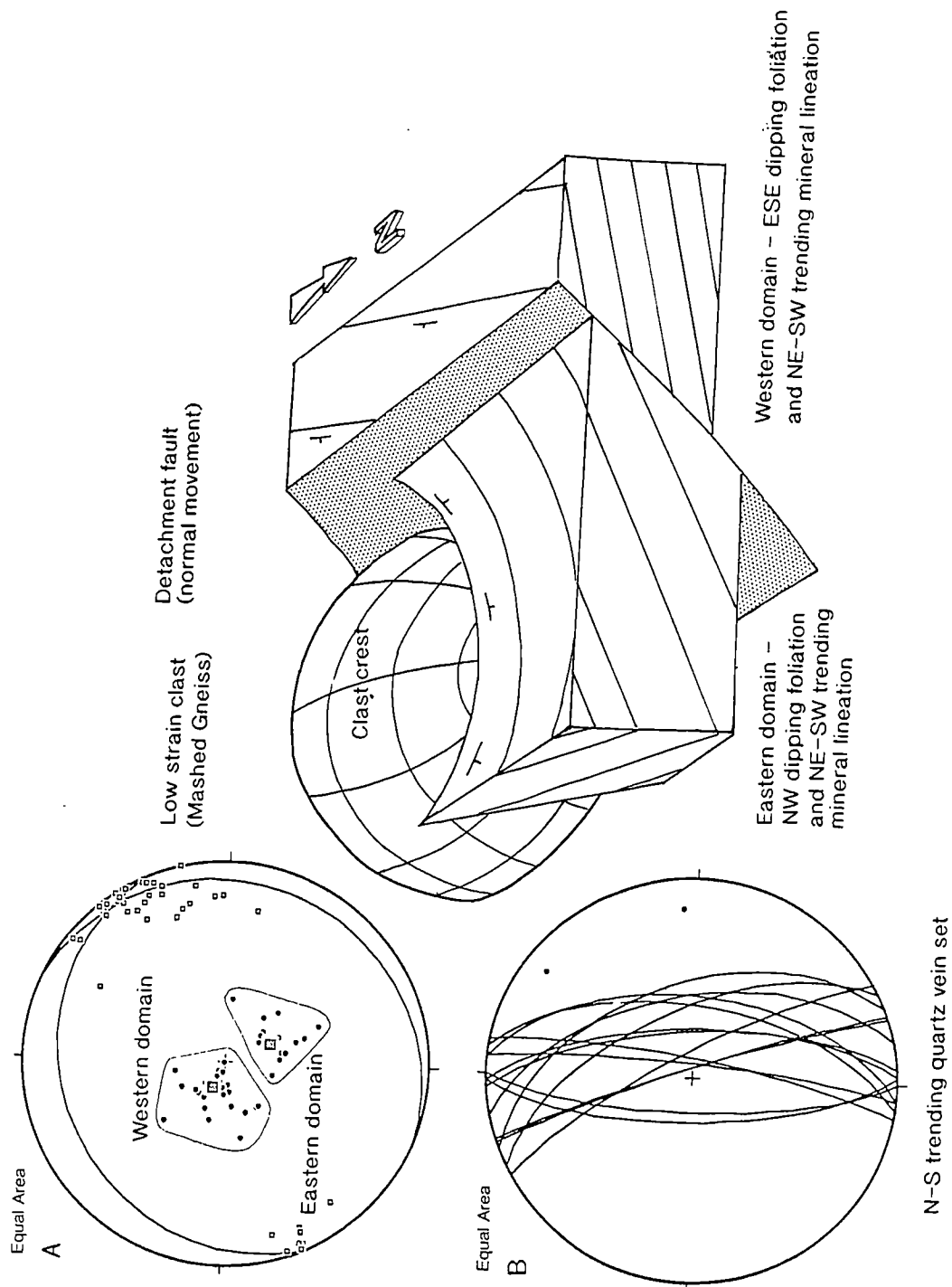


Figure 4.65. Summary block diagram of structural relationships at Rubha Bolum, S.Uist. Equal area stereonets of: A) Poles to two populations of phyllonitic foliation (dots) with mean great circles and mineral lineations (boxes); and B) extension-related quartz veins (great circles) and vein fibres (dots).

A set of discontinuous 1-2mm thick quartz veins are present in the phyllonite, cross-cutting the phyllonitic foliation (Fig. 4.65b). They trend roughly N-S and dip moderately or steeply east. Fibrous quartz within the veins suggests vein opening was dominantly ENE-WSW. The relative timing of faulting and vein opening is not known, but may be penecontemporaneous; the vein opening direction is broadly consistent with the overall extension direction inferred from detachment faulting.

4.4.9. Stuley

The island of Stuley (NF 830235) (Fig. 4.66) is unique in the southern segment because it displays an extremely well developed second foliation related to regional extension. The foliation previously described from all other southern segment localities (and hereafter referred to as 'S1') is only discernible on Stuley where it has been folded by 'D2 lag' folds (using the terminology of Sibson (1977b).

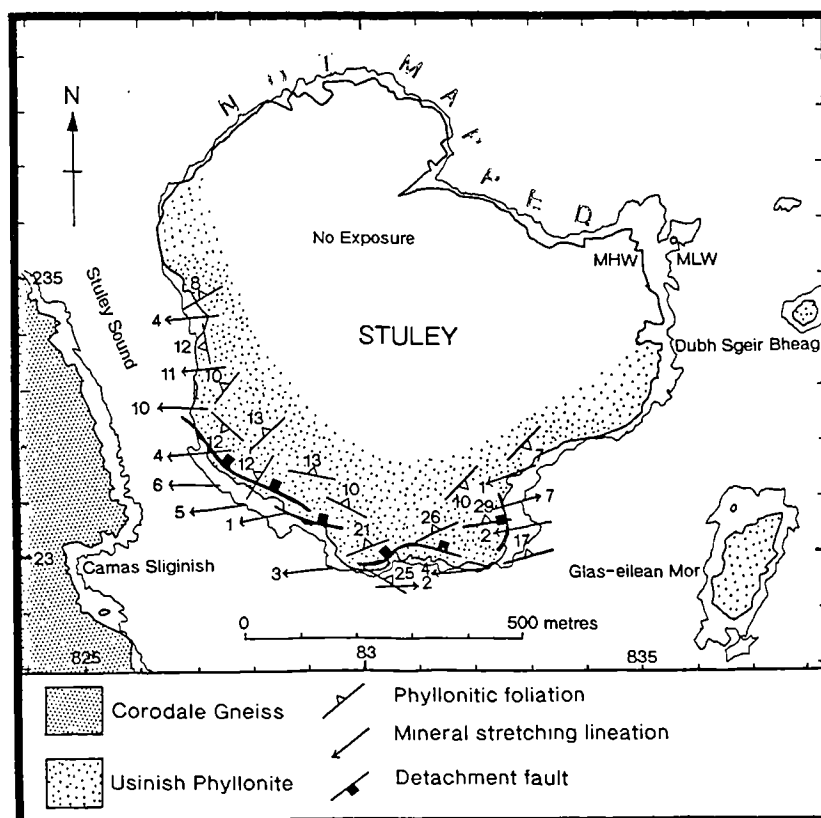


Figure 4.66. Geological map of the island of Stuley.

The S2 foliation is defined by ribboned quartz and phyllosilicate alignments, and is subhorizontal or dips N or NW at very low angles (Fig. 4.67). A very well developed mineral elongation lineation, defined by quartz rods, is present on many S2 surfaces, and trends between E-W and ENE-WSW (Plate 4.14c). Kinematic

indicators parallel to this lineation include cm-scale asymmetric extensional shear bands, displacing top-to-the-E or ENE. The fissile S2 surfaces tend to form present-day outcrop topography, making the characteristics of the sub-parallel earlier S1 foliation difficult to determine. A strong E-W-trending intersection lineation results from the intersection of S1 and S2.

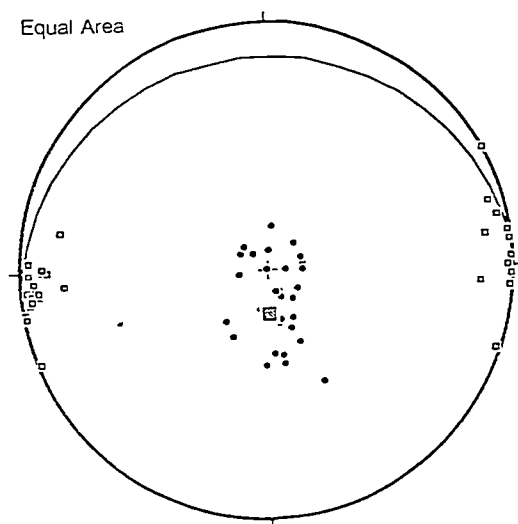


Figure 4.67. Equal area stereonet of poles to phyllonitic foliation (dots) with mean great circle, and mineral lineations (boxes) from Stuley.

The nature of the earlier S1 foliation can only usually be discerned in the hinge regions of tight or isoclinal minor D2 folds, to which S2 is axial planar. It is defined by elongate quartz/ feldspar aggregates and phyllosilicate alignments. Very occasionally, concordant veins of quartz pick out the S1 foliation and are folded by cm -scale D2 folds (Plate 4.14d). The folds, which strongly resemble the extension-related chevron folds described from Eigneag Bheag (NF 922600), are found disparately along the southern coast of Stuley. They usually have straight limbs and angular (occasionally rounded) hinges and are recumbent or gently inclined. Their axial planes dip to the N or NW, and their axes trend between NE-SW and E-W (Fig. 4.68a). Fold vergence is variable between S and SE, although some NW vergences also occur. This latter trend is probably due to minor folding on the short limb of a larger SE-verging fold, where the vergence direction is reversed (see Fig. 4.52). Rarely, the surfaces of folded S1 planes are present (e.g. folded quartz vein hinges), and a poorly preserved mineral lineation is present, defined by elongate quartz rods. This early lineation is always parallel to the D2 fold axes, and varies between NE-SW and E-W. The west side of Stuley shows a tendency to preserve E-W trending linear structures (D2 fold hinges and L1 mineral lineations) whilst the east side of the island preserves more evidence for NE-SW trending linear

structures. The relationship between the S2 foliation/ L2 mineral lineation and the folded S1 foliation/ L2 mineral lineation are summarised in in Fig. 4.68.

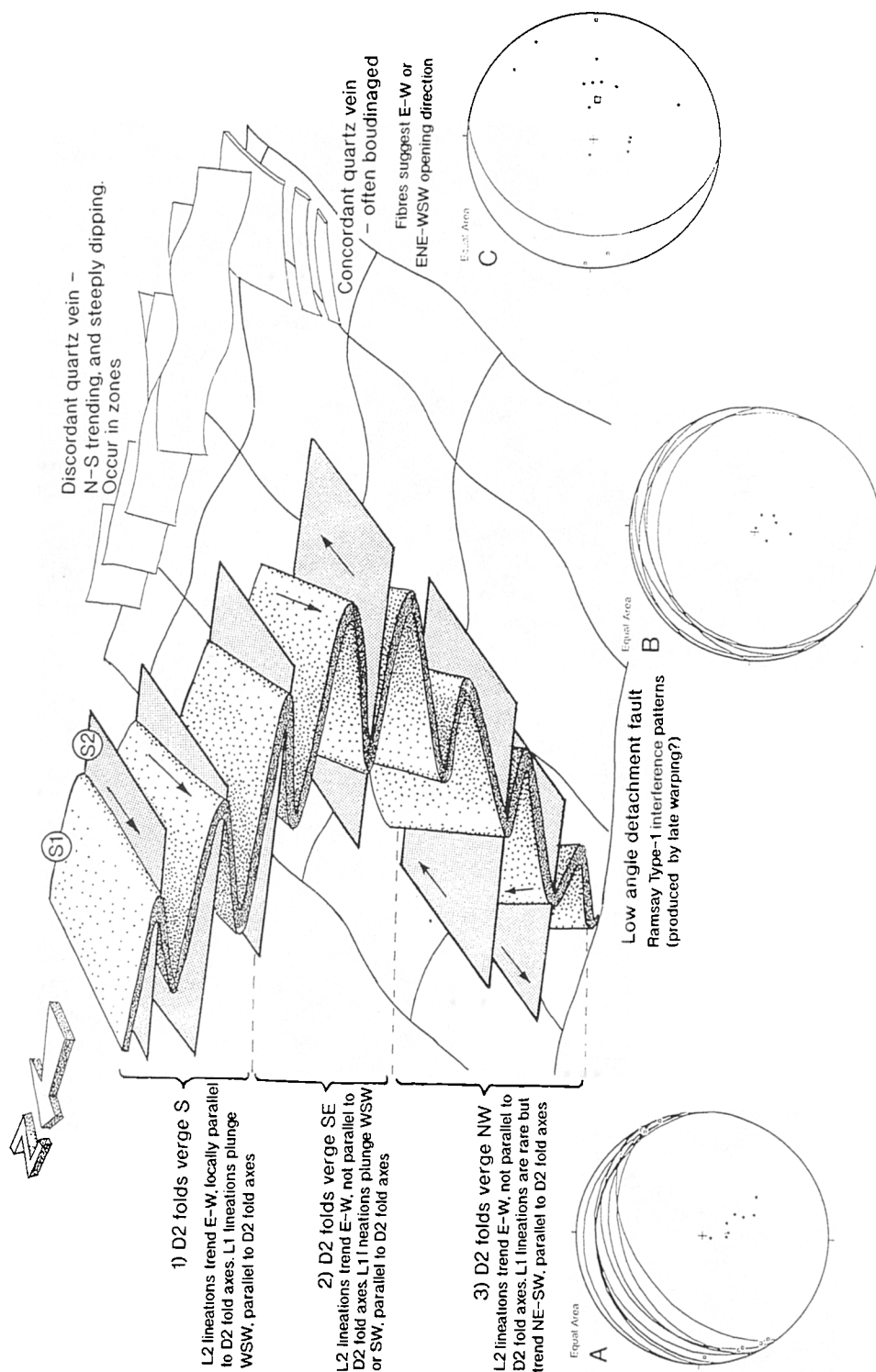


Figure 4.68. Summary block diagram of fold and fault geometries from Stuley. Equal area stereonet of: A) Extension-related fold axial planes (great circles) with poles (dots) and fold axes (boxes); B) Detachment faults (great circles) and poles (dots); and C) poles to quartz veins (dots) with mean great circle and vein fibres (boxes).

The variation in fold vergence direction between S and SE on Stuley can be explained by the following three models:

- Strike-slip related S1 is folded during further strike-slip. Extension-related S2 disrupts the early folds, leaving occasional vestiges (Fig 4.69 model A).
- Extension-related S1 is folded by D2 during further extension, and S2 is superimposed (Fig 4.69 model B). The curvilinear hinge is caused by clockwise rotation during dextral differential shear.
- Strike-slip-related S1 is folded by extension-related D2, and S2 is superimposed (Fig 4.69 model C). The curvilinear hinge is caused by clockwise rotation during dextral differential shear.

Model A does not require an additional component of dextral differential shear to account for the preponderance of south verging D2 folds. It is thought to be unlikely however, because no strike-slip related lineations are observed to be folded by the early D2 folds. Model B explains the curvilinearity of observed fold hinges, but again, does not explain the lack of observed folded lineations. Model C is regarded as the most probable origin for the variable fold vergence directions, because the strike-slip-related mineral lineation is always parallel to the fold axes. The origin of imposed dextral differential shear that this model requires can only be speculated upon, but may be due to the presence of a large E-propagating sheath fold, the northern (sinistral differential shear) side of which is unexposed.

Low angle detachment faults are also present on Stuley and are concordant to the S2 and S1 foliations (Fig. 4.68b). Sense-of-shear indicators directly associated with the detachments have not been found, but evidence for contemporaneous extension comes from zones of late, subvertical, N-S trending quartz veins with E-W oriented vein fibres (Fig. 4.68c). These quartz veins both cut, and are cut by, detachment faults. The earlier set of concordant quartz veins which are folded by D2, are boudinaged during extensional shearing on the S2 foliation surfaces. Displaced marker horizons suggest top-to-the-E movement has occurred.

A phase of extremely open upright folding (described as 'warps' by Coward 1969), is apparent, and locally affects the orientation of foliations, lineations and detachments. This flexuring occurs on a variety of scales (10's of cm to 10's of m), and is markedly non-cylindrical, producing 'Type 1' (dome-and-basin) interference patterns (using the terminology of Ramsay 1962). It is thought that this 'warping' is only readily observed at this locality because the foliation is subhorizontal. This

deformation post-dates extension-related detachment faulting, and is therefore relatively late in the structural history.

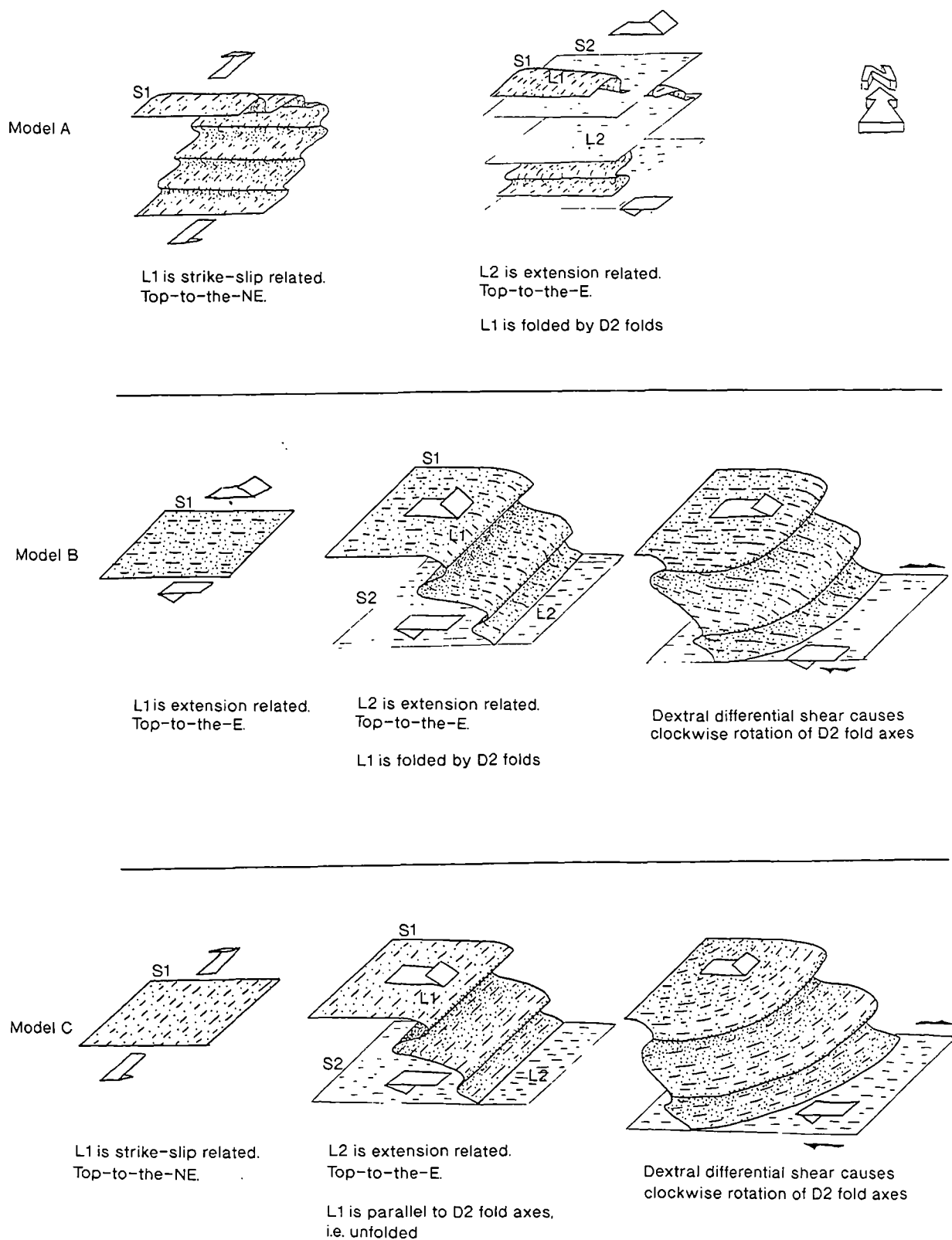


Figure 4.69 Three models for the possible evolution of the Stuley region during low-angle extension.

4.4.10. Conclusions and discussion on extensional movement in the southern segment

Conclusions

A suite of structures including faults and asymmetric folds overprint and therefore post-date the strike-slip related structures. These new structures relate to a phase of extensional reactivation, which has focused into the most highly strained and retrogressed phyllonitic areas. This suggests that the phyllonites are a profound mechanical weakness, and able to localise subsequent deformation.

Kinematic regime

In most phyllonite belts, the geometries of structures which post-date those produced during sinistral strike-slip motion are indicative of regional extension. Folds are asymmetric and display a ruck-like geometry, verging down the dip of the pre-existing foliation, suggesting a sticking point on the extensional slip surface has caused localised hangingwall compression. Most fold packages display fold vergence directions consistent with extension to the E or SE. Occasionally, however, the pre-existing foliation dips NW, and where this occurs, the extension direction is also towards the NW.

Conditions of deformation

The retrograde, low-greenschist facies mineral assemblage generated prior to extension have not been significantly metamorphically modified during the extension event. The presence of fibrous chlorite in a new 'down-dip' orientation suggests that the phyllonites were still acting as a DMT sink during extension. The presence of a pressure solution cleavage axial planar to some folded phyllonites suggests that deformation may have been partly accommodated by the removal of material via DMT source mechanisms. The brittle-ductile behaviour of the phyllonites during extension, the low greenschist facies mineral assemblages preserved from strike-slip-related metamorphism, and the low-greenschist facies minerals precipitated from solution during extension, suggests that deformation occurred at low greenschist facies during reactivation. The more brittle-ductile style of deformation during extension compared with the consistently ductile deformation during sinistral strike-slip may be the result of a slight drop in P/T conditions between these two deformation phases.

Discussion

The change from strike-slip to extension

The clockwise rotation from NE-SW-trending mineral lineations in the protophyllonites to E-W or SE-NW in many phyllonites is believed to show the effects of extensional overprinting. Prior to extension, all the phyllonitised material probably possessed strike-parallel mineral lineations as a result of the imposed sinistral shear associated with phyllonite development. During extension, however, deformation focussed into the highest strain and/ or retrogressed areas, re-orientating or overprinting the existing mineral lineation in these areas whilst the earlier movement indicators remain relatively unaffected in the less phyllonitic parts of the zone. The orientation of mineral lineations is not bimodal however, and the spread of lineation data through c. 50°, could indicate that a change from strike-slip to extension occurred gradually via a transtensional phase of movement. This interpretation is corroborated to some extent by the orientation of extensional shear bands and cross-cutting quartz/ chlorite veins. Extensional shear bands within the phyllonite are often oriented markedly anticlockwise of the regional foliation strike. These shear bands displace top-to-the ENE. Furthermore, fluids released during the extensional movement phase in the phyllonite belts were injected into the immediate phyllonitic and local protophyllonitic material, to form tensional veins or vein arrays of quartz and/ or chlorite, whose orientation is also indicative of ENE-directed extension (Fig. 4.70). Extension was accommodated largely by shearing, folding and faulting *within* the phyllonites, with relatively little extension accommodated outside the belts. Thus, continued extensional movement may have reworked the earlier injected veins in the phyllonite whilst promoting the generation of new ones. Outside the phyllonite belts, quartz veins remain intact without reworking. It is notable that the earlier reworked veins commonly trend NW-SE, consistent with early sinistral ?transtensional displacements, whilst the N-S orientation of the dominant, non-reworked veins are consistent with pure extension. Late vein orientations may therefore provide an indication of the later evolution of the OHFZ in the region, and appear to suggest a change from NE-SW sinistral transtension to E-W extension.

Some reworked veins within the phyllonites at Eigneag Bheag (NF 922600), show thrust-sense compressional offsets parallel to the foliation and displacing top-to-the-west. It is not known to what extent this post-extensional/ veining phase of thrusting is significant in the region. No similar features have been observed elsewhere, and it is not thought to be regionally significant.

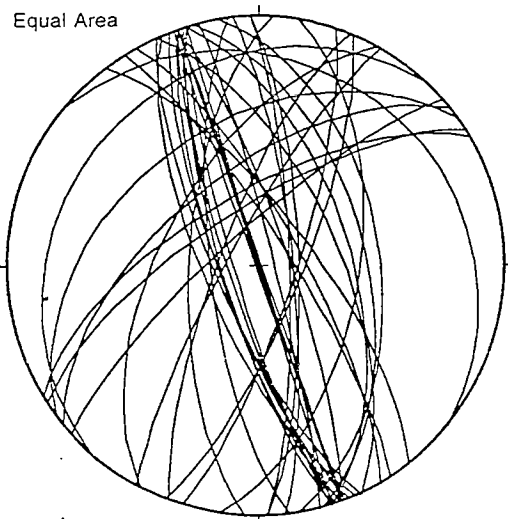


Figure 4.70. Equal area stereonet of quartz veins (great circles) from Burrival, Eigneag Bheag and south Eaval.

The Usinish Phyllonite (width versus extension)

The Usinish Phyllonite belt of South Uist appears to undergo a gradual increase in outcrop width from north to south. At its northernmost exposure of Ornish (NF 858376), the belt is c. 10 m thick, whilst at its southernmost exposure of Stuley (NF 830235) the belt is *at least* c. 200m thick (Fig. 4.42).

It should be noted that for reasons outlined in section 4.3.8, the writer disagrees with the BGS map of Fettes et al. (1981), in that at Rubha Bolum (NF 828284), the upper contact of the phyllonite belt is regarded by the present work as being unexposed. The 'Mashed Gneiss' purported to be exposed on Bolum Island (NF 829284) by Fettes et al. (1981) lies at a structural level which is *below* phyllonitic material and is therefore regarded as a low strain 'clast' within the belt.

The lateral change in width coincides with a marked change in the style of extensional deformation. In the northern part of the belt, the phyllonite fabric (S1), generated during strike-slip, is *directly* reactivated by extensional movement, and a rotation in the mineral elongation lineation occurs. Folds of the S1 foliation become more frequent further south, and the development of an incipient crenulation cleavage is apparent. At the southernmost exposures of Usinish Phyllonite, e.g. at Rubha Bolum (NF 828284) and Stuley (NF 830235), the crenulation cleavage (S2) is fully developed, and at Stuley, it is the dominant fabric. At this locality a new E-dipping mineral lineation has been generated on the S2 surfaces and it is thought that the S2 foliation accommodates more extension-related deformation than the overprinted S1. This lateral change in style of extensional deformation is believed

to relate to an increase in the magnitude of extension from north to south, and thus, may have affected the overall width of the belt.

4.4.11 Summary

- Brittle-ductile deformation, forming ruck folds, faults and localised fabrics, overprints and therefore post-dates deformation relating to sinistral strike-slip.
- Extensional deformation has preferentially focused into the most phyllonitic belts, with relatively little extension accommodated elsewhere.
- The pre-existing chlorite grade metamorphic assemblages in the phyllonites are not altered significantly by the extension event, and new chlorite is associated with extension, suggesting low greenschist facies metamorphism occurred during extension.
- Diffusive mass transfer (DMT), crystal plastic, and brittle fracturing deformation mechanisms dominate during extensional movement.
- Kinematic indicators associated with down-dip plunging mineral elongation lineations give consistent down-dip, normal senses of shear, irrespective of the overall dip direction.
- The extension directions are 'passively' controlled by the orientation and geometries of the pre-existing fabric, suggesting extension may have resulted from gravitational collapse.
- More extension is believed to have been accommodated in the southern part of the Usinish Phyllonite than in the north, due to the more advanced state of overprinting by an extension-related foliation
- A phase of sinistral transtension may separate purely strike-slip deformation from purely extensional deformation, with the implication that these two kinematic 'events' may be closely timed.
- Quartz veining is common during extension and is penecontemporaneous with 'collapse' folding.
- Very late laterally continuous subvertical faults cross-cut all structures

4.5. Chapter conclusions

The southern Outer Hebrides region has undergone a polyphase deformation history. Following the Scourian and Laxfordian deformation phases in the basement complex, early motion on the OHFZ occurred. This commenced with large-scale brittle thrusting, causing the imposition of a roughly NNE-SSW trending

and ESE dipping structural trend, which acted as a zone of preferential failure during subsequent reactivations.

Kinematic history and distribution of fault rocks

The distribution of fault rocks in the southern segment of the OHFZ is geographically variable and contrasts with the distribution of fault rocks in the northern segment of the OHFZ. The earliest fault rocks in the southern segment are a roughly N-S trending belt of brittle rocks up to 5km wide, including cataclasites and pseudotachylites. These rocks were generated in response to E-W compression and the generation of a major west-directed thrust zone. Brittle rocks occur throughout the eastern side of the southern islands and often occur locally in regions up to 20 km west of the main thrust belt.

The style of brittle faulting is laterally variable. In the northernmost and southernmost parts of the region (primarily North Uist and Barra respectively), brittle deformation is dominantly manifested as zones of abundant brittle fracturing and cataclasis, with relatively small amounts of pseudotachylite generated. In the central part of the region however (primarily South Uist and the Eaval region of North Uist), brittle deformation occurs by the generation of large pseudotachylite/ultracataclasite crush zones, as well as by brittle fracturing. This lateral change is due to the localisation of 'multiple jerk' pseudotachylite injection and cataclasite generation in the central part of the fault zone segment. By contrast, 'multiple jerk' pseudotachylite injection in the northern and southern parts of the fault zone segment is more diffuse. The reason for this lateral increase in strain localisation in the central part of the fault zone segment may, in part, relate to the prominent pre-existing anisotropy which occurred between the Western Gneiss and the Corodale Gneiss and/or the local orientation of the pre-existing gneissose banding, prior to fault inception.

The wide belt of localised brittle failure which occurs throughout the southern Outer Hebrides, and the relatively narrow zone of intense brittle failure near to the fault trace in the eastern part of the islands can be respectively regarded as the result of diffuse microfracturing during initial compression, and the final localisation of microfractures along the main failure surface close to the point of ultimate failure stress (Sibson 1977b).

The phyllonitic and protophyllonitic rocks of the southern OHFZ segment always overprint the brittle rocks related to thrusting. These rocks are spatially coincident with the eastern side of the main thrust belt, trending mainly N-S or NNE-SSW. They are concordant to the larger pre-existing thrust surfaces, and probably represent thrusts that have undergone localised and intense retrogression to

chlorite-bearing greenschist facies. metamorphic hydration reactions, caused by fluid flux along enhanced permeability pathways (relict faults), have caused the main phase changes.

The lateral distribution of phyllonite and protophyllonite is variable in the southern Outer Hebrides. In the northern islands (e.g. North Uist and Ronay), the phyllonitic rocks occur as braided anastomosing networks, separating low strain protophyllonitic 'clasts' which lead to local deformation complexities. By contrast, in the southern islands (e.g. South Uist), the phyllonitic rocks occur as a single belt (the Usinish Phyllonite), with mainly gradational margins into protophyllonitic gneisses. In Barra, phyllonitic rocks are completely absent. Like the lateral change in brittle thrust structures, this lateral change in phyllonite geometry is also believed to result from the existence of pre-existing anisotropies. In North Uist, brittle deformation is somewhat diffuse, with abundant large-scale brittle 'topographic' fractures available to channel fluids. In South Uist, the presence of the Corodale Gneiss has localised brittle deformation into the marginal areas, hence the lack of suitable anastomosing faults and available fluid channelways. In Barra, the non-existence of phyllonitic material may be due to its location, some 10 km west of the inferred offshore lateral continuation of the Usinish Phyllonite of South Uist.

Brittle-ductile faults and folds, associated with extensional reactivation are focused into the most phyllonitic zones of the southern OHFZ segment. This relationship suggests that there is a profound rheological contrast between the relatively strong protophyllonitic and gneissose regions, and the relatively weak phyllonitic regions. Again, a lateral change in structures related to extension can be attributed to the distribution of pre-existing structures: In the north, the anastomosing phyllonite belts are host to 'down-dip' extending faults and folds, irrespective of the phyllonite belt orientation. This strongly suggests that extension was 'passive' and driven by gravitational collapse rather than by tectonic extension. In the south, the single Usinish Phyllonite belt is host to 'down-dip' collapsing faults and folds which are progressively overprinted southwards by a new phyllonitic foliation which takes up most of the deformation by inter-layer slip.

No evidence for steep extensional faulting like that observed in the northern segment of the OHFZ has been found onshore in the southern segment. This is probably due to their development entirely offshore. This suggestion is corroborated to some extent by seismic studies (e.g. McQuillin and Binns 1973), which locate the steeply dipping, extensional Minch Fault a few kilometres east of, and parallel to the onshore trace of the OHFZ

There is abundant field evidence to suggest that some of the kinematic 'events' were not necessarily exclusive. A phase of sinistral transpression may have

separated the early brittle thrusting from later sinistral strike-slip. This transpressional phase may be interpreted from the coexistence of localised low-grade thrust-sense fabrics in the west of the North Uist Crush Melange, with contemporaneous, widespread, low-grade strike-slip-sense fabrics throughout the rest of the melange.

Similarly, the change from sinistral strike-slip to extension may have been facilitated by a mid-stage of sinistral transtension. The spread of mineral lineation data, shear band orientations and quartz vein patterns from many phyllonite belts in both North and South Uist, suggest a gradual change in the fault zone movement vector may have occurred. The kinematic history of the entire southern segment of the OHFZ is summarised in figures 4.71 and 4.72.

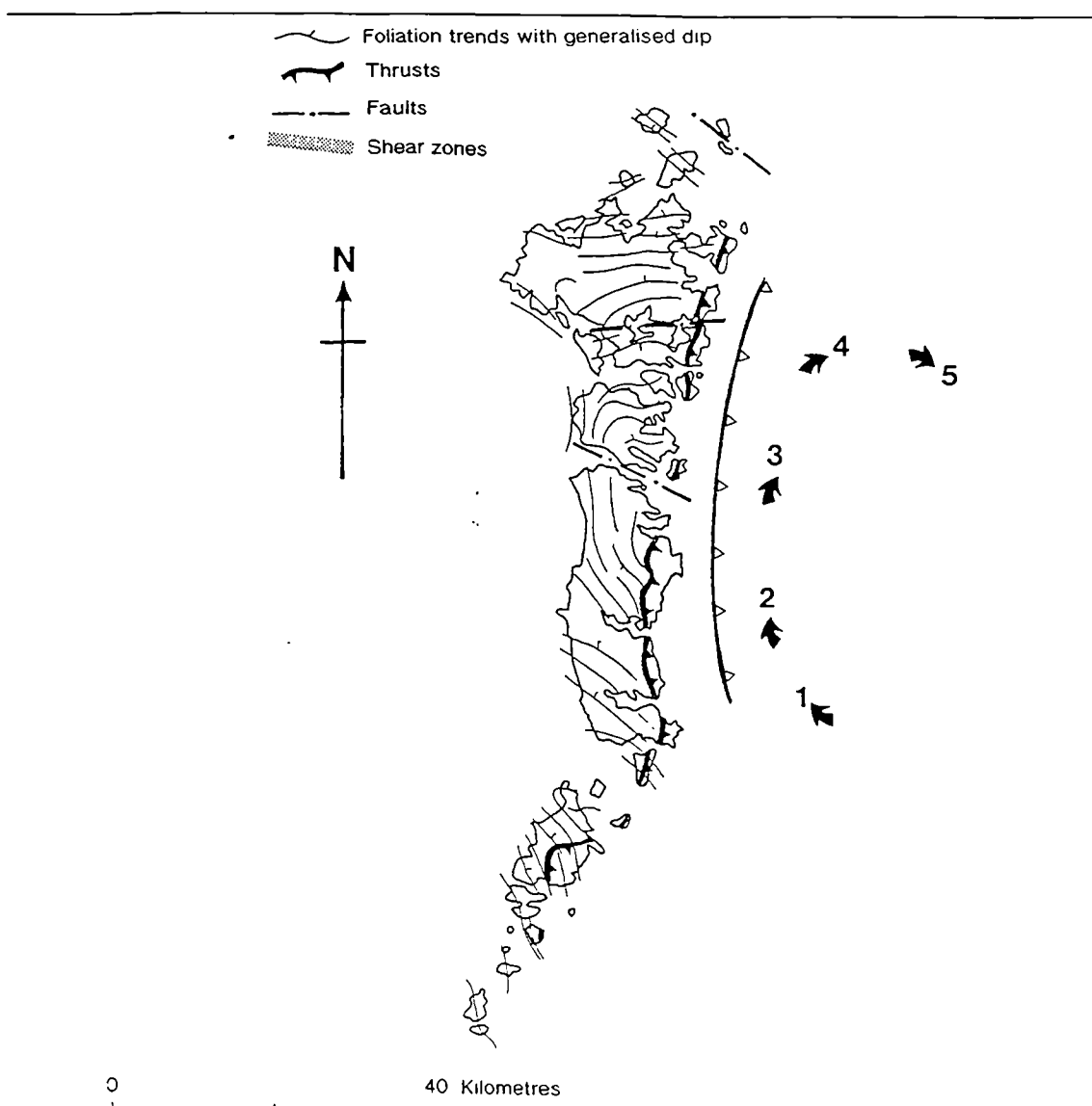


Figure 4.71. Map of the southern Outer Hebrides showing the inferred motion of the hangingwall block. Magnitudes of displacement are not known and are not implied by the diagram.

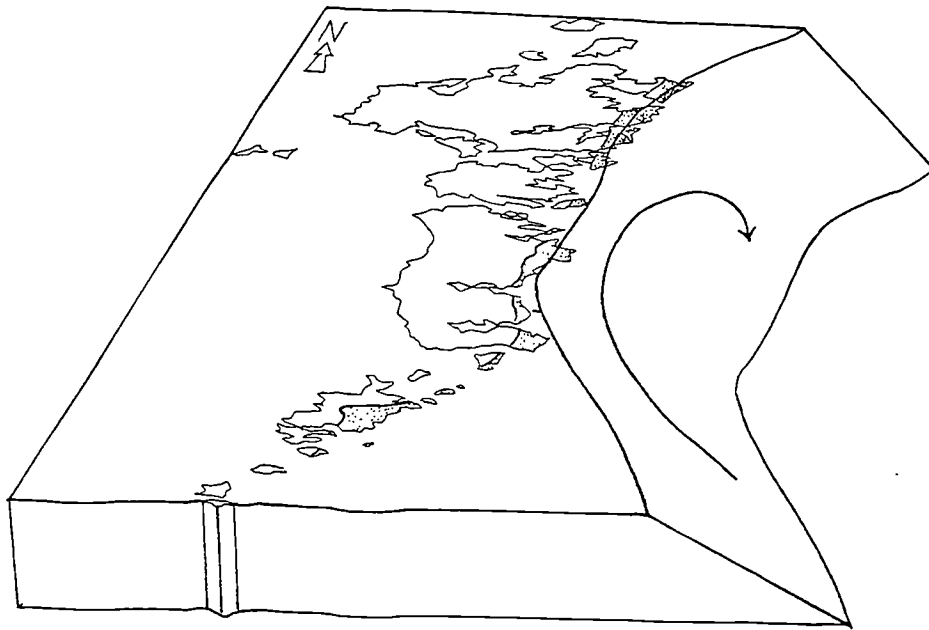


Figure 4.72. 3-D block diagram of the kinematic evolution of the onshore trace of the southern segment of the OHFZ, prior to offshore motion on the Minch Fault. The footwall block and the motion vector on the hangingwall block are shown.

Changes in deformation conditions

The earliest fault rocks in the southern segment of the OHFZ are superficially unusual in that they preserve mineral assemblages which show very little retrogression from the original amphibolite facies gneiss protoliths, but also show extremely brittle styles of deformation, dominated by fracture/ cataclastic deformation mechanisms. The P/T conditions at which both these features normally form are very different. This paradox can be attributed to either:

1. Deformation occurring at low grades ($<300^{\circ}\text{C}$) in the absence of hydrous fluids, promoting brittle deformation mechanisms. The high grade mineral assemblages are not in equilibrium (i.e. metastable) but are not retrogressed due to the fluid-absent conditions: or
2. Deformation occurred at higher grades, with assemblages in equilibrium, but the strain rates were sufficiently high to cause brittle rather than ductile deformation in most phases (including quartz).

The widespread development of pseudotachylites may indicate fluid-absent conditions during brittle deformation (Sibson 1975), but this is not completely reliable (e.g. see Magloughlin 1992) (see section 4.2.12). There is also evidence to suggest that deformation did not occur at amphibolite facies, based on the lack of any ductile overprint which should have formed as strain rates decreased (see section 4.2.12). Thus, the former explanation is preferred. However, high strain rate episodes may be responsible for pseudotachylite generation. The exact P/T conditions for early brittle deformation are unknown but probably equate to greenschist facies.

During subsequent strike-slip motion, both the mineral assemblages and the style of deformation change. Ductile deformation mechanisms become dominant including fluid-assisted transfer of material by diffusion (DMT), crystal-plastic deformation and intercrystalline slip. All are linked to the change in fault zone rheology, as the amphibolite grade gneissose assemblages are retrogressed to low greenschist facies, chlorite/ sericite- bearing assemblages. The change to a weaker rheology effectively shallows the brittle-ductile transition zone, so that the rocks deform in a ductile manner. No increase in P/ T conditions is necessary to account for the change in deformation conditions. These low-greenschist facies phyllonites probably formed at c. 300°C and c. 2-3 kb.

Brittle, semi-brittle and ductile deformation occurs during extension, and it seems likely that this phase of fault zone movement occurred at low-grade conditions around the brittle-ductile transition for phyllonites. In contrast to the P/ T/ fluid conditions prevalent during earlier, mainly ductile strike-slip movements, slightly lower P/T conditions probably prevailed during extension, to account for the increase in brittle deformation. The generation of a widespread pressure solution cleavage, axial planar to the deformed phyllonite foliation, and the relative rarity of deposited extension-related precipitates (e.g. fibrous chlorite) suggests that the phyllonites acted as both a DMT source and sink during extension.

PART THREE - SYNTHESIS

Chapter Five A kinematic model for the OHFZ

5.1. Introduction

Field evidence from the northern and southern segments of the OHFZ suggests a broadly similar kinematic history exists along the entire length of the fault zone as outlined in Table 5.1 and Fig. 5.1. The fault zone has been divided into two segments, separating Lewis/Harris to the north and North Uist/ South Uist to the south, because some important structural differences exist (see section 5.2).

Northern Segment	Southern segment
Thrust-sense ductile mylonites Top-to-the NW	No equivalent deformation exposed
Thrust-sense brittle deformation, including moderate to locally intense development of cataclasite and pseudotachylite Top-to-the W or NW	Thrust-sense brittle deformation, including widespread intense development of cataclasite and pseudotachylite Top-to-the W or NW
Sinistral strike-slip forming isolated phyllonitic shear zones Top-to-the NE	Sinistral strike-slip forming anastomosing or isolated phyllonitic shear zones Top-to-the NE
Low-angle extension (gravitational collapse), utilising pre-existing fabrics Top-to-the S or SE	Low-angle extension (gravitational collapse), utilising pre-existing fabrics top-to-the SE or E
High-angle extension , cross-cutting pre-existing fabrics, and with syn-tectonic sedimentation Top-to-the SE	No equivalent deformation exposed onshore, but may occur offshore (the Minch Fault) Top-to-the E?

Table 5.1. The kinematic history of the OHFZ, based on field observations during the present study. A fundamental division exists between Lewis/ Harris (the northern segment) and Uist/ Barra (the southern segment).

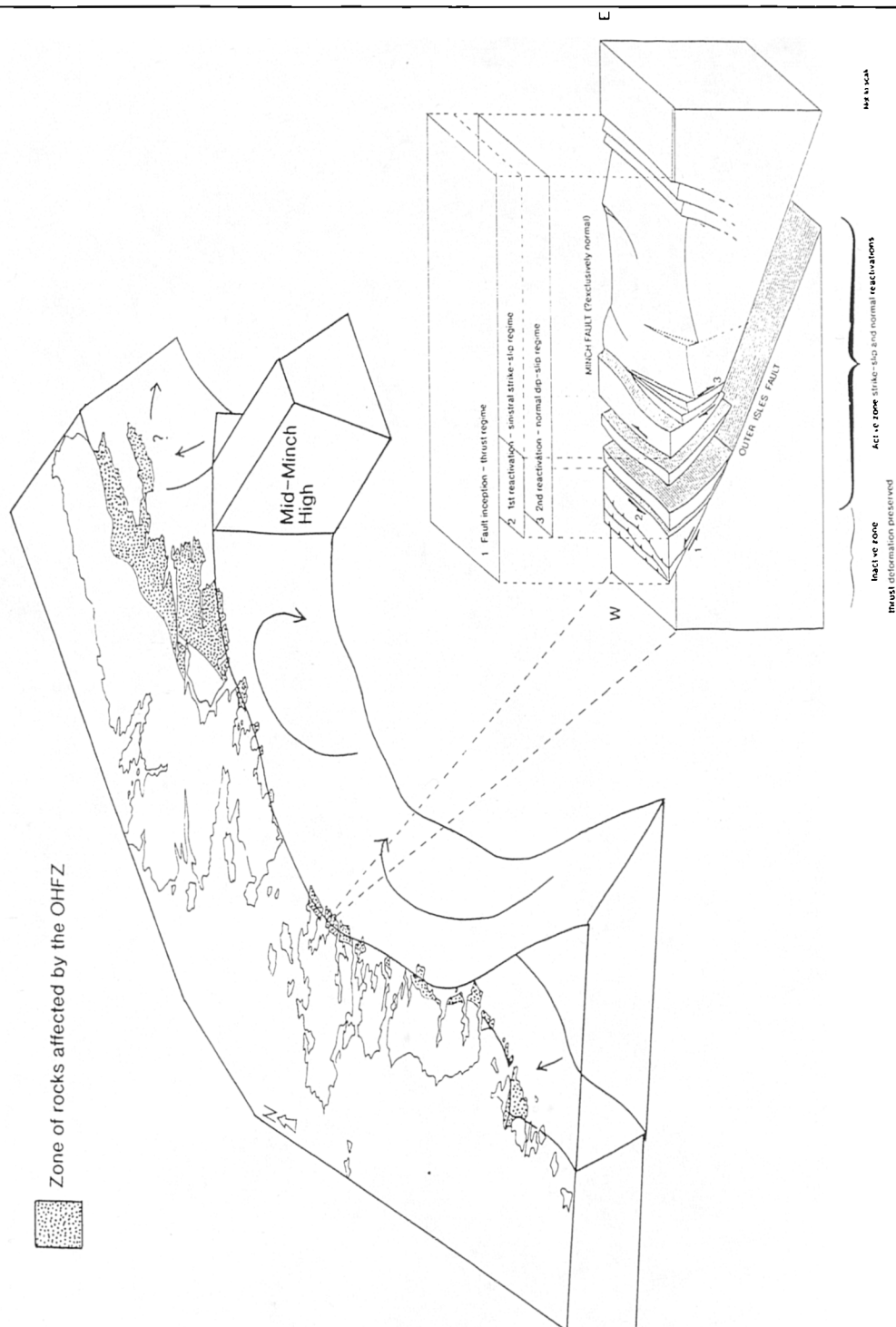


Figure 5.1 3-D block diagram of the kinematic evolution of the onshore trace of the entire OHFZ, prior to offshore motion on the Minch Fault. The footwall block and the motion vectors of the hangingwall blocks are shown. Inset is a 3-D block diagram showing the onshore evolution of the fault zone (from N.Uist). Initial deformation is preferentially preserved in the west, whilst later deformation reactivates the fault zone progressively further east (modified from Stein 1988)

5.1.1 Timing of movements

Ductile thrusting (northern segment only)

Scourie dykes and Laxfordian pegmatites are cut by early mylonites associated with early ductile movement on the OHFZ (see Lailey et al. 1989, for an alternative interpretation and section 3.2.5 of the present work for a critique of this alternative). This suggests that all ductile thrusting occurred after their intrusion, and sets an upper age limit on onshore OHFZ movement of c. 1700 Ma. Ductile thrust fabrics are overprinted by the effects of brittle thrusting (e.g. Loch Sgibacleit; see section 3.2.2), setting a lower age limit (c. 430 Ma: see below), on movements, but in the absence of other geological or geochronological data, the age of this event cannot be constrained more precisely.

Brittle thrusting

Brittle deformation cross-cuts both Scourie dykes (Younger Basics), whose intrusion is believed to have occurred at c. 2.4 - 2.2 Ga (Fettes and Mendum 1987), and Laxfordian pegmatites, whose intrusion is believed to have occurred at c. 1700 Ma (Fettes and Mendum 1987). Undeformed Permo-Carboniferous lamprophyre dykes (c. 300 Ma.) south of Eaval, North Uist (NF 894587) cross-cut the Crush Melange. This gives a possible age range of brittle movement of c. 1400 Ma.

Direct isotopic age dates of brittle deformation products also exist. A high precision laser probe ^{40}Ar - ^{39}Ar investigation of thrust-related pseudotachylites from Grimsay has recently been published (Kelley et al. 1994). These authors suggest that pseudotachylite generation occurred at 430 \pm 6 Ma. This age corresponds well with published ages for movements along the Moine Thrust in mainland Scotland (Kelley 1988), and appears to suggest that Caledonian-age thrust movement has occurred along the OHFZ. However, field relationships cannot constrain with certainty whether all pseudotachylite along the OHFZ was formed during the Caledonian, or whether more than one phase of generation is developed.

Sinistral strike-slip

On theoretical grounds, Sibson (1977b) argued that all pseudotachylites must be post-dated by the deformation responsible for the formation of the phyllonitic shear zones. This suggestion appears to be consistent with all field observations made during the present study (see sections 3.3 and 4.3). An upper limit of c. 430 Ma may therefore be placed on the onset of strike-slip displacements along the OHFZ. Sibson

(1977b) also reports the results of a pilot whole-rock K-Ar study of cataclastic and phyllonitic rocks which yielded ages between 100 \pm 40 Ma and 394 \pm 16 Ma, with a mean age of c.400 Ma. It should be noted that all but one of the phyllonitic rocks, which post-date the thrusting episode, fall between 471 Ma. and 394 Ma, broadly consistent with late Caledonian (mid to late Silurian) sinistral movements noted elsewhere in the Caledonian orogen of Scotland and adjacent regions (Soper et al. 1992).

Low-angle extension

The absolute age of extensional movement is not known but must fall between the known age of earliest thrusting (430 Ma, Kelley et al. 1994) and the intrusion of Permo-Carboniferous dykes (c. 300 Ma.); a period of c. 130 Ma. If the K-Ar dates of c. 400 Ma, cited by Sibson (1977b) for the formation of the phyllonites, are regarded as reliable ages for the onset of sinistral strike-slip, the age range of possible extensional movements is reduced to 100 Ma.

High-angle extension

There is evidence to suggest that the Stornoway Formation is syntectonic with high-angle extensional faulting (see section 3.5.3). These rocks are believed to be Permo-Triassic in age from palaeomagnetic studies (Storetvedt and Steel, 1977), and therefore date the onshore extension at c. 235 Ma.

The presence of fault-rock clasts within the Stornoway Formation conglomerates, and the lack of cross-cutting deformation in the succession, suggests that no onshore deformation post-dates the deposition of the Stornoway Formation. Thus, a possible total age range of c.1465 Ma. exists for all onshore movement along the OHFZ. Offshore movements probably continued after onshore movement ceased, because sedimentation of Jurassic sediments was controlled by the partially reactivated splay of the OHFZ; the Minch Fault.

5.2. Along-strike differences in the kinematic evolution of the OHFZ

Several important differences in the along-strike behaviour of the OHFZ are apparent and suggest that the fault zone movements may be compartmentalised, especially during its early history. Each compartment appears to have experienced a different fault zone evolution. These along-strike differences include:

1. The distribution of thrust-sense, *ductile* mylonites
2. The heterogeneous intensity of thrust-sense, *brittle* deformation
3. The distribution and geometry of phyllonite belts
4. The distribution and direction of low-angle extension
5. The distribution and direction of late, steep, normal faulting

5.2.1 The distribution of ductile, thrust-related mylonites

The belt of ductile, thrust-related mylonites observed in Lewis and Scalpay in the northern segment of the OHFZ has not been observed in the southern segment of the OHFZ (Fig. 5.2a). This suggests that either:

- the belt of thrust-related mylonite is laterally discontinuous and has died out between Scalpay and North Uist;
- the belt of mylonite is laterally continuous, but lies offshore to the SE and is not exposed onshore; or
- the belt is laterally continuous, but has been significantly displaced by faults/ shear zones oriented at a high angle to the OHFZ, so that the southern part of the mylonite belt is no longer exposed along strike from the northern part.

The most southerly exposure of mylonite in the northern segment is on Scalpay, where the mylonite belt is c. 600m thick. At Loch Sgibacleit c. 22km further north, the mylonite belt is c. 350m thick. Assuming a linear relationship between lateral extent and the thickness of the belt, a southwards lateral *thickening* of c. 12m per km is implied. In contrast, the lack of mylonitic material in North Uist, would imply a southward lateral *thinning* of at least 18m per km, in order for the belt to have pinched out completely. Given that the mylonite appears to be undergoing southward thickening at Scalpay, it is thought that this amount of southward thinning is unlikely.

The belt of mylonite is not thought to occur to the SE of the southern islands because in the nearest exposures of the OHFZ (in Scalpay), the mylonites define the western margin of the fault zone. All brittle deformation occurs further east. The reverse of this situation would have to be true in order to account for mylonites lying to the SE of the southern islands. Whilst this is a possibility, the following explanation is preferred for reasons explained below.

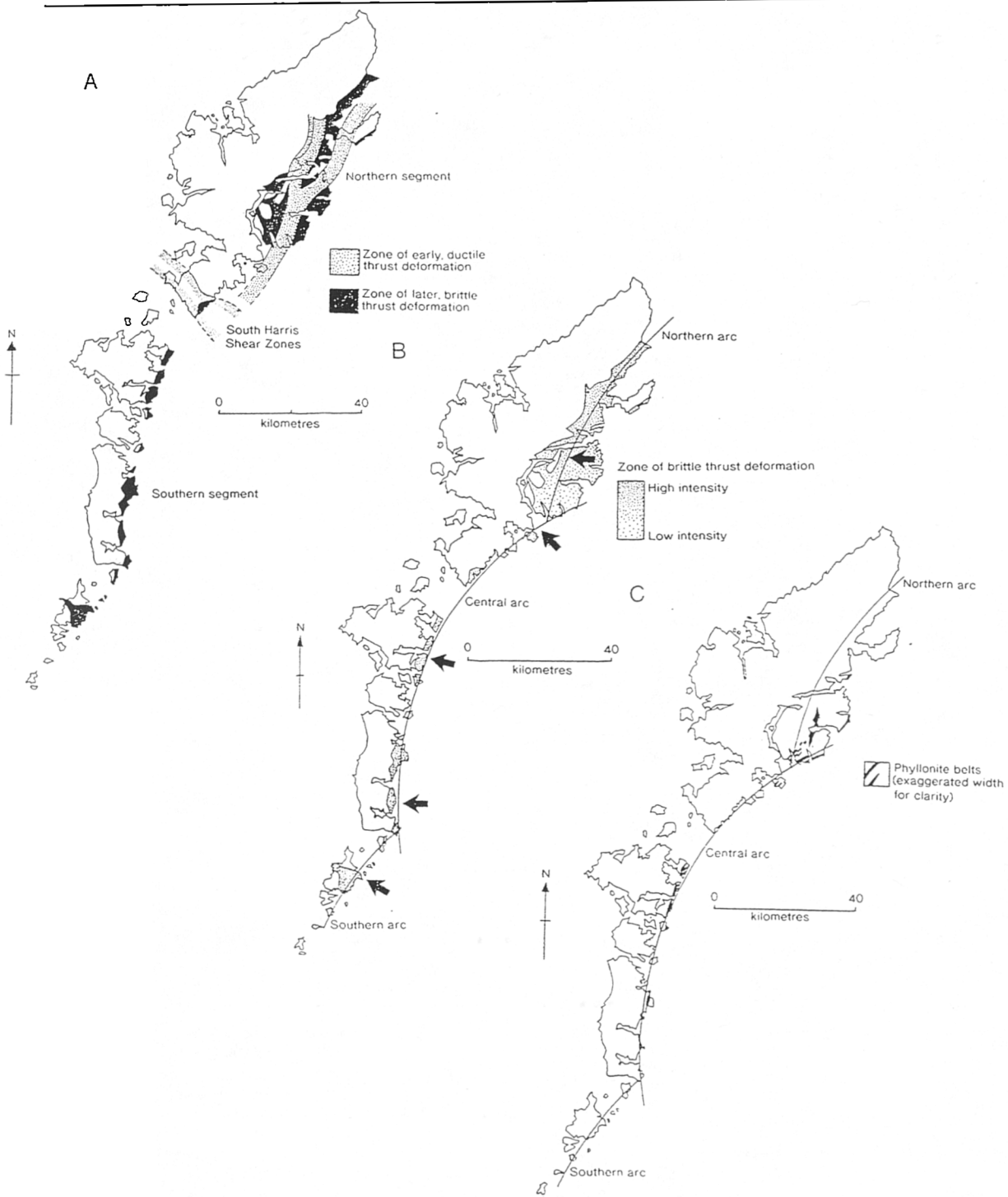


Figure 5.2 Simplified geological maps of the Outer Hebrides showing: A) onshore extent of ductile and brittle deformation associated with thrusting; B) onshore extent of brittle deformation associated with thrusting, and mean movement vectors; and C) onshore extent of ductile deformation associated with sinistral strike-slip along the OHFZ

The mylonite belt has probably been displaced by either transfer faults/shear zones active during thrusting or faults/ shear zones oriented at a high angle to the OHFZ, active after thrusting. The location and geometry of the shear zones of South Harris (Fig. 5.2a) are consistent with this hypothesis. The possible role of these shear zones in compartmentalising the early fault zone history is discussed at greater length in section 5.3.

5.2.2 The distribution of thrust-related brittle rocks

The distribution of thrust-related brittle rocks along the OHFZ is also markedly heterogeneous, but in contrast with the preceeding ductile rocks, they are found along the entire length of the fault zone. Brittle thrusting appears to be focused along three arcuate fault traces which are concave to the east, as first noted by Sibson (1977b). In general, brittle deformation and the generation of pseudotachylite and/or ultracataclasite decreases in intensity from south to north along the OHFZ, although in Lewis, the reverse appears to be true (Fig. 5.2b). The intensity of brittle deformation is thought to be related to the magnitude and frequency of local fault-slip events and unrelated to compartmentalisation. It is significant to note that in areas where large amounts of pseudotachylite and ultracataclasite are generated in discrete 'crush zones', (specifically in Barra and South Uist), a contrast in the composition of footwall and hangingwall rock types occurs. In the footwall 'western gneisses' of Barra and South Uist, amphibolite-grade banded gneisses are the dominant lithology. By contrast, in the hangingwall 'eastern gneisses', granulite-grade, pyroxene-bearing metadiorites are dominant. A zone of high contact strain between the two lithologies may have focused the majority of slip events and generated the observed brittle fault products. The displacement magnitude may also be higher in these regions. Focusing of deformation at lithological contacts has been observed in both ductile and brittle rocks, on outcrop and thin section scales, and is regarded as a viable mechanism to account for the large amount of pseudotachylite and ultracataclasite generated in these areas.

5.2.3 The geometry of phyllonite belts

Several along-strike differences in the geometry and extent of phyllonite belts are apparent. It is significant to note that the central arc (as defined in Fig. 5.2c), of the OHFZ, contains the greatest amount of phyllonitic material onshore. Phyllonites have not been observed south of Stuley (see section 4.3.9), and are therefore absent from

the Barra Isles. Similarly, significant amounts of phyllonite have not been positively identified from north of Eishken (see section 3.3.3), despite the *phyllonite-like* appearance of a small belt of calcareous mylonites at Port Beag (see section 3.3.5). It therefore appears that phyllonitisation was spatially restricted, chiefly to the central arc of the OHFZ. The possible reason for this lateral discontinuity is examined in chapter 6.

The geometry of phyllonite belts is laterally variable. In **Lewis and Scalpay**, phyllonite belts are narrow and isolated and occur between large areas of protophyllonitic material. They form in one of two trends (Fig. 5.3):

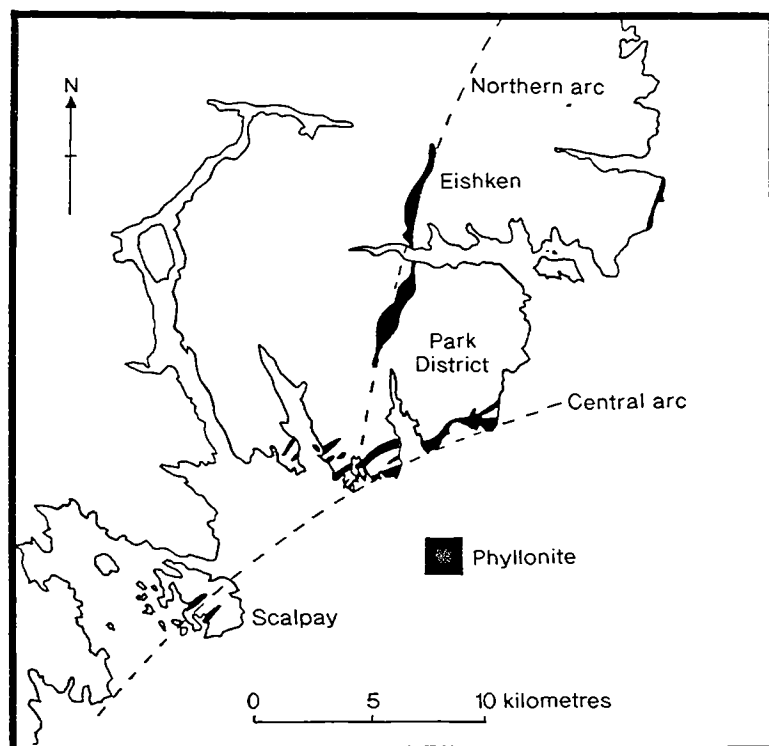


Figure 5.3. Simplified geological map of SE Lewis, showing extent of phyllonite related to sinistral strike-slip.

1. A moderately NE-SW-striking, SE-dipping trend, exemplified by the belts on Scalpay and around Loch Bhallamus. This trend swings gradually from NE to ENE from south to north, and traces the shape of the central OHFZ arc; or
2. A N-S striking, and E dipping trend, exemplified by the belt at Eishken, and Kebock Head further east (not visited during the present study) (Fettes et al. 1992).

These two different trends are regarded as the effects of pre-existing thrust geometry on the subsequent evolution of the fault zone. In the three arcuate, brittle, thrust-related zones, the density of brittle fractures adjacent to thrust faults is locally higher than in the surrounding gneisses, and the grain size is locally reduced by brittle comminution. Retrogression, related to hydrous fluid influx during subsequent strike-slip motion, focused mainly along these pre-existing thrusts. Thus the trend of the phyllonite belts is an inherited feature.

By contrast, in **North and South Uist**, phyllonite belts occur as either:

1. Anastomosing braided networks separating large areas of protophyllonitic material (see Fig 4.27). These belts strike between N-S and NE-SW, with the latter subordinate to the former. The networks probably represent high strain 'wrapping' of low strain 'clasts', and local dip magnitudes and dip directions are affected by the present-day erosion level ; or
2. An isolated, southward thickening belt, striking N-S and dipping E (see Fig. 4.42). Very little protophyllonitic material occurs away from the belts except in the immediately adjacent hangingwall and footwall regions

The geometric relationship between thrusts and phyllonite belts is illustrated by the observed parallelism between 'topographic' faults, (where cataclasis and microfracturing are preserved), and phyllonite belts, (where these brittle fault products have been effectively replaced), in the Crush Melange of North Uist (Fig. 5.4). This parallelism also shows that fluid flux was spatially restricted on a regional scale, preferentially occurring in the east of the Crush Melange, allowing the preservation of original thrust-related features to the west of the fault zone. A possible reason for the preservation of original thrust-sense features in the west of the fault zone, whilst phyllonitic overprinting occurs in the east of the fault zone, is discussed in chapter 6.

The southward lateral change in phyllonite geometry is probably an inherited feature. In North Uist, where phyllonite belts anastomose around low-strain 'clasts', no compositional contrast exists between footwall and hangingwall rocks, and as a result, pre-existing brittle thrusts developed diffusely throughout the Crush Melange. Subsequent phyllonitisation picked out the areas of densest fracturing

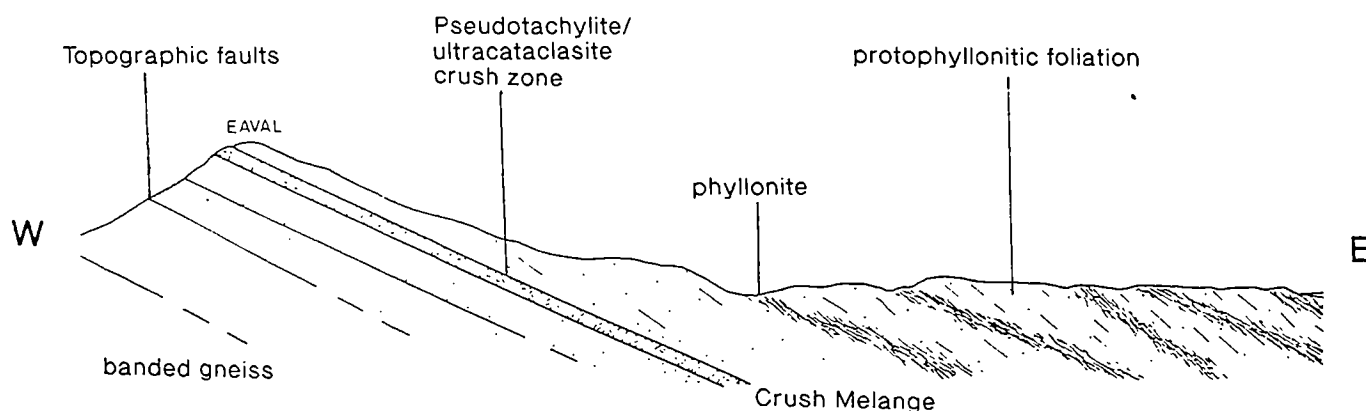


Figure 5.4 Geological cross-section (W-E) through the Crush Melange and phyllonite belts of N.Uist (from Sibson 1977b).

In South Uist, however, the presence of the granulite facies 'Corodale Gneiss' below the amphibolite facies 'Mashed Gneiss' may have generated a region of high contact strain and focused brittle thrusting, albeit above the main thrust 'base'. Enhanced fault zone permeability by the increased fracture density and reduction in grain size, resulted. Phyllonites were therefore focused into a single N-S trending belt.

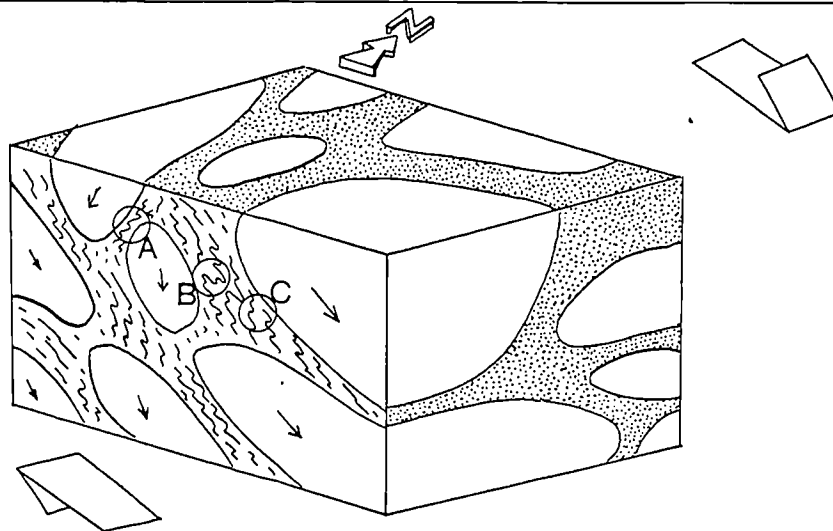
5.2.4 The distribution and direction of low-angle extension

Comparatively few effects of regional extension occur outside the regions where phyllonites developed. The effects of extension are therefore most readily observed onshore in the central fault zone arc, and the phyllonite belt geometry governs the extension direction over most of the region.

In South Uist, the single N-S striking, and E-dipping belt possesses E or SE-verging folds and E-dipping normal faults, indicative of down-dip extension. The amount of extension is believed to increase to the south, indicated by the increasing dominance of a second extension-related foliation over the first strike-slip-related foliation. Differential shear may have occurred during extension, so that folds are often curvilinear (see section 4.4.9).

In North Uist, the complex anastomosing phyllonite network exerts a similar control on the extension direction. In E-dipping portions of the phyllonite belt network, faults and folds show geometries consistent with down-dip extension to the east (marked C on Fig. 5.5). Similarly, extension on SE-dipping portions is down to the SE, and on NW dipping portions, extension is down to the NW (marked A on Fig. 5.5). Only in areas where (2nd order) folds are parasitic on larger (1st order) folds, are 'up-dip' vergences encountered (marked B on Fig. 5.5). This strong fabric control on the

extension direction, is probably due to 'passive' gravitational 'collapse' (see also Sibson 1977b), rather than 'active' extension or 'active' underthrusting (cf. Fettes et al. 1992).



- A) Down-dip, NW-verging folds
- B) Up-dip, NW-verging folds
- C) Down-dip, SE-verging folds

Figure 5.5 Schematic 3-D block diagram of N. Uist phyllonite network, showing protophyllonitic 'clasts' in anastomosing phyllonite belts with extensional overprint.

In contrast, the geometric control on extension in phyllonite belts from Lewis and Scalpay is less obvious. In the Park district of Lewis, folds verge to the S or SE, at 90° to strike, but low-angle extensional faults are absent, either within the belts or along their margins. It is thought that the phyllonite belts at this locality were not in the ideal orientation for reactivation. The southward-directed extensional 'collapse' vector is also apparent at Eishken, despite the N-S strike of the belt at this locality. Here the result of extension is a dextral differential shear component and a clockwise reorientation of the phyllonitic foliation within the phyllonite belt. Clearly, the pre-existing fabric exerts much less of a control on the 'collapse' vector during later extension in the northernmost phyllonites. In Scalpay, phyllonites possess extension-related folds which show an anomalous SW vergence. This also relates to southward-directed extension and a component of dextral differential shear, but in contrast to the Eishken and Bhallamus phyllonites, 'collapse' fold axes, as well as the phyllonitic foliation, are rotated significantly clockwise during extension. In the Lewis / Scalpay region, the control on the extension direction is regional, rather than local, and may relate to presence of the Mid-Minch High (see below and the discussion in section 3.4.6).

In the remainder of the northern and southern arcs of the OHFZ, extensional collapse is less obvious, due the lack of phyllonitic rocks in these regions. D2 folds are occasionally apparent from the early mylonites at Loch Sgibacleit, but the bulk of extension is believed to have been accommodated on large 'topographic' faults, and at "competence boundaries" between different lithologies (Sibson 1977b). In Barra, evidence for extension is rare, but the large, laterally continuous topographic break, which defines the trace of the OHFZ, may be a relatively late (and possibly extensionally reactivated) structure.

A marked change in the direction of the extensional collapse vector is apparent along strike. A dominantly S to SE direction occurs in the phyllonites of the central fault zone arc, whereas a dominantly NE direction occurs on the brittle faults of north Lewis (Fig. 5.1). The cause of this bimodal collapse vector can only be speculated upon, but a roughly E-W-trending region of positive topography from which gravitational collapse may have occurred in more than one direction, may have been present. The location of the Mid-Minch High, a positive region of Lewisian and Torridonian rocks which separates the Sea of the Hebrides and North Minch Basins, clearly visible on seismic reflection profiles (Stein 1988) (see section 2.8.2), suggests that this may have been the causal structure. This hypothesis cannot be proven as extension-related data in the northernmost part of the OHFZ are sparse.

5.2.5 The distribution and direction of late, steep normal faulting

An obvious lateral contrast in the distribution of late, steep normal faulting also exists. In Lewis, high-angle normal faults are common, and are seen to partially reactivate pre-existing thrusts, by hangingwall short-cut faults (e.g. see Fig. 3.24). This phase of deformation probably occurred synchronously with the deposition of the Stornoway Formation (see section 3.5.3). Further south, however, very little high-angle normal faulting is apparent onshore. Most of the normal faulting associated with sedimentation and the Sea of Hebrides Basin development probably occurred offshore. Partial reactivation of the OHFZ, by a hanging-wall short-cut, normal fault (the Minch Fault) (see section 2.8.1) offshore, is a mechanism, much cited in the existing literature, for accommodating normal motion without any onshore expression (Stein 1988, Huyghe and Mugnier 1990). Topographic faults may be locally reactivated during late extension, however, because their lateral extent and cross-cutting relationships with phyllonite belts (see Fig. 4.36 Lochportain map) suggests that they moved very late in the sequence of fault zone movement events.

The movement vector associated with late, high-angle, normal faulting appears to show a bimodal pattern, similar to that outlined in section 5.2.4. In the north of Lewis, steep, extensional faults display top-to-the-NE movements, whilst in the south of Lewis and in Scalpay, they display top-to-the-E or SE movements. The Mid-Minch High (see section 2.8.2), may once again be related to this divergence. In general, the extensional movement vectors during this late event are similar to those during the earlier, low-angle extension event, implying the same underlying control of a pre-existing structural geometry.

5.2.6. Summary

Although much of the deformation along the OHFZ is heterogenous along-strike, those related to later phases of OHFZ movement, (i.e. the distribution and geometry of phyllonite belts, the distribution and direction of low angle extension, and the distribution and direction of late, steep normal faulting) are probably controlled by pre-existing differences in the along-strike geometry of the OHFZ. The most important along-strike difference in fault zone deformation, and the one which requires a more thorough discussion, is the apparent absence of early, thrust-related, ductile mylonites from the southern segment. This difference can be explained by interaction of the OHFZ with the shear zones of South Harris.

5.3 The role of the South Harris Shear Zones

5.3.1 A possible interaction between the OHFZ and the SHSZ

The early ductile mylonitisation event in the northern segment is apparently offset in the region of South Harris before it reaches the along-strike trace of the OHFZ in the southern segment. In contrast, however, brittle deformation is not displaced across this region, but continues along the entire length of the fault zone. Subsequent kinematic 'events' along the OHFZ, including the development of phyllonites during strike-slip motion and deformation of phyllonites during gravitational 'collapse' also effectively ignore the South Harris Shear Zones. It therefore appears that if the SHSZ was a controlling factor in the evolution of the OHFZ, this only applies prior to brittle thrust motion.

There are two viable scenarios to explain the present distribution of ductile and brittle thrust-related deformation:

1. **One stage of thrusting on the OHFZ, with syn-kinematic displacement on the SHSZ.** In this scenario, ductile and brittle faulting are inferred to be the *same* age, separated by a brittle-ductile transition zone at depth. The ductile and brittle styles of deformation are the products of *one* progressive thrusting event along the OHFZ. Dip-slip motion on the South Harris Shear Zones (SHSZ) during thrusting may have uplifted the northern segment of the OHFZ through the brittle-ductile transition, thus exposing deeper level ductile rocks to brittle deformation, juxtaposing them against brittle rocks of the southern segment at the same crustal level (Fig. 5.6a).
2. **Two stages of thrusting on the OHFZ separated by displacement on the SHSZ.** In this scenario, ductile and brittle faulting are inferred to be *different* ages and the products of *two* completely separate thrusting events along the OHFZ. These events were separated by a component of lateral displacement on the SHSZ (Fig. 5.6b). Ductile mylonites in the southern segment are therefore displaced to a region of no exposure (now lying offshore). Uplift of the entire fault zone, through the brittle-ductile transition, occurs prior to the commencement of the second phase of (brittle) thrusting. During brittle thrusting, the mylonites of the northern segment focused brittle deformation and may have acted as a 'stress guide' (using the terminology of Dixon et al.1987), for the along-strike development of brittle fault rocks in the isotropic basement of the southern segment. This process may be analogous to the lateral continuation of present-day faults (e.g. oceanic transform faults), along-strike from ancient faults/ shear zones (e.g. continental suture zones) (Fletcher 1978, Sykes 1978, see section 1.3.4).

The isotopic dating of pseudotachylite related to thrusting (Kelley et al. 1994, see section 5.1.1) suggests that some, if not all, brittle, thrust-related deformation is Caledonian. The age of ductile thrusting is less certain, and field evidence leaves a large possible age range for movements between the late Laxfordian (c. 1700 Ma), and the Caledonian (c. 430m Ma) (see section 5.1.1). If one thrusting event occurred, all reverse movements would therefore probably be Caledonian. If two thrusting events occurred, Caledonian brittle deformation (c. 430 Ma) may be preceeded by ductile movements between 1700Ma and c. 430 Ma. Four models are possible (labelled A to D on Table 5.2).

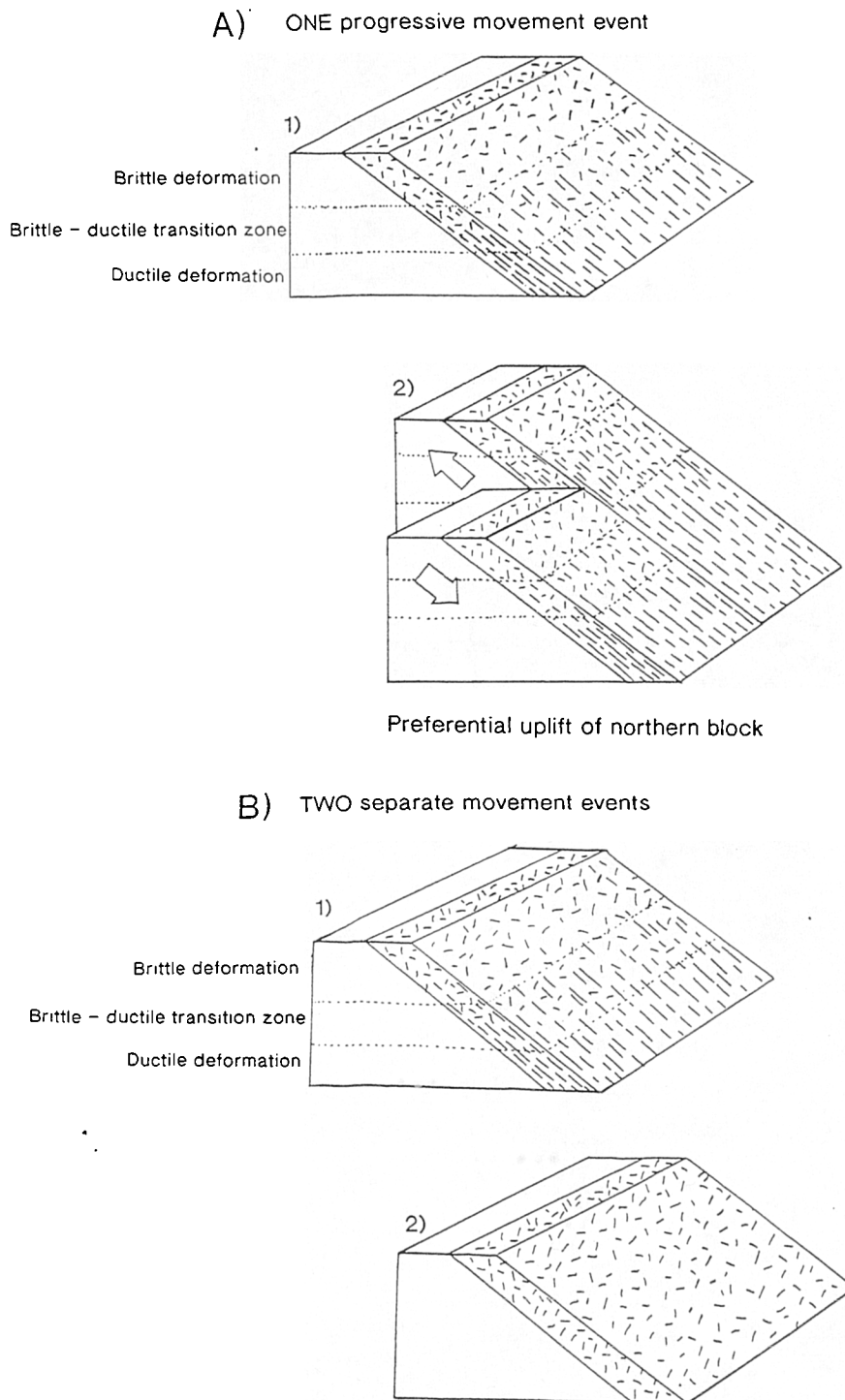


Figure 5.6 Schematic block diagrams illustrating a large thrust zone which occurs in ductile and brittle deformation regimes: A) one progressive movement event; and B) two separate movement events.

1 progressive event on the OHFZ	2 discrete events on the OHFZ
A) <u>Caledonian</u> ductile thrusting on the OHFZ, <u>Caledonian</u> transfer motion on the SHSZ, <u>Caledonian</u> brittle thrusting on the OHFZ.	B) <u>Precambrian</u> ductile thrusting on the OHFZ, <u>Precambrian</u> transfer motion on the SHSZ, <u>Caledonian</u> brittle thrusting on the OHFZ.
	C) <u>Precambrian</u> ductile thrusting on the OHFZ, <u>Precambrian to Caledonian</u> apparent lateral displacement on the SHSZ, <u>Caledonian</u> brittle thrusting on the OHFZ.
	D) <u>Early Caledonian</u> ductile thrusting on the OHFZ, <u>mid-Caledonian</u> apparent lateral displacement on the SHSZ, <u>late Caledonian</u> brittle thrusting on the OHFZ

Table 5.2. Four alternative kinematic models for interaction between the OHFZ and the SHSZ. A Caledonian age for brittle thrusting is assumed, based on Kelley et al. (1994).

In the absence of isotopic age dates for *both* ductile and brittle thrusting along the OHFZ, an alternative method of determining whether one or two thrusting events occurred must be sought. In either scenario, some interaction between the OHFZ and the South Harris Shear Zones is implied, and examination of the kinematic evolution of the SHSZ may be the only way to discern whether one or two thrusting episodes occurred. If one thrusting episode occurred, a very specific movement vector on the SHSZ should be apparent: The northern segment (Lewis block) should not only be uplifted relative to the southern segment (Uist block), but should move sinistrally towards the NW, in order for the ductile mylonites to remain along strike from brittle rocks of the southern block. If two thrusting episodes occurred, dip-slip or strike-slip motion may be apparent on the SHSZ, provided that the ductile mylonites are displaced to a region of no exposure (offshore?).

5.3.2 A preliminary investigation of the kinematic evolution of the SHSZ

South Harris is one of the most geologically complex regions in the Outer Hebrides, and has been documented at length by several workers (e.g. Jehu and Craig 1927, Dearnley 1963, Coward et al. 1969, Myers 1971, Van Breemen et al. 1971,

Graham 1980, Cliff et al. 1983, and Fettes et al. 1992). Most of this work has concentrated on the South Harris Igneous Complex (briefly outlined in section 2.2.2), (e.g. Dearnley 1963), the granite-migmatite complex which occurs in the adjacent Grey Gneiss (Myers 1971), and the metasediments which bound the igneous complex (e.g. Coward et al. 1969). Comparatively little work has been concentrated on the shear zones of the South Harris region, with the exception of a detailed study by Graham (1980). The following account reports the results of a preliminary investigation of the region carried out during the present study. It is not intended to be a definitive account of the structural evolution of the region.

The South Harris shear zones occur within, and immediately adjacent to, the gneisses of the South Harris Igneous Complex (Fig. 5.7). There are two main shear zones in the region:

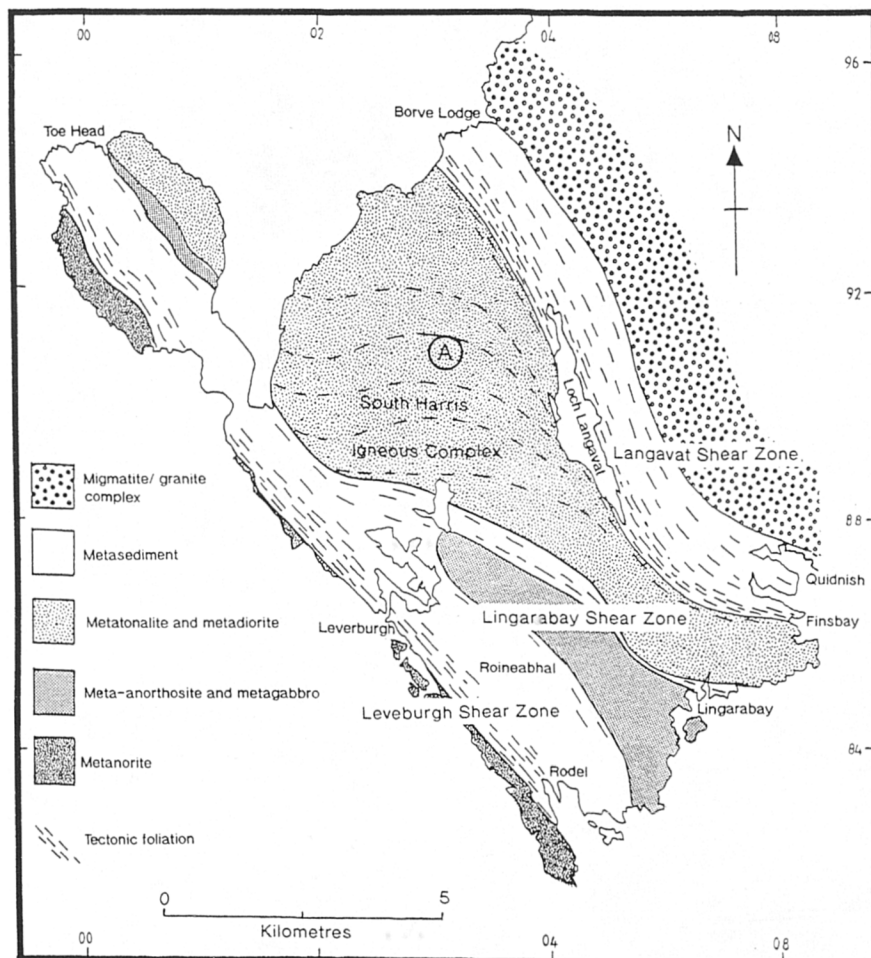


Figure 5.7 Geological map of the South Harris region (modified from Graham 1980 and Fettes et al. 1992).

1. The Langavat Shear Zone
2. The Leverburgh Shear Zone

These shear zones are steeply dipping, NW-SE trending structures, developed within the Langavat Belt metasediments and the Leverburgh Belt metasediments, which respectively form the NW and SE flanks of the igneous complex. The Leverburgh Shear Zone is subordinate to the Langavat Shear Zone in both lateral extent and thickness, but both can be traced laterally for c. 10 - 12km. The metasediments which host the shear zones are gneissose or schistose and include marbles, calc-silicate gneisses, psammites, pelites and semi-pelites (Coward et al. 1969). They are often characterised by an ochre weathering colour, due to the oxidation of iron. The paragneisses are not described at length here and the reader should refer to the work of Dearnley (1963) and Coward et al. (1969) for detailed lithological descriptions of the constituent units.

A third, similarly oriented shear zone occurs in the Lingarabay region (NG 062853), *within* the igneous complex, separating the meta-anorthosite and metagabbros of the Roineabhal region (NG 040860) to the SW, from the metatonolite and metadiorite which constitute the bulk of the rest of the complex to the NE. This shear zone is subordinate to those developed in the paragneisses, and will not be discussed here, (see Graham 1980 for a full discussion).

The paragneiss-hosted shear zones have variable dimensions, but typically form belts of flaggy, ductile mylonites and protomylonites between 1 and 2 km thick. These are often colour banded reflecting the highly variable composition of the protolith. The strong foliation is usually defined by elongate quartz/ feldspar aggregates and/ or aligned amphiboles. The kinematic history of the two main shear zones is different and each is described separately below. In each description, two phases of motion are recognised. The terms 'early' and 'late' are applied to distinguish between the *overprinted* and the *overprinting* deformations.

The Langavat Shear Zone

'Early' movement

The Langavat shear Zone trends NW-SE from Borge Lodge (NG 035950) to N of Finsbay (NG 080870), undergoing a sigmoidal strike-swing between Loch Langavat (NG 055890) and Quidnish (NG 090870) (Fig. 5.7). The fabric within the shear zone, defined by quartzofeldspathic and amphibolitic banding, and made fissile by the

abundance of muscovite and biotite, is subvertical or dips steeply SW. It often possesses a well defined mineral elongation lineation, defined by aligned hornblendes, and occasionally elongate quartzo-feldspathic aggregates and quartz ribbons, plunging at moderate angles towards the SE (Fig. 5.8) (Plate 5.1a). This lineation is believed to represent the movement vector of the shear zone during early deformation. The assemblages present in this shear zone are rich in biotite, muscovite, epidote and hornblende (see Coward et al. 1969 for a full petrological description), and are consistent with deformation at amphibolite facies. The assemblages also contain plagioclase (andesine or oligoclase) which deforms in a ductile manner, suggesting that P/T conditions of at least amphibolite facies prevailed (Fitz Gerald and Stunitz 1993).

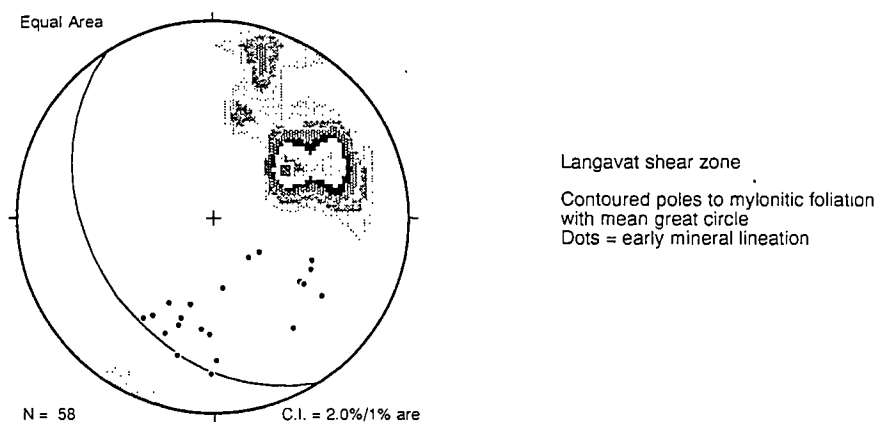
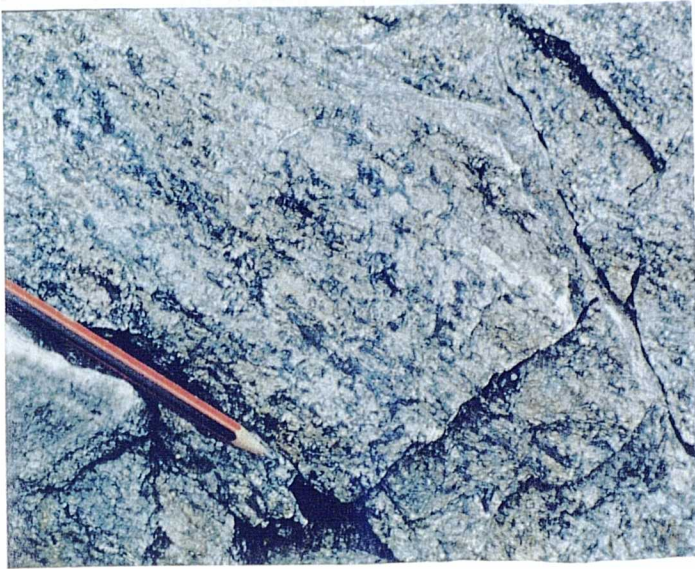


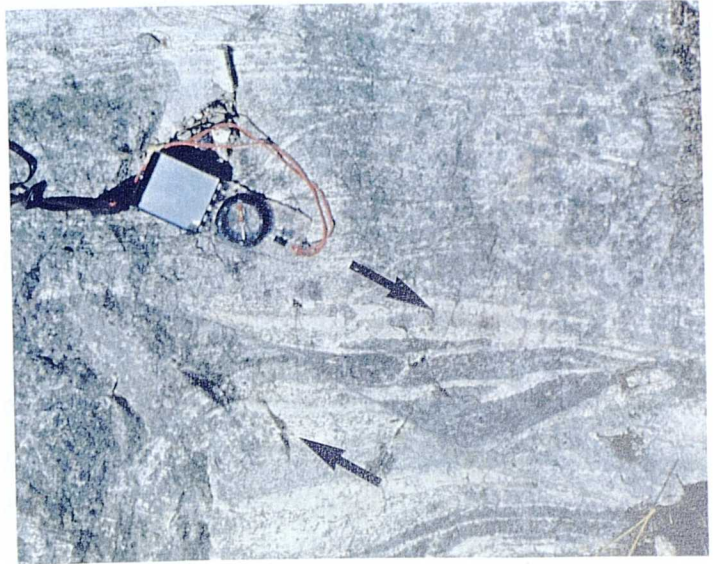
Figure 5.8 Equal area stereonet showing contoured poles to mylonitic foliation and 'early' mineral lineation (dots), from Langavat shear zone.

Shear-sense indicators are common in the Langavat Shear Zone and include small cm-scale shear zones with offset marker bands (Plate 5.1b), and/or an asymmetric foliation swing and asymmetric folds, e.g. at (NG 056883). Most kinematic indicators suggest that oblique dextral/ reverse motion occurred, consistent with previous interpretations (e.g. Coward 1984). Graham (1980) suggests that a dextral displacement of at least 14 km occurred on the Langavat Shear Zone, based on the angular relationship between the shear plane and a reoriented earlier fabric (marked A on Fig. 5.7) which he regarded as Scourian igneous layering, and entirely earlier than the dextral motion event. This estimate should be treated with caution however, for three reasons:

1. The model assumes dextral simple shear, whilst many of the included tectonic pods show apparent flattening (Graham 1980).



a)



b)



c)



d)

Plate 5.1 Langavat Shear Zone

a) Early, SE-plunging mineral stretching lineation defined by aligned hornblendes in mylonites of the Langavat Shear Zone (from NG 069863).

b) Dextral shear indicated by offset mafic marker bands during 'early' motion on the Langavat Shear Zone (from NG 069863).

c) Late, NW-plunging slickenfibres in the mylonites of the Langavat Shear Zone (from NG 070865).

d) Non-rotated σ porphyroblast of feldspar in mylonitised Laxfordian pegmatite from the Langavat Shear Zone (from 056878).

2. The model assumes a purely strike-slip movement vector. This is thought to be unlikely because the associated mineral lineation has a significant amount of plunge. The present work has shown that the shear zone has accommodated probable oblique dextral/ reverse motion.
3. The model assumes a single phase of deformation when at least one phase of reactivation has occurred (see below, and Coward and Park 1987).

'Late' movement

A later phase of lower grade reactivation is indicated by the widespread presence of a new overprinting mineral elongation lineation defined by aligned epidote and chlorite fibres (e.g. at NG 070865), and/ or a slickenfibres growth (Plate 5.1c). These lineations occur on existing foliation surfaces, phyllosilicate-rich, discrete, cm-scale mylonitic zones, and concordant brittle and semi-brittle faults. The new lineations have a markedly different orientation from the earlier lineation. Chlorite fibres, possibly derived from hydrated amphibole and indicative of low-greenschist facies retrograde metamorphism, plunge moderately NW (Fig. 5.9). Biotite is occasionally present (e.g. at NG 069863) and suggests metamorphic grades may have been locally higher. In contrast to the 'early' deformation, plagioclase deforms in a brittle manner, forming fractured and rounded porphyroclasts in a ductile quartz/ phyllosilicate-rich matrix. This suggests that P/T conditions did not exceed greenschist facies (Burg et al. 1984, Obee and White 1985). Mylonitised (ribboned) quartz is often 'blackened' as a result of high dislocation densities ('cold working') within grains.

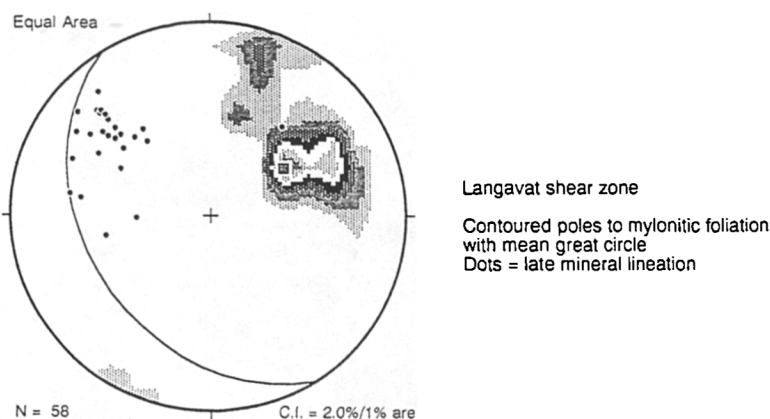


Figure 5.9 Equal area stereonet showing contoured poles to mylonitic foliation and 'late' mineral lineation (dots), from Langavat shear zone.

Kinematic indicators, include asymmetric shear bands (e.g. at NG 069863), asymmetric wrapping of non-rotated σ porphyroclasts and rotated δ porphyroclasts (e.g. at NG 069864 and NG 056878; Plate 5.1d), displaced markers and rare C-S fabrics. These are consistent with dextral oblique normal motion, causing the NE side of the shear zone to be uplifted relative to the SW side.

Very occasionally (e.g. at NG 069874), cm-scale, SE-dipping, brittle faults are present in the Langavat metasediments which host concordant, pseudotachylite fault and injection veins. The sense of shear, demonstrated by the asymmetry of pseudotachylite-bearing T-fractures relative to the fault surface along these veins, is consistent with normal motion to the SW. It is not known whether this brittle deformation occurred coevally with the 'late' deformation described above, but no evidence to contradict this possibility has been found. The exact timing of the 'early' and 'late' motion events on the Langavat Shear Zone are discussed below.

The Leverburgh Shear Zone

'Early' movement

The Leverburgh Shear Zone stretches NW-SE from Toe Head (NF 955946) to Rodel (NG 048828), and is subvertical or dips steeply NE. The well foliated, flaggy, mylonitic rocks which form the shear zone do not undergo the sigmoidal strike swing noted in the Langavat belt. The metamorphic assemblages are comparable to that of the Langavat belt during 'early' deformation, being quartzo-feldspathic, and rich in hornblende, garnet and epidote. Garnets (up to 1cm across) are often wrapped by quartz and feldspar aggregates. A linear fabric is present on some mylonitic surfaces and is defined by elongate quartz-feldspar aggregates and aligned hornblendes (Plate 5.2a). This lineation plunges moderately to the SE. (Fig. 5.10). Graham (1980) does not take account of the plunge component of this mineral lineation and assumes pure strike-slip motion to have affected the belt. Shear sense indicators associated with the plunging lineation include cm-scale asymmetric shear band fabrics, displaced marker bands, σ and δ wrapping of asymmetric porphyroclasts and cm-scale asymmetric folds. Graham (1980), notes the dominance of sinistral shear asymmetry over dextral in the Leverburgh Shear Zone but most kinematic evidence suggests that oblique sinistral/ reverse motion occurred.

The metamorphic conditions during shear zone deformation approximate amphibolite facies, although granulite facies assemblages are present in adjacent metagneous rocks (metanorite to the SW and meta-anorthosite to the NE). In the



Plate 5.2 Leverburgh Shear Zone

a) Early, SE plunging mineral elongation lineation in mylonites of the Leverburgh Shear Zone (from NG 053841).

b) Late NW-plunging slickenfibres lineation in the mylonites of the Leverburgh Shear Zone (from NG 018859).

c) Concordant fault vein of pseudotachylite in the mylonites of the Leverburgh Shear Zone (from NG 021855).

Langavat region, granulite facies assemblages in the igneous rocks undergo northeastward retrogression to amphibolite facies, so that within the shear zone itself, no evidence for the higher grade is preserved. By contrast, in the Leverburgh metasediments, localised regions of granulite facies assemblages *are* preserved (Coward et al. 1969).

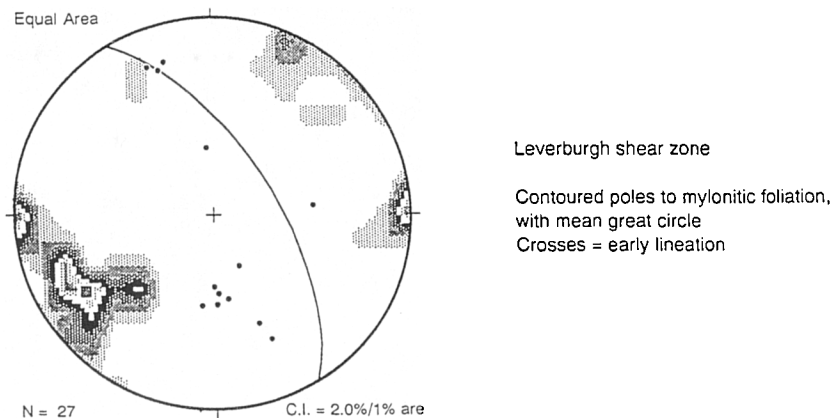


Figure 5.10 Equal area stereonet showing contoured poles to mylonitic foliation and 'early' mineral lineation (dots), from Leverburgh shear zone.

'Late' movement

The Leverburgh shear Zone has also undergone some degree of reactivation under lower P/T conditions. A new, moderately NW-plunging mineral elongation lineation and/or slickenfibres orientation, defined by fibrous chlorite and commonly epidote, is widespread and overprints the earlier lineation on existing foliation surfaces. (Fig. 5.11) (Plate 5.2b). Kinematic indicators parallel to this lineation, including asymmetric shear bands, displaced markers and slickenfibres asperities, show that an oblique dextral motion occurred, accompanied by a component of apparent reverse motion. This caused the NE side of the shear zone to be uplifted relative to the SW side, consistent with the movement sense from the similar, low greenschist facies fabrics in the Langavat belt.

Pseudotachylite is also present in the paragneisses of the Leverburgh Shear Zone in veins up to 5 cm thick (Plate 5.2c). These usually occur on concordant, NE-dipping brittle faults developed within the well-foliated mylonites. Discordant injection veins in T-shear orientations indicate reverse (NE side-up) motion. Although the development of pseudotachylite has not been proved to be synchronous with the 'late'

deformation described above, these pseudotachylite veins, by nature of their orientation and shear sense, are not thought to relate to the extensive brittle crushing in the SE part of the anorthosite body (e.g. at NG 060835). The pseudotachylites present in the latter region have been attributed to the onshore development of the OHFZ (Macaudiere and Brown 1982).

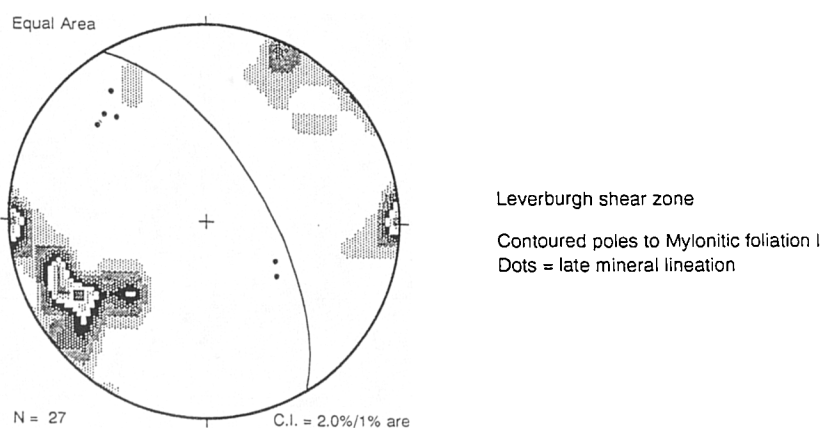


Figure 5.11 Equal area stereonet showing contoured poles to mylonitic foliation and 'late' mineral lineation (dots), from Leverburgh shear zone.

The relative timing of movements

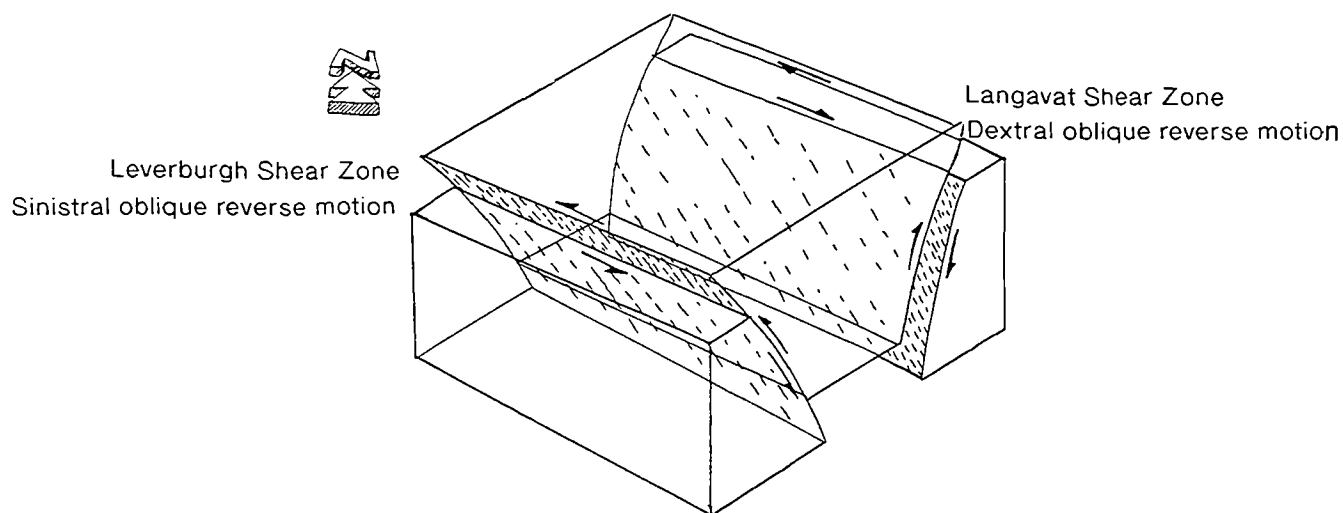
Although no conclusive evidence has been found which proves that early amphibolite facies motion on the Langavat Shear Zone occurred synchronously with early amphibolite facies motion on the Leverburgh Shear Zone, the common movement vectors and metamorphic state suggests that a roughly contemporaneous displacement is likely (Fig. 5.12a). Similarly, greenschist facies movements on both shear zones are also thought to be roughly the same age (Fig. 5.12b).

The age of early, bulk compressional motion under amphibolite facies (model A), causing oblique dextral/ reverse motion on the Langavat belt, and oblique sinistral reverse motion on the Leverburgh belt, can be constrained by cross-cutting relationships with igneous intrusions. The bulk of the preserved shear zone structures are younger than the age of emplacement of the South Harris Igneous Complex but older than the intrusion of Laxfordian pegmatites. This relationship is exemplified by:

- The presence of SE-plunging mineral stretching lineations and dextral amphibolite facies kinematic indicators on metagabbroic pods and slivers within the Langavat Shear Zone (e.g. south of Finsbay at NG 072865 and E of Loch Langavat NG

055883), suggesting that emplacement of the igneous complex preceded deformation.

A 1) Early compressional event



B 2) Later extensional/dextral event

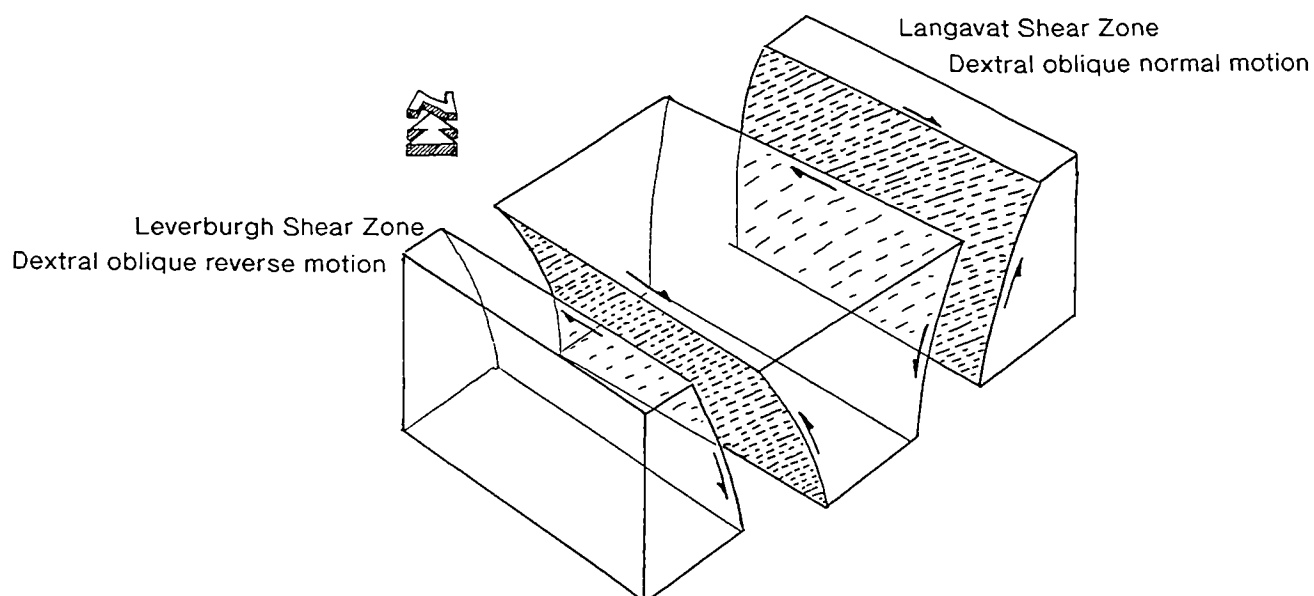


Figure 5.12 Schematic block diagrams illustrating: A) 'Early' movements on the Langavat and Leverburgh shear zones; and B) 'Late' movements on the Langavat and Leverburgh shear zones.

- The presence of undeformed pegmatites cross-cutting deformed paragneisses close to Finsbay church (NG 076871). A SE plunging mineral lineation is *never* observed in deformed pegmatites, suggesting that this phase of deformation preceded pegmatite intrusion. Some authors (e.g. Coward 1984) consider the intrusion of the late Laxfordian granite injection complex to have resulted from melting of the Lewisian in the thickened region beneath the shear zone.

'Early' deformation on the Langavat belt therefore occurred between the late Scourian (c. 2250) and the late Laxfordian (c. 1700 Ma). An early Laxfordian age of deformation is favoured by some authors (e.g. Coward 1984, Coward and Park 1987), based on the age of the earliest high strain fabrics in the igneous complex (marked A on Fig. 5.7). These fabrics preserve granulite facies metamorphic assemblages. The age of the granulite facies metamorphism has been dated at c. 1900 Ma (early Laxfordian), using Sm-Nd isotopes (Cliff et al. 1983). Coward (1984) regards the early high strain fabric as generated during shear zone movement, and therefore suggests that early motion on the shear zones is probably early Laxfordian.

The shear belts are probably most likely to have initiated in the Inverian (c. 2600 Ma), consistent with the interpreted ages for similarly oriented shear zones in mainland Scotland (Coward and Park 1987). The igneous complex was emplaced at least 350 Ma later, between 2250 and 1840 Ma. (Cliff et al. 1983) and the shear zones may have therefore acted as a major controlling element on the evolution of the South Harris Igneous Complex.

The later bulk extensional motion (*model B*), causing *oblique dextral*/ *normal* motion with SW-side-down, on the Langavat Shear Zone, is somewhat ambiguous. Coward and Park (1987) regard this motion as late Laxfordian. Pegmatites, interpreted as late Laxfordian in age, are often severely deformed by, and may even focus, this phase of deformation, e.g. south of Loch Langavat (NG 056878), suggesting that deformation must be synchronous with, or post-date, late Laxfordian granite/ pegmatite intrusion (c. 1400 Ma). No evidence has been found which suggests that this motion predates pegmatite intrusion, and Coward and Park's interpretation can not be confirmed.

Evidence for post-Laxfordian deformation has been cited by Cliff and Rex (1989). These authors present evidence from a Rb-Sr biotite age study, along a 50 km traverse across the northern Outer Hebrides, which implies that kilometre-scale vertical displacements may have occurred on the Langavat Shear Zone at around 1100 Ma.

Their evidence shows that biotites south of the Langavat Shear Zone (including the South Harris Igneous Complex), have been reset at ages older than 1300 Ma (late Laxfordian). By contrast, biotite ages to the north of the Langavat shear zone, are close to 1100 Ma (ranging from 950 Ma to 1210 Ma). It therefore appears that only the northern block of the Outer Hebrides (including north Harris and Lewis) *shows evidence for a* reheating event at around 1100 Ma, which reset the biotite ages. Differential uplift of the northern block, via NE-side-up motion on the Langavat Shear Zone, has the correct sense of motion to account for the 200 Ma. jump in biotite ages. In addition to the two Laxfordian events on the SHSZ proposed by Coward and Park (1987), Cliff and Rex (1989) suggest a third, Grenvillian motion event, is necessary to account for biotite age jump.

There seems little evidence to support the argument that three (Laxfordian or younger) movement events occurred on the Langavat shear zone. There also seems little evidence to suggest that the 'late' SHSZ movement event was late Laxfordian in age. The present study proposes that the 'late' event was not late Laxfordian (cf. Coward 1984 and Coward and Park 1987), but Grenvillian (c. 1100 Ma) consistent with the isotopic evidence cited by Cliff and Rex (1989).

The revised chronology of South Harris deformation events can therefore be summarised as follows:

1. Inverian (c. 2600 Ma) inception of the NW-SE-trending SHSZ, similar to shear zones in mainland Scotland. No kinematic evidence of this episode is preserved;
2. South Harris Igneous Complex emplacement in the late Scourian (c. 2250 -1840 Ma) (Cliff et al 1983), with a possible early igneous fabric with granulite facies assemblages (Graham 1980);
3. Early Laxfordian (c. 1900 Ma) bulk compression on the SHSZ, causing oblique dextral/ reverse motion on the Langavat shear zone and oblique sinistral/ reverse motion on the Leverburgh Shear Zone at amphibolite facies (Fig. 5.12a);
4. Grenvillian (c. 1100 Ma) bulk extension on the SHSZ, causing km-scale oblique dextral/ normal motion on the Langavat shear Zone and oblique dextral/ reverse motion on the Leverburgh Shear Zone at low greenschist facies. This phase of motion causes differential uplift of the NE side (the northern segment of the outer Hebrides) (Fig. 5.12b)

5.3.3 An integrated kinematic model for the OHFZ and SHSZ interaction

The kinematic information provided by the South Harris Shear zones can be used to elucidate whether one or two thrusting events occurred on the OHFZ.

In order to account for syn-thrust *transfer* and uplift of the northern segment of the OHFZ (Table 5.2, models A and B) (see section 5.3.1), a very specific movement vector on the SHSZ is required. The mineral lineation associated with this movement should plunge SE and displacement should combine sinistral, and 'NE-side-up' motion, so that ductile and brittle deformation of the northern segment lies directly along-strike from brittle deformation in the southern segment (see Fig. 5.6a). The kinematic histories of the Langavat and Leverburgh Shear Zones, are incompatible with this requirement (see Fig. 5.12 a and b).

It can be argued that sinistral/ 'NE-side-up' motion is possible during the 'early' (amphibolite grade), phase of SHSZ motion, provided that more displacement occurs on the Leverburgh Shear Zone than on the Langavat Shear Zone. However, the early ductile thrusting on the OHFZ is constrained by cross-cutting relationships with Laxfordian pegmatites (see section 3.2.5), and can not occur before the late Laxfordian (c. 1700 Ma). Early SHSZ motion (which is thought to be early Laxfordian) therefore pre-dates early ductile thrusting along the OHFZ.

These observations have several important implications regarding the four possible OHFZ-SHSZ interaction models (Table 5.2):

- A single progressive thrusting event on the OHFZ (model 'A') is extremely unlikely;
- Models involving transfer motion on the SHSZ synchronous with thrusting on the OHFZ (model 'B') are impossible to accommodate using the kinematic evidence;
- Oblique-slip motion on the SHSZ must therefore separate *two* distinct thrust motion phases on the OHFZ.

The age of ductile thrusting may therefore be Precambrian to Caledonian (model C) or Caledonian (model D) (see table 5.2). However, the latter is thought to be unlikely because no equivalent Caledonian structures of this orientation occur elsewhere in the UK. As noted previously, published Rb-Sr age dates for Lewisian basement in the Outer Hebrides (Cliff and Rex 1989), show a marked change in age across the Langavat Shear Zone. These authors suggest that km-scale dip-slip displacements on the Langavat Shear Zone during the Grenville 'event' at c. 1100 Ma, would account for the younger age dates in the differentially uplifted northern Outer Hebrides. The 'late'

kinematic history of the SHSZ, including the Langavat Shear Zone, (Fig. 5.12b), has the correct sense of displacement to account for the age jump. I propose therefore, that the ductile, thrust-related mylonites were displaced by this late (Grenvillian) movement on the SHSZ, and would favour a model C in which Precambrian age (1700-1100Ma), ductile, thrust-sense mylonites in the southern segment of the OHFZ were displaced dextrally to a region of no exposure, probably offshore to the west. The differential exhumation of the northern block of the Outer Hebrides during the Grenville event could also provide a source for the Torridonian sediments to the SE (Cliff and Rex 1989), and may explain the occasional presence of Grenville age detritus within the Torridonian of mainland Scotland (Moorbath et al. 1967).

The revised kinematic history of the OHFZ and its interaction with the South Harris Shear Zones are summarised in Table 5.3.

Structure	Movement sense	Fault products	Metamorphic grade	Age of motion
SHSZ	Oblique dextral / reverse on Langavat SZ and oblique sinistral reverse on Leverburgh SZ	Platy mylonites	Amphibolite facies (very locally granulite facies)	c. 1900 Ma (early Laxfordian)
OHFZ	Top-to-the-NW ductile thrusting not exposed in the southern segment due to subsequent SHSZ displacement	Platy mylonites	High Greenschist facies	between c. 1700 Ma (late Laxfordian) and c. 1100 Ma (Grenvillian)
SHSZ	Oblique dextral / normal motion on the Langavat SZ and oblique dextral reverse motion on the Leverburgh SZ	Overprinting linear fabrics on ductile mylonite foliations. pseudotachylite very locally	Low greenschist facies	c. 1100 MA (Grenvillian)
OHFZ	Top-to-the NW brittle thrusting	Cataclasites and pseudotachylites	Low greenschist facies	c. 430 Ma (Caledonian)
OHFZ	Top-to-the-NE ductile sinistral strike-slip	Platy phyllonites	Low greenschist facies	Post-430 Ma ? Caledonian
OHFZ	Top to the S, or SE, low-angle, brittle-ductile extension	Faults and folds in existing foliated rocks especially phyllonites	Low greenschist facies	Late Caledonian
OHFZ	Top to the E or NE, high-angle brittle extension	Steep brittle faults	? Near surface	Mesozoic (Permo-Triassic)

Table 5.3 An integrated kinematic history for the OHFZ and SHSZ, based on the present work and previously published age dates.

It is conceivable that displacements other than those shown in Table 5.3 may have occurred along the OHFZ. Most authors (e.g. Binns et al. 1974, 1975, Blundell 1984, Stein 1988, O'Neill and England, 1994) suggest a large thickness of Torridonian exists offshore and at depth below the Sea of The Hebrides Basin. Although the presence of this unit is not thought to relate to syn-depositional movements on the OHFZ (see Nicholson 1992 and O'Neill and England 1994), these offshore data suggest that Caledonian thrusting on the OHFZ was relatively minor (see section 5.4.2.

5.4 Estimates of displacement magnitudes on the OHFZ

5.4.1 Ductile thrust displacements

Previous attempts to quantify the amount of displacement in the ductile rocks of the OHFZ, have relied upon the shape of deformed strain markers (e.g. Sibson 1977b), especially amphibolitic boudins. *Sibson's estimate for finite thrust displacement of 10 +/- 5 km*, is regarded as unreliable for three reasons:

1. The pre-deformation shape of the strain markers is assumed to be spherical, whereas most amphibolites in unmylonitised Lewisian banded gneiss often have large aspect ratios.
2. The estimates are based on simple shear models. Apparent flattening of the boudins suggest a significant amount of layer-parallel extension may have occurred (see sections 3.2.1 and 3.2.2).
3. Strain is markedly heterogeneous throughout the belt.

Nevertheless, the mylonite belt is a major structural feature, achieving thicknesses of up to 600 m on Scalpay. A direct correlation between mylonite thickness and displacement is difficult to quantify due to the heterogeneous nature of the deformation, but displacements in the order of several kilometres are thought to be likely based on comparisons with mylonite zones associated with major fault zones of known displacements elsewhere (Hobbs et al. 1976).

5.4.2 Brittle Thrust displacements

The absence of stratigraphic marker horizons associated with the OHFZ make estimates of displacement difficult. Large-scale structures which are present in the footwall rocks are rarely present in the hangingwall rocks, and for this reason direct estimates of displacements have been confined to regions where these occur. Estimates based on the displacement of a Laxfordian F3 fold axis have been suggested by previous workers for the Barra region (Francis 1969, Francis 1973, Francis and Sibson 1973) (see section 2.4.2). This estimate suggests that c. 4. - 8 km of displacement has occurred. There are problems with this reconstruction however:

- There is no evidence to suggest that the two displaced axes were at one time part of the same fold structure that was continuous across the fault;
- This finite displacement estimate assumes the most direct route between the two displaced markers;
- The extent to which normal motion has reactivated the major thrust of the region is not considered
- The displacement estimate requires c. 30° of clockwise hangingwall rotation, and examination of gneissose banding from footwall and hangingwall country rocks (see discussion in section 4.2.12) suggests that no rotation has occurred.
- There is some doubt about the exact fault zone trace in Barra (see discussion in section 4.2.12), with the consequence that the fold axes are probably two entirely different structures, both of which occur in the hangingwall meaning that they do not traverse the fault trace.

Coward (1969) approached the same problem differently. He estimated that E-W shortening in the S. Uist region must have been at least 2 - 3 km, based on the thickness of pseudotachylite and ultracataclasite crush zones. Although the thickness/displacement ratio is not a particularly reliable indication of finite displacement, a brittle displacement in the order of several kilometres is regarded as likely, based on the difference in metamorphic grade of gneisses across the fault. It is important to stress that brittle thrust deformation along the OHFZ cannot be large because Torridonian sediments occur in the hangingwall region presently beneath the Sea of the Hebrides Basin (see section 5.3.3). If brittle deformation was in the order of several kilometres, the Torridonian should have been displaced and eroded.

5.4.3 Sinistral strike-slip displacements

Several previous studies have attempted to quantify the apparent mismatch and offset of mainland Lewisian structures with Lewisian structures in the Outer Hebrides (e.g. Dearnley 1962, Francis 1969, Coward 1969, Coward and Park 1987, Piper 1992 and Lisle 1992). A major sinistral displacement along the (unexposed) Minch Fault has usually been cited as a probable cause for such displacement. The present study reveals for the first time that a sinistral strike-slip movement phase did ^{occur} along the onshore trace of the OHFZ. In the revised structural chronology, the inception of the Minch Fault post-dates strike-slip motion, so most of the strike-slip displacements are probably accommodated along the OHFZ and *not* the Minch Fault.

The following strike-slip estimate is based on a re-evaluation of regional correlations across the Minch proposed by previous workers (summarised in Table 5.4).

	Displacement estimate	Evidence for displacement	Stated or implied correlations of S. Harris shear zones with mainland shear zones
Dearnley (1962)	c. 125 km	Regional correlation of 3 metamorphic zones in mainland Scotland (Sutton and Watson 1951 with 3 metamorphic zones in the Outer Hebrides)	Langavat Shear Zone correlated with Laxford Shear Zone
Park (1962), in discussion of Dearnley (1962)	c. 60 km	Regional correlation of major dextral shear zones and large early Proterozoic basic masses	South Harris Shear Zones correlated with Gairloch Shear Zone
Coward and Park (1987)	none	Lack of correspondence between flanking zones either side of Gairloch and S.Harris Shear Zones, and a necessity for 'too great a strike-slip displacement in the Minch'	South Harris shear zones correlated with a region of no Lewisian exposure in Skye
Piper (1992)	95 km	Comparison of populations of Paleomagnetic components	Langavat Shear Zone correlated with Laxford Shear Zone. Leverburgh Shear Zone correlated with Canisp Shear Zone
Lisle (1993)	34-145 km (best estimate is 84 km)	Regional correlation of Scourie dyke trends	None stated, but South Harris Shear Zones lie roughly along strike from Canisp Shear Zone

Table 5.4. Previous work on attempted correlations of regional structures across the Minch.

Re-examination of the published evidence shows that there are only four, main, viable, along-strike correlations of the South Harris Shear zones with mainland Shear Zones (Fig. 5.13 a,b,c and d).

These are:

1. Correlation with unexposed basement in Skye (e.g. Coward and Park 1987), Fig. 5.13a;
2. Correlation with the Canisp Shear Zone (e.g. Piper 1992), Fig. 5.13b;
3. Correlation with the Laxford shear Zone (e.g. Dearnley 1962), Fig. 5.13c;
4. Correlation with the Gairloch shear Zone (e.g. Park 1962), Fig. 5.13d;

A correlation of the South Harris shear zones with unexposed basement under the Tertiary cover sequence of Skye (i.e. the present day position, Fig. 5.13a) has the consequence of positioning the mainland Gairloch and Diabaig Shear Zones along strike from Lewis where no NW-SE trending shear zones are exposed. Coward and Park (1987) suggest that the Outer Hebrides block is a major shear zone 'flat' which has been uplifted relative to the mainland, and that the mainland shear zones are lateral ramps which root into this region. Note that the postulated shear zone flat would have to be a Laxfordian or older structure, therefore pre-dating the (post-1700 Ma) ductile thrust mylonites of the OHFZ. No evidence to either support or discount this interpretation has been found.

A correlation between the South Harris Shear Zones and the Canisp Shear Zone (Fig. 5.13b) seems unlikely. Attfield (1987) reports two major phases of motion on the Canisp Shear Zone, the latter of which occurred in the Laxfordian. The sense of shear on this structure at this time is interpreted to be largely dextral strike-slip with a small downthrow to the N, consistent with the sense of shear on the Langavat Shear Zone during the 'early' phase of motion in the early Laxfordian. No evidence is reported by Attfield (1987), however, for a later, dextral/ oblique NE-side-up motion event on the Canisp Shear Zone, and the absence of this event makes the correlation suspect.

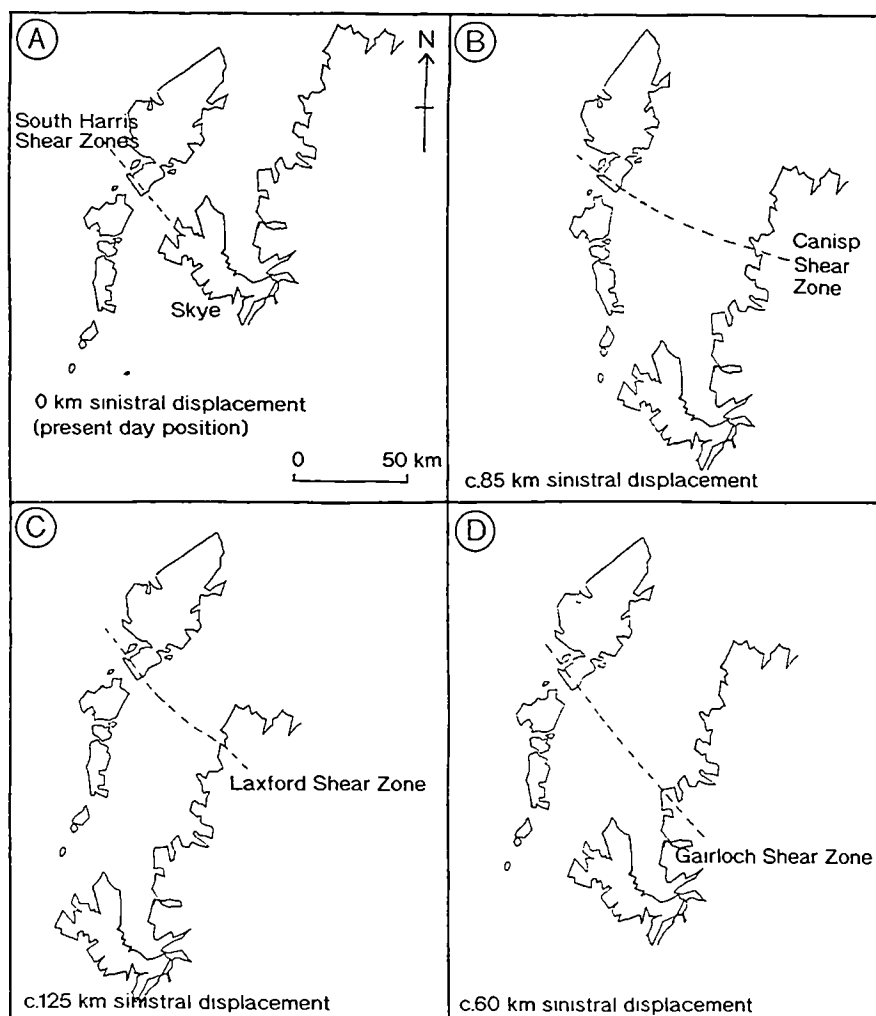


Figure 5.13 Four possible regional correlations of the South Harris Shear Zones across the Minch.

A correlation between the South Harris Shear Zones and the Laxford Shear Zone (Fig. 5.13c) is regarded as extremely unlikely. Beach et al. (1974) and Coward (1984) report a sinistral/ oblique normal sense-of-shear with a 'S-side down' component on this structure. This is inconsistent with any of the deformation events observed in the South Harris region. In addition, a large-scale Laxfordian synform adjacent to the South Harris Shear Zones (the South Harris synformal zone), does not correspond well to the marginal zones of intense deformation along the Laxford Shear Zone (Coward et al. 1970). In contrast, the folding next to the Laxford shear zone is interpreted as monoclinial rather than synformal (Sutton and Watson 1962). These interpretations imply that the South Harris Shear Zones and the Laxford Shear Zone are different structures.

Whilst a strike-slip displacement estimate along the OHFZ is inevitably speculative, the present work favours the interpretation of Park (1962), that the South Harris shear zones are the lateral continuation of the Gairloch Shear Zone (Fig. 5.13d), for several reasons, outlined below.

- The Gairloch region has patterns of high strain Laxfordian synforms (e.g. the Loch Maree synform) and low strain Laxfordian antiforms (e.g. Tollie antiform) which are comparable with those of the South Harris region (e.g. South Harris synformal zone) (Coward et al. 1970).
- Steeply dipping shear zones at Gairloch and Torridon, have a NW-SE trending mineral lineation and a dextral sense of shear (Park and Cresswell 1973), consistent with 'early' dextral motion on the Langavat shear zone.
- Later deformation on the Gairloch Shear Zone (between 1400 Ma and 1100 Ma), involved localised greenschist facies retrograde metamorphism, and cataclastic deformation with pseudotachylite development (Park et al. 1987). This is consistent with the interpreted Grenvillian age of retrograde greenschist facies metamorphism and pseudotachylite development from the South Harris Shear Zones.
- The mainland supracrustal rocks (the Loch Maree Group metavolcanics), lie directly along strike from the main belts of Outer Hebridean supracrustal rocks (the Langavat and Leverburgh belts), and published ages of the two units (O'Nions et al. 1983, Cliff 1989) suggest that they are broadly coeval.

A less direct approach to the problem of strike-slip displacement estimation also suggests that the Gairloch Shear Zone is the most likely along-strike continuation of the South Harris Shear Zones. This approach involves the sinistral displacement of the South Harris Igneous Complex, which does not crop out in mainland Scotland. If the shear zone bounded South Harris Igneous Complex is sinistrally displaced by the OHFZ during the Caledonian, it should occur several kilometres further north in the Minch. Commercial seismic reflection profiles shot along the long axis of the Minch, show that an upstanding ridge of Lewisian and Torridonian basement (the Mid-Minch High) occurs immediately along strike from the Gairloch/ Gruinard Bay region of the mainland (Stein 1988) (see section 2.8.2). Stein (1988) suggests that the Mid-Minch High is a NW-SE trending fault block bounded by Lewisian Shear Zones. He proposes that the northern margin of the basement high is the lateral continuation of the transition zone between granulite-grade Scourian rocks to the N and amphibolite grade

Laxfordian rocks to the S, and the southern margin of the basement 'high' is the lateral continuation of the Gairloch Shear Zone/ Loch Maree Fault. This gives rise to the possibility that the Mid-Minch High and bounding shear zones in the Gairloch region are the sinistrally displaced lateral continuations of the South Harris Igneous Complex and South Harris Shear Zones. Conclusive evidence is lacking but a sinistral displacement estimate_{including offshore movement} of c. 60 km is implied. This displacement estimate is well within the 90% confidence limits of Lisle (1993) who used the correlation of laterally variable Scourie dyke orientations to estimate the sinistral component of displacement at c. 84 km.

5.4.4 Extension estimates

it is difficult to separate the effects of early low-angle extensional 'collapse' from the effects of later, high angle normal faulting and basin formation. Direct estimates of extension rely primarily on seismic profiles, and are therefore likely to record the Mesozoic or younger extension responsible for the main phase of basin development. The amount of extension is probably variable along the length of the OHFZ (Brewer and Smythe 1986), but examination of existing seismic profiles from the Sea of Hebrides Basin suggests that extension is in the order of 1-2 km.

5.4.5 The relationship between fault kinematics and Caledonian plate motions

The kinematic history, which is mostly common to both segments of the OHFZ, (Fig. 5.1) appears to agree well with recent models of ancient plate motions during the Silurian and Devonian (Fig. 5.14a, b and c). During brittle thrust deformation on the OHFZ at c. 430 Ma (Kelley et al. 1994), Scotland occupied an area on the eastern Laurentian margin (Soper et al. 1992), separated from the western part of Baltica by the Northern Iapetus Ocean (Fig. 5.14a). The onset of convergence of these two continents in the early Silurian (c. 440 Ma) led to the closure of Iapetus, which continued into the late Silurian (c. 420 Ma). Mid-way through closure, the convergence of Laurentia and Baltica was markedly oblique, causing crustal scale imbrication and major sinistral strike-slip displacements on faults in Scandinavia, East Greenland and Scotland. The onset of sinistral strike-slip motion along the OHFZ, could very plausibly have occurred at this time. Gravitational collapse of the orogen in Scotland and Ireland is thought to have occurred around 400 Ma, after the completed docking of Avalonia and newly formed Laurussia (Laurentia and Baltica). Strike-slip movements at this time had effectively ceased. The onset of gravitationally induced 'collapse' structures along the OHFZ may have occurred at this time.

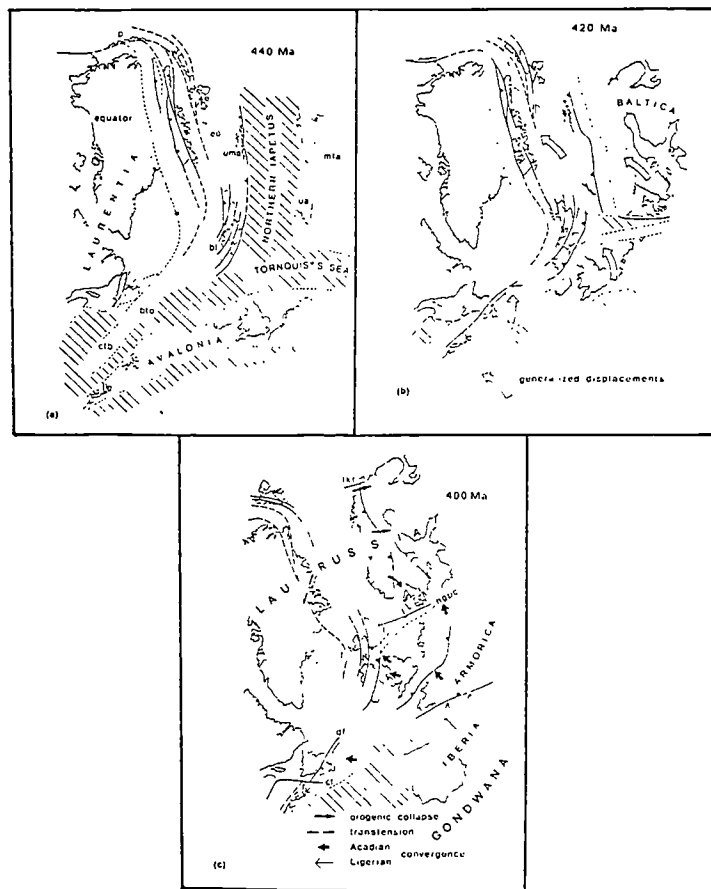


Figure 5.14 Cartoon reconstructions to illustrate the Silurian closure of Iapetus at: a) 440 Ma; b) 420 Ma; and c) 400 Ma. (from Soper et al. 1992).

5.5 Summary of the kinematic evolution of the OHFZ

- Inception of the OHFZ occurred between c. 1700 Ma (late Laxfordian) and c. 1100 Ma (Grenvillian). Initial movement was top-to-the-NW, ductile thrusting, forming platy, high greenschist facies mylonites. The extent of these mylonites is uncertain due to later displacement, but they are inferred to have occurred along the length of the Outer Hebrides.
- The early mylonites are inferred to have been cut into two segments at c. 1100 Ma (Grenvillian), by oblique dextral, 'south-side-down' displacements reactivating the South Harris Shear Zones. The northern segment of the Outer Hebrides (the Lewis and Harris block) was uplifted and may have provided a source area for Torridonian

sedimentation to the SE. The thrust-sense mylonites of the southern segment of the OHFZ were probably displaced to the NW^{towards the Atlantic,} are are presently unexposed.

- Subsequent thrusting on the OHFZ, at c. 430 Ma (Caledonian) caused the generation of widespread, brittle deformation, including catclasis and pseudotachylite generation. These low grade rocks were focused into the ductile mylonites of the northern segment, and also occur directly along-strike in the unmylonitised gneisses of the southern segment. The distribution of brittle thrusting can be described as forming three fault zone arcs, concave to the east, and not coinciding with the earlier segmentation of the fault zone. Displacements are not thought to be large because Torridonian sediments are inferred to be present in the fault zone hangingwall.
- A change of kinematics to sinistral strike-slip, probably during the late Caledonian (post-430 Ma), reactivated the brittle thrusts, mainly in the east of the fault zone, and mainly along the central arc. The change in kinematics was coincident with widespread fluid influx and retrogression, and belts of low-greenschist facies phyllonite were formed along several earlier brittle thrust zones.
- In the early Devonian (?), low-angle, top-to-the-S or SE, extensional movement (possibly connected with the gravitationally-induced collapse of the Caledonian orogen) mainly reactivated the phyllonite belts because of their absolute and relative weakness. This low-greenschist facies deformation produced extensional fault and fold packages in the phyllonites, and low angle brittle normal faults in other lithologies.
- The final stage of *onshore* reactivation was associated with top-to-the E or NE, steep, normal faulting in the Mesozoic. Permo-Triassic sedimentation was syn-tectonic with this event and formed the large offshore basins to the east. Subsequent normal faulting during the rest of the Mesozoic was concentrated offshore, on the hangingwall short-cut of the OHFZ; the Minch Fault.

Chapter Six

Possible causes of weakness and reactivation of the OHFZ

6.1 Introduction

Faults reactivate because they are weaker than the surrounding intact regions of crust. It is clear from the evidence presented in this thesis that the OHFZ has acted as a zone of crustal weakness for a long period of geological time. This weakness is manifested in three main ways:

- A repeated history of fault zone movement
- The focusing of most onshore extension into pre-existing discrete zones of phyllonite
- The apparent similarity between the offshore Mesozoic basin architecture and the geometry of the onshore fault zone

The purpose of this section is to briefly review the reasons why faults undergo weakening and to examine in greater detail, those weakening mechanisms which are pertinent to the OHFZ.

6.2 Why are faults weak?

Recent studies of the San Andreas Fault, a long-lived fault zone, have suggested that it is mechanically very weak, both in an *absolute* sense (moving under very low shear stresses), and in a *relative* sense (surrounded by much stronger crust) (Rice 1992).

If a hypothetical fault/shear zone traverses most of the crust, it will simultaneously exist in brittle (seismic), brittle-ductile, and ductile (aseismic) states at different depths (Fig. 6.1). As a result, there are likely to be several reasons why this fault/shear zone may remain weak. The most obvious method of considering these criteria is to separately discuss weakening mechanisms operating in the brittle (frictional) and ductile (quasi-plastic) regimes. This division is somewhat unrealistic however, since processes occurring in one regime may influence behaviour in the other, and several processes may occur together in the broad transition zone between the two.

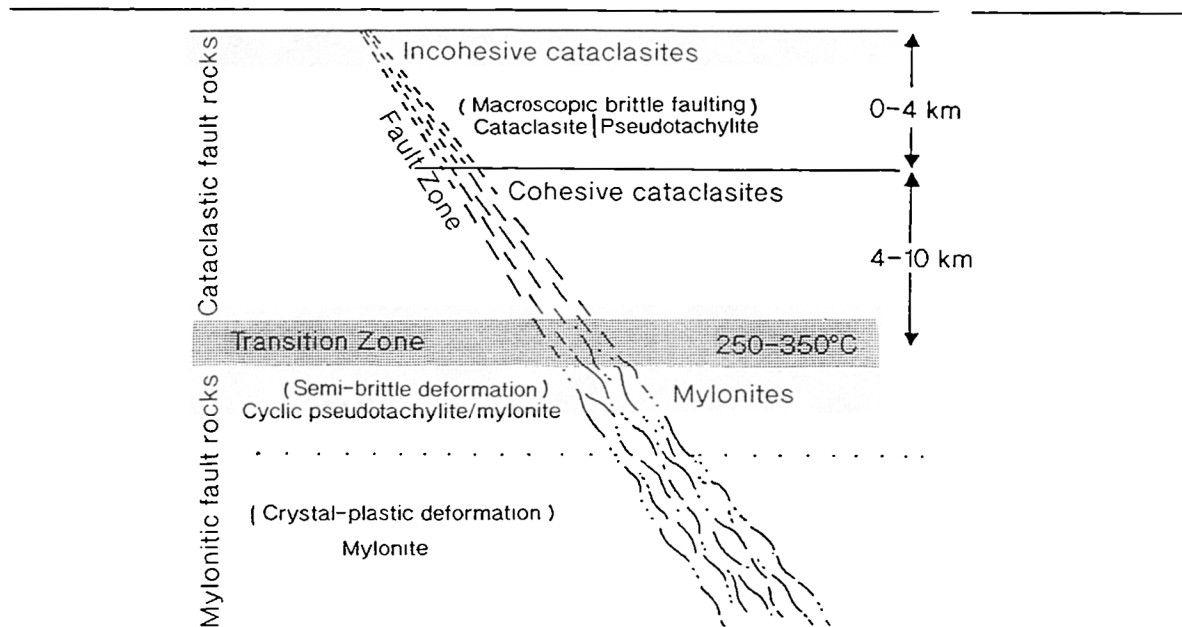


Figure 6.1. Hypothetical fault/shear zone showing the approximate depths and temperatures for different types of fault rock, and the brittle-ductile transition (modified from Sibson 1977b)

A more convenient division exists between *transient* weakening mechanisms which alter fault zone rheology at the time of deformation and *long-lived* weakening mechanisms which keep fault zones weak over long geological timescales. Table 6.1 shows the processes which alter fault zone rheology to favour reactivation.

Long-lived weakening mechanisms	Favourable orientation of a Pre-existing anisotropy
	Fabric softening and the formation of CPO's
	Grain size reduction
	Thermal perturbations
Transient weakening mechanisms	Fluid enhanced
	Permanent reaction softening
	Fluids required
	Permeability pathways
	Changes in pore fluid pressure
	Fluid assisted DMT
	Pore fluid chemistry
	Transient fine grained reaction products
Transient weakening mechanisms	The introduction of melt
	Shear heating
	Transformational plasticity

Table 6.1 Processes involved in the weakening of fault zone rheology, leading to fault zone reactivation. Transient and long-lived weakening mechanisms are separated and the processes which require, or are enhanced by the presence of fluids are highlighted.

6.2.1 Transient, syn-tectonic mechanisms of rheological change

According to the existing literature, most recently summarised by Rubie (1990), these transient mechanisms include:

1. Fluid -related processes:
 - a) Changes in pore fluid pressure
 - b) Fluid assisted diffusive mass transfer (DMT)
 - c) Pore fluid chemistry
2. The generation of transient fine grained reaction products
3. The introduction of melt
4. Shear heating
5. Transformational plasticity

1 Fluid related processes:

There is abundant evidence for hydrous fluid flux along the OHFZ at certain times during its evolution. During early ductile and later brittle thrusting, fluids were largely absent, as exemplified by the lack of syntectonic retrogression in the mylonites and cataclasites (see section 3.2.2) and the generation of large volumes of pseudotachylite, which many authors believe (e.g. Sibson 1977a), are indicative of dry conditions (see section 4.2.12 for a full discussion).

During subsequent strike-slip, however, large volumes of fluid are thought to have infiltrated the fault zone. The amphibolite facies mineral assemblages of the Lewisian gneisses which remained largely unaltered during thrusting were strongly retrogressed to low greenschist facies. The main mineralogical changes involve hydration reactions, such as the alteration of feldspars to white mica / epidote, and mafic minerals (e.g. hornblende) to chlorite. This retrogression is associated with phyllonitic fabrics which ultimately form a network of phyllonite belts. There is good geochemical evidence to suggest that retrogression was associated with the influx of hydrous fluids. Walker (1990) suggests that warm, aqueous fluids, rich in dissolved Fe and Mg were flushed through the brittle fault zone, depositing silica as they cooled. In addition, fibrous mineral overgrowth textures are widespread, suggesting that diffusive mass transfer (DMT) mechanisms were operative (see sections 3.3 and 4.3). There is good evidence to suggest that these DMT textures (and hence fluid influx) were syntectonic with respect to sinistral strike-slip displacements. In particular, fibrous growths of retrograde minerals that define strike-parallel stretching lineations in protophyllonites and phyllonites, have the same assemblages as formed by

retrogression in the phyllonites as a whole, i.e. an incongruent pressure solution microstructure (Beach 1982, Rubie 1990).

During later extension, the generation of tensional quartz veins is common, and requires both the presence of fluid and elevated pore fluid pressures. Elevated pore fluid pressures are also implied by the presence of tensionally fractured porphyroclasts, containing fibrous minerals. Thus, there is good evidence for the presence of widespread hydrous fluids during the strike-slip and low-angle extensional phases of movement along the OHFZ

a) Changes in Pore Fluid Pressure

Perhaps the most frequently cited cause of transient fault zone weakening is elevated pore fluid pressure. An increase in pore fluid pressure causes a decrease in the effective normal stress across the pre-existing surface, and therefore a decrease in the critical shear stress needed for frictional sliding. Thus, high pore fluid pressure in a pre-existing fault lowers the differential stress necessary to cause failure, which may occur in a stress state that is otherwise stable at zero pore fluid pressure (Byerlee 1978).

In the case of the San Andreas Fault, the pore pressure distribution is highest in the fault zone and decreases with distance into the adjacent crust. This is consistent with the observed *absolute* and *relative* weaknesses (Rice 1992) of this structure. In the OHFZ, high pore fluid pressures probably served to weaken the fault zone *during* sinistral strike-slip and extension, but it is difficult to explain the long term weakness of the OHFZ by this model, because an additional mechanism is required to maintain the high pore fluid pressure over a very long timespan from the first reactivation (Caledonian) to the last reactivation (Permo-Triassic). No such mechanism is known.

b) Fluid assisted Diffusive mass transfer

High pore fluid pressures have an indirect effect on the reactivation potential of a fault/shear zone by increasing the rates of mass transfer, diffusion and hydrolytic weakening, thereby reducing the shear strength of the material (Etheridge et al. 1984). When fluid is present under pressure, shear zones may deform by mass transfer mechanisms at lower shear stresses than the surrounding rock with a lower pore fluid pressure (Beach 1976). Given the widespread evidence for the operation of DMT processes in the phyllonites, the rates of these processes were probably enhanced during times of high pore fluid pressure on the OHFZ. Once again, however, it is

difficult to envisage how these processes would be important over the long term in the absence of a mechanism by which elevated pore fluid pressures may be maintained.

c) Pore Fluid Chemistry

The creep properties of minerals are sensitive to the metamorphic fluid environment (Brodie and Rutter 1985). In most cases of fluid chemistry affecting rock deformation, e.g. during water - silicate interaction, a weakening effect occurs. In quartz for example, the strength of the mineral is sensitive to the concentration of crystal lattice-bound, or intergranular water (Kronenberg and Tullis 1984), and if a metamorphic reaction modifies the metamorphic fluid environment, the creep properties of quartz change. Experiments have shown that in olivine, the amount of iron in solid solution governs the defect state of the mineral, so that in any olivine phase other than pure forsterite (Mg_2SiO_4), the deformation is dependent on the syn-tectonic environmental chemistry (Ricoult and Kohlstedt 1983). In the absence of geochemical analyses of the OHFZ fluids, the effect of pore fluid chemistry is unknown, but this process is likely to be important, given the widespread mineralogical changes observed during phyllonite development.

2 The generation of transient, fine-grained reaction products

During metamorphism, the production of fine-grained materials at the start of a reaction can also cause appreciable weakening (Rutter and Brodie 1985). Deformation by grain boundary sliding accommodated by diffusive mass transfer is greatly enhanced by ultrafine-grained transient reaction products which occur at the onset of metamorphic reactions (Brodie and Rutter 1985). These authors cite Rubie (1983) in an example of preferential deformation of fine grained reaction products (quartz and jadeite) from the prograde metamorphism of feldspar in quartz diorite from the western Alps. Although this process may be applicable at the onset of phyllonitisation along the OHFZ, detailed SEM / TEM studies are required to assess whether ultra-fine grained reaction products are present. This process does not explain the profound weakness of the fault zone over the long term.

3 The introduction of melt

Hollister and Crawford (1986) and Davidson et al. (1994) have suggested a link exists between magma emplacement and the weakening of the crust, and more significantly, the concentration of strain where melt is present. In addition, laboratory experiments have shown that partial melting significantly alters the rheology of rocks

(Arzi 1978) and may promote cataclasis. Scholz (1990) suggests the frictional resistance of a brittle fault may be abruptly dropped if the fault is filled with melt or hot fluids. The presence of silicate melt (despite its high viscosity) may therefore be a syn-tectonic cause of weakening in active fault/shear zones (Scholz 1990). Although small quantities of melt are added to the OHFZ during thrusting, in the form of pseudotachylite veins, this effect is extremely short lived and there is no evidence to suggest that this process assists reactivation; no pseudotachylites are generated during strike-slip or extensional reactivations.

Igneous melt appears to be entirely absent from the OHFZ, although Walker (1990) suggests that the SE-dipping Tertiary sills close to Lochmaddy in North Uist (Mackinnon 1974) may be synchronous with widespread fluid flow and phyllonitisation (see section 4.3.1). These sills are undeformed, however, and are entirely post-tectonic.

4 Shear heating

If localised deformation is very rapid, a syn-tectonic cause of weakening may be shear heating. Scholz (1990) cites evidence for comparatively recent resetting of K-Ar dates from Mesozoic schists close to the Alpine Fault in New Zealand. These dates decrease as the fault zone is approached, showing that the heat generated by faulting was responsible for the loss of radiogenic argon from adjacent rocks. The syntectonic generation of sufficient heat in a fault zone has the effect of allowing deformation at lower shear stresses than in the surrounding cooler rock. Whilst syn-tectonic weakening of the OHFZ may be enhanced by this process, (and is possibly manifested in the continued focusing of brittle deformation into large pseudotachylite/ultracataclasite crush zones), the onset and focusing of later reactivations, after a long period of time after inception, is not explained by this process.

5 Transformational plasticity

Metamorphic phase change may enhance the plasticity of a rock by promoting a volume change at the transition from one phase to another. This volume change may create local stresses which assist intracrystalline plastic flow (Brodie and Rutter 1985). This process may occur during phyllonitisation along the OHFZ, where the growth of reaction products (sericite, chlorite and epidote) has occurred in fine grained cataclasites and coarser grained gneisses. Here, the reactants cease to deform by brittle processes and plastic flow is promoted. The generation of large strains by this

process seems unlikely, however because repeated cycling through the phase change is required (Brodie and Rutter 1985).

Summary

The most important transient weakening mechanisms along the OHFZ are likely to be those related to the presence of hydrous fluids inferred to exist from geochemical and textural evidence. These fluids are thought to have first gained access into the fault zone during sinistral displacements and appear to have continued to remain important thereafter. However, the transient weakening mechanisms are only effective at the time of deformation, and as the OHFZ has been reactivated over a long timespan, a permanent mechanism(s) must also occur.

6.2.2 Long-lived mechanisms of rheological change

According to the published literature, summarised most recently by Rubie (1990) these include:

1. Favourable orientation of a pre-existing anisotropy
2. Permanent reaction softening
3. Fabric softening and the formation of CPO's
4. Grain size reduction
5. Thermal perturbations
6. Permeability pathways

1 Favourable orientation of a pre-existing anisotropy

The orientation of an existing fault/shear zone with respect to the newly imposed stress regime is likely to fundamentally control reactivation if it exists as a crustal weakness in the long-term. Some authors suggest that reactivation in the brittle regime may only occur if the fault lies in a near ideal orientation to the stress-field because the difference in strength may be very small (e.g. Etheridge 1986), whilst others (e.g. Donath 1961), suggest that faults fail under a much greater variety of angles for the same stress.

The failure criterion of most rocks is approximately the same, because most rocks share similar frictional properties. This failure criterion is termed the *Coulomb Fracture Criterion* (Byerlee 1978). The potential for reactivation of the fault which results at failure can be assessed by comparing the coefficient of internal friction for the fault with the intact rock (Donath and Cranwell 1981, Etheridge 1986). If the fault

occurs at high crustal levels, the fracture plane is subsequently weaker than the surrounding rock because the rock possesses no cohesion across the fault (Jamison and Cook 1980). Even if the fault contains gouge, the cohesion across the fault is less than the intact rock because these fault products are intrinsically weak (Byerlee and Savage 1992). At low confining pressures, subsequent deformation will therefore occur by frictional sliding along the pre-existing fracture. With increasing depth (and confining pressure), however, it soon becomes easier to form another fracture than to produce sliding, so the rock deforms by repeated brittle fracture (cataclasis) (Byerlee 1978) (Fig. 6.2).

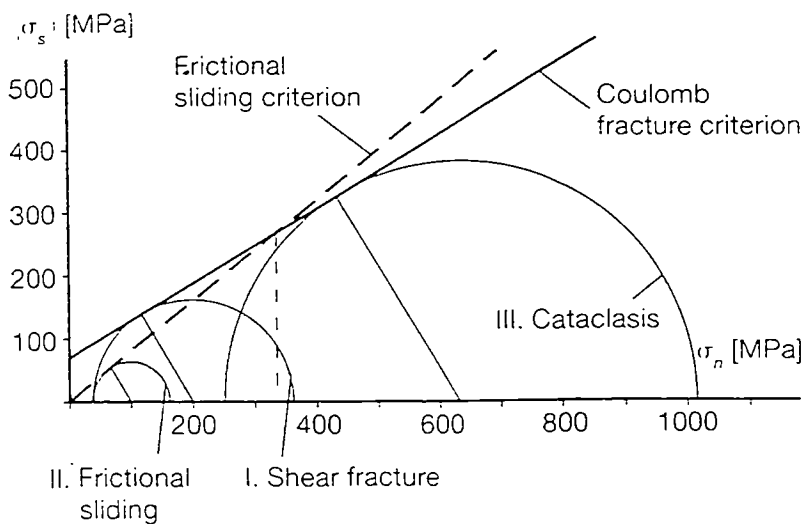


Figure 6.2. Mohr - Coulomb diagram for fracture (solid line) and for frictional sliding on a pre-existing fault surface (dashed line). (Data from Weber sandstone)

Circle I - critical stress for shear fracture

Circle II - critical stress for frictional sliding on the fracture plane at low confining pressure

Circle III - critical stress for cataclastic flow during which fracturing requires a lower differential stress than frictional sliding at the same confining pressure.

(From Twiss and Moores 1992 after Byerlee 1975)

At low confining pressure, the onset of this frictional sliding depends on Amontons's law (which approximates the Coulomb failure criterion for a pre-existing fracture). This states that:

$$\tau = \mu \sigma'_n = \mu(\sigma_n - P)$$

Where τ and σ are the shear and normal stresses to the plane respectively, and μ is the coefficient of internal friction (which from laboratory experiment on crustal rocks is 0.6 - 0.9 and is usually taken to be c. 0.75) (Sibson 1985). The angle of the fault to be reactivated shows a relationship with the stress ratio required to cause reactivation

(assuming a coefficient of internal friction of 0.75) (Sibson 1985) This may be written as:

$$R = \left(\frac{\sigma_1}{\sigma_3} \right) = \left(\frac{1 + \mu \cot \theta}{1 - \mu \tan \theta} \right)$$

where σ_1 is the maximum principal stress, σ_3 is the minimum principal stress and θ is the angle between σ_1 and the fault plane (the reactivation angle) or graphically as shown in figure. 6.3 (Sibson 1985).

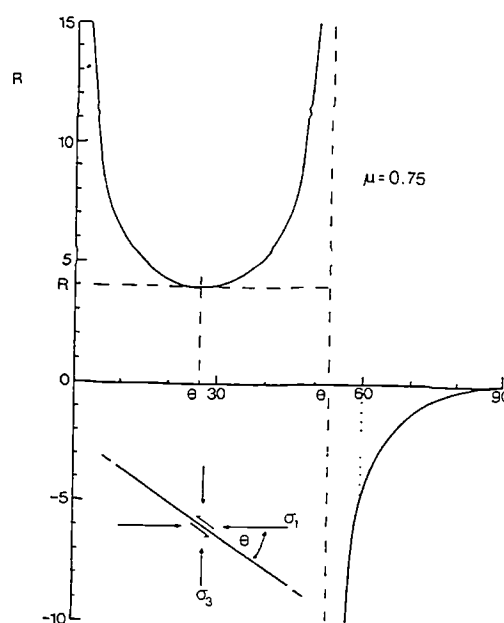


Figure 6.3. Stress ratio required for frictional reactivation $R = \sigma_1/\sigma_3$ of an existing fault with a reactivation angle θ . As θ deviates from the optimum angle of 26.5, reactivation requires a greater differential stress to occur, so that at a θ angle of 60° (as is required for complete fault movement reversal in this simplified Andersonian model) the ratio (R) required is c. -5 (with σ_3 effectively tensile). n.b. The fault is cohesionless, with its normal lying in the σ_1 , σ_3 plane. (From Sibson 1985).

For μ of 0.75, the minimum possible value of R is 4, occurring at the optimum angle for reactivation (θ^*) of 26.5°. Any deviation from this optimum angle will increase the value of R , leading to reactivation only at higher ratios of σ_1 to σ_3 . If the angle of reactivation is greater than 2 θ , the ratio (R) becomes less than 0. This means σ_3 must be less than 0 (i.e. effectively tensile) in order to allow reactivation to occur.

For typical values of internal friction, faults develop at c. 30° to σ_1 , so that normal faults (with σ_1 vertical) dip at 60° from the horizontal, whilst thrusts (with σ_1

horizontal) dip at 30° from the horizontal (Fig. 6.4a). If these maximum principal stress directions are interchanged, as is feasible in rifts experiencing collision or mountain belts experiencing extension, these faults may be potentially reactivated. In either case, the reactivation angle (θ) is 60° (the angle between σ_1 and the fault plane) (Fig. 6.4b). A θ of 60° requires R to be less than 0 (Fig. 6.3) (i.e. with a tensile σ_3 or a much lower μ than 0.75) and may require conditions of high pore fluid pressure or the presence of very weak fault rocks.

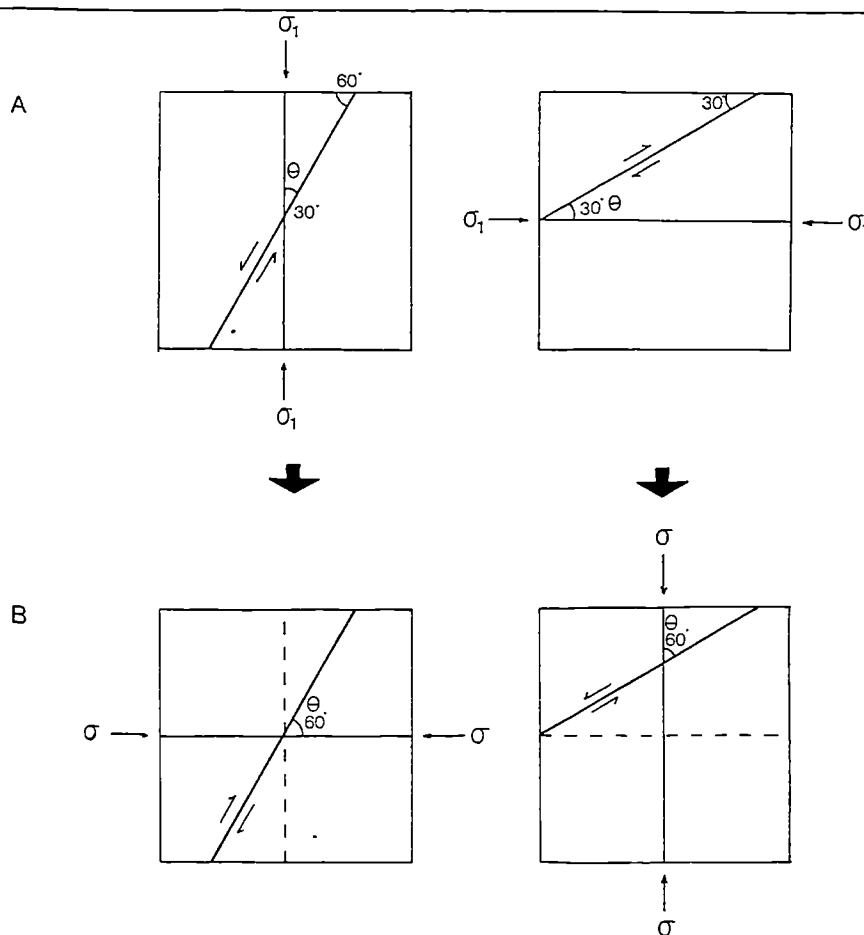


Figure 6.4. Simple two-dimensional Andersonian fault block models showing the relationship between σ_1 and a given fault surface before and after complete movement reversal in both normal and reverse precursors.

A) Before reactivation the normal fault dips at 60° from the horizontal and the reverse fault dips at 30° from the horizontal. In both cases the σ_1 direction forms a θ angle of 30° with the fault surface. (after Anderson 1951).

B) After reactivation (with a reversal of the maximum and minimum principal stress directions) the σ_1 direction forms a θ angle of 60° with the existing surface in both the normal and reverse fault precursors. Such a high angle of reactivation is not possible without an effectively tensile σ_3 .

If such a model applies to the OHFZ, then, as extensional reactivation during gravitationally induced 'collapse' reactivates low angle (c. 30°) phyllonitic shear zones, the reactivation angle is c. 60°, and requires R to be less than 0. High pore fluid pressure could conceivably be important in the short term, (causing an apparently tensile σ_3), but there is also clear evidence that the phyllonites formed remarkably weak fault rocks. However, this discussion assumes faulting occurs in the brittle regime, using Coulomb fracture criteria. The deformation in the OHFZ during low-angle extension, however, is often ductile in nature. Thus, the foregoing model cannot be strictly applied in a quantitative sense. Nevertheless, the concept of favourably oriented zones of weakness may be generally applicable to those regions of the lower crust and mantle, where ductile flow laws operate. The size of the range of favourable orientations, and how it may change with depth and/or dominant deformation mechanism is presently unknown.

2 Permanent reaction softening

The mineralogy of faults/shear zones may be altered to a permanently weaker rheology by the effects of metamorphism in dry or wet conditions, but is greatly assisted by the presence of fluids (e.g. by hydration of silicate bonds). Fluids also serve to speed up reaction rates, especially if pore fluid pressures are elevated periodically. The presence of hydrothermal fluids, even without a high pore fluid pressure can retrogress the rocks within and adjacent to the fault/shear zone, altering the mineralogy to water-swelling montmorillonite clays or zeolites with a permanent frictional strength reduction (Byerlee 1978), or phyllosilicates oriented for easy grain-boundary sliding. Retrogressed mineral assemblages such as the phyllonites resulting from a Lewisian gneiss protolith along the Moine Thrust Zone (White 1982) incur a permanent strength decrease by about a factor of 10 (White et al. 1986) because mica aggregates deform more easily than granitic protolith. This has the effect of increasing the reactivation potential.

A very similar process has operated during the development of the phyllonite fabrics in the OHFZ; original K-feldspar and plagioclase have been altered to sericite and epidote; amphiboles and biotites have been altered to chlorite; cataclasites have been altered to aggregates of chlorite epidote and white mica. These reaction products are mechanically weaker than the reactants and may deform by crystal plastic processes and/or fluid assisted DMT and/or grain boundary sliding at lower stresses than the surrounding unretrogressed material. It is thought that the presence of

mechanically weak phyllonites is probably the single most important cause of the permanent weakness of the OHFZ.

3 Fabric softening and the formation of CPO's

In ductile rocks, fabric softening will occur as the foliation rotates into parallelism with the shear zone margins, especially if phyllosilicate minerals are present (see above) oriented for easy grain boundary sliding. Quartz grain boundaries may also be similarly oriented (White et al. 1986). In the OHFZ, this process is believed to have occurred during two separate episodes. Firstly, during early, ductile thrusting, a strong mylonitic foliation, defined by quartz-feldspar aggregates, aligned amphiboles and quartz ribbons, was produced. The presence of this mylonitic foliation (which may be significantly older than any subsequent deformation (see section 5.1.1)) may control the localisation of subsequent brittle thrusting. Secondly, during sinistral strike-slip on the OHFZ, a well defined phyllosilicate foliation, defined by aligned sericite and chlorite flakes, was generated in phyllonitic shear zones. This foliation allows inter-layer slip and also serves to lower the internal friction of the fault zone. Once this phyllosilicate-rich foliation had been produced, the fault zone became permanently weak, relative to the surrounding gneisses, and therefore susceptible to reactivation during the later, low-angle extensional 'collapse' phase, giving rise to profound strain localisation.

The formation of a crystallographic preferred orientation (CPO) occurs during ductile deformation and results in the alignment of the crystallographic directions of a particular phase (e.g. the parallel alignment of [0001] of calcite normal to the foliation in marbles (Hobbs et al. 1976)). The alignment requires either an element of rotation of the crystallographic directions towards their preferred orientation by slip on their particular slip systems (Twiss and Moores 1992), particularly at low temperatures and/or high strain rates, or the growth of a preferred orientation during recrystallisation. The growth of 'type-2b' quartz ribbons with a CPO (using the terminology of Boullier and Bouchez 1978) during the early ductile thrusting along the OHFZ, may have added to the effect of the well-defined mylonitic foliation, in rendering the fault zone more susceptible to subsequent brittle failure than the surrounding gneisses.

4 Grain size reduction

Grain size reduction in a shear zone, whether by comminution or recrystallisation, can have several effects. The surface area available for reaction will be increased by a finer grain size and chemical weakening processes will be enhanced (Brodie and Rutter 1985), and a change from grain size insensitive to grain size

sensitive deformation mechanisms may be promoted (Schmid et al. 1977). These effects appear to be borne out by the OHFZ, where the phyllonitic shear zones occur parallel to, and appear to have localised on, topographic faults (see section 5.2.3). The increased brittle comminution and high density of fractures in the topographic fault regions had the effect of:

- reducing the grain size, increasing the surface area available for reaction;
- Increasing the local permeability, promoting fluid-assisted weakening mechanisms.

Diffusion rates are therefore increased in these regions and grain size sensitive deformation mechanisms such as fluid-assisted DMT are promoted. Thus, these regions became the favoured sites for hydration reactions and retrogression, ultimately culminating in the generation of phyllonite. The phyllonite belts are therefore thought to be the expression of the largest topographic faults where microfracturing, cataclasis and grain size reduction are at their maximum.

5 Thermal perturbations

The syn-tectonic processes which involve a release of thermal energy, such as the introduction of melt and/or hot fluids and/or shear heating, have the effect of locally rising the geotherm in the region of the fault/shear zone. This thermal perturbation may be long-lived and makes the fault/shear zone more susceptible to continued reactivation because deformation is facilitated at lower shear stresses in the relatively hot fault/shear zone than in the surrounding cooler rock. There is no evidence to suggest that a locally higher geotherm existed in the region of the OHFZ, and this long-term effect seems unlikely as an operative weakening mechanism along the OHFZ.

6 Permeability pathways

Because the sinistral shear zones along the OHFZ are the sites of selective retrogression involving hydration, they imply an increased water permeation along the shear zones relative to permeation sideways into the surrounding rock. The enhanced permeability may occur as a result of grain size/shape contrasts with the undeformed rock, or active creation of permeable voids in the shear zone (Rutter and Brodie 1985), and field evidence from the OHFZ suggests both factors may have contributed. The enhanced permeability probably occurs both as a short-lived, syn-tectonic effect of deformation mechanisms which involve dilatancy, such as cataclasis, and as a long-lived, post-tectonic effect of grain size reduction, which generate a greater density of

diffusion pathways in finer grains. It is therefore no coincidence that the main belts of phyllonite correspond to those regions of the OHFZ that have undergone greater degrees of cataclasis during earlier fault movements.

It is often difficult however, to distinguish the case of syn-tectonic permeability enhancement and hydration, from the case of *long-lived, permeability-enhanced* hydration (Rutter and Brodie 1985). It is clear however, that both may contribute to the weakening of faults and shear zones.

6.2.3 Conclusions on weakening processes: the importance of fluids

A combination of transient and permanent weakening mechanisms have led to the localisation of deformation and reactivation of the OHFZ. Field and thin section observations consistently indicate the crucial role played by fluids, both mechanically (by changes in pore fluid pressure), and chemically (by permanent reaction softening and processes which accompany metamorphic phase changes). These fluid-enhanced weakening processes are highlighted in Table 6.1 and are a commonly observed feature in other reactivated fault zones: Bruhn et al. (1982) suggest that a combination of hydrothermal fluid effects initiated and maintained movement on the joint surfaces which became low-angle normal faults in the Basin and Range Province. Although they state that a low coefficient of friction was largely responsible for this reactivation (lowered by inter-layer water in some clay minerals), the alteration of the primary mineralogy, by fluid-enhanced retrogression, facilitated this movement. A high pore fluid pressure may have been maintained by the growth of new phyllosilicates which reduced the permeability by increasing the volume. The influence of fluids to reactivation is widely considered to be fundamentally important. Etheridge (1986) for example, states that "fluids within fault zones may well be the single most important factor influencing their tendency to be reactivated".

6.3. The link between kinematics and fluid flow

If phyllonite development along the OHFZ is simply caused by localised retrogression in the immediate vicinity of the largest brittle faults, (where grain size is finest and brittle fractures are at their densest), two problems arise:

1. The fault zone has remained apparently 'dry' until the onset of sinistral strike-slip movement;

2. Thrust-related brittle deformation with cataclasis and grain comminution is ubiquitous along the entire length of the OHFZ, whereas phyllonite development and therefore fluid flow is spatially restricted in two ways:
- Phyllonite development is restricted to the eastern part of the fault zone, whilst unphyllonitised thrust sense topographic faults are preserved further west (e.g. see section 4.3.1).
 - On a larger scale, phyllonites are mainly restricted to the central fault zone arc and the most southerly part of the northern fault zone arc (see Fig. 5.2c).

In simple terms, the fault zone, by nature of its pre-existing deformation, has the ability to accommodate fluid movement along its *entire* length and width, but clearly, it has not.

Sibson (1993) has suggested that fluid flux in the vicinity of a fault may be influenced by the kinematics of the fault. In *thrust* faults, the frictional strength of the fault will increase as the normal stress across the fault increases (load-strengthening). In *normal* faults, however, the frictional strength of the fault will decrease as the normal stress across the fault decreases (load-weakening) (Fig. 6.5). Strike-slip faults may show either type of behaviour. Rock dilatancy and permeability is inversely proportional to mean normal stresses, so load-weakening faults are more likely to allow fluid influx during the interseismic period than load-strengthening faults. Once the fluids have gained access to the rock on a grain scale, they are then able to cause hydration reactions, retrogression and weakening in the vicinity of the fault.

In the OHFZ, I propose that only fault strands which have experienced brittle, load-weakening behaviour eventually formed phyllonite belts. Fluid influx, from an unknown source, is demonstrably syn-tectonic with strike-slip behaviour, and may have occurred at the change in kinematics from thrusting to strike-slip motion (Butler et al. 1995). If strike-slip motion was restricted to the central OHFZ arc, and regions in the east of the Crush Melange, as appears from field evidence, it is possible that no fluids were allowed into faults which did not experience strike-slip motion, and hence phyllonites are rarely present outside this central arc.

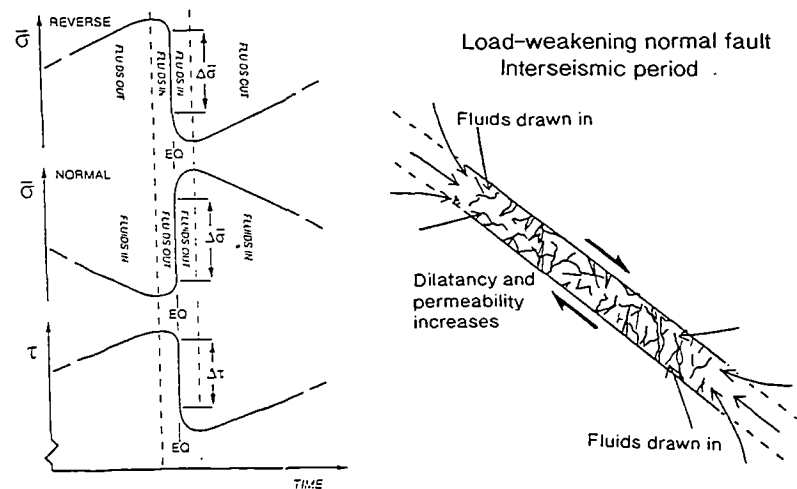


Figure 6.5 Coupled relationships between shear stress, τ , and mean stress σ , on optimally oriented reverse and normal faults, illustrating expected changes in fluid migration accompanying pre-seismic and post-seismic slip, and a hypothetical load-weakening fault in the pre-seismic state, (from Sibson 1993).

This process may be aided by the pattern of dilatancy during the seismic period (Sibson 1989). In dip-slip faults, asperities on fault surfaces cause dilational jogs which have their long axes oriented horizontally (Fig. 6.6). Fluid flow up or down the fault zone is inhibited by a tortuous route. In strike-slip faults, however, dilational jogs are oriented parallel to dip, and fluid flow up or down the fault zone is less tortuous (Sibson 1989). Fluid enhanced weakening processes would therefore be favoured by strike-slip movements along faults. The observations of retrogression, inferred fluid flow and fault kinematics in the OHFZ, confirms that a relationship exists between fluid flux and the kinematic regime.

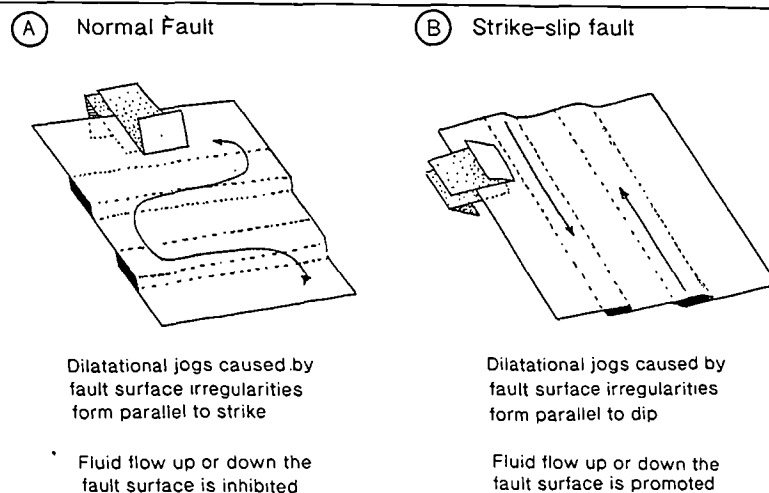


Figure 6.6 Hypothetical faults with irregular surfaces. A) Normal fault B) Strike-slip fault.

6.4 Implications for other reactivated basement faults

The present study has implications for the understanding of reactivation processes in continental basement rocks. Three processes are of particular significance:

- The development of retrograde phyllosilicate assemblages appears to be a major cause of long term weakness. Such hydrated assemblages are probably typical of reactivated faults.
- Hydrous fluids are important in both a physical and chemical sense, effectively controlling the fault zone rheology in both the short-term (syn-tectonically) and the long-term (permanently).
- The kinematic evolution of a fault zone may be crucial in determining its fluid flow, retrogression and future ability to reactivate. In particular, strike-slip movements, leading to fluid influx, may be a precursor to the development of long term weakening.

These processes should form the basis for future work on reactivated basement faults.

References cited in the text

- Anderson, E.M.**, 1951. *The Dynamics of Faulting*, (2nd edition). Oliver & Boyd, Edinburgh. 206pp.
- Aggarwal, Y.P., and Sykes, L.R.**, 1978. Earthquakes, faults and nuclear power plants in southern New York - northern New Jersey. *Science* **200**, 425-429.
- Arthurton, R.S., Gutteridge, P. and Nolan S.C.**, 1989. *The role of tectonics in Devonian and Carboniferous sedimentation in the British Isles*. The Yorkshire Geological Society (Occasional publication No. 6), 258pp.
- Arzi, A.A.**, 1978. Critical phenomena in the rheology of partially melted rocks. *Tectonophysics*, **44**, 173-184.
- Attfield, P.** 1987. The structural history of the Canisp Shear Zone. In Park, R.G. and Tarney, J. (eds). *Evolution of the Lewisian and Comparable Precambrian High Grade Terrains*, Geological Society Special Publication, **27**, 165-173.
- Badley, M.E., Price, J.D., and Backshall, L.C.**, 1989. Inversion, reactivated faults and related structures: seismic examples from the southern North sea. In Cooper, M.A., and Williams G.D., (eds) 1989a. *Inversion Tectonics*. Geological Society Special Publication, **44** 201-219.
- Basham, P.W., Forsyth, D.A., and Wetmiller, R.J.**, 1977. The seismicity of northern Canada. *Canadian Journal of Earth sciences*, **14**, 1646-1667.
- Beach, A.**, 1976. The interrelations of fluid transport, deformation, geochemistry and heat flow in early Proterozoic shear zones in the Lewisian complex. *Philosophical Transactions of the Royal Society of London*, **A 280**, 529-604.
- Beach, A.**, 1982. Deformation mechanisms in some cover thrust sheets from the external French Alps. *Journal of Structural Geology*, **4**, 137-149.
- Beach, A., Coward, M.P., and Graham, R.**, 1974. An interpretation of the structural evolution of the Laxford front, NW Scotland. *Scottish Journal of Geology*, **9**, 297-308.
- Berlenbach, J.W., and Roering, C.**, 1992. Sheath-fold-like structures in pseudotachylytes. *Journal of Structural Geology*, **14**, 847-856.
- Berthe, D., Choukroune, P. and Jegouzo, P.**, 1979. Orthogneiss, mylonite and non-coaxial deformation of granites: the example of the South Armorican Shear Zone. *Journal of Structural Geology* **1**, 31-42.
- Binns, P.E., McQuillin, R. and Kenolty, N.**, 1974. *The geology of the Sea of the Hebrides*. Report of the Institute of Geological Sciences **73/14** 44pp.
- Binns, P.E., McQuillin, R., Fannin, N.G.T., Kenolty, N. and Ardu, D.A.**, 1975. Structure and stratigraphy of sedimentary basins in the Sea of the Hebrides and the Minches. In Woodland, A.W. (ed) *Petroleum and the Continental Shelf of NW Europe*. **1**, Applied science publishers Ltd, 93-102.
- Blight, D.F., Compston, W., and Wilde, S.A.**, 1981. The Logue Brook Granite: age and significance of deformation zones along the Darling Scarp. *Western Australia Geological Survey Annual Report for 1980*, 72-81.

- Blundell, D.J.**, 1976. Active faults in west Africa. *Earth and Planetary Science Letters*, **31**, 287-290.
- Blundell, D.J.**, 1984. Deformation of the Caledonide lithosphere of northwest Scotland. *Tectonophysics*, **109**, 137-145.
- Bott, M.H.P.**, 1971. *The interior of the earth*. E. Arnold, London, 316pp.
- Boullier, A.M., and Bouchez, J.L.**, 1978. Le quartz en rubans dans le mylonites. *Bulletin de la Societe Geologique, de France*, **7**, 253-262.
- Bowes, D.R., and Hopgood, A.M.**, 1969. The Lewisian Gneiss Complex of Mingulay, Outer hebrides Scotland. *Memoir of the Geological Society of America*, **115**, 317-356
- Brace, W.F., and Kohlstedt, D.L.**, 1980. Limits on lithospheric stress imposed by laboratory experiments. *Journal of Geophysical Research*, **B11 85**, 6248-6252.
- Brewer, J.A., Matthews, D.H., Warner, M.R., Hall, J., Smythe, D.K. and Whittington, R.J.**, 1983. BIRPS deep seismic reflection studies of the British Caledonides. *Nature*, **305**, 206-210.
- Brewer, J.A. and Smythe, D.K.**, 1984. MOIST and the continuity of crustal reflector geometry along the Caledonian-Appalachian orogen. *Journal of the Geological society of London*, **141**, 105-120.
- Brewer, J.A. and Smythe, D.K.**, 1986. The BIRPS WINCH profile: deep structure of the foreland to the Caledonian orogen, NW scotland. *Tectonics*, **5**, 171-194.
- Briden, J.C., Whitcombe D.N., Stuart, G.W., Fairhead, J.D., Dorbath, C., and Dorbath, L.**, 1981. Depth of geological contrast across the West African craton margin. *Nature*, **292**, 123-137.
- Bridgewater, D., Escher, A., and Watterson, J.** 1973. Dyke swarms and the persistence of major geological boundaries in Greenland. In Park, R.G. and Tarney, J. (eds), *The early Precambrian of Scotland and related rocks of Greenland*. University of Keele, 137-141.
- Brodie, K. and Rutter, E.H.**, 1985. On the relationship between deformation and metamorphism with special reference to the behaviour of basic rocks. In Thompson, A.B. and Rubie, D. (eds), *Kinetics, Textures and Deformation, Advanced Physical Geochemistry*, **4**, 138-179.
- Bruhn, R.L., Yusas, M.R., and Huertas, F.** 1982. Mechanics of low-angle normal faulting: an example from Roosevelt Hot springs geothermal area, Utah. *Tectonophysics*, **86**, 343-361.
- Brunel, M.**, 1980. Quartz fabrics in shear zone mylonite: evidence for a major imprint due to late strain increments. *Tectonophysics*, **64**, 33-44.
- Bubb, J.N., and Hayash, J.M.**, 1980. Techniques in a seismic interpretation for hydrocarbon assessment: Assessment of undiscovered oil and gas. *Committee for the Co-ordination of Joint Prosperity for Mineral Resources in Asian Offshore areas. Technical Publications*, **10**, Bangkok.
- Burg, J.P., Brunel, M., Gapais, D., Chen, G.M., and Liu, G.H.**, 1984. Deformation of leucogranites of the crystalline main central sheet in southern Tibet (China). *Journal of Structural Geology*, **6**, 535.

- Butler, C.A., Holdsworth, R.E., and Strachan, R.A.**, 1993. Kinematics and controls of the distribution of extension along the Outer Isles Fault Zone, NW Scotland. *In* Seranne, M. and Malavielle J., (eds). *Late orogenic extension in mountain belts*. Doc. BRGM Fr., **219**, 32-33
- Butler, C.A., Holdsworth, R.E., and Strachan, R.A.**, 1995. Evidence for Caledonian sinistral strike-slip motion and associated fault zone weakening, Outer Hebrides Fault Zone, NW Scotland. *Journal of the Geological Society of London*, **152**, 743-746.
- Butler, R.W.H.**, 1989. The influence of pre-existing basin structure on thrust system evolution in the Western Alps. *In* Cooper, M.A., and Williams G.D., (eds) 1989 *Inversion Tectonics*, Geological Society Special Publication, **44**, 105-122.
- Byerlee, J.D.**, 1978. Friction of rocks. *Pure and Applied Geophysics*, **116**, 615-626.
- Byerlee, J.D., and Savage, J.C.**, 1992. Coulomb plasticity within the fault zone. *Geophysical Research Letters*, **19**, 2341-2344.
- Cashman, P.H.**, 1990. Evidence for extensional deformation during a collisional orogeny, Rombak window, north Norway. *Tectonics*, **9**, 859-886.
- Chapman, H.J.**, 1979. 2,390 Myr Rb-Sr whole-rock age for the Scourie dykes of north-west Scotland. *Nature*, **277**, 642-643.
- Chen, W.P., and Molnar, P.**, 1983. Focal depths of intracontinental and intraplate earthquakes and their implications for the thermal and mechanical properties of the lithosphere. *Journal of Geophysical Research*, **88**, 4183-4214.
- Chesher, J.A., and Smythe, D.K.**, 1986. Little Minch Sheet 57°N-08°W 1:250,000 series, solid geology. British Geological Survey.
- Chesher, J.A., Smythe, D.K., and Bishop, P.**, 1983. *The geology of the Minches, Inner Sound and Sound of Raasay*. Report of the Institute of Geological Sciences **83/6**, 29pp
- Chester, F.M., Friedman, M., and Logan, J.M.**, 1985. Foliated Cataclasites. *Tectonophysics*, **111** 139-146.
- Cliff, R.A.**, 1989. Proterozoic evolution in the northern Outer Hebrides, NW Scotland. *Terra Abstracts*, **1**, 4
- Cliff, R.A., Gray, C.M., and Huhma, H.**, 1983. A Sm-Nd isotope study of the South Harris Igneous Complex, the Outer Hebrides. *Contributions to Mineralogy and Petrology*, **82**, 91-98.
- Cliff, R.A. and Rex, D.C.**, 1989. Evidence for a 'Grenville' event in the Lewisian of the northern Outer Hebrides. *Journal of the Geological Society of London*, **146**, 921-924.
- Coney, P.J., and Harms, T.A.**, 1984. Cordilleran metamorphic core complexes: Cenozoic extensional relics of Mesozoic compression. *Geology*, **12**, 550-555.
- Cooper, M.A., Williams, G.D., de Graciansky, P.C., Murphy, R.W., Needham, T., de Paor, D., Stoneley, R., Todd, S.P., Turner, J.P., and Ziegler, P.A.**, 1989. Inversion tectonics: a discussion. *In* Cooper, M.A., and Williams G.D., (eds) 1989. *Inversion Tectonics*. Geological Society Special Publication, **44**, 335-347.
- Coward, M.P.**, 1969. *The structural and metamorphic geology of South Uist, Outer Hebrides*. Unpublished PhD thesis, University of London.
- Coward, M.P.**, 1972. The Eastern Gneisses of South Uist. *Scottish Journal of Geology*, **8**, 1-12.

- Coward, M.P.**, 1973. Heterogeneous deformation in the development of the Laxfordian complex of South Uist, Outer Hebrides. *Journal of the Geological Society of London*, **129**, 137-160.
- Coward, M.P.**, 1976. Large scale Paleozoic shear zone in Australia and present extension to the Antarctic Ridge. *Nature*, **259**, 648-649.
- Coward, M.P.**, 1984. Major shear zones in the Precambrian crust: examples from NW Scotland and southern Africa and their significance. In Kroner, A., and Greiling, S.R., (eds). *Precambrian Tectonics Illustrated*, Stuttgart. 207-235.
- Coward, M.P., Enfield, M.A., and Fischer M.W.**, 1989. Devonian basins of Northern Scotland: extension and inversion related to Late Caledonian - Variscan tectonics. In Cooper, M.A., and Williams G.D., (eds) 1989. *Inversion Tectonics*. Geological Society Special Publication, **44**, 275-308.
- Coward, M.P., Francis, P.W., Graham, R.H., Myers, J.S., and Watson, J.**, 1969. Remnants of an early metasedimentary assemblage in the Lewisian complex of the Outer Hebrides. *Proceedings of the Geologists Association*, **80**, 387-408.
- Coward, M.P., Francis, P.W., Graham, R.H., and Watson, J.**, 1970. Large-scale Laxfordian structures of the Outer Hebrides in relation to those of the Scottish Mainland. *Tectonophysics*, **10**, 425-435.
- Coward, M.P., and Park, R.G.**, 1987. The role of mid-crustal shear zones in the Early Proterozoic evolution of the Lewisian. In Park, R.G., and Tarney, J., (eds), *Evolution of the Lewisian and Comparable High Grade Terrains*. Geological Society Special Publication, **27**, 127-138.
- Dalmayrac, B., and Molnar, P.**, 1981. Parallel thrusts and normal faulting in Peru and the state of stress. *Earth and Planetary Science Letters*, **55**, 473-481.
- Daly, M.C., Chorowicz, J., and Fairhead, J.D.**, 1989. Rift basin evolution in Africa: the influence of reactivated steep basement shear zones. In Cooper, M.A., and Williams G.D., (eds) 1989. *Inversion Tectonics*. Geological Society Special Publication, **44** 309-334.
- Dalziel, I.W.D.**, 1989. Inversion of circum-Pacific marginal basins. In Cooper, M.A., and Williams G.D., (eds) 1989. *Inversion Tectonics*. Geological Society Special Publication, **44**, 351.
- Davidson, C., Schmid, S.M., Hollister, L.S.**, 1994. Role of melt during deformation in the deep crust. *Terra Nova*, **6**, 133-142.
- Davies, F.B., Lisle, R.J., and Watson, J.V.** 1975. The tectonic evolution of the Lewisian Complex in Northern Lewis. *Proceedings of the Geologists Association*, **86**, 45-61.
- Dearnley, R.**, 1962. An outline of the Lewisian complex of the Outer Hebrides in relation to that of the Scottish mainland. *Quarterly Journal of the Geological Society of London*, **118**, 143-176.
- Dearnley, R.**, 1963. The Lewisian complex of South Harris; with some observations on the metamorphosed basic intrusions of the Outer Hebrides, Scotland. *Quarterly Journal of the Geological Society of London*, **119**, 243-312.
- Dearnley, R., and Dunning, F.W.**, 1968. Metamorphosed and deformed pegmatites and basic dykes in the Lewisian complex of the Outer Hebrides and their geological significance. *Quarterly Journal of the Geological Society of London*, **123**, 335-378.

de Graciansky, P.C., Dardeau, G., Lemoine, M. and Tricart, P., 1989. The inverted margin of the French alps and foreland basin inversion. *In* Cooper, M.A., and Williams G.D., (eds) 1989. *Inversion Tectonics*. Geological Society Special Publication, **44** 87-104.

Dewey, J.F., 1988. Extensional collapse of orogens. *Tectonics*, **7**, 1123-1139.

Dewey, J.F., Hempton, M.R., Kidd, W.S.F., Saroglu, F., and Sengör, A.M.C., 1986. Shortening of continental lithosphere: The neotectonics of Eastern Anatolia - a young collision zone. *In* Coward, M.P., and Ries, A.C. (eds), *Collision Tectonics*. Geological Society of London Special Publication No. **19** 3-36.

Dixon, T., Stern, R.J., and Hussein, I.M., 1987. Control of Red Sea Rift geometry by Precambrian structures. *Tectonics*, **6**, 551-571.

Donath, F.A., 1961. Experimental study of shear failure in anisotropic rocks. *Bulletin of the Geological Society of America*, **72**, 985-990.

Donath, F.A. and Cranwell, J., 1981. Probabilistic treatment of faulting in geologic media. *In*: Carter, N.L., Friedman, M., and Logan, J.M. (eds), *Mechanical behaviour of crustal rocks*. American Geophysical Union, Washington DC, 231-241.

Doser, D.I., 1987. The Ancash, Peru, earthquake of 1946 November 10: evidence for low angle normal faulting in the high Andes of northern Peru. *Geophysical Journal of the Royal Astronomical Society*, **91**, 57-71.

Dougal, J.W., 1928. Observations on the geology of Lewis. *Transactions of the Edinburgh Geological Society*, **12**, 12-18.

Eaton, G.P., Christiansen, R.L., Iyer, H.M., Pitt, A.M., Mabey, D.R., Blank Jr, H.R., and Gettings, M.E., 1975. Magma beneath Yellowstone Park, *Science*, **188**, 787-796.

Emeleus, C.H., 1983. Tertiary igneous activity. *In* Craig, G.Y., (ed). *Geology of Scotland*. Scottish Academic Press, Edinburgh.

Etheridge, M.A., 1986. On the reactivation of extensional fault systems. *Philosophical Transactions of the Royal Society of London A* **317**, 179-194.

Etheridge, M.A., Wall, V.J., Cox, S.F., and Vernon, R.H., 1984. High fluid pressures during regional metamorphism and deformation: Implications for mass transport and deformation mechanisms. *Journal of Geophysical research*, **B 89**, 4344-4358.

Etheridge, M.A., and Wilkie, J.C., 1979. Grainsize reduction, grain boundary sliding and the flow strength of mylonites. *Tectonophysics*, **58**, 159-178.

Eskola, P., 1915. On the relations between the chemical and mineralogical composition in the metamorphic rocks of the Orijarvi region in southwestern Finland. *Bulletin de la Commission Geologique de Finlande*, No. **44**.

Evans, D., Hallsworth, C., Jolley, D.W., and Morton, A.C., 1991. Late Oligocene terrestrial sediments from a small basin in the Little Minch. *Scottish Journal of Geology*, **27**, 33-40.

Fettes, D.J., and Mendum, J.R., 1987. The evolution of the Lewisian complex in the Outer Hebrides. *In* Park, R.G., and Tarney, J., (eds), *Evolution of the Lewisian and Comparable High Grade Terrains*. Geological Society Special Publication, **27**, 27-44.

Fettes, D.J., Mendum, J.R., Smith, D.I., and Watson, J.V., 1981. *British Geological Survey, Sheets (solid edition) Lewis and Harris, Uist and Barra (Scotland)*. HMSO.

- Fettes, D.J., Mendum, J.R., Smith, D.I., and Watson, J.V., 1992.** Geology of the Outer Hebrides. *Memoir of the British Geological Survey, Sheets* (solid edition) Lewis and Harris, Uist and Barra (Scotland). HMSO. 197pp.
- Fitch, T.J., Worthington, M.H. and Everingham I.B., 1973.** Mechanisms of Australian earthquakes and contemporary stress in the Indian Ocean plate. *Earth and Planetary Science Letters*, **18**, 345-356.
- Fitz Gerald, J.G., and Stunitz, H., 1993.** Deformation of granitoids at low metamorphic grade, 1. Reactions and grain size reduction. *Tectonophysics*, **221**, 169-297.
- Fletcher, J.B., Sbar M.L., and Sykes L.R., 1978.** Seismic trends and travel time residuals in eastern North America and their tectonic implications. *Bulletin of the Geological Society of America*, **89**, 1656-1676.
- Fossen, H., 1992.** The role of extensional tectonics in the Caledonides of south Norway. *Journal of Structural Geology* **14**, 1033-1046.
- Fountain, D.M., Hurich, C.A., and Smithson, S.B., 1984.** Seismic reflectivity of mylonite zones in the crust. *Geology*, **12**, 195-198.
- Francis, P.W., 1969, Some aspects of the Lewisian Geology of the Isle of Barra and adjacent small islands.** Unpublished PhD thesis, University of London.
- Francis, P.W., 1973.** Scourian-Laxfordian relationships in the Barra Isles. *Journal of the Geological Society of London*, **129**, 161-189.
- Francis, P.W., and Sibson, R.H., 1973.** The Outer Hebrides Thrust. In Park, R.G., and Tarney, J., (eds). *The early Precambrian of Scotland and related rocks of Greenland*. University of Keele, 95-104.
- Fuller, A.O., 1971.** South Atlantic fracture zones and lines of old weakness in southern Africa. *Nature, Physical Science*, **231**, 84-85.
- Garson, M.S., and Krs, M., 1976.** Geophysical and geological evidence of the relationship of Red Sea transverse tectonics to ancient fractures. *Geological society of America Bulletin*, **87**, 169-181.
- Gawthorpe, R.L., Getteridge, P., and Leeder, M.R., 1989.** Late Devonian and Dinantian basin evolution in northern England and North Wales. In Arthurton, R.S., Gutteridge, P. and Nolan S.C., (eds), *The role of tectonics in Devonian and Carboniferous sedimentation in the British Isles*. The Yorkshire Geological Society (Ocrasional publication No. 6) 1-23.
- Gifkins, R.C., 1976.** The effect of grain size and stress upon grain-boundary sliding. *Metallurgical Transactions*, **8A** 1507-1516.
- Gillchrist, R., Coward, M.P., Trudgill, B., Pecher, A., and Mugnier, J.L., 1989.** Structural inversion in the external French Alps. In Cooper, M.A., and Williams G.D., (eds) 1989. *Inversion Tectonics*. Geological Society Special Publication, **44**, 354.
- Glennie, K.W., and Boegner, P.L.E., 1981.** Sole Pit inversion tectonics. In Illing, L.V., and Hobson, G.D. (eds), *Petroleum Geology of the Continental Shelf of North-west Europe*. Institute of Petroleum, London, 110-120.
- Goodwin, L.B., and Wenk, H.R., 1990.** Intracrystalline folding and cataclasis in biotite of the Santa Rosa mylonite zone, HVEM and TEM observations. *Tectonophysics*, **172**, 201-214.

- Gorini, M.A., and Bryan, G.M.,** 1976. The tectonic fabric of the equatorial Atlantic and adjoining continental margins: Gulf of Guinea to northeastern Brazil. *An. Acad. Brazil. Cienc.* **48**, 101-119.
- Graham, D.K., Harland, R., Gregory, D.M., Long, D., and Morton, A.C.,** 1990. The biostratigraphy and chronostratigraphy of BGS borehole 78/4, North Minch. *Scottish Journal of Geology*, **26**, 65-75.
- Graham, R.H.,** 1980. The role of shear belts in the structural evolution of the South Harris igneous complex. 29-37 In Carreras, J., Cobbold, P.R., Ramsay, J.G., and White, S.H. (eds). Shear zones in rocks. *Journal of Structural Geology*, **2**, 29-37.
- Griggs, D.T.,** 1967. Hydrolytic weakening of quartz and other silicates. *Geophysical Journal of the Royal Astronomical Society*, **14**, 19-31.
- Griggs, D.T., and Blacic, J.D.,** 1965. Quartz: anomalous weakness of single crystals. *Science*, **147**, 292-295.
- Grocott, J.,** 1981. Fracture geometry of pseudotachylite generation zones: a study of shear fractures formed during seismic events. *Journal of Structural Geology*, **3**, 169-178.
- Haller, J., and Kulp, J.L.,** 1962. Absolute age determinations in east Greenland. *Medd. Groenland*, **171**, 1-77.
- Handy, M.R.,** 1990. The Solid-State Flow of Polymineralic Rocks. *Journal of Geophysical Research*, **95**, 8647-8661.
- Hanmer, S., and Passchier, C.,** 1991. *Shear Sense Indicators: a review*. Geological Survey of Canada, Paper **90-17**, 71pp.
- Hayward, A.B. and Graham, R.H.,** 1989. Some Geometrical characteristics of inversion. in Cooper, M.A., and Williams G.D., (eds) 1989 *Inversion Tectonics*. Geological Society Special Publication, **44**, 17-39.
- Heaman, L.M. and Tarney, J.,** 1989. U-Pb baddeleyite ages for the Scourie dyke swarm, Scotland: evidence for two distinct intrusion events. *Nature*, **340**, 705-708.
- Heard, H.C.,** 1960. Transition from brittle fracture to ductile flow in Solenhofen limestone as a function of temperature, confining pressure and interstitial fluid pressure. In Griggs, D., and Handin, J. (eds), *Rock Deformation. Memoir of the Geological Society of America*, **79**, 193-226.
- Heddle, M.F.,** 1888. Notes, In Harvie-Brown, J.A., and Buckley, T.E., *A Vertebrate Fauna of the Outer Hebrides*.
- Helwig, J.,** 1976. Shortening of continental crust in orogenic belts and plate tectonics. *Nature*, **260**, 768-770.
- Hills, E.S.,** 1946. Some aspects of the tectonics of Australia. *Proceedings of the Royal Society of New South Wales*, **79**, 67-91.
- Hills, E.S.,** 1960. Morphotectonics and the geomorphological sciences with special reference to Australia. *Quarterly Journal of the Geological Society*, **465**, 77-89.
- Hirth, G., and Tullis, J.,** 1992. Dislocation creep regimes in quartz aggregates. *Journal of Structural Geology*, **14**, 145-159.

- Hobbs, B.E., Means, W.D., and Williams, P.F., 1976.** *An Outline of Structural Geology*. John Wiley, New York. 571pp.
- Holdsworth, R.E., 1989.** Late brittle deformation in a Caledonian ductile thrust wedge: new evidence for gravitational collapse in the Moine thrust sheet, Sutherland Scotland. *Tectonophysics*, **170**, 17-28.
- Holdsworth, R.E., 1994.** Structural evolution of the Gander-Avalon terrane boundary: a reactivated transpression zone in the NE Newfoundland Appalachians. *Journal of the Geological Society of London*, **151**, 629-646.
- Holdsworth, R.E., and Grant, C.J., 1990.** Convergence-related 'dynamic spreading' in a mid-crustal ductile thrust zone: a possible orogenic wedge model. In Knipe, R.J., and Rutter, E.H., (eds), *Deformation Mechanisms, Rheology and Tectonics*,. *Special Publication of the Geological Society of London*, **54**, 491-500.
- Hollister, L.S., and Crawford, M.A., 1986.** Melt-enhanced deformation: a major tectonic process. *Geology*, **14**, 558-561.
- Hopgood, A.M., 1964.** *Structure and tectonic history of Lewisian Gneiss - Isle of Barra*. Unpublished PhD thesis, University of St. Andrews.
- Hopgood, A.M., and Bowes, D.R., 1972.** Application of structural sequence to the correlation of Precambrian gneisses, Outer Hebrides, Scotland. *Bulletin of the Geological Society of America*, **83**, 107-127.
- Hudson, J.D., 1964.** The petrology of the sandstones of the Great Estuarine Series, and the Jurassic Palaeogeography of Scotland. *Proceedings of the Geologists Association*, **75**, 499-528.
- Husebye E.S., Gjoystdal, H., Bungum H., and Eldholm O., 1975.** The seismicity of the Norwegian and Greenland seas and adjacent continental shelf areas. *Tectonophysics*, **26**, 55-70.
- Huyghe, P. and Mugnier, J.L., 1992.** The influence of depth on reactivation in normal faulting. *Journal of Structural Geology*, **14**, 991-998.
- Jackson, J., and McKenzie, D., 1983.** The geometrical evolution of normal fault systems. *Journal of Structural Geology*, **5**, 471-482.
- Jackson, J.A., 1980.** Reactivation of basement faults and crustal shortening in orogenic belts. *Nature*, **283**, 343-346.
- Jamison, D.B., and Cook, N.G.W., 1980.** Note on measured values for the state of stress in the Earth's crust. *Journal of Geophysical Research*, **85**, 1833-1838.
- Jehu, T.J., and Craig, R.M., 1923.** Geology of the Outer Hebrides, Part I, The Barra Isles. *Transactions of the Royal Society of Edinburgh*, **53**, 419-441.
- Jehu, T.J., and Craig, R.M., 1925.** Geology of the Outer Hebrides, Part II, South Uist and Eriskay. *Transactions of the Royal Society of Edinburgh*, **53**, 615-641.
- Jehu, T.J., and Craig, R.M., 1926.** Geology of the Outer Hebrides, Part III, North Uist and Benbecula. *Transactions of the Royal Society of Edinburgh*, **54**, 467-489.
- Jehu, T.J., and Craig, R.M., 1927.** Geology of the Outer Hebrides, Part IV, South Harris. *Transactions of the Royal Society of Edinburgh*, **55**, 457-488.

- Jehu, T.J., and Craig, R.M.**, 1934. Geology of the Outer Hebrides, Part V, North Harris and Lewis. *Transactions of the Royal Society of Edinburgh*, **57**, 839-874.
- Johnstone, G.S., and Mykura, W.**, 1989. British Regional Geology: The Northern Highlands of Scotland. HMSO, London, 219pp
- Kelley, S.P.** 1988. The relationship between K-Ar mineral ages, mica grain sizes and movement on the Moine Thrust Zone, NW Highlands, Scotland. *Journal of the Geological Society of London*, **145**, 1-10.
- Kelley, S.P., Reddy, S.M., and Maddock, R.H.**, 1994. Laser Probe $^{40}\text{Ar}/^{39}\text{Ar}$ investigation of a pseudotachylite and its host rock from the Outer Isles Thrust, Scotland. *Geology*, **22**, 443-446.
- Kennedy, W.Q.**, 1946. The Great Glen Fault. *Quarterly Journal of the Geological Society of London*, **102**, 41-76.
- Kennedy, W.Q.**, 1965. The influence of basement structure on the evolution of the coastal (Mesozoic and Tertiary) basins of Africa. In: *Salt basins around Africa*, Elsevier, New York. 7-16.
- Killick, A.M.**, 1990. Pseudotachylite generated as a result of drilling "burn-in". *Tectonophysics*, **171**, 221-227
- Knipe, R.J.**, 1989. Deformation mechanisms - recognition from natural tectonites. *Journal of Structural Geology*, **11**, 127-146.
- Knipe, R.J., and Wintsch, R.P.**, 1985. Heterogeneous deformation, foliation development, and metamorphic processes in a polyphase mylonite. In Thompson, A.B., and Rubie, D.C. (eds). *Metamorphic Reactions: Kinetics, Textures and Deformation. Advanced Physical geochemistry* **4**, 180-201.
- Kronenberg, A.K., Kirby, S.H., Aines, R.D., and Rossman, G.R.**, 1986. Solubility and diffusional uptake of hydrogen in quartz at high water pressures: implications for hydrolytic weakening. *Journal of Geophysical Research*, **91**, 12723-12744.
- Kronenberg, A.K., and Tullis, J.** 1984. Flow strengths of quartz aggregates: grain size and pressure effects due to hydrolytic weakening. *Journal of Geophysical Research*, **89**, 4281-97.
- Kurstén, M.**, 1957. The metamorphic and tectonic history of parts of the Outer Hebrides. *Transactions of the Edinburgh Geological Society*, **17**, 1-31.
- Lailey, M., Stein, A.M., and Reston, T.J.**, 1989. The Outer Hebrides fault: a major Proterozoic structure in NW Britain. *Journal of the Geological Society of London*, **146**, 253-259.
- Lilwall, R.C.**, 1976. Seismicity and seismic hazard in Britain. *Seismology Bulletin*, **4**, HMSO, London.
- Lisle, R.J.**, 1993. Strike-slip motion in the Minches, NW Scotland, deduced from the trends of the Scourie dyke swarm. *Journal of the Geological Society of London*, **150**, 653-656.
- Lister, G.S., and Snoke, A.W.**, 1984. S-C mylonites. *Journal of Structural Geology*, **6**, 617-638.
- Lister, G.S., and Williams, P.F.**, 1983. The partitioning of deformation in flowing rock masses. *Tectonophysics* **92**, 1-33.

- Lloyd G. and Knipe, R.J.**, 1992. Deformation mechanisms accommodating faulting of quartzite under upper crustal conditions. *Journal of Structural Geology*, **14**, 127-143.
- Macaudiere, J. and Brown, W.L.** 1982. Transcrystalline shear fracturing and pseudotachylite generation in a meta-anorthosite (Harris, Scotland). *Journal of Structural Geology*, **4**, 395-406.
- MacCulloch, J.**, 1819. A description of the Western Isles of Scotland including the Isle of Man (3 vols.), London.
- MacKinnon, A.**, 1974. The Madadh Rocks: A Tertiary olivine dolerite sill in the Outer Hebrides. *Scottish Journal of Geology*, **10**, 67-70.
- Maddock, R.H.**, 1986. The petrogenesis of some fault-generated pseudotachylites. Unpublished PhD thesis, University of London.
- Maddock, R.H.**, 1992. Effects of lithology, cataclasis and melting on the composition of fault-generated pseudotachylites in Lewisian gneiss, Scotland. *Tectonophysics*, **204**, 261-278.
- Magloughlin, J.F.**, 1992. Microstructural and chemical changes associated with cataclasis and frictional melting at shallow crustal levels: the cataclasis - pseudotachylite connection. *Tectonophysics*, **204**, 243-260.
- McClay, K.R., Norton M.G., Coney, P. and Davis G.H.**, 1986. Collapse of the Caledonian orogen and the Old Red Sandstone. *Nature*, **323** 147-149.
- McClay, K.R., and Buchanan, P.G.**, 1992. Thrust faults in inverted extensional basins. In McClay, K.R., (ed). Thrust Tectonics, Chapman and Hall, London, 93-104.
- McConnell, R.B.**, 1972. Geological development of the rift system of eastern Africa. *Bulletin of the Geological society of America*, **83**, 2549- 2572.
- McKenzie, D.P.**, 1969. Speculations on the consequences and causes of plate motions. *Geophysical Journal of the Royal Astronomical Society*, **18** 1-32.
- McKenzie, D.P.**, 1972. Active tectonics of the Mediterranean Region. *Geophysical Journal of the Royal Astronomical Society*, **30**, 109- 185
- McKenzie, D.P.**, 1978. Active tectonics of the Alpine-Himalayan belt: the Aegean Sea and surrounding regions. *Geophysical Journal of the Royal Astronomical Society*, **55**, 217-254.
- McQuillin, R., and Binns, P.E.**, 1973. Geological structure in the Sea of the Hebrides. *Nature, Physical Science*, **241**, 2-4.
- Means, W.D.**, 1987. A newly recognised type of slickenside striation. *Journal of Structural Geology*, **9**, 585-590.
- Mixon, R.B., and Newell, W.L.**, 1977. Stafford fault system: structures documenting Cretaceous and Tertiary deformation along the fall line in northeastern Virginia. *Geology*, **5**, 437-440.
- Molnar, P.**, 1988. Continental tectonics in the aftermath of plate tectonics. *Nature* **335** 131-137.
- Molnar, P., and Tapponier, P.**, 1975. Cenozoic tectonics of Asia: Effects of a continental collision. *Science* **189**, 419-426.

- Moorbath, S., Stewart, A.D., Lawson, D.E., and Williams, G.E.**, 1967. Geochronological studies of the Torridonian sediments of NW Scotland. *Scottish Journal of Geology*, **5**, 154-170.
- Moorbath, S., Powell, J.L., and Taylor, P.N.**, 1975. Isotopic evidence for the age and origin of the grey gneiss complex of the southern Outer Hebrides, Scotland. *Journal of the Geological Society of London*, **131**, 213-222.
- Myashiro, A.** 1994. *Metamorphic petrology*. U.C.L, London.
- Myers, J.S.**, 1970. Gneiss types and their significance in the repeatedly deformed and metamorphosed Lewisian Complex of Western Harris, Outer Hebrides. *Scottish Journal of Geology*, **6**, 186-199.
- Myers, J.S.**, 1971. The late Laxfordian granite-migmatite complex of western Harris, Outer Hebrides. *Scottish Journal of Geology*, **7**, 254-284.
- Nicholson, P.G.**, 1992. Northwestern Britain (Hebriddean Scotland): Mid to Late Proterozoic. In Cope, J.C.W., Ingham, J.K. and Rawson, P.F. (eds). *Atlas of Paleaeogeography and Lithofacies. Memoir of the Geological Society of London*, **13**, 5-6.
- Nuttli, O.W.**, 1973. The Mississippi Valley earthquakes of 1811 and 1812: intensities, ground motion and magnitudes. *Bulletin of the Seismological Society of America*, **63**, 227-248.
- Obee, H.K., and White, S.H.**, 1985. Faults and associated fault of the southern Arunta block, Alice Springs, Central Australia. *Journal of Structural Geology*, **7**, 701-712.
- O'Hara, M.J.**, 1961. Petrology of the Scourie dyke, Sutherland. *Mineralogy Magazine*, **32**, 848-865.
- O'Neill, P.S. and England, R.W.**, 1994. The structure of the Sea of the Hebrides Basin: an integrated gravity and seismic model. *Scottish Journal of Geology*, **30**, 1-9.
- O'Nions, R.K., Hamilton, P.J. and Hooker, P.J.** 1983. A Nd Isotope investigation of sediments related to crustal development in the British Isles. *Earth and Planetary Science Letters*, **63**, 229-240.
- Oxburgh, E.R.**, 1972. Flake tectonics and continental collision. *Nature*, **239**, 202-204.
- Park, R.G.**, 1962. A discussion of Dearnley, R., 1962. An outline of the Lewisian complex of the Outer Hebrides in relation to that of the Scottish mainland. *Quarterly Journal of the Geological Society of London*, **118**, 143-176.
- Park, R.G.**, 1970. Observations on Lewisian chronology. *Scottish Journal of Geology*, **6**, 379-399.
- Park, R.G., Crane, A., and Niamatullah, M.**, 1987. Early Proterozoic structure and kinematic evolution of the southern mainland Lewisian. In Park, R.G., and Tarney, J., (eds), *Evolution of the Lewisian and Comparable High Grade Terrains*. Geological Society Special Publication, **27**, 139-151.
- Park, R.G., and Cresswell, D.**, 1973. The dykes of the Laxfordian belts. In: Park, R.G. and Tarney, J. (eds). *The Early Precambrian of Scotland and related rocks of Greenland*. University of Keele, 119-130.
- Park, R.G., Cliff, R.A., Fettes, D.J., and Stewart, A.D.**, 1994. Precambrian rocks in northwest Scotland west of the Moine thrust: the Lewisian complex and Torridonian. In

- Gibbons, W. and Harris, A.L. (eds). *A revised correlation of Precambrian rocks in the British Isles*. Special Report of the Geological Society of London, **22**, 6-22.
- Park, R.G., and Tarney, J.**, 1987. The Lewisian complex: a typical high-grade gneiss terrain? In Park, R.G., and Tarney, J., (eds), *Evolution of the Lewisian and Comparable High Grade Terrains*. Geological Society Special Publication, **27**, 13-25.
- Passchier, C.W., Hoek, J.D., Bekendam, R.F., and de Boorder, H.**, 1990. Ductile reactivation of Proterozoic brittle fault rocks; an example from the Vestfold Hills, East Antarctica. *Precambrian Research*, **47**, 3-16.
- Passchier, C.W., and Simpson, C.**, 1986. Porphyroclast systems as kinematic indicators. *Journal of Structural Geology*, **8**, 831-844.
- Paterson, M.S.**, 1969. The ductility of rocks. In Argon, A.S. (ed), *Strength and Plasticity*, The M.I.T. Press, Cambridge, MA, 377-392.
- Peach, B.N. and Horne, J.**, 1930. *Chapters on the geology of Scotland*. Oxford University Press, London, 232pp.
- Peddy, C.P.**, 1984. Displacement of the Moho by Outer Isles Thrust shown by seismic modelling. *Nature*, **312**, 628-630.
- Peterson, T.A., Brown, R.D., Cook, F.A., Kaufman, S., and Oliver, J.E.**, 1984. Structure of the Riddleville basin from COCORP seismic data and implications for reactivation tectonics. *Journal of Geology*, **92**, 261-271.
- Petit, J.P.**, 1987. Criteria for the sense of movement on fault surfaces in brittle rocks. *Journal of Structural Geology*, **9**, 597-608.
- Philcox, M.E., Sevastopulo, G.D., and MacDermot, C.V.**, 1989. Intra-Dinantian tectonic activity on the Curlew Fault, north-west Ireland. In Arthurton, R.S., Gutteridge, P. and Nolan S.C., (eds). *The role of tectonics in Devonian and Carboniferous sedimentation in the British Isles*. The Yorkshire Geological Society (Occasional publication No. 6) 55-66.
- Piper, J.D.A.**, 1992. Post-Laxfordian magnetic imprint in the Lewisian metamorphic complex, and strike-slip motion in the Minches, NW Scotland. *Journal of the Geological Society of London*, **149**, 127-137.
- Ramsay, J.G.**, 1962. Interference patterns produced by the superposition of folds of similar types. *Journal of Geology*, **70**, 466-481.
- Ramsay, J.G., and Graham, R.H.**, 1970. Strain variation in shear belts. *Canadian Journal of Earth Sciences*, **7**, 786-813.
- Ratcliffe, N.M.**, 1971. The Ramapo fault system in New York and adjacent northern New Jersey: A case of tectonic heredity. *Geological Society of America Bulletin*, **82**, 125-142.
- Ratcliffe, N.M., Burton, W.C., D'Angelo, R.M., and Costain, J.K.**, 1986. Low angle extensional faulting, reactivated mylonites, and seismic reflection geometry of the Newark basin margin in eastern Pennsylvania. *Geology*, **14**, 766-770.
- Reston, T.J.**, 1987. Spatial interference, reflection character and the structure of the lower crust under extension. Results from 2-D seismic modelling. *Annales Geophysicae*, **5B**, 339-348.
- Rice, J.R.**, 1992. Fault stress states, Pore Pressure Distributions, and the weakness of the San Andreas Fault. In Evans, B. and Wong, T.F., (eds), *Fault mechanics and Transport Properties of Rocks*. Academic Press, 476-503.

- Ricoult, D.L., and Kohlstedt, D.L.**, 1983. Structural width of low angle grain boundaries in olivine. *Physical Chemistry and mineralogy*, **9**, 133-138.
- Riedel, W.**, 1929. Zur mechanik geologischer Brucherscheinungen. *Zentralblatt fur Mineralogie Geologie und Palaeontologie*. Abhandlung **B**, 343-368.
- Roberts, D.G., Bott, M.H.P., and Uruski, C.**, 1983. Structure and origin of the Wyville-Thomson Ridge. In, Bott, M.H.P., Saxon, S., Talwani, M and Thiede, J. (eds). *Structure and Evolution of the Greenland, Iceland, Faroe Ridge*. Plenum Press, New York. 133-159.
- Rubie, D.C.**, 1983. Reaction enhanced ductility; the role of solid-solid univariant reactions in the deformation of the crust and mantle. *Tectonophysics*, **96**, 331-352.
- Rubie, D.C.**, 1990. Mechanisms of reaction-enhanced deformability in minerals and rocks. In Barber, D.J. and Meredith, P.G. (eds). *Deformation processes in minerals, ceramics and rocks*. Cambridge University press, 262-294
- Rutter, E.H.**, 1976. The kinetics of rock deformation by pressure solution. *Philosophical Transactions of the Royal Society of London*, **A283**, 203-219.
- Rutter, E.H.**, 1983. Pressure solution in nature, theory and experiment. *Journal of the Geological Society of London*, **140**, 725-740.
- Rutter, E.H., & Brodie, K.H.**, 1985. Experimental deformation of serpentinite under conditions of syntectonic dehydration. *Abstracts of the international conference on tectonics and structural processes, utrecht* 45- 46.
- Sadowski, G.R.**, 1978. Platform activation in South America and the South Atlantic fracture zones. In Sykes L.R., 1978. Intraplate seismicity, reactivation of preexisting zones of weakness, alkaline magmatism, and other tectonism postdating continental fragmentation. *Reviews of Geophysics and Space Physics* **16** 621-688.
- Sanderson, D.J.**, 1982. Models of strain variation in nappes and thrust sheets: a review. *Tectonophysics*, **88**, 201-233.
- Schmid, S.M., Boland, J.N., and Paterson, M.S.**, 1977. Superplastic flow in fine grained limestones. *Tectonophysics*, **43**, 257-292.
- Scholz, C.H.**, 1968. Microfracturing and inelastic deformation of rock in compression. *Journal of Geophysical Research*, **73**, 1417-1432.
- Scholz, C.H.**, 1990. *The mechanics of earthquakes and faulting*. Cambridge University Press, 433pp.
- Shihe, L., and Park, R.G.**, 1993. Reversals of movement sense in the Lewisian brittle-ductile shear zones at Gairloch, NW Scotland, in the context of Laxfordian kinematic history. *Scottish Journal of Geology*, **29**, 9-19.
- Sibson, R.H.**, 1973. Interactions between temperature and pore-fluid pressure during earthquake faulting - a mechanism for partial or total stress relief. *Nature - Physical Science*, **243**, 66-68.
- Sibson, R.H.**, 1974. Frictional constraints on thrust, wrench and normal faults. *Nature*, **249**, 542-543.
- Sibson, R.H.**, 1975. Generation of pseudotachylite by ancient seismic faulting. *Geophysical Journal of the Royal Astronomical Society*, **43**, 775-794.

- Sibson, R.H.**, 1977a. Fault rocks and fault mechanisms. *Journal of the Geological society of London*, **133**, 191-213.
- Sibson, R.H.**, 1977b. *The Outer Hebrides Thrust: Its Structure, Mechanism and Deformation Environment*. Unpublished PhD thesis, University of London, 254pp.
- Sibson, R.H.**, 1980. Transient discontinuities in ductile shear zones. *Journal of Structural Geology*, **2**, 165-171.
- Sibson, R.H.**, 1985. A note on fault reactivation. *Journal of structural Geology*, **7**, 751-754.
- Sibson, R.H.**, 1989. Earthquake faulting, induced fluid flow, and fault-hosted gold-quartz mineralization. In Bartholomew, M.J., Hyndman, D.W., Mogk, D.W., and Mason, R.(eds). *Basement Tectonics 8: Characterisation and comparison of Ancient and Mesozoic Continental Margins*. Proceedings of the 8th International Conference on Basement Tectonics. 603-614.
- Sibson R.H.**, 1993. Load-strengthening vs load-weakening faults. *Journal of Structural Geology*, **15**, 123-128.
- Simpson, C.**, 1985. Deformation of granitic rocks across the brittle-ductile transition. *Journal of Structural Geology*, **7**, 503-511.
- Simpson, C.** 1986. Fabric development in brittle-to-ductile shear zones. *Pageoph*, **124**, 269-288.
- Simpson, C. and Schmid, S.M.**, 1983. An evaluation of criteria to deduce the sense of movement in sheared rocks. *Geological Society of America Bulletin*, **94**, 1281-1288.
- Simpson, I.R., Gravestock, M., Ham, D., Leach, H., and Thompson, S.D.**, 1989. Notes and cross-sections illustrating inversion tectonics in the Wessex basin. In Cooper, M.A., and Williams G.D., (eds) 1989. *Inversion Tectonics*. Geological Society Special Publication, **44**, 123-129.
- Smale, J.L., Thurnell, R.C., and Schamel, S.**, 1988. Sedimentological evidence for early Miocene fault reactivation in the Gulf of Suez. *Geology*, **16**, 113-116.
- Smithson, S.B., Brewer, J.A., Kaufman, S., Oliver, J.E., and Hurich C.A.**, 1979. Structure of the Laramide Wind River uplift, Wyoming, from COCORP deep reflection data and from gravity data. *Journal of Geophysical Research*, **84**, 5955-5972.
- Smythe, D.K.**, 1982. Results of the Moine Outer Isles Seismic Traverse (MOIST) (abs.) *Newsletter of the Geological Society of London*, **11**, 11.
- Smythe, D.K.**, 1987. Deep seismic reflection profiling of the Lewisian foreland. In Park, R.G., and Tarney, J., (eds), *Evolution of the Lewisian and Comparable High Grade Terrains*. Geological Society Special Publication, **27**, 193-203.
- Smythe, D.K., Dobinson, A., McQuillin, R., Brewer, J.A., Matthews, D.H., Blundell, D.J. and Kelk, B.**, 1982. Deep structure of the Scottish Caledonides revealed by the MOIST reflection profile. *Nature*, **299**, 338-340.
- Smythe, D.K. and Kenolty, N.** 1975. Tertiary sediments in the Sea of the Hebrides. *Journal of the Geological Society of London* **131**, 227-233.
- Soper, N.J., Strachan, R.A., Holdsworth, R.E., Gayer, R.A., and Greiling, R.O.**, 1992. Sinistral transpression and the Silurian closure of Iapetus. *Journal of the Geological Society of London*, **149**, 871-880.

- Steavenson, A.G.**, 1928. Some geological notes on three districts of Northern Scotland. *Transactions of the Geological Society of Glasgow*, **18**, 193-233.
- Steel, R.J.**, 1971. New Red Sandstone movement on the Minch Fault. *Nature, Physical Science*, **234** 158-159.
- Steel, R.J., and Wilson, A.C.**, 1975. Sedimentation and tectonism (?Permo-Triassic) on the margin of the North Minch Basin, Lewis. *Journal of the Geological Society of London*, **131**, 183-202
- Stein, A.M.**, 1988. Basement controls upon basin development in the Caledonian foreland, NW Scotland. *Basin Research*, **1**, 107-119.
- Steltonpohl, M.G., and Bartley, J.M.**, 1993. Postcollisional extension of the Caledonide orogen in Scandanavia: Structural expressions and tectonic significance: Comment and reply. *Geology*, 476-477.
- Stocklin, J.**, 1968. Structural history and tectonics of Iran: a review. *Bulletin of the American Association of Petroleum Geologists*, **52**, 1229-58.
- Stoneley, R.**, 1982. The structural development of the Wessex Basin. *Journal of the Geological society of London* **139**, 545-552.
- Storetvedt, K.M., and Steel, R.J.**, 1977. Palaeomagnetic evidence for the age of the Stornoway Formation. *Scottish Journal of Geology*, **13**, 263-269.
- Sutton, J., and Watson, J.**, 1951. The pre-Torridonian metamorphic history of the Loch torridon and Scourie areas in the north-west Highlands, and its bearing on the chronological classification of the Lewisian. *Journal of the Geological Society of London*, **104**, 241-307
- Sutton, J., and Watson, J.** 1962. Further observations on the margin of the Laxfordian complex of the Lewisian near Loch Laxford, Sutherland. *Transactions of the Royal Society of Edinburgh*, **65**, 89-106.
- Swanson, M.T.**, 1988. Pseudotachylite-bearing strike-slip duplex structures in the Fort Foster Brittle Zone, S. Maine. *Journal of Structural Geology*, **10**, 813-828.
- Sykes L.R.**, 1978. Intraplate seismicity, reactivation of preexisting zones of weakness, alkaline magmatism, and other tectonism postdating continental fragmentation. *Reviews of Geophysics and Space Physics* **16** 621-688.
- Talwani, P., and Howell, D.E.**, 1976. Crustal structure of South Carolina; some speculations. *Geological Society of America abstracts program*, **8**, 284.
- Techmer, K.S., Ahrendt, H. and Weber, K.**, 1992. The development of pseudotachylite in the Ivrea-Verbarno Zone of the Italian Alps. *Tectonophysics*, **204**, 307-322.
- Twiss, R.J.**, 1977. Theory and applicability of a recrystallised grain size palaeopiezometer. *Pure and Applied Geophysics*, **115**, 227-224.
- Twiss, R.J., and Moores, E.M.**, 1992. *Structural Geology*. W.H. Freeman & Co, New York, 532pp.
- Van Breemen, O., Aftalion, M., and Pidgeon, R.T.**, 1971. The age of the granitic injection complex of Harris Outer Hebrides. *Scottish Journal of Geology*, **7**, 139-152.
- Van Breemen, O., Aftalion, M., and Johnson, M.R.W.**, 1979. Age of the Loch Borrolan complex, Assynt, and the late movements along the Moine Thrust Zone. *Journal of the Geological Society of London*, **136**, 489-497.

Vink, G.E., Morgan, W.J., and Zhao, W.L., 1984. Preferential rifting of continents: a source of displaced terranes. *Journal of Geophysical research*, **89**, B12, 10072-10076.

Walker, J., 1990. *A study of the deformation environment of the Outer Hebrides Fault Zone*. Unpublished PhD thesis, University of London. 419pp.

Watterson, J., 1975. Mechanisms for the persistence of tectonic lineaments. *Nature*, **253**, 520-521.

Weaver, B.L., and Tarney, J., 1980. Rare earth geochemistry of Lewisian granulite facies gneisses, northwest Scotland: implications for the petrogenesis for the Archaean lower continental crust. *Earth and Planetary Science Letters*, **51**, 279-296.

Wernicke, B., 1986. Whole-lithosphere normal simple shear: an interpretation of deep-reflection profiles in Great Britain. In Barazangi, M. and Brown, L.D. (eds). *Reflection seismology: the continental crust*. American Geophysical Union Geodynamics Series, **14**, 331-339.

White, S.H., 1982. Fault rocks of the Moine Thrust Zone: a guide to their nomenclature. *Textures and microstructures*, **5**, 211-221.

White, S.H., Bretan, P.G., and Rutter, E.H., 1986. Fault-zone reactivation: kinematics and mechanisms. *Philosophical Transactions of the Royal Society of London*, **A 317** 81-97.

White, S.H., and Glasser, J., 1987. The Outer Hebrides Fault Zone: evidence for normal movements. In Park, R.G., and Tarney, J., (eds), *Evolution of the Lewisian and Comparable High Grade Terrains*. Geological Society Special Publication, **27**, 175 - 183.

White, S.H., and Green P.F., 1985. Tectonic development of the Alpine fault zone, New Zealand: A fission track study. *Geology*, **14**, 124-127.

White, S.H., and Muir, M.D., 1989. Multiple reactivation of coupled orthogonal fault systems: An example from the Kimberley region in north Western Australia. *Geology*, **17**, 618-621.

Whitehouse, M.J., 1993, Age of the Corodale Gneisses, South Uist. *Scottish Journal of Geology*, **39**, 49-58.

Williams, G.D., Powell, C.M., and Cooper, M.A., Geometry and kinematics of inversion tectonics. In Cooper, M.A., and Williams G.D., (eds) 1989. *Inversion Tectonics*. Geological Society Special Publication, **44**, 3-15.

Williams, P.F., 1990. Differentiated layering in metamorphic rocks. *Earth Science Review*, **29**, 267-281.

Williams, P.F., Goodwin, L.B., and Ralser, S., 1994. Ductile Deformation Processes. In, Hancock, P.L., (ed). *Continental Deformation*, Pergamon Press, Oxford, 1-27.

Wilson, J.T., 1966. Did the Atlantic close and then re-open? *Nature*, **211**, 676-681.

Winslow, M.A., 1981. Mechanisms for basement shortening in the Andean foreland fold belt of southern South America. In McClay, K.R. and Price, N.J. (eds). *Thrust and Nappe Tectonic*. Special Publication of the Geological Society of London, **9**, 513-528.

Wise, D.U., Dunn, D.E., Engelder, J.T., Geiser, P.A., Hatcher, R.D., Kish, S.A., Odom, A.L., and Schamel, S., 1984. Fault-related rocks: Suggestions for terminology. *Geology*, **12**, 391-394.

Woolard, G.P., 1958. Areas of tectonic activity in the United States as indicated by earthquake epicenters. *Eos Transactions AGU*, **39** 1135-1150.

Yardley, B.W.D., 1989. *An introduction to metamorphic petrology*. Longman, U.K., 248pp.

Ziegler, P.A., 1983. Inverted basins in the Alpine foreland. In Bally, A.W., (ed). *Seismic Expression of Structural Styles - A Picture and Work Atlas*. American Association of Petroleum Geologists, *Studies in Geology, Series No. 15*, **3**, 3.3.3-3.3.12.

Zoback, M.L. and Zoback, M.D., 1980. Faulting patterns in North-Central Nevada and strength of the crust. *Journal of Geophysical Research*, **85** (No B1), 275-284.